University of Florida
Civil and Coastal Engineering

Final Report   Deliverable 8, September 2020

Geo-statistical Deep Foundation Design Software

Principal investigator:
Michael T. Davidson

Co-Principal investigators:
Michael C. McVay, Gary R. Consolazio

Lead User Interface Developer:
Clinton J. Monari

Project Consultant:
Michael A. Faraone

Bridge Software Institute
Engineering School of Sustainable Infrastructure & Environment
College of Engineering
University of Florida
P.O. Box 116580
Gainesville, Florida 32611

Sponsor:
Florida Department of Transportation (FDOT)

Project Manager:
Rodrigo Herrera

Contract:
FDOT BDV31-977-108
UF Project No. 0118651

DISCLAIMER

UNIT CONVERSION

APPROXIMATE CONVERSIONS TO SI UNITS

SYMBOL	WHEN YOU KNOW	MULTIPLY BY	TO FIND	SYMBOL
LENGTH				
in	inches	25.4	millimeters	mm
ft	feet	0.305	meters	m
yd	yards	0.914	meters	m
mi	miles	1.61	kilometers	km

SYMBOL	WHEN YOU KNOW	MULTIPLY BY	TO FIND	SYMBOL
AREA				
in²	square inches	645.2	square millimeters	mm²
ft²	square feet	0.093	square meters	m²
yd²	square yard	0.836	square meters	m²
mi²	square miles	2.59	square kilometers	km²

SYMBOL	WHEN YOU KNOW	MULTIPLY BY	TO FIND	SYMBOL
VOLUME				
fl oz	fluid ounces	29.57	milliliters	mL
ft³	cubic feet	0.028	cubic meters	m³
yd³	cubic yards	0.765	cubic meters	m³
NOTE: volumes greater than 1,000 L shall be shown in m³				

SYMBOL	WHEN YOU KNOW	MULTIPLY BY	TO FIND	SYMBOL
MASS				
oz	ounces	28.35	grams	g
lb	pounds	0.454	kilograms	kg
T	short tons (2,000 lb)	0.907	megagrams (or "metric ton")	Mg (or "t")

SYMBOL	WHEN YOU KNOW	MULTIPLY BY	TO FIND	SYMBOL
TEMPERATURE (exact degrees)				
°F	Fahrenheit	5 (F-32)/9 or (F-32)/1.8	Celsius	°C

SYMBOL	WHEN YOU KNOW	MULTIPLY BY	TO FIND	SYMBOL
ILLUMINATION				
fc	foot-candles	10.76	lux	lx
fl	foot-Lamberts	3.426	candela/m²	cd/m²

SYMBOL	WHEN YOU KNOW	MULTIPLY BY	TO FIND	SYMBOL
FORCE and PRESSURE or STRESS				
lbf	pound force	4.45	newtons	N
kips	kips	4,448.22	newtons	N
lbf/in²	pound force per square inch	6.89	kilopascals	kPa
ksi	kips per square inch	6,894.76	kilopascals	kPa
tsf	tons (short) per square foot	95.67	kilopascals	kPa
pcf	pound force per cubic foot	156.967	newtons per cubic meter	N/m³

APPROXIMATE CONVERSIONS TO ENGLISH UNITS

SYMBOL	WHEN YOU KNOW	MULTIPLY BY	TO FIND	SYMBOL
		LENGTH		
mm	millimeters	0.039	inches	in
m	meters	3.28	feet	ft
m	meters	1.09	yards	yd
km	kilometers	0.621	miles	mi

SYMBOL	WHEN YOU KNOW	MULTIPLY BY	TO FIND	SYMBOL
		AREA		
mm^2	square millimeters	0.0016	square inches	in^2
m^2	square meters	10.764	square feet	ft^2
m^2	square meters	1.195	square yards	yd^2
ha	hectares	2.47	acres	ac
km^2	square kilometers	0.386	square miles	mi^2

SYMBOL	WHEN YOU KNOW	MULTIPLY BY	TO FIND	SYMBOL
		VOLUME		
mL	milliliters	0.034	fluid ounces	fl oz
L	liters	0.264	gallons	gal
m^3	cubic meters	35.314	cubic feet	ft^3
m^3	cubic meters	1.307	cubic yards	yd^3

SYMBOL	WHEN YOU KNOW	MULTIPLY BY	TO FIND	SYMBOL
		MASS		
g	grams	0.035	ounces	oz
kg	kilograms	2.202	pounds	lb
Mg (or "t")	megagrams (or "metric ton")	1.103	short tons (2,000 lb)	T

SYMBOL	WHEN YOU KNOW	MULTIPLY BY	TO FIND	SYMBOL
		TEMPERATURE (exact degrees)		
°C	Celsius	1.8C+32	Fahrenheit	°F

SYMBOL	WHEN YOU KNOW	MULTIPLY BY	TO FIND	SYMBOL
		ILLUMINATION		
lx	lux	0.0929	foot-candles	fc
cd/m^2	candela/m^2	0.2919	foot-Lamberts	fl

SYMBOL	WHEN YOU KNOW	MULTIPLY BY	TO FIND	SYMBOL
		FORCE and PRESSURE or STRESS		
N	newtons	0.225	pound force	lbf
N	newtons	0.000224809	kips	kips
kPa	kilopascals	0.145	pound force per square inch	lbf/in^2
kPa	kilopascals	0.000145	kips per square inch	ksi
kPa	kilopascals	0.000145038	kips per square inch	ksi
N/m^3	newtons per cubic meter	0.0104526	pound force per cubic foot	pcf

*SI is the symbol for International System of Units. Appropriate rounding should be made to comply with Section 4 of ASTM E380. (Revised March 2003).

TECHNICAL REPORT DOCUMENTATION PAGE

1. Report No.	2. Government Accession No.	3. Recipient's Catalog No.

4. Title and Subtitle	5. Report Date
Geo-statistical Deep Foundation Design Software	September 2020
	6. Performing Organization Code

7. Author(s)	8. Performing Organization Report No.
Davidson, M. T., McVay, M. C., Consolazio, G. R., Monari, C. J., Patil, A., and Faraone, M. A.	

9. Performing Organization Name and Address	10. Work Unit No. (TRAIS)
Bridge Software Institute	
University of Florida	11. Contract or Grant No.
1949 Stadium Rd. Room 365	
P.O. Box 116580	BDV31-977-108
Gainesville, FL 32611	

12. Sponsoring Agency Name and Address	13. Type of Report and Period Covered
Florida Department of Transportation	
605 Suwannee Street, MS 30	Final Report
Tallahassee, FL 32399	03/12/2019 - 09/30/2020
	14. Sponsoring Agency Code

15. Supplementary Notes

16. Abstract

Significant portions of overall design and construction costs for Florida bridges are typically attributed to deep foundation components. Such costs arise because soils are highly variable materials; measured soil properties typically exhibit spatial variability across a given site, both with respect to depth and horizontal position. In addition, empirical methods by which measured and lab-determined soil properties are correlated to design-relevant soil resistance quantities introduce a separate form of uncertainty into the design process. Directly accounting for these two distinct sources of uncertainty (spatial variability, method error) in bridge foundation design can bring about improved (1) soil or rock layering as well as zones or regions to reduce coefficients of variation and (2) increased reliability-based foundation configurations for given boring and strength data. As part of previous FDOT-funded research, geostatistical techniques and method-error characterizations were coded into a prototype software tool. The current project was undertaken to transition the software from a research tool into a design tool, referred to as GeoStat. Detailed in this report are efforts and outcomes associated with (1) establishing an input file format and data read/write operations; (2) automation of calls to pre-existing pile/shaft axial capacity calculation software; (3) quality assurance testing; (4) development of an installation package and licensing; (5) development of a software user manual; (6) development of a software technical manual; and, (7) deployment of the software. Accordingly, the GeoStat software is ready to be officially deployed so that it can be made use of by practicing engineers.

17. Key Words	18. Distribution Statement
Deep foundation design; Geostatistics; Spatial variability; Method error; Pile and shaft axial capacity	No restrictions.

19. Security Classif. (of this report)	20. Security Classif. (of this page)	21. No. of Pages	22. Price
Unclassified	Unclassified	336	

ACKNOWLEDGEMENTS

EXECUTIVE SUMMARY

Deep foundations can consume substantial portions of overall design and construction costs for Florida bridges. Such costs arise because soils are highly variable materials. For example, measured soil properties typically exhibit spatial variability (both horizontally and vertically) across a given site. Further, empirical methods by which measured soil properties are correlated to design-relevant pile/shaft-soil resistance introduce a separate form of uncertainty into the design process. These uncertainties present challenges in determining if sufficient site data have been gathered as part of required geotechnical investigations and also can result in non-uniform practices when making use of geotechnical site data to empirically estimate soil resistance for deep foundation member design. Therefore, quantifying these two distinct sources of uncertainty (spatial variability, method error) can lead to (1) efficient distribution of boring or coring locations during geotechnical investigations; (2) conservative, reliability-based foundation designs; and, (3) economical allocation of construction materials to the multiple foundation systems within bridges.

The benefits of quantifying spatial variability and method error and incorporating the phenomena into bridge foundation designs were investigated as part of previously completed FDOT research (BDK75-977-23). Therein, it was demonstrated that geostatistical techniques— which may be thought of as statistical interpolation—are viable for quantifying soil-spatial variability of site measurements (e.g., SPT-N values and rock unconfined compressive strengths). Additionally, the FDOT-funded research produced methodologies for estimating method error. The statistical techniques and methodologies were ultimately bundled into a prototype software package.

The objective of the current project was to transform the software package developed in BDK75-977-23 from a research tool into a design tool, referred to as GeoStat, which computes pile or shaft axial resistance (and the associated descriptive statistics), given site data. More specifically, the program accepts a collection of borings/corings pertinent to a site of interest, performs both spatial variability analysis and method error estimation and permits generation of location-specific output such as through-depth resistance profiles and associated resistance factors. Foundation design data generated in this manner overcome significant simplifications typical of current practice, where phenomena such as spatial variability are either ignored or indirectly accounted for via significantly more conservative (and more costly) configurations.

The design software, GeoStat, allows for statistical methods to be leveraged by practicing engineers in a robust manner and also facilitates estimations of pile/shaft axial resistance quantities, variability, and uncertainty. Transitioning the software from a prototype tool to a deployable package for use by practicing engineers entails (1) establishing an input file format and data read/write operations; (2) automation of calls to pre-existing pile/shaft axial capacity calculation software; (3) quality assurance testing; (4) development of an installation package and licensing; (5) development of a software user manual; (6) development of a software technical manual; and, (7) deployment of the software. Documented in the following are the outcomes associated with each of the seven items listed above.

TABLE OF CONTENTS

LIST OF FIGURES

LIST OF TABLES

CHAPTER 1
INTRODUCTION

1.1 Introduction

Due in part to intrinsic variability of soil and rock materials, design and construction of deep foundations typically comprise significant costs for Florida bridges. Measured soil properties exhibit spatial variability across a given site (both with respect to depth and horizontal position), while empirical methods by which measured soil properties are correlated to design-relevant soil or rock resistances introduce a separate form of uncertainty into the design process. These sources of uncertainty present challenges in determining layering and distinct zones as well as if sufficient site data have been gathered as part of required geotechnical investigations, which can result in non-representative (unconservative, overly conservative) estimates of Load and Resistance Factor Design (LRFD) resistances (as a function of embedment depth) of deep foundation members. Quantifying these distinct sources of uncertainty (spatial variability, method error) allows for better determination of whether or not sufficient geotechnical site data have been gathered and also makes clear the level of uncertainty that can be attributed to predicted resistance of deep foundation members. By making analysis and design tools available to characterize these forms of uncertainty, more efficient design efforts and more economical allocation of construction materials can potentially be realized for bridge substructure configurations (Rivers, 2018).

The benefits of quantifying uncertainties due to spatial variability and method error and incorporating them into bridge foundation designs were investigated as part of previously completed FDOT-funded research (McVay et al. 2009; Klammler et al. 2010). It was subsequently demonstrated (McVay et al. 2012; Faraone, 2014) that geostatistical techniques—which may be thought of as statistical interpolation—are viable for quantifying soil-spatial variability of site measurements (e.g., SPT, unconfined compressive strength). Additionally, the FDOT-funded research allowed for gathering and production of methodologies for estimating method error. In McVay et al. (2012), the statistical techniques and methodologies were ultimately bundled into a prototype software tool, referred to as GS-Deep.

In the present research, the previously developed research tool (GS-Deep) is enhanced and streamlined into a deployable software package, referred to as GeoStat, for use by practicing engineers. GeoStat is intended for computing pile or shaft axial capacity, the associated uncertainty of those estimates, and Load and Resistance Factor Design (LRFD) resistance factors (ϕ) over a selected range of member embedment lengths for given site data and engineer-selected layering and zones. More specifically, the program accepts a collection of borings/corings pertinent to a site of interest, the engineer divides the site into zones and, for each zone, determines the layering. The software is then used to perform both spatial-variability analysis and method error estimation on a pile/shaft, resulting in generation of location-specific output such as through-depth resistance profiles and associated resistance factors (ϕ).

Foundation design data generated in this manner overcome significant simplifications typical of current practice, where phenomena such as rock layering and area zones (i.e., spatial variability) are either ignored or indirectly accounted for via significantly more conservative (and more costly) configurations. By incorporating this type of software into the design process,

quantitative indicators of scope and sufficiency will become available for budgeting, and conducting, geotechnical investigations. Also, the ability to quantify variability in foundation resistance quantities (e.g., the effect of pile/shaft lengths on LRFD resistance factors, ϕ), in turn, allows practicing engineers to achieve more optimized (and cost-effective) foundation designs.

1.2 Motivation

For geotechnical design methods to provide reliable estimates of foundation resistance, the soil or rock parameters used in design must reflect subsurface conditions as accurately as possible. Considering the small volume of soil or rock analyzed in-situ and recovered for laboratory testing, geotechnical engineers are faced with having to assess variability and uncertainty for each project with a very limited amount of data. For the purposes of this work, the term variability is used to describe the change in subsurface characteristics with respect to distance (vertical or horizontal), and the term uncertainty is used to describe the lack of knowledge regarding how the magnitude of a specific parameter changes throughout a project site (vertically or horizontally).

To make a clear distinction on terminology, variability can be thought of as a non-homogenous subsurface profile that could result from either manmade or natural processes, such as soil or rock layering and/or the presence of zones. Uncertainty is related to the engineer's limited knowledge of how rock strength varies within the volume of interest. One of the more challenging tasks for geotechnical engineers is the assessment of variability and uncertainty between points of exploration (e.g., standard penetration test, SPT, boring). The issue is compounded by the fact that there is no method of assessment that is universally adopted by either local or national codes, resulting in either inconsistent assessments or a complete lack of acknowledgement of these sources of variability (and uncertainty) during design. Currently, the approach that is most widely used to address the issue is specifying a minimum amount of subsurface exploration that must be conducted. This approach (as useful as it is) is still restricted however, since only a limited number of discrete points can be used for testing and sampling. In practice, the question of how engineering parameters and geological stratification changes between test points remains.

Given that some quantity of geotechnical investigation data are available for a site, the GeoStat software can be used to compute descriptive statistics (mean; standard deviation; and coefficient of variation, COV) of location-specific pile or shaft axial (skin, tip) resistance, over the range of embedded member lengths considered. In addition, the software allows the engineer to separate the site into layers and zones to minimize individual pile/shaft COVs for direct estimates of the associated LRFD resistance factors. In turn, direct estimates of LRFD resistance factors allow for comparisons to the factors required in provisions such as the FDOT Structures Design Guidelines (FDOT 2019) and AASHTO (2017). Computed foundation design resistances, the associated uncertainty, and resistance factors (ϕ) that are generated in this manner improve upon deterministic approaches typical of current practice, where phenomena such as spatial variability are either ignored or indirectly accounted for via significantly more conservative (and potentially more costly) configurations.

The remainder of the current report documents outcomes from the major steps taken towards making the statistical methods housed within GeoStat available for use by practicing engineers. Major outcomes include quality assurance testing of the program user interface (UI)

and underlying analysis routines. In addition, two manuals (that accompany the software) are presented. Namely, a Help Manual is provided (Appendix A) for installing and licensing the software; formatting of model file input; and, navigating all controls contained within the UI. In addition, a Technical Manual is provided in Appendix B, which provides review of relevant statistical concepts; and, two comprehensive, illustrative examples of modeling and simulating member axial resistances.

1.3 Objective and Supporting Tasks

The focus of the current research is to build upon prototype software, GS-Deep, developed in FDOT BDK75 977-23 and establish a streamlined design tool, referred to as GeoStat, for use by practicing engineers. The current research project includes seven major thrusts: (1) Defining an input file format and data read/write operations; (2) Automation of calls to pre-existing pile/shaft axial capacity calculation software; (3) Quality assurance testing; (4) Development of an installation package and licensing; (5) Development of a software user manual; (6) Development of a software technical manual; and, (7) Deployment of the software. A brief summary of each task, and the associated outcome, is provided below.

1.3.1 Task 1 – Establish Input File Format and Data Read/Write

Task 1 focused upon item (1) above: establishing an input file format and data read/write operations. As context, intended program usage of GeoStat is such that engineers work from left to right across a "tabbed" interface. An advantage of the tabbed interface is that it visually presents engineers with an intuitive progression of program usage, gradually transitioning from data input (leftmost tabs) to analysis, and ultimately, to presentation of results (rightmost tabs). Given that the leftmost program tabs pertain to data input, engineers making use of GeoStat will typically begin program usage by creating a new input file, or by opening a pre-existing input file.

A major component of Task 1 consisted of establishing a standardized input file format. The standardized input file format is in the form of non-programmed (i.e. non-VBA) Microsoft® Excel sheets. The input file is organized such that there is one Excel worksheet tab dedicated to each major component of the GeoStat UI. Also, one additional Excel worksheet tab is reserved for each boring or coring location applicable to a given site (i.e., for each unique location throughout the site at which geotechnical investigation data are available). For this latter category of input data, the formatting is structured to match that of pre-existing axial capacity calculation software (FB-Deep). An additional component of the Task 1 efforts is implementation of input file read and file write capabilities in the program UI.

Outcomes from the efforts of Task 1 were packaged into portions of the GeoStat Help Manual (Ch.3 of Appendix A). Documented therein are the standardized format of GeoStat input files. More specifically, all input associated with each applicable UI component is documented (e.g., tab, input box, table), across combinations of structural member type, soil type, and analysis method.

1.3.2 Task 2 – Automate Calls to Axial Capacity Software, FB-Deep

Task 2 focused upon item (2) above: automation of calls to pre-existing pile/shaft axial capacity calculation software. Within the tabbed interface of GeoStat, the "Simulation" tab is located within the central region of the overall left-to-right tabbed program layout, which signifies that the "Simulation" tab pertains to analysis (as opposed to input or presentation of results). In particular, the "Simulation" tab involves statistical sampling and creation of a corresponding number of individual FB-Deep input files (e.g., 2,000), where FB-Deep is a separate software package used by bridge engineers to calculate design axial capacities of driven piles and drilled shafts.

In order to streamline GeoStat usage for practicing engineers, Task 2 consisted of automating the numerous analysis calls to FB-Deep. Further, as part of Task 2, the process of importing the collective FB-Deep output data back into GeoStat is automated. As an outcome from Task 2, the GeoStat Help Manual contains details (Ch. 5 of Appendix A) of the various forms of interaction between geostatistical software (GeoStat) and axial capacity calculation software (FB-Deep). The nature of such program-to-program interfacing includes: automatic generation of FB-Deep model files from within GeoStat; batch mode analysis of FB-Deep models; and, bulk post-processing of FB-Deep analysis output. As a critical step in propelling GeoStat towards viable use by practicing engineers, all such program-to-program interfacing has been streamlined or automated, as detailed in the Help Manual.

1.3.3 Task 3 – Conduct Quality Assurance Testing

Task 3 focused upon item (3) above: quality assurance testing. In order to promote and sustain widespread adoption of the GeoStat software by practicing engineers, program robustness is assessed across multiple input sets. More specifically, quality assurance testing is carried out to ensure that the program possesses the ability to maintain data integrity when writing to (or reading) files; detect and alert engineers when non-viable data are input; form FB-Deep input files; post-process the collection of FB-Deep output files; pass data to the analytical engine; obtain data from the analytical engine; and, display descriptive statistics of axial capacity.

Task 3 consisted of passing several data sets through all program tabs, verifying that data integrity is upheld for each data set, and that end-user notifications are issued in the event that improper data are input at any location within the UI. Also, as part of Task 3, error detection is implemented to prevent program crashes.

Outcomes associated with Task 3 are documented in Ch. 2 through Ch. 4 of the current report. Documentation includes UI data validation efforts and quality assurance testing of engineering calculation routines. Those efforts documented herein, and pertaining to Task 3, constitute a critical step in ensuring that GeoStat can be used with confidence by practicing engineers.

1.3.4 Task 4 – Develop Installation Package and Licensing

Task 4 focused upon item (4) above: development of an installation package and licensing. As a necessary part of making GeoStat available to practicing engineers, the software components (e.g., UI executable, supporting dynamic link libraries, help manual files) are collected into an installation package. Further, to ensure that practicing engineers utilize the program in a consistent manner and only within the intended scope of program usage, program licensing documentation is established.

As outcomes from Task 4, Ch. 1 of the Help Manual documents listings of program files that, collectively, comprise the GeoStat software. In addition, the manner by which the program can be installed and licensed is detailed. The efforts pertaining to Task 4 constitute a critical step in ensuring that GeoStat can, upon completion of the current research, be conveniently deployed to practicing engineers in a uniform manner.

1.3.5 Task 5 – Develop Software User Manual

Task 5 focused upon item (5) above: development of a software user manual. The scope of the Help Manual includes documentation of program dialogs and windows, and instructions on usage of the dialogs. Importantly, the Help Manual is identified as a distinct document from the Technical Manual (which is associated with Task 6, discussed below).

As the primary outcome from Task 5, the efforts and documentation from Tasks 1 through Task 4 are combined to form the GeoStat Help Manual, which is presented in Appendix A of the current report. Intended as a standalone document, the Help Manual, details program installation and licensing procedures, input file layout, and all UI controls. Alternatively stated, the Help Manual documents the *what* and the *where* of the GeoStat software. Accessible directly from within the Geostat UI, the Help Manual provides a centralized resource that engineers can reference for installing, licensing, and navigating through all input file and UI controls while making use of the GeoStat software for bridge design.

1.3.6 Task 6 – Develop Software Technical Manual

Task 6 focused upon item (6) above: development of a software technical manual. This document (along with the Help Manual) is included as part of the GeoStat installation and is accessible directly from within the GeoStat UI. The Technical Manual is a self-contained (i.e., standalone) document. Housed therein is documentation of the underlying algorithms that are utilized within the analysis portions of the GeoStat software. These underlying algorithms are illustrated via two unique case-studies, where data are selected to be representative relative to what would be measured across Florida bridge sites.

Presented in Appendix B of the current report is the GeoStat Technical Manual. As an outcome of the Task 6 effort, and complementary to the Help Manual, the Technical Manual documents the *why* and the *how* of the GeoStat software. For each of the two case studies,

summaries are provided for the associated geotechnical site data. Additionally, the process by which the data are packaged into GeoStat input is illustrated. Usage of relevant tabs within GeoStat are also documented (from input, to analysis, to presentation of results). Emphasis is placed upon documenting underlying algorithms and concepts that are implemented in the geostatistical and method error calculations.

1.4 Scope

Organization of the report is as follows:

- In Chapter 2, documentation is provided for data validation of all input controls and output displays located throughout the GeoStat interface.

- In Chapter 3, verification of engineering routines is discussed, with focus given to calculations of layer-specific descriptive statistics and spatial correlation structures (variograms).

- In Chapter 4, verification of engineering routines is further discussed, with emphasis on verification of geostatistical simulation processes and ensembles of axial capacity calculations.

- In Chapter 5, a summary is given of the project efforts for Tasks 1 through 6. In addition, recommendations for practice and future research are provided.

- Presented in Appendix A is the GeoStat Help Manual.

- Presented in Appendix B is the GeoStat Technical Manual.

CHAPTER 2
DATA VALIDATION OF USER INTERFACE (UI) CONTROLS

2.1 Overview

Documented in Ch. 2 is data validation of the GeoStat UI controls. In this context, a "control" is defined as any clickable component within the UI that stores or displays data, and including input boxes, table cells, plots, buttons, and tabs. Further, "data validation" signifies that, when an engineer interacts with a given control, that the UI conducts a check to ensure that the as-input data (or action) do not lead to undesirable behaviors (e.g., program crashes). In Sec. 2.2 through Sec. 2.8, data validation of controls located in each of the seven program tabs is documented (in order, from left to right). See Ch. 4 of the Help Manual (in Appendix A) for additional details regarding the tab ordering and individual tab layouts. Also, note that data shown throughout all screenshots of UI components of Ch. 2 are shown solely for illustrative purposes.

2.2 Project Information Tab

Shown in Fig. 1 is the first of seven program tabs, referred to as the Project Information tab. This portion of the GeoStat UI allows for the positions of any subset (or all) borings/corings across the site to be plotted in plan view. Also, a scatterplot of through-depth measurements is provided for available soil parameters of interest. Two data validation checks of note are located on the Project Information tab. Note that data associated with the currently selected boring (in the table) are highlighted in both the plan view and elevation plots. The desired soil or rock parameter data can be viewed in the elevation plot.
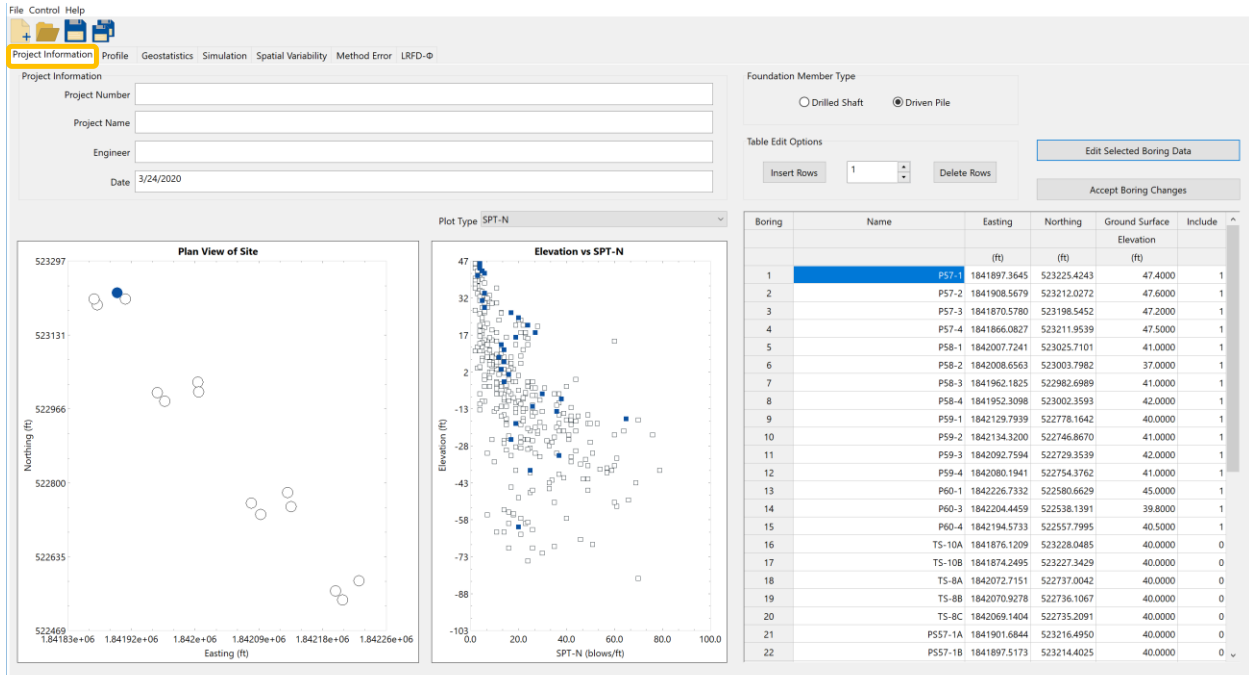
Figure 1. Project Information tab

As the first of two items: for the creation of one or more boring or coring locations, said number of locations can be specified, and the Insert Rows button can then be clicked. Upon clicking the Insert Rows button, the UI issues a warning (and takes no other action) if the number of rows to be inserted is less than 1. Second, note that the rightmost column of the boring or coring location table (Fig. 1, right) houses the Include column. Here, a value of 1 signifies that the boring or coring location is to be included in the analysis (i.e., included in the data structures built up and operated upon in subsequent program tabs). A value of 0 indicates that the boring or coring location is to be excluded from the analysis. To protect against program crashes, any other values input in these locations are interpreted as 0 (exclude), and a value of 0 is saved for these entries upon the next file save event.

2.2.1 Edit Selected Boring Data Dialog

Shown in Fig. 2 is the Boring Data dialog, which is accessed by clicking the Edit Selected Boring Data button from the Project Information tab (recall Fig. 1). This dialog permits bulk input of boring or coring data (e.g., from Excel). Upon clicking the OK button within the Boring Data dialog, the program checks that the depth values (highlighted in Fig. 2) are input in increasing order. In addition, note that GeoStat adopts the integer mapping to soil types, consistent with the convention implemented in axial capacity calculation software, FB-Deep. Accordingly, if integer values other than 1 through 5 are input beneath the Soil Type column for any row in the Boring Data dialog table, then (upon clicking OK), the program issues a warning and recommends input of revised values. For any row of data input in the Boring Data dialog (Fig. 2), the required inputs are Depth and Soil Type (with permitted integer values between 1 and 5). Inputs for all other columns are optional. This approach (as discussed in the Technical Manual, Appendix B) provides flexibility to engineers when only partial sets of geotechnical site data are available.
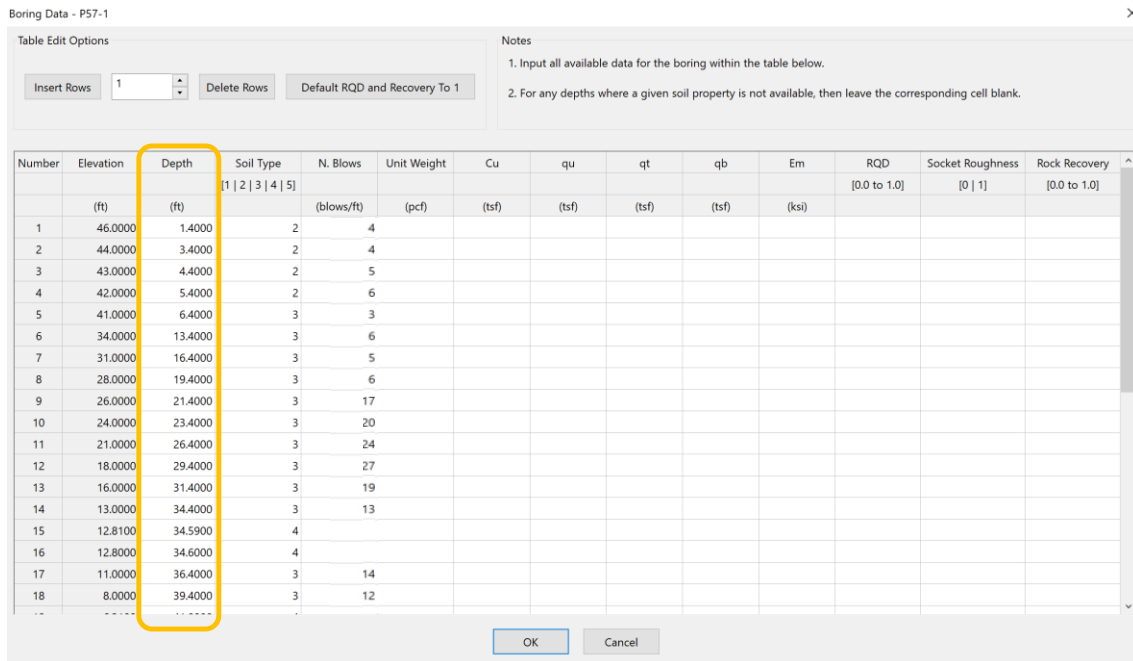
Figure 2. Boring Data dialog

2.3 Profile Tab

The second of seven program tabs is the Profile tab (Fig. 3). Given a collection of included borings/corings (as decided upon from within the Project Information tab), the Profile tab facilitates estimation of representative soil or rock layerings for a given location of interest. For the creation of one or more layers (Fig. 3, top-center), the number of locations can be specified, and the Insert Rows button can then be clicked. Immediately after clicking the Insert Rows button, the UI issues a warning (and take no other action) if the number of rows to be inserted is less than 1. The desired soil or rock data can be viewed in elevation view within each plot.
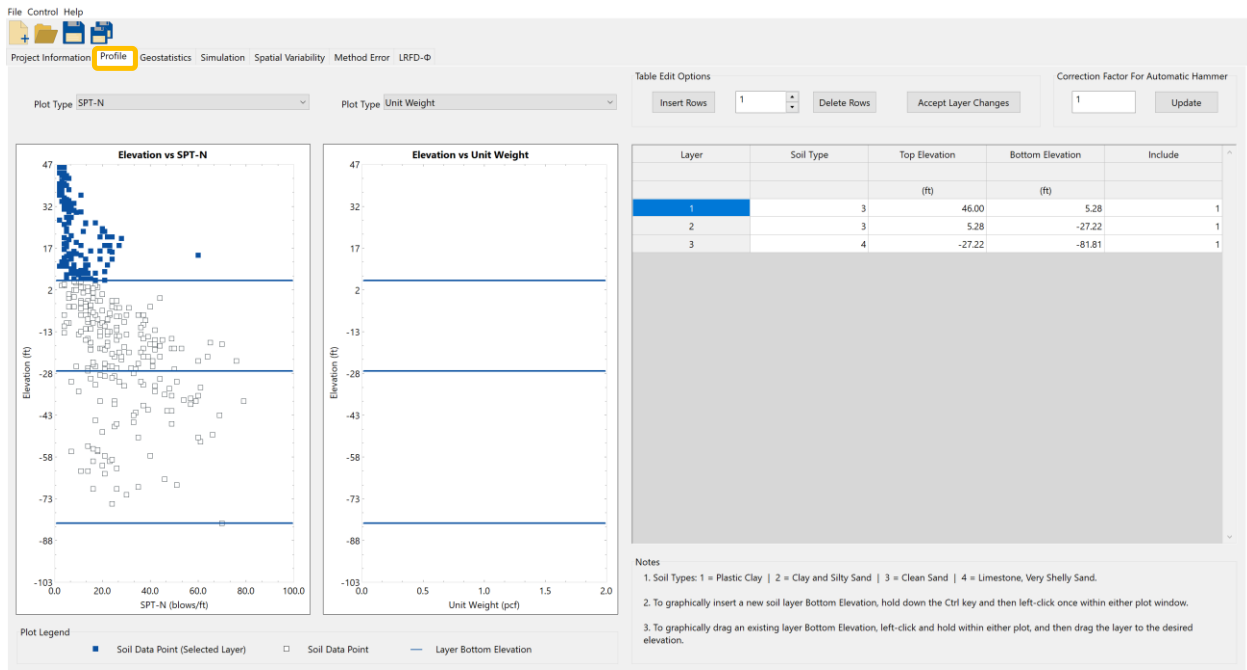
Figure 3. Profile tab

2.3.1 Layer Profile Table

Soil or rock layering can be graphically defined from within the Profile tab by interacting with through-depth scatterplots (shown in the left and center of Fig. 3). In addition, top and bottom elevations of soil layers can be input from within the Soil Layer table, as shown in Fig. 4. If integer values other than 1 through 4 are input beneath the Soil Type column, then the program will issue a warning message. The rightmost column of the Layer Profile table houses the Include column. Here, a value of 1 signifies that the layer is to be included in the analysis. A value of 0 indicates that layer is to be excluded from the analysis. To protect against program crashes, any other values input in these locations are interpreted as 0 (exclude), and a value of 0 is saved for these entries upon the next file save event. Upon clicking the Accept Layer Changes button (Fig. 3, top-right), the program checks that all Top Elevation (and separately, Bottom Elevation) values are in decreasing order. For intermediate layers (e.g., Layer 2 in Fig. 4), the program ensures that the Top Elevation (of each intermediate layer) matches the Bottom Elevation of the layer above.

Similarly, the program checks that the Bottom Elevation of each intermediate layer matches the Top Elevation of the layer below.

Layer	Soil Type	Top Elevation	Bottom Elevation	Include
		(ft)	(ft)	
1	3	46.00	5.28	1
2	3	5.28	-27.22	1
3	4	-27.22	-81.81	1

Figure 4. Layer profile table

2.4 Geostatistics Tab

Spatial correlation structures are determined for included soil or rock layers (based on layering defined in the Profile tab) using controls distributed throughout the Geostatistics tab (Fig. 5). Several input parameters, found in the Layer Variograms table (Fig. 5, top) are utilized in forming the horizontal and vertical variograms for each layer. Upon clicking any of the Generate Variogram, Variogram Data, or Process Layers buttons, the program will issue a warning message (and indicate the specific issue) in the event that variogram points cannot be generated for a given layer. When valid data are input and variograms can be formed, the two bottom-right plots of Fig. 5 (horizontal and vertical variograms, respectively) are populated with plot points. The size of each point symbol (diamond) within the variogram plots is scaled to reflect the respective number of pairs associated with that point. Specifically, the point symbols are scaled depending on interquartile ranges of the associated pairs (larger symbols indicate relatively more pairs). See the Technical Manual (in Appendix B) for additional details regarding the underlying concepts.
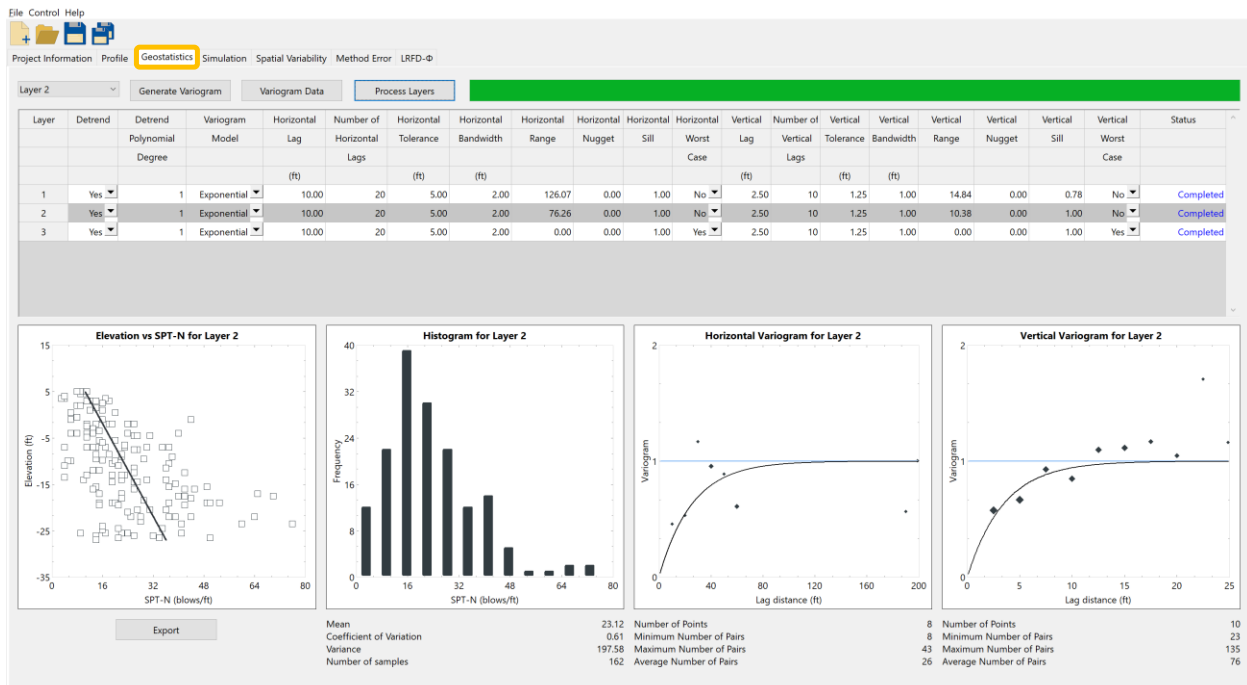
Figure 5. Geostatistics tab

2.4.1 Layer Variograms Table

An inset of the Layer Variograms table is presented in Fig. 6. Two particularly essential parameters for generating variograms are the lag distance (the distance interval at which to search for pairs of data points) and the number of lag intervals. Accordingly, if any one of the Horizontal Lag, Number of Horizontal Lags, Vertical Lag, or Number of Vertical Lags are input as non-positive, then the program issues a warning upon any attempts at generating variogram data for the offending layer(s).

Layer	Detrend	Detrend Polynomial Degree	Variogram Model	Horizontal Lag (ft)	Number of Horizontal Lags	Horizontal Tolerance	Horizontal Bandwidth (ft)	Horizontal Range (ft)	Horizontal Nugget	Horizontal Sill	Horizontal Worst Case	Vertical Lag (ft)	Number of Vertical Lags	Vertical Tolerance (ft)	Vertical Bandwidth (ft)	Vertical Range	Vertical Nugget	Vertical Sill	Vertical Worst Case	Status
1	Yes	1	Exponential	10.00	20	5.00	2.00	126.07	0.00	1.00	No	2.50	10	1.25	1.00	14.84	0.00	0.78	No	Completed
2	Yes	1	Exponential	10.00	20	5.00	2.00	76.26	0.00	1.00	No	2.50	10	1.25	1.00	10.38	0.00	1.00	No	Completed
3	Yes	1	Exponential	10.00	20	5.00	2.00	0.00	0.00	1.00	Yes	2.50	10	1.25	1.00	0.00	0.00	1.00	Yes	Completed

Figure 6. Layer Variograms table

2.5 Simulation Tab
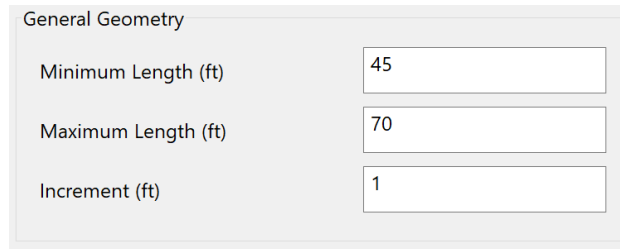
Shown in Fig. 7 is the fourth of seven program tabs, the Simulation tab, wherein controls are dedicated to defining the foundation member configuration and conducting statistical simulation. Data validation checks on input controls specific to the foundation member definition are carried out upon clicking the Run Simulation button (Fig. 7, bottom-center). For each grouping of input controls on the Simulation tab, the associated data validation checks are provided in Sec. 2.5.1 through Sec. 2.5.5.

Figure 7. Simulation tab

2.5.1 General Geometry Frame

Located in the upper-left portion of the Simulation tab is the General Geometry frame (an inset is shown in Fig. 8). Within the frame are the controls that dictate the range and increment of embedment lengths to consider during simulation. To protect against formation of improper data in the numerous FB-Deep model files (generated as part of the statistical simulation), only positive values are permitted to be entered. In addition, the program ensures that the range of embedment lengths fall within the soil or rock profile (as defined using controls on the Profile tab, recall Fig. 3). Specific to GeoStat models of pile members, and depending on the soil or rock layering, the program further ensures that adequate soil or rock layering is available given the input value of Maximum Length (e.g., 3.5 pile diameters below and 8.0 pile diameters above for end bearing calculations).
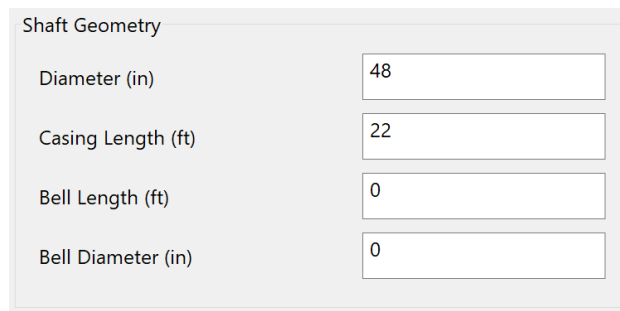
General Geometry

Minimum Length (ft)	45
Maximum Length (ft)	70
Increment (ft)	1

Figure 8. General Geometry frame

2.5.2 Shaft Geometry Frame

For GeoStat models of drilled shafts, controls within the Shaft Geometry frame (Fig. 9) are enabled. The program enforces input of only positive-valued entries for Diameter. However, inputs for Casing Length, Bell Length, and Bell Diameter are permitted to be input as equal to or greater than zero.
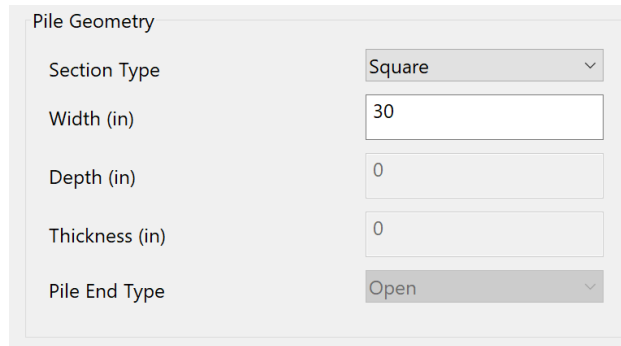
Shaft Geometry

Diameter (in)	48
Casing Length (ft)	22
Bell Length (ft)	0
Bell Diameter (in)	0

Figure 9. Shaft Geometry frame

2.5.3 Pile Geometry Frame

For modeling of driven piles in GeoStat, certain controls within the Pile Geometry (Fig. 10) are enabled. More specifically, depending on the selection of Section Type, only those parameters required to populate the FB-Deep model portions (during simulation) become enabled. For example, for square piles, only the Width parameter is required. Regardless of which input parameters are required for a pile cross-section, the program accepts only those that are positive (and otherwise issues a warning). Similar descriptions for all available pile types are provided in Ch. 4 of the Help Manual (in Appendix A).
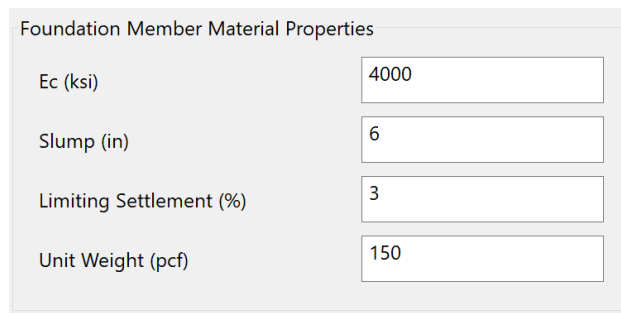
Figure 10. Pile Geometry frame

2.5.4 Foundation Member Material Properties Frame

Material properties of foundation members are specified in the Foundation Member Material Properties frame (Fig. 11). For drilled shaft models, all four parameters are required. In contrast, only Unit Weight must be supplied when modeling driven piles (the other three controls are disabled in this case). Regardless of the foundation member type, all enabled controls within this frame are checked to prevent input of non-positive values.
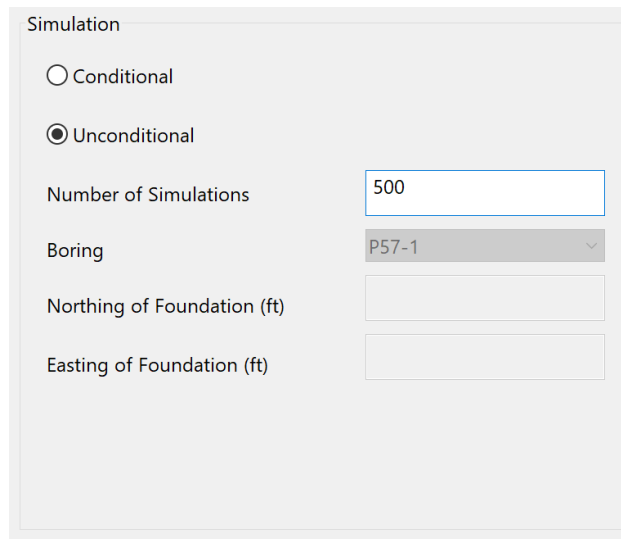
Figure 11. Foundation Member Material Properties frame

2.5.5 Simulation Frame

Two simulation options are available from within the Simulation frame: Conditional, Unconditional. The differences between these two options are discussed in the Technical Manal (Appendix B). Input controls pertaining to the type of simulation (conditional, unconditional) and number of simulations (i.e., number of FB-Deep models to generate and analyze) are shown in Fig. 12. If the Unconditional radio button is selected, then only the Number of Simulations is required, and all other controls are disabled. Otherwise, if the Conditional radio button is selected, then the Boring pulldown list, Northing of Foundation, and Easting of Foundation controls also become enabled. Regardless of the type of simulation being conducted, upon clicking the Run Simulation button (recall Fig. 7, bottom-center), the program checks that a value greater than zero has been supplied for the Number of Simulations.

Figure 12. Simulation frame

2.6 Spatial Variability Tab

Plots of axial capacity are located on the Spatial Variability tab (Fig. 13). The plots shown on this tab reflect the boring or coring data, soil or rock layering, spatial correlation structures, and foundation member configuration defined on previously discussed UI tabs. Data validation of controls on this page are carried out when the Import FB-Deep Output button is clicked (Fig. 13, top-left).

2.6.1 Import FB-Deep Output Dialog

Upon clicking the Import FB-Deep Output button, a dialog opens for the purpose of selecting the desired set of output to post-process (Fig. 14). As a convenience, during a given program session, the folder associated with the most recent simulation is automatically highlighted

within the dialog. However, if a folder containing no valid FB-Deep model files is selected, then the program (GeoStat) issues a warning. Further, if one or more FB-Deep model files containing invalid data are identified during creation of the Spatial Variability results plots, then GeoStat excludes the offending files and notifies the engineer of the total number of valid file reads.
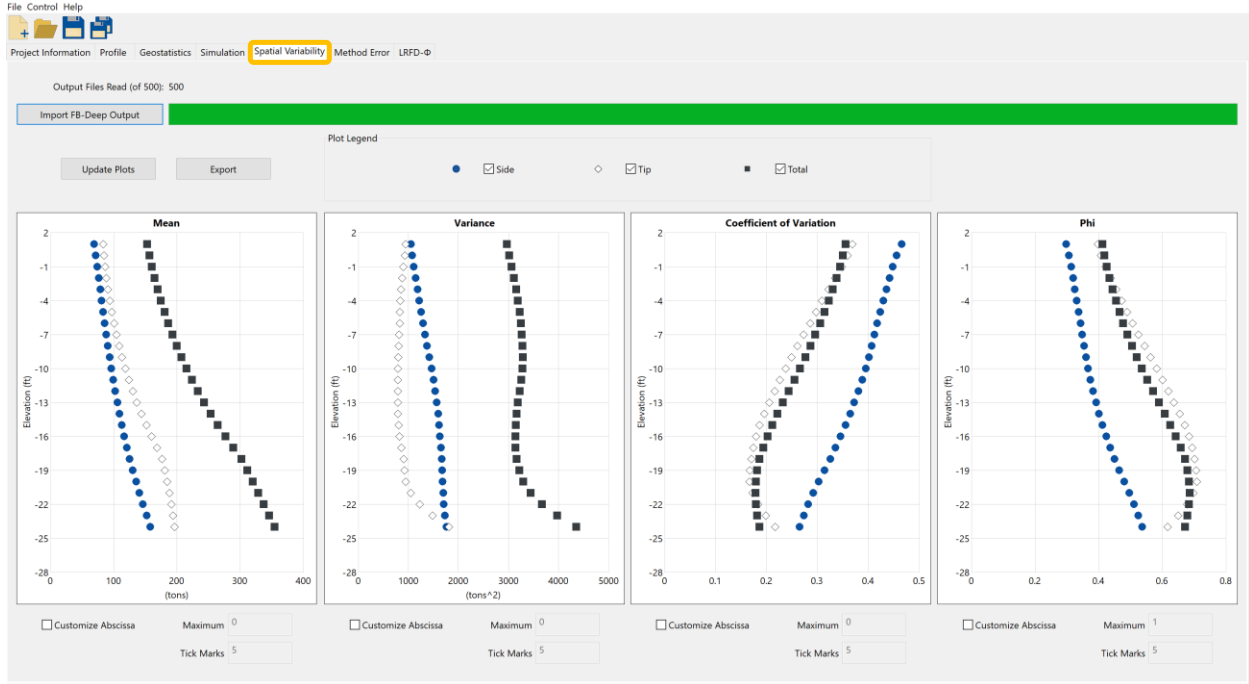
Figure 13. Spatial Variability tab
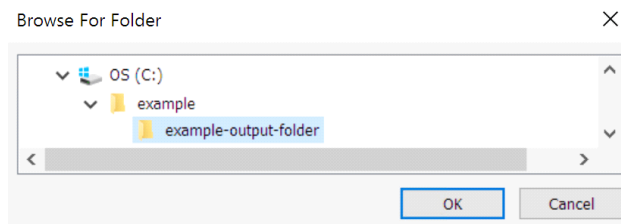
Figure 14. Import FB-Deep Output dialog

2.7 Method Error Tab

Shown in Fig. 15 is the Method Error tab, which allows for either default or custom adjustments (e.g., those based on load test data) to be made on the simulation results. In turn, these adjustments (intercept, slope, and dispersion) provide a means of accounting for the uncertainty associated with use of various empirical methods for calculating axial resistance. The Method Error tab includes three tables (Fig. 15, center-left): the topmost table applies to driven piles, the middle table applies to skin friction of drilled shafts, and the bottom table applies to end bearing

of drilled shafts. The approach illustrated in Sec. 2.7.1 is implemented in GeoStat to ensure that only relevant data are entered (when required) for a given type of foundation member.
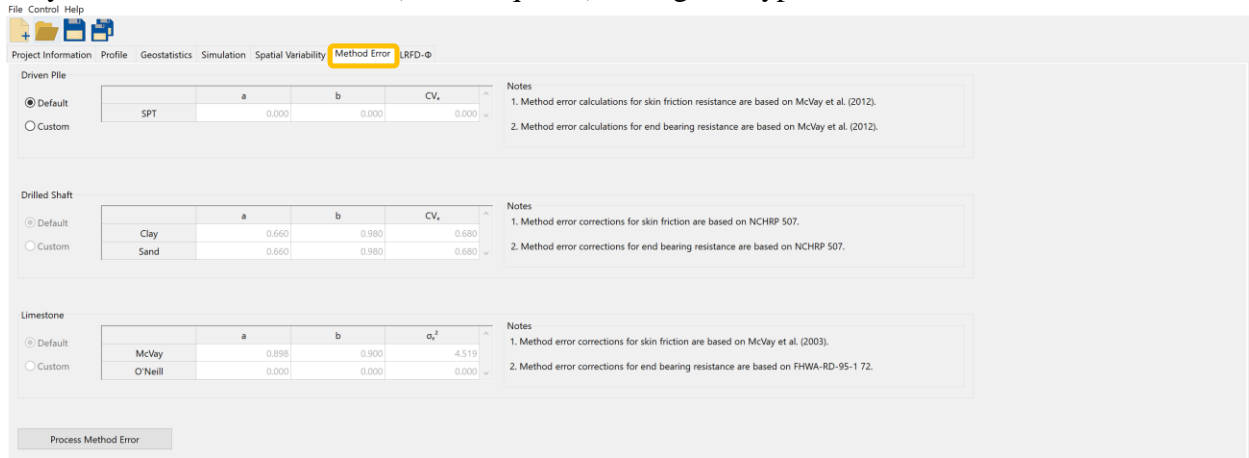
Figure 15. Method Error tab

2.7.1 Process Method Error

An example inset of the Method Error tab, applicable to pile models, is presented in Fig. 16. Only the topmost table (pertaining to piles) is enabled, while controls associated with drilled shafts (the middle and bottom tables) are disabled. As discussed further in the Technical Manual (Appendix B), tables in the Method Error tab allow engineers to perform linear bias correction (of piles and shafts) through "a" and "b" coefficients and also permit introduction of method error (CV_ε), as shown in Fig. 16. Engineers may make use of Default values or supply Custom values. For instance, in the example inset, the Custom radio button is selected (Fig. 16, top-left). Only when the Custom radio button is selected are the table cells made editable. Otherwise, when the Default radio button is selected, no other input values are required. A similar approach is taken for the two tables associated with drilled shaft members. Once the input set for this tab is complete, then the Process Method Error button must be clicked.
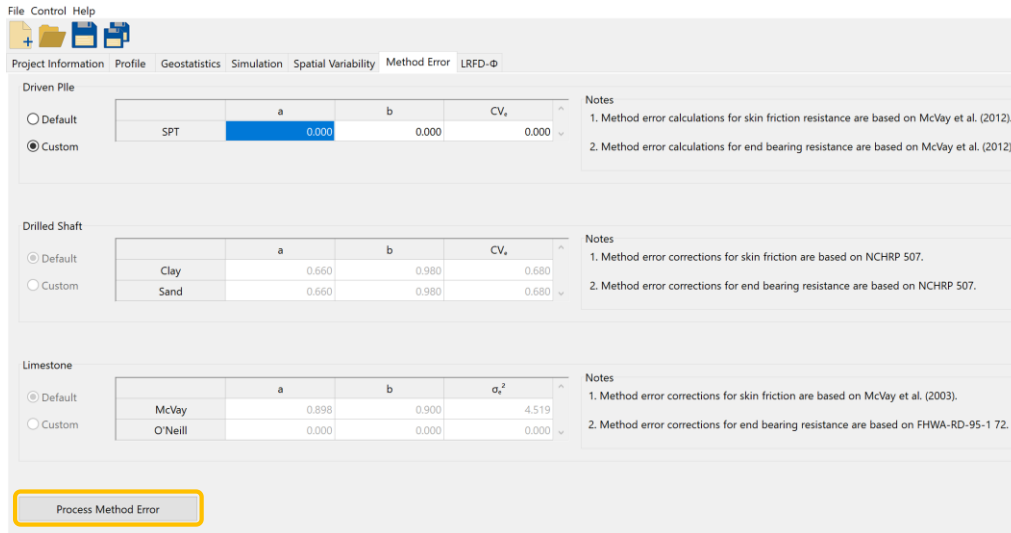
Figure 16. Process Method Error button

2.8 LRFD-ϕ Tab

The seventh (leftmost) tab in the GeoStat UI (Fig. 17) is the LRFD-ϕ tab, which contains profile plots of mean-valued resistance, site-specific resistance factors, and factored resistance. Further, the plots on this tab include both the axial resistance quantities associated with spatial variability as well as those of combined spatial variability and method error. Note that resistance (ϕ) factors generated in association with use of GeoStat should only be applied in conjunction with Owner's guidelines.

If adequate post-processing has not occurred upon reaching this tab, then the UI will issue a warning message in lieu of attempting to generate the summary plots. Examples of inadequacies in post-processing that are detected (when present) include: no results data have been loaded from the Spatial Variability page (recall Fig. 13); the method error has not been processed (recall Fig. 15).

17
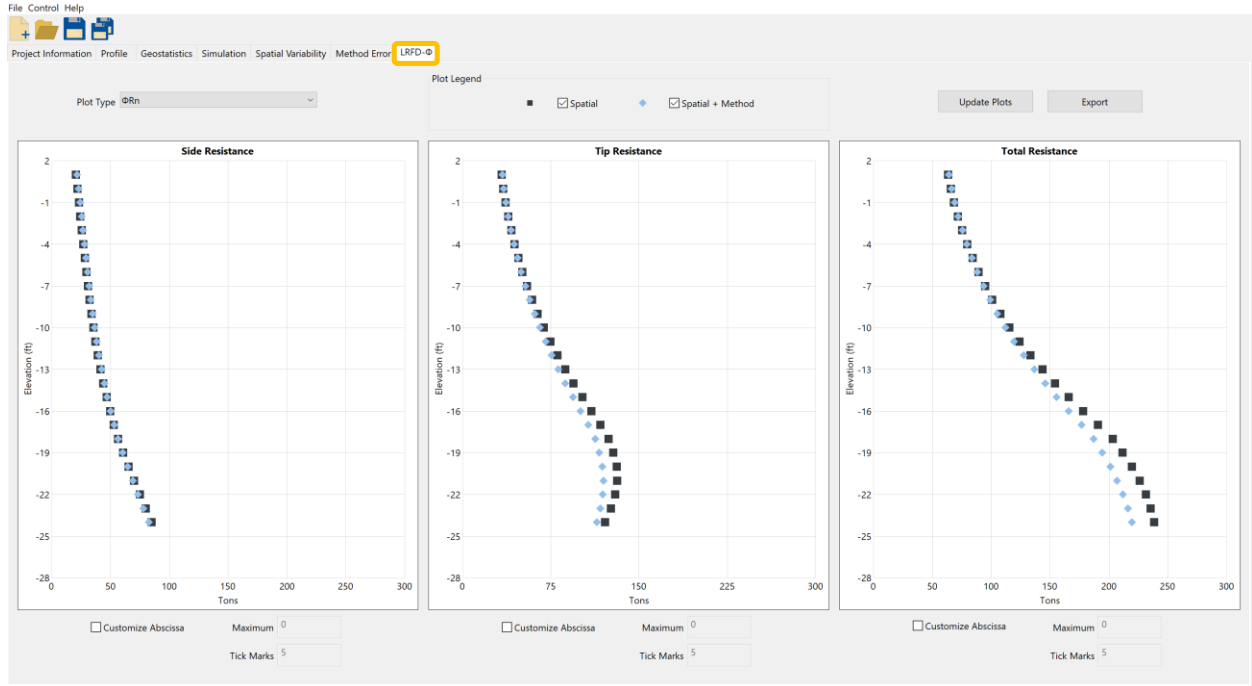
Figure 17. LRFD-ϕ tab

CHAPTER 3
VERIFICATION OF DESCRIPTIVE STATISTICS AND SPATIAL CORRELATION CALCULATIONS USING GEOTECHINCAL SITE DATA

3.1 Overview

Presented in Ch. 3 are verification efforts pertaining to program-generated descriptive statistics for soil or rock layers of GeoStat models. Also, verification of spatial correlation calculations (variograms, in particular) is documented. Reported in Sec. 3.2 are comparisons between manually calculated histogram data and that generated within GeoStat using physically measured site data. Descriptive statistics associated with the same data set are then documented in Sec. 3.3, where again, comparisons are made between manually calculated and program-generated values. The final section of Ch. 3, Sec. 3.4, is devoted to verification of variogram calculations in GeoStat, where both synthetic and physically measured data sets are investigated.

3.2 Histogram

Plotted in Fig. 18 is histogram data for 99 physically measured values of unconfined compressive strength (q_u), which were accumulated from examination of six boring locations for a bridge site located in South Florida. The binning convention adopted in GeoStat is such that values equal to or greater than the bin lower boundary and values less than the bin upper boundary are attributed to a given histogram bin. Identical histograms are formed when using this binning convention to manually form the histogram, as compared to those histogram values obtained from GeoStat.
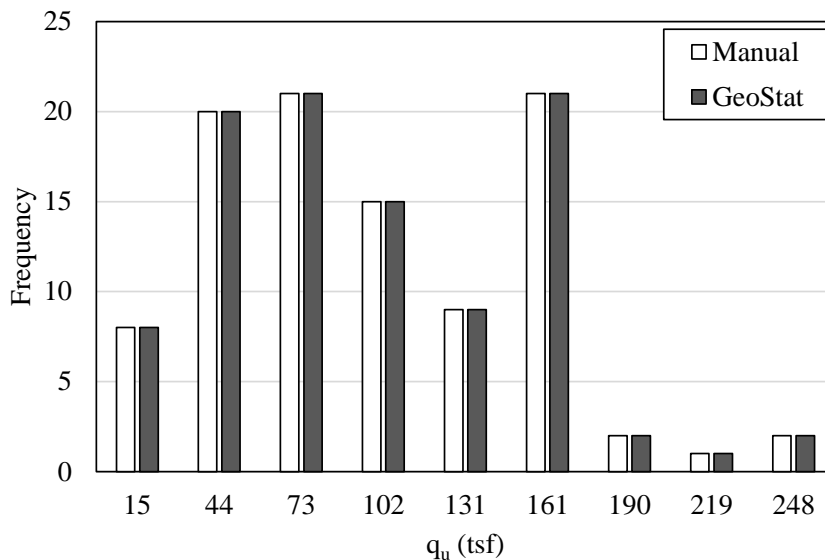
Figure 18. Manually calculated versus computed histograms for measured values of unconfined compressive strength (q_u)

3.3 Descriptive Statistics

An inset of the histogram plot—excerpted from the Geostatistics tab (recall Fig. 5) when operating on the 99 values of unconfined compressive strength (q_u)—is presented in Fig. 19. Included in the inset is the program-generated histogram and descriptive statistics: mean, coefficient of variation (COV), variance, and number of samples. Listed in Table 1 are manually calculated descriptive statistics as compared to those displayed in Fig. 19. Exact agreement is observed for all compared quantities. Note that the geometric mean is additionally reported in GeoStat.

Mean (Arithmetic, Geometric)	98.19, 80.56
Coefficient of Variation	0.57
Variance	3132.48
Number of samples	99
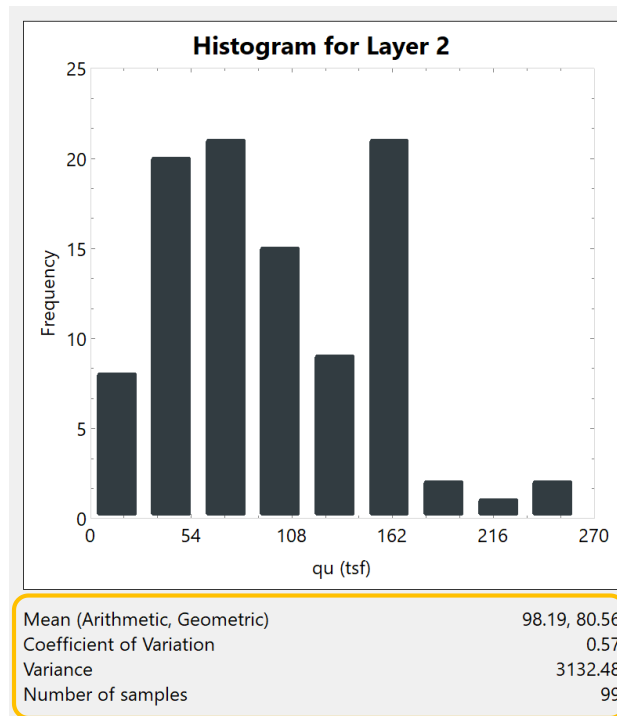
Figure 19. Histogram and descriptive statistics excerpted from the Geostatistics tab

Table 1. Descriptive statistics for measured values of unconfined compressive strength (q_u)

Statistical measure	Manual	GeoStat
Sample size	99	99
Mean	98.19	98.19
Variance	3132.48	3132.48
COV	0.57	0.57

3.4 Variograms

Spatial correlation structures in GeoStat are packaged into layer-specific variograms. In turn, these graphical constructs, which characterize how covariance within a given layer changes with respect to distance between data points, are drawn upon in forming multitudes of soil parameter profiles during statistical simulation. Depending on the type of foundation member and

20

soil (or rock) layer, SPT blow counts or unconfined compressive strengths (q_u) values are utilized when forming the corresponding variograms. Additional discussion of geostatistical processes in GeoStat is provided in the Technical Manual (Ch. 2 of Appendix B). Germane to the discussion immediately below is verification of variograms generated using GeoStat.

3.4.1 SPT Blow Counts

Documented in Sec. 3.4.1 is verification of variograms generated (within GeoStat) using SPT blow count values, where comparisons are made to manual calculations. Shown in Fig. 20a are the plan view of 50 boring locations and a through-depth scatterplot of 5,050 (synthetic) SPT blow count values. Plotted in Fig. 20b is the corresponding histogram.

a)

b)
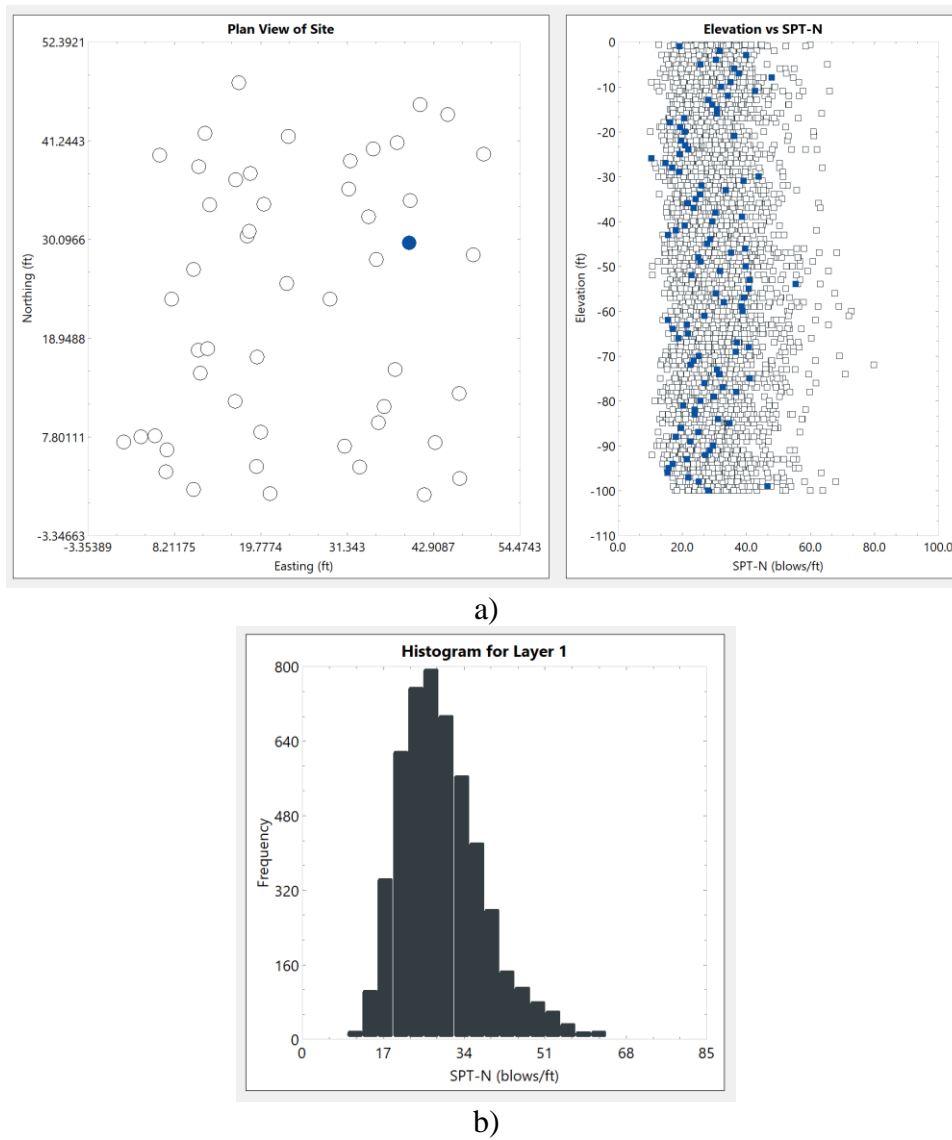
Figure 20. Synthetic SPT blow count values for use in verification of horizontal and vertical variograms: a) Plan view and through-depth scatterplot; b) Histogram

21

Manually determined and program-generated descriptive statistics are compared in Table 2, where exact agreement is found across all statistical quantities. Comparative plots (manual vs program-generated) of horizontal variograms are presented in Fig. 21. Excellent agreement is observed for the variogram ordinates and the data pairs found at each lag distance.

Table 2. Descriptive statistics for synthetic values of SPT blow counts

Statistical measure	Manual	GeoStat
Sample size	5,050	5,050
Mean	29.59	29.59
Variance	80.59	80.59
COV	0.30	0.30
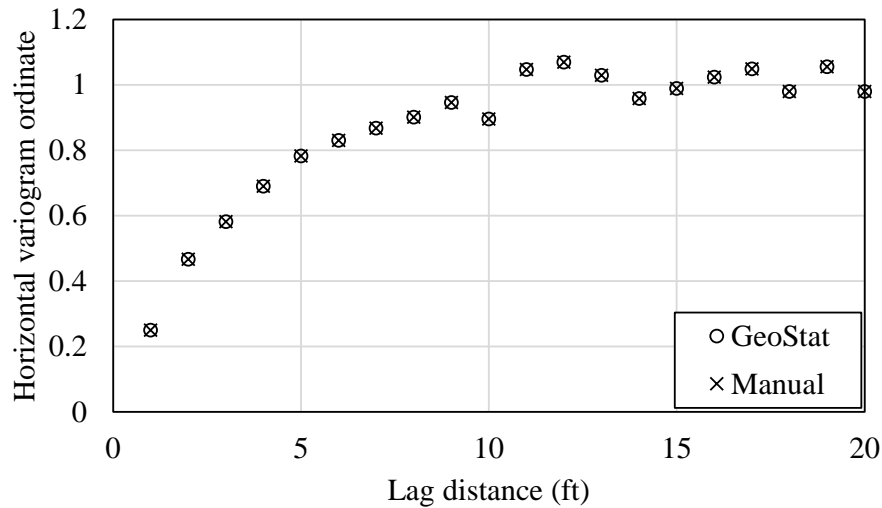
a)
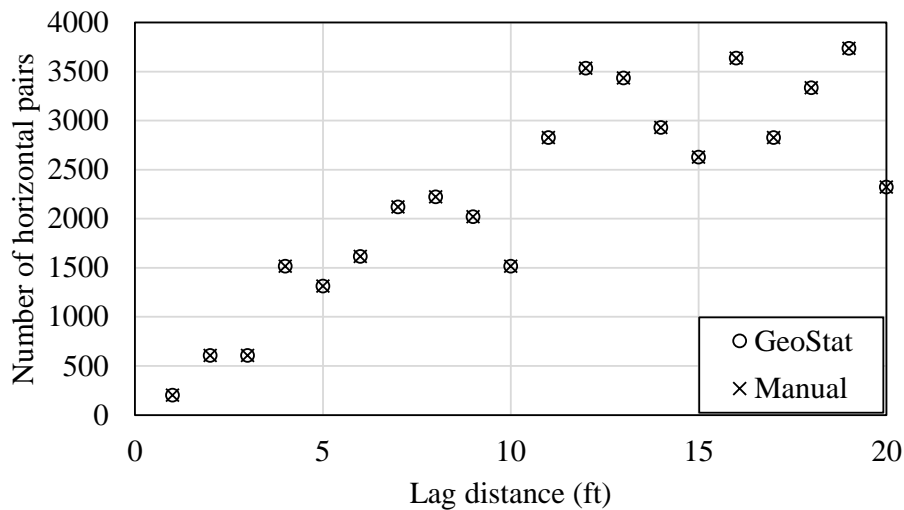
b)

Figure 21. Comparison of horizontal variograms for synthetic SPT blow count values, manual versus computed using GeoStat: a) Variogram ordinates; b) Variogram pairs

Vertical variograms associated with the synthetic SPT blow counts are plotted in Fig. 22. Manual versus computed (using GeoStat) variogram ordinates indicate practically identical agreement across all lag distances considered (Fig. 22a). Likewise, the intensities associated with each variogram ordinate (i.e., the number of data pairs found at each lag distance) show excellent agreement (Fig. 22b). The collective comparisons between manual and program-generated statistical quantities (Fig. 21, Fig. 22, and Table 2) serve to verify the generation of variograms, when operating on SPT blow count values, using GeoStat.
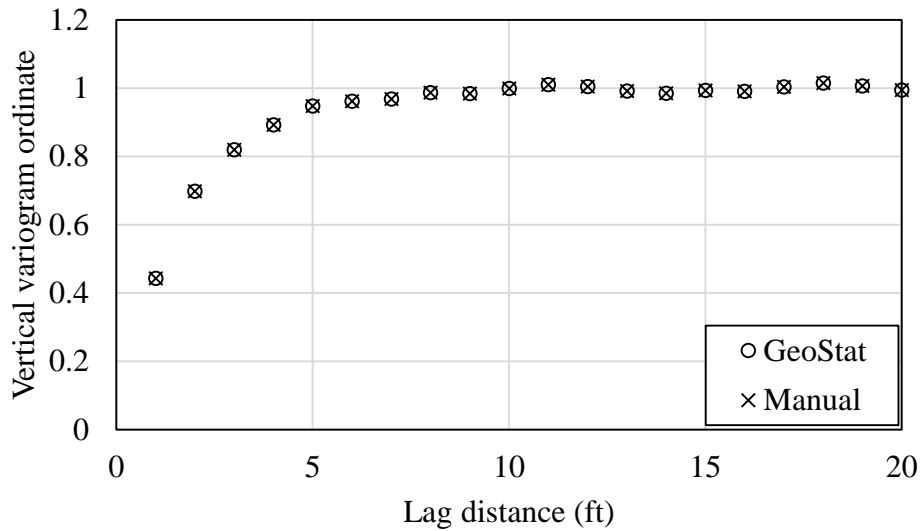
a)
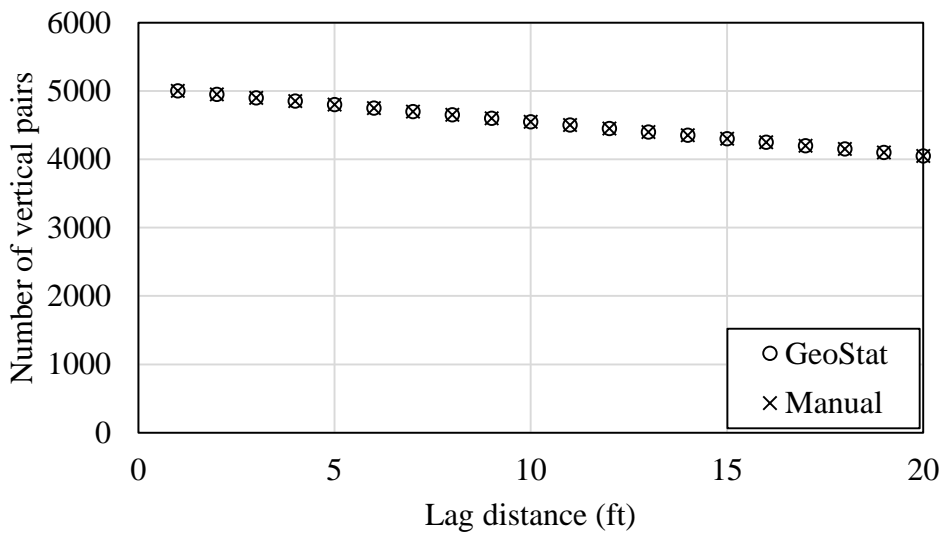
b)

Figure 22. Comparison of vertical variograms for synthetic SPT blow count values, manual versus computed using GeoStat: a) Variogram ordinates; b) Variogram pairs

3.4.2 Unconfined Compressive Strength (q_u)

Verification of variograms generated using unconfined compressive strength values (q_u) is focused upon in Sec. 3.4.2. For this portion of the verification effort, the data set consisting of 99 unconfined compressive strength (q_u) values is revisited (recall Sec. 3.2 and Sec. 3.3). Further, comparisons are made between GeoStat and those quantities obtained from use of the prototype software (referred to as GS-Deep), which was developed in McVay et al. (2012). Shown in Fig. 23 are plots excerpted from the GeoStat UI. In particular, the plan view of 6 coring locations and a through-depth scatterplot of the 99 measured q_u values are displayed in Fig. 23a. Both the scatterplot and histogram of the data set, assigned to Layer 2, are shown in Fig. 23b.

a)

b)
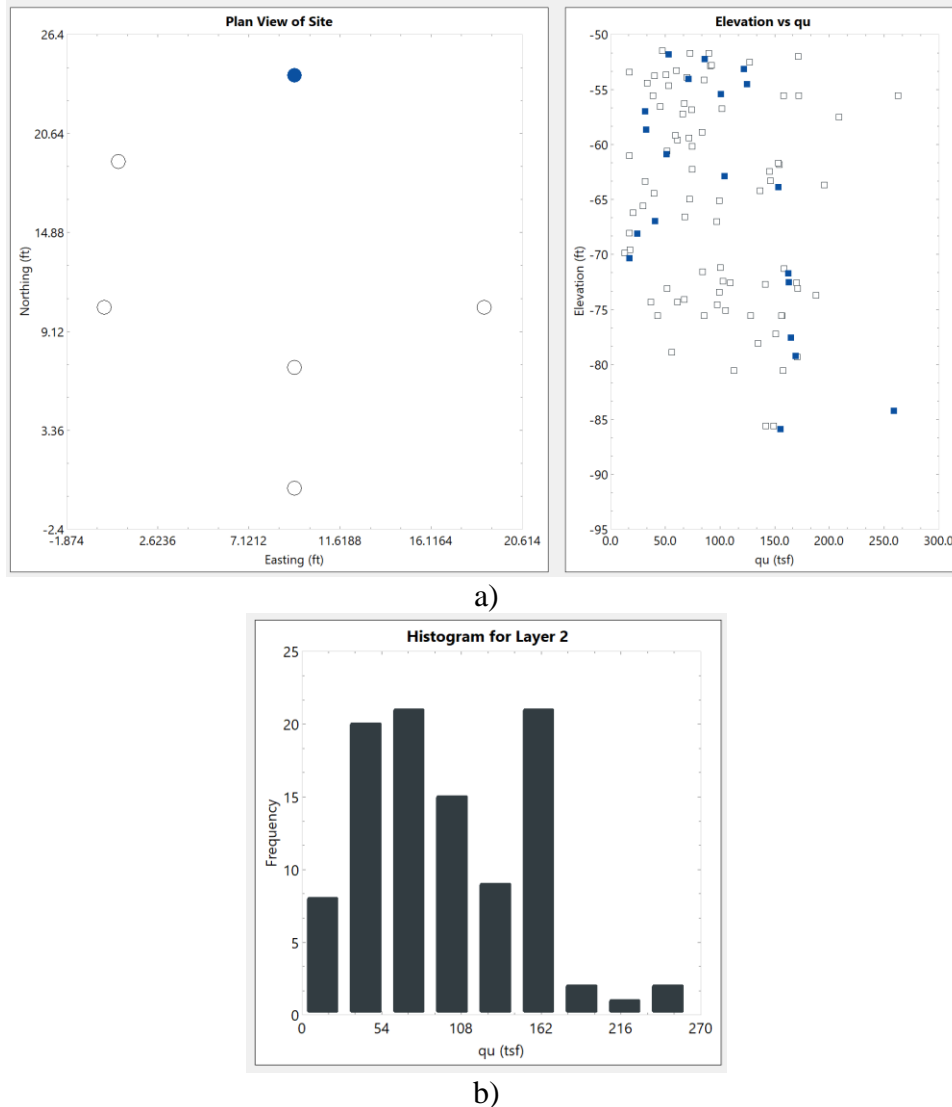
Figure 23. Measured q_u values for use in verification of horizontal and vertical variograms: a) Plan view of coring locations and profile-view scatterplot; b) Histogram

Recall that descriptive statistics for the 99 q_u values (manual versus program-generated) are listed in Table 1. Comparative plots (GS-Deep vs GeoStat) of horizontal variograms are shown in Fig. 24a, and indicate nearly exact agreement across the seven lag distances considered. Likewise, exact agreement is observed when comparing data pairs found at each lag distance (Fig. 24b).
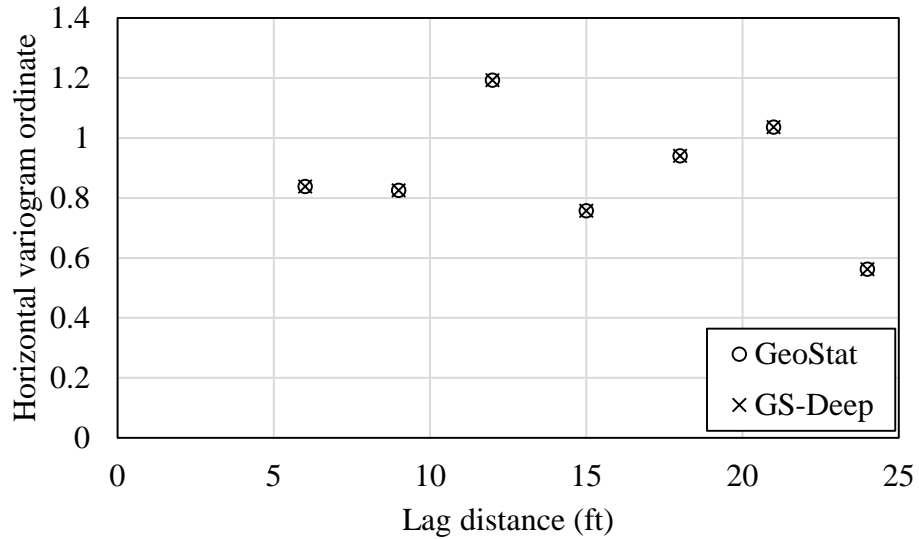
a)
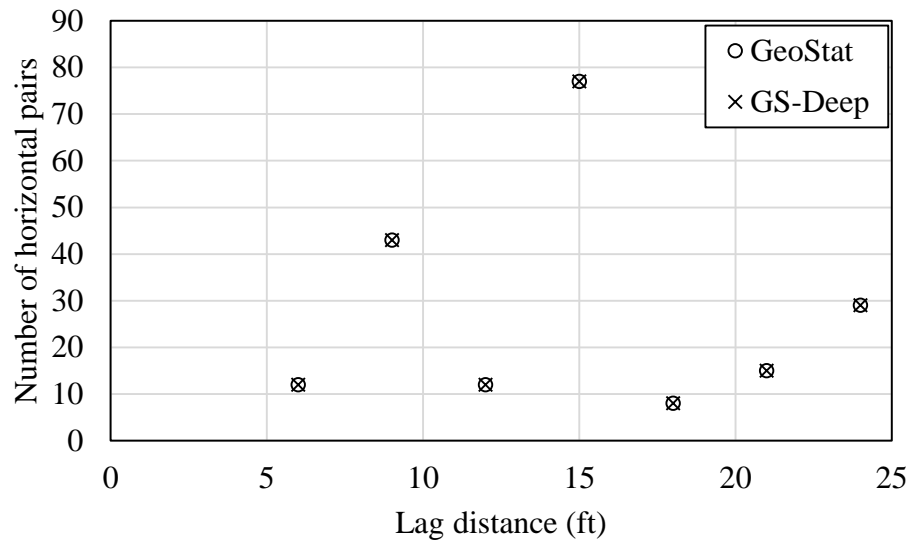
b)

Figure 24. Comparison of horizontal variograms for q_u values, computed using GeoStat and GS-Deep: a) Variogram ordinates; b) Variogram pairs

Presented in Fig. 25 are comparative plots of variogram quantities obtained when using GS-Deep, and separately, GeoStat. Plotted variogram ordinates (Fig. 25a) and data pairs (Fig. 25b) exhibit excellent agreement across the 20 lag distances considered. As exceptions, the variogram

ordinates and the number of data pairs at lag distances of 2 ft and 3 ft indicate differences of less than 2% (Fig. 25b). These exceptions are attributed to slight differences in the spatial coordinates (particularly, the elevations) within the GS-Deep model file versus those of the GeoStat model file. The generally excellent agreement found across the horizontal and vertical variogram comparisons provides verification of GeoStat, when unconfined compressive strength values (q_u) are being operated upon.
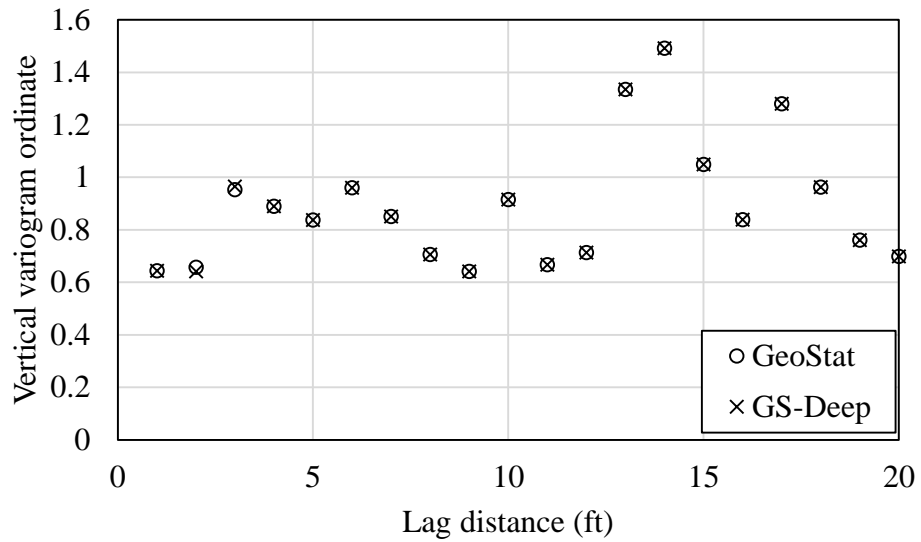
a)
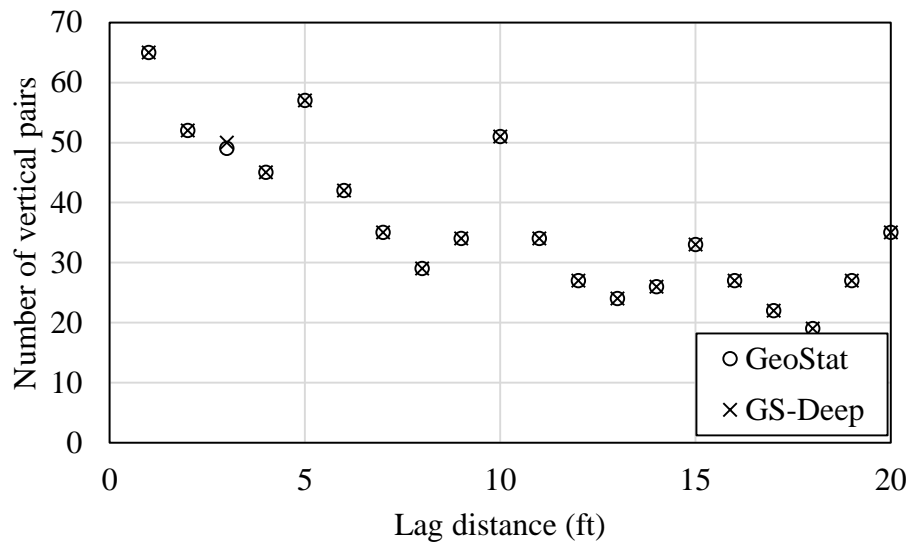
b)

Figure 25. Comparison of vertical variograms for q_u values, computed using GeoStat and GS-Deep: a) Variogram ordinates; b) Variogram pairs

CHAPTER 4
VERIFICATION OF GEOSTATISTICAL SIMULATION

4.1 Overview

Documented in Ch. 4 are verification efforts pertaining to geostatistical simulation of axial resistances for foundation members, when using GeoStat. Simulations involving drilled shafts are discussed in Sec. 4.2, where comparisons are made between results obtained from use of the prototype software (GS-Deep, McVay et al. 2012) and GeoStat. Similarly, verification of GeoStat (relative to GS-Deep) is reported for simulations involving driven pile members in Sec. 4.3.

4.2 Drilled Shafts

The collection of 99 physically measured values of unconfined compressive strength (q_u), as accumulated from six boring locations for a bridge site located in South Florida, are again revisited for verification purposes (recall Sec. 3.2, Sec. 3.3, and Sec. 3.4.2). As plotted above in Fig. 23a, the range of elevations encompassed by the 99 q_u values extends from (approximately) -50 ft to -85 ft. Further, the ground surface elevation associated with this data set is 0 ft. Accordingly, candidate embedment lengths that fall within the elevation range (i.e., embedment lengths of 55 ft to 80 ft) are considered for the verification cases documented in Sec. 4.2. GeoStat permits both unconditional and conditional simulations (see Ch. 2 of the Technical Manual in Appendix B for additional details), one verification case is carried out for each type of simulation in the following (Sec. 4.2.1 and Sec. 4.2.2, respectively).

4.2.1 Unconditional Simulation

Plotted in Fig. 26 are comparisons of through-depth quantities pertaining to drilled shaft axial capacity, as obtained when using GS-Deep versus GeoStat to carry out unconditional simulation on a 48-in. diameter shaft. Good agreement is found along the profile of mean-valued total resistance (Fig. 26a), where for example, the two programs produce values of total resistance that differ by 2% at an elevation of -80 ft. Relatively small differences that are present among the two plots are attributed to utilization of different random number seeds between the two programs.

As plotted in Fig. 26b, strong agreement is also present among the computed values of COV, which indicates that the variability (as contributed to by both spatial variability and method error) manifests in a consistent manner between GS-Deep and GeoStat. Both the mean-valued resistances and COV values factor into calculation of the resistance factor (ϕ), as plotted in Fig. 26c. As comprehensive verification of GeoStat (for unconditional simulation of drilled shaft members), the product of values plotted in Fig. 26a (mean) and Fig. 26c (ϕ) is displayed in Fig. 26d (factored total resistance).

Figure 26. Comparison of drilled shaft response profiles obtained from unconditional simulation using GeoStat and GS-Deep: a) Total resistance; b) Coefficient of variation; c) Resistance factor; d) Factored total resistance

4.2.2 Conditional Simulation

Presented in Fig. 27 are comparative results plots for conditional simulation on a 48-in shaft. In this context, "conditional" signifies that realizations of profiles of soil parameters are

generated relative to the positioning of a specified coring location (taken as that highlighted above in Fig. 23a). Good agreement (within 5% or better) is generally exhibited among the computed profiles of mean total resistance, COV, resistance factor, and factored total resistance (Fig. 27a through Fig. 27d, respectively). Differences that are present between the two sets of results plots are attributed to: 1) minor differences in elevations of the q_u values that arise during processing of the XML model file in GS-Deep, versus the approach of directly inputting elevations in GeoStat; and, 2) differences between the random number seeds used in the two programs.

Figure 27. Comparison of drilled shaft response profiles obtained from conditional simulation using GeoStat and GS-Deep: a) Total resistance; b) Coefficient of variation; c) Resistance factor; d) Factored total resistance

4.3 Driven Piles

Presented in Fig. 28 are 15 boring locations and 318 SPT blow counts pertaining to a bridge site located in Northwest Florida. In the following, this data set is utilized for verification of a conditional simulation on a 32-in. square pile, using both GS-Deep and GeoStat. Four layers are defined for this verification case, where layers 2 (Fig. 29) through 4 (Fig. 31) are assumed to appreciably contribute to the pile axial resistance. Descriptive statistics, as obtained from both programs, are listed for layers 2 through 4 in Table 3 through Table 5, respectively. For all layers considered, comparisons of the descriptive statistics (GS-Deep versus GeoStat) indicate excellent agreement.
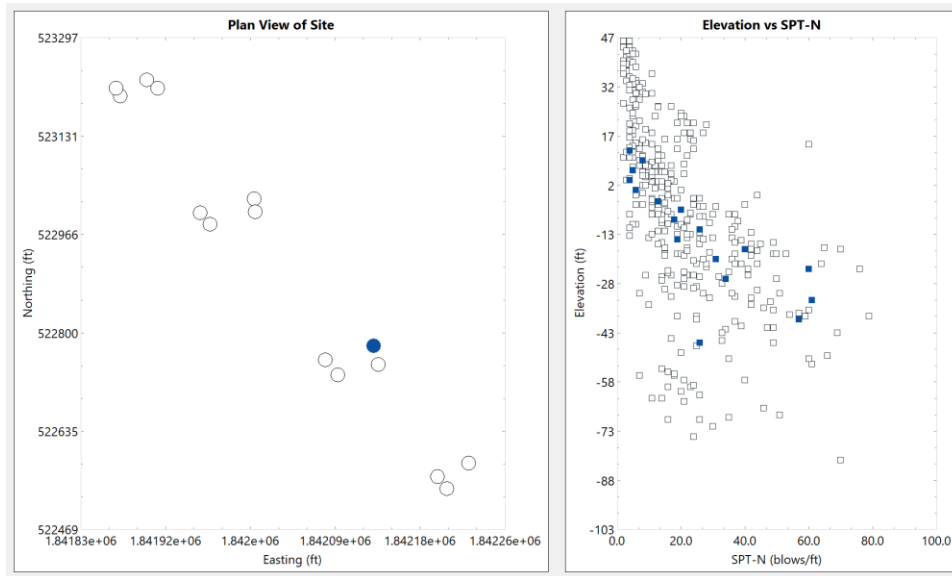
Figure 28. Plan view of boring locations and profile-view scatterplot for driven pile verification case
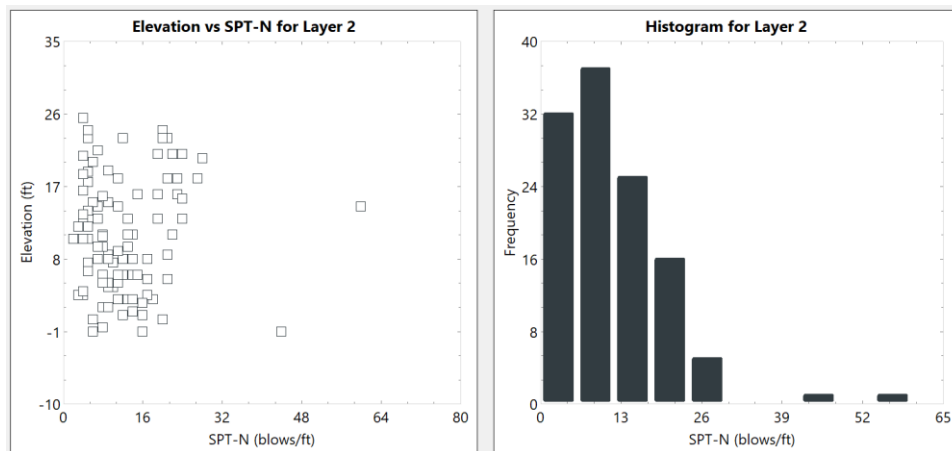
Figure 29. Layer 2 scatterplot and histogram of SPT blow count values

Table 3. Descriptive statistics for measured values of SPT blow counts in Layer 2

Statistical measure	GS-Deep	GeoStat
Sample size	117	117
Mean	11.41	11.41
Variance	75.31	75.31
COV	0.76	0.76
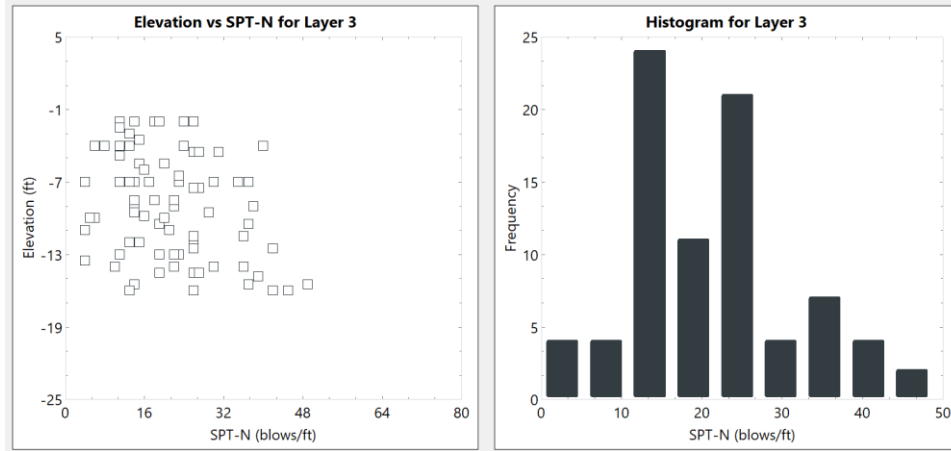
Figure 30. Layer 3 scatterplot and histogram of SPT blow count values

Table 4. Descriptive statistics for measured values of SPT blow counts in Layer 3

Statistical measure	GS-Deep	GeoStat
Sample size	81	81
Mean	21.31	21.31
Variance	109.44	109.44
COV	0.49	0.49
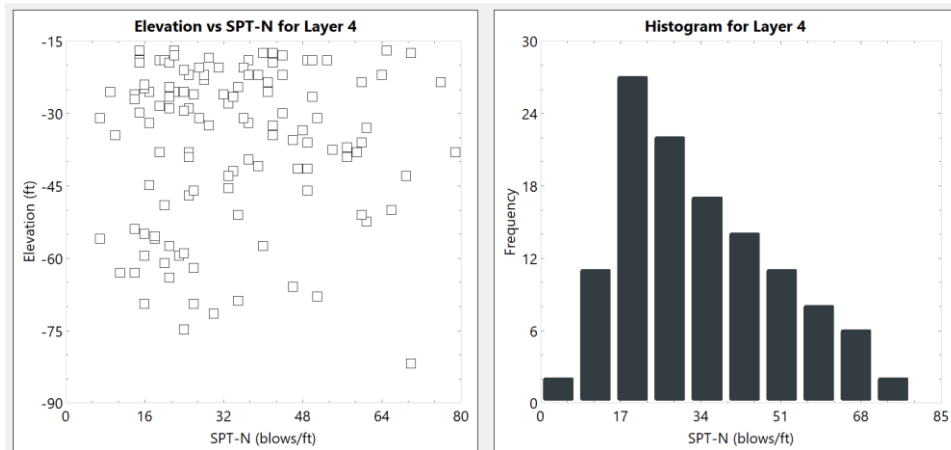
Figure 31. Layer 4 scatterplot and histogram of SPT blow count values

Table 5. Descriptive statistics for measured values of SPT blow counts in Layer 4

Statistical measure	GS-Deep	GeoStat
Sample size	120	120
Mean	33.74	33.74
Variance	281.49	281.49
COV	0.50	0.50

Results profiles pertaining to axial capacity—obtained by conducting conditional simulation (see the highlighted boring location in Fig. 28)—are plotted in Fig. 32 for candidate pile lengths of 50 ft to 100 ft. Excellent agreement is shown among the GS-Deep (versus GeoStat) results profiles: mean-valued total resistance (Fig. 28a), COV (Fig. 28b), resistance factor (Fig. 28c), and factored total resistance (Fig. 28d). More specifically, response quantities obtained using the two programs fall within approximately 1% of one another. Differences that are present are attributed to differences in the random number seed utilized in GS-Deep versus that utilized in GeoStat. Regardless, such strong agreement serves as verification of GeoStat for the purpose of simulating driven pile axial capacities.
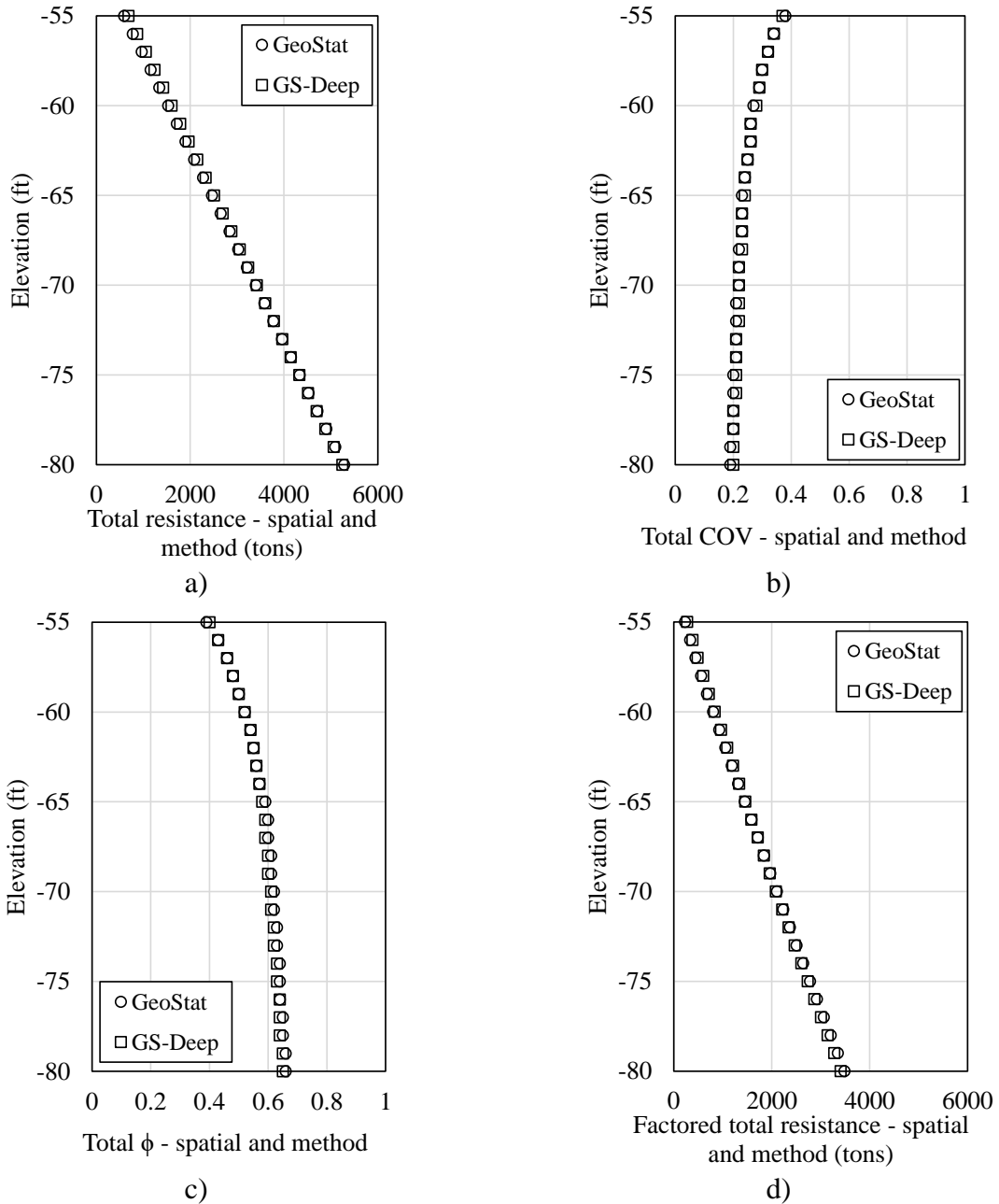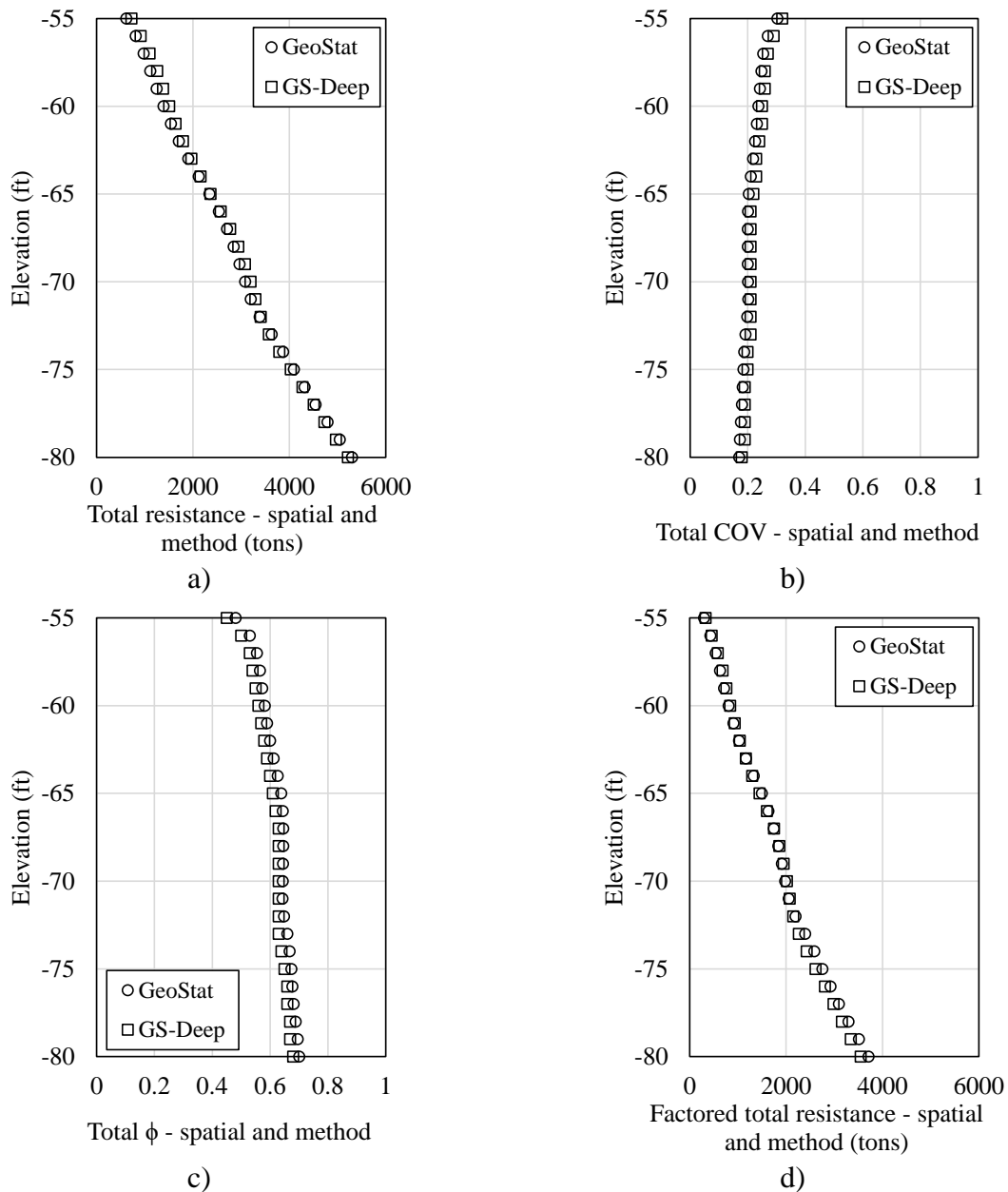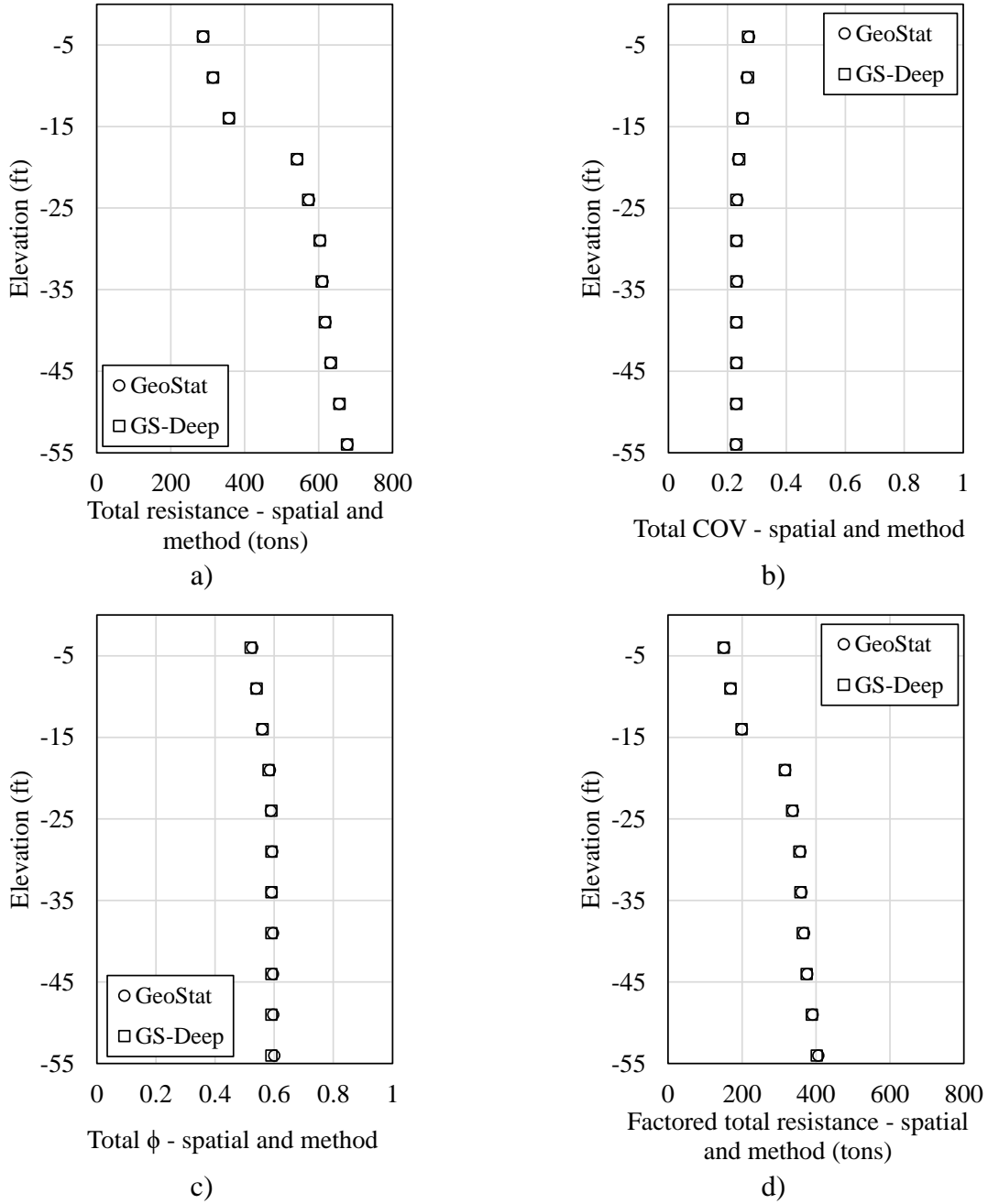
Figure 32. Comparison of driven pile response profiles obtained from conditional simulation using GeoStat and GS-Deep: a) Total resistance; b) Coefficient of variation; c) Resistance factor; d) Factored total resistance

CHAPTER 5
SUMMARY AND CONCLUSIONS

5.1 Summary of Work Completed

The current project was undertaken to transition a previously developed research prototype tool into a design tool, referred to as GeoStat, for use in bridge foundation design. This transition would subsequently allow for spatial variability and method error computation algorithms contained within GeoStat to be employed by practicing engineers. In turn, more informed selections of deep foundation configurations could then be made as part of bridge design processes. The project tasks included: (1) Establishing an input file format and data read/write operations; (2) Automation of calls to pre-existing pile/shaft axial capacity calculation software; (3) Quality assurance testing; (4) Development of an installation package and licensing; (5) Development of a software user manual; (6) Development of a software technical manual; and, (7) Deployment of the software. Summaries of the efforts and outcomes specific to items (1) through (6) are provided below.

5.1.1 Summary of Task 1 Work Completed

The primary objective of Task 1 was to establish an input file format and data read/write operations for the GeoStat software. Given the volume of data associated with geotechnical investigations for a site and the additional data necessary to evaluate both spatial correlation and method error the Microsoft® Excel worksheet was selected as the GeoStat input file type. To facilitate adherence to standardized input formatting, the worksheets were established as non-programmed (i.e., absent of Visual Basic for Applications and worksheet equations). Further, to bring about consistency with the tabbed GeoStat User Interface (UI), the input file was organized such that one Excel worksheet tab was dedicated to each major component (tab) of the GeoStat user interface (UI). Worksheet tabs for geotechnical investigation site data were also housed within the GeoStat input file, where one worksheet tab was populated for each boring location, and the boring data were organized consistent with that of pre-existing pile (or shaft) axial capacity calculation software. Task 1 (with outcomes documented in Ch. 2 of Appendix A) detailed the format and syntax for each input control in the GeoStat UI, as well as the inputs pertaining to geotechnical investigation site data. As part of the Task 1 efforts, file read and write operations such as "Open", "Close", "Save", and "Save As" were incorporated into the GeoStat code base.

5.1.2 Summary of Task 2 Work Completed

The primary objective of Task 2 was to automate calls to the pre-existing pile/shaft axial capacity calculation software, FB-Deep. The efforts to streamline and automate the manner in which GeoStat engaged FB-Deep were divided into three parts: 1) Automate calls from within GeoStat that are dedicated to forming FB-Deep model files; 2) Automate the process of carrying out batch-mode analysis of the FB-Deep model files; and, 3) Automate bulk importing of the FB-Deep analysis output. Outcomes from Task 2 were documented in Ch. 5 of the Help Manual (Appendix A), and detailed the manner in which GeoStat can be utilized to carry out each of the

three task components. Completion of this task constituted a major step in making GeoStat more convenient for use by practicing engineers.

5.1.3 Summary of Task 3 Work Completed

The primary objective of Task 3 was to conduct quality assurance on the GeoStat software. A beta version of the program was produced as part of this effort (referred to as GeoStat v0.1.0) and supplied to FDOT for review. The manner in which quality assurance was carried out for GeoStat was divided into three parts: 1) data validation of user interface controls (tabs, dialogs, tables, input boxes, results plots); 2) verification of engineering routines associated with calculation of descriptive statistics and spatial correlation structures (variograms); and, 3) verification of engineering routines associated with geostatistical simulation processes for both drilled shaft and driven pile foundation members. The quality assurance efforts were documented in Ch. 2 through Ch. 4 of the current report, and demonstrated that GeoStat possesses substantial protection against program crashes. Furthermore, the GeoStat software was verified against manual calculations and by making comparisons to the previously developed prototype tool, GS-Deep. Completion of this portion of the overall GeoStat development efforts constituted a major step in establishing GeoStat as a tool that can be used with confidence by practicing engineers

5.1.4 Summary of Task 4 Work Completed

The primary objective of Task 4 was to establish the means by which geostatistical analysis software can be deployed on the computers of practicing engineers. As a necessary part of making the software (GeoStat) available, the software components (user interface, or UI; graphical assets displayed within the UI; supporting dynamic link libraries; help manual files) were combined into an installation package. Further, to ensure that practicing engineers utilize the program in a consistent manner and only within the intended scope of program usage, program licensing (and documentation) was established. Completion of this task constituted a major step in establishing GeoStat as a tool that can be deployed with ease, confidence, and uniformity by practicing engineers.

5.1.5 Summary of Task 5 Work Completed

The primary objective of Task 5 was to establish a software user manual, referred to as the GeoStat Help Manual. As presented in Appendix A of the current report, the Help Manual was created as a distinct document from the Technical Manual (the latter of which is presented in Appendix B). The Help Manual included instructions on program installation and licensing activities; listings of input file contents; and, details concerning all user interface (UI) menu options, tabs, dialogs, plots, and controls. Completion of this task constituted establishment of a centralized resource for installation and licensing of the GeoStat software, creation of input files, and navigation across all controls distributed throughout the program UI.

5.1.6 Summary of Task 6 Work Completed

The primary objective of Task 6 was to establish a software technical manual. As presented in Appendix B of the current report, the GeoStat Technical Manual was created as a distinct document from the Help Manual (the former of which is presented in Appendix A). The Technical Manual included illustrative examples regarding selection of modeling parameters for, in turn, assessing bridge deep foundation member axial capacities. Site data from two unique locations, representative of soil or rock strengths and variability relative to those that would be found in Florida bridge sites, are utilized in the illustrative examples. In addition, for each site, technical guidance was provided concerning characterization of relevant parameters that described spatial variability of soil or rock resistance from within GeoStat. Furthermore, underlying engineering calculations carried out when modeling foundation members using GeoStat software were reviewed. Completion of this task constituted establishment of a centralized resource to aid in organizing site data through use of GeoStat; making selections for representative profiles; characterizing site spatial variability (and method error) phenomena; and, interpreting profiles of pile/shaft axial resistance.

5.2 Recommendations

Two categories of recommendations arose through the course of the project efforts. Namely, recommendations pertaining to design practice were identified; and additional recommendations pertaining to future research efforts were accumulated.

5.2.1 Recommendations for Design

GeoStat is uniquely suited to quantify spatial variability of site geotechnical data and uncertainties that routinely accompany geotechnical design processes. Further, the software produces quantitative predictions of axial resistance for deep foundation members, in combatting such uncertainties. The software may be particularly valuable in scenarios (or during design phases) where only limited site information is available. For example, member length estimates made using limited (e.g., historical-only) data during the pre-bid phase of design-build projects can benefit from use of GeoStat, as compared to use of deterministic pile/shaft axial capacity calculation software. In addition, from the perspective of the Owner, GeoStat can potentially lead to a means of objectively deciding whether or not a sufficient quantity of site data have been gathered for a given bridge site (e.g., via evaluation of capacity variance, or site-specific estimates of resistance factors, ϕ).

Given the above observations, the following recommendations are put forth for the purpose of potentially leading to improvements in bridge design:

- Use of GeoStat, in practice, is recommended for analysis of axial resistance of pile/shaft foundations embedded in homogenous or layered media (including clays, silty sands, sands, and limestone materials);

- The GeoStat software should be considered as an alternative to, or at least complementary to, use of deterministic pile/shaft axial capacity calculation software; and,

- Analysis output such as site-specific resistance factors (ϕ) should be considered (with Owner approval) for use in member design, or at least, in determining if sufficient geotechnical data have been gathered for a given bridge site.

5.2.2 Recommendations for Potential Future Research

During completion of the project tasks, several potential future enhancement items were identified, which could further increase the utility of GeoStat software in foundation design applications. The accumulated list of enhancement items may be undertaken, in part or in whole, as part of potential future research efforts.

- Development of training materials may raise awareness of the merits of the statistical approach to assessing pile/shaft resistances using GeoStat;

- Building on FDOT-funded research efforts such as BDV31-820-006, implementation of parameters associated with Measuring While Drilling (MWD), and further, associated calculations of axial resistance.

- Implementation of CPT parameters (e.g., for driven piles) and associated calculations of axial resistance.

- If significant volumes of load test data have been gathered since the development of the prototype software in 2012, then such data may be identified and utilized in investigating methodologies (e.g., Bayesian updating) for characterizing site-specific bias.

- Implementation of options for the engineer to specify desired empirical correlations for parameters such as undrained shear strength for cohesionless soils and mass modulus for limestone.

- Implementation of auto-calculation of unit weights (mean, COV) assigned to layers (when data are available) for analysis of drilled shaft members.

- Implementation of the option for automatic variogram curve fits to raw variogram data.

REFERENCES

AASHTO. (2017). *LRFD bridge design specifications, 8th Ed*. Washington D.C.

Faraone, M. A. (2014). *Geostatistical Analysis for Reliability Based Design of Foundations*, Dissertation, University of Florida, Gainesville, FL.

FB-Deep [Computer software]. Bridge Software Institute (BSI), University of Florida, Gainesville, FL.

FDOT. (2019). *Structures Design Guidelines, Structures Manual, Vol. 1*, Tallahassee, FL.

Klammler, H., McVay, M., Horhota, D., and Lai, P. (2010). "Influence of Spatially Variable Side Friction on Single Drilled Shaft Resistance and LRFD Resistance Factors", *ASCE Journal of Geotechnical and Geoenvironmental Engineering*, 136(8), 1114-1123.

McVay, M., Klammler, H., Bloomquist, D., Otero, J., Faraone, M. A. (2009). *Modifications of LRFD Resistance Factors Based on Site Variability*, FDOT Research Report BD-545 RPW76, Tallahassee, FL.

McVay, M., Klammler, H., Faraone, M. A., Krishmarao, D., Jenneisch, C. (2012). *Development of Variable LRFD ϕ Factors for Deep Foundation Design Due to Site Variability*, FDOT Research Report BDK75 977-23, Tallahassee, FL.

Rivers, B. (2018). Advanced Geotechnical Methods in Exploration (The A-GaME), *49th Annual Southeastern Transportation Geotechnical Engineering Conference (STGEC)*, Louisville, KY, Oct. 8-11.

Rodgers, M., McVay, M. C., Horhota, D. (2019). *Measuring While Drilling for Florida Site Investigation (FLMWD)*, BDV31-820-006, FDOT Geotechnical Research in Progress Meeting, Gainesville, FL, Aug. 15.

APPENDIX A
GEOSTAT HELP MANUAL

Presented below is the Help Manual for the GeoStat software, which is included as a standalone document, and is accessible from within the GeoStat UI. The Help Manual integrates work carried out during project Task 1 through Task 4, and contains documentation of program installation and licensing; input file formatting; and, all UI controls. A companion manual, which focuses on geotechnical engineering concepts, selection of modeling parameters, and underlying engineering calculations that are carried out when using the GeoStat software, is provided in Appendix B.

GeoStat

Help Manual

DISCLAIMER

No warranty, expressed or implied, is made by the Florida Department of Transportation or the University of Florida as to the accuracy and functioning of any programs or the results they produce, nor shall the fact of distribution constitute any such warranty, and no responsibility is assumed by the Florida Department of Transportation or the University of Florida in any connection therewith.

TABLE OF CONTENTS

CHAPTER 1
INTRODUCTION

1.1 Introduction

Due in part to intrinsic variability of soil and rock materials, design and construction of deep foundations typically comprise significant costs for bridges. Measured soil properties exhibit spatial variability across a given site (both with respect to depth and horizontal position), while empirical methods by which measured soil properties are correlated to design-relevant soil or rock resistances introduce a separate form of uncertainty into the design process. These sources of uncertainty present challenges in determining layering, distinct zones, as well as if sufficient site data have been gathered as part of required geotechnical investigations, which can result in non-representative (i.e., overly conservative or unconservative) estimates of Load and Resistance Factor Design (LRFD) resistances (ϕ) of deep foundation members. Quantifying these distinct sources of uncertainty (spatial variability, method error) allows for better determination of whether or not sufficient geotechnical site data have been gathered, and also, makes clear the level of uncertainty that can be attributed to predicted resistance of deep foundation members.

The GeoStat software allows engineers to characterize these forms of uncertainty, more efficiently carry out design efforts, and potentially arrive at more economical allocation of construction materials for bridge substructure configurations. GeoStat can be used to compute pile or shaft (axial) soil resistance, the associated uncertainty of those estimates, and LRFD resistance (ϕ) factors over a selected range of member embedment lengths, for given site data and engineer-selected layering and zones. The program accepts a collection of borings/corings pertinent to a site of interest, the engineer divides the site into zones, and for each zone, determines the layering. GeoStat is then used to perform both spatial-variability analysis and method error estimation on a pile/shaft, resulting in generation of through-depth resistance profiles and associated resistance (ϕ) factors.

1.2 Software Description

The GeoStat user interface (UI), which is a tabbed interface, guides engineers through the process of: 1) cataloging site data (borings, corings); 2) permitting zone definitions (i.e., subsets of the collected site data, i.e., zones); 3) permitting definitions of soil or rock layering; 4) forming spatial correlation structures given the subset of site data and soil or rock layering; 5) simulating numerous realizations of through-depth soil strength parameters; 6) computing through-depth axial resistance for each realization; 7) adjusting axial capacities using appropriate method error correlations; and, 8) reporting descriptive statistics (e.g., mean, variance, and COV) of resistance throughout the site and location-specific LRFD resistance (ϕ) factors.

Foundation design data generated in this manner overcome significant simplifications typical of current practice, where phenomena such as rock layering, area zones (i.e., spatial variability) are either ignored or indirectly accounted for via significantly more conservative (and more costly) configurations. By incorporating GeoStat into the design process, quantitative indicators of scope and sufficiency can be made available for budgeting, and conducting, geotechnical investigations. Also, the ability to quantify variability in foundation resistance quantities (e.g., the effect of pile/shaft lengths on LRFD resistance ϕ factors) can enable practicing engineers to achieve more optimized (and cost-effective) foundation designs.

1.3 Help Manual Scope

Program documentation for the GeoStat software is divided into two components: 1) a Help Manual; and, 2) a Technical Manual. Accordingly, the GeoStat Help Manual is a standalone document that details the program installation and licensing procedures, input file layout, and all user interface (UI) controls. In contrast, as a separate document, the GeoStat Technical Manual focuses on underlying engineering calculations (originally developed in McVay et al. 2012 and Faraone, 2014), and utilizes representative anonymized data from bridge sites to provide guidance and recommendations for establishing GeoStat model files (and interpreting results).

The present document, the GeoStat Help Manual, provides engineers with a centralized resource to aid in navigating through all input file contents and UI controls while making use of the GeoStat software for bridge foundation design. Organization of remaining chapters of the GeoStat Help Manual is as follows:

- In Chapter 2, step-by-step guides are provided for program installation and licensing.

- In Chapter 3, all input parameters (and formatting) making up GeoStat input files are identified and described.

- In Chapter 4, listings and descriptions are provided for all controls that comprise the GeoStat UI.

- In Chapter 5, the means by which analysis model files are created (for analysis) and parsed (for results viewing) are documented.

CHAPTER 2
PROGRAM INSTALLATION AND LICENSING

2.1 Installation

Documented in Section 2.1 are the GeoStat installation package contents and the procedure for installing the software.

2.1.1 Installation Package Overview

Sec. 2.1.2 delineates the various program executable, support, license, and settings files that collectively make up the GeoStat software package. A step-by-step guide for installing GeoStat is provided in Sec. 2.1.3.

2.1.2 Installation Package Contents

The GeoStat installation package, created using InstallShield (Flexera, Itasca, IL), streamlines the creation and placement of all required program components on a target machine. For the GeoStat program (a Microsoft Windows desktop application) to work properly, appropriate components need to be installed in "Program Files (x86)" and "Users" directories. As part of the software installation operations, all necessary ActiveX Controls are also registered. In addition, program shortcuts are created in the Windows Start Menu and Desktop.

The installation package (GeoStat_ins.exe) contents consist of three major parts: program prerequisites, program execution files, and program settings files. In particular, the installation procedure ensures that a prerequisite "Microsoft Visual C++ 2017 Redistributable Package (x86)" is present on the target machine. This perquisite redistributable contains runtime libraries that, in turn, are required for the GeoStat program to function properly. If not found, then the installation package installs the redistributable package prior to carrying out remaining stages in the installation procedure.

After prerequisite files have been placed on (or confirmed to preexist on) a target machine, program files are created. Shown in Fig. 1 are the files that are placed within the "Program Files (x86)" directory during installation. These files are needed to carry out the functioning and display of the UI, as well as for performing engineering calculations.

Figure 1. Program files included in the GeoStat installation package

By default, program files are installed in "C:\Program Files (x86)\BSI\GeoStat". However, as shown later, a custom installation location can be specified. Program files include: program documentation (Help and Technical manuals); user interface (UI) graphical resources (images); a support executable (eoul.exe); the executable UI (GeoStat.exe); a support library (libxl.dll); and, ActiveX control (NTGraphGS.ocx). The ActiveX control is registered during the installation process.

Shown in Fig. 2 are program settings files generated by the GeoStat software during the first program session after the installation package is run. These files are located in "C:\Users\Public\Documents\BSI\GeoStat", and consist of wider software settings (GeoStat.ini) and within-UI settings (ProgramSettings.ini). Also included here is a folder containing illustrative program example files (one for driven piles and one for drilled shafts). As discussed later, for GeoStat deployments with machine-locked (standalone) licensing, the software license file also resides here.

Figure 2. Program settings files generated during the first GeoStat session

2.1.3 Step-by-Step Installation Guide

Installation of the GeoStat software can be carried out by following the nine steps listed below, where many of the steps are guided by an Installation Wizard tool:

1. Download the installation package executable (GeoStat_ins.exe) from the BSI website.

4

2. Double-click the installer executable, and click "Yes", when asked for permission to install the program (Fig. 3).

3. If prerequisite program files are not present on the machine, then the necessary files will be installed prior to proceeding any further with the GeoStat installation.

4. The Installation Wizard will appear (Fig. 4). Click "Next" to proceed.

5. The software End User License Agreement (EULA) will be displayed for review (Fig. 5), where example language contained within the EULA is given in Appendix A. Click "Next" to accept the terms of the EULA and proceed with the GeoStat installation.

6. As shown in (Fig. 6), the program installation directory can be selected. The default location is "C:\Program Files (x86)\BSI\GeoStat". If it is desired to modify the default location, click the "Change…" button and provide the new destination folder location. Click "Next" to proceed.

7. If any settings were not assigned as intended, then click "Back" (Fig. 7). Otherwise, click "Install" to proceed with the GeoStat installation.

8. The installation progress is updated in real-time on the progress page (Fig. 8). After all files have been created, and all supporting libraries (or controls) registered, the Completed page will appear (Fig. 9). Click "Finish" to complete the installation.

9. A desktop shortcut for the GeoStat software will be located on the Desktop. Double-click the newly created GeoStat shortcut to run the program.

Figure 3. User Account Control message box for initiating program installation

Figure 4. Welcome page in the Installation Wizard
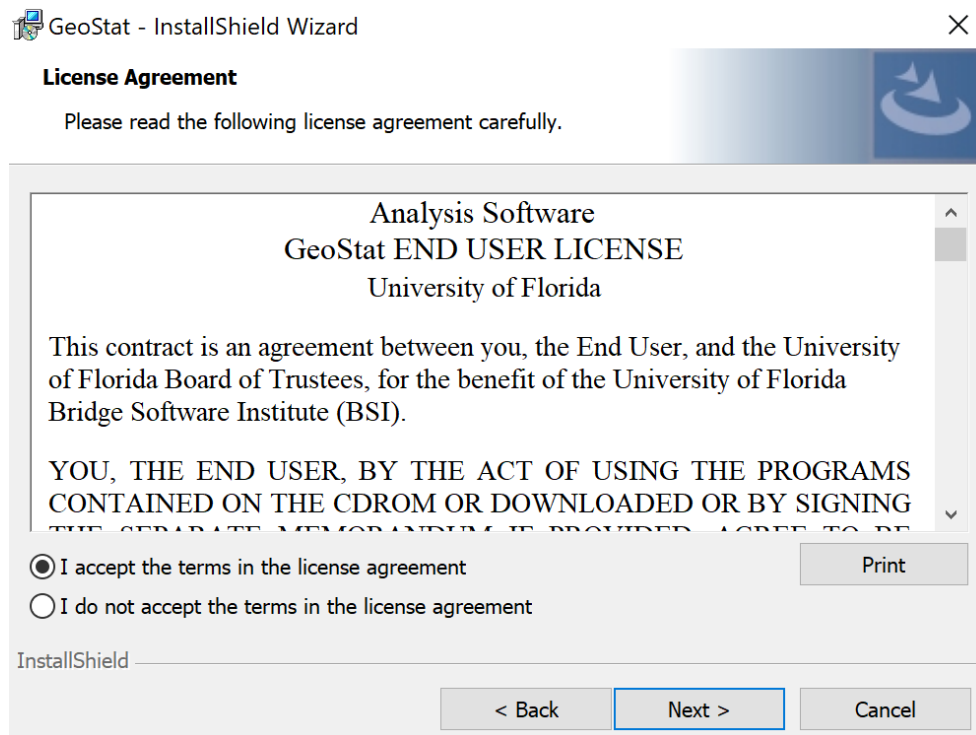
Figure 5. End User License Agreement (EULA) page in the Installation Wizard
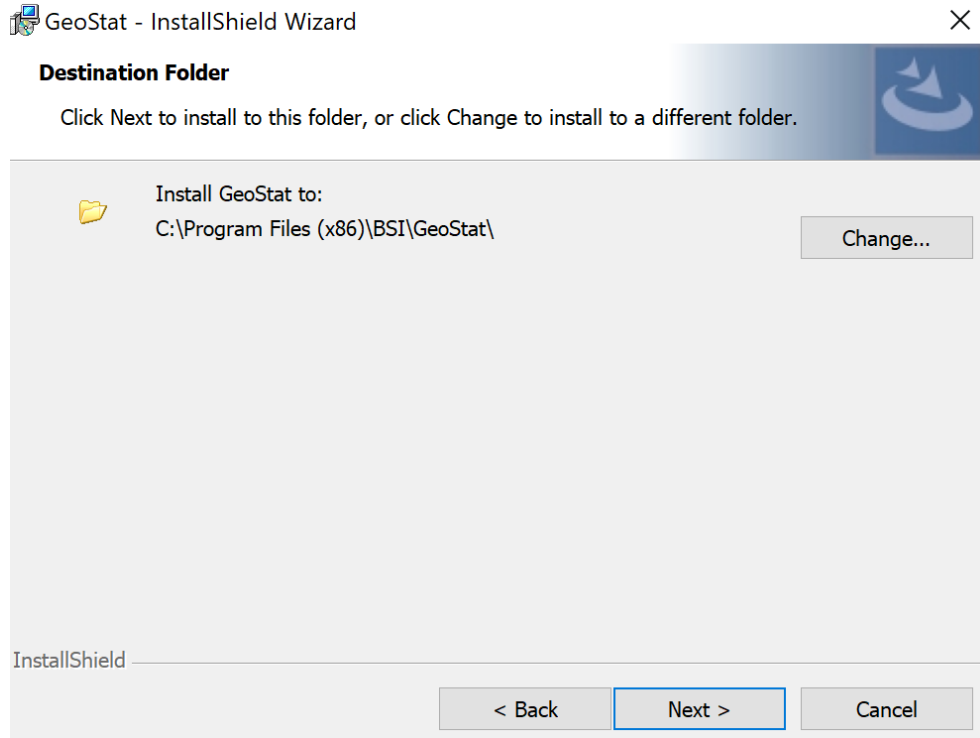
Figure 6. Destination Folder page in the Installation Wizard
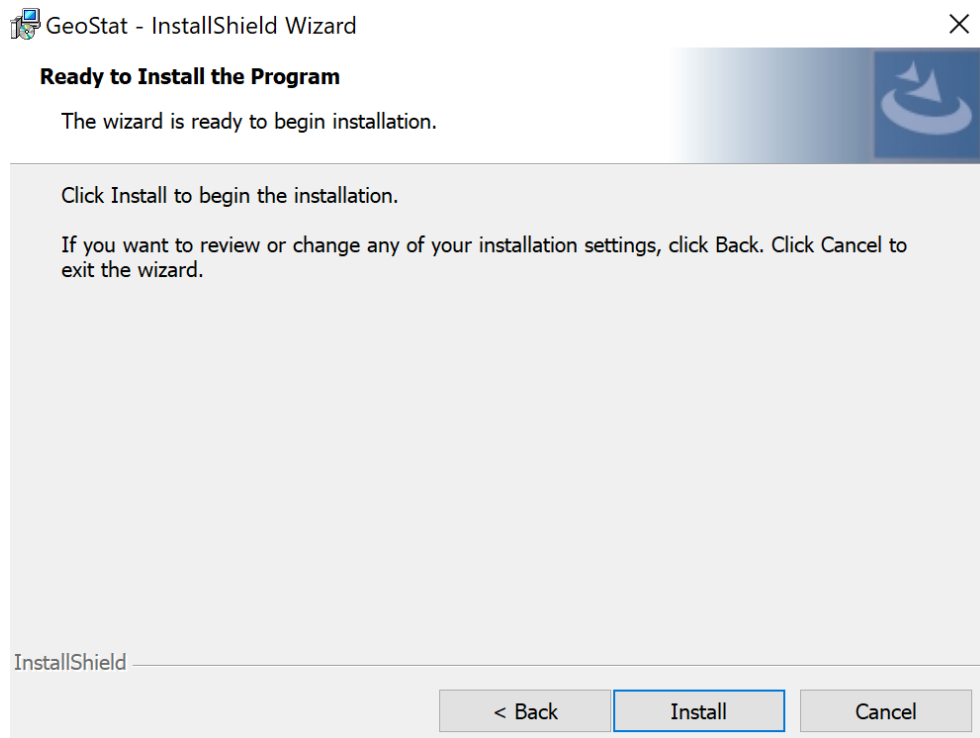
Figure 7. User Account Control page in the Installation Wizard
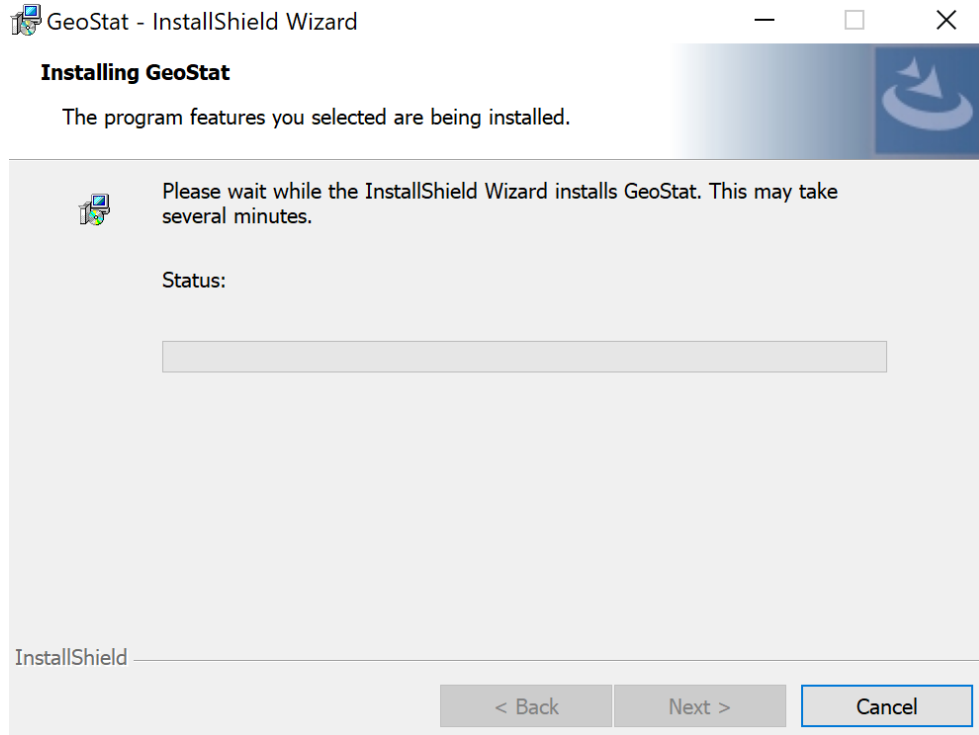
Figure 8. Installing GeoStat progress page in the Installation Wizard
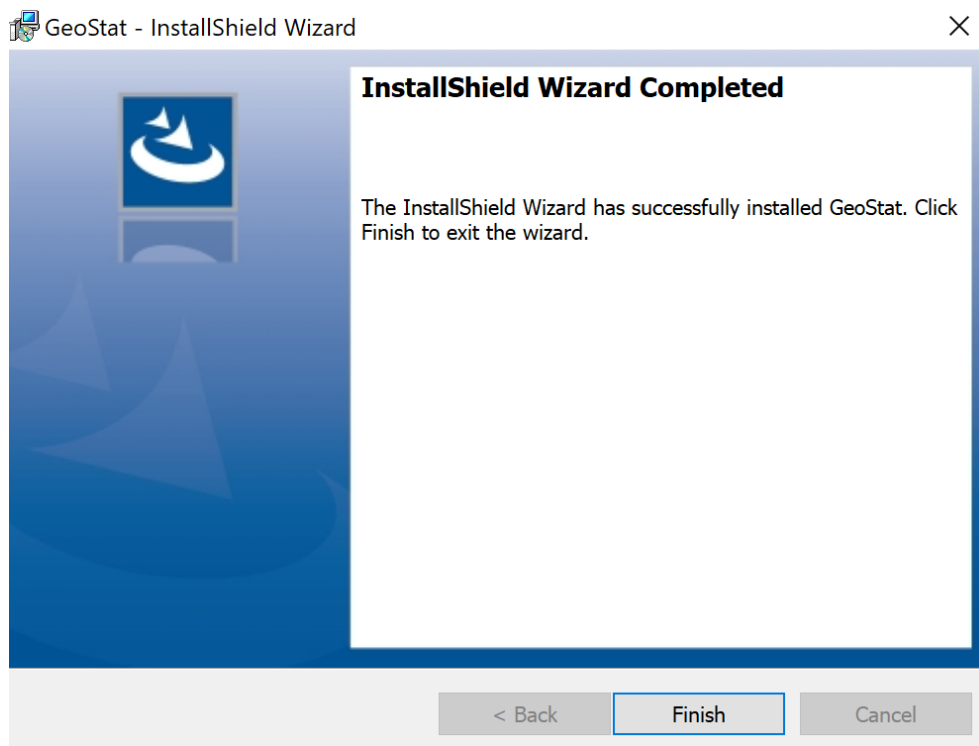
Figure 9. Completed page in the Installation Wizard

2.2 Licensing

Presented in Sec. 2.2 is documentation concerning licensing of the GeoStat software.

2.2.1 Licensing Overview

In Sec. 2.2.2, step-by-step guides are provided for accessing a program License Wizard. Also, guides are provided for program deployments under machine-locked (standalone, Sec. 2.2.2.1) and networked (Sec. 2.2.2.2) license scenarios. Guides for making various modifications to the licensing file (custom path, transfer to another machine) are provided in Sec. 2.2.3 through Sec. 2.2.5.

2.2.2 Step-by-Step Licensing Guide

A licensing system has been implemented in the GeoStat software, as a means of restricting program access, such that only authorized users can access the program. Central to this licensing system is the license file (GeoStat.lfx). The license file is inspected during each GeoStat session to ensure the user has permission to operate the software. Examples of the types of license file authentication performed include ensuring that the computer or network is authorized to run GeoStat.

Upon initial installation of GeoStat on a target machine, and by design, a license file will not exist. During the first program session, however, GeoStat will create a license with a 30-day duration. This license will allow GeoStat to run in Demo mode, which greatly limits program functionality. To convert the Demo license to a Standard (full) license, a license update must be performed. Performing a license update requires action to be taken on the part of the end user. To facilitate this process, a License Wizard can be utilized. Through use of the License Wizard and initial contact with BSI, licensed use of the program can be achieved.

2.2.2.1 Accessing the License Wizard

The License Wizard is accessible directly from within the GeoStat UI. To access the License Wizard, click the Help menu item (Fig. 10). Then, select the Update Software License sub-item (Fig. 11).

The License Wizard provides a centralized set of pages for performing various license operations, as accessed from the Select Type of License Update page (Fig. 12). There are five license modification modes: Update Standalone License; Update Network License; Set License File Path for Standalone License; Set License File Path for Network License; and, Transfer License to Different Computer. Guides for operating within each mode are given below.
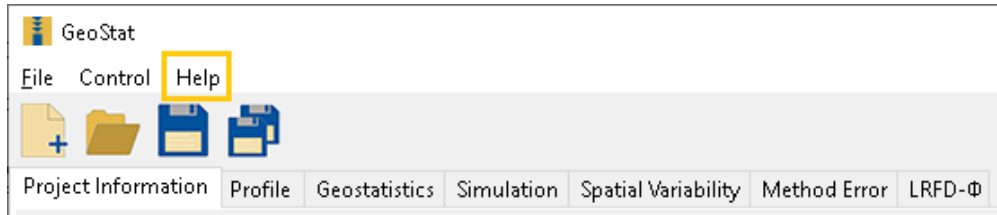
Figure 10. Help file menu item in the GeoStat UI
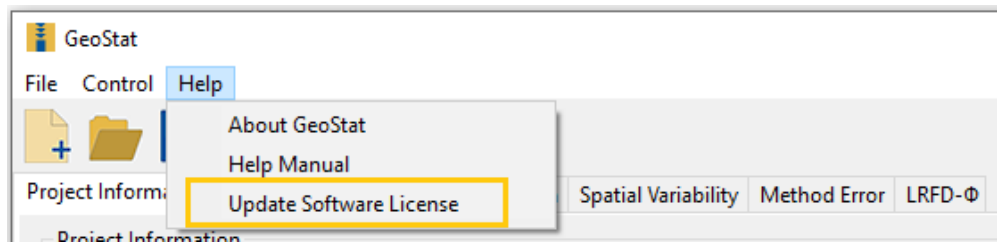
Figure 11. Update Software License file menu sub-item in the GeoStat UI
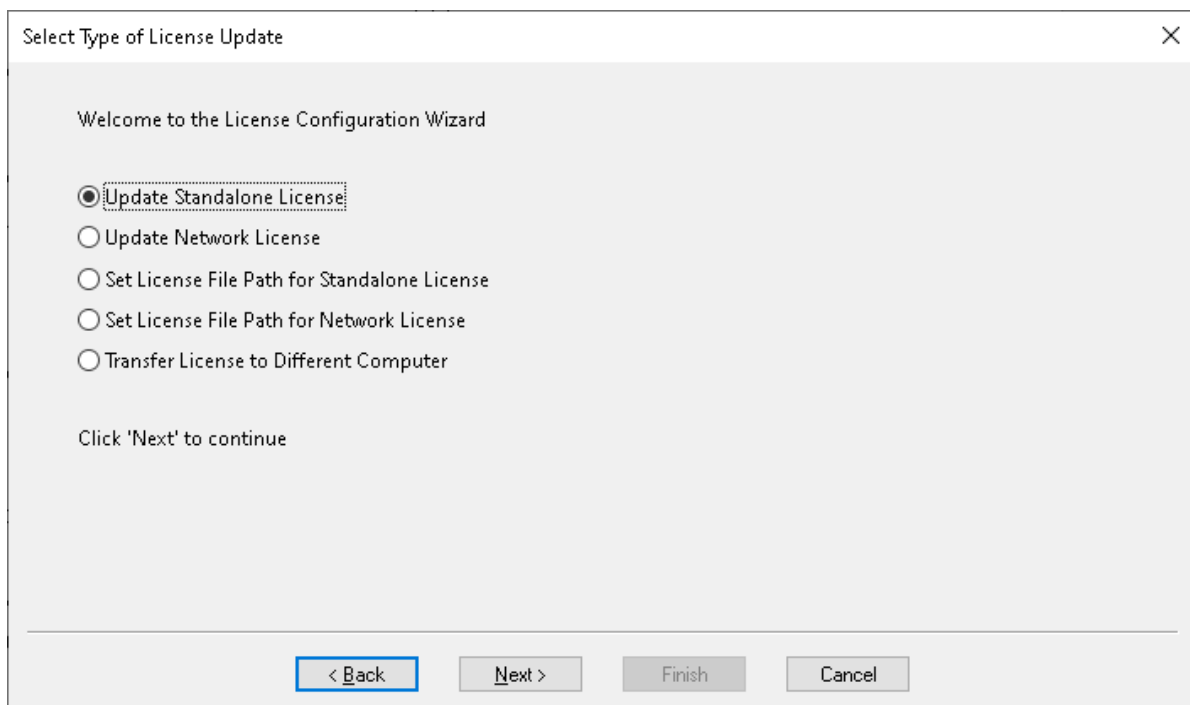
Figure 12. Select Type of License Update page in License Wizard

2.2.2.2 Configuring a Standalone License

The Update Standalone License option is used to update a license file when both the license file and GeoStat program files are located on the same machine. The Update Standalone

License option is used to put additional time on the license file, for example to extend the license expiration by one year. To use this option, select the Update Standalone License radio button (Fig. 13), and click the "Next" button (Fig. 14). The License Codes page displays the Session Code and Machine ID (Fig. 15). At this juncture, contact with BSI must be made to continue the license update, where the Session Code and Machine ID are emailed to bsi@ce.ufl.edu. For convenience and accuracy in copying these codes into an email, the Copy Codes to Clipboard button can be clicked (Fig. 16) to transfer the Session Code and Machine ID to the clipboard.

Upon receiving the codes, BSI will email back seven required unlocking codes. These seven codes will need to be selected, copied, and then pasted into the seven text boxes on the License Codes page (Fig. 17). Similar to using the Copy Codes to Clipboard button, the Paste Codes from Clipboard button can be used to transfer all seven codes into the License Wizard at one time. Copy the seven unlocking codes from the email (sent from BSI) to the clipboard. Then, paste all seven codes into the License Update page (at once) by clicking the Paste Codes from Clipboard button (Fig. 18). After the codes are copied into the License Codes page, click the "Finish" button to complete the license update (Fig. 19). The GeoStat program will then automatically close. Upon reopening the program, the updated license file will be utilized.
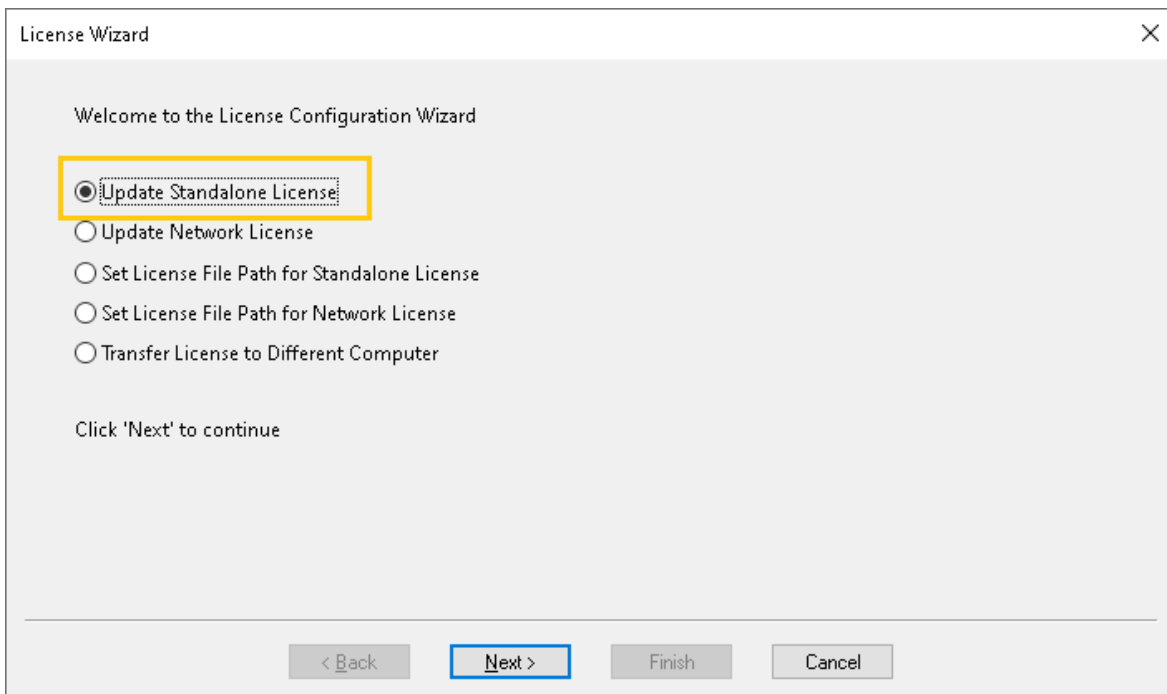
Figure 13. Update Standalone License radio button
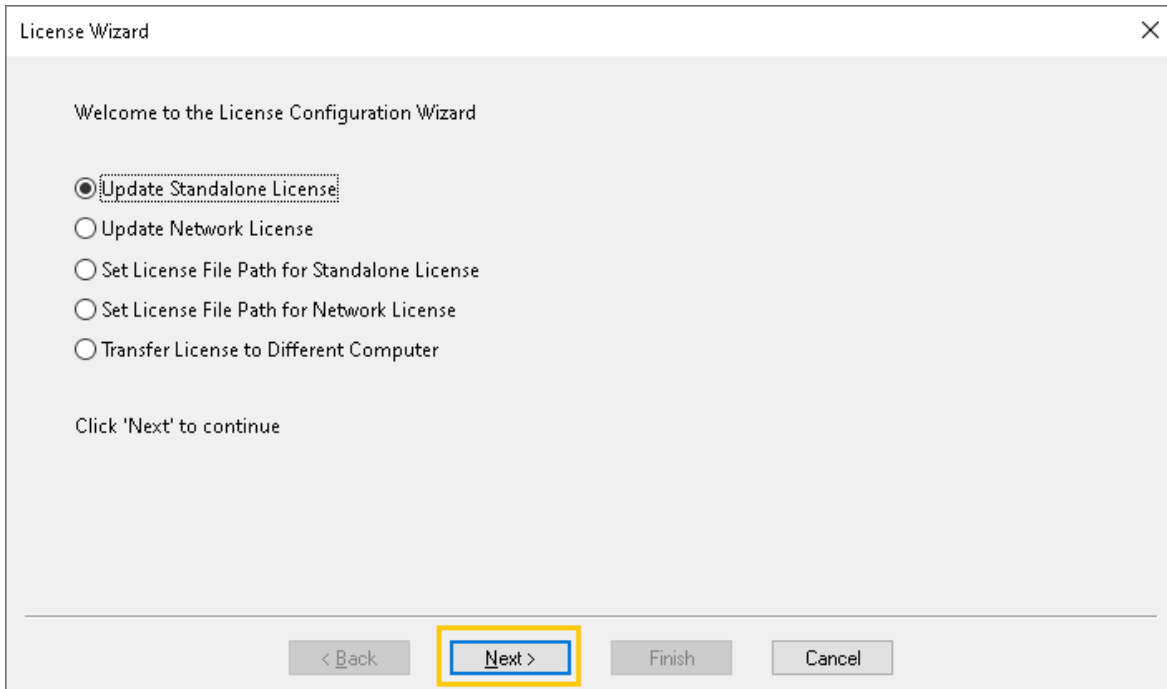
Figure 14. Next button in Update Standalone License process
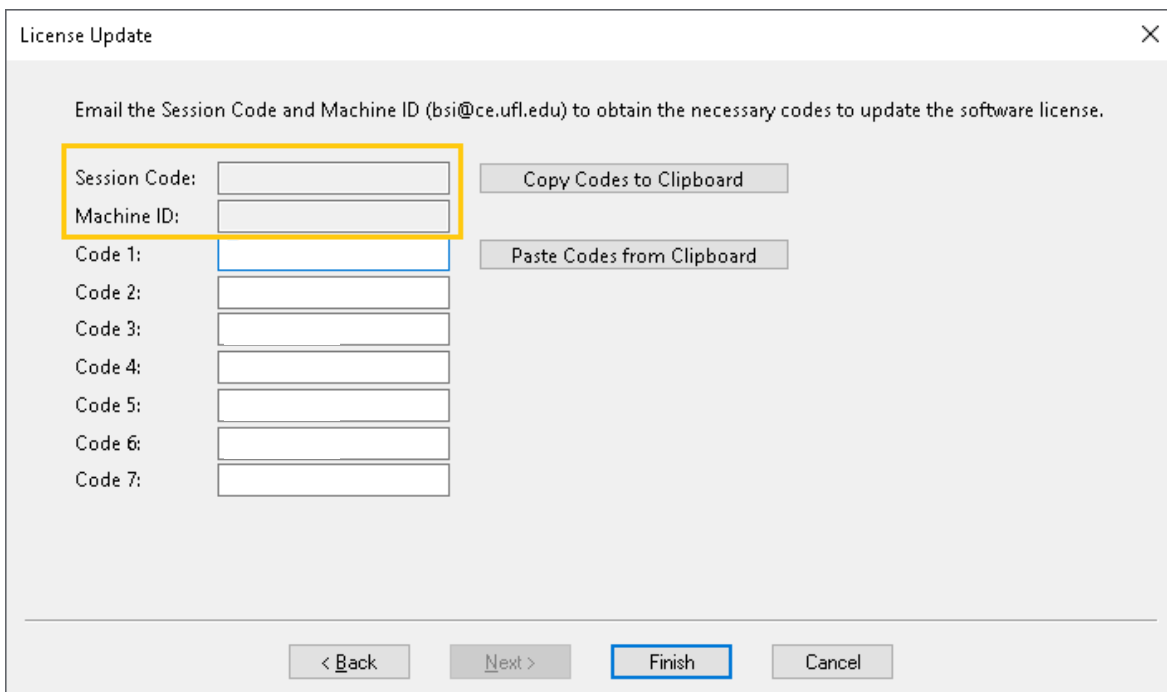
Figure 15. License Update page with Session Code and Machine ID (for standalone license)
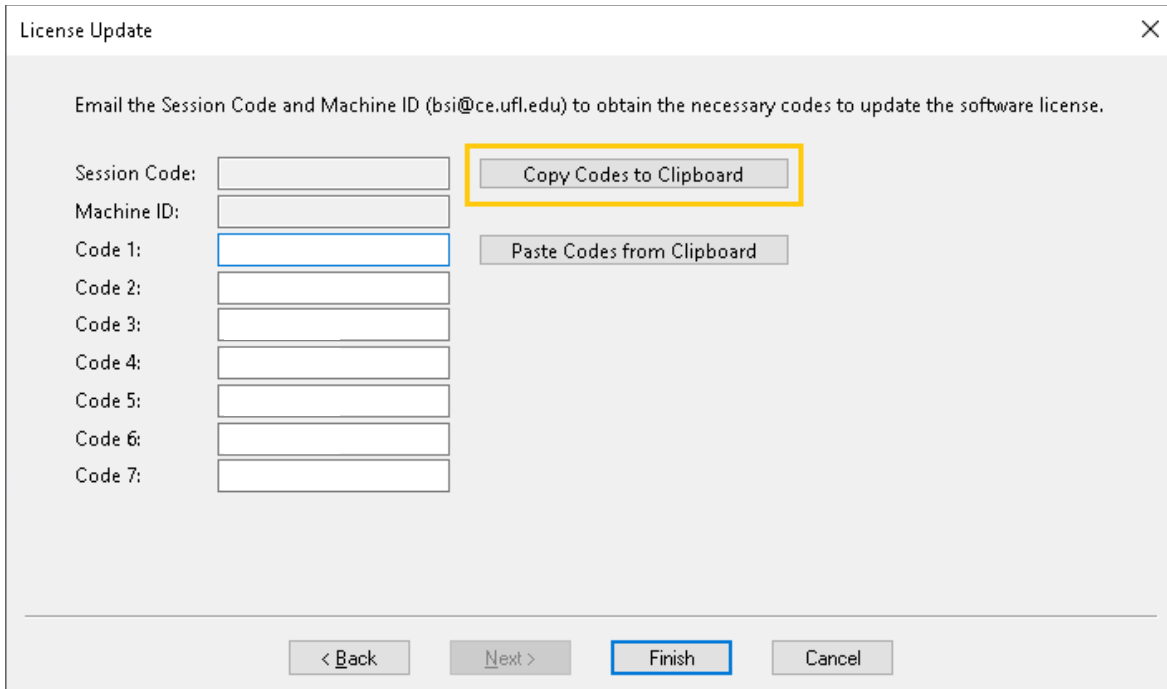
Figure 16. Copy Codes to Clipboard button (for standalone license)
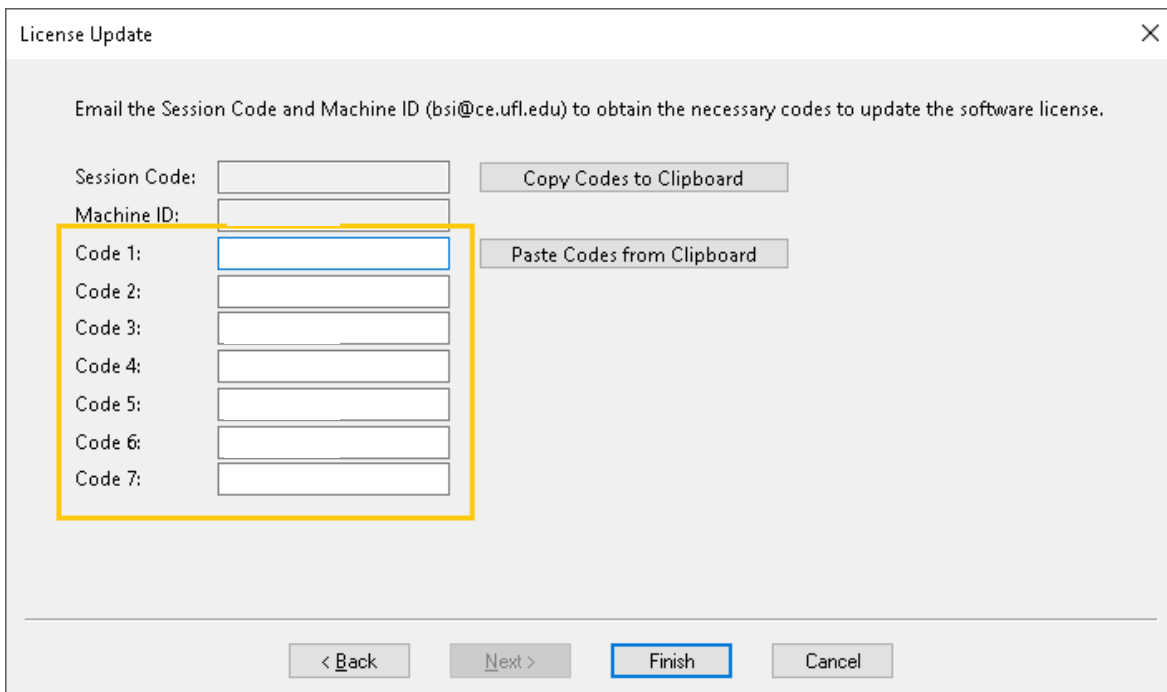
Figure 17. Unlocking codes for Standalone License Update
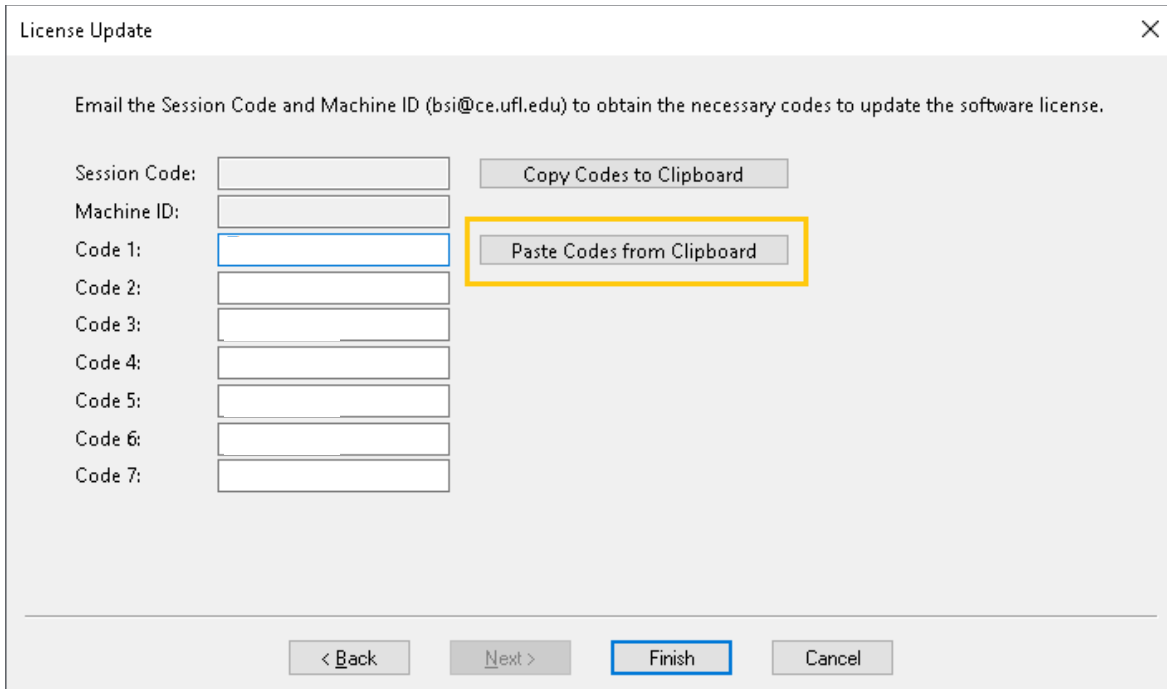
Figure 18. Paste Codes from Clipboard button (for standalone license)
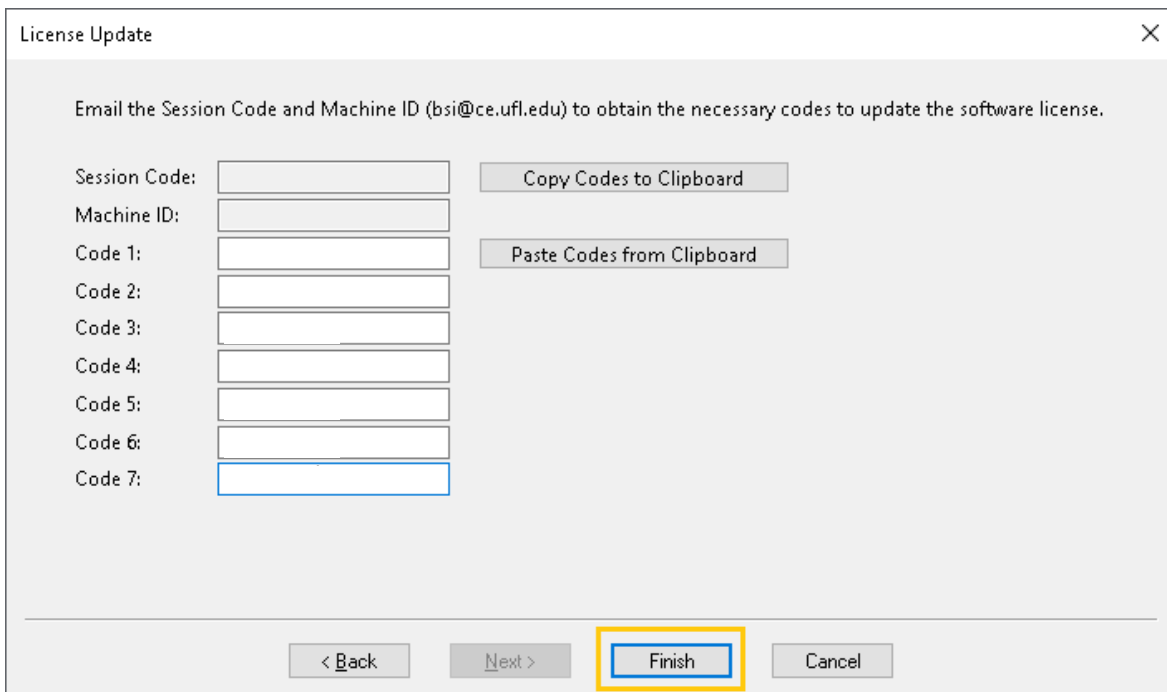
Figure 19. Finish button on License Update page (for standalone license)

14

2.2.2.3 Configuring a Network License

The Update Network License option is used to update a license file when the license file is hosted on a network server (e.g., serving a Local Area Network). This is known as a Network license configuration. In this type of installation, a number of workstations, each with an installed copy of GeoStat, point to the license file (located on the network server). The Update Network License option is used to put additional time on the license file, for example to extend the license expiration by one year, or to add to or subtract from the number of seats that can be used concurrently on the Network license. To use the Update Network License option, select the Update Network License radio button (Fig. 20) and click the "Next" button (Fig. 21). The License Codes page displays the Session Code and Machine ID (Fig. 22).

At this juncture, contact with BSI must be made to continue the license update. Email the Session Code and Machine ID to bsi@ce.ufl.edu. For convenience and accuracy in copying these codes into an email, the Copy Codes to Clipboard button can be clicked (Fig. 23) to transfer the Session Code and Machine ID to the clipboard.

Upon receiving the codes, BSI will email back the seven required unlocking codes. These seven codes will need to be selected, copied, and then pasted into the seven text boxes on the License Codes page (Fig. 24). Similar to using the Copy Codes to Clipboard button, the Paste Codes from Clipboard button can be used to simultaneously transfer (all seven) codes into the License Wizard.
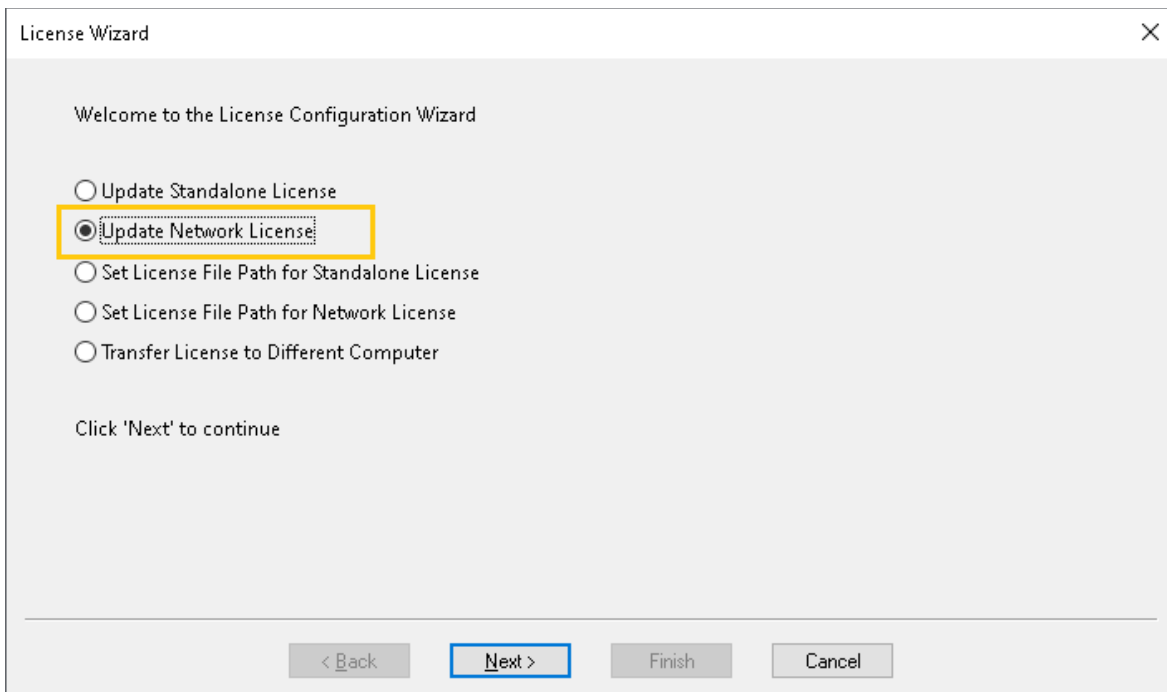
Figure 20. Update Network License radio button
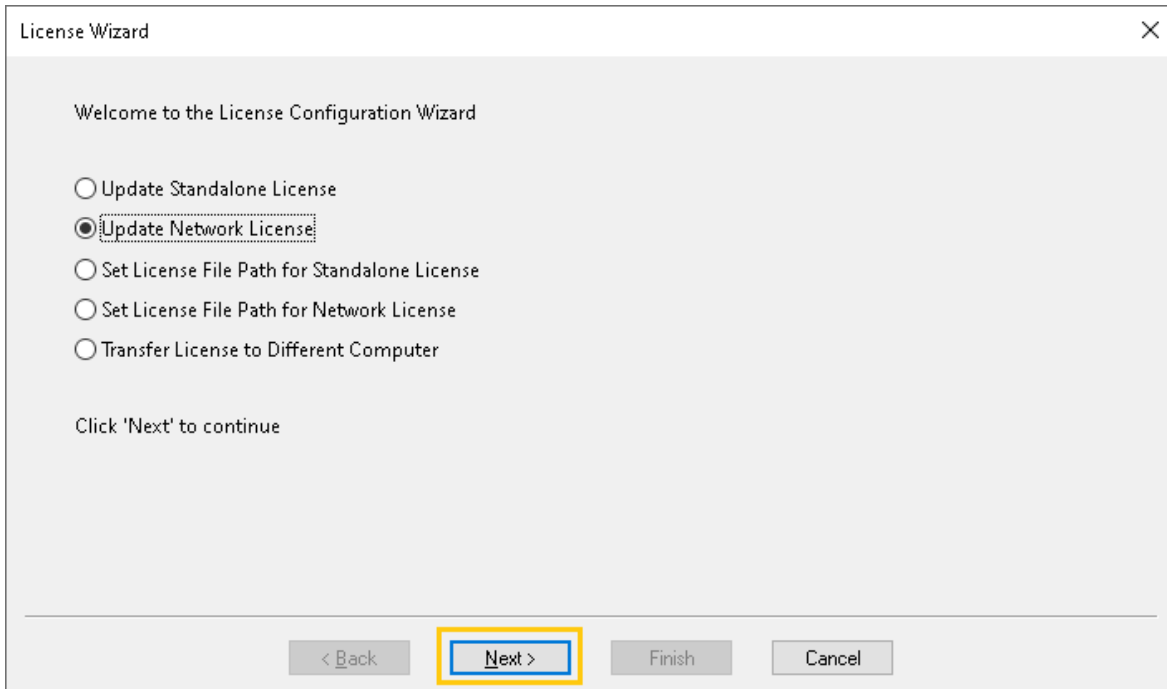
Figure 21. Next button to update a network license
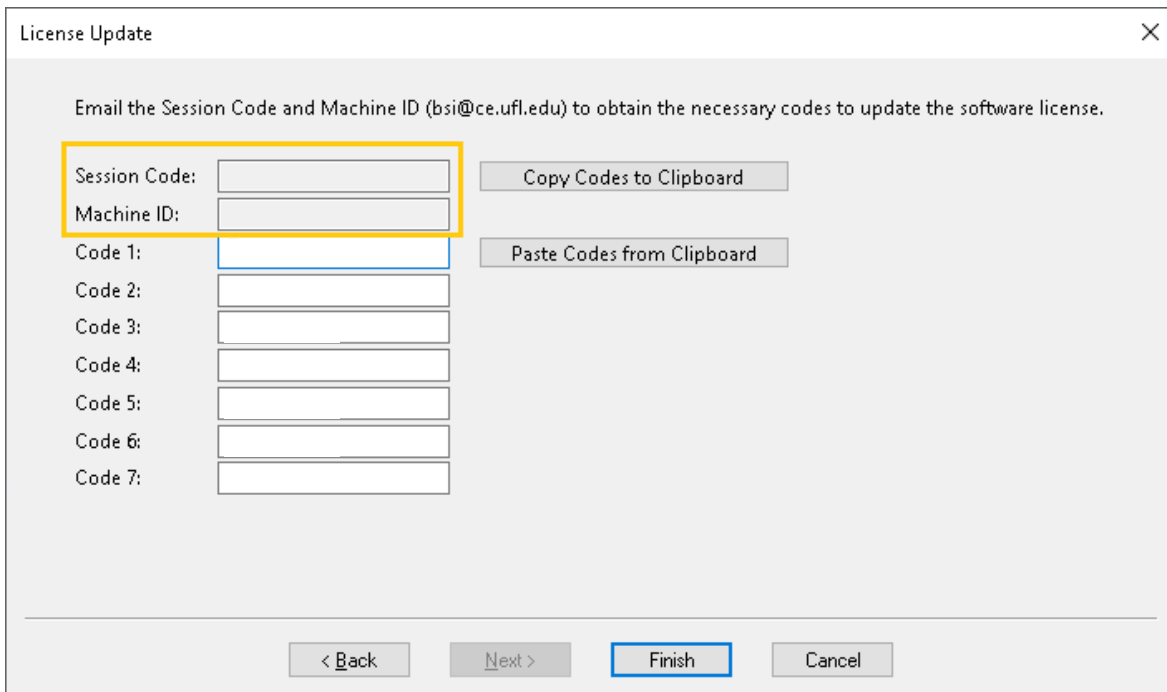
Figure 22. License Update page with Session Code and Machine ID (for network license)
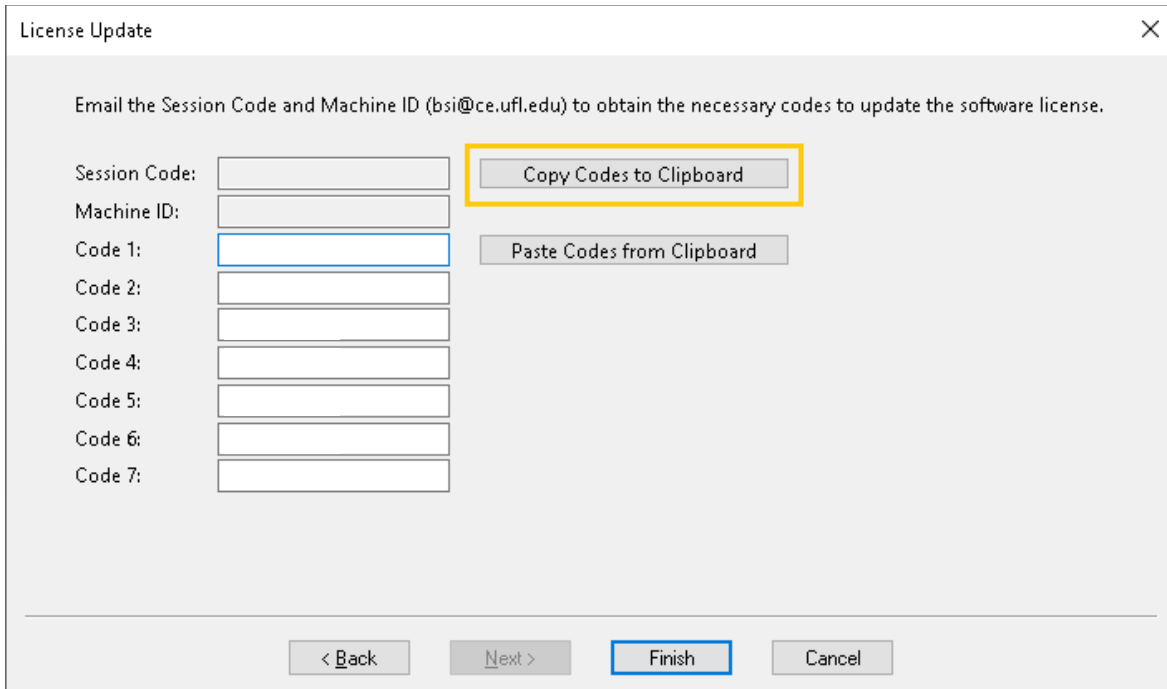
Figure 23. Copy Codes to Clipboard button (for network license)
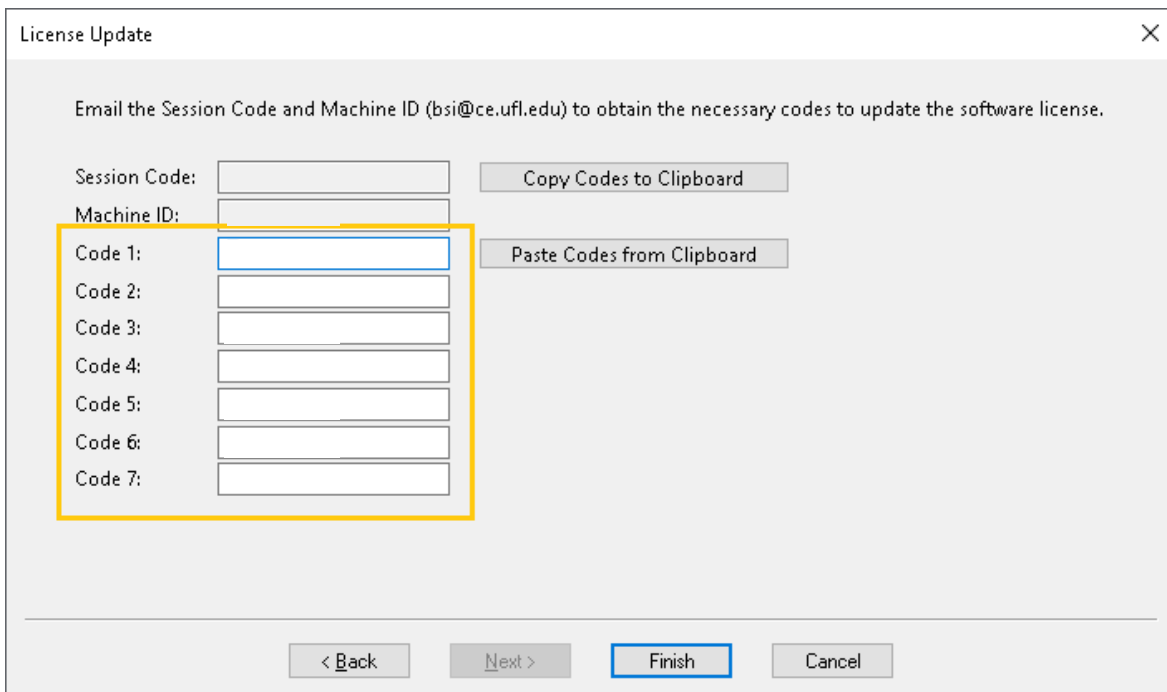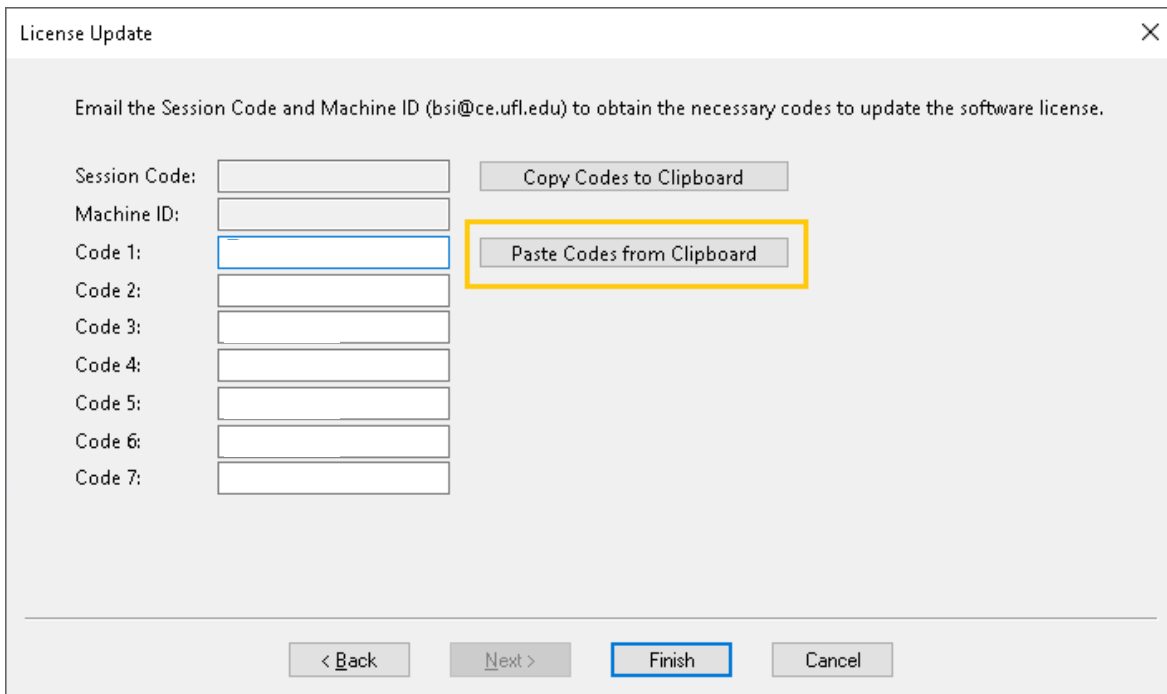
Figure 24. Unlocking codes for Network License Update
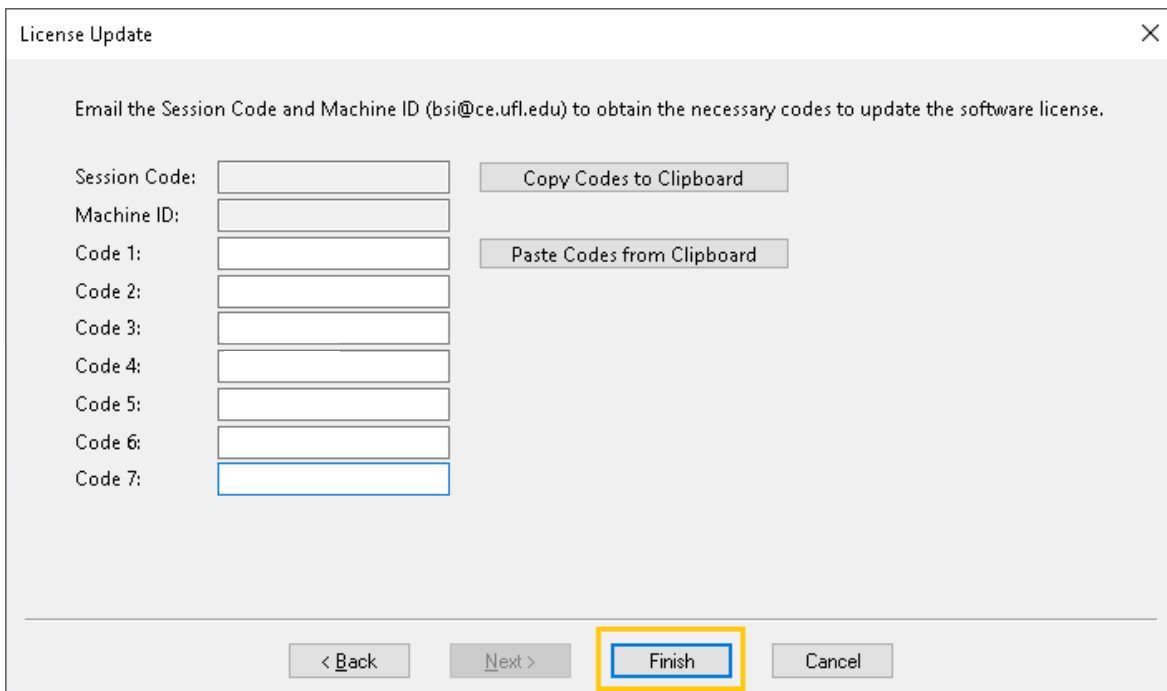
Copy the seven unlocking codes from the email (sent from BSI) to the clipboard. Then, paste all seven codes into the License Update page by clicking the Paste Codes from Clipboard

button (Fig. 25). After the codes are copied into the License Codes page, click the "Finish" button to complete the license update (Fig. 26).

Figure 25. Paste Codes from Clipboard button (for network license)

Figure 26. Finish button on License Update page (for network license)

Upon clicking the "Finish" button, the GeoStat program will automatically close. Upon reopening the program, the update license file will be used. This license update will affect all workstations pointing to the license file that is hosted on the network server. Thus, this update does not need to performed once per workstation, but instead only once per network.

2.2.3 Setting a Custom License File Path for a Standalone License

The license file (GeoStat.lfx) by default is positioned in the "Users" public directory at the following location: "C:\Users\Public\Documents\BSI\GeoStat". However, if it is so desired, the license file location can be set to a custom location. The Set License File Path for Standalone License option is used to specify the location of the GeoStat license file on a workstation (Fig. 27).
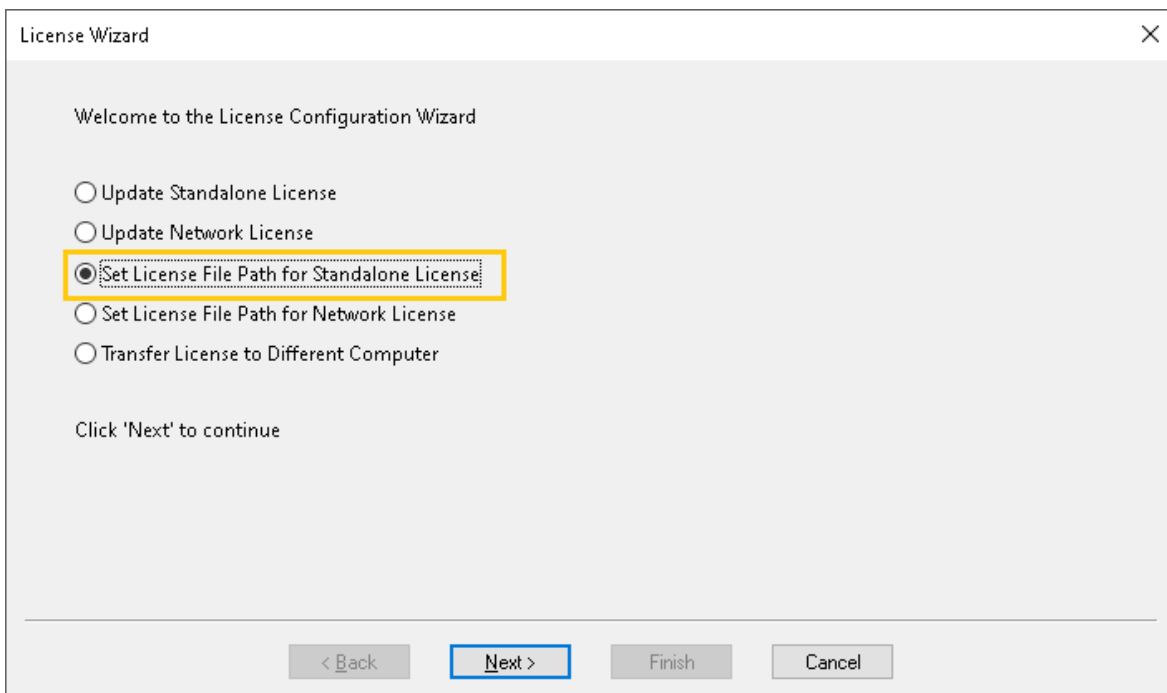
Figure 27. Set License File Path for Standalone License radio button

Though the location of the license file can be changed by using the Set License File Path for Standalone License option, the license file must reside in a folder for which the user has full permissions (read, write, execute). This scope of folder permissions is necessary so that the license file can be manipulated as necessary during operation of the GeoStat software.

To make use of the option for customizing the license file location, select the Set License File Path for Standalone License radio button (as indicated above in Fig. 27). Then, click the "Next" button (Fig. 28). This action will, in turn, launch the "Set License File Path - Standalone" page

(Fig. 29). Then, click the "Browse" button to specify the desired location of the license file (Fig. 30).
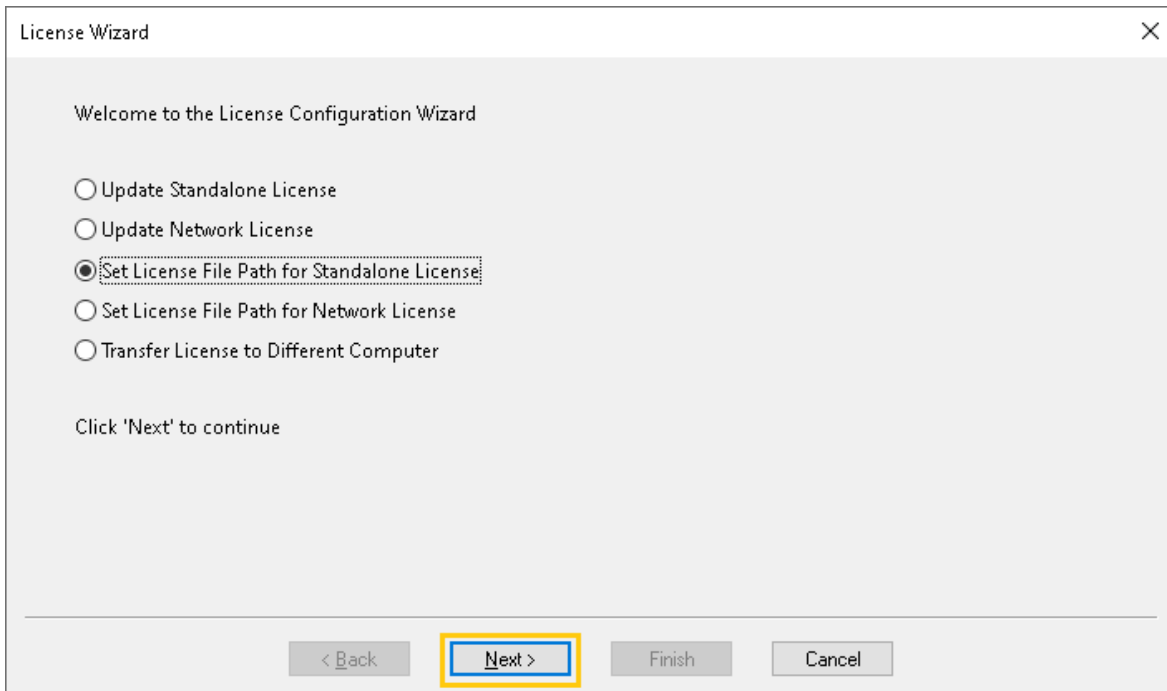
Figure 28. Next button to Set License File Path for Standalone License
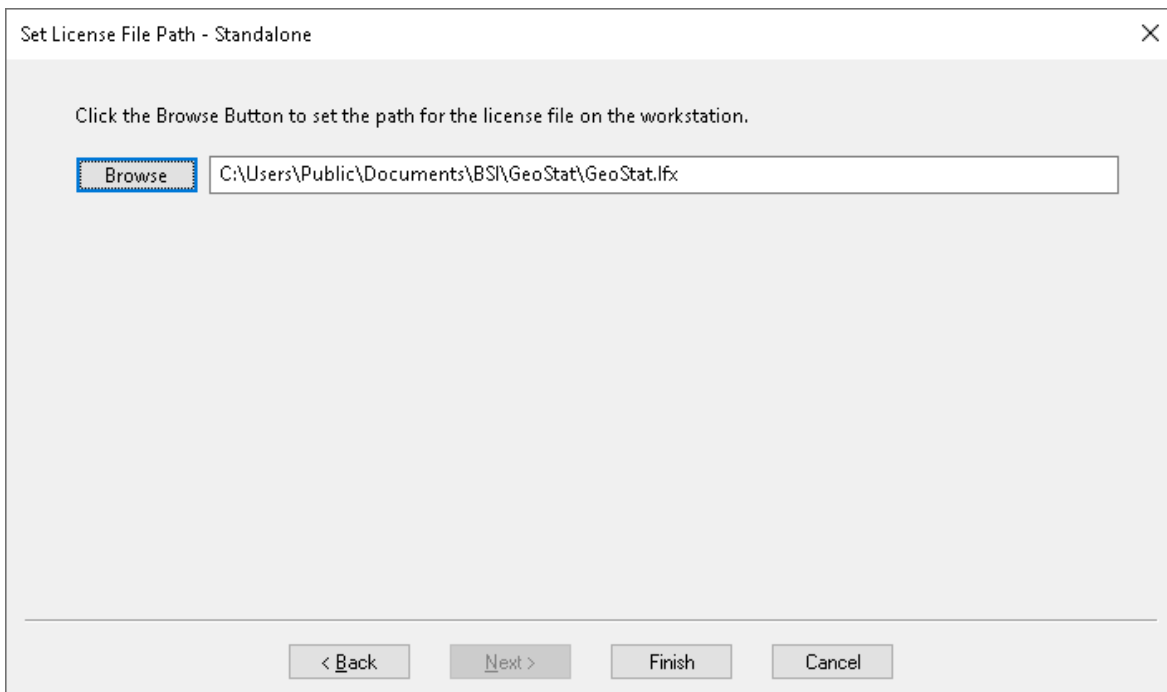
Figure 29. Set License File Path - Standalone page
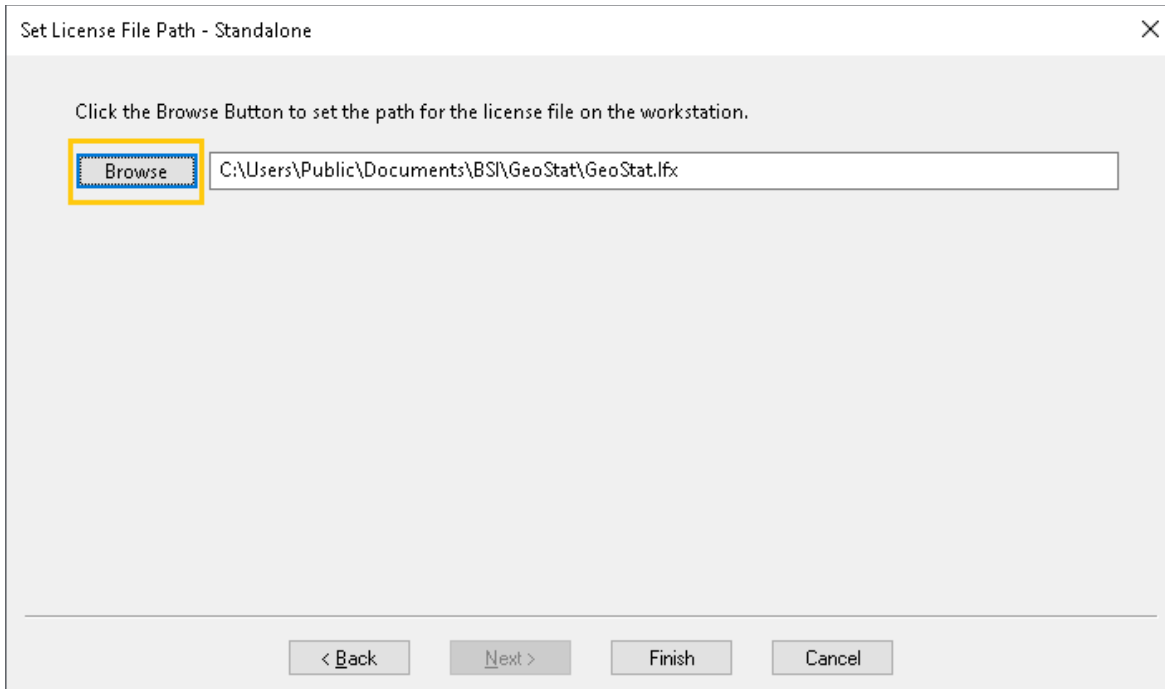
Figure 30. Browse button on Set License File Path - Standalone page

The path to the license file must include, and end with, the name of the license file itself (GeoStat.lfx). As an example of the full (filename included) path: "C:\PathToLicenseFile\GeoStat.lfx". After the path has been specified, click the "Finish" button. The GeoStat program will automatically close. Upon reopening the program, the updated license file path will be used.

2.2.4 Setting the License File Path for a Network License

The Set License File Path for Network License option is used to specify the location of the GeoStat license file on a network server serving a Local Area Network. The license file (GeoStat.lfx) by default is positioned on the local machine, not on a network server. In particular, the default location is in the "Users" public directory with the following full path: "C:\Users\Public\Documents\BSI\GeoStat".

When changing the default path to a desired location on a network server, please note that the license file must reside in a folder for which the user has full permissions (read, write, edit). In this way, the license file can be manipulated as necessary during execution of the GeoStat program. To use this option, select the Set License File Path for Network License radio button (Fig. 31). Then click the "Next" button (Fig. 32). This action launches the "Set License File Path - Network" page (Fig. 33). Then, click the "Browse" button to specify the desired location of the license file.

The specified path must end with the name of the license file (GeoStat.lfx), for example: "\\serverName\BSI\GeoStat\GeoStat.lfx". Note also that adherence to the universal naming convention (UNC) is required in specifying the server name (Fig. 34).
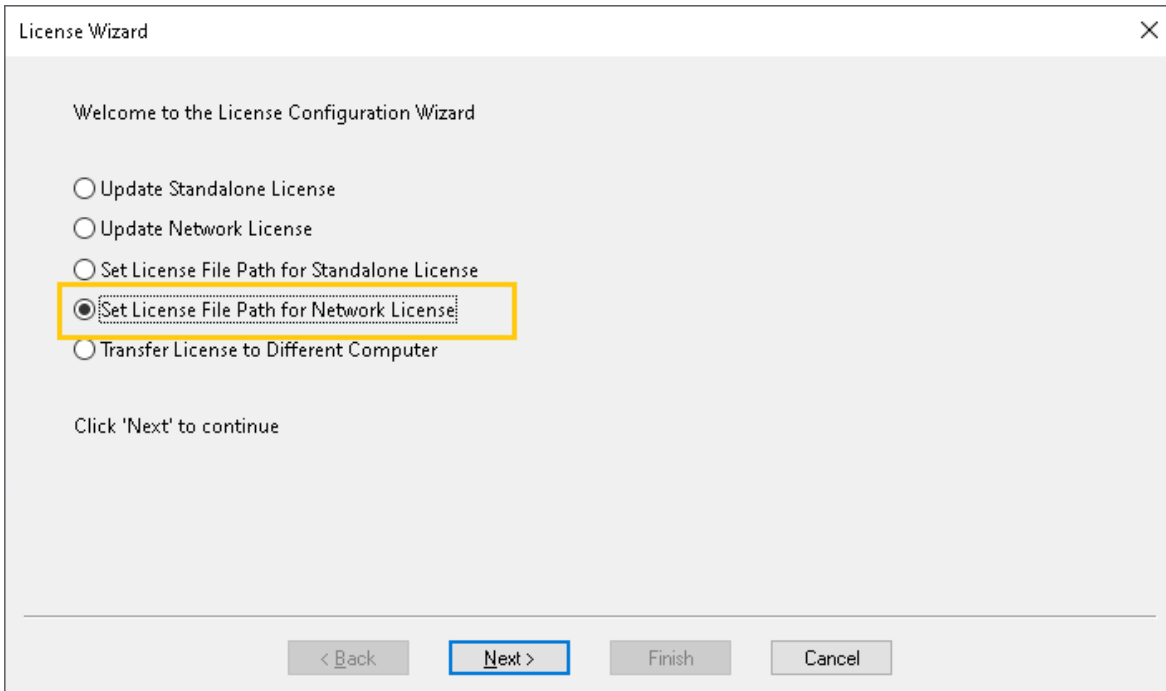
Figure 31. Set License File Path for Network License radio button
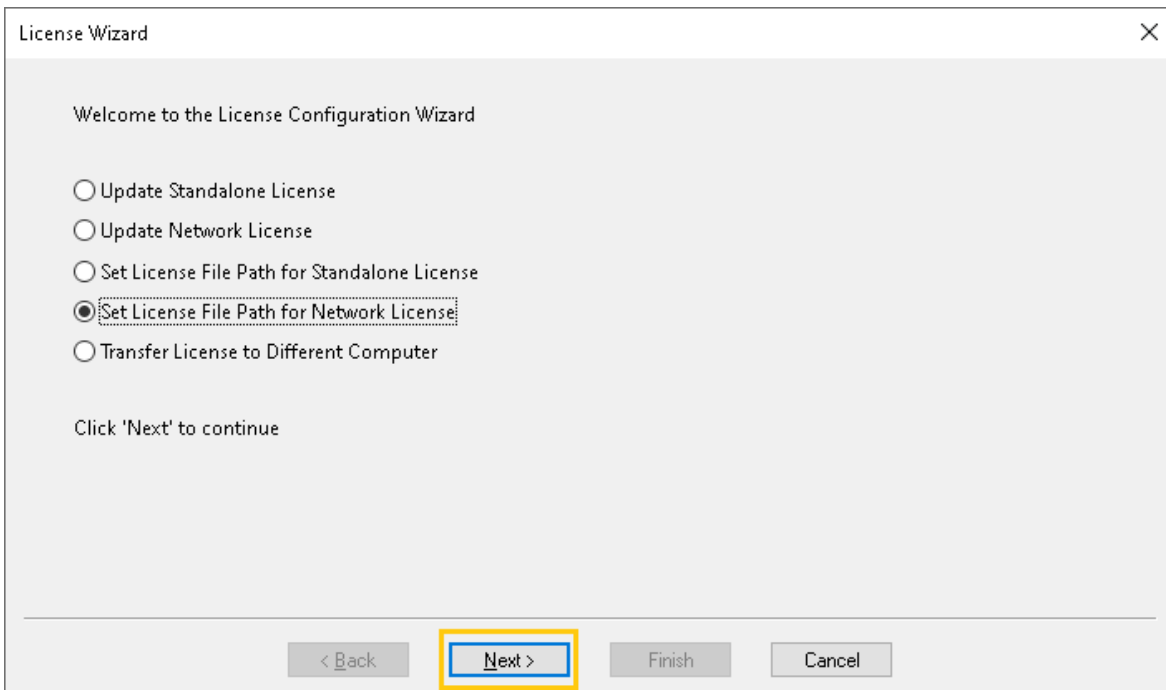
Figure 32. Next button to Set License File Path for Network License
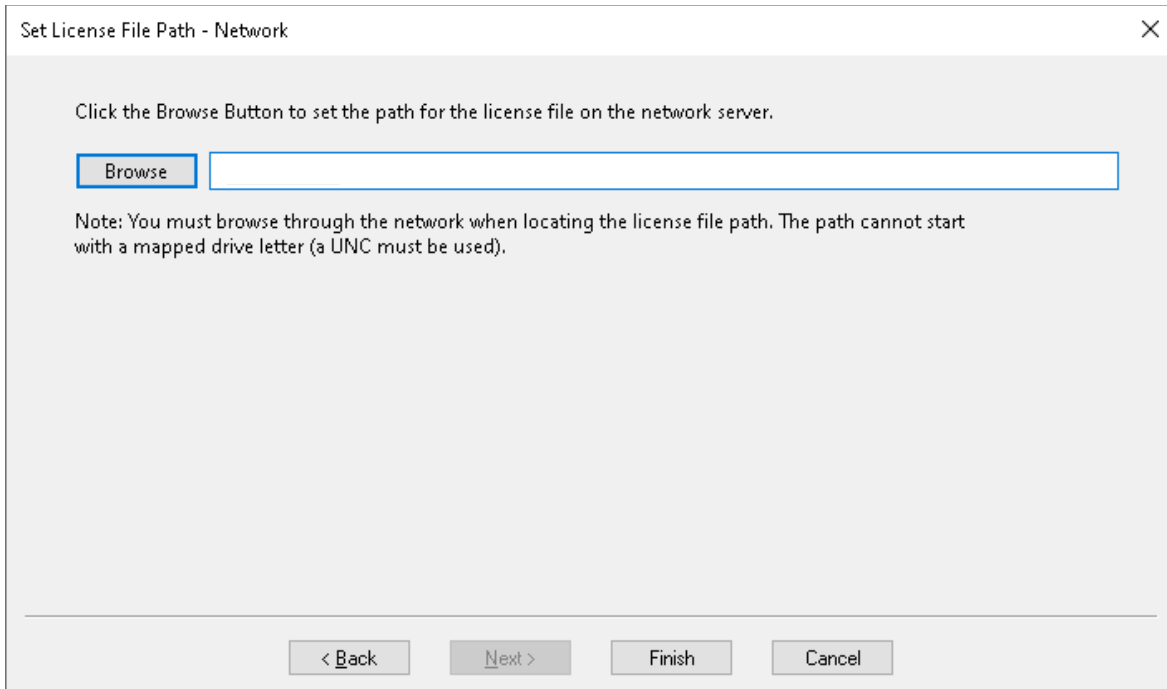
Figure 33. Set License File Path - Network page
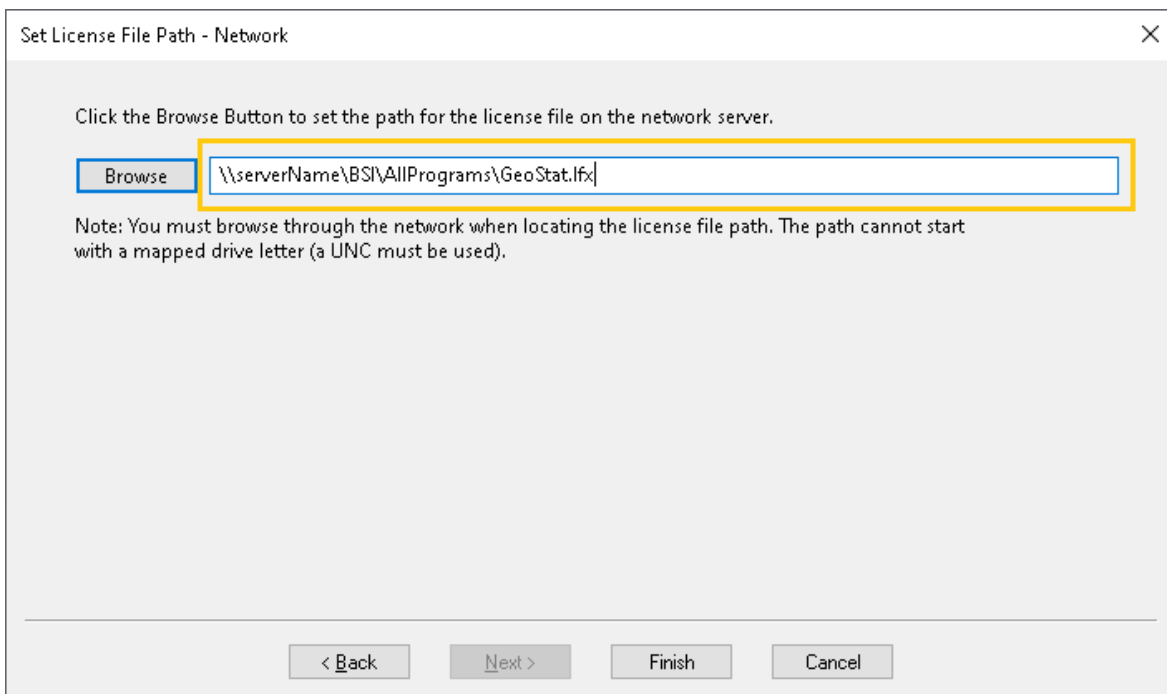
Figure 34. Example of License File path text box using UNC for server name

After the path has been specified, click the "Finish" button (Fig. 35). The GeoStat program will automatically close. Upon reopening the program, the updated license file path will be used.

Using the Set License File Path for Network License option sets the network path to the license file for the workstation from which this type of license action was performed. So as to use the license file's new position for all workstations on the LAN, each workstation on the network must repeat this process of using the "Set License File Path – Network" option from the GeoStat license wizard (recall Fig. 31).
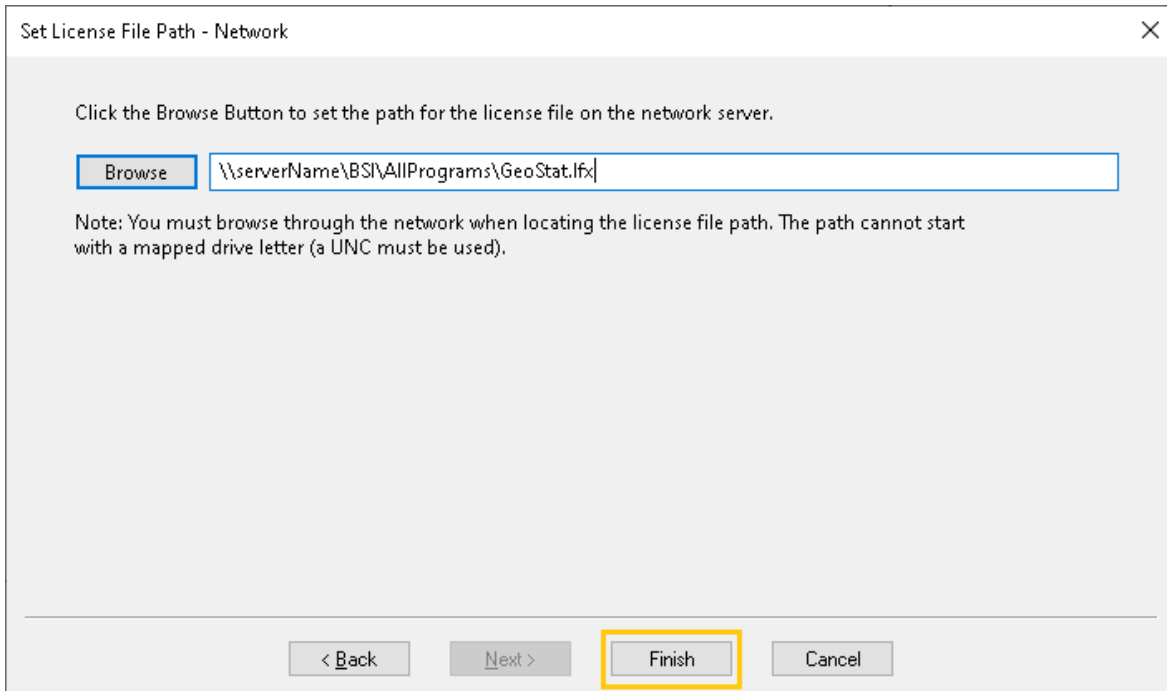
Figure 35. Finish button on Set License File Path - Network page

2.2.5 Transfer a License to a Different Computer

The Transfer License to Different Computer option (Fig. 36) is used to facilitate changing the system on which the GeoStat software is used. License transfers can be performed to change which workstation or which network server hosts the license file. To use this option, select the Transfer License to Different Computer radio button (Fig. 36), and then click the "Next" button (Fig. 37). The License Transfer page will then appear (Fig. 38).

Next, check the "Check to remove the license from the computer" checkbox (Fig. 39). This action will cause the Verification Code for Session page to display (Fig. 40). At this juncture, contact with BSI must be made to continue with the license transfer. Email the Verification Code for Session to bsi@ce.ufl.edu.

BSI will respond with an approval for the license transfer. Then click the "Finish" button (Fig. 41). The GeoStat program will automatically close. Upon reopening the program (from the same workstation in a Standalone license configuration, or any workstation using a network license that has been transferred), program access will not be granted by design. To once

24

again achieve program access, BSI will need to be contacted to perform a license update on the machine to which the licensing is to transfer.
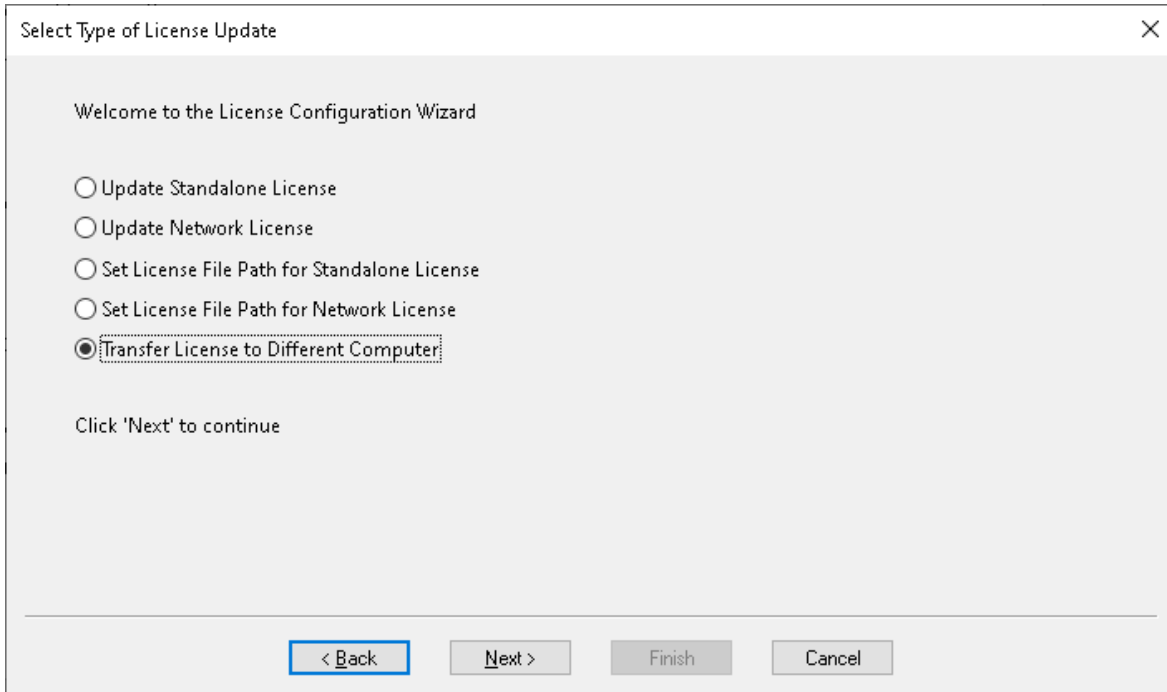
Figure 36. Transfer License to Different Computer radio button
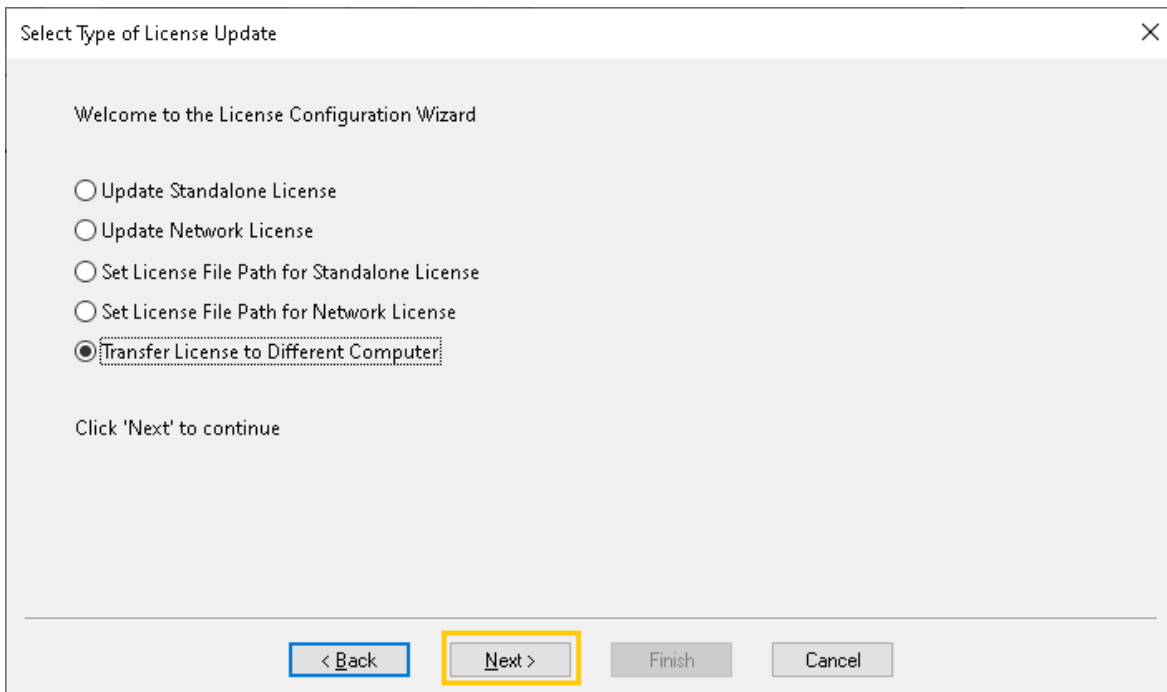
Figure 37. Next button to transfer the license to a different computer
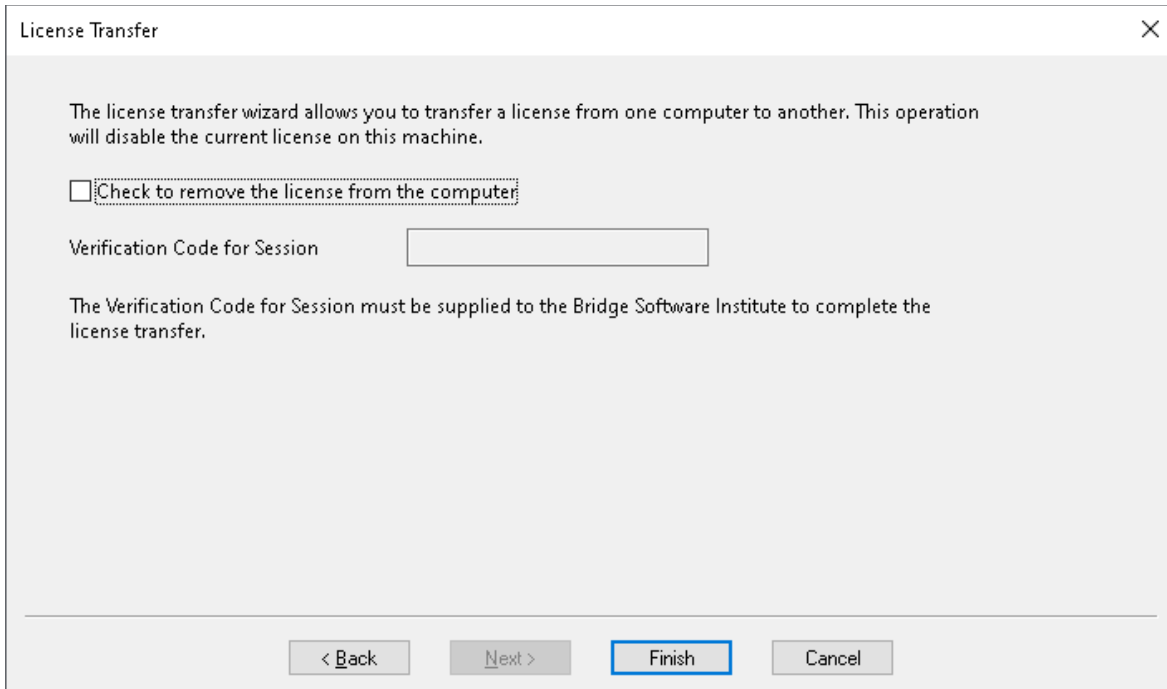
Figure 38. Transfer License to Different Computer page
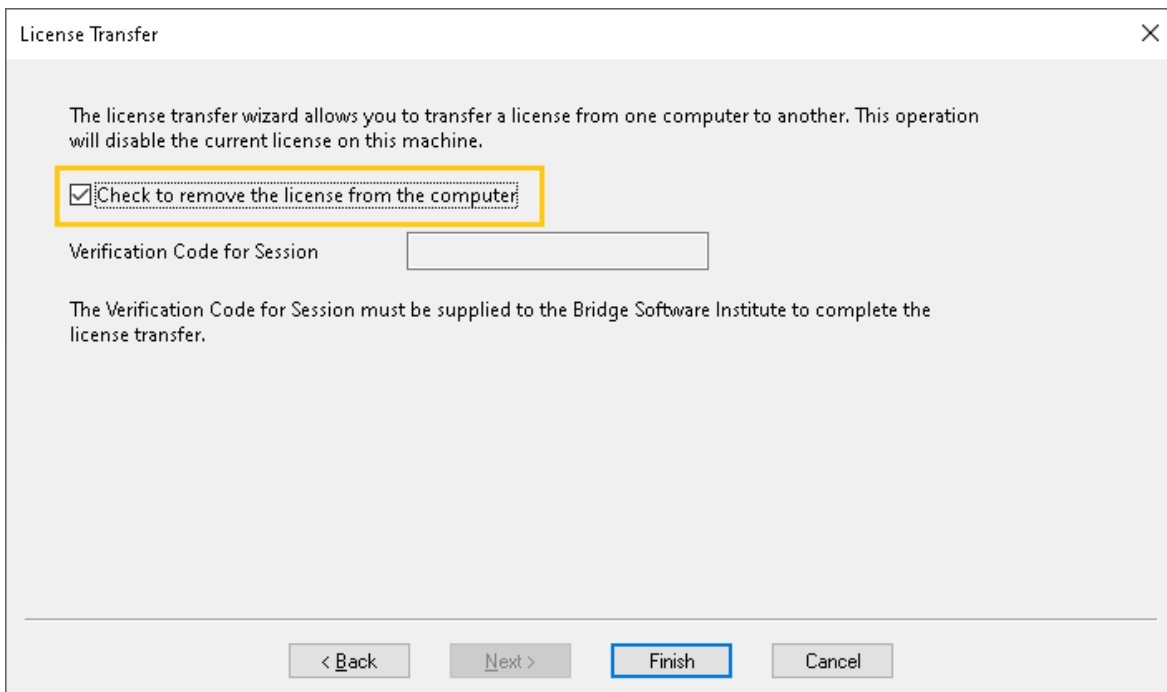
Figure 39. Check to remove the license from the computer checkbox
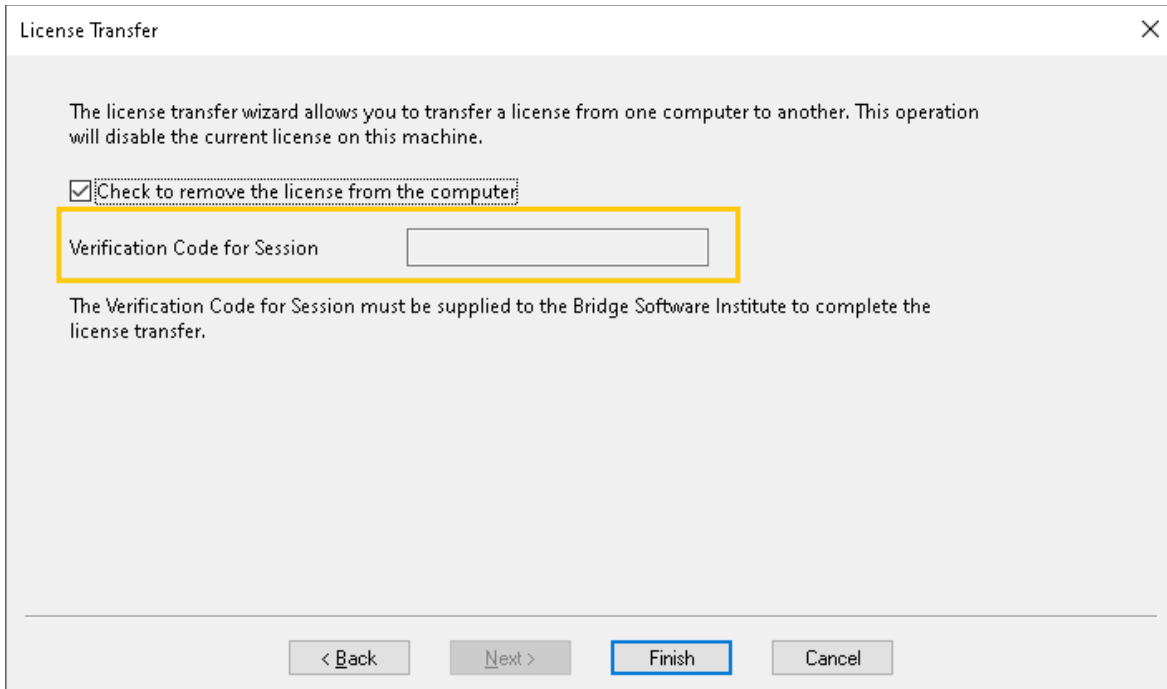
Figure 40. Verification Code for Session on License Transfer page
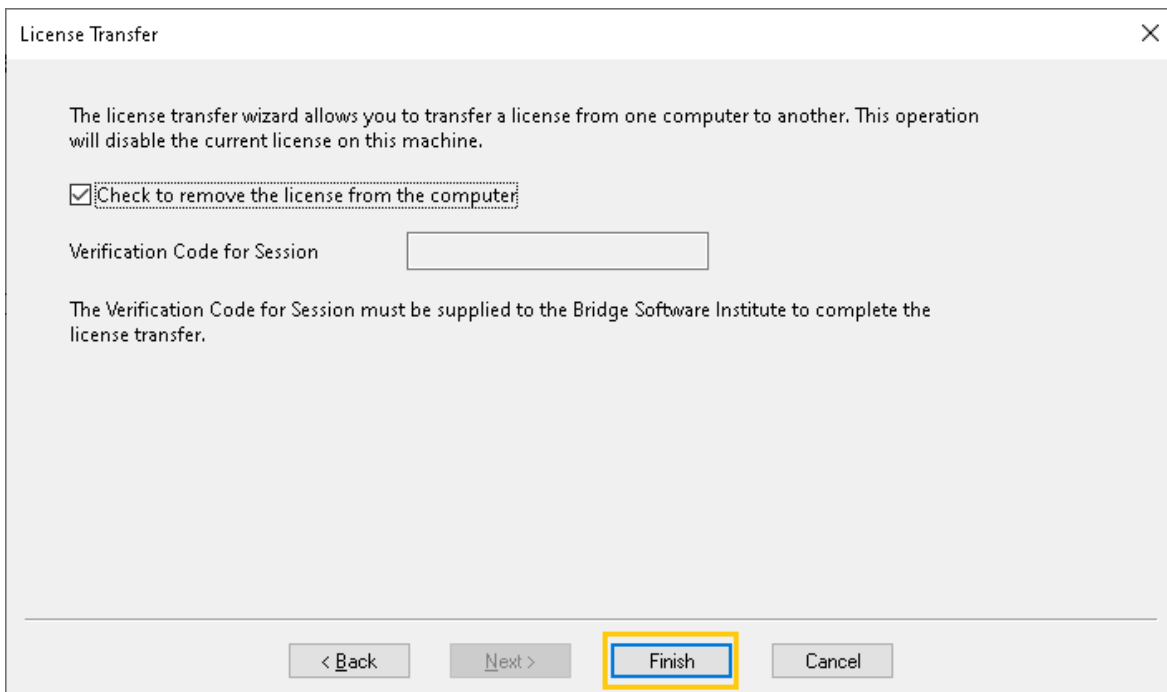
Figure 41. Finish Button on License Transfer page

CHAPTER 3
INPUT FILE FORMAT

3.1 Overview

Regarding GeoStat input file formatting, two overarching categories of data are recognized: (1) Parameters necessary to define the of-interest deep foundation member configuration and conditions (pile or shaft; cross-section and length; soil or rock zones; soil or rock layering; spatial correlation structure; and, empirical method for calculating resistance); and, (2) Geotechnical investigation data acquired for a given site. Documentation pertaining to these two data categories is provided in Sec. 3.2 and Sec. 3.3, respectively.

Given the considerable amount of data typically associated with geotechnical investigations of bridge sites (e.g., blow counts, unit weights, coring data) and, further, the additional inputs required to define the foundation member configuration and conditions, Microsoft® Excel is utilized for housing the contents of GeoStat input files. The standardized input file format is in the form of a non-programmed Excel worksheet, which signifies that no Visual Basic for Applications (VBA) or embedded formulas are present across the entire input deck. This approach allows for convenient tabulation of (potentially) large data sets, but also (due to being "non-programmed") ensures that uniformity is upheld in practice, with respect to the standard input file format. In addition, the input file format adopted here adheres to a 1:1 mapping between a given tab within the GeoStat UI (see Ch. 4) and a dedicated Excel worksheet tab in the input file itself. Purely illustrative sets of input data are utilized throughout Ch. 3 solely to aid in documentation of the standard input formatting.

3.2 Input Format for Data Pertaining to Member Configuration and Conditions

Documented in Sec. 3.2 is the input file formatting for those parameters that are necessary to define the of-interest deep foundation member configuration and conditions (including member type and section, layering, zones, geostatistics parameters, and method error parameters). Documentation of input file formatting is subdivided into the corresponding UI tab (where UI controls found on each tab are detailed in Ch. 4).

3.2.1 Project Information Tab

A template of the Excel input file format pertaining to the "Project Information" tab is shown in Fig. 42, where illustrative input values are supplied. Note that this Excel worksheet tab must be named "1. Project Information". In the event that the model file input data are being supplied directly from within Excel (as opposed to from within the UI), data contained within the "1. Project Information" worksheet tab must be populated prior to loading the input file in GeoStat.

There are three distinct regions of tab-specific input data in Fig. 42, and the Excel input data contained within each region of the worksheet tab are subdivided into: (1) Program Data; (2) Project Data; and, (3) Geotechnical Investigation Site Data Locations. Listings of the template input file content within the "1. Project Information" worksheet tab, and how the various inputs are organized, are presented in Sec. 3.2.1.1 through Sec. 3.2.1.3.

	A	B	C	D	E
1	This tab must be populated with data prior to loading GeoStat.				
2					
3	Program Data	Input Options	Units	Value	
4	Version				
5	Time				
6	Date				
7	Random Seed			1	
8					
9	Project Item	Input Options	Units	Value	
10	Project Number				
11	Project Name				
12	Engineer				
13	Unit System	[English | SI]	ft | m	English	
14	Foundation Type	[Drilled | Driven]		Drilled	
15					
16	Boring Name	Easting	Northing	Ground Surface Elevation	Include
17					[1 | 0]
18		ft | m	ft | m	ft | m	
19	1	39.69572565	29.68719491	0	1
20	2	23.51011394	41.72421117	0	1
21	3	10.85878194	1.862512196	0	1
22	4	23.30608022	25.0954102	0	1
23	5	20.22832195	34.07028903	0	1
24	6	46.3900801	12.67391202	0	1
25	7	34.84509306	40.30333808	0	1
26	8	11.4851696	17.56046431	0	1
27	9	35.5552953	9.414533586	0	1
28	10	44.83948954	44.2006293	0	1
29	11	34.22587081	32.62235497	0	1
30	12	6.317031341	39.57006516	0	1
31	13	7.120414135	3.885231141	0	1
32	14	39.77515924	34.46696213	0	1
33	15	1.465124715	7.199877994	0	1
34	16	35.28721863	27.82690599	0	1
35	17	11.7349542	14.99744533	0	1
36	18	48.25595703	28.32406735	0	1
37	19	5.683502345	7.931451435	0	1
38	20	21.04854635	1.404033452	0	1

Figure 42. "1. Project Information" worksheet tab with illustrative data set (only the first 20 out of 50 total boring locations are displayed)

3.2.1.1 Program Data

Occupying cells A3 through D7 of the "1. Project Information" worksheet tab (Fig. 42) is the Program Data input. As listed in Table 1, the "Program Data" inputs consist of general

29

information about the program version and a fundamental program setting. Namely, the program version is housed here, along with the time and date of the most recent file save operation. In addition, the program setting (the random seed) is included among this input group, where the random seed dictates the sequence of pseudo-random numbers that are generated as part of geostatistical calculations. Reproducibility of program results is ensured by including a record of the random seed value among the file input set. Note that input values only need to be supplied within the "Value" column for this subset of input data.

Table 1. "Program Data" input from within the "1. Project Information" worksheet tab

Program Data	Input Options	Units	Value
Version			
Time			
Date			
Random Seed			1

3.2.1.2 Project Data

Cells A9 through D14 of the "1. Project Information" worksheet tab (Fig. 42) are reserved for the "Project Data" input. This subset of input data, listed in Table 2, allows for retention of records such as the project number, project name, and the engineer developing the GeoStat model. Note that, again, input values only need to be supplied within the "Value" column for this subset of input data. Also included among the inputs here are the "Unit System" and "Foundation Type". For these latter two inputs, valid input is constrained to those options given within the "Input Options" column. For example, the input supplied under the "Value" column for "Unit System" must be one of "English" or "SI". Likewise, either "Drilled" (for drilled shaft) or "Driven" (for driven pile) must be specified for the "Foundation Type".

Table 2. "Project Data" input from within the "1. Project Information" worksheet tab

Project Item	Input Options	Units	Value
Project Number			
Project Name			
Engineer			
Unit System	[English | SI]	ft | m	English
Foundation Type	[Drilled | Driven]		Drilled

3.2.1.3 Geotechnical Investigation Site Data Locations

Beginning in row 16 of the "1. Project Information" worksheet tab (Fig. 42) is GeoStat input on basic information of locations at which geotechnical investigation data have been gathered throughout the site. For each boring (and/or coring) to be housed within the

GeoStat input file, one row of data should be populated within this region of the "1. Project Information" worksheet tab; additionally, one Excel worksheet tab must be created for each populated data row. As an illustration, fifty boring locations are listed in Table 3, and therefore, fifty additional worksheet tabs should be included in the Excel input file, where the fifty worksheet tabs are named "1", "2", "3", ... , "50". Data stored within the rows of Table 3 include the Boring Name, Northing, Easting, and Ground Surface Elevation, where units of "ft" or "m" should be used in a consistent manner.

Also, in Column E, is an option ("1" or "0") to "Include" the boring in the specific GeoStat analysis; entering "1" means that the boring will be included and entering "0" means that the boring will not be included in the GeoStat analysis. This option is provided so that all of the geotechnical investigation data for a site can be housed within a single Excel file. In addition, this option allows the engineer to make use of all the data for the site when calculating axial resistance for a pile or shaft located within a specific zone within the site. For instance, the engineer may wish to separate the site into multiple zones (e.g., land versus navigable waterway) with separate layering, correlation, and LRFD resistance assessment.

Table 3. "Geotechnical Investigation Site Data Locations" input from within the "1. Project Information" worksheet tab (20 of 50 total boring locations are displayed)

Boring Name	Easting	Northing	Ground Surface Elevation	Include
				[1 | 0]
	ft | m	ft | m	ft | m	
1	39.69572565	29.68719491	0	1
2	23.51011394	41.72421117	0	1
3	10.85878194	1.862512196	0	1
4	23.30608022	25.0954102	0	1
5	20.22832195	34.07028903	0	1
6	46.3900801	12.67391202	0	1
7	34.84509306	40.30333808	0	1
8	11.4851696	17.56046431	0	1
9	35.5552953	9.414533586	0	1
10	44.83948954	44.2006293	0	1
11	34.22587081	32.62235497	0	1
12	6.317031341	39.57006516	0	1
13	7.120414135	3.885231141	0	1
14	39.77515924	34.46696213	0	1
15	1.465124715	7.199877994	0	1
16	35.28721863	27.82690599	0	1
17	11.7349542	14.99744533	0	1
18	48.25595703	28.32406735	0	1
19	5.683502345	7.931451435	0	1
20	21.04854635	1.404033452	0	1

3.2.2 Profile Tab

A template of the Excel input file format pertaining to the "Profile" tab is shown in Fig. 43, where illustrative input values are supplied. Note that this Excel worksheet tab must be named "2. Profile". Also, as indicated in cell A1 of the template worksheet tab, data may be input directly from within the Excel worksheet or through the GeoStat UI.

The Excel input data contained within each region of the worksheet tab are subdivided into: (1) Hammer Correction Factor; and, (2) Layering. While input pertaining to "Hammer Correction Factor" always occupies the same range of cells in the worksheet tab, the number of rows making up the "Layering" data is model-specific. Listings of the template input file content within the "2. Profile" worksheet tab, and how the various inputs are organized, are presented in Sec. 3.2.2.1 through 3.2.2.2.

	A	B	C	D	E	F	G
1	Tabs 2. through 7. can be populated here or from within GeoStat.						
2							
3	Profile Variable	Input Options	Units	Value			
4	Hammer Correction Factor			1			
5							
6	Layer	Soil Type	Top Elevation	Bottom Elevation	Mean Unit Weight	Coefficient of Variation	Include
7		[1 | 2 | 3 | 4 | 5]					[1 | 0]
8			ft | m	ft | m	pcf | kN/m^3		
9	1	1	0	-105	110	0.7	1

Figure 43. Excel input file "2. Profile" worksheet tab

3.2.2.1 Hammer Correction Factor

Contained within cells A3 through D4 of the "2. Profile" worksheet tab (Fig. 43) is input pertaining to the "Hammer Correction Factor". This subset of input data is listed in Table 4 and contains the adjustment to soil-profile layer data (e.g., SPT values) due to automatic versus safety hammers. The correction factor is unitless and is input within the "Value" column. When a value other than 1.0 is supplied for the "Hammer Correction Factor", then values of geotechnical investigation site data such as SPT-N values will be adjusted by the correction factor as statistical processes are carried out.

Table 4. "Hammer Correction Factor" input from within the "2. Profile" worksheet tab

Profile Variable	Input Options	Units	Value
Hammer correction factor			1

3.2.2.2 Layering

Beginning in row 6 of the "2. Profile" worksheet tab (Fig. 43) is GeoStat soil layer data. One row of data should be populated (generally, through use of the GeoStat UI) for each layer. Included in each row (Table 5) is the "Layer" number, along with "Top Elevation" and "Bottom Elevation" (in units of either ft or m). Also input for each row is the "Soil Type", where an

32

integer value between 1 and 5 must be supplied. The range of permissible input values corresponds to the mapping of soil types within the axial capacity software package, referred to as FB-Deep: 1 = Plastic clay; 2 = Clay and silty sand; 3 = Clean sand; 4 = Limestone, very shelly sand; and, 5 = Void.

Table 5. "Layering" input from within the "2. Profile" worksheet tab

Layer	Soil Type	Top Elevation	Bottom Elevation	Mean Unit Weight	Coefficient of Variation	Include
	[1 | 2 | 3 | 4 | 5]					[1 | 0]
		ft | m	ft | m	pcf | kN/m^3		
1	1	0	-105	110	0.7	1

Columns E and F of the "Layering" input (Fig. 43) pertain to the layer "Mean Unit Weight" and corresponding "Coefficient of Variation", where the former parameter is in units of either pcf or kN/m^3. Note that input of the mean, and COV values of unit weight (Table 5) are only required if the "Foundation Type" is input as "Drilled" on the "1. Project Information" worksheet tab (recall Table 2). Stated alternatively, the "Mean Unit Weight" and "Coefficient of Variation" input parameters are not required for analysis of driven piles in GeoStat. Also, in Column G, is an option ("1" or "0") to "Include" the layer in the specific GeoStat analysis; entering "1" means that the layer will be included and entering "0" means that the layer will not be included in either the GeoStat analysis for determining spatial correlation structures, or in the model analysis files (with FB-Deep formatting) for calculating axial capacities.

3.2.3 Geostatistics Tab

A template of the Excel input file format pertaining to the "Geostatistics" tab in GeoStat is shown in Fig. 44 (columns A through D), Fig. 45 (columns E through L), and Fig. 46 (columns M through T), along with illustrative input values. Note that this Excel worksheet tab must be named "3. Geostatistics". Also, as indicated in cell A1 of the template worksheet tab, data contained within the "3. Geostatistics" worksheet tab can be directly input into the worksheet, or the data can be populated from within the GeoStat UI. Generally, input data for this worksheet tab should be populated through use of the GeoStat UI. Input data contained within the Excel worksheet tab are subdivided into: (1) Layer Detrending; (2) Horizontal Variograms; and, (3) Vertical Variograms. Template input file content within the "3. Geostatistics" worksheet tab, and how the various inputs are organized, are presented in Sec. 3.2.3.1 through Sec. 3.2.3.3.

	A	B	C	D
1	Tabs 2. through 7. can be populated here or from within GS-Deep.			
2				
3	Layer	Detrend	Detrend Polynomial Degree	Variogram
4		[Yes | No]	[1 | 2]	[Spherical | Exponential]
5				
6	1	No		Exponential

Figure 44. Excel input file "3. Geostatistics" worksheet tab, columns A through D

	E	F	G	H	I	J	K	L
1								
2								
3	Horizontal Lag	Number of Horizontal Lags	Horizontal Tolerance	Horizontal Bandwidth	Horizontal Range	Horizontal Nugget	Horizontal Sill	Horizontal Worst Case
4								[Yes | No]
5	ft | m		ft | m	ft | m				
6	1	20	0.5	0	10	0	1	No

Figure 45. Excel input file "3. Geostatistics" worksheet tab, columns E through L

	M	N	O	P	Q	R	S	T
1								
2								
3	Vertical Lag	Number of Vertical Lags	Vertical Tolerance	Vertical Bandwidth	Vertical Range	Vertical Nugget	Vertical Sill	Vertical Worst Case
4								[Yes | No]
5	ft | m		ft | m	ft | m				
6	1	20	0.5	0	5	0	1	No

Figure 46. Excel input file "3. Geostatistics" worksheet tab, columns M through T

3.2.3.1 Layer Detrending

Input data pertaining to detrending of soil layer properties begins in row 3, and occupies columns A through D, of the "3. Geostatistics" worksheet tab (Fig. 44). Consistent with layer data from the "2. Profile" worksheet tab (recall Fig. 43), one row of data should be populated (Fig. 44) for each defined layer. Note that, generally, this subset of input data is populated through use of the GeoStat UI. Included in each row (Table 6) is the "Layer" number and an indicator ("Yes" or "No") of whether or not detrending is to be performed on the layer data. For any layers that are to be detrended, an integer value (1 or 2) of the polynomial degree to which detrending should be carried out must also be input. Otherwise, the corresponding cell within the "Detrend Polynomial Degree" column can remain blank. Input data located within column D, "Variogram", dictates the form of the mathematical fit to the variograms generated for each layer, which consist of "Spherical" and "Exponential".

34

Table 6. "Layer Detrending" input from within the "3. Geostatistics" worksheet tab

Layer	Detrend	Detrend Polynomial Degree	Variogram
	[Yes | No]	[1 | 2]	[Spherical | Exponential]
1	No		Exponential

3.2.3.2 Horizontal Variograms

Columns E through L of the "3. Geostatistics" worksheet tab (Fig. 45) are reserved for input of "Horizontal Variograms" data (one row per layer). See Sec. 4.5.3 and the program Technical Manual for definitions and additional details regarding these parameters. Note that this subset of input data is generally populated through use of the GeoStat UI, rather than from within the Excel worksheet. Included in each row (as listed in Table 7) is the "Horizontal Lag" distance (ft, m); "Number of Horizontal Lags"; "Horizontal Tolerance" (ft, m); and, "Horizontal Bandwidth" (ft, m). Additional inputs include (Table 8): "Horizontal Range"; "Horizontal Nugget"; "Horizontal Sill"; and, an indicator of whether or not ("Yes" or "No") the "Horizontal Worst Case" is to be considered for use when an acceptable horizontal variogram cannot be formed.

Table 7. "Horizontal Variograms" input from within the "3. Geostatistics" worksheet tab

Horizontal Lag	Number of Horizontal Lags	Horizontal Tolerance	Horizontal Bandwidth
ft | m		ft | m	ft | m
1	20	0.5	0

Table 8. Continued "Horizontal Variograms" input from within the "3. Geostatistics" tab

Horizontal Range	Horizontal Nugget	Horizontal Sill	Horizontal Worst Case
			[Yes | No]
10	0	1	No

3.2.3.3 Vertical Variograms

Columns M through T of the "3. Geostatistics" worksheet tab (Fig. 46) are reserved for input of "Vertical Variograms" data. See Sec. 4.5.3 and the program Technical Manual for additional details regarding these parameters. Note that one row of data is populated per soil layer. As with all other input data on the "3. Geostatistics" worksheet tab, the "Vertical Variograms" input parameters are intended to be populated through use of the GeoStat UI, rather than from within the Excel worksheet. For each layer (i.e., for each row), inputs listed in Table 9 must be supplied, including: "Vertical Lag" distance (ft, m); "Number of Vertical Lags"; "Vertical

Tolerance" (ft, m); and, "Vertical Bandwidth" (ft, m). Additional inputs (Table 10) include: "Vertical Range"; "Vertical Nugget"; "Vertical Sill"; and, an indicator of whether or not ("Yes" or "No) the "Vertical Worst Case" is to be considered for use when an acceptable vertical variogram cannot be formed.

Table 9. "Vertical Variograms" input from within the "3. Geostatistics" worksheet tab

Vertical Lag	Number of Vertical Lags	Vertical Tolerance	Vertical Bandwidth
ft | m		ft | m	ft | m
1	20	0.5	0

Table 10. Continued "Vertical Variograms" input from within the "3. Geostatistics" tab

Vertical Range	Vertical Nugget	Vertical Sill	Vertical Worst Case
			[Yes | No]
5	0	1	No

3.2.4 Simulation Tab

A template of the Excel A template of the Excel input file format pertaining to the "Simulation" tab in GeoStat is shown in Fig. 47, along with illustrative input values. Note that this Excel worksheet tab must be named "4. Simulation". As noted in cell A1 of the template worksheet tab, data contained within the "4. Simulation" worksheet tab may be input directly from within the Excel environment, or via the GeoStat UI. However, it is generally intended that this collection of parameters would be input from within the GeoStat UI.

The various inputs are organized into several data subsets in the "4. Simulation" worksheet tab: (1) Pile Geometry; (2) Shaft Geometry; (3) Shaft/Pile Length; (4) Shaft/Pile Material; (5) Soil; and, (6) Simulation. Listings of the template input file content within the "4. Simulation" worksheet tab, and how the various inputs are organized, are presented in Sec. 3.2.4.1 through 3.2.4.6. For all inputs contained within the "4. Simulation" worksheet tab, input values need only be supplied within column D, which is labeled as the "Value" column (Fig. 47).

3.2.4.1 Pile Geometry

Contained within cells A3 through D8 of the "4. Simulation" worksheet tab (Fig. 47) are inputs pertaining to "Pile Geometry". This subset of input data is listed in Table 11 and contains the "Width" (ft, m), "Section Type" ("Square" or "Round" or "Cylinder" or "Pipe" or "H-Section"), "Depth", "Thickness", and "Pile End Condition" of the pile. If the pile "Section" is input as "Round" or Square", then the pile diameter should be input for "Width". If the pile "Section" is input as "Cylinder" or "Pipe", then the pile diameter should be input for "Width", the wall

thickness input for "Thickness", and the pile end condition input for "Pile End Condition" (0 signifies open, 1 signifies closed). If the pile "Section" is input as "H-Section", then the pile width should be input for "Width" and the pile depth should be input for "Depth.

Input data is only required in cells A3 through D8 if the "Foundation Type" parameter is input as "Driven" (i.e., driven pile) on the "1. Project Information" worksheet tab (Fig. 42). Recalling the "1. Project Information" worksheet tab (Fig. 42), and the illustrative data set, the "Foundation Type" is input as "Driven" (i.e., driven pile). Consequently, input pertaining to "Pile Geometry" is required in this instance.

	A	B	C	D
1	Tabs 2. through 7. can be populated here or from within GeoStat.			
2				
3	Pile Geometry	Input Options	Units	Value
4	Width		in | mm	0
5	Section	[Square | Round | Cylinder | Pipe | H-Section]		Square
6	Depth		in | mm	0
7	Thickness		in | mm	0
8	Pile End Condition	[0 | 1]		0
9				
10	Shaft Geometry	Input Options	Units	Value
11	Diameter		in | mm	48
12	Casing Length		ft | m	0
13	Bell Length		ft | m	0
14	Bell Diameter		in | mm	0
15				
16	Shaft/Pile Length	Input Options	Units	Value
17	Minimum Length		ft | m	52
18	Maximum Length		ft | m	80
19	Length Increment		ft | m	1
20				
21	Shaft/Pile Material	Input Options	Units	Value
22	Unit Weight		pcf | kN/m^3	150
23	Elastic Modulus		ksi | MPa	4000
24	Slump		in | mm	6
25	Limiting Settlement		%	3
26				
27	Soil	Input Options	Units	Value
28	Water Elevation		ft | m	0
29	Reserved	[Yes | No]		
30				
31	Simulation Settings	Input Options	Units	Value
32	Number of Simulations			1500
33	Conditional	[Yes | No]		No
34	Nearest Boring			B4
35	Northing		ft | m	24
36	Easting		ft | m	9.37
37	Layer Separation	[1 | 2 | 5]		5
38	Unit Weight		pcf | kN/m^3	0
39	SPT-N		blows/ft | blows/300mm	0
40	Cu		tsf | kPa	0

Figure 47. Excel input file "4. Simulation" worksheet tab

Table 11. "Pile Geometry" input from within the "4. Simulation" worksheet tab

Pile Geometry	Input Options	Units	Value
Width		in | mm	24
Section	[Square | Round | Cylinder | Pipe | H-Section]		Square
Depth		in | mm	0
Thickness		in | mm	0
Pile End Condition	[0 | 1]		0

3.2.4.2 Shaft Geometry

Contained within cells A10 through D14 of the "4. Simulation" worksheet tab (Fig. 47) are inputs specific to "Shaft Geometry". This input data (Table 12) includes shaft "Diameter" (ft, m); "Casing Length" (ft, m); "Bell Length" (ft, m); and, "Bell Diameter" (ft, m). Note that if attributes such as casing or bell are not present, then the corresponding entries in the worksheet tab can be supplied as "0" or left blank. For the illustrative data set, a driven pile is modeled, and so, no input is required for "Shaft Geometry".

Table 12. "Shaft Geometry" input from within the "4. Simulation" worksheet tab

Shaft Geometry	Input Options	Units	Value
Diameter		in | mm	48
Casing Length		ft | m	0
Bell Length		ft | m	0
Bell Diameter		in | mm	0

3.2.4.3 Shaft/Pile Length

Contained within cells A16 through D19 of the "4. Simulation" worksheet tab (Fig. 47) are inputs specific to "Shaft/Pile Length". The length-related input data (Table 13) includes "Minimum Length" (ft, m); "Maximum Length" (ft, m); and, "Length Increment" (ft, m). The latter input parameter, "Length Increment" allows for several trial embedment lengths to be analyzed between the "Minimum Length" considered and "Maximum Length" considered. "Shaft/Pile Length" data must be input regardless of the foundation type being modeled.

Table 13. "Shaft/Pile Length" input from within the "4. Simulation" worksheet tab

Shaft/Pile Length	Input Options	Units	Value
Minimum Length		ft | m	52
Maximum Length		ft | m	80
Length Increment		ft | m	1

3.2.4.4 Shaft/Pile Material

Contained within cells A21 through D25 of the "4. Simulation" worksheet tab (Fig. 47) are inputs specific to "Shaft/Pile Material". The corresponding inputs (Table 14) include "Elastic Modulus" (ksi, kPa); "Slump" (in, mm); "Limiting Settlement" (%); and, "Unit Weight" (pcf, kN/m^3). While input values must always be supplied for "Unit Weight", the "Slump" and "Elastic Modulus" parameters must only be supplied when modeling drilled shafts (and can remain blank otherwise). Further, regarding the "Limiting Settlement" input, which is technically a limiting parameter concerning member-level response to loading, will be defaulted during analysis of drilled shafts to 5% if input as "0" or left blank.

Table 14. "Shaft/Pile Material" input from within the "4. Simulation" worksheet tab

Shaft/Pile Material	Input Options	Units	Value
Unit Weight		pcf | kN/m^3	150
Elastic Modulus		ksi | MPa	4000
Slump		in | mm	6
Limiting Settlement		%	3

3.2.4.5 Soil

Contained within cells A27 through D29 of the "4. Simulation" worksheet tab (Fig. 47) are general inputs concerning the "Soil" at the location in which the pile (or shaft) is being installed. The corresponding input (Table 15) is "Water Elevation" (ft, m).

Table 15. "Soil" input from within the "4. Simulation" worksheet tab

Soil	Input Options	Units	Value
Water Elevation		ft | m	0
Reserved			

3.2.4.6 Simulation Settings

Contained within cells A31 through D40 of the "4. Simulation" worksheet tab (Fig. 47) are "Simulation Settings" inputs, which are also listed in Table 16. The integer-valued input "Number of Simulations" dictates the number of realizations to generate (i.e., number of unique FB-Deep models to create) for computing descriptive statistics (e.g., mean, variance) of the pile (or shaft) soil resistance. The sample size (number of realizations) can be "Conditional" (if input as "Yes") upon the nearest boring, or unconditional (if "No" is input). If "Yes" is input for the "Conditional" option, then a value must also be supplied for the "Nearest Boring". Note that the input under the "Value" column for the "Nearest Boring" must exactly match one of the input values beneath the "Boring Name" column from the "1. Project Information" worksheet tab (recall Fig. 42). For instances when the "Conditional" option is set to "Yes", then the "Northing" (ft, m) and "Easting" (ft, m) of the foundation must also be

supplied. Otherwise, if the "Conditional" option is input as "No", then the "Nearest Boring", "Northing", and "Easting" values may be left blank.

Table 16. "Simulation Settings" input from within the "4. Simulation" worksheet tab

Simulation Settings		Units	Value
Number of Simulations			1500
Conditional	[Yes | No]		No
Nearest Boring			
Northing		ft | m	
Easting		ft | m	
Layer Separation	[1 | 2 | 5]		5
Unit Weight		pcf | kN/m^3	0
SPT-N		blows/ft | blows/300 mm	0
Cu		tsf | kPa	0

In the event that a layered soil profile is modeled, then there may be layers of the same soil type positioned directly atop (or below) one another. To ensure treatment of the two layers as separate entities, a fictitious (thin) soil layer (i.e., a "Layer Separation") can be inserted between the two real layers. As listed in Table 16, the "Layer Separation" can specified in the convention of soil types established in the axial capacity software, FB-Deep, where 1 signifies plastic clay; 2 signifies clay and silty sand; and, 5 signifies a void. The default value for this input parameter, if left blank, is 5 (void). If "Layer Separation" is input as 1 (plastic clay), then a value of undrained shear strength, "Cu" (tsf, kPa), must also be supplied. Similarly, if "Layer Separation" is input as 2 (clay and silty sand), then an uncorrected blow count value, "SPT-N" (blows/ft, blows/300 mm), must additionally be provided.

3.2.5 Spatial Variability Tab

A template of the Excel input file format pertaining to the "Spatial Variability" tab is shown in Fig. 48, along with illustrative input values. Note that this Excel worksheet tab must be named "5. Spatial Variability". Also, as indicated in cell A1 of the template worksheet tab, data contained within the "5. Spatial Variability" worksheet tab can be directly input into the worksheet, or the data can be populated from within the GeoStat UI. Generally, input data for this worksheet tab should be populated through use of the GeoStat UI. Template input file content within the "5. Spatial Variability" worksheet tab, and how the various inputs are organized, are presented in Sec. 3.2.5.1.

	A	B	C
1	**Tabs 2. through 7. can be populated here or from within GeoStat.**		
2			
3	**Display Side Data**	**Display Tip Data**	**Display Total Data**
4	[Yes | No]	[Yes | No]	[Yes | No]
5			
6	Yes	Yes	Yes

Figure 48. Excel input file "5. Spatial Variability" worksheet tab

3.2.5.1 Plot Display Settings

Contained within cells A3 through C6 of the "5. Spatial Variability" worksheet tab (Fig. 48) are plot settings for display of computed axial capacity data, which in turn, reflect spatial variability phenomena associated with the foundation being analyzed. The plot settings (Table 17) include "Display Side Data", "Display Tip Data", and "Display Total Data", where input options consist of "Yes" or "No" for each plot setting. The three plot settings, respectively, signify whether or not to display the progressions of side resistance, tip resistance, and total resistance as a function of embedment length.

Table 17. "Plot Display Settings" input from within the "5. Spatial Variability" worksheet tab

Display Side Data	Display Tip Data	Display Total Data
[Yes | No]	[Yes | No]	[Yes | No]
Yes	Yes	Yes

3.2.6 Method Error Tab

A template of the Excel input file format pertaining to the "Method Error" tab is shown in Fig. 49, along with illustrative input values. Note that this Excel worksheet tab must be named "6. Method Error". Also, as indicated in cell A1 of the template worksheet tab, data contained within the "6. Method Error" worksheet tab can be directly input into the worksheet, or the data can be populated from within the GeoStat UI. Generally, input data for this worksheet tab should be populated through use of the GeoStat UI. For GeoStat models associated with drilled shafts, two regions of input data are located within the "6. Method Error" worksheet tab. These regions pertain to method error parameter input for: (1) "Drilled Shaft" foundations; and, (2) "Limestone" layers. For driven pile foundations, a unique input region can also be found in the "6. Method Error" worksheet tab, and this tab-specific subset of input data is referred to as "Driven Pile" input. Listings of the template input file content within the "6. Method Error" worksheet tab, and how the various inputs are organized, are presented in Sec. 3.2.6.1 through Sec. 3.2.6.4

Figure 49. Excel input file "6. Method Error" worksheet tab.

3.2.6.1 Method Error Options

Contained within cells A3 through C6 of the "6. Method Error" worksheet tab (Fig. 49) are inputs specific to "Method Error Options". The input data (Table 18) pertains to the use of default or custom values for the method errors associated with "Driven Pile" foundations, "Drilled Shaft" Foundations, and layers used by the "Limestone Model". To use the default method error parameters in GeoStat, the input in column C must be "Default". To use custom method error parameters, the input in column C must be "Custom" and the desired parameters entered into the relevant method error section, described in Sec. 3.2.6.2 through Sec. 3.2.6.4.

Table 18. "Method Error Options" input from within the "6. Method Error" worksheet tab

Method Error Options	Input Options	Value
Driven Pile	[Default | Custom]	Default
Drilled Shaft	[Default | Custom]	Default
Limestone Model	[Default | Custom]	Default

3.2.6.2 Driven Pile

Contained within cells A8 through D11 of the "6. Method Error" worksheet tab (Fig. 49) is method error input data specific to driven pile foundations. As presented in McVay et al. 2012, method error parameters operate on "SPT" values, and include an "Intercept", "Slope", and

42

"Coefficient of Variation". Input values may be left blank or input as zero if the foundation type being considered is not that of driven piles (as listed in Table 19). However, if a driven pile foundation is being considered, then these values can be set to default values from within the GeoStat UI.

Table 19. "Driven Pile" input from within the "6. Method Error" worksheet tab

Driven Pile	Intercept	Slope	Coefficient of Variation
SPT	0	0	0

3.2.6.3 Drilled Shaft

Contained within cells A13 through D17 of the "6. Method Error" worksheet tab (Fig. 49) is method error input data specific to drilled shaft foundations. As presented in McVay et al. 2012, method error parameters operate on one (or both) of "Clay" layer data and/or "Sand" layer data. Inputs include an "Exponent for Exponential", "Exponent for Power", and "Coefficient of Variation". If a given soil type is not present among the layering being considered for a drilled shaft foundation, then the corresponding row-specific input values may be left blank or input as zero. For example, as listed in Table 20, if "Sand" layers are defined, but no "Clay" layers are defined, then zero-valued entries can be supplied in the corresponding data row, while non-zero values should be supplied for the method error parameters associated with computed resistances within the "Sand" layers. Note that, for driven pile foundations, this subset of input data (both for "Clay" and "Sand") can be input as zero-valued or can remain blank.

Table 20. "Drilled Shaft" input from within the "6. Method Error" worksheet tab

Drilled Shaft	Exponent for Exponential	Exponent for Power	Coefficient of Variation
Clay	0.66	0.98	0.68
Sand	0.66	0.98	0.68

3.2.6.4 Limestone Model

Contained within cells A19 through D23 of the "6. Method Error" worksheet tab (Fig. 49) is method error input data for when one or more layers of "Limestone" are defined in the soil layer profile of the GeoStat model. As presented in McVay et al. 2012, method error parameters make use of the "McVay" approach for side resistance and the "O'Neill" approach

for end resistance. Inputs for these two approaches include an "Intercept", "Slope", and "Method Error" value. If no limestone layers are defined for the foundation soil layering, then all values within this data subset may be left blank or input as zero. The template input, populated with illustrative data, is listed in Table 21, where (just for illustration) values are taken directly from Ch. 3 of McVay et al. (2012).

Table 21. "Limestone" input from within the "6. Method Error" worksheet tab

Limestone Model	Intercept	Slope	Method Error
McVay	0.898	0.9	4.519
O'Neill	0	0	0

3.2.7 LRFD-φ Tab

A template of the Excel input file format pertaining to the "LRFD-φ" tab is shown in Fig. 50, along with illustrative input values. Note that this Excel worksheet tab must be named "7. LRFD-phi" (where "phi" is spelled out instead of presented as a symbol). Also, as indicated in cell A1 of the template worksheet tab, data contained within the "7. LRFD-phi" worksheet tab can be directly input into the worksheet, or the data can be populated from within the GeoStat UI. Generally, input data for this worksheet tab should be populated through use of the GeoStat UI. Template input file content within the "7. LRFD-phi" worksheet tab, and how the various inputs are organized, are presented in Sec. 3.2.7.1.

Figure 50. Excel input file "7. LRFD-phi" worksheet tab

3.2.7.1 Plot Type

Contained within cells A3 through A6 of the "7. LRFD-phi" worksheet tab (Fig. 50) is the input that dictates the type of design resistance versus elevation plot to display within the respective tab of the GeoStat UI. Namely, the "Plot Type" can be selected from among the "Mean", "COV" (coefficient of variation), "Phi" (resistance factor), or "PhiRn" (product of the resistance factor and nominal resistance). The template input, populated with illustrative data, is listed in Table 22.

44

Table 22. "Plot Type" input from within the "7. LRFD-phi" worksheet tab

Plot Type
[Mean | COV | Phi | PhiRn]
PhiRn

3.3 Input Format for Geotechnical Investigation Site Data

The GeoStat software makes use of geotechnical investigation site data to aid in: (1) Estimation of the profile of soil layering at a location of interest for a pile or shaft within the site; (2) Quantitative characterization of spatial variability (i.e., formation of spatial correlation structures); and, (3) Realization of many (e.g., thousands) of possible soil-pile (or soil-shaft) configurations for analysis in axial capacity calculation software. Presented in Sec. 3.3 is the input format for data acquired through geotechnical investigation of distinct locations across a given site.

3.3.1 Overview

Soil boring (and/or coring) parameters intended for use in estimating soil layer divisions are identified in Sec. 3.3.4, while those parameters dedicated to formation of spatial correlation structures are identified in Sec. 3.3.5. Boring data inputs (depth, soil type) common to both items are discussed in Sec. 3.3.2 and Sec. 3.3.3. Two illustrative input sets, each for a distinct location within a bridge site, are utilized to illustrate the input format for geotechnical investigation site data (Fig. 51 through Fig. 53).

Recall that, in the GeoStat input file, the worksheet tab "1. Project Information" (Fig. 42) requires input of all boring (and/or coring) locations associated with a given site. Further, one unique worksheet tab is required within the GeoStat input file for each boring location, where the name of the worksheet tab must match a respective boring name specified in the "1. Project Information" worksheet tab (recall Table 2). In the following, geotechnical investigation site data associated with borings "1" (the name of which is listed among the example input in Table 2) and "2" are used to illustrate the standard input format for GeoStat input files. As emphasis, a complete GeoStat input file requires one unique worksheet tab for each boring location across the site. The geotechnical site data can be input directly from within the UI (see Ch. 4), or designated cells can be input from within Excel prior to opening the model file within GeoStat.

For a given boring (e.g., "1"), the site-acquired data is input in a manner that is consistent with the tabulated input format of the axial capacity calculation software, FB-Deep. This approach is adopted to provide convenience in making use of the geotechnical site data (measured field data) in either software package (GeoStat, FB-Deep). Accordingly, data distributed across the worksheet tab consist of depth, soil type, and measured (or estimated) soil properties.

Depth (column A) and soil type (column B) inputs are discussed in Sec. 3.3.2 and Sec. 3.3.3, respectively, and must be supplied for each data row within the worksheet tab. Worksheet column C through E (Fig. 51, Table 23 and Fig. 54, Table 26) pertain to soils, while data in columns F through H (Fig. 52, Table 24 and Fig. 55, Table 27) and columns I through L (Fig. 53, Table 25 and Fig. 56, Table 28) pertain to rock (data within these columns are discussed in Sec. 3.34 and Sec. 3.3.5).

	A	B	C	D	E
1	This tab must be populated with data prior to loading GeoStat.				
2					
3	Depth	Soil Type	N. Blows	Unit Weight	Cu
4		[1 | 2 | 3 | 4 | 5]			
5	ft | m		blows/ft | blows/300mm	pcf | kN/m^3	tsf | kPa
6	0	4	0		
7	2.5	4	0		
8	5	4	13		
9	7.5	4	14		
10	10	4	19		
11	12.5	4	16		
12	15	4	19		
13	17.5	4	7		
14	20	4	8		
15	22.5	4	0		
16	25	4	0		
17	27.5	4	0		
18	30	4	10		
19	32.5	4	11		
20	35	4	15		
21	37.5	4	28		
22	40	4	34		
23	42.5	4	22		
24	45	4	25		
25	47.5	4	24		
26	50	4	24		
27	52.5	4	50		
28	55	4	50		
29	57.5	4	50		
30	60	4	50		
31	62.5	4	50		
32	65	4	50		
33	67.5	4	50		
34	70	4	50		
35	72.5	4	50		

Figure 51. Example input file worksheet tab for boring "1", columns A through E (the first 30 out of 100 data rows are displayed)

Note that only those soil (or rock) parameter values that are available need to be input, while cells associated with unavailable (or not applicable) data should remain blank (unpopulated). For brevity, four selected data rows (i.e., four distinct depths) are excerpted in Tables 23-25

and Tables 26-28, and are focused upon in the following sections. In the actual GeoStat input file, one data row should be populated for each depth throughout the boring (as depicted in Fig. 51-53 and Fig. 54-56).

	F	G	H
1			
2			
3	qu	qt	qb
4			
5	tsf	kPa	tsf	kPa	tsf	kPa
6			
7			
8			
9			
10			
11			
12			
13			
14			
15			
16			
17			
18			
19			
20			
21			
22			
23			
24			
25			
26			
27			
28			
29			
30			
31			
32			
33			
34			
35			

Figure 52. Example input file worksheet tab for boring "1", columns F through H (the first 30 out of 100 data rows are displayed)

	I	J	K	L
2				
3	**Em**	**RQD**	**Socket Roughness**	**Rock Recovery**
4		[0.0 to 1.0]	[0 | 1]	[0.0 to 1.0]
5	**ksi | MPa**			
6				
7				
8				
9				
10				
11				
12				
13				
14				
15				
16				
17				
18				
19				
20				
21				
22				
23				
24				
25				
26				
27				
28				
29				
30				
31				
32				
33				
34				
35				

Figure 53. Example input file worksheet tab for boring "1", columns I through L (the first 30 out of 100 data rows are displayed)

	A	B	C	D	E
1	**This tab must be populated with data prior to loading GeoStat.**				
2					
3	**Depth**	**Soil Type**	**N. Blows**	**Unit Weight**	**Cu**
4		[1 | 2 | 3 | 4 | 5]			
5	**ft | m**		**blows/ft | blows/300mm**	**pcf | kN/m^3**	**tsf | kPa**
6	0	4			
7	1	4			
8	2	4			
9	3	4			
10	4	4			
11	5	4			
12	6	4			
13	7	4			
14	8	4			
15	9	4			
16	10	4			
17	11	4			
18	12	4			
19	13	4			
20	14	4			
21	15	4			
22	16	4			
23	17	4			
24	18	4			
25	19	4			
26	20	4			
27	21	4			
28	22	4			
29	23	4			
30	24	4			
31	25	4			
32	26	4			
33	27	4			
34	28	4			
35	29	4			
36	30	4			

Figure 54. Example input file worksheet tab for boring "2", columns A through E (the first 30 out of 100 data rows are displayed)

	F	G	H
1			
2			
3	qu	qt	qb
4			
5	tsf | kPa	tsf | kPa	tsf | kPa
6			
7			
8		0.26	
9	1.71		
10	1.73		
11	1.96		
12		0.29	
13	2.21		
14		0.04	
15	2.41		
16	1.93		
17	1.98		
18		0.09	
19		0.10	
20		0.30	
21	1.72		
22	2.21		
23	2.36		
24	2.36		
25		0.21	
26		0.25	
27	1.96		
28	2.19		
29	2.19		
30	2.39		
31		0.11	
32	2.34		
33		0.29	
34	2.24		
35	1.64		

Figure 55. Example input file worksheet tab for boring "2", columns F through H (the first 30 out of 100 data rows are displayed)

	I	J	K	L
1				
2				
3	**Em**	**RQD**	**Socket Roughness**	**Rock Recovery**
4		[0.0 to 1.0]	[0 | 1]	[0.0 to 1.0]
5	**ksi | MPa**			
6				
7				
8				
9		0.57		0.99
10				
11				
12				
13		0.1		0.53
14				
15		0.71		0.98
16				
17				
18		0.43		0.67
19				
20				
21				
22				
23				
24				
25				
26				
27		0.17		0.23
28				
29				
30				
31		0.1		0.18
32				
33		0.74		0.99
34				
35				

Figure 56. Example input file worksheet tab for boring "2", columns I through L (only the first 30 out of 100 data rows are displayed)

Table 23. Soil properties within the example boring "1" worksheet tab, columns A through E

Depth	Soil Type	N. Blows	Unit Weight	Cu
	[1 | 2 | 3 | 4 | 5]			
ft | m		blows/ft | blows/30 cm	pcf | kN/m^3	tsf | kPa
0	4	0		
2.5	4	0		
5	4	13		
7.5	4	14		

51

Table 24. Soil properties within the example boring "1" worksheet tab, columns F through H

qu	qt	qb
tsf | kPa	tsf | kPa	tsf | kPa

Table 25. Soil properties within the example boring "1" worksheet tab, columns I through L

Em	RQD	Socket Roughness	Rock Recovery
	[0.0 to 1.0]	[0 | 1]	[0.0 to 1.0]
ksi | kPa			

Table 26. Soil properties within the example boring "2" worksheet tab, columns A through E

Depth	Soil Type	N. Blows	Unit Weight	Cu
	[1 | 2 | 3 | 4 | 5]			
ft | m		blows/ft | blows/30 cm	pcf | kN/m^3	tsf | kPa
0	4			
1	4			
2	4			
3	4			

Table 27. Soil properties within the example boring "2" worksheet tab, columns F through H

qu	qt	qb
tsf | kPa	tsf | kPa	tsf | kPa
	0.26	
1.71		

Table 28. Soil properties within the example boring "2" worksheet tab, columns I through L

Em	RQD	Socket Roughness	Rock Recovery
	[0.0 to 1.0]	[0 | 1]	[0.0 to 1.0]
ksi | kPa			
	0.57		0.99

3.3.2 Depth

The first (leftmost, or column A) parameter encountered within the "1" and "2" worksheet tabs (Tab 1: Fig. 51 and Table 23; Tab 2: Fig. 54 and Table 26) is that of "Depth" (ft, m). The "Depth" magnitude should be taken relative to the "Ground Surface Elevation" parameter input in the "1. Project Information" worksheet tab (recall Table 2). For example, for "1" the "Ground Surface Elevation" is input as 0 ft. Therefore, a depth of 0 ft corresponds to an elevation of 0 ft. As noted above, one data row in the worksheet tab should correspond to one measurement point within the boring. In addition, cells within column A cannot be left blank (from the topmost depth to the bottommost depth).

3.3.3 Soil Type

The second (from left, or column B) parameter encountered within the "1" and "2" worksheet tabs (Tab 1: Fig. 51 and Table 23; Tab 2: Fig. 54 and Table 26) is that of "Soil Type", which can be input as an integer value ranging from 1 through 5. As indicated previously, GeoStat adheres to the soil-type mapping established in FB-Deep, where for data input in column B: 1 = Plastic clay; 2 = Clay and silty sand; 3 = Clean sand; 4 = Limestone, very shelly sand; and, 5 = Void. As with the "Depth" input data, each populated data row within column B of the worksheet tab must contain an input value of soil type (i.e., one input value of soil type must be provided at each input depth).

3.3.4 Properties for Determining Layer Divisions

The remaining columns in the "1" and "2" worksheet tabs (columns C through L) can be used to estimate soil layer divisions for a candidate pile or shaft location within the site. Plots of soil properties versus elevation and a table of soil profile divisions are located within the GeoStat "Profile" tab (see Ch. 4). Specifically, soil properties (versus elevation) available for plotting include (Table 23, Table 26): SPT-N blow count, "N.Blows" (blows/ft, blows/300 mm); "Unit Weight" (pcf, kN/m^3); and, undrained shear strength, "Cu" (tsf, kPa).

While input values for data such as blow count ("N. Blows") and "Unit Weight" can pertain to the various soil types considered, certain other parameters are only applicable to specific soil

types. For example, values of undrained shear strength are typically only applicable to plastic clays ("Soil Type" 1) and clay and silty sand ("Soil Type" 2). Specific to those layer depths associated with rock ("Soil Type" 4), soil properties that can be plotted for layer determination include (Table 24, Table 25 and Table 27, Table 28): unconfined compressive strength, "q_u" (tsf, kPa); tensile strength, "q_t" (tsf, kPa); unit end bearing resistance, "q_b" (tsf, kPa); mass modulus, "E_m" (ksi, MPa); rock quality designation, "RQD" (0.0 to 1.0); "Socket Roughness" (0 for smooth or 1 for rough); and, "Rock Recovery" (0.0 to 1.0). Note that, for data within columns C through L, only those data available should be input, while other cells within columns C through L should remain blank.

3.3.5 Properties for Determining Spatial Variability

Among the soil property inputs distributed among columns C through L, SPT blow counts "N. Blows" (column C, Table 23 and Table 26) are utilized for all soil types in forming soil spatial correlation structures. For data rows that are associated with rock ("Soil Type" 4), input values of unconfined compressive strength "q_u" (column F, Table 24 and Table 27) are employed in forming spatial variability structures at the candidate pile (or shaft) location. Only populated cells within these columns are carried forward into the statistical calculations, while blank cells are ignored. In other words, only available SPT or q_u data should be input within the respective data rows, while other cells within these columns should remain blank.

CHAPTER 4
USER INTERFACE CONTROLS

4.1 Overview

The GeoStat UI takes into account a set (or subset) of site geotechnical data (borings/corings) and guides engineers through calculation of pile/shaft axial capacities, with direct consideration of both spatial-variability analysis and method error estimation. Further, for a given pile or shaft member and soil or rock layering, GeoStat generates through-depth profiles of factored axial resistance and the uncertainty of each computed resistance within the profiles.

In particular, the GeoStat UI is organized into seven tabs, which guides engineers through the process of: 1) selecting a foundation type and identifying a set or subset of borings/corings of interest throughout a given site; 2) defining a representative soil or rock layering given the set (or subset) of borings/corings; 3) selecting geostatistical parameters and establishing spatial correlation structures for each layer; 4) simulating numerous realizations of through-depth soil strength parameters and determining the associated axial resistances; 5) viewing through-depth profiles of spatially varying resistance; 6) adjusting axial resistance calculations using appropriate method error correlations; and, 7) viewing profile plots of descriptive statistics based on the simulations conducted (e.g., mean, variance, COV, LRFD resistance ϕ factors), as well as factored axial resistance.

The focus of Ch. 4 is to document all controls that are accessible from within the GeoStat UI. Given in Sec. 4.2 are all program file menu and toolbar items. Additionally, UI tabs (and the associated controls) corresponding to each of the seven items listed above are discussed in Sec. 4.3 through Sec. 4.9, respectively.

4.2 File Menu and Toolbar

The GeoStat UI, along with an illustrative set of site data, is shown in Fig. 57. The File Menu and Toolbar controls (highlighted in Fig. 57) are always visible and accessible from within the GeoStat UI, regardless of which of the seven program tabs are being accessed. File main menu items include File, Control, and Help, and are discussed in Sec. 4.2.1 through Sec. 4.2.3. Further, the File Menu controls allow engineers to open, save, and close a project file; modify program settings, modify project settings; access the program manuals, and update the software license. Program toolbar buttons include actions such as New, Open, Save, and Save As, and are discussed in Sec. 4.2.5.
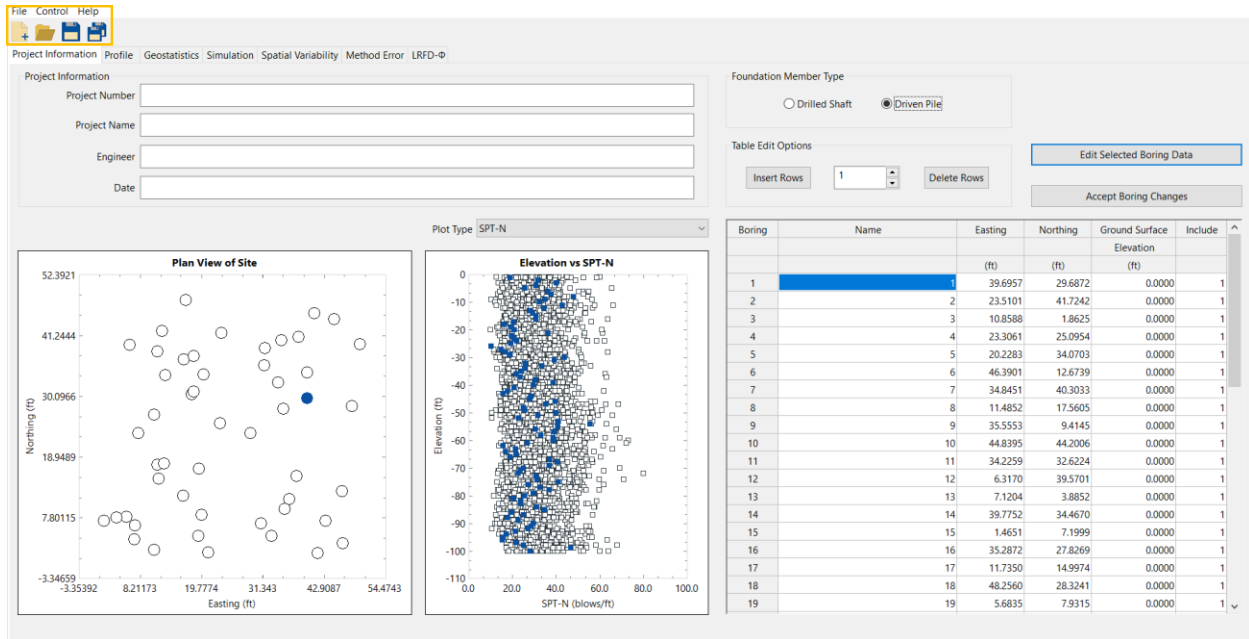
Figure 57. File menu and toolbar controls

4.2.1 File

The File dropdown menu component of the File Menu section of the GeoStat UI (shown in Fig. 58)—and moving from the top of the list downwards—allows for the engineer to create a new GeoStat model; open an existing model file (with Excel format); open an example file (driven pile or drilled shaft foundation); close the current model file; save the current model file to its current directory; save the current model file to a new directory, or, exit GeoStat.
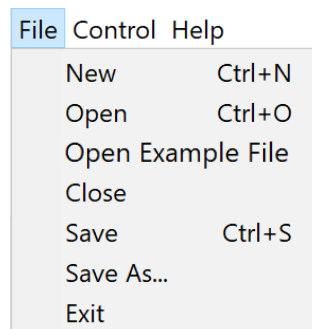
Figure 58. File dropdown menu

4.2.2 Control

The Control dropdown menu component of the File Menu section of the GeoStat UI is shown in Fig. 59. The associated menu options allow for engineers to view and edit high-level program and project (i.e., model-specific) settings.
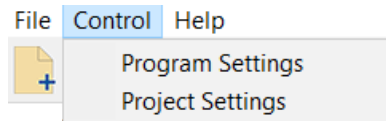
Figure 59. Control dropdown menu

The Program Settings (Fig. 60) dialog allows for selection of whether or not scaling intelligence is used for sizing and positioning of controls throughout the UI (by means of checking the Apply Scaling Intelligence checkbox). Also, the option whether or not to display a message box when the simulation output does not correspond to the current model file. In addition, a custom file path can be specified for use in analyzing all analysis model files that are generated from within GeoStat. Analysis files are always generated in accordance with input format requirements of the axial capacity software, FB-Deep. Also, note that the name of the executable must be included in the path (e.g., "FB-Deep.exe").
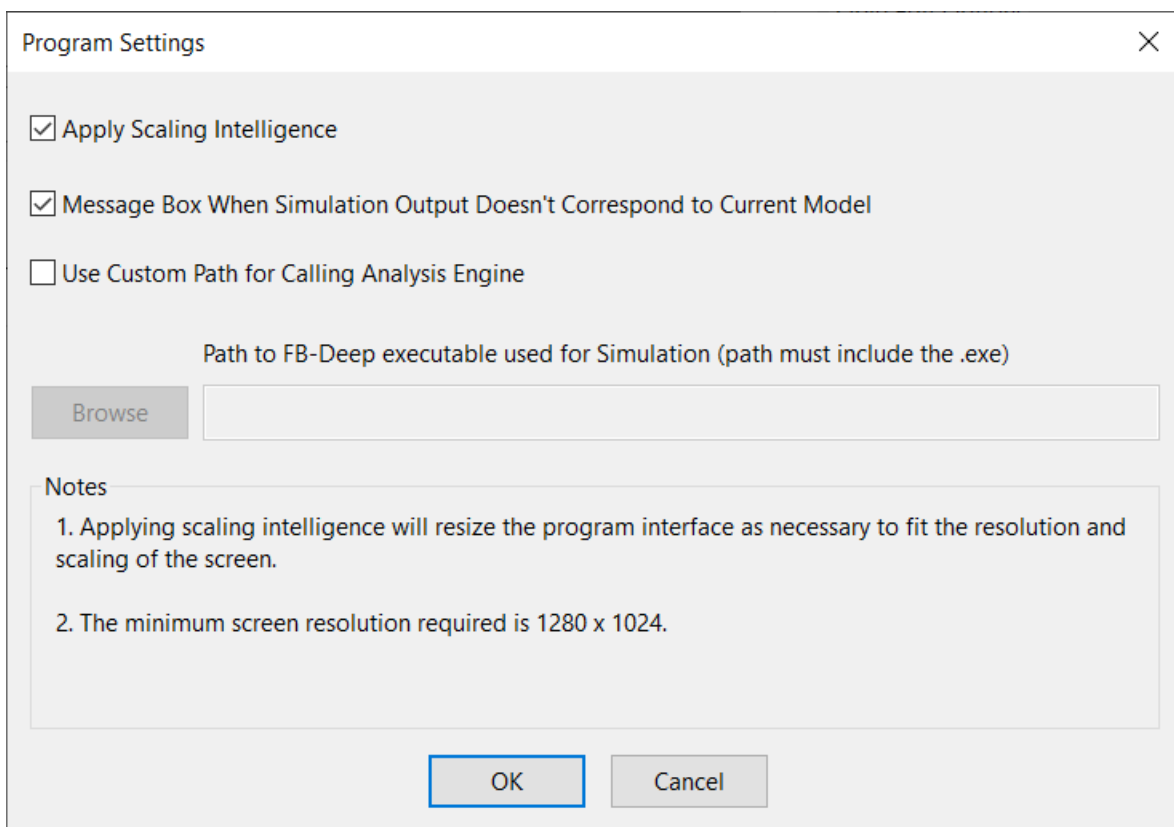
Figure 60. Program Settings dialog

The Project Settings (Fig. 61) dialog allows specification of the Random Seed and Units convention (English or SI) used by GeoStat. The random seed dictates the sequence of

pseudo-random numbers that are generated as part of geostatistical calculations. Reproducibility of program results is ensured by including a record of the random seed value among the file input set.
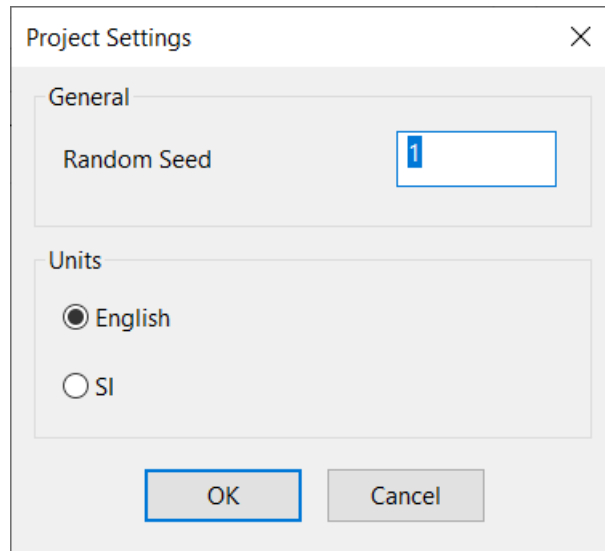
Figure 61. Project Settings dialog

4.2.3 Help

The Help dropdown menu component of the File Menu section of the GeoStat UI is shown in Fig. 62. Moving from the top of the list downwards, available options within the Help menu item include: access the Help Manual, access the Technical Manual, update the software license (see Ch. 2), and display an About GeoStat dialog.
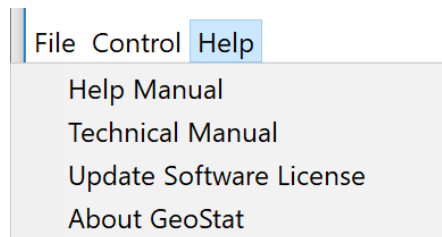
Figure 62. Help dropdown menu

4.2.4 Toolbar Buttons

Four toolbar buttons are available from within the GeoStat UI (Fig. 63). Moving from left to right, the buttons allow for the engineer to create a New model, Open an existing input file, save the currently loaded GeoStat input file, and perform a Save As operation on the currently loaded input file.

Figure 63. Toolbar buttons

4.3 Project Information Tab

Shown in Fig. 64 is the first of seven program tabs, referred to as the Project Information tab. This portion of the GeoStat UI allows for the positions of any subset (or all) borings/corings across the site to be plotted in plan view. Also, a scatterplot of through-depth measurements is provided for available soil parameters of interest. In addition, boring or coring locations can be created and/or deleted and the data within individual borings/corings modified. There are five distinct regions (or frames) of user input data in this tab: (1) Project Information; (2) Foundation Member Type; (3) Table Edit Options; (4) Edit Selected Boring Data; and, (5) Geotechnical Investigation Site Data Locations. Each of the five frames are highlighted in Fig. 64. There are also two distinct plot regions in this tab: (6) Plan View of Site and (7) Plot of Soil Properties vs. Elevation (as highlighted in Fig. 64). All input control and plot regions are discussed in Sec. 4.3.1 through Sec. 4.3.7
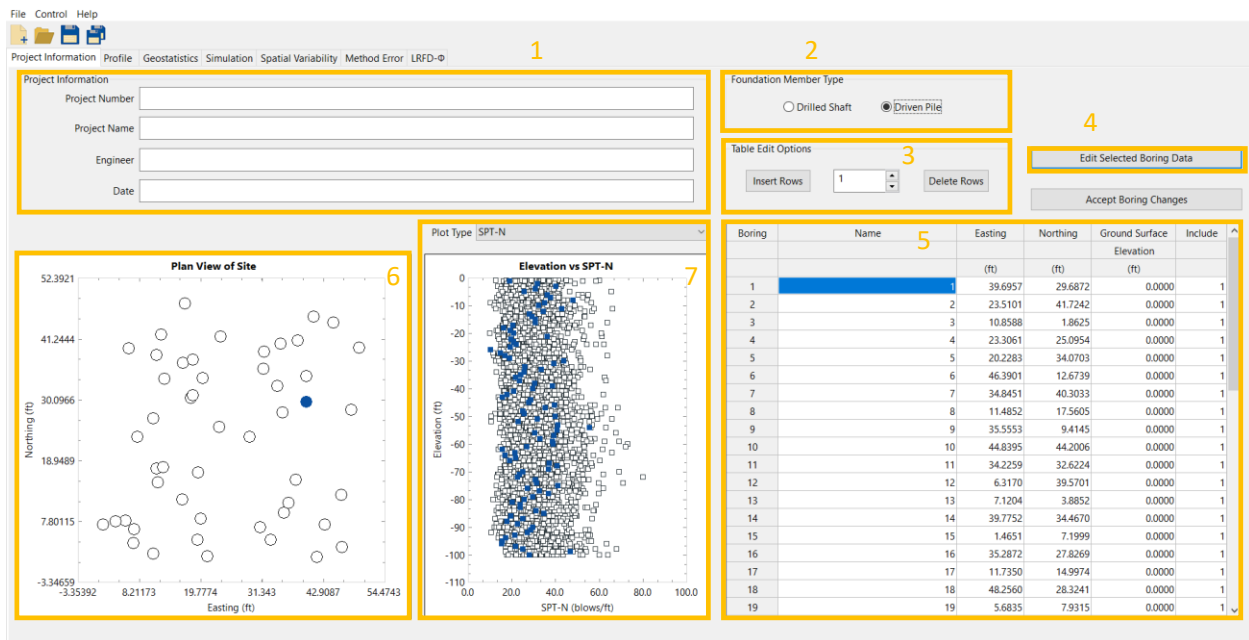
Figure 64. Project Information tab

4.3.1 Project Information Frame

Shown in Fig. 65 is the Project Information frame, where the Project Number, Project Name, Engineer, and Date may be specified. Upon saving the file, the Date field is automatically populated with the current date.

Figure 65. Project Information frame

4.3.2 Foundation Member Type Frame

Shown in Fig. 66 is the Foundation Member Type frame, where the engineer can specify the type of foundation member being considered (Drilled Shaft or Driven Pile).
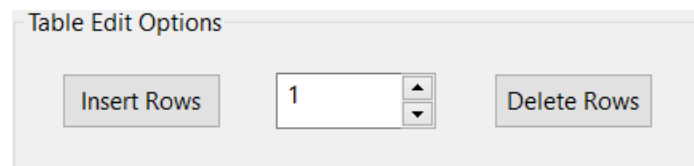
Figure 66. Foundation Member Type frame

4.3.3 Table Edit Options Frame

Shown in Fig. 67 is the table edit options frame, where the user may create and/or delete boring or coring locations. For the creation of one or more boring or coring locations, said number of locations can be specified, and the Insert Rows button can then be clicked. Upon clicking the Insert Rows button, the UI issues a warning (and takes no other action) if the number of rows to be inserted is less than 1. For the deletion of one or more boring or coring locations, said number of locations can be specified, and the Delete Rows button can then be clicked. Upon clicking the Delete Rows button, the UI issues a warning (and takes no other action) if the number of rows to be deleted is less than 1.

Figure 67. Table Edit Options frame

4.3.4 Edit Selected Boring Data Dialog

Shown in Fig. 68 is the Boring Data dialog, which is accessed by clicking the Edit Selected Boring Data button from the Project Information tab (recall Fig. 64). This dialog permits bulk input of boring or coring data (e.g., from Excel). Upon clicking the OK button within the Boring Data dialog, the program checks that the depth values (highlighted in Fig. 68) are input in increasing order. GeoStat adopts the integer mapping to soil types, consistent with the convention implemented in the axial capacity calculation software FB-Deep. Accordingly, if integer values other than 1 through 5 are input beneath the Soil Type column for any row in the Boring Data dialog table, then (upon clicking OK), the program issues a warning and recommends input of revised values. For any row of data input in the Boring Data dialog, the required inputs are Depth and Soil Type (with permitted integer values between 1 and 5). Inputs for all other columns are optional.

Figure 68. Boring Data dialog for a driven pile with illustrative data

Shown in Fig. 69 is the Boring Data dialog associated with a purely illustrative data set for modeling of a drilled shaft. Note the presence of data in columns "q_u", "q_t", "RQD", and "Rock Recovery". With regard to pairing together parameters such as q_u and q_t with RQD and Rock Recovery, two optional input methods are available: values of (for example) q_u and RQD can either be input at the same elevation, or alternatively, at unique elevations. If values of (again, for example) q_u and RQD are input at the same elevation, then these two values will be paired

together during analysis. However, for any q_u (or q_t) values that do not contain RQD (and/or Rock Recovery) values at the same elevation, then the RQD (and/or Rock Recovery) values are selected from the general set of values defined across all currently enabled boring locations.

Boring Data - 1   ✕

Table Edit Options

| Insert Rows | 1 ⏶⏷ | Delete Rows | Default RQD and Recovery To 1 |

Notes
1. Input all available data for the boring within the table below.
2. For any depths where a given soil property is not available, then leave the corresponding cell blank.

Number	Elevation	Depth	Soil Type [1|2|3|4|5]	N. Blows	Unit Weight	Cu	qu	qt	qb	Em	RQD [0.0 to 1.0]	Socket Roughness [0 | 1]	Rock Recovery [0.0 to 1.0]
	(ft)	(ft)		(blows/ft)	(pcf)	(tsf)	(tsf)	(tsf)	(tsf)	(ksi)			
1	0.0000	0.0000	4				1.1958	0.1794			0.0393		0.0964
2	-1.0000	1.0000	4				1.2839	0.1926			0.1566		0.3836
3	-2.0000	2.0000	4				2.1167	0.3175			0.6261		1.0000
4	-3.0000	3.0000	4				2.6752	0.4013			0.4495		1.0000
5	-4.0000	4.0000	4				2.0486	0.3073			0.3999		0.9798
6	-5.0000	5.0000	4				1.7190	0.2579			0.2928		0.7174
7	-6.0000	6.0000	4				2.4208	0.3631			0.0560		0.1372
8	-7.0000	7.0000	4				2.5175	0.3776			0.6563		1.0000
9	-8.0000	8.0000	4				3.1986	0.4798			0.4845		1.0000
10	-9.0000	9.0000	4				2.3460	0.3519			0.1600		0.3921
11	-10.0000	10.0000	4				2.1561	0.3234			0.5868		1.0000
12	-11.0000	11.0000	4				2.8526	0.4279			0.3193		0.7822
13	-12.0000	12.0000	4				2.2976	0.3446			0.2442		0.5982
14	-13.0000	13.0000	4				1.8812	0.2822			0.5985		1.0000
15	-14.0000	14.0000	4				1.9627	0.2944			0.2610		0.6394
16	-15.0000	15.0000	4				2.0672	0.3101			0.5967		1.0000
17	-16.0000	16.0000	4				2.0633	0.3095			0.4088		1.0000
18	-17.0000	17.0000	4				1.3792	0.2069			0.3953		0.9684
19	-18.0000	18.0000	4				1.0929	0.1639			0.1751		0.4291

| OK | Cancel |

Figure 69. Boring Data dialog with illustrative data for a drilled shaft

4.3.5 Table Of Geotechnical Investigation Site Data Locations

Shown in Fig. 70 is the table of Geotechnical Investigation Site Data Locations. For each boring or coring present in current input data file this table displays its name, easting, northing, and ground surface elevation. Any of these values may be changed by selecting the appropriate cell, deleting the old value, and entering the new value.

Note that the rightmost column of the boring or coring location table (highlighted in Fig. 70) houses the Include column. Here, a value of 1 signifies that the boring or coring location is to be included in the analysis (i.e., included in the data structures built up and operated upon in subsequent program tabs). A value of 0 indicates that the boring or coring location is to be excluded from the analysis. To protect against program crashes, any other values input in these locations are interpreted as 0 (exclude), and a value of 0 is saved for these entries upon the next file save event.

Boring	Name	Easting	Northing	Ground Surface Elevation	Include
		(ft)	(ft)	(ft)	
1	1	39.6957	29.6872	0.0000	1
2	2	23.5101	41.7242	0.0000	1
3	3	10.8588	1.8625	0.0000	1
4	4	23.3061	25.0954	0.0000	1
5	5	20.2283	34.0703	0.0000	1
6	6	46.3901	12.6739	0.0000	1
7	7	34.8451	40.3033	0.0000	1
8	8	11.4852	17.5605	0.0000	1
9	9	35.5553	9.4145	0.0000	1
10	10	44.8395	44.2006	0.0000	1
11	11	34.2259	32.6224	0.0000	1
12	12	6.3170	39.5701	0.0000	1
13	13	7.1204	3.8852	0.0000	1
14	14	39.7752	34.4670	0.0000	1
15	15	1.4651	7.1999	0.0000	1
16	16	35.2872	27.8269	0.0000	1
17	17	11.7350	14.9974	0.0000	1
18	18	48.2560	28.3241	0.0000	1
19	19	5.6835	7.9315	0.0000	1

Figure 70. Table of geotechnical investigation site data locations

4.3.6 Plan View of Site

Shown in Fig. 71 is the plan view of the site containing the positions of all borings/corings included in the current analysis. The borings/coring plotted as a solid blue circle signifies the borings/coring that is currently selected within the table of Geotechnical Investigation Site Data Locations (recall Fig. 70).
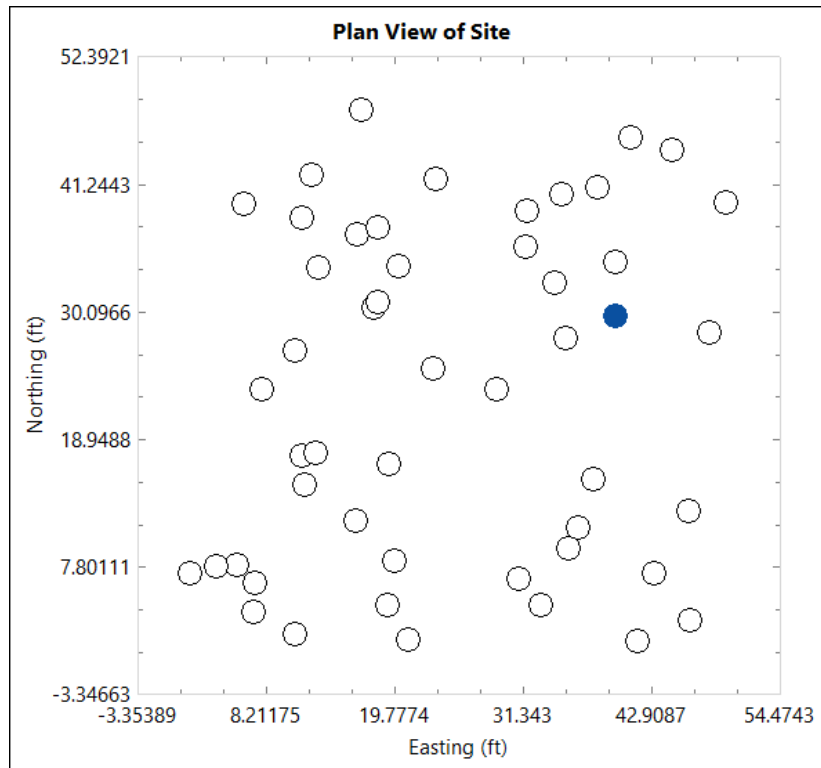
Figure 71. Plan view of site boring or coring locations

4.3.7 Soil Properties vs. Elevation

Shown in Fig. 72 is a plot of elevation vs. SPT-N for each data point across all borings/corings included for the current analysis. The data points rendered in solid blue represent those data points corresponding to the boring(s)/coring(s) currently selected within the table of Geotechnical Investigation Site Data Locations (recall Fig. 70).

Shown in Fig. 73 is a plot of elevation vs. q_u for an illustrative data file, where these values are of particular use when modeling drilled shafts embed in limestone/very shelly sand. Shown in Fig. 74 are the different options available for the soil property that is to be plotted against elevation. To view the plot of a different soil property vs. elevation, select the desired soil property from the dropdown menu to the right of the Plot Type label.
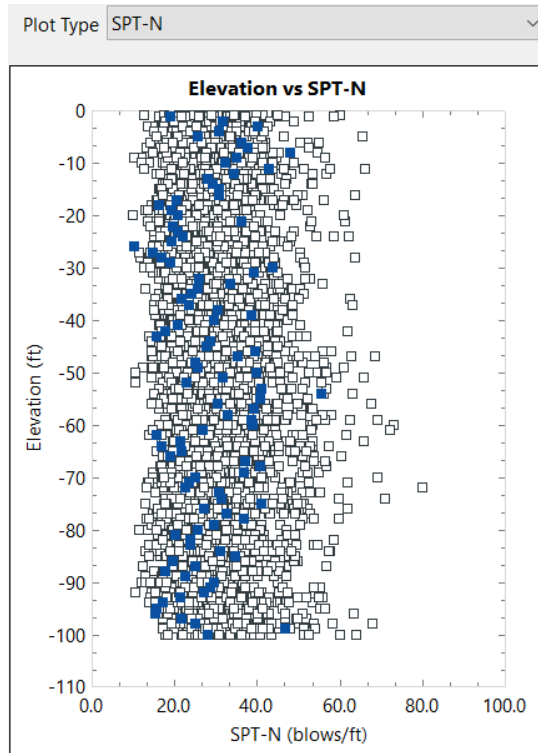
Figure 72. Plot of elevation vs. SPT-N
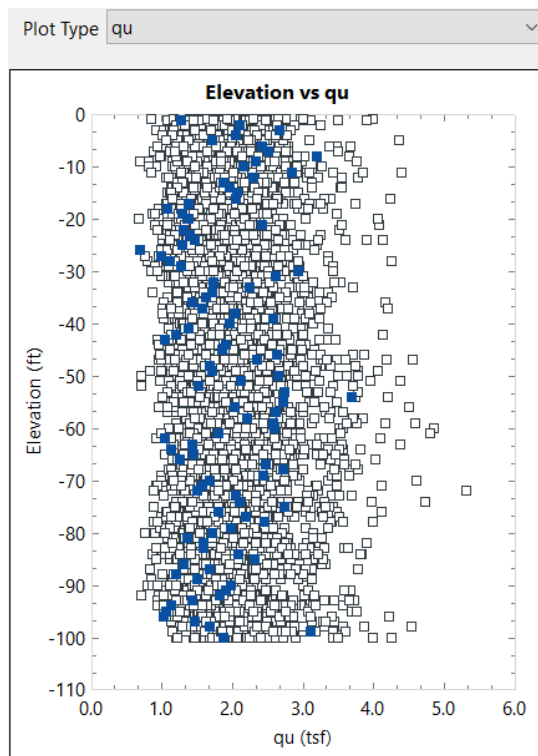
Figure 73. Plot of elevation vs. q_u
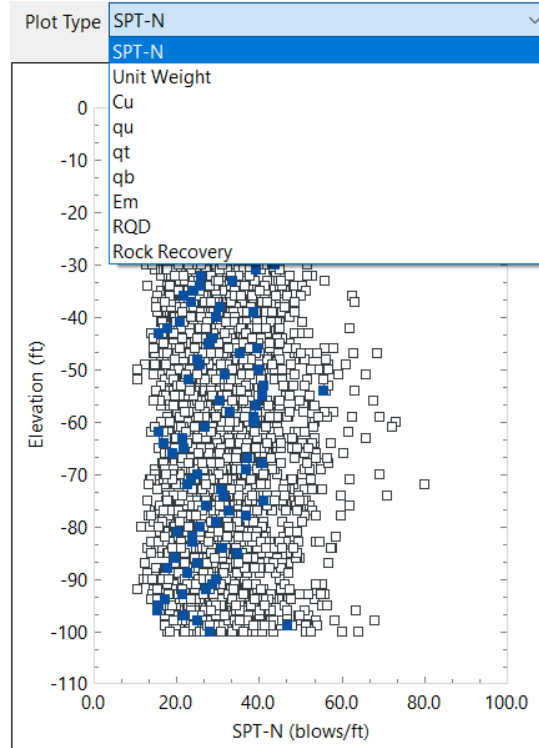
Figure 74. Menu of soil parameters that can be plotted against elevation

4.4 Profile Tab

The second (from left) tab encountered when navigating the GeoStat UI is the "Profile" tab (Fig. 75). Given a collection of included borings/corings (as decided upon from within the Project Information tab), the Profile tab facilitates estimation of representative soil or rock layers for a given location of interest.

There are three distinct regions (frames) of user input data in this tab: (1) Table Edit Options; (2) Correction Factor for Automatic Hammer; and, (3) Layer Profile table (as highlighted in Fig. 75). There is also a distinct region of plots in the left portion of the Profile tab (also highlighted in Fig. 75), which consists of two independent plots of soil properties vs. elevation. All input frames and plot regions are discussed in Sec. 4.4.1 through Sec. 4.4.4.
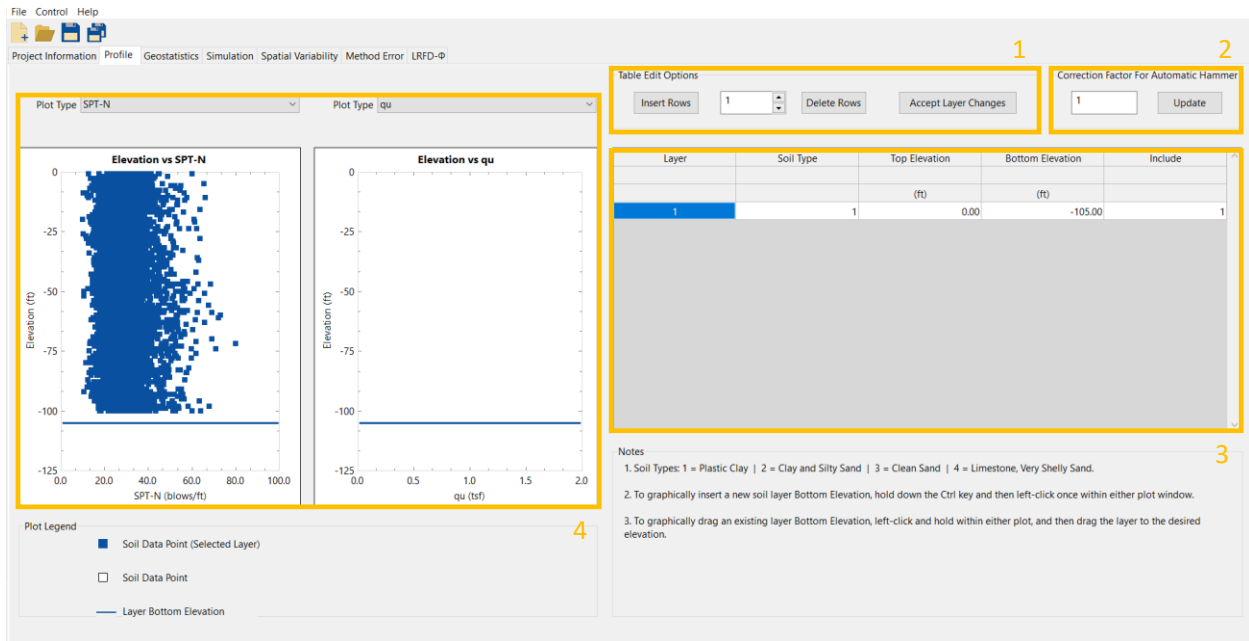
Figure 75. Profile tab

4.4.1 Table Edit Options Frame

Shown in Fig. 76 is the Table Edit Options frame, where the user may create and/or delete layers. For the creation of one or more layers, said number of layers can be specified, and the Insert Rows button can then be clicked. Upon clicking the Insert Rows button, the UI issues a warning (and takes no other action) if the number of rows to be inserted is less than 1. For the deletion of one or more layers, said number of layers can be specified, and the Delete Rows button can then be clicked. Upon clicking the Delete Rows button, the UI issues a warning (and takes no other action) if the number of rows to be deleted is less than 1.

Upon clicking the Accept Layer Changes button, the program checks that all Top Elevation (and separately, Bottom Elevation) values are in decreasing order. For intermediate layers, the program ensures that the Top Elevation (of each intermediate layer) matches the Bottom Elevation of the layer above. Similarly, the program checks that the Bottom Elevation of each intermediate layer matches the Top Elevation of the layer below.
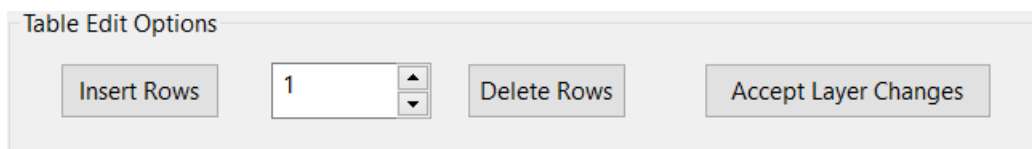
Figure 76. Table Edit Options frame for defining soil or rock layers

4.4.2 Correction Factor for Automatic Hammer Frame

Shown in Fig. 77 is the Correction Factor for Automatic Hammer frame, where the user inputs the adjustment to soil-profile layer data (e.g., SPT values) due to automatic versus safety hammers. The correction factor is unitless and is modified by entering a new value into the text box and pressing the "Update" button. When a value other than 1.0 is supplied for the "Hammer Correction Factor", then values of geotechnical investigation site data such as SPT-N values are adjusted by the correction factor as statistical processes are carried out.

Figure 77. Correction Factor for Automatic Hammer frame

4.4.3 Layer Profile Table

Shown in Fig. 78 are examples of the Layer Profile table, which contains the layering that is to be used during simulation. In addition, top and bottom elevations of soil layers can be input from within the Layer Profile table, as shown in Fig. 78. If integer values other than 1 through 4 are input beneath the Soil Type column, then the program will issue a warning message. The rightmost column of the Layer Profile table houses the Include column. Here, a value of 1 signifies that the layer is to be included in the analysis. A value of 0 indicates that layer is to be excluded from the analysis. To protect against program crashes, any other values input in these locations are interpreted as 0 (exclude), and a value of 0 is saved for these entries upon the next file save event. Note that if a drilled shaft foundation is being considered, then the Mean Unit Weight and Coefficient of Variation must also be specified. After finalizing any changes made within the layering table, clicking the Accept Layer Changes button (Fig. 76, right) will cause the program to perform several checks which ensure that the input layers are valid (the checks are detailed in Sec. 4.4.1).

Layer	Soil Type	Top Elevation	Bottom Elevation	Include
		(ft)	(ft)	
1	1	0.00	-105.00	1

a)

Layer	Soil Type	Top Elevation	Bottom Elevation	Mean Unit Weight	Coefficient of Variation	Include
		(ft)	(ft)	(pcf)		
1	1	0.00	-105.00	110.00	0.70	1

b)

Figure 78. Layer Profile Table: a) Driven pile foundations; b) Drilled shaft foundations

4.4.4 Elevation vs. Soil Parameter Plots

Shown in Fig. 79 is a plot of elevation vs. SPT-N (left side of Fig. 79) and a plot of elevation vs. unit weight (right side of Fig. 79) for each data point within the borings/corings included in the current analysis. The data points highlighted blue represent the data points located within the currently selected layer(s) in the layer profile table (recall Fig. 78). The horizontal lines present in the plots indicate the divisions between distinct layers, as specified in the layer profile table. In addition, moving any of these horizontal lines by dragging them with the cursor will change the layering of the analyses to reflect the new positions of the layer divisions. Changes made to layering within these plots will be reflected in the layer profile table (Fig. 78).
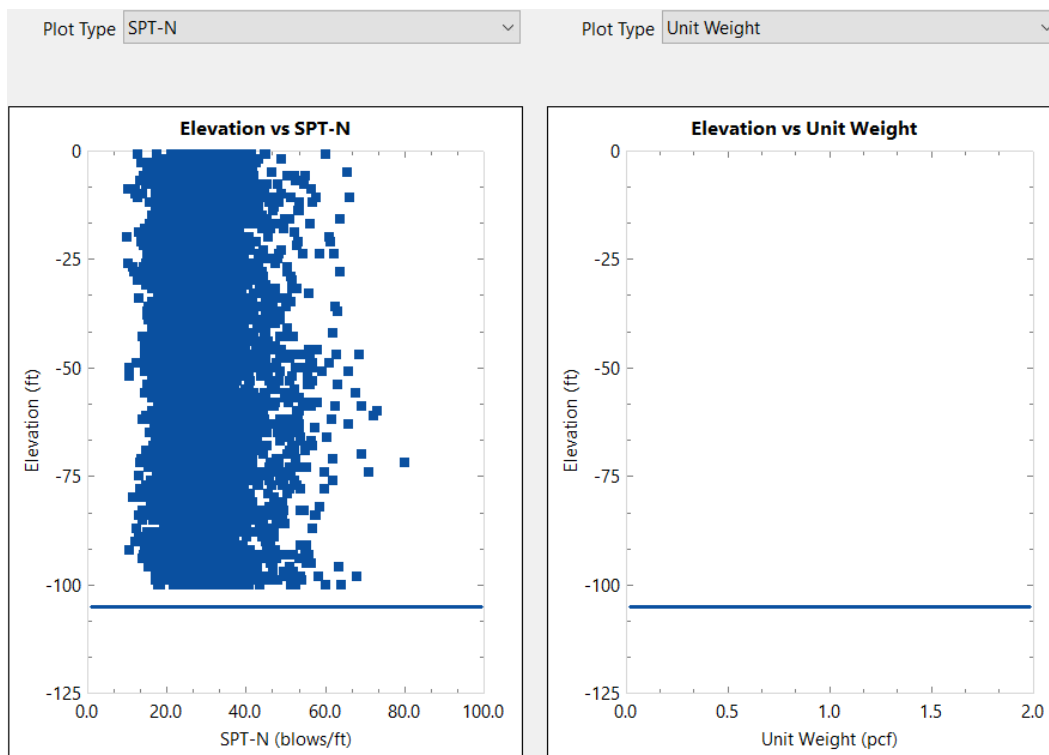
Figure 79. Plots of elevation vs. SPT-N (left) and elevation vs. Unit Weight (right)

Shown in Fig. 80 is a plot of elevation vs. RQD (left side of Fig. 80) and a plot of elevation vs. q_u (right side of Fig. 80) for an illustrative data file associated with a drilled shaft analysis. Shown in Fig. 81 are the different options available for the soil property that is to be plotted against elevation for the plot on the left side of Fig. 79 and Fig. 80. To view the plot of a different soil property vs. elevation, select the desired soil property from the dropdown menu to the right of the label Plot Type. Changing the plot type in this manner can be performed independently for the plot on the left side and the plot on the right side of Fig. 79 and Fig. 80, respectively. See the discussion in Sec. 4.3.4 for options regarding how q_u (and/or q_t) values are paired with RQD (and/or Rock Recovery).
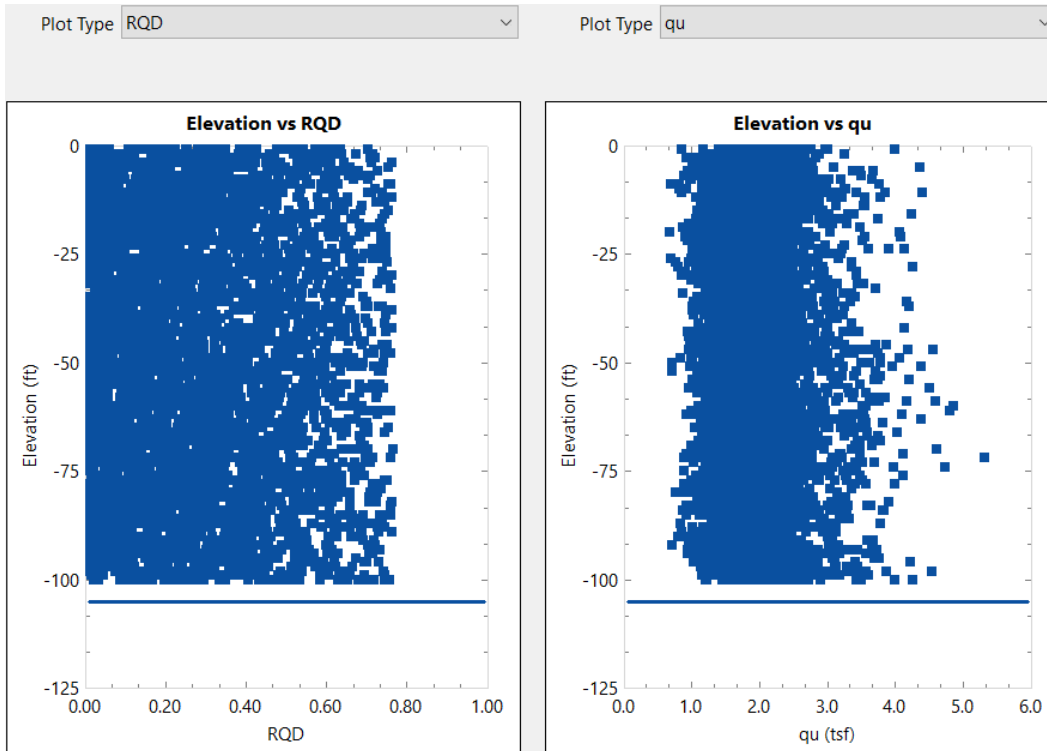
Figure 80. Plots of elevation vs. RQD and elevation vs. q_u
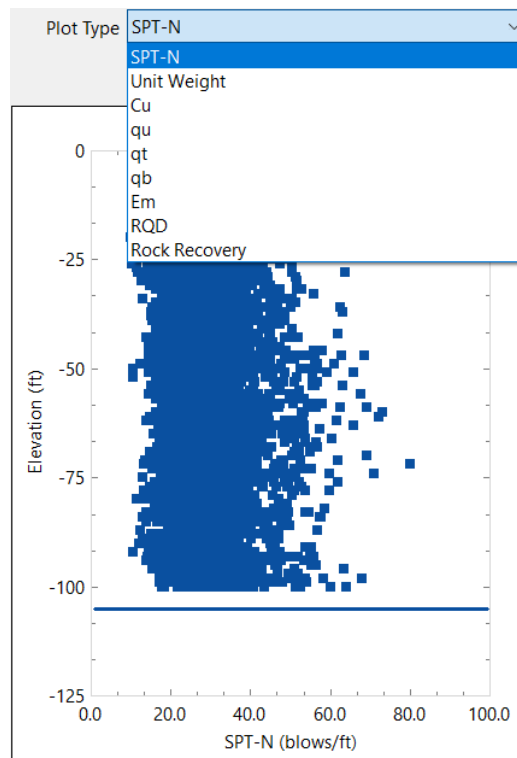
Figure 81. Menu of soil parameters that can be plotted against elevation

4.5 Geostatistics Tab

Spatial correlation structures are determined for included soil or rock layers (based on layering defined in the Profile tab) using controls distributed throughout the Geostatistics tab (Fig. 82). There are three distinct regions of user input data in this tab: (1) Layer Selection and Generate Variogram; (2) Process Layers Frame; and, (3) Layer Variograms table (all highlighted in Fig. 82). There are also five distinct regions of output in this tab: (4) Variogram Data button; (5) Elevation vs. soil parameter plot; (6) Histogram plot; (7) Horizontal Variogram plot; (8) Vertical Variogram plot; and, (9) Export frame (all highlighted in Fig. 82). The nine regions of the Geostatistics tab are discussed in Sec. 4.5.1 through Sec. 4.5.9.
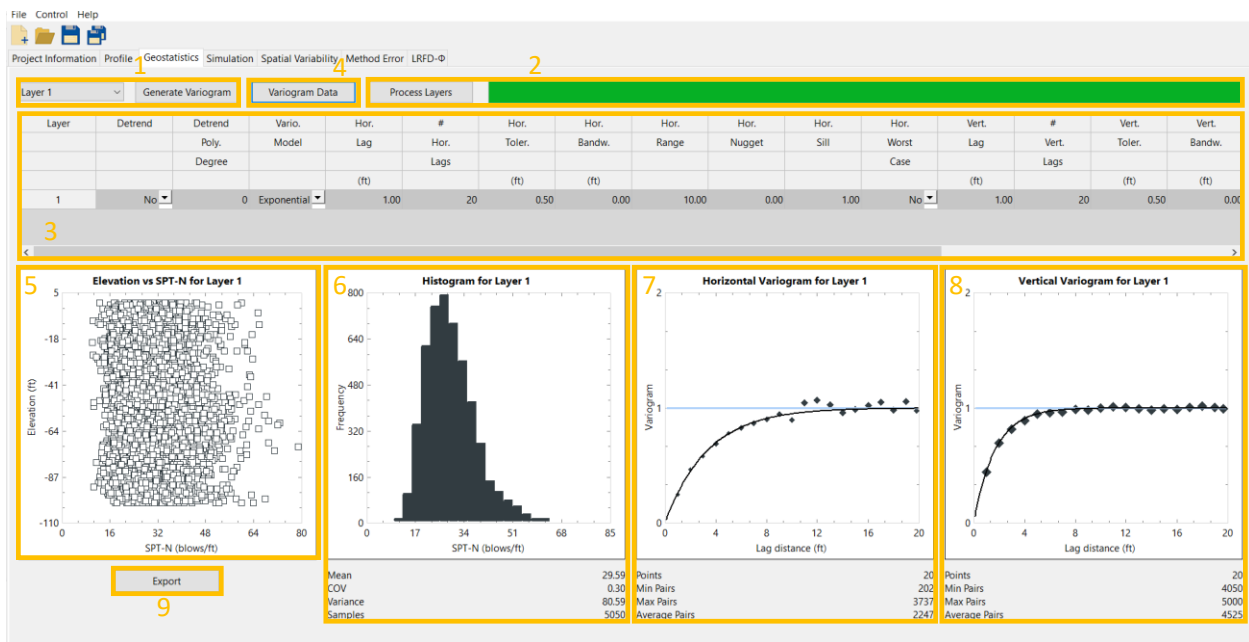
Figure 82. Geostatistics tab

4.5.1 Layer Selection and Generate Variogram Controls

Located in the upper-left portion of the Geostatistics tab are the Layer Selection and Generate Variogram controls (Fig. 83). Soil-spatial parameters are computed for the layer selected in the dropdown menu present on the left side of this frame by pressing the Generate Variogram button. Upon clicking the Generate Variogram button, the program issues a warning message (and indicate the specific issue) in the event that variogram points cannot be generated for a given layer. When valid data are input and variograms can be formed, the two bottom-right plots of Fig. 82 (horizontal and vertical variograms, respectively) are populated with plot points.

71

Figure 83. Layer Selection and Generate Variogram frame

4.5.2 Process Layers Button

Located in the upper-middle and upper-right portions of the Geostatistics tab is the Process Layers frame and an associated progress bar (Fig. 84). Upon clicking the Process Layers button, the program issues a warning message (and indicates the specific issue) in the event that variogram points cannot be generated for a given layer. When valid data are input and variograms can be formed, the two bottom-right plots of Fig. 82 (horizontal and vertical variograms, respectively) are populated with plot points After this operation is complete, the progress bar to the right of Process Layers will become fully green. Note that the Process Layers button only needs to be pressed one time, regardless of the number of layers that are defined (and included) for analysis.

Figure 84. Process Layers button and progress bar

4.5.3 Layer Variograms Table

Insets of the Layer Variograms table are presented in Fig. 85 and Fig. 86, with additional context provided in Fig. 87. Two particularly essential parameters for generating variograms are the lag distance (the distance interval at which to search for pairs of data points) and the number of lag intervals. Note that the site data pertaining to each layer (e.g., SPT, q_u) can also be detrended, where this concept is further discussed in the Technical Manual.

Layer	Detrend	Detrend Polynomial Degree	Variogram Model	Horizontal Lag (ft)	Number of Horizontal Lags	Horizontal Tolerance	Horizontal Bandwidth (ft)	Horizontal Range	Horizontal Nugget	Horizontal Sill	Horizontal Worst Case
1	No	0	Exponential	1.00	20	0.50	0.00	10.00	0.00	1.00	No

Figure 85. Layer Variograms table (left portion)

Vertical Lag (ft)	Number of Vertical Lags	Vertical Tolerance	Vertical Bandwidth (ft)	Vertical Range	Vertical Nugget	Vertical Sill	Vertical Worst Case	Status
1.00	20	0.50	0.00	5.00	0.00	1.00	No	Completed

Figure 86. Layer Variograms table (right portion)

Geometric parameters given in the Layer Variograms table are used for searching out and identifying pairs of data points, where the geometric search terms are defined in the schematic of Fig. 87. Searches for pairs of data points are divided into discrete distances ranging from the lag distance up to, and including, the product of the lag distance and number of lags.

Both the tolerance and bandwidth terms are used to define the search domain associated with a given, current lag distance. Tolerance is parallel to the search direction while bandwidth is perpendicular to the search direction. The tolerance is generally limited to one half of the respective base lag distance (i.e., one half of the Horizontal Lag, one half of the Vertical Lag). For case studies reported in McVay et al. (2012), the recommended bandwidth magnitude is 1 ft (up to 2 ft) for horizontal searches, and 0 ft for vertical searches.

With respect to each applicable search direction (horizontal, vertical), the search process is repeated for every data point to identify point pairs. Variogram ordinate values are then computed by operating on distances between pairs of data points. Additional details are found in McVay et al. (2012) and provided in the program Technical Manual.
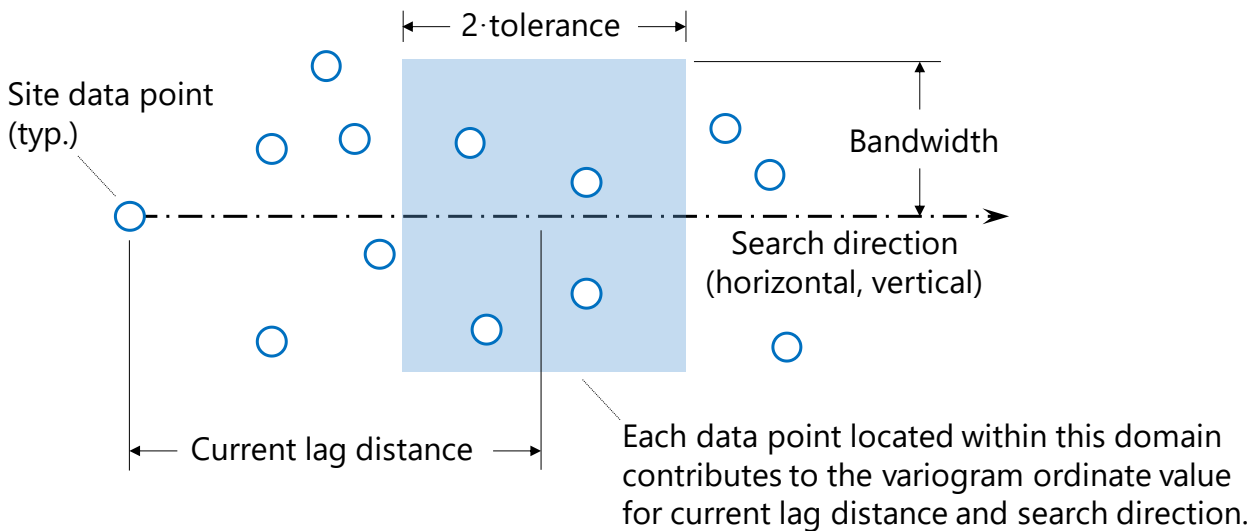
Figure 87. Geometric search terms in Layer Variograms table (adapted from McVay et al. 2012)

If any one of the Horizontal Lag, Number of Horizontal Lags, Vertical Lag, or Number of Vertical Lags are input as non-positive, then the program issues a warning upon any attempts at generating variogram data for the offending layer(s). After successful generation of variograms the Status column in the Layer Variograms table (Fig. 86) indicates that layer processing has "Completed".

4.5.4 Variogram Data Dialog

Located in the upper-left portion of the Geostatistics tab is the Variogram Data button, which when clicks, causes the Variogram Data dialog to appear. Upon clicking the Variogram Data button, the Variogram Data dialog appears (Fig. 88), which displays the horizontal and vertical variogram data associated with the currently selected layer in the Layer Variograms table. For both the horizontal and vertical variograms, the Variogram Data dialog lists computed values of Lag Distance, the Variogram Value at each distance, and the number of pairs found at each lag distance.

Variogram Output

Horizontal Variogram				Vertical Variogram		
Lag Distance	Variogram Value	Pairs		Lag Distance	Variogram Value	Pairs
(ft)				(ft)		
1.0000	0.2504	202		1.0000	0.4426	5000
2.0000	0.4667	606		2.0000	0.6976	4950
3.0000	0.5813	606		3.0000	0.8192	4900
4.0000	0.6900	1515		4.0000	0.8921	4850
5.0000	0.7829	1313		5.0000	0.9473	4800
6.0000	0.8303	1616		6.0000	0.9616	4750
7.0000	0.8678	2121		7.0000	0.9683	4700
8.0000	0.9015	2222		8.0000	0.9870	4650
9.0000	0.9458	2020		9.0000	0.9838	4600
10.0000	0.8954	1515		10.0000	0.9988	4550
11.0000	1.0472	2828		11.0000	1.0103	4500
12.0000	1.0691	3535		12.0000	1.0043	4450
13.0000	1.0289	3434		13.0000	0.9915	4400
14.0000	0.9580	2929		14.0000	0.9851	4350
15.0000	0.9894	2626		15.0000	0.9934	4300
16.0000	1.0241	3636		16.0000	0.9904	4250
17.0000	1.0489	2828		17.0000	1.0037	4200

OK   Cancel

Figure 88. Variogram Data dialog

4.5.5 Elevation vs. Soil Properties Plot

Positioned in the lower-left portion of the Geostatistics tab is a scatterplot, which displays profiles of soil data for a selected layer. For most instances, the relevant type of soil data is that of SPT-N values. As an exception, for drilled shaft foundations, and when a layer of the type Limestone/Very Shelly Sand is active, then unconfined compression strength (q_u) values are displayed instead. Shown in Fig. 89 is a plot of elevation vs. SPT-N using a purely illustrative set of layer data. In the case of a drilled shaft analysis, the Elevation vs. Soil Properties plot will become a plot of elevation vs. SPT-N for each data point within the borings/corings present in the layer currently selected in the Layer Selection and Generate

74

Variogram frame (recall Fig. 83). Shown in Fig. 90 is such a plot, generated from an input data file intended for use in a drilled shaft analysis.
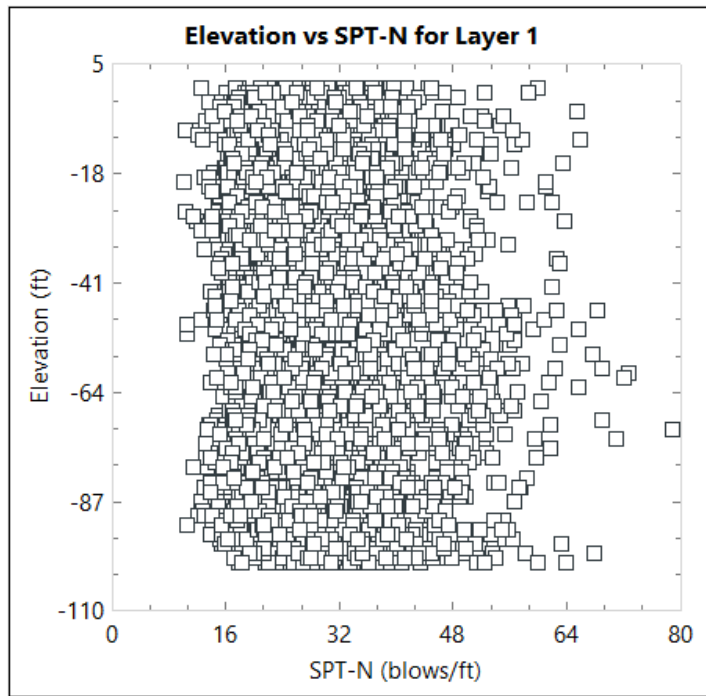
Figure 89. Plot of elevation vs. SPT-N for a selected layer
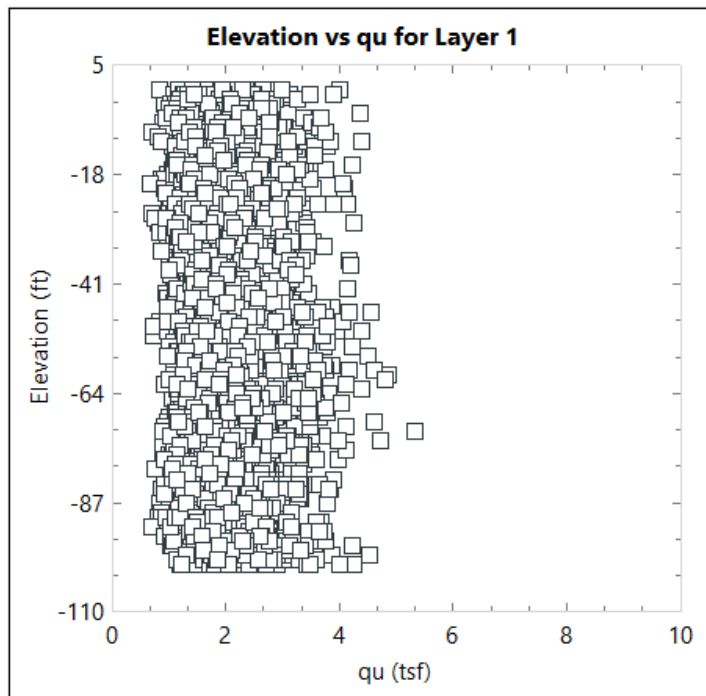
Figure 90. Plot of elevation vs. q_u for a selected layer

4.5.6 Histogram Plot

Shown in Fig. 91 is a histogram of SPT-N (blow count) values for the borings/corings corresponding to the scatterplot (using purely illustrative data) displayed in Fig. 89. Displayed immediately below the histogram are corresponding values of mean (arithmetic, geometric), covariance, variance, and number of samples pertaining to the selected layer.

Mean (Arithmetic, Geometric)	29.59, 28.35
Coefficient of Variation	0.30
Variance	80.59
Number of samples	5050
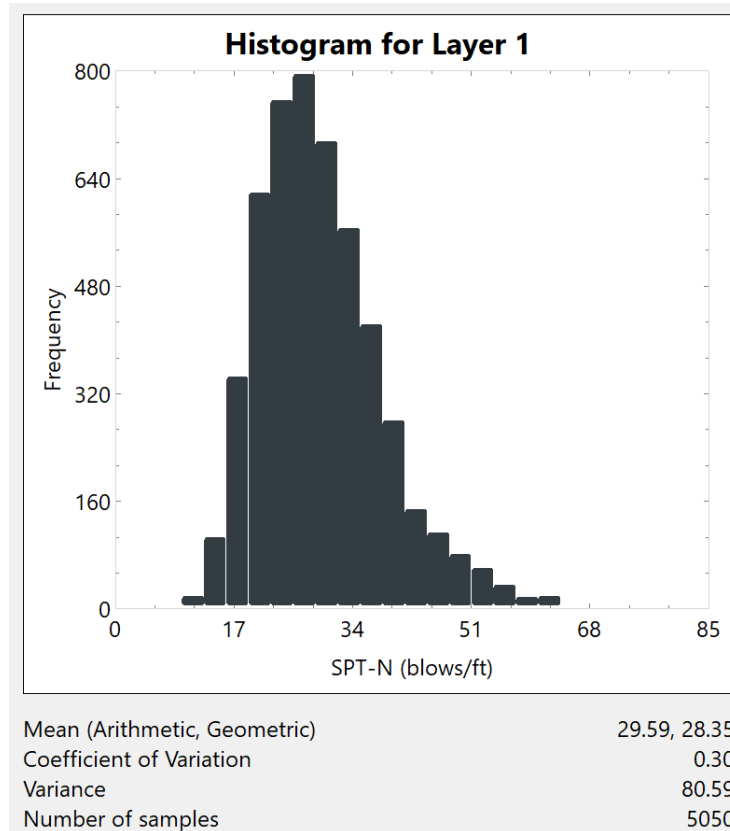
Figure 91. Histogram of SPT-N values

For instances where a drilled shaft foundation is being considered, and the currently selected layer is that of Limestone/Very Shell Sand, the histogram displays values of q_u for the borings/corings present in the layer currently selected. Shown in Fig. 92 is an example histogram, generated using the same illustrative data set as that displayed (in scatterplot form) in Fig. 90.

Histogram for Layer 1

Mean (Arithmetic, Geometric)	1.97, 1.96
Coefficient of Variation	0.30
Variance	0.36
Number of samples	5050
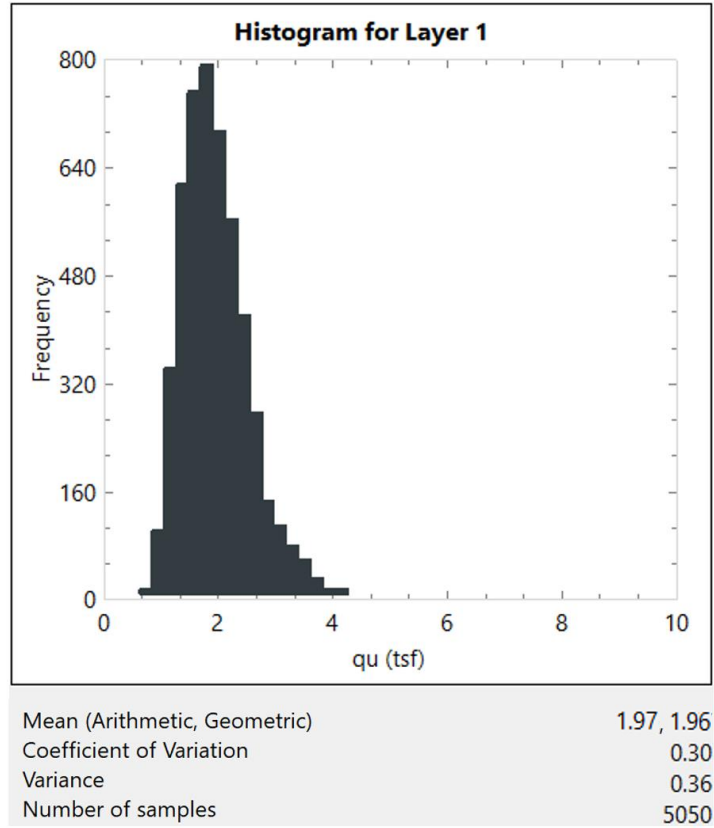
Figure 92. Histogram of q_u values

4.5.7 Horizontal Variogram Plot

Shown in Fig. 93 is the horizontal variogram of the layer currently selected in the Layer Selection and Generate Variogram frame (recall Fig. 83). Displayed below the plot are the number of points, minimum number of pairs per point, maximum number of pairs per point, and average number of pairs per point. Dragging the black curve upwards will increase the horizontal sill (and vice versa), and dragging the black curve to the right will increase the horizontal range (and vice versa). These changes are reflected in real-time in the Layers Variogram table (recall Fig. 85).

Three distinct curves are displayed in the horizontal variogram plot. Solid black diamonds indicate the horizontal variogram points obtained from processing the layer-specific data with respect to the horizontal lag distances. Note that the size of each black diamond reflects the number of pairs that are associated with the respective plot point. In addition, the normalized sill of 1.0 is displayed as a constant-valued, soft blue line. Third, the thin black line indicates the current mathematical fit (either exponential or spherical) to the horizontal variogram data points.

Horizontal Variogram for Layer 1

Points	20
Min Pairs	202
Max Pairs	3737
Average Pairs	2247
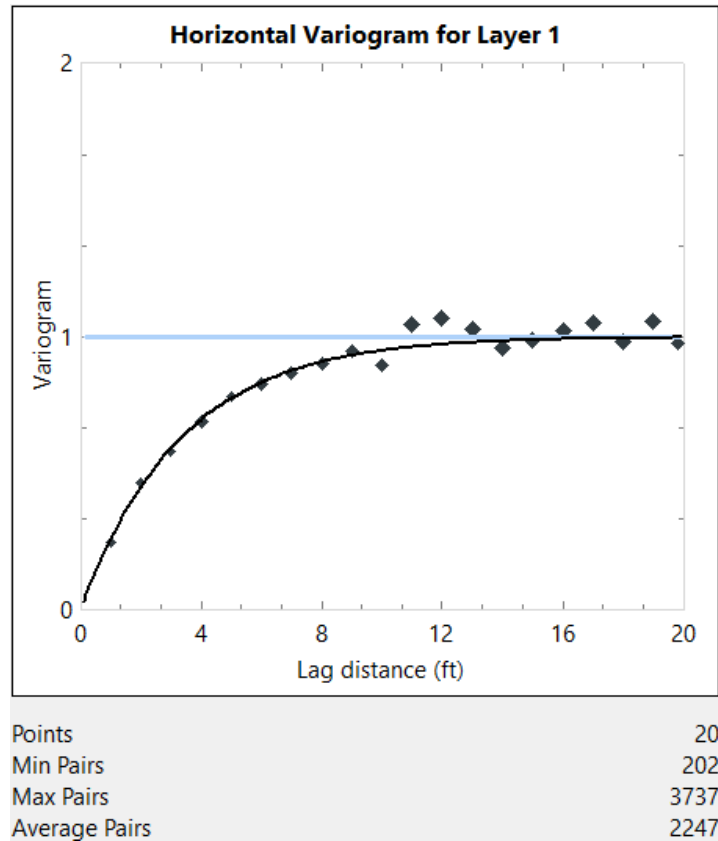
Figure 93. Horizontal variogram for a selected layer

4.5.8 Vertical Variogram Plot

Shown in Fig. 94 is the vertical variogram of the layer currently selected in the Layer Selection and Generate Variogram frame (recall Fig. 83). Displayed below the plot are the number of points, minimum number of pairs per point, maximum number of pairs per point, and average number of pairs per point. Dragging the black curve upwards will increase the vertical sill (and vice versa), and dragging the black curve to the right will increase the vertical range (and vice versa). These changes are reflected in real-time the corresponding row of the Layers Variogram table (recall Fig. 85).

Three distinct curves are displayed in the vertical variogram plot. Solid black diamonds indicate the vertical variogram points obtained from processing the layer-specific data with respect to the vertical lag distances. Note that the size of each black diamond reflects the number of pairs that are associated with the respective plot point. In addition, the normalized sill of 1.0 is displayed as a constant-valued, soft blue line. Third, the thin black line indicates the current mathematical fit (either exponential or spherical) to the vertical variogram data points.
.

78
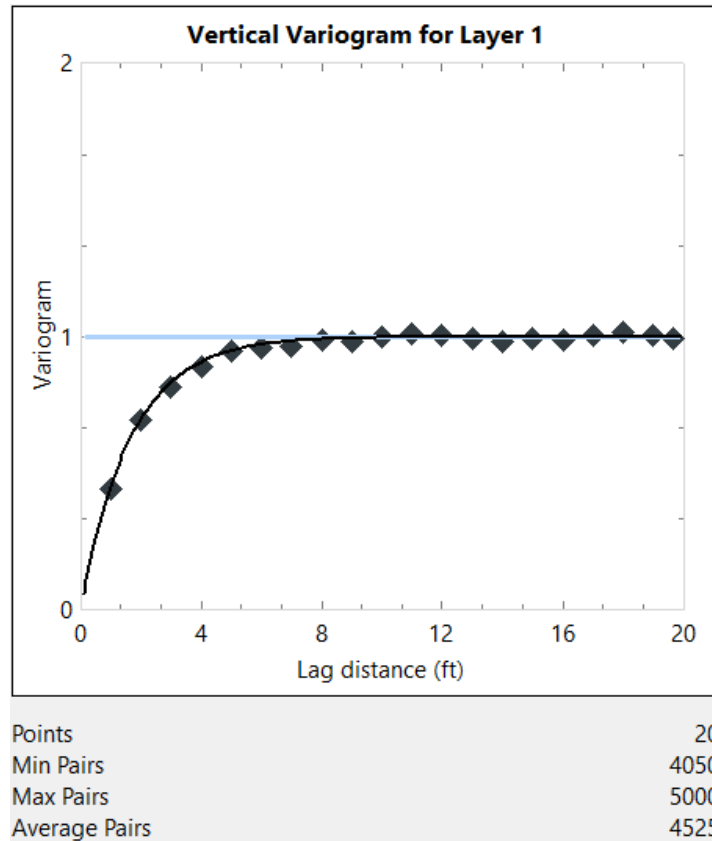
Figure 94. Vertical variogram for a selected layer

4.5.9 Export Layer Data

Clicking the Export button on the Geostatistics tab (Fig. 82, bottom-left) generates and opens an Excel file containing the values used in generating the elevation vs. soil properties scatterplot (e.g., Fig. 89, Fig. 90) and histogram plot (e.g., Fig. 91, Fig. 92). The Excel workbook tab titled "Scatter" contains the elevation of a given data point in column "A" and the value of the data point in column "B". For instances where driven piles are being considered, or drilled shafts in clayey or sandy soils are considered, then column "B" will display SPT-N values (as displayed for an illustrative data set in Fig. 95). For instances where Limestone/Very Shell Sand layers are being considered for drilled shaft foundation, then column "B" will display q_u values (such as those shown for illustrative purposes in Fig. 96).

	A	B
1		
2	**Elevation**	**SPT-N**
3	**(ft | m)**	**(blows/ft | blows/300mm)**
4	0.0000	29
5	0.0000	34
6	0.0000	30
7	0.0000	21
8	0.0000	24
9	0.0000	45
10	0.0000	25
11	0.0000	34
12	0.0000	29
13	0.0000	24
14	0.0000	34
15	0.0000	26
16	0.0000	32
17	0.0000	31
18	0.0000	24
19	0.0000	26
20	0.0000	27
21	0.0000	32
22	0.0000	28
23	0.0000	31
24	0.0000	27
25	0.0000	24
26	0.0000	17
27	0.0000	39
28	0.0000	44
29	0.0000	41
30	0.0000	39
31	0.0000	22
32	0.0000	24
33	0.0000	25
34	0.0000	29
35	0.0000	36
36	0.0000	41
37	0.0000	29
38	0.0000	22
39	0.0000	23

Figure 95. "Scatter" worksheet tab for an illustrative driven pile data set (the first 35 out of 5050 total data points are displayed)

	A	B
1		
2	**Elevation**	qu
3	(ft | m)	(tsf | kPa)
4	0.0000	1.9340
5	0.0000	2.3018
6	0.0000	2.0344
7	0.0000	1.4094
8	0.0000	1.6425
9	0.0000	3.0011
10	0.0000	1.7284
11	0.0000	2.3103
12	0.0000	1.9858
13	0.0000	1.6612
14	0.0000	2.2669
15	0.0000	1.7538
16	0.0000	2.1807
17	0.0000	2.0891
18	0.0000	1.6194
19	0.0000	1.7951
20	0.0000	1.8593
21	0.0000	2.1765
22	0.0000	1.9256
23	0.0000	2.1297
24	0.0000	1.8325
25	0.0000	1.6116
26	0.0000	1.1667
27	0.0000	2.6522
28	0.0000	2.9808
29	0.0000	2.7668
30	0.0000	2.6251
31	0.0000	1.4957
32	0.0000	1.6436
33	0.0000	1.6822
34	0.0000	1.9342
35	0.0000	2.4441
36	0.0000	2.7391
37	0.0000	1.9587
38	0.0000	1.5256
39	0.0000	1.5597

Figure 96. "Scatter" worksheet tab for an illustrative data set involving Limestone/Very Shell Sand layer and a drilled shaft foundation (only the first 35 out of 5050 total data points are displayed)

The workbook tab titled "Histogram" contains consecutive, non-overlapping ranges of data in Column "A" and the frequency of data between those interval bounds in column "B". For instances where driven piles are being considered, or drilled shafts in clayey or sandy soils are considered, then column "A" will display interval bounds for SPT-N values (as displayed for an illustrative data set in Fig. 97). For instances where Limestone/Very Shell Sand layers are being considered for drilled shaft foundation, then column "A" will display interval bounds for q_u values (such as those shown for illustrative purposes in Fig. 98).

	A	B
1		
2	SPT-N	Frequency
3	(blows/ft | blows/300mm)	
4	1	0
5	4	0
6	7	0
7	11	16
8	14	103
9	17	343
10	20	616
11	23	754
12	27	797
13	30	693
14	33	563
15	36	420
16	39	277
17	43	145
18	46	110
19	49	79
20	52	58
21	55	32
22	59	14
23	62	16
24	65	5
25	68	5
26	71	3
27	75	0
28	78	1

These values indicate histogram bin extents (left-open, right closed)

Figure 97. "Histogram" worksheet tab for an illustrative driven pile data set (note: the SPT-N blow count values listed indicate the histogram bin extents with a left-open, right closed convention)

	A	B
1		
2	qu	Frequency
3	(tsf | kPa)	
4	0.1065	0
5	0.3195	0
6	0.5324	0
7	0.7454	16
8	0.9584	103
9	1.1714	343
10	1.3843	616
11	1.5973	754
12	1.8103	797
13	2.0232	693
14	2.2362	563
15	2.4492	420
16	2.6622	277
17	2.8751	145
18	3.0881	110
19	3.3011	79
20	3.5141	58
21	3.7270	32
22	3.9400	14
23	4.1530	16
24	4.3659	5
25	4.5789	5
26	4.7919	3
27	5.0049	0
28	5.2178	1

Figure 98. "Histogram" worksheet tab for a drilled shaft data set (within a Limestone/Very Shelly Sand layer)

4.6 Simulation Tab

Shown in Fig. 99 is the fourth of seven program tabs, the Simulation tab, wherein controls are dedicated to defining the foundation member configuration and conducting statistical simulation. There are eight distinct regions of user input data in this tab: (1) General Geometry frame; (2) Shaft Geometry frame; (3) Pile Geometry frame; (4) Foundation Member Material Properties frame; (5) Soil frame; (6) Layer Separation frame; (7) Simulation frame; and, (8) Run Simulation controls (all highlighted in Fig. 99). There is also one distinct region of display-only (i.e., non-editable) output in this tab: (9) Soil-Spatial Parameters (also highlighted in Fig. 99). The nine regions of the Simulation tab are discussed in Sec. 4.6.1 through Sec. 4.6.9.
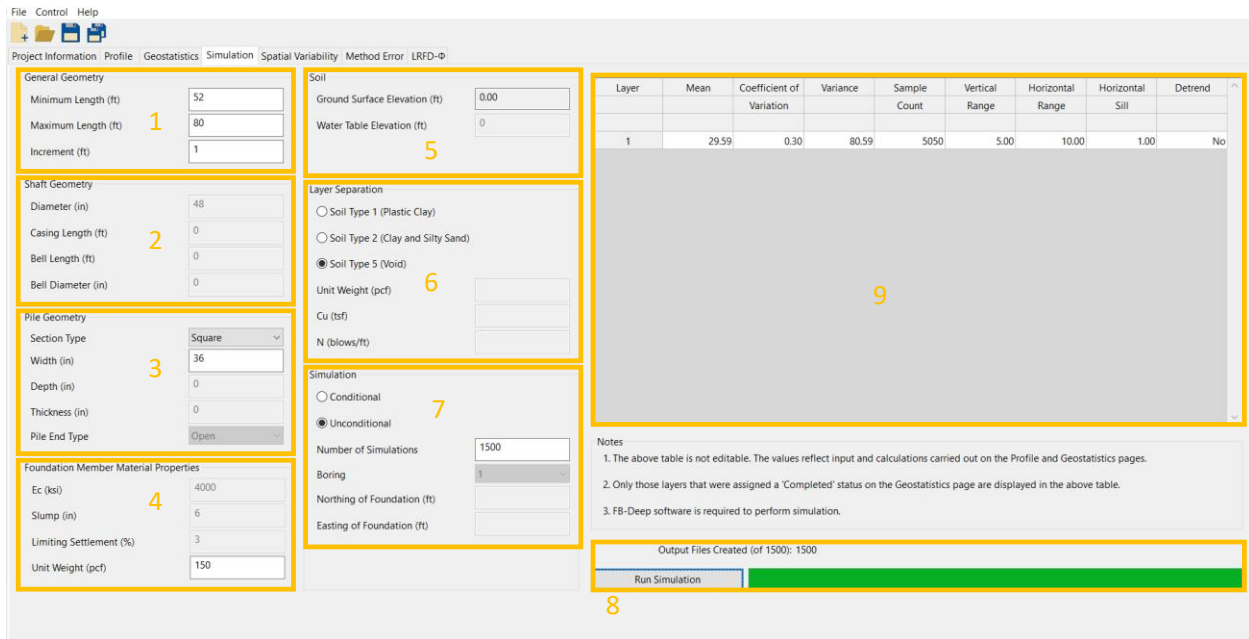
Figure 99. Simulation tab

4.6.1 General Geometry Frame

Located in the upper-left portion of the Simulation tab is the General Geometry frame (an inset is shown in Fig. 100). Within the frame are the controls that dictate the range and increment of embedment lengths to consider during simulation. To protect against formation of improper data in the numerous analysis model files (generated as part of the statistical simulation), only positive values are permitted to be entered. In addition, the program ensures that the range of embedment lengths fall within the soil or rock profile (as defined using controls on the Profile tab, recall Fig. 75). Specific to GeoStat models of pile members, and depending on the soil or rock layering, the program further ensures that adequate soil or rock layering is available given the input value of Maximum Length (e.g., 3.5 pile diameters below and 8.0 pile diameters above for end bearing calculations).
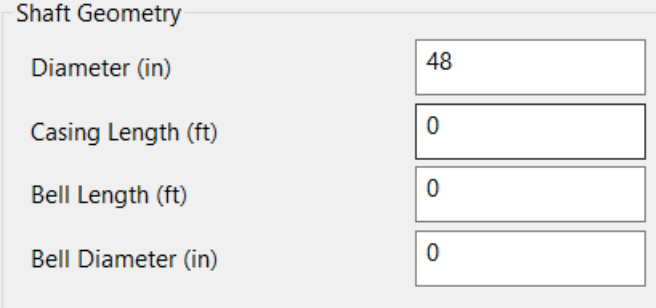
Figure 100. General Geometry frame

84

4.6.2 Shaft Geometry Frame

For models involving drilled shaft foundations, controls within the Shaft Geometry frame (Fig. 101) are enabled. The program enforces input of only positive-valued entries for Diameter. However, inputs for Casing Length, Bell Length, and Bell Diameter are permitted to be input as equal to or greater than zero.
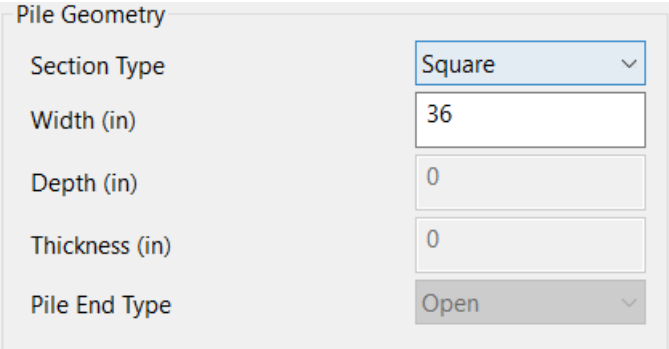
Figure 101. Shaft Geometry frame

4.6.3 Pile Geometry Frame

For modeling of driven piles, certain controls within the Pile Geometry frame (Fig. 102) are enabled. More specifically, depending on the selection of Section Type, only those parameters required to describe the cross-section (for the purposes of soil or rock axial-capacity simulations) become enabled. The section types that can be considered include: Square, Round, Pipe, Cylinder, and H-Section. For square piles, only the Width parameter is required. Regardless of which input parameters are required for a pile cross-section, the program accepts only those that are positive (and otherwise issues a warning). For round piles, only the Width parameter is required (Fig. 103). For a pipe pile, only the Width and Thickness parameters are required (Fig. 104). For a cylindrical pile, only the Width, Thickness, and Pile End Type parameters are required (Fig. 105). For a pile with an H-Section geometry, only the Width and Depth parameters are required (Fig. 106).

Figure 102. Pile Geometry frame for square piles

Figure 103. Pile Geometry frame for round piles

Figure 104. Pile Geometry frame for pipe piles

Figure 105. Pile Geometry frame for cylindrical piles

Figure 106. Pile Geometry frame for piles with an H-Section Geometry

4.6.4 Foundation Member Material Properties Frame

Material properties of foundation members are specified in the Foundation Member Material Properties frame (Fig. 107 and Fig. 108). Only Unit Weight (Fig. 107) must be supplied when modeling driven piles (the other three controls are disabled for such cases). In contrast, for drilled shaft models (Fig. 108), four parameters are required (modulus of elasticity, Ec; Slump; Limiting Settlement; and, Unit Weight). Regardless of the foundation member type being modeled, all enabled controls within this frame are checked to prevent input of non-positive values.
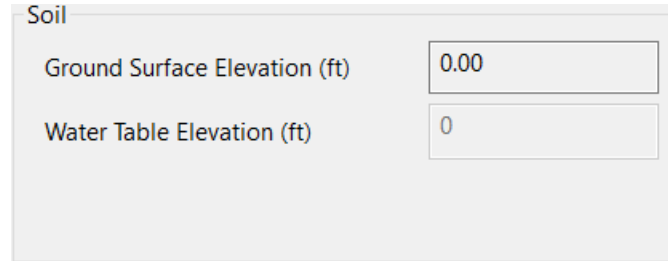
Figure 107. Foundation Member Material Properties frame for a driven pile

Figure 108. Foundation Member Material Properties frame for a drilled shaft

4.6.5 Soil Frame

In order to establish relative positioning of the pile/shaft within the user-defined soil or rock layering, the Ground Surface Elevation must be taken into account. Although this parameter is automatically calculated by the program based on data input on the Profile tab, it is displayed within the Soil frame as a convenience to the engineer (Fig. 109). For drilled shafts, the input box for the Water Table Elevation will be enabled and must also be input.
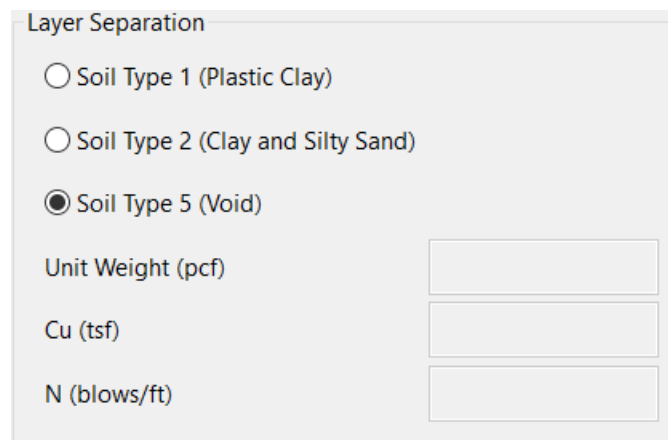
Figure 109. Soil frame

4.6.6 Layer Separation Frame

Recall that soil or rock layerings are defined from within the UI Profile tab, and can be defined as consisting of any of four soil or rock types (as well as a fifth type corresponding to a void). For generation of analysis model files, the layerings are subdivided into 0.5-ft increments (referred to in this context as sublayers). A subset of the available layer types may be specified for defining those sublayers that fall at the boundaries of layers that are defined on the Profile tab. By default, and as a conservative measure, these "bounding" sublayers (or, layer separators) are designated as Soil Type 5 (Void). If the layer separation consists of a void (Soil Type 5), then the engineer is not required to specify any additional properties. (Fig. 110).

Figure 110. Layer Separation frame inputs for Soil Type 5 (Void)

If the layer separation is defined as Soil Type 1 (Plastic Clay), then the engineer must additionally specify representative values of Unit Weight and undrained shear strength, Cu (Fig. 111). If the layer separation is defined as Soil Type 2 (Clay and Silty Sand), then the engineer must specify the Unit Weight and N of the soil (Fig. 112). Note that these latter two selections should be made with caution as use of non-representative parameter values may lead to unconservative predictions of member resistance.

Figure 111. Layer Separation frame inputs for Soil Type 1 (Plastic Clay)
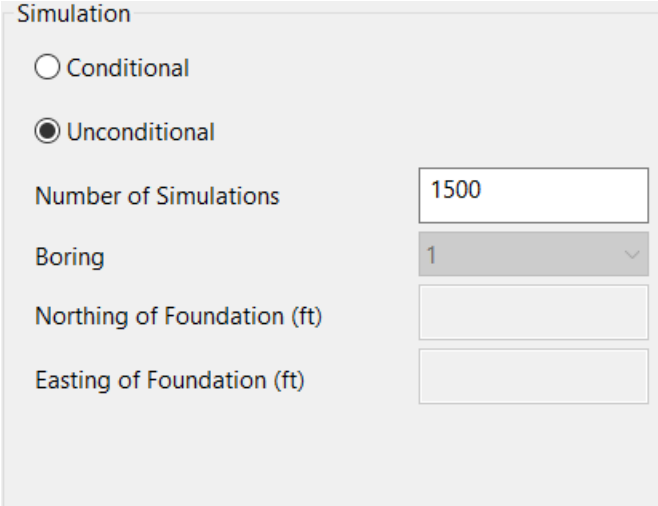
Figure 112. Layer Separation frame inputs for Soil Type 2 (Clay and Silty Sand)

4.6.7 Simulation Frame

Positioned in the lower right portion the Simulation tab is the Simulation frame (Fig. 113). The Simulation frame contains input controls that determine the overall nature of the probabilistic simulation. Namely, either a Conditional (data from nearby borings) or Unconditional (pile/shaft outside of correlation length) simulation can be conducted. In the case of an Unconditional simulation, a value is only needed for Number of Simulations. This parameter
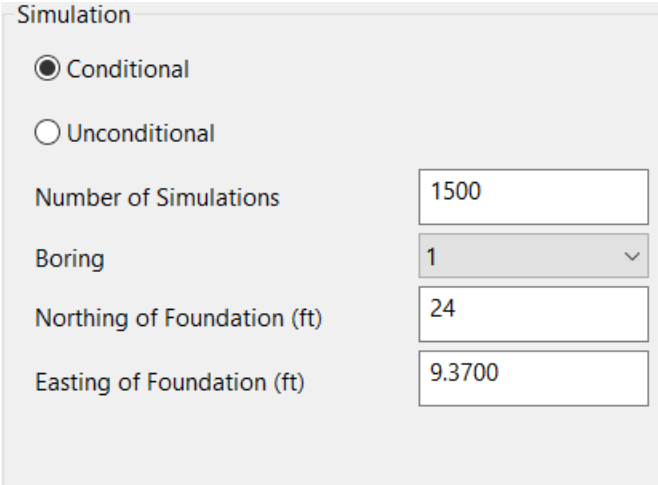
dictates the total number of realizations to be generated and then packaged (along with pile/shaft data) into model analysis files, which adhere to FB-Deep input format requirements.

Figure 113. Simulation frame with selection of Unconditional simulation

For Conditional simulations, the Number of Simulations is also required. In addition, the boring nearest to the foundation location being analyzed must be selected from the Boring dropdown menu (Fig. 114). After selecting a boring, the respective positioning values of Northing and Easting will be displayed, and can be further adjusted as appropriate.

Figure 114. Simulation frame with selection of Conditional simulation

Faraone (2014) recommended that a minimum of 1000 realizations be considered when conducting stochastic simulation. As reported in McVay et al. (2012), a recommended number of simulations is 2000. For use of GeoStat in design applications, it is recommended that 2000 realizations be considered. See the Technical Manual for additional details.

4.6.8 Run Simulation Button

Positioned in the lower-right portion of the Simulation tab is the Run Simulation button (Fig. 115). Clicking the Run Simulation button prompts GeoStat to first generate the many realizations of soil or rock profiles, taking into account spatial variability phenomena. Next, a folder is created in the same directory as the GeoStat model file and is subsequently populated with model analysis files (one realization corresponds to one input file). Note that the folder name issued is identical to the name of the currently loaded GeoStat model file. Also, the model analysis files satisfy input format requirements required for analysis using the geotechnical axial capacity software, FB-Deep.

Figure 115. Run Simulation button and progress bar

The numerous model analysis files, all stored within the newly created folder, are named using a sequential numbering convention. Therefore, it is useful to save a unique GeoStat input file for each unique instance of carrying out the simulations. Additional details on creation of the model analysis files, and interfacing of the GeoStat UI with analysis executables are provided in Ch. 5.

4.6.9 Soil-spatial Parameters Table

Positioned in the upper right portion the Simulation tab is the Soil-spatial Parameters table (Fig. 116). This table contains soil-spatial parameters for each active layer, given the input selections made from within the Profile tab (Fig. 75) and Geostatistics tab (Fig. 82). Values listed within the table are not editable. Rather, the listings serve as an intermediate summary of layer data, which in turn, can aid in determining whether or not to proceed with simulations (or alternatively, revisit the Profile and/or Geostatistics tabs to adjust the model data).

Layer	Mean	Coefficient of Variation	Variance	Sample Count	Vertical Range	Horizontal Range	Horizontal Sill	Detrend
1	29.59	0.30	80.59	5050	5.00	10.00	1.00	No

Figure 116. Soil-spatial Parameters table

4.7 Spatial Variability Tab

For any complete sets of simulation files, plots of pile/shaft axial resistance can subsequently be viewed from within the Spatial Variability tab (e.g., the illustrative data plotted in Fig. 117). Plots shown on this tab reflect the boring or coring data, soil or rock layering, spatial correlation structures, and foundation member configuration defined on those UI tabs discussed in Sec. 4.1 through Sec. 4.6. There are two distinct regions of user input data in this tab: (1) Import FB-Deep Output button; and, (2) Plot Legend Frame (both highlighted in Fig. 117). Also, five distinct regions of output controls are located within the Spatial Variability tab: (3) Update Plots and Export buttons; (4) Mean Plot; (5) Variance Plot; (6) Coefficient of Variation Plot; and, (7) Phi Plot (as highlighted in Fig. 117). These seven tab regions are discussed in Sec. 4.7.1 through Sec. 4.7.7.

Figure 117. Spatial Variability tab

4.7.1 Import FB-Deep Output Button

Positioned in the upper portion of the Spatial Variability tab is the Import FB-Deep Output button and a paired progress bar (Fig. 118). Pressing the Import FB-Deep Output button opens a menu which allows for the directory containing the model analysis output files of interest to be selected. After the files are imported, the progress bar will become fully green.

Figure 118. Import FB-Deep Output button and progress bar

4.7.2 Plot Legend Frame

The Plot Legend frame allows for the user to select whether or not Side (side friction), Tip (end bearing), and/or Total (total resistance) data points appear on the plots of mean, variance, coefficient of variation, and phi (Fig. 119).
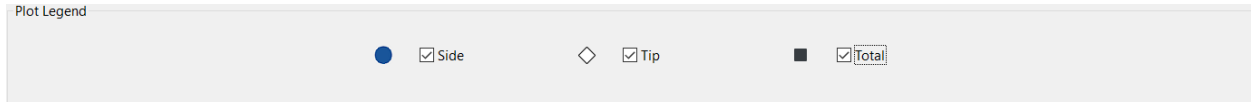
Figure 119. Plot Legend frame

4.7.3 Mean Plot

The Mean plot displays through-depth mean values of one or more of side friction, end bearing, and total resistance. A plot obtained using an illustrative data set is given in Fig. 120. Checking the Custom Abscissa box allows for the abscissa axis to be redrawn using the values input for Max and number of Tick Marks.
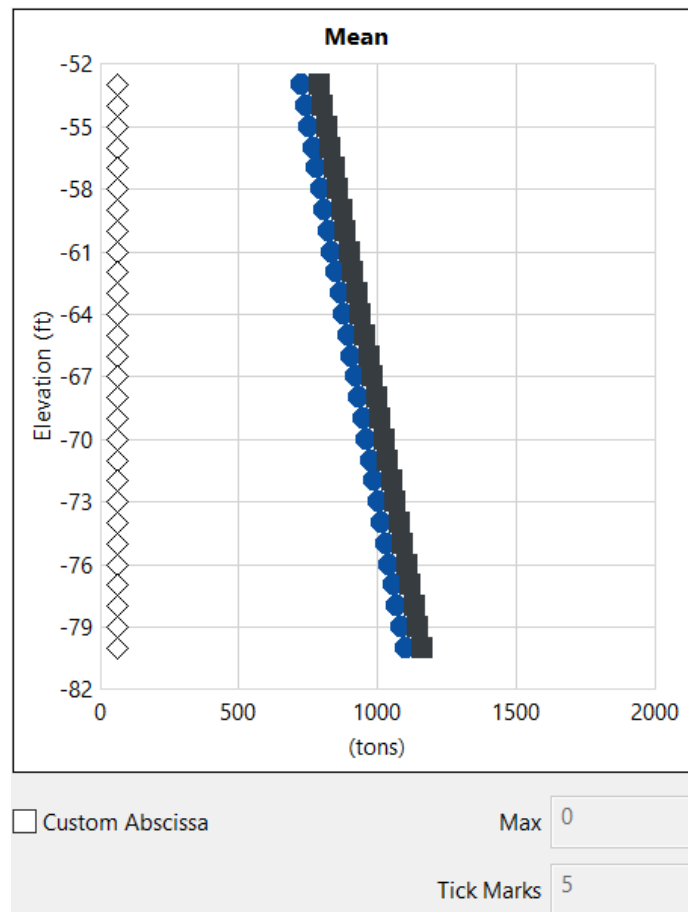
Figure 120. Elevation vs. mean value of axial resistance plot (data for illustration only)

4.7.4 Variance Plot

The Variance plot displays through-depth variances for any (or all) of side friction, end bearing, and total resistance. A plot obtained using an illustrative data set is given in Fig. 121. Checking the Custom Abscissa box allows for the abscissa axis to be redrawn using the values input for Max and number of Tick Marks.
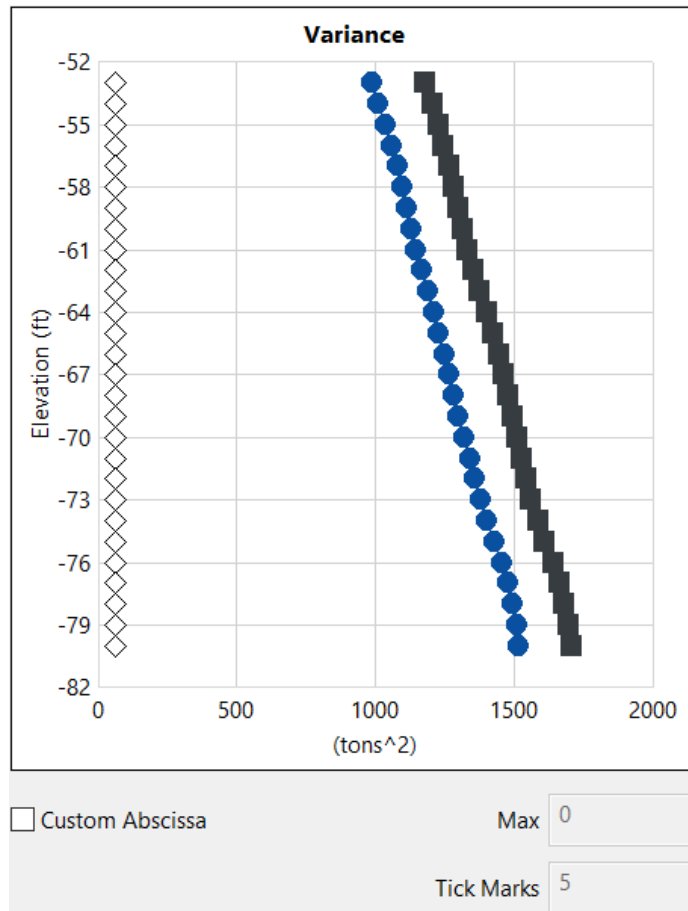
Figure 121. Elevation vs. variance of axial resistance plot (data for illustration only)

4.7.5 Coefficient of Variation Plot

The Coefficient of Variation plot displays through-depth coefficients of variation for side friction, end bearing, and total resistance (or any combination thereof). A plot obtained using an illustrative data set is given in Fig. 122. Checking the Custom Abscissa box allows for the abscissa axis to be redrawn using the values input for Max and number of Tick Marks.
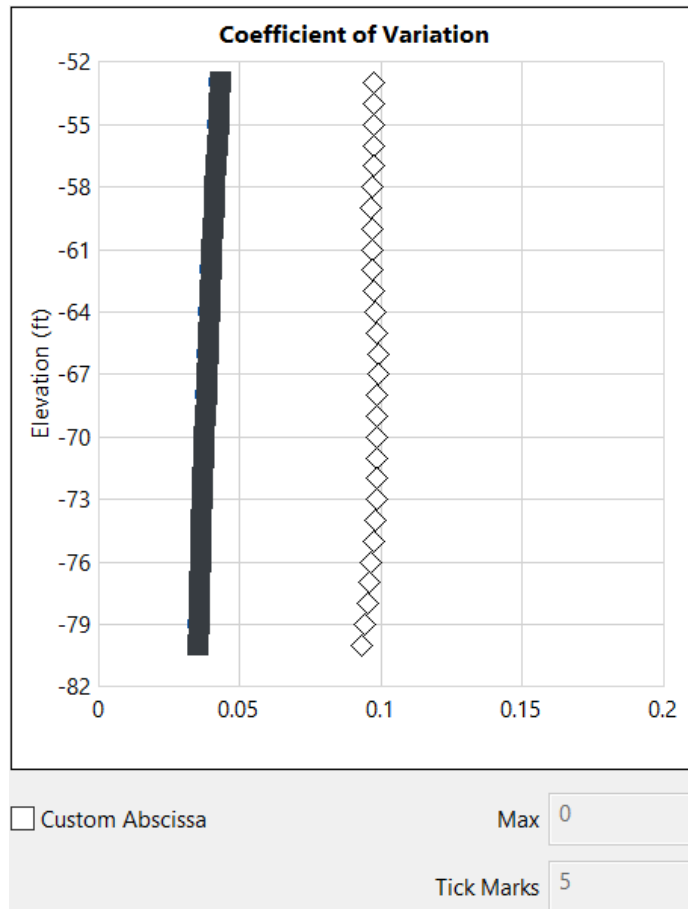
Figure 122. Elevation vs. coefficient of variation of axial resistance plot (data for illustration only)

4.7.6 Phi Plot

The Phi plot displays through-depth mean values of any one (or more) of side friction, end bearing, and total resistance. A plot obtained using an illustrative data set is given in (Fig. 123). Checking the Custom Abscissa box allows for the abscissa axis to be redrawn using the values input for Max and number of Tick Marks.

Note that the resistance (i.e., phi, or φ) factors plotted on the Spatial Variability page only take into account the spatial correlation structures associated with the selected site data (and given some layering and set of foundation member parameter values). Calculation and plotting of quantities that incorporate both spatial variability and method error phenomena are documented in Sec. 4.9.
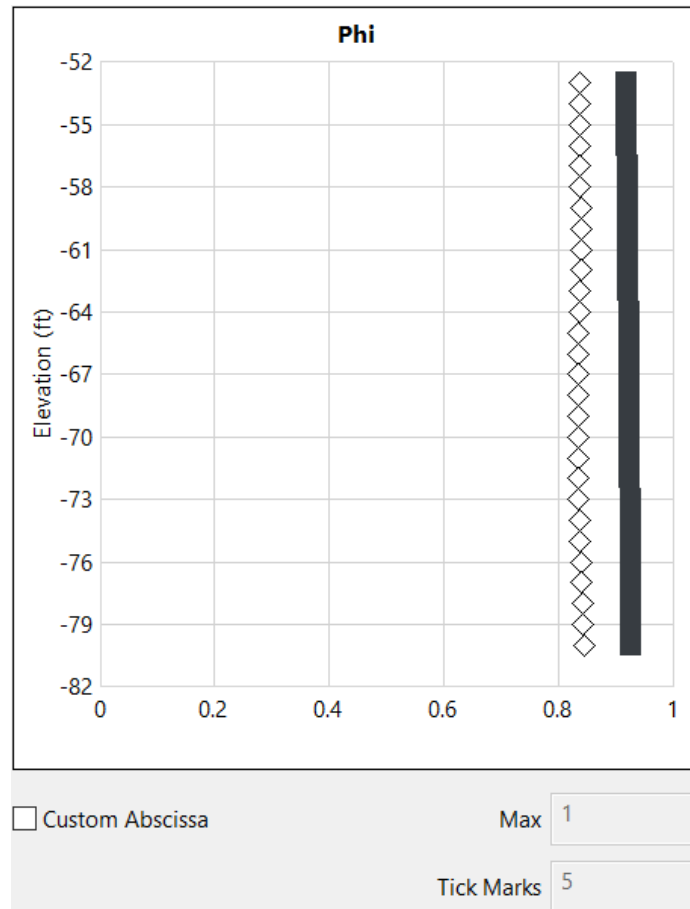
Figure 123. Elevation vs. soil resistance factor (Phi) plot based on soil-spatial variability (data for illustration only)

4.7.7 Update Plots and Export Buttons

The Update Plots button (Fig. 124, left) allows for the engineer to, respectively, update the Mean, Variance, Coefficient of Variation, and Phi plots (recall Fig. 120 to Fig. 123) to account for plot view modifications, such as those that can be made in the Plot Legend frame (Fig. 119). Upon pressing the Update Plots button, all plots in the Spatial Variability tab are redrawn.

Figure 124. Update Plots and Export buttons

Data presented in all plots of the Spatial Variability page can be exported to an Excel file by pressing the Export button (Fig. 124, right). The generated Excel file is exported to the same folder as the model analysis files. Further, the Excel file is populated with four worksheet tabs: "Mean", "Variance", "Coefficient of Variation", and "Phi".

The "Mean" Excel tab contains elevation in column "A", mean side resistance in column "B", mean tip resistance in column "C", and mean total resistance in column "D". Listings obtained using an illustrative data set are given in Fig. 125.

	A	B	C	D
1				
2	Elevation	Side	Tip	Total
3	ft | m	(tons | kN)	(tons | kN)	(tons | kN)
4	-52.0000	715.3307	61.9803	777.3112
5	-53.0000	729.0517	62.0192	791.0708
6	-54.0000	742.8179	62.0541	804.8722
7	-55.0000	756.5368	62.0878	818.6249
8	-56.0000	770.3263	62.0573	832.3836
9	-57.0000	784.1080	62.0116	846.1195
10	-58.0000	797.8517	62.0092	859.8608
11	-59.0000	811.5721	62.0089	873.5810
12	-60.0000	825.3808	61.9884	887.3695
13	-61.0000	839.1620	61.9827	901.1446
14	-62.0000	852.9217	61.9952	914.9170
15	-63.0000	866.7356	62.0091	928.7446
16	-64.0000	880.5876	62.0093	942.5970
17	-65.0000	894.4061	62.0070	956.4128
18	-66.0000	908.1557	62.0115	970.1673
19	-67.0000	921.7966	62.0420	983.8387
20	-68.0000	935.4840	62.0665	997.5504
21	-69.0000	949.2276	62.0803	1011.3079
22	-70.0000	962.9460	62.1057	1025.0515
23	-71.0000	976.6798	62.1474	1038.8273
24	-72.0000	990.4689	62.1539	1052.6227
25	-73.0000	1004.3102	62.1309	1066.4413
26	-74.0000	1018.1675	62.0752	1080.2428
27	-75.0000	1031.9536	62.0237	1093.9774
28	-76.0000	1045.7255	61.9982	1107.7240
29	-77.0000	1059.5263	61.9943	1121.5206
30	-78.0000	1073.3043	61.9856	1135.2901
31	-79.0000	1087.0880	61.9718	1149.0599
32	-80.0000	1100.8621	61.9463	1162.8083

Figure 125. "Mean" Excel tab (data for illustration only)

The "Variance" Excel tab contains elevation in column "A", variance in side resistance in column "B", variance in tip resistance in column "C", and variance in total resistance in column "D". Example listings, obtained using illustrative data, are provided in Fig. 126.

	A	B	C	D
1				
2	Elevation	Side	Tip	Total
3	ft | m	(tons^2 | kN^2)	(tons^2 | kN^2)	(tons^2 | kN^2)
4	-52.0000	965.0134	36.7392	1154.9273
5	-53.0000	987.6280	36.7297	1179.7413
6	-54.0000	1012.7749	36.7383	1204.5806
7	-55.0000	1040.4072	36.6237	1228.9500
8	-56.0000	1062.3999	36.5102	1247.0316
9	-57.0000	1082.3146	36.5054	1265.3348
10	-58.0000	1100.7550	36.1815	1284.0508
11	-59.0000	1116.9145	36.0011	1302.0908
12	-60.0000	1131.3511	36.0277	1317.9376
13	-61.0000	1146.7989	36.0126	1333.2580
14	-62.0000	1167.9382	36.0090	1354.6643
15	-63.0000	1188.7063	36.4458	1376.7382
16	-64.0000	1211.7584	36.8556	1402.0266
17	-65.0000	1231.3897	37.5451	1425.8630
18	-66.0000	1248.4511	37.8737	1446.6519
19	-67.0000	1264.6017	37.6864	1464.1869
20	-68.0000	1283.0687	37.6949	1481.7883
21	-69.0000	1301.2852	37.5781	1496.3628
22	-70.0000	1322.7690	37.5485	1512.7106
23	-71.0000	1341.6561	37.6498	1527.3092
24	-72.0000	1359.9350	37.7574	1544.3529
25	-73.0000	1380.6204	37.6971	1563.6453
26	-74.0000	1403.8766	37.0751	1587.4032
27	-75.0000	1429.2978	36.4488	1612.4476
28	-76.0000	1457.3072	35.9770	1641.6782
29	-77.0000	1477.7763	35.4927	1662.9760
30	-78.0000	1495.9105	34.8781	1679.9448
31	-79.0000	1510.4487	34.0947	1695.4904
32	-80.0000	1520.0179	33.4580	1707.3147

Figure 126. "Variance" Excel tab (data for illustration only)

The "Coefficient of Variation" tab contains elevation in column "A", coefficient of variation for side resistance in column "B", coefficient of variation for tip resistance in column "C", and coefficient of variation for total resistance in column "D". Example data are listed (for illustration) in Fig. 127.

	A	B	C	D
1				
2	Elevation	Side	Tip	Total
3	ft | m			
4	-52.0000	0.0434	0.0978	0.0437
5	-53.0000	0.0431	0.0977	0.0434
6	-54.0000	0.0428	0.0977	0.0431
7	-55.0000	0.0426	0.0975	0.0428
8	-56.0000	0.0423	0.0974	0.0424
9	-57.0000	0.0420	0.0974	0.0420
10	-58.0000	0.0416	0.0970	0.0417
11	-59.0000	0.0412	0.0968	0.0413
12	-60.0000	0.0408	0.0968	0.0409
13	-61.0000	0.0404	0.0968	0.0405
14	-62.0000	0.0401	0.0968	0.0402
15	-63.0000	0.0398	0.0974	0.0400
16	-64.0000	0.0395	0.0979	0.0397
17	-65.0000	0.0392	0.0988	0.0395
18	-66.0000	0.0389	0.0992	0.0392
19	-67.0000	0.0386	0.0989	0.0389
20	-68.0000	0.0383	0.0989	0.0386
21	-69.0000	0.0380	0.0987	0.0383
22	-70.0000	0.0378	0.0987	0.0379
23	-71.0000	0.0375	0.0987	0.0376
24	-72.0000	0.0372	0.0989	0.0373
25	-73.0000	0.0370	0.0988	0.0371
26	-74.0000	0.0368	0.0981	0.0369
27	-75.0000	0.0366	0.0973	0.0367
28	-76.0000	0.0365	0.0967	0.0366
29	-77.0000	0.0363	0.0961	0.0364
30	-78.0000	0.0360	0.0953	0.0361
31	-79.0000	0.0358	0.0942	0.0358
32	-80.0000	0.0354	0.0934	0.0355

Figure 127. "Coefficient of Variation" Excel tab (data for illustration only)

The "Phi" tab contains listings of elevation in column "A", phi for side resistance in column "B", phi for tip resistance in column "C", and phi for total resistance in column "D". The worksheet layout and illustrative data are depicted in Fig. 128.

	A	B	C	D
1				
2	**Elevation**	**Side**	**Tip**	**Total**
3	**ft | m**			
4	-52.0000	0.9196	0.8375	0.9193
5	-53.0000	0.9200	0.8377	0.9196
6	-54.0000	0.9202	0.8377	0.9199
7	-55.0000	0.9205	0.8381	0.9203
8	-56.0000	0.9208	0.8383	0.9207
9	-57.0000	0.9212	0.8382	0.9211
10	-58.0000	0.9216	0.8389	0.9215
11	-59.0000	0.9220	0.8394	0.9219
12	-60.0000	0.9225	0.8392	0.9223
13	-61.0000	0.9229	0.8393	0.9227
14	-62.0000	0.9232	0.8393	0.9230
15	-63.0000	0.9235	0.8383	0.9233
16	-64.0000	0.9237	0.8373	0.9235
17	-65.0000	0.9240	0.8357	0.9238
18	-66.0000	0.9244	0.8349	0.9241
19	-67.0000	0.9247	0.8355	0.9244
20	-68.0000	0.9250	0.8355	0.9247
21	-69.0000	0.9253	0.8358	0.9250
22	-70.0000	0.9255	0.8360	0.9253
23	-71.0000	0.9258	0.8358	0.9256
24	-72.0000	0.9260	0.8356	0.9259
25	-73.0000	0.9262	0.8357	0.9262
26	-74.0000	0.9264	0.8370	0.9264
27	-75.0000	0.9266	0.8383	0.9265
28	-76.0000	0.9267	0.8394	0.9266
29	-77.0000	0.9269	0.8405	0.9269
30	-78.0000	0.9272	0.8420	0.9271
31	-79.0000	0.9274	0.8439	0.9273
32	-80.0000	0.9277	0.8454	0.9276

Figure 128. "Phi" Excel tab (data for illustration only)

4.8 Method Error Tab

Shown in Fig. 129 is the Method Error tab, which allows for either default or custom adjustments (e.g., those based on load test data) to be made on the simulation results. In turn, these adjustments (intercept, slope, and dispersion) provide a means of accounting for the uncertainty associated with use of various empirical methods for calculating axial resistance.

There are four distinct regions of user input data in this tab: (1) Driven Pile frame; (2) Drilled Shaft frame; (3) Limestone frame; and, (5) Process Method Error button (all highlighted in Fig. 129). The five regions of the Method Error tab are discussed in Sec. 4.8.1 through Sec. 4.8.4.
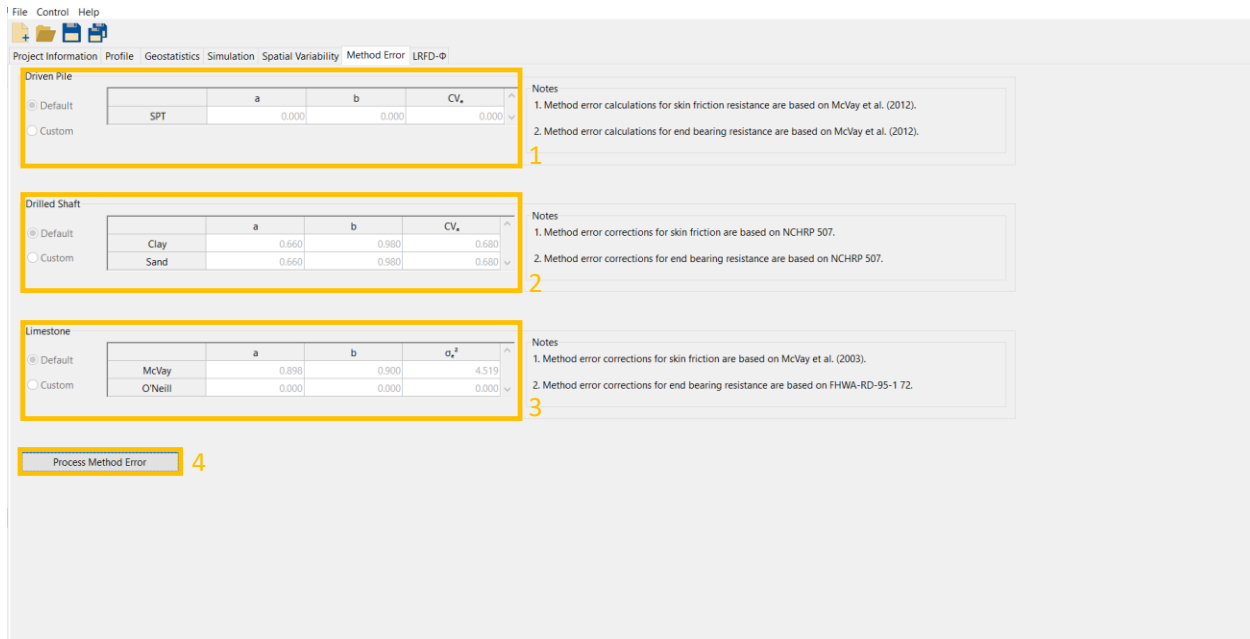
Figure 129. Method Error tab

4.8.1 Driven Pile Frame

Contained within the Driven Pile frame (Fig. 130) is method error input data specific to driven pile foundations. As presented in McVay et al. (2012), and implemented in GeoStat, method error parameters for driven piles operate on "SPT" values. The form of the method error adjustments for driven piles includes an intercept (a), slope (b), and coefficient of variation (CV_e). If the foundation type being considered is a driven pile, then either default or custom values (i.e., corrections derived from load-tests) for the method error parameters may be entered by selecting "Custom" and then entering the desired values. If the Default radio button is selected, then the parameters table will be disabled, signifying that no additional input is required. Further, input controls located within the Driven Pile frame are not enabled if the foundation type being considered is not that of driven pile.
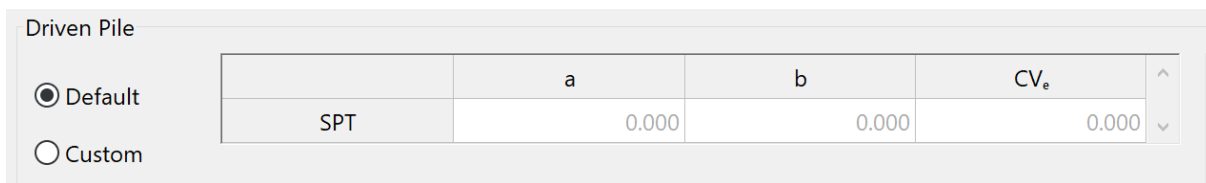
Figure 130. Driven Pile frame

4.8.2 Drilled Shaft Frame

Contained within the Drilled Shaft frame (Fig. 131) is method error input data specific to drilled shaft foundations embedded in Clay or Sand layers. Accordingly, method error parameters, as identified in McVay et al. (2012), operate on one (or both) of "Clay" layer data and/or "Sand"

101

layer data. Inputs include an "Exponent for Exponential" (a), "Exponent for Power" (b), and "Coefficient of Variation" (CV_e). Note that "CV_e" is used here instead of "COV" to distinguish that this instance of coefficient of variation is specific to method error calculations. If the foundation type being considered is a drilled shaft, then default or custom values (i.e., from load-test data) for the method error parameters may be entered by selecting "Custom" and then entering the desired values (no values are required to be input otherwise). Controls located within the Drilled Shaft frame are not enabled if the foundation type being considered is not that of drilled shaft.

Figure 131. Drilled Shaft frame

4.8.3 Limestone Frame

Contained within the Limestone frame (Fig. 132) is method error input data for when one or more layers of "Limestone" are defined in the soil layer profile of the GeoStat model, and a drilled shaft foundation is being considered. The GeoStat software adopts a method error approach based on that documented in McVay et al. (2012) for limestone layers of drilled shaft foundations. More specifically, parameters make use of the "McVay" approach for side resistance and the "O'Neill" approach for end resistance. As an exception, the O'Neill term for "a" is defaulted to zero. The default value of zero is used here to prevent potentially unconservative adjustments to computed capacities when tip resistance does not significantly contribute to total resistance.

Figure 132. Limestone frame

Inputs for these two approaches include intercept ("a"), slope ("b"), and method error ("σ_e^2") values. If no limestone layers are defined for the foundation soil layering, then all values within this data subset may be left blank or input as zero. If there are limestone layers defined for the foundation soil layering (and the foundation type being considered is that of drilled shaft), then custom values for the method error parameters may be entered by selecting "Custom" and then entering the desired values. In this context, custom values are often based on load tests.

102

4.8.4 Process Method Error Button

The Process Method Error button (recall Fig. 129, bottom) is used to accept the applicable inputs present in the Driven Pile frame, Drilled Shaft frame, and the Limestone frame.

4.9 LRFD-ɸ Tab

The seventh and final (rightmost) tab in the GeoStat UI (Fig. 133) is the LRFD-ɸ tab, which contains profile plots of mean-valued resistance, coefficients of variation, resistance (ɸ) factors, and factored resistance. Further, plots located within the LRFD-ɸ tab include both the axial resistance quantities associated with spatial variability as well as those of combined spatial variability and method error. If adequate post-processing has not occurred upon reaching this tab, then the UI will issue a warning message in lieu of attempting to generate the summary plots. Examples of inadequacies in post-processing that are detected (when present) include: no results data have been loaded from the Spatial Variability tab; or, the method error has not yet been processed.

There are two distinct regions of user input data in LRFD-ɸ tab: (1) Plot Type dropdown menu (2) Plot Legend frame (both highlighted in Fig. 133). There are also four distinct regions of output in this tab: (3) Update Plots and Export buttons; (4) Side Resistance plot; (5) Tip Resistance plot; and, (6) Total Resistance plot (all highlighted in Fig. 133). The six tab regions are discussed in Sec. 4.9.1 through Sec. 4.9.6.
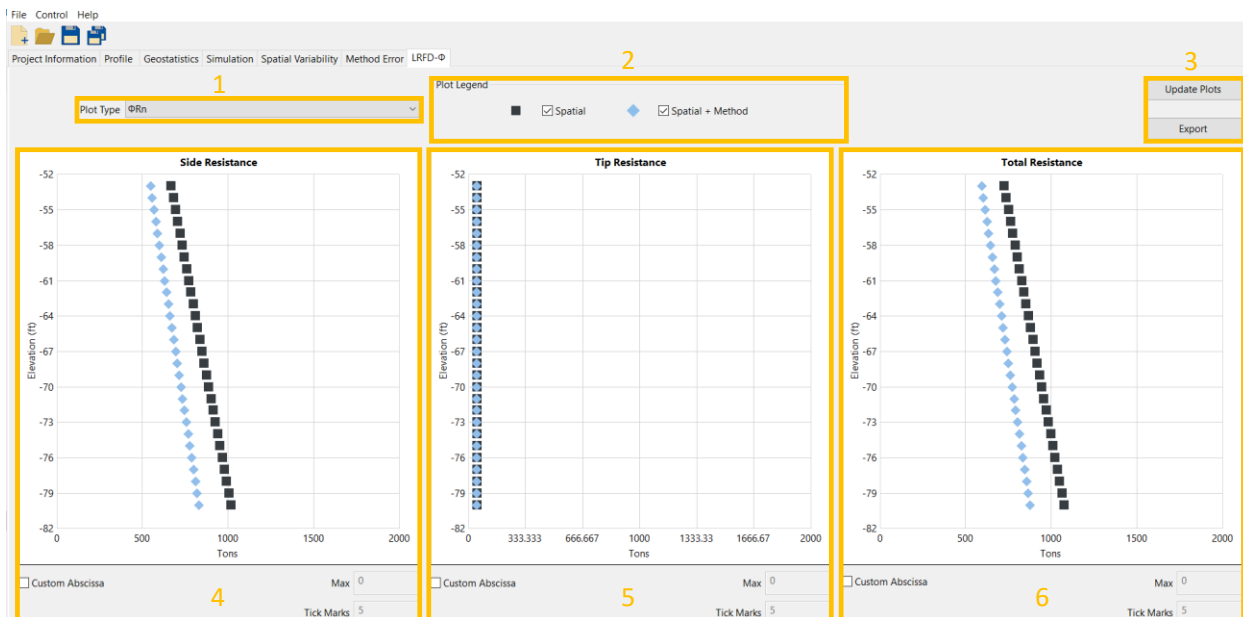
Figure 133. LRFD-ɸ tab

4.9.1 Plot Type

The Plot Type dropdown menu (Fig. 134) allows for the engineer to select which type of data is to be presented in the Side Resistance plot (see Sec. 4.9.3), the Tip Resistance plot (Sec. 4.9.4), and the Total Resistance plot (Sec. 4.9.5). The options available for plot type are Mean, Coefficient of Variation, Estimated ϕ, and ϕRn.
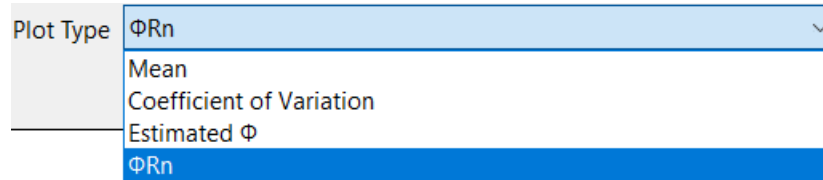
Figure 134. Plot Type dropdown menu

4.9.2 Plot Legend Frame

The Plot Legend frame (Fig. 135) allows for the engineer to select any combination of the Spatial and/or Spatial + Method curves for display in the side, tip, and total resistance plots.
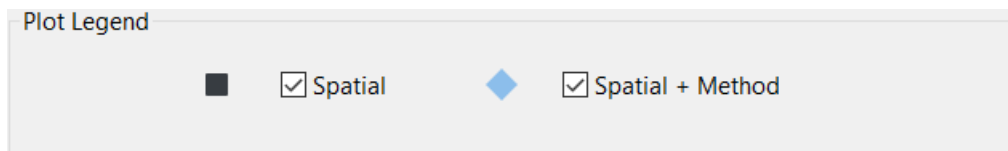
Figure 135. Plot Legend frame

4.9.3 Side Resistance Plot

The Side Resistance plot (Fig. 136) displays the mean, variance, coefficient of variation, or Phi for side resistance. The plots are generated with respect to elevation, and may include only spatial variability and/or combined spatial variability and method error. The curves displayed in the Side Resistance plot vary depending on which settings are chosen in the Plot Type dropdown menu (Fig. 134) and the Plot Legend frame (Fig. 135). In addition, checking the Custom Abscissa box (Fig. 136, bottom-left) allows for the curve(s) to be redrawn along an updated abscissa axis using the values input for Max and number of Tick Marks. Note that program-generated resistance (ϕ) factors should only be used in conjunction with Owner's guidelines.

104
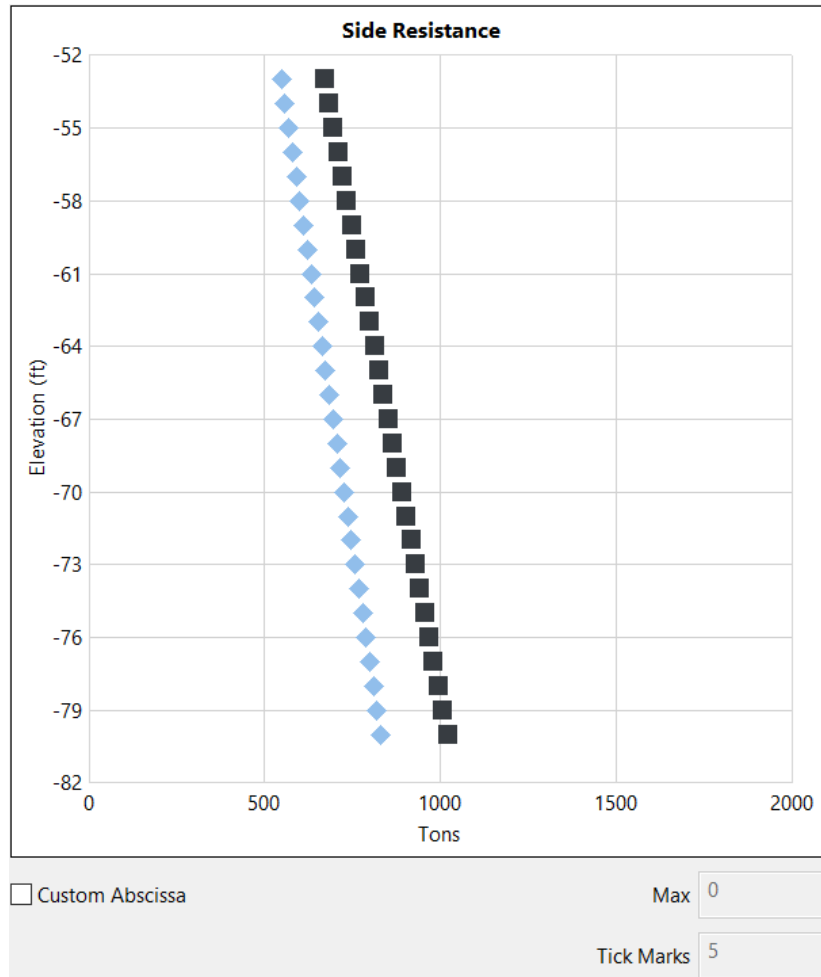
Figure 136. Side Resistance plot (data for illustration only)

4.9.4 Tip Resistance Plot

The Side Resistance plot (Fig. 137) displays the mean, variance, coefficient of variation, or Phi for side resistance. The plots are generated with respect to elevation, and may include only spatial variability and/or combined spatial variability and method error. The curves displayed in the Tip Resistance plot vary depending on which settings are chosen in the Plot Type dropdown menu (Fig. 134) and the Plot Legend frame (Fig. 135). In addition, checking the Custom Abscissa box (Fig. 137, bottom-left) allows for the curve(s) to be redrawn along an updated abscissa axis using the values input for Max and number of Tick Marks. Note that program-generated resistance (ϕ) factors should only be used in conjunction with Owner's guidelines. Also, note that the illustrative plot here indicates relatively low tip resistance. For driven piles and drilled shafts that terminate in sand and clay layers, tip resistance is determined based on realizations of through-depth profiles of SPT blow counts. For drilled shafts terminating in rock, mass modulus (E_m) influences computed tip resistance. See Ch. 5 and the Technical Manual for additional details.
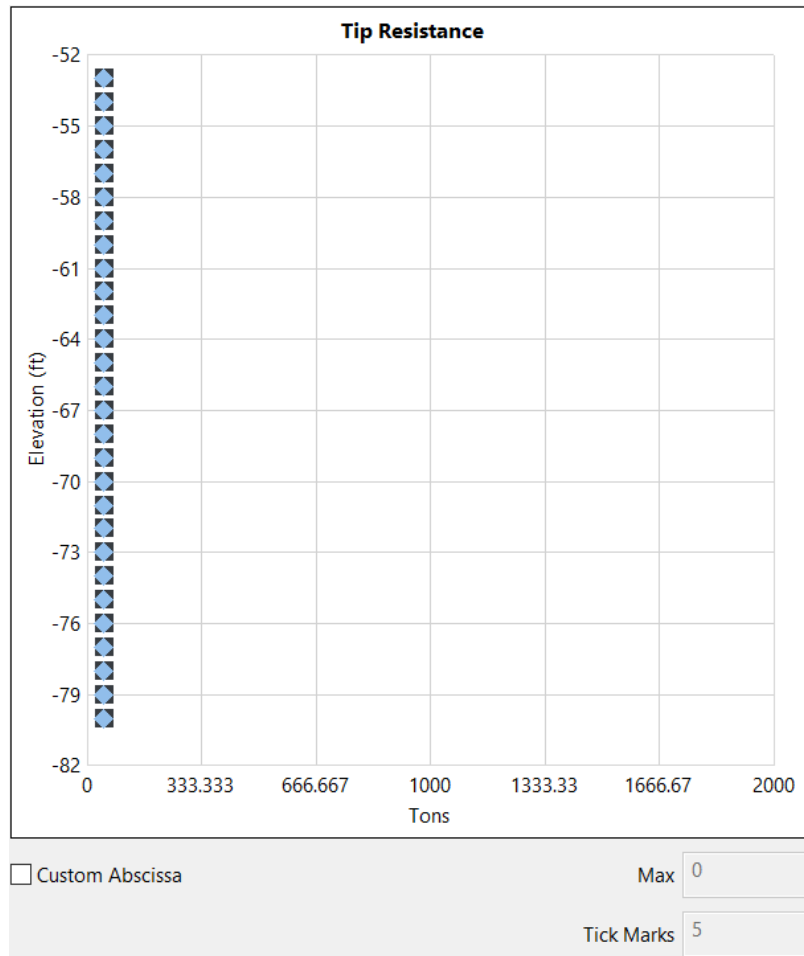
Figure 137. Tip Resistance plot (data for illustration only)

4.9.5 Total Resistance Plot

The Total Resistance plot (Fig. 138) displays the mean, variance, coefficient of variation, or Phi for total resistance. The plots are generated with respect to elevation, and may include only spatial variability and/or combined spatial variability and method error. Note that the total resistance curves are not produced via simple summation of side and tip resistance curves, but rather, total resistances are determined for each model analysis file analyzed, and only then are total resistance quantities (e.g., mean values vs. elevation) formed.

The curves displayed in the Tip Resistance plot vary depending on which settings are chosen in the Plot Type dropdown menu (Fig. 134) and the Plot Legend frame (Fig. 135). In addition, checking the Custom Abscissa box (Fig. 138, bottom-left) allows for the curve(s) to be redrawn along an updated abscissa axis using the values input for Max and number of Tick Marks. Note that program-generated resistance (ϕ) factors should only be used in conjunction with Owner's guidelines.

106
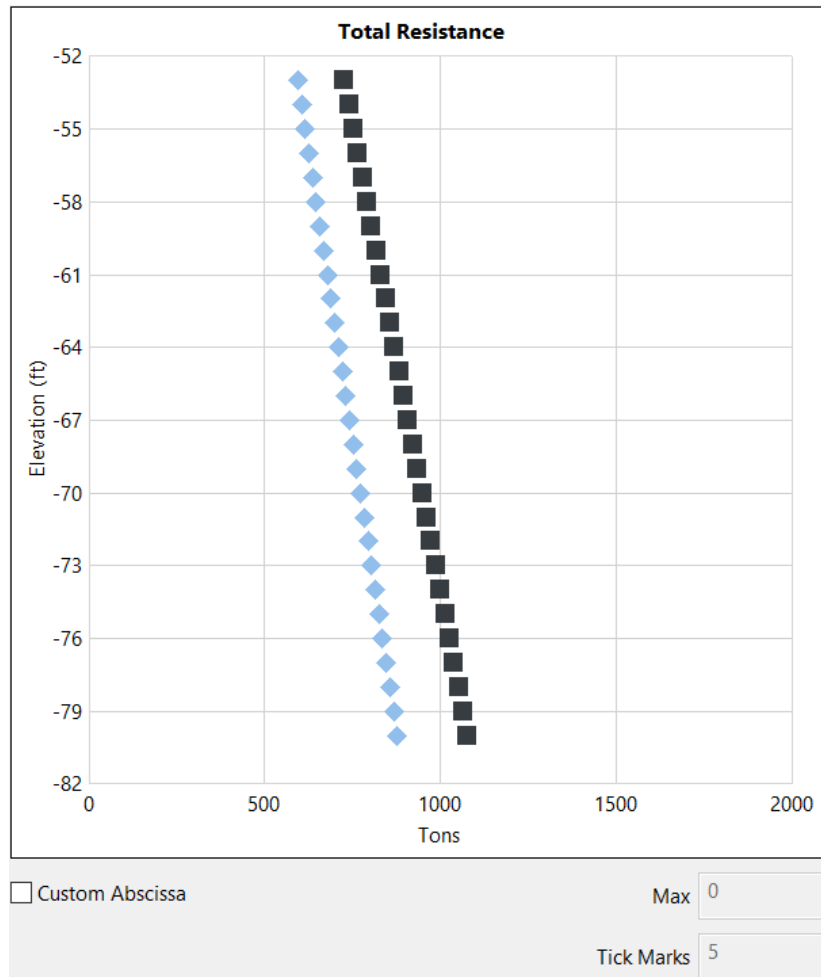
Figure 138. Total Resistance plot (data for illustration only)

4.9.6 Update Plots and Export Buttons

The Update Plots button (Fig. 139, left) allows for the engineer to, respectively, update the Side, Tip, and Total resistance plots (recall Fig. 136 to Fig. 138) to account for plot view modifications, such as those that can be made in the Plot Legend frame (Fig. 135). Upon pressing the Update Plots button, all plots in the LRFD-ϕ tab are redrawn.

Figure 139. Update Plots and Export button

Data plotted in the LRFD-ϕ tab can be exported to an Excel file by pressing the Export button (Fig. 139, right). The generated Excel file is exported to the same folder as the model analysis

files. Further, four worksheet tabs are contained within the Excel worksheet: "Mean", "Coefficient of Variation", "Phi", and "PhiRn".

The "Mean" Excel tab contains the elevation in column "A"; mean side resistance (spatial only) in column "B"; mean side resistance with both spatial variability and method error in column "C"; mean tip resistance (spatial only) in column "D"; mean tip resistance with both spatial variability and method error in column "E"; mean total resistance (spatial only) in column "F", and, the mean total resistance with both spatial variability and method error in column "G". The Excel tab format, along with a listing of illustrative data, is provided in Fig. 140.

	A	B	C	D	E	F	G
1							
2	Elevation	Side Spatial	Side Spatial + Method	Tip Spatial	Tip Spatial + Method	Total Spatial	Total Spatial + Method
3	ft | m	(tons | kN)	(tons | kN)	(tons | kN)	(tons | kN)	(tons | kN)	(tons | kN)
4	-52.0000	715.3307	847.8850	61.9803	73.4656	777.3112	921.3507
5	-53.0000	729.0517	864.1485	62.0192	73.5117	791.0708	937.6601
6	-54.0000	742.8179	880.4657	62.0541	73.5531	804.8722	954.0189
7	-55.0000	756.5368	896.7268	62.0878	73.5930	818.6249	970.3201
8	-56.0000	770.3263	913.0716	62.0573	73.5568	832.3836	986.6284
9	-57.0000	784.1080	929.4070	62.0116	73.5026	846.1195	1002.9096
10	-58.0000	797.8517	945.6975	62.0092	73.4998	859.8608	1019.1972
11	-59.0000	811.5721	961.9603	62.0089	73.4994	873.5810	1035.4598
12	-60.0000	825.3808	978.3278	61.9884	73.4752	887.3695	1051.8034
13	-61.0000	839.1620	994.6628	61.9827	73.4684	901.1446	1068.1310
14	-62.0000	852.9217	1010.9723	61.9952	73.4832	914.9170	1084.4555
15	-63.0000	866.7356	1027.3459	62.0091	73.4996	928.7446	1100.8455
16	-64.0000	880.5876	1043.7648	62.0093	73.4999	942.5970	1117.2649
17	-65.0000	894.4061	1060.1439	62.0070	73.4971	956.4128	1133.6407
18	-66.0000	908.1557	1076.4413	62.0115	73.5026	970.1673	1149.9440
19	-67.0000	921.7966	1092.6100	62.0420	73.5387	983.8387	1166.1488
20	-68.0000	935.4840	1108.8337	62.0665	73.5677	997.5504	1182.4013
21	-69.0000	949.2276	1125.1241	62.0803	73.5841	1011.3079	1198.7081
22	-70.0000	962.9460	1141.3845	62.1057	73.6142	1025.0515	1214.9985
23	-71.0000	976.6798	1157.6633	62.1474	73.6636	1038.8273	1231.3270
24	-72.0000	990.4689	1174.0076	62.1539	73.6713	1052.6227	1247.6788
25	-73.0000	1004.3102	1190.4138	62.1309	73.6441	1066.4413	1264.0581
26	-74.0000	1018.1675	1206.8389	62.0752	73.5781	1080.2428	1280.4170
27	-75.0000	1031.9536	1223.1796	62.0237	73.5170	1093.9774	1296.6968
28	-76.0000	1045.7255	1239.5035	61.9982	73.4867	1107.7240	1312.9907
29	-77.0000	1059.5263	1255.8617	61.9943	73.4822	1121.5206	1329.3438
30	-78.0000	1073.3043	1272.1927	61.9856	73.4719	1135.2901	1345.6648
31	-79.0000	1087.0880	1288.5307	61.9718	73.4555	1149.0599	1361.9862
32	-80.0000	1100.8621	1304.8572	61.9463	73.4252	1162.8083	1378.2823

Figure 140. "Mean" Excel tab (data for illustration only)

The "Coefficient of Variation" Excel tab contains the elevation in column "A"; coefficient of variation for side resistance (spatial only) in column "B"; coefficient of variation for side resistance with both spatial variability and method error in column "C"; coefficient of variation for tip resistance (spatial only) in column "D"; coefficient of variation for tip resistance with both spatial variability and method error in column "E"; coefficient of variation for total resistance (spatial only) in column "F", and, the coefficient of variation for total resistance with both spatial variability and method error in column "G". The Excel tab format and illustrative data are provided in Fig. 141.

	A	B	C	D	E	F	G
2	Elevation	Side Spatial	Side Spatial + Method	Tip Spatial	Tip Spatial + Method	Total Spatial	Total Spatial + Method
3	ft | m						
4	-52.0000	0.0434	0.2071	0.0978	0.2249	0.0437	0.2071
5	-53.0000	0.0431	0.2070	0.0977	0.2248	0.0434	0.2071
6	-54.0000	0.0428	0.2070	0.0977	0.2248	0.0431	0.2070
7	-55.0000	0.0426	0.2069	0.0975	0.2247	0.0428	0.2070
8	-56.0000	0.0423	0.2069	0.0974	0.2247	0.0424	0.2069
9	-57.0000	0.0420	0.2068	0.0974	0.2247	0.0420	0.2068
10	-58.0000	0.0416	0.2067	0.0970	0.2245	0.0417	0.2067
11	-59.0000	0.0412	0.2066	0.0968	0.2244	0.0413	0.2066
12	-60.0000	0.0408	0.2065	0.0968	0.2244	0.0409	0.2066
13	-61.0000	0.0404	0.2065	0.0968	0.2244	0.0405	0.2065
14	-62.0000	0.0401	0.2064	0.0968	0.2244	0.0402	0.2064
15	-63.0000	0.0398	0.2063	0.0974	0.2247	0.0400	0.2064
16	-64.0000	0.0395	0.2063	0.0979	0.2249	0.0397	0.2063
17	-65.0000	0.0392	0.2062	0.0988	0.2253	0.0395	0.2063
18	-66.0000	0.0389	0.2062	0.0992	0.2255	0.0392	0.2062
19	-67.0000	0.0386	0.2061	0.0989	0.2254	0.0389	0.2062
20	-68.0000	0.0383	0.2061	0.0989	0.2254	0.0386	0.2061
21	-69.0000	0.0380	0.2060	0.0987	0.2253	0.0383	0.2061
22	-70.0000	0.0378	0.2060	0.0987	0.2252	0.0379	0.2060
23	-71.0000	0.0375	0.2059	0.0987	0.2253	0.0376	0.2059
24	-72.0000	0.0372	0.2059	0.0989	0.2253	0.0373	0.2059
25	-73.0000	0.0370	0.2058	0.0988	0.2253	0.0371	0.2058
26	-74.0000	0.0368	0.2058	0.0981	0.2250	0.0369	0.2058
27	-75.0000	0.0366	0.2058	0.0973	0.2247	0.0367	0.2058
28	-76.0000	0.0365	0.2057	0.0967	0.2244	0.0366	0.2058
29	-77.0000	0.0363	0.2057	0.0961	0.2241	0.0364	0.2057
30	-78.0000	0.0360	0.2057	0.0953	0.2238	0.0361	0.2057
31	-79.0000	0.0358	0.2056	0.0942	0.2233	0.0358	0.2056
32	-80.0000	0.0354	0.2056	0.0934	0.2230	0.0355	0.2056

Figure 141. "Coefficient of Variation" Excel tab (data for illustration only)

The "Phi" Excel tab contains the elevation in column "A"; phi (ϕ) for side resistance (spatial only) in column "B"; phi (ϕ) for side resistance with both spatial variability and method error in column "C"; phi (ϕ) for tip resistance (spatial only) in column "D"; phi (ϕ) for tip resistance with both spatial variability and method error in column "E"; phi (ϕ) for total resistance (spatial only) in column "F", and, the phi (ϕ) for total resistance with both spatial variability and method error in column "G". Excel tab formatting and illustrative data are provided in Fig. 142.

	A	B	C	D	E	F	G
2	Elevation	Side Spatial	Side Spatial + Method	Tip Spatial	Tip Spatial + Method	Total Spatial	Total Spatial + Method
3	ft | m						
4	-52.0000	0.9196	0.6344	0.8375	0.6035	0.9193	0.6343
5	-53.0000	0.9200	0.6345	0.8377	0.6035	0.9196	0.6344
6	-54.0000	0.9202	0.6346	0.8377	0.6036	0.9199	0.6345
7	-55.0000	0.9205	0.6347	0.8381	0.6037	0.9203	0.6346
8	-56.0000	0.9208	0.6348	0.8383	0.6038	0.9207	0.6348
9	-57.0000	0.9212	0.6349	0.8382	0.6037	0.9211	0.6349
10	-58.0000	0.9216	0.6351	0.8389	0.6041	0.9215	0.6350
11	-59.0000	0.9220	0.6352	0.8394	0.6042	0.9219	0.6352
12	-60.0000	0.9225	0.6354	0.8392	0.6042	0.9223	0.6353
13	-61.0000	0.9229	0.6355	0.8393	0.6042	0.9227	0.6354
14	-62.0000	0.9232	0.6356	0.8393	0.6042	0.9230	0.6355
15	-63.0000	0.9235	0.6357	0.8383	0.6038	0.9233	0.6356
16	-64.0000	0.9237	0.6358	0.8373	0.6034	0.9235	0.6357
17	-65.0000	0.9240	0.6359	0.8357	0.6027	0.9238	0.6358
18	-66.0000	0.9244	0.6360	0.8349	0.6024	0.9241	0.6359
19	-67.0000	0.9247	0.6361	0.8355	0.6026	0.9244	0.6360
20	-68.0000	0.9250	0.6362	0.8355	0.6026	0.9247	0.6361
21	-69.0000	0.9253	0.6363	0.8358	0.6028	0.9250	0.6362
22	-70.0000	0.9255	0.6364	0.8360	0.6028	0.9253	0.6363
23	-71.0000	0.9258	0.6365	0.8358	0.6028	0.9256	0.6364
24	-72.0000	0.9260	0.6365	0.8356	0.6027	0.9259	0.6365
25	-73.0000	0.9262	0.6366	0.8357	0.6027	0.9262	0.6366
26	-74.0000	0.9264	0.6367	0.8370	0.6032	0.9264	0.6367
27	-75.0000	0.9266	0.6367	0.8383	0.6038	0.9265	0.6367
28	-76.0000	0.9267	0.6368	0.8394	0.6042	0.9266	0.6367
29	-77.0000	0.9269	0.6368	0.8405	0.6047	0.9269	0.6368
30	-78.0000	0.9272	0.6369	0.8420	0.6053	0.9271	0.6369
31	-79.0000	0.9274	0.6370	0.8439	0.6061	0.9273	0.6370
32	-80.0000	0.9277	0.6371	0.8454	0.6067	0.9276	0.6371

Figure 142. "Phi" Excel tab (data for illustration only)

The "PhiRn" (i.e., the product of mean resistance and resistance factor, φ) Excel tab contains the elevation in column "A"; factored resistance for side resistance (spatial only) in column "B"; factored resistance for side resistance with both spatial variability and method error in column "C"; factored resistance for tip resistance (spatial only) in column "D"; factored resistance for tip resistance with both spatial variability and method error in column "E"; factored resistance for total resistance (spatial only) in column "F", and, the factored resistance for total resistance with both spatial variability and method error in column "G". Excel tab formatting and illustrative data are provided in Fig. 143.

	A	B	C	D	E	F	G
1							
2	Elevation	Side Spatial	Side Spatial + Method	Tip Spatial	Tip Spatial + Method	Total Spatial	Total Spatial + Method
3	ft | m	(tons | kN)	(tons | kN)	(tons | kN)	(tons | kN)	(tons | kN)	(tons | kN)
4	-52.0000	657.8182	537.8953	51.9100	44.3339	714.5639	584.4011
5	-53.0000	670.6927	548.3154	51.9507	44.3658	727.4759	594.8512
6	-54.0000	683.5707	558.7543	51.9848	44.3932	740.4306	605.3342
7	-55.0000	696.3654	569.1416	52.0358	44.4284	753.3481	615.7837
8	-56.0000	709.3271	579.6226	52.0217	44.4123	766.3699	626.2769
9	-57.0000	722.3171	590.1118	51.9761	44.3760	779.3656	636.7507
10	-58.0000	735.2950	600.5814	52.0216	44.3976	792.3599	647.2259
11	-59.0000	748.2866	611.0473	52.0480	44.4105	805.3433	657.6885
12	-60.0000	761.3894	621.5913	52.0234	44.3922	818.4238	668.2159
13	-61.0000	774.4485	632.1072	52.0199	44.3887	831.4974	678.7352
14	-62.0000	787.3999	642.5719	52.0331	44.3990	844.4814	689.2178
15	-63.0000	800.4105	653.0810	51.9824	44.3783	857.5101	699.7395
16	-64.0000	813.4256	663.6066	51.9221	44.3487	870.5197	710.2631
17	-65.0000	826.4597	674.1266	51.8186	44.2968	883.5156	720.7670
18	-66.0000	839.4647	684.6082	51.7752	44.2767	896.4945	731.2403
19	-67.0000	852.3774	695.0110	51.8334	44.3147	909.4366	741.6667
20	-68.0000	865.3021	705.4365	51.8569	44.3337	922.4159	752.1233
21	-69.0000	878.2845	715.9066	51.8880	44.3533	935.4776	762.6301
22	-70.0000	891.1987	726.3399	51.9181	44.3758	948.5019	773.1167
23	-71.0000	904.1635	736.7991	51.9455	44.4019	961.5780	783.6361
24	-72.0000	917.1897	747.3040	51.9364	44.3993	974.6414	794.1580
25	-73.0000	930.2350	757.8366	51.9219	44.3852	987.6990	804.6867
26	-74.0000	943.2635	768.3689	51.9566	44.3856	1000.6861	815.1809
27	-75.0000	956.1978	778.8364	51.9968	44.3898	1013.5949	825.6182
28	-76.0000	969.0884	789.2811	52.0408	44.4037	1026.4674	836.0459
29	-77.0000	982.1028	799.7856	52.1090	44.4360	1039.4829	846.5493
30	-78.0000	995.1241	810.2838	52.1921	44.4739	1052.5227	857.0514
31	-79.0000	1008.1942	820.8033	52.2961	44.5203	1065.5784	867.5598
32	-80.0000	1021.3131	831.3380	52.3668	44.5467	1078.6544	878.0677

Figure 143. "PhiRn" Excel tab (data for illustration only)

110

CHAPTER 5
GENERATION AND BATCH PROCESSING OF MODEL ANALYSIS FILES

5.1 Overview

Documented in Ch. 5 are those features implemented in the GeoStat software that serve to automate the process of creating analysis model files, and perform batch mode computation of the models to determine pile/shaft axial capacities. Those GeoStat UI controls that result in issuance of the system (batch) commands are identified in Sec. 5.2. Documentation is provided in Sec. 5.3 regarding necessary system commands that are issued (automatically) to "silently" perform analyses from within GeoStat. In addition, Ch. 5 documents the manner in which bulk post-processing of the analysis files is automatically carried out by the GeoStat software.

All analysis files created from within the GeoStat UI adhere to the input and output (ASCII) file formats of the pile/shaft axial-capacity calculation software, FB-Deep. Details regarding specific regions of interest within the output files for post-processing of pile analyses are given in Sec. 5.4. Similarly, Sec. 5.5 documents regions of interest in output files for post-processing of shaft analyses.

5.2 Generating Model Analysis Files

Positioned in the lower right portion the Simulation tab is the Run Simulation button (Fig. 144). Clicking the Run Simulation button prompts GeoStat to first generate the many realizations of soil or rock profiles, taking into account spatial variability phenomena. Next, a folder is created in the same directory as the GeoStat model file and is subsequently populated with model analysis files (one realization corresponds to one file). Note that the folder name issued is identical to the name of the currently loaded GeoStat model file. When combined with file saving features (such as "Save As"), engineers gain the ability to revisit or edit previously created GeoStat model files, and also, keep track of which GeoStat model file corresponds to a given collection of model analysis files (and analysis results).

The numerous model analysis files, all stored within the newly created folder, are named using a sequential numbering convention. For example, if 2,000 simulations are to be conducted, then files "1.in" through "2000.in" are created and stored within the dedicated folder for that batch of analyses. Note that if the folder already exists, then any pre-existing files within the folder are deleted prior to population of the model files. Therefore, it is useful to save a unique GeoStat input file for each unique instance of carrying out the simulations.
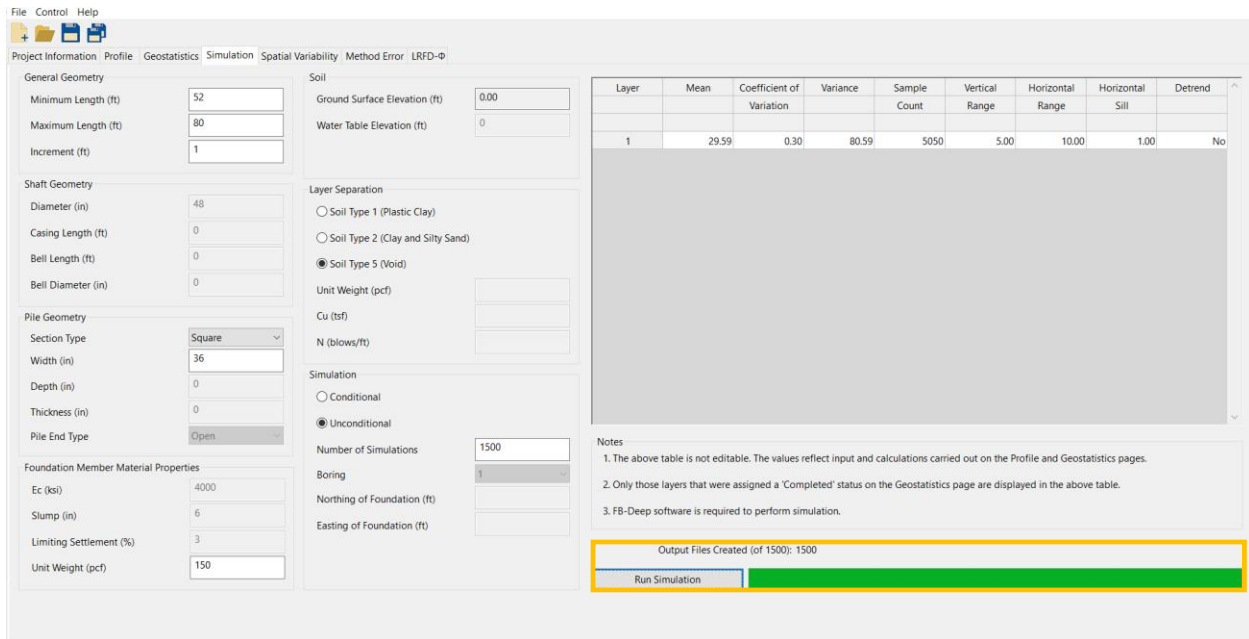
Figure 144. Generation (and analysis) of model analysis files in the Simulation tab

5.3 Running Batch Mode Analysis

As highlighted in Fig. 144, clicking the Run Simulation button performs the action of issuing the "silent" call to carry out batch mode analysis of all newly created analysis files. Clicking the Run Simulation button instructs the GeoStat software to carry out the desired number of realizations, package relevant parameters from each realization into model analysis files (which adhere to the formatting requirements of the FB-Deep software), and then issue the "silent" batch mode analysis command. Approximately 400-500 simulations can be completed per minute for both pile and shaft configurations (including consideration for generating realizations, creating the model analysis files, and running the analyses).

5.3.1 Batch Mode Syntax

By default, a call to "silently" perform batch mode analysis is issued through use of system commands. This "silent" functionality is leveraged in GeoStat to directly perform batch mode analysis (see the Program Settings options detailed in Ch. 1 for alternative approaches). Consequently, GeoStat can effectively employ axial capacity calculation algorithms such as those contained within software packages such as FB-Deep without requiring the engineer to manually open and operate external software packages (including the FB-Deep software).

The syntax of the system command is:

[*executable path*] B:1 N:[*number of simulations*] I:[*1.in path*]

112

where [*executable path*] is the full path to the executable performing the analysis, including the name of the executable file; [*number of simulations*] is the total number of simulations to conduct; [*1.in path*] is the full path to the model file named "1.in" (recall the discussion in Sec. 5.2), including the filename (1.in). The flag characters "B", "N", and "I" are required in all instances for the purpose of distinguishing each component of the command syntax.

5.4 Parsing Output for Pile Analysis

Highlighted in Fig. 145 is the region of interest within analysis output files (created during batch operations) that is specific to analysis of piles, and is used for the purpose of bulk importing data into the GeoStat UI. All data of interest reside within the output (.out) file region entitled "Driven Pile Capacity". More specifically, the Test Pile Length, Ultimate Side Friction, and Mobilized End Bearing quantities are parsed from the output file. Note that the output file formatting is consistent with that of FB-Deep output for driven pile analysis.

```
Driven Pile Capacity:
=====================


                        Section Type:  Round
                        Pile Width:    48.00 (in)



    Test    Pile   Ultimate  Mobilized  Estimated  Allowable   Ultimate
    Pile   Width      Side        End   Davisson       Pile       Pile
  Length           Friction    Bearing  Capacity   Capacity   Capacity
    (ft)    (in)     (tons)     (tons)    (tons)     (tons)     (tons)
   -----  ------  ---------- ---------- ---------- ---------- ----------
   50.00    48.0     553.86     601.35   1155.20     577.60    2357.90
   51.00    48.0     560.34     599.81   1160.16     580.08    2359.79
   52.00    48.0     566.82     598.39   1165.21     582.60    2362.00
   53.00    48.0     573.15     597.95   1171.10     585.55    2367.01
   54.00    48.0     579.47     597.54   1177.01     588.51    2372.10
   55.00    48.0     585.79     597.11   1182.90     591.45    2377.13
```

Figure 145. Example excerpt of pile analysis output that is read-in from the Spatial Variability tab

5.5 Parsing Output for Shaft Analysis

Depicted in Fig. 146 and Fig. 147 are excerpts from an illustrative output file, which was generated as part of analyzing a shaft foundation member (again, the output file formatting matches that of FB-Deep output files). For the purpose of post-processing data from within GeoStat, shaft geometric properties reported beneath the "SHAFT INFORMATION" header are parsed and retained. Also, both elevation and shaft axial resistance quantities residing beneath the "Skin friction capacity" sub-header are parsed as part of the data importation

(including the tabulated columns of Top Elev., Ult. Skin Friction, and integer mapping values of FB-Deep soil types). Further, the ultimate skin friction in the bearing layer is included among the imported data.

```
SHAFT INFORMATION (Shaft ID = 1)
================================
 Diameter      =    48.00(in)
 Base Diameter =    48.00(in)
 Length        =    50.00(ft)
 Tip elevation =    32.00(ft)
 Case length   =    22.20(ft)
 Bell length   =     0.00(ft)

 Skin friction capacity
 ----------------------
   Strength reduction factor for skin-friction = 1.00

   Layer  Top            Ult Skin
    ID    Elev.  Thick. Friction         Soil Type
          (ft)   (ft)    (Tons)
   -----  ------ ------ -------- -----------------------------
     1     82.00  0.50    0.00 5- Cavity layer
     2     81.50 12.50    0.00 2- Clay and silty sand
     3     69.00  0.50    0.00 5- Cavity layer
     4     68.50  6.50    0.00 2- Clay and silty sand
     5     62.00  0.50    0.00 5- Cavity layer
     6     61.50  6.50  106.77 2- Clay and silty sand
     7     55.00  0.50    0.00 5- Cavity layer
     8     54.50  4.50   96.33 1- Plastic Clay
     9     50.00  0.50    0.00 5- Cavity layer
    10     49.50 14.50  258.15 2- Clay and silty sand
    11     35.00  0.50    0.00 5- Cavity layer
    12     34.50 26.00         4- Lime Stone/Very shelly sand <--- Bearing layer
   (* IN LAYERS ABOVE BEARING LAYER)

   Ultimate skin friction in layers above bearing layer =  461.25(tons)
   Ultimate skin friction in bearing layer              =  178.63(tons)
   Total Skin Friction                                  =  639.87(tons)
```

Figure 146. Example excerpt of shaft analysis output that is read-in from the Spatial Variability tab

While the aforementioned elevation and resistance quantities pertain primarily to skin friction resistance, a second region of interest located among the analysis output is scanned and parsed for the purpose of building up estimates of end bearing resistance. In particular, settlement data found beneath the "Settlement curve" sub-header are focused upon. Recall that one of the GeoStat input parameters associated with modeling of shafts is the Limiting Settlement (%). As part of the data importation from within GeoStat, the end bearing reaction (i.e., Q_b) corresponding to the input value of Limiting Settlement is parsed and retained. Note that linear interpolation is carried out during importation in the event that the input value of Limiting Settlement (from GeoStat) does not exactly match any value found among the reported R(%) values in the model analysis output files.

```
  Settlement curve:
  ----------------
***** Capacity is NOT modified by the strength reduction factors *****
              ---

 User-Defined Settlement = 3.00%
 Shaft capacity at user-defined settlement =  492.89(tons)


      R(%)      Settl.(in)   Qs(tons)    Qb(tons)    Qt(tons)
    ------------ ------------ ------------ ------------ ------------
      0.1        0.048        231.65        4.08       235.73
      0.2        0.096        344.15        6.50       350.65
      0.4        0.192        421.65       10.34       431.99
      0.6        0.288        458.53       13.57       472.10
      0.8        0.384        473.89       16.45       490.34
      1.0        0.480        468.49       19.10       487.60
      1.5        0.720        453.53       25.06       478.60
      2.0        0.960        436.84       30.39       467.23
      2.5        1.200        445.48       35.29       480.77
      3.0        1.440        453.02       39.88       492.89
      4.0        1.920        465.51       48.36       513.87
      5.0        2.400        475.45       56.15       531.61
      6.0        2.880        483.55       63.45       547.00
      7.0        3.360        490.28       70.35       560.63
      8.0        3.840        495.95       76.94       572.89
```

Figure 147. Example excerpt of shaft settlement output that is read-in from the Spatial Variability tab

CHAPTER 6
REFERENCES

Faraone, M. A. (2014). *Geostatistical Analysis for Reliability Based Design of Foundations*, Dissertation, University of Florida, Gainesville, FL.

FB-Deep [Computer software]. Bridge Software Institute (BSI), University of Florida, Gainesville, FL.

McVay, M., Klammler, H., Faraone, M. A., Krishmarao, D., Jenneisch, C. (2012). *Development of Variable LRFD ϕ Factors for Deep Foundation Design Due to Site Variability*, FDOT Research Report BDK75 977-23, Tallahassee, FL.

APPENDIX B
GEOSTAT TECHNICAL MANUAL

Presented below is the Technical Manual for the GeoStat software, which is included as a standalone document, and is accessible from within the GeoStat UI. The Technical Manual integrates work carried out during project Task 2, Task 3, and Task 6. The manual reviews relevant geotechnical engineering concepts associated with use of the GeoStat software. In addition, illustrative examples and technical guidance are provided regarding selection of modeling parameters when developing site and foundation model components within GeoStat. Site data from two unique locations, representative of Florida bridges, are utilized in the illustrative examples. Furthermore, underlying engineering calculations that are carried out when using the GeoStat software are reviewed.

GeoStat

Technical Manual

DISCLAIMER

No warranty, expressed or implied, is made by the Florida Department of Transportation or the University of Florida as to the accuracy and functioning of any programs or the results they produce, nor shall the fact of distribution constitute any such warranty, and no responsibility is assumed by the Florida Department of Transportation or the University of Florida in any connection therewith.

TABLE OF CONTENTS

CHAPTER 1
INTRODUCTION

1.1 Introduction

Spatial variability is exhibited among collections of soil and rock properties that are measured across a given bridge site, which casts some level of uncertainty upon properties at locations between those same measurements. Also, when soil (or rock) properties are utilized in estimating design resistances of deep foundation members via empirical methods, an additional component of uncertainty is introduced. Therefore, two sources of uncertainty that factor into estimations of foundation-member soil resistance are spatial variability and method error.

Determination of axial capacities for deep foundation members, absent considerations for these two forms of uncertainty, can lead to either unconservative or overly conservative bridge foundation layouts. In contrast, incorporation of geostatistics into design calculations facilitates characterization of both forms of uncertainty, particularly when estimating axial capacities of deep foundation members such as piles and drilled shafts.

The GeoStat software contains geostatistical analysis features and guides engineers through processes such as: 1) identification of geological zones across a given site; 2) selection of representative layers for a foundation location of interest; 3) characterization of spatial variability intrinsic to available site data; 4) assessment of pile/shaft axial resistance (and variability of the assessment), along with incorporation of both spatial variability and method error phenomena; and, 5) estimation of site-specific Load and Resistance Factor Design, LRFD, resistance (ϕ) factors. Furthermore, the GeoStat software is intended for use in: 1) characterization of whether or not adequate site data have been collected; 2) bringing about increased uniformity of design methodologies in practice; and, 3) improved economy of bridge foundation designs. Consequently, the GeoStat software is a suitable tool for design scenarios where determination of deep foundation member resistance (and characterization of resistance uncertainty) is of interest.

1.2 Background

Development of geostatistical techniques and synthesis of relevant load-test data for establishing method error estimations was previously carried out as part of Florida Department of Transportation (FDOT) research (documented in McVay et al. 2009; Klammler et al. 2010). Subsequently, the advantages of directly accounting for spatial variability and method error phenomena were investigated in Faraone (2014). In the aforementioned studies, focus was given to determining axial capacities of pile and drilled shaft members. Also, focus was given to finding the means to estimate site-specific resistance (ϕ) factors, for comparison

to those prescribed in design provisions such as the AASHTO LRFD bridge design specifications (AASHTO 2017) and the FDOT Structures Design Guidelines (FDOT 2020).

In addition to the above, FDOT-funded research was carried out by McVay et al. (2012) to synthesize geostatistical techniques, identify correlations for use in method error calculations, and create prototype software for conducting geostatistical analysis. The prototype software was configured to operate on collections of geotechnical site data and produce statistical estimates of pile (or shaft) axial capacity along candidate embedment depths. In addition, the software permitted delineation of the influence of spatial variability and method error (as well as the combined influence) on through-depth resistance calculations. Building upon these past research efforts, including software prototyping, has led to the development of the GeoStat software.

Deployment of analysis and design tools that aid in characterizing uncertainty and the soil or rock strata at a given location within a bridge site can bring about benefits with respect to both safety and economy of bridge designs (Rivers, 2018). Accordingly, by accounting for the influences that spatial variability and method error have on estimates of foundation member resistances, several aspects of foundation design can be improved upon through use of GeoStat. Namely, these include: determination of representative soil or rock layering at a location of interest; identification of spatial zones (when present) throughout the site; and, assessment of whether or not additional site data need to be collected. In current practice, deep foundation member design typically entails simplified treatments of (or wholly ignoring) phenomena such as soil or rock layering, spatial zones, and spatial variability among sets of measured soil or rock strength data.

Foundation design data generated in this manner overcome significant simplifications typical of current practice, where phenomena such as rock layering, area zones (i.e., spatial variability) are either ignored or indirectly accounted for via significantly more conservative (and more costly) configurations. By incorporating the GeoStat software into bridge design processes, quantitative indicators of scope and sufficiency can be produced for budgeting, and conducting, geotechnical investigations. Also, the ability to quantify variability in foundation resistance quantities (e.g., the effect of pile/shaft lengths on LRFD resistance factors, ϕ), in turn, allows practicing engineers to achieve more optimized and cost-effective foundation designs.

1.3 Technical Manual Scope

Program documentation for the GeoStat software is divided into two components: 1) a Help Manual; and, 2) a Technical Manual. The present report, the GeoStat Technical Manual, is a standalone document, which details engineering calculations originally developed and/or synthesized in McVay et al. 2012 and Faraone, 2014. In addition, presented in the Technical Manual are representative (but anonymized) sets of data obtained from geotechnical

investigations of Florida bridge sites. The site data are utilized to provide guidance and recommendations for establishing GeoStat model files and interpreting results.

The Technical Manual provides engineers with a centralized resource to aid in understanding of the underlying algorithms that are utilized during site analysis, realizations of soil or rock layerings, calculations of pile/shaft axial resistances, and calculations of the associated uncertainty. These underlying algorithms are illustrated via two unique case-studies, where data are selected to be representative relative to what would be measured across Florida bridge sites. In addition, for each site, technical guidance is provided concerning characterization of relevant parameters that describe spatial variability of soil or rock resistance from within GeoStat.

Organization of remaining chapters of the GeoStat Technical Manual is as follows:

- Provided in Chapter 2 is a review of statistical and spatial variability concepts that hold relevance with respect to the analysis and simulation algorithms implemented in the GeoStat software. Emphasis is placed on a graphical technique for characterizing spatial variability (referred to as the variogram).

- In Chapter 3, details are provided concerning the various method error formulations available for use.

- Presented in Chapter 4 is a modeling guide, which makes use of data collected from a Florida bridge site, referred to as Example Site A. The guide walks engineers through pertinent technical concepts associated with usage of the GeoStat software.

- In Chapter 5, data from a second site, Example Site B, is made use of to provide an additional instance of an illustrative modeling guide.

CHAPTER 2
SPATIAL VARIABILITY ANALYSIS

2.1 Overview

The GeoStat software is intended for use in guiding engineers through the processes of characterizing the spatial variability associated with geotechnical site data, quantifying foundation member axial resistance, and quantifying the total uncertainty of axial resistance quantities. To make a clear distinction on terminology, variability can be thought of as a non-homogenous subsurface profile that could result from either manmade or natural processes, such as soil or rock layering and/or the presence of zones. In contrast, uncertainty is related to the engineer's limited knowledge of how rock strength varies within the volume of interest. One of the more challenging tasks for geotechnical engineers is the assessment of variability and uncertainty between points of exploration (e.g., standard penetration test, SPT-N, boring).

The focus of Ch. 2 is on those statistical concepts and analytical techniques that are implemented in GeoStat for characterizing spatial variability phenomena and the associated uncertainty in geotechnical engineering applications. Introduced in Sec. 2.2 is an illustrative data set, which is included solely to facilitate elucidation of the requisite statistical concepts. Documented in Sec. 2.3 is the manner by which descriptive statistics are calculated using geotechnical site data. The concept of spatial correlation is introduced and reviewed in Sec. 2.4. Further, both the concepts and graphical techniques that are applied when forming spatial correlation structures of site data, via variograms, are reviewed in Sec. 2.5.

Subsequent to formation of spatial correlation structures, stochastic simulation—or, in this context, statistical interpolation—can be utilized to form point estimates of pile/shaft axial resistance. Technical aspects of the associated simulation processes, as implemented in the GeoStat software, are discussed in Sec. 2.6. Listings of the types of layers available for modeling in GeoStat, along with the associated soil or rock parameters (and empirical relationships) are documented in Sec. 2.7. Presented in Sec. 2.8 is the mathematical form in which uncertainty is summarily expressed for a given estimate of foundation axial resistance (via the resistance factor, ϕ).

2.2 Illustrative Set of Geotechnical Site Data

To illustrate concepts associated with determining both descriptive statistics and geostatistical quantities, an illustrative data set is drawn upon. Plotted in plan-view in Fig. 1 are 40 locations from an idealized site, where locations are expressed as pairs of eastings and northings. In this context, each location is associated with a through-depth profile of boring (or coring) data, with corresponding subsets of site measurements (e.g., SPT-N; unconfined compression strength, q_u). Although illustrative in nature, the locations and accompanying profiles of measurements fall into clusters so as to mimic distributions of boring locations that

4

would be selected for geotechnical investigation prior to bridge construction (e.g., within or near the footprints of substructures along the bridge).

In the following, illustrative site data associated with these 40 locations, and in particular, ensembles of SPT-N blow count values accumulated across various elevation ranges, are utilized to conceptually convey various statistical phenomena. Note that, although SPT-N blow counts are utilized for illustrative purposes in the next several subsections, the statistical constructs discussed below can generally be formed for any set of measurements taken across a bridge site (e.g., q_u).
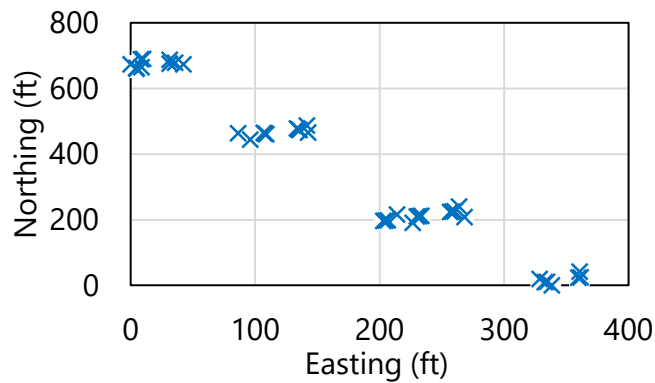
Figure 1. Plan view of illustrative set of 40 boring (and coring) locations

2.3 Site Descriptive Statistics

Descriptive statistics relevant to analysis of geotechnical site data (including histogram, mean, and variance quantities) are discussed throughout Sec. 2.3. See Sec. 2.4 for extension of the descriptive statistics concepts, as pertaining to spatial correlation. In addition, descriptive statistics discussed immediately below are further utilized in Sec. 2.5, where technical documentation is provided concerning the vital graphical concept of variograms.

2.3.1 Histograms

Recalling the 40 illustrative boring (and coring) locations from Fig. 1, consider a scenario where all SPT-N values measured throughout the site are cataloged with respect to elevation. One manner of graphically representing these values is that of the scatterplot, which allows for initial insights to be made regarding the presence of spatial relationships among the data set. For example, an illustrative scatterplot of 88 SPT-N values attributed to an idealized soil layer is provided in Fig. 2. The values fall within elevations ranging between 10 ft and -10 ft.

The SPT-N values (Fig. 2) exhibit appreciable variation (i.e., dispersion, scatter, spread) at a given elevation. Further, a trend is qualitatively observable, where blow count values tend to increase with decreasing elevation (increasing depth). While the scatterplot is extremely useful for gaining insights into spatial phenomena for collections of soil resistance measurements,

5

data presented in this form do not readily reveal aspects of the ensemble that are related to frequency (i.e., relative likelihood of occurrence).
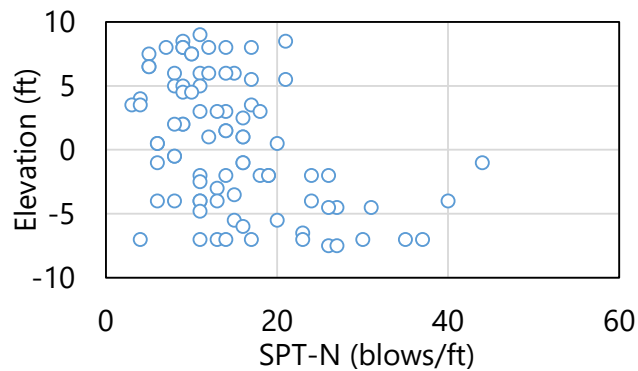
Figure 2. Scatterplot of illustrative set of 88 SPT-N blow counts (elevation range: 10 ft to -10 ft)

As an alternative graphical formation, consider a histogram of the same set of 88 SPT-N blow count values (Fig. 3). The histogram provides a visual representation of the distribution of the data with respect to frequency. The histogram is formed by first calculating a number of intervals (bins, or ranges of SPT-N values). As implemented in the GeoStat software, the following equation is used to calculate the number of bins:

$$n_{bins} = \sqrt{n} \qquad (1)$$

where n_{bins} is the integer number of bins and n is the number of points (measurements) in the data set.
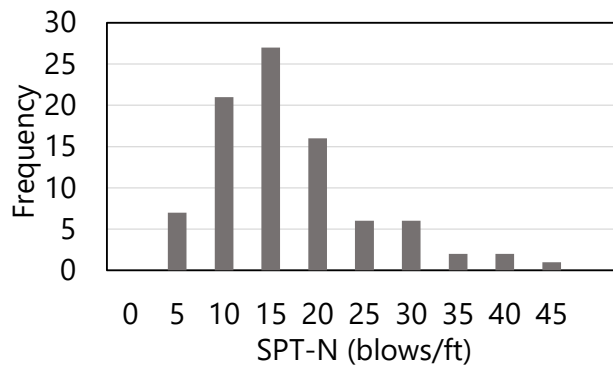
Figure 3. Histogram of illustrative set of 88 SPT-N blow counts (elevation range: 10 ft to -10 ft)

At least two bins—and no more than 25 bins—are permitted when forming histograms in GeoStat. Additionally, the "left-open, right closed" convention is adopted for assigning measured values (q) to bins. This convention signifies adoption of the following two criteria

6

for assigning a measured value (q) to a bin. Namely, the value must be: 1) equal to or greater than a bin left extent; and, 2) less than right extent of the same bin. As an exception, the rightmost (maximum-value) bin is always "left-open, right-open".

The maximum bin value (bin_{max}), which lies at the center of the rightmost interval is then determined by:

$$bin_{max} = max(\{q\}) \tag{2}$$

where $max()$ denotes the operation of finding the maximum value of an array, and $\{q\}$ is the set of measured values (e.g., SPT-N).

For the 88 SPT-N values, evaluations of Eqn. 1 and Eqn. 2, respectively, give 9 bins and a bin_{max} (center of rightmost interval) value of 45 blows/ft. As the next step in forming the histogram, each of the 88 measured values are then assigned a bin. The cumulative number of values that fall within each bin interval comprise the histogram plotted in Fig. 3.

When data are plotted in histogram form, it is apparent that the distribution of the SPT-N blow count values tend to fall within the range of approximately 10 to 20 blows/ft. In addition, the distribution of the data is such that a skew exists, with a relatively steep reduction in frequency for blow counts less than approximately 10 blows/ft, and a relatively more gradual reduction in frequency for blow counts exceeding approximately 20 blows/ft.

2.3.2 Mean, Median, Standard Deviation, and Variance

From examination of the scatterplot (Fig. 2) and histogram (Fig. 3) of the 88 illustrative SPT-N values (10 ft to -10 ft), it is evident that scatterplots aid in making initial observations regarding spatial characteristics of the data, while histograms aid in assessing data frequency (or how often the data, proportionally, fall within a given range of values). However, scalar-valued descriptive statistics also prove complementary to the above plots for assessing spatial variability, likelihood of occurrence (frequency), and uncertainty of geotechnical site data.

2.3.2.1 Mean and Median

For example, the (arithmetic) mean of the data gives an indicator of expected value, and is expressed as:

$$\mu = \frac{1}{n}\sum_{i=1}^{n} q_i \tag{3}$$

where μ is the mean; and is determined by summing the values of each of q_i measurements (1 through n), and then dividing that summation by the total number of measurements (n). Note that the geometric mean is the product of the q_i measurements taken to the nth root. While both arithmetic and geometric means are made use of in GeoStat, the former is utilized in computing resistance (ϕ) factors, while the latter serves to aid in qualitatively characterizing the skew present in distributions of layer-specific data.

In contrast to the mean is the median, which separates the bottom and top halves of the data set. While the mean of the 88 SPT-N blow count values is 15 blows/ft, the median is 13 blows/ft. The median is identified by: 1) sorting the 88 values in increasing order; and, 2) selecting the 44th value from the sorted list.

Recalling the presence of skew in the histogram of Fig. 3, roughly speaking, this is comparable to stating that the mean does not equal the median. This phenomenon is one (among others) that distinguishes idealized histogram shapes. As further illustration, consider two idealized distributions that are germane to geotechnical applications: normal and lognormal distributions (Fig. 4). The normal distribution plotted in Fig. 4a exhibits symmetry (i.e., the mean and median are equal), whereas the distribution in Fig. 4b exhibits right-skew.

These two types of distributions (normal, lognormal) are made frequent use of throughout the present report. For example, the positive and negative residual errors associated with data sets may, in some instances, be characterized as normally distributed. Physical measurements such as unconfined compression strength, q_u, are always positive and tend to exhibit right-skew distributions (characterized as log-normally distributed).
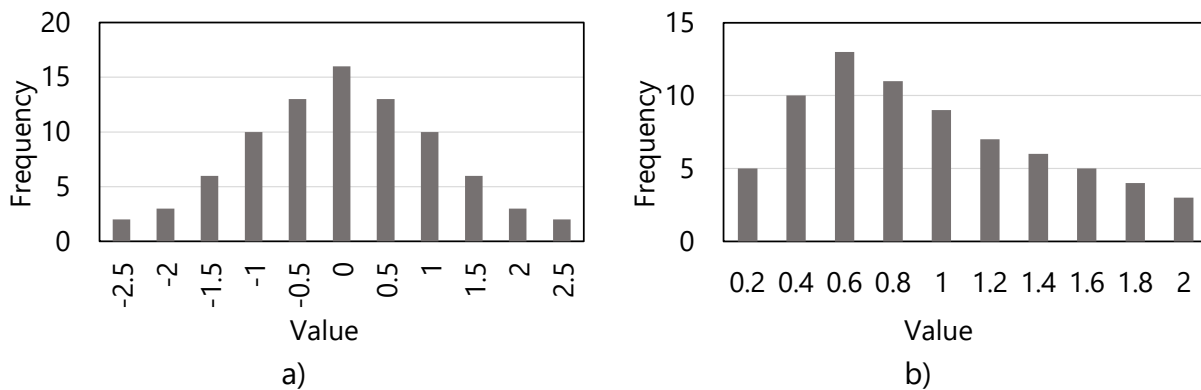
Figure 4. Idealized distribution shapes: a) normal; b) lognormal

2.3.2.2 Standard Deviation and Variance

While descriptive statistics such as the mean (μ) provide point-estimate summary values for the data set, the spread or dispersion of the data set is often quantified using standard deviation, σ:

$$\sigma = \sqrt{\frac{1}{n-1}\sum_{i=1}^{n}(q_i - \mu)^2} \qquad (4)$$

The standard deviation is, roughly, an average of the sum of the differences between each measured value (q_i) and the mean (μ). Another common quantitative representation for the dispersion of the data is that of the variance, which is simply the square of the standard deviation, or σ^2. Both quantities provide absolute indicators of how far the data extends away from the mean.

2.3.2.3 Coefficient of Variation

A descriptive statistic that provides a relative indication of how much dispersion is present in the data is that of the coefficient of variation, COV:

$$\text{COV} = \frac{\sigma}{\mu} \qquad (5)$$

where, for example, a COV value of 1.0 indicates that the magnitude of the data spread is comparable to the magnitude of the mean. The COV for a set of site data has the largest influence on LRFD resistance factors, ϕ, for piles/shafts (and therefore pile/shaft design side friction and end bearing). The larger the COV value, the lower the LRFD-ϕ (or, again, pile/shaft design side friction and end bearing). Scenarios that may lead to relatively high COV values (e.g., values greater than unity) are: 1) too few samples; 2) presence of outlier data (exacerbated by squaring of difference terms in Eqn. 4); 3) not breaking up the site into layers or zones—where each constituent data set possesses unique mean and standard deviation (and tends to produce relatively, smaller values of COV). Alternatively stated, the COV value associated with a collection of site data (or that of candidate zones from within a site) is critical to differentiating and identifying layers and zones

For the illustrative set of 88 SPT-N blow count values, the descriptive statistics are listed in Table 1. The mean (μ) is qualitatively reinforced by referring back to the histogram (Fig. 3). In addition, the coefficient of variation (COV) is 0.6, which indicates that the data dispersion is substantial relative to (i.e., 60% as large as) the magnitude of the mean.

Table 1. Descriptive statistics for illustrative set of 88 SPT-N blow counts (elevation range: 10 ft to -10 ft)

Descriptive statistic	Value	Units
Mean (μ)	15.0	blows/ft
Median	13	blows/ft
Standard deviation (σ)	8.3	blows/ft
Variance (σ^2)	68.8	blows^2/ft^2
Coefficient of variation (COV)	0.6	N/A

2.4 Spatial Correlation

As demonstrated above, initial inferences regarding variability and distributions of geotechnical site data are afforded by examination of scatterplots, histograms, and descriptive statistics. However, more explicit statistical assessments are available for characterization of spatial variability phenomena. Introduced in Sec. 2.4 is the concept of spatial correlation and the covariance function, where the latter is used to assess the variability of a mean (e.g., pile/shaft capacities). As an extension of this concept, subsequently introduced in Sec. 2.5 is the key graphical construct for assessing spatial variability from within GeoStat, which is that of the variogram.

2.4.1 Conceptual Illustration

Spatial correlation is a quantitative indication of the strength of the relationship between two physical measurements. One approach to assessing spatial correlation is to plot value pairs for a series of physical distances (McVay et al. 2012). As illustration, three scatterplots of subsets of the 88 SPT-N blow counts at three different prescribed distances are presented in Fig. 5. Also note, even though the illustrative subsets of data are obtained by examining vertical distances between physical measurements, the discussion below also generally applies with respect to horizontal distance.
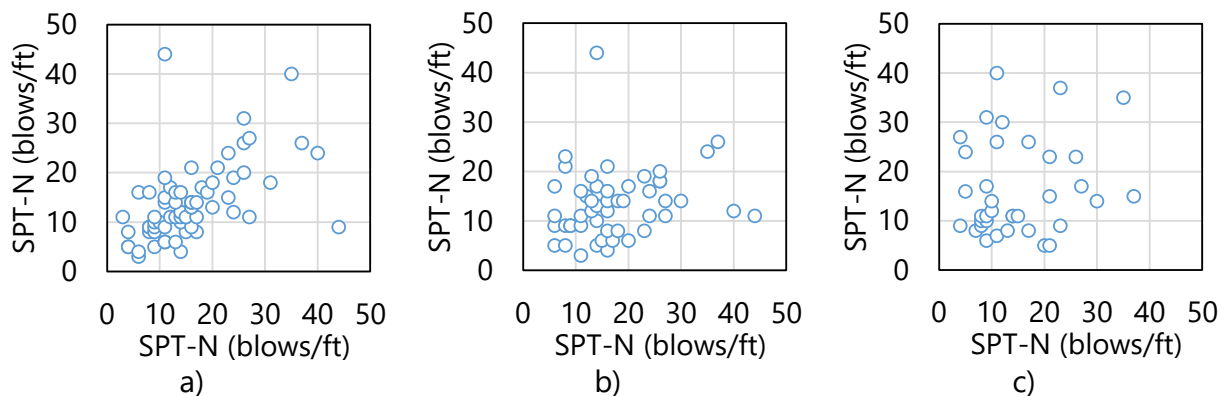
Figure 5. Pairs of illustrative SPT-N blow counts that are separated by a specified vertical distance (elevation range: 10 ft to -10 ft): a) 2.5 ft, 68 pairs; b) 5 ft, 50 pairs; c) 12.5 ft, 41 pairs

Among the 88 measurements, there are 68 pairs of data points that lie approximately 2.5 ft apart. That is, the paired values are positioned at vertical distances of approximately 2.5 ft (typical SPT spacing) with respect to one another (Fig. 5a). At an offset distance (or lag distance, h) of 5 ft, 50 pairs are identified (Fig. 5b). As shown in Fig. 5c, 41 pairs are identified at a lag distance (h) of 12.5 ft. When pairs are formed in this manner, a given point (q_i) is

assigned as a member of a pair for every instance where another point (q_j) satisfies the lag distance criterion.

Of particular note when visually scanning from Fig. 5a to Fig. 5c is that the discernibility of correlation (i.e., similar magnitudes) between each paired value steadily degrades with increasing physical distance (lag, h) between points. A clear trend is qualitatively observed (i.e., 45° line) in Fig. 5a (h = 2.5 ft), where increasing values of SPT-N blow counts at one location correspond to (correlate with) increasing values of the respective paired values of SPT-N blow counts at distance, h. In contrast, in Fig. 5c (h = 12.5 ft) the pairs of points more qualitatively resemble "white noise", or an illustrative data subset with near-zero correlation.

2.4.2 Covariance

Within the context of geostatistics, the covariance is typically used when quantifying the strength of correlation between pairs of points that satisfy a given lag distance (h). More specifically, covariance is expressed as a function of lag distance (and only accepts points that are physically separated in accordance with lag distance, h):

$$C(h) = \frac{1}{n_{pairs}} \sum_{i,j=1}^{n_{pairs}} (q_i - \mu)^2 \cdot (q_j - \mu)^2 \tag{6}$$

where $C(h)$ is the covariance of the subset of points that are paired; and, n_{pairs} is the number of pairs. When pairs of data are perfectly correlated (i.e., $q_i = q_j$), then the covariance converges to the variance (σ^2) of the data subset (q). When point pairs are not correlated, covariance is 0. In the context of analyzing geotechnical site data—and because correlation tends to decrease with increasing lag distance (h)—the covariance function, $C(h)$ likewise tends to decrease with increasing lag distance (McVay et al. 2012).

2.4.3 Correlation Coefficient

As an additional means of quantifying correlation, a correlation coefficient can be defined as:

$$R(h) = \frac{C(h)}{\sigma^2} \tag{7}$$

where the correlation coefficient, $R(h)$, expressed in this form is dimensionless and is bounded between 0.0 and 1.0. For correlation coefficient values of 1.0, pairs of values are perfectly correlated. A correlation coefficient of 0.0 indicates that no linear relationship exists between the paired points.

11

2.5 Variograms

Effective use of variograms is critical to successfully characterizing spatial correlation structures that are present among geotechnical site data. Therefore, the next several subsections (within Sec. 2.5) are devoted to formally defining variograms; reviewing common characteristics of variogram curves (e.g., anisotropy); and, delineation of how variograms are computed when using GeoStat.

2.5.1 Variogram Definition

Semi-variograms (commonly referred to as "variograms") are highly effective constructs for summarily assessing spatial correlations among sets (or subsets) of geotechnical site data. Variograms can be expressed in the following form:

$$v(h) = \frac{1}{2 \cdot n_{pairs}} \sum_{i,j=1}^{n_{pairs}} (q_i - q_j)^2 \tag{8}$$

where the variogram ordinate, $v(h)$, is a function of lag distance (h). Defining the variogram as presented in Eqn. 8 includes direct use of the paired physical measurements (q_i, q_j). In particular, differences between the measured values are summed across the number of point pairs (n_{pairs}) identified from a wider set of site data. Alternatively stated, the number of pairs, n_{pairs}, is the total number of pairs of physical measurements that were obtained from the site at a distance approximately equal to lag distance, h. In the case of no trend in the data (e.g., increasing values with depth), then the variogram may be given as:

$$v(h) = \sigma^2 - C(h) \tag{9}$$

Here, the variogram is expressed in a form that simultaneously relates lag distance (h) to both covariance, $C(h)$, and variance (σ^2) of all the paired data. Note that the variance (σ^2) of a set of recorded physical measurements is constant, while the covariance, $C(h)$, is a function (among other variables) of lag distance. Further, recall that covariance (Eqn. 6) tends to *decrease* with increasing lag distance (McVay et al. 2012). Consequently, the variogram function tends to *increase* with increasing lag distance.

For a more visual interpretation of variograms, consider the conceptual schematics shown in Fig. 6. Specifically, as shown in Fig. 6a, the variogram indicates a relatively sharp increase (i.e., a sharp reduction in correlation) at small lag distances. With increasing lag distance (h), the idealized variogram of Fig. 6a exhibits asymptotic behavior. Ultimately, the variogram function converges to an ordinate, which in turn, corresponds to the variance (σ^2) of the full data set (i.e., n_{total} pairs of measurements) and covariance $C(h)$ approaches zero.
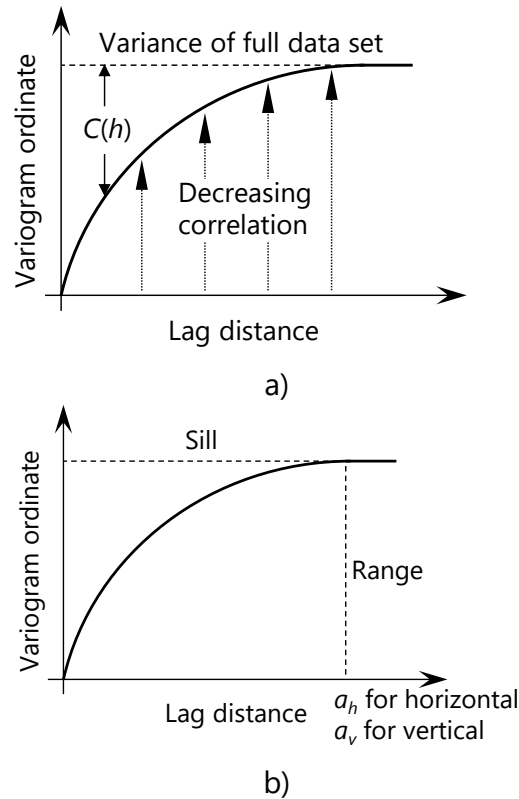
Figure 6. Overview of variograms: a) Conceptual schematic; b) Curve components

Annotations of basic features of variograms are provided in Fig. 6b. The variogram ordinate that corresponds to the variance of the full data set is referred to as the sill. The corresponding lag distance (variogram abscissa value) at which convergence to the sill is attained is referred to as the range (a_h for horizontal, a_v for vertical). Additional features that are commonly present within variograms are discussed in Sec. 2.5.2.

2.5.1.1 Experimental vs Theoretical Variograms

The schematic variogram depictions from Fig. 6 above include continuous, smooth curves to represent the idealized variograms. However, as a distinction, variogram values computed using site data are generally discrete in nature. Discrete collections of variogram points that are directly obtained from sets of physically measured site data are referred to as experimental variograms (Fig. 7a). In contrast, continuous mathematical functions (which are intended for best-fit representations of experimental variogram points) are referred to as theoretical variograms (Fig. 7b). Theoretical variograms, rather than experimental variograms, are used for conducting stochastic simulation to determine deep foundation member axial resistance. Therefore, an important aspect of site modeling within GeoStat is that of ensuring that experimental variograms are appropriately fitted with theoretical variograms.
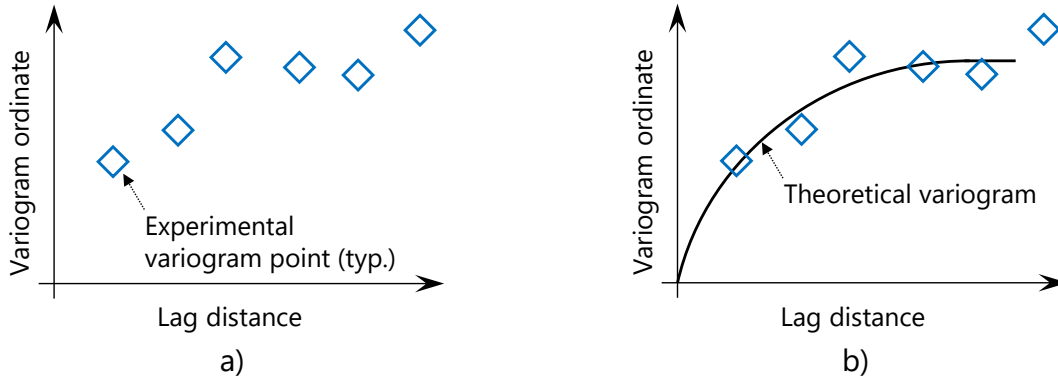
Figure 7. Overview of variograms: a) Experimental variogram; b) Theoretical variogram

Two forms of theoretical functions are available to choose from when modeling spatial correlation structures in GeoStat. A spherical form is expressed as:

$$v_{theoretical}(h) = \left\{ \begin{array}{c} \sigma^2 \cdot \left(1.5\frac{h}{a} - 0.5\left(\frac{h}{a}\right)^3\right); \ h < a \\ \sigma^2; h \geq a \end{array} \right\} \tag{10}$$

where $v_{theoretical}(h)$ is the ordinate of the theoretical variogram function; and, a is the range (recall Fig. 6b). The exponential form is expressed as:

$$v_{theoretical}(h) = \sigma^2 \cdot (1 - exp(\frac{-3.0|h|}{a})) \tag{11}$$

where both of the theoretical expressions typically conform to the overall curve shapes shown in Fig. 7b. When the lag distance (h) approaches the range (a), evaluations of Eqn. 10 and Eqn. 11 approach the variance, σ^2. The form of the variogram (spherical or exponential) is used to ensure that an estimate (e.g., SPT-N blow count value, q_u) at any location is possible.

2.5.2 Anisotropy

In the context of geotechnical site data, spatial variability phenomena are often direction dependent. More specifically, unique variograms are often necessary to describe spatial correlations in horizontal and vertical directions. For such instances, the soil data is spatially categorized as anisotropic, where several forms of anisotropy are possible.

In rare instances, the same variogram curve may be suitable for describing spatial variability in both the horizontal and vertical directions (isotropic, Fig. 8a). More often, geotechnical site data possess spatial correlation characteristics such that either the range (a), the sill, or both features differ with respect to variogram direction (as shown in the schematics of Fig. 8b through Fig. 8d).

14
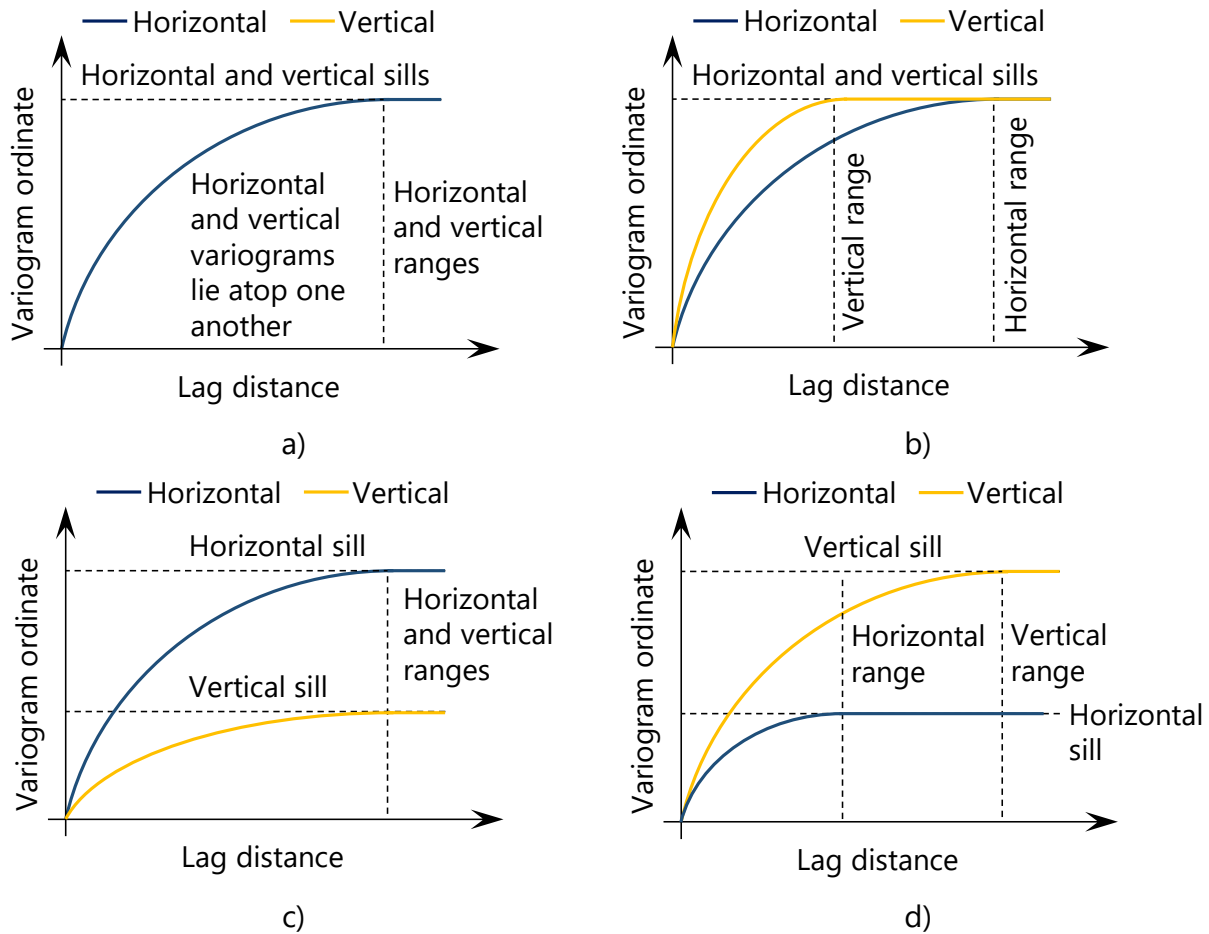
Figure 8. Variogram isotropy and anisotropy: a) Isotropy; b) Geometric anisotropy; c) Zonal anisotropy; d) Geometric and zonal anisotropy (i.e., layering)

When the horizontal and vertical variograms have the same sill, but different range values (a), the condition is referred to as geometric anisotropy (Fig. 8b). The material has a shorter correlation range vertically than horizontally as a result of the soil formation process. Zonal anisotropy (Fig. 8c) signifies that the material has less variability vertically than horizontally, and suggests that the site should be broken into zones to reduce COV (i.e., variability). Combined forms of anisotropy can also occur. As illustration, Fig. 8d shows less variability horizontally than vertically, and is a clear indicator of soil or rock layering.

Of particular note, when data sets exhibit zonal anisotropy (Fig. 8c), then the corresponding variances (σ^2) are also direction dependent. Per McVay et al. (2012), it is very important to identify zonal anisotropy because the overall variance of the data may adversely affect estimation of the data uncertainty when calculating LRFD resistance factors (ϕ). Furthermore, when zonal anisotropy occurs, it may signify that the data set being considered encompasses

multiple geological zones, and requires further division such that one data subset is defined for each zone.

2.5.2.1 Additional Variogram Features

Additional features and phenomena that may appear when constructing variograms are presented in the schematics of Fig. 9. For instances where errors in measurement have occurred, or where only a relatively small number of data pairs are available (McVay et al. 2012), the corresponding variogram (in a given direction) may exhibit the "nugget effect" (Fig. 9a).
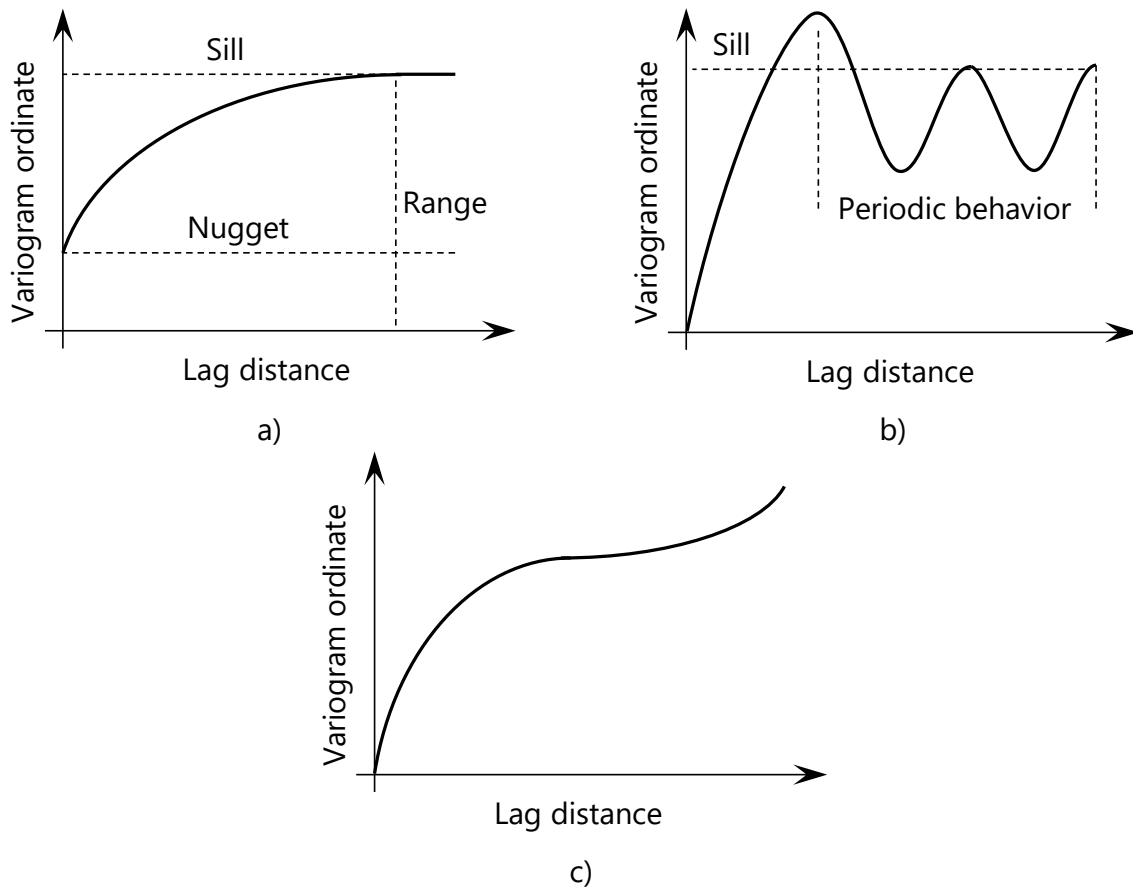
Figure 9. Additional variogram phenomena: a) Nugget effect; b) Cyclicity; c) Non-asymptotic behavior

The phenomenon of cyclicity is depicted in Fig. 9b. This variogram feature corresponds to use of a data set, that physically, includes spatially periodic bands (i.e., layers) in the facies (Gringarten and Deutsch 2001). For such instances, particularly for vertical varigorams, the data subset may need to be further subdivided (broken up into smaller ranges of elevations). Data which has a trend (e.g., SPT-N or q_u increasing with depth) exhibits non-asymptotic

behavior (Fig. 9c). Therefore, the data violates Eqn. 9 and detrending is necessary (discussed in Sec. 2.5.4).

2.5.3 Variogram Formation

From a computational standpoint, additional considerations are necessary when forming the points of experimental variograms. For example, it is not practical to use only pairs of measurements that exactly satisfy a given lag distance when determining the number of pairs within a data set. Therefore, when forming an experimental variogram in a given direction, a search domain is considered for identifying pairs of measurements (Fig. 10). Searches for pairs of data points are divided into discrete distances ranging from the lag distance (h) up to, and including, the product of the lag distance and number of lags (n_{lags}).
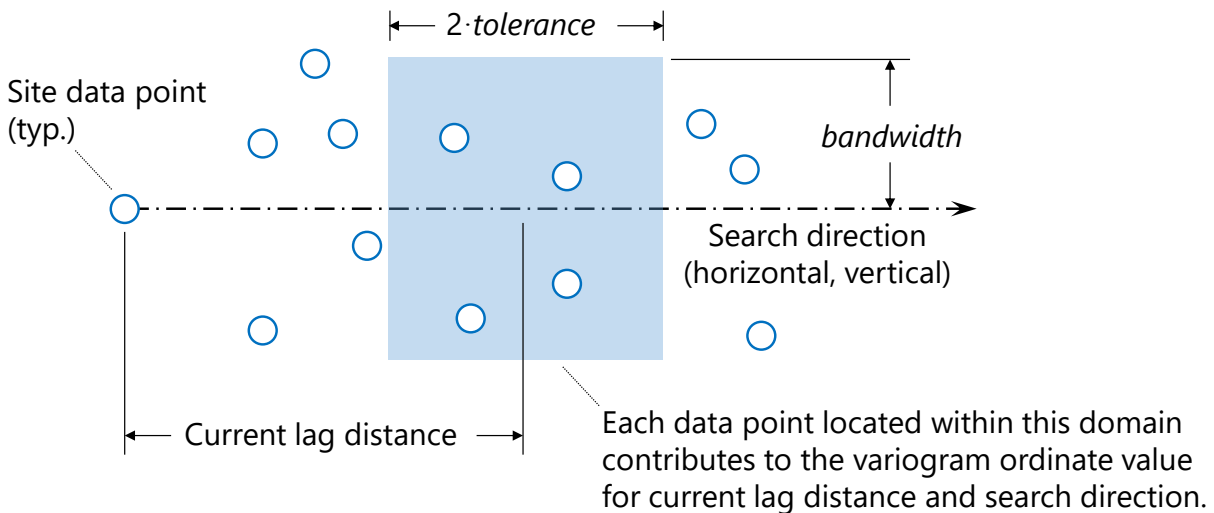
Figure 10. Geometric search terms for forming variograms

Both the tolerance (*tolerance*) and bandwidth (*bandwidth*) terms are used to define the search domain associated with a given, current search distance. Tolerance is parallel to the search direction and bandwidth is perpendicular to the search direction. The tolerance is limited to one half of the respective base lag distance (h). In the case of horizontal searches, bandwidth should be less than or equal to the tolerance, whereas for vertical searches the bandwidth is generally smaller (0 ft to 1 ft) due to prescribed distances between SPT-N profiles and core drilling specimens. With respect to each applicable search direction (horizontal, vertical), the search process is repeated for n data points to identify point pairs (n_{pairs}). Variogram ordinate values are then computed by operating on distances between pairs of data points. The procedures for forming variograms in the horizontal and vertical directions are delineated in Fig. 11 and Fig. 12, respectively.

Horizontal variogram formation

Given {Z_{score}}, {$northing$}, {$easting$}, and {$elevation$} for n site data points
Select h, n_{lags}, $bandwidth$, and $tolerance$
For i = 1, n_{lags}
  n_{pairs} = 0
  ε_{Zscore} = 0
  For j = 1, n
    For k = 1, n
      Δ_{north} = {$northing$}$_j$ - {$northing$}$_k$
      Δ_{east} = {$easting$}$_j$ - {$easting$}$_k$
      Δ_{elev} = {$elevation$}$_j$ - {$elevation$}$_k$
      $\Delta_{horizontal}$ = ($\Delta_{north} \cdot \Delta_{north} + \Delta_{east} \cdot \Delta_{east}$)$^{0.5}$
      If $|\Delta_{elev}| \leq 0.5 \cdot bandwidth$
        If $\Delta_{horiz} \leq h \cdot i + tolerance$ & $\Delta_{horiz} \geq h \cdot i - tolerance$
          ε_{Zscore} = ε_{Zscore} + ($Z_{score\,j}$ - $Z_{score\,k}$)^2
          n_{pairs} = n_{pairs} + 1
    End of loop on k
  End of loop on j
  Determine variogram point:
    Abscissa = $h \cdot i$
    Ordinate = $0.5 \cdot \varepsilon_{Zscore} / n_{pairs}$
    Corresponding Pairs = $0.5 \cdot n_{pairs}$
End of loop on i

Figure 11. Horizontal variogram formation

Vertical variogram formation

Given {Z_{score}}, {$northing$}, {$easting$}, and {$elevation$} for n site data points
Select h, n_{lags}, $bandwidth$, and $tolerance$
For i = 1, n_{lags}
  n_{pairs} = 0
  ε_{Zscore} = 0
  For j = 1, n
    For k = 1, n
      Δ_{north} = {$northing$}$_j$ - {$northing$}$_k$
      Δ_{east} = {$easting$}$_j$ - {$easting$}$_k$
      Δ_{elev} = {$elevation$}$_j$ - {$elevation$}$_k$
      Δ_{horiz} = ($\Delta_{north} \cdot \Delta_{north} + \Delta_{east} \cdot \Delta_{east}$)$^{0.5}$
      If $\Delta_{horiz} \leq 0.5 \cdot bandwidth$
        If $|\Delta_{elev}| \leq h \cdot i + tolerance$ & $|\Delta_{elev}| \geq h \cdot i - tolerance$
          ε_{Zscore} = ε_{Zscore} + ($Z_{score\,j}$ - $Z_{score\,k}$)^2
          n_{pairs} = n_{pairs} + 1
    End of loop on k
  End of loop on j
  Determine variogram point:
    Abscissa = $h \cdot i$
    Ordinate = $0.5 \cdot \varepsilon_{Zscore} / n_{pairs}$
    Corresponding Pairs = $0.5 \cdot n_{pairs}$
End of loop on i

Figure 12. Vertical variogram formation

As initial steps in the variogram formation process, data values and corresponding positions for n points are cataloged. The position terms include arrays of northing, {*northing*}; easting, {*easting*}; and, elevation, {*elevation*}. Note that the "raw" measurements of data are not used in variogram formation in GeoStat. Rather, consistent with McVay et al. (2012), a normal distribution standard score (z-score) is assigned to each measurement, relative to the ensemble descriptive statistics of the n data points. The z-scores are cataloged, as {Z_{score}}, where array entries correspond to those of the positioning arrays. Formation of z-scores for an illustrative data set is given in Sec. 2.5.4.

As the next step in variogram formation, selections are made for lag distance (h), number of lags (n_{lags}), *bandwidth*, and *tolerance*. (recall that the latter two parameters are depicted in Fig. 10 above). Then, for each of n_{lags}, a double loop on the number of data points (n) is iterated upon. For the innermost loop over n data points (the loop on k in both Fig. 11 and Fig. 12), changes in northing (Δ_{north}), easting (Δ_{east}), elevation (Δ_{elev}), and horizontal distance (Δ_{horiz}) are calculated between candidate pairs of data points.

Subsequently, the distance between the two data points being considered is compared to the search domain (recall Fig. 10) for the current search distance. For horizontal variogram searches, horizontal distance (Δ_{horiz}) is associated with *bandwidth*, while elevation (Δ_{elev}) is associated with both the current search distance and *tolerance*. In contrast, for vertical variogram searches, elevation (Δ_{elev}) is associated with *bandwidth*; horizontal distance (Δ_{horiz}) is associated with both the current search distance and *tolerance*.

For each search distance considered, and for pairs of data points that satisfy the search criteria, a squared-difference term (ε_{Zscore}) is calculated from the z-scores of the data pairings. The squared-difference term is accumulated each time a pairing is identified. In addition, the pair count (n_{pairs}) is incremented each time a pairing is identified.

After the double loop on n data points is iterated through, the variogram point associated with the current search distance is calculated as shown in the bottom portions of Fig. 11 and Fig. 12. To prevent double-counting of point pairs, the n_{pair} term is divided by 2 at this point in the variogram formation process. After iterating through n_{lags}, the experimental variogram is taken as the catalog of the variogram points.

2.5.3.1 Illustrative Example of Variogram Formation

An illustrative example is given in the following of vertical variogram formation. However, the same general concepts apply with respect to formation of horizontal variograms. Recall from Fig. 2 the illustrative data set consisting of (n = 88) SPT-N blow counts, over the elevation range 10 ft to -10 ft. Consider (for illustration) selection of a lag distance (h) of 2.5 ft, six lags (n_{lags} = 6), and use of recommended values for *bandwidth* (0 ft) and *tolerance* (half of h, 1.25 ft)

in accordance with McVay et al. (2012). Using the procedure listed above in Fig. 12, vertical variogram abscissa values, ordinates, and pairs (n_{pairs}) of the experimental variogram are produced, as listed in Table 2 and plotted in Fig. 13a.

Table 2. Vertical variogram data for illustrative set of 88 SPT-N blow counts (elevation range: 10 ft to -10 ft)

Abscissa (ft)	Ordinate	Pairs
2.5	0.45	68
5.0	0.77	50
7.5	0.6	27
10.0	0.76	36
12.5	0.83	25
15.0	1.06	12
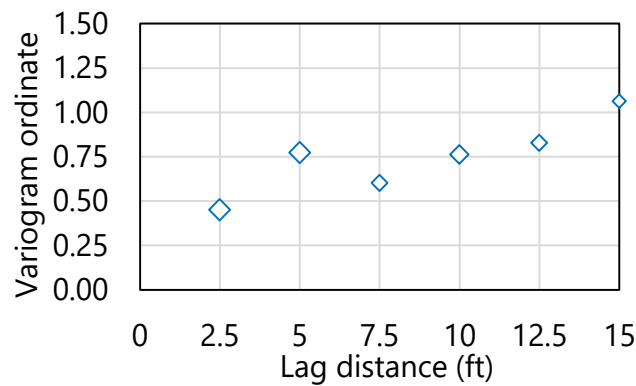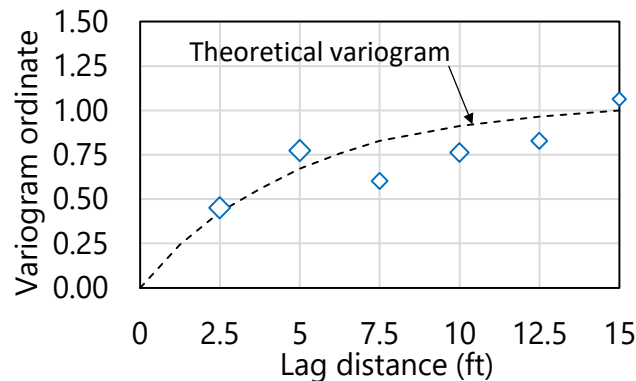
Figure 13. Vertical variogram for illustrative set of 88 SPT-N blow counts (elevation range: 10 ft to -10 ft): a) Variogram points; b) Variogram points and theoretical fit

GeoStat facilitates interactive graphical selection of theoretical variogram fits, given some experimental variogram (see Ch. 4 of the GeoStat Help Manual for additional details). An overlay of an exponential (theoretical) variogram, with use of Eqn. 11, a range (*a*) of 15 ft, and

20

sill of 1.0 is plotted in Fig. 13b. A sill value of 1.0 is selected because the z-scores ($v(h)/\sigma^2$) of the data set are utilized in forming the variogram.

Such use of z-scores, as implemented in GeoStat, is consistent with McVay et al. (2012) and serves to conveniently normalize variogram ordinate values. In this way, a sill value of 1.0 signifies that, for all points separated at a distance equal to or greater than the range (a), the spatial relationship between said data points is no more informative than that of the variance (σ^2) of the n_{pairs} of points that were selected during the pairing process. Stated alternatively (and recalling Eqn. 9), the covariance, $C(h)$, reaches zero at distances equal to or greater than the range (a), and so, only the covariance (σ^2) remains as a non-trivial contributor to the variogram ordinate values.

As an additional observation for this illustrative example, consider the listing of distance-dependent paired values in Table 2, where pair counts range from 12 to 68. It is recommended in McVay et al. (2012) that, ideally, 30 or more pairs should be obtained for each point along the experimental variogram. However, given typical volumes of geotechnical site data, this may not feasible for all points of experimental variograms. Accordingly, visual emphasis is placed upon those points that are associated with pair counts exceeding 30. More specifically, as implemented in GeoStat and shown in Fig. 13 above, the sizes of plotted experimental variogram points increase in proportion to the number of associated pairs. Therefore, when fitting theoretical variograms to experimental variograms within GeoStat, it is recommended that the theoretical variogram should favor proximity to more prominently drawn (larger) data points rather than smaller data points.

2.5.4 Additional Considerations for Variogram Formation

Discussed immediately below are additional considerations pertaining to variogram formation. First, the concept of data detrending is reviewed, where this operation holds relevance both with respect to variogram formation and stochastic simulation (the latter of which is discussed in Sec. 2.6). In addition, the manner by which normal score (z-score) values are determined and utilized is reviewed. An illustrative data set of SPT-N blow counts is utilized to aid in elucidating the conceptual discussions.

2.5.4.1 Data Detrending

As is discussed in Sec. 2.6, the GeoStat software makes use of stochastic simulation to produce estimates of deep foundation member axial resistance, along with associated characterizations of variability and uncertainty. It is assumed that both the correlation structure and frequency distribution of a given data set (e.g., geotechnical data concentrated within a selected range of elevations, or soil or rock data within a layer) remain approximately constant along the direction of interest (horizontal, vertical). When a data set exhibits these qualities, it is referred to as stationarity. Also, because of the critical role that variograms play

in performing stochastic simulation (discussed later), stationarity is a necessary attribute for data to possess when said data are utilized in forming variograms.

To illustrate the significance (and procedure) of data detrending, recall the illustrative set of 40 borings for an idealized site (Fig. 1). Further, consider an illustrative set of 51 SPT-N blow counts, measured across the elevation range of 30 ft to 10 ft (Fig. 14a). Descriptive statistics for the 51 SPT-N blow counts are listed in Table 3.
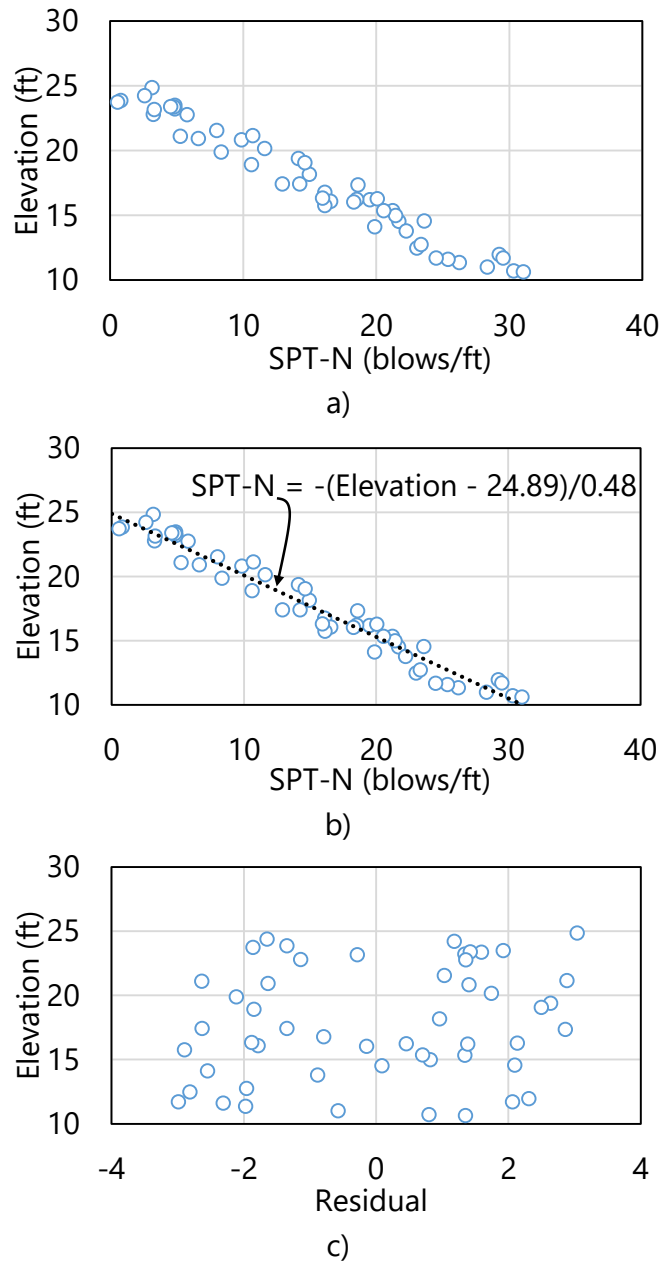
Figure 14. Detrending of illustrative set of 51 SPT-N blow counts (elevation range: 30 ft to 10 ft): a) Scatterplot; b) Scatterplot with inverted trend line; c) Residual

22

Table 3. Descriptive statistics for illustrative set of 51 SPT-N blow counts (elevation range: 30 ft to 10 ft)

Descriptive statistic	Value	Units
Mean (μ)	14.9	blows/ft
Standard deviation (σ)	8.9	blows/ft
Variance (σ^2)	80.1	blows^2/ft^2
Coefficient of variation (COV)	0.6	N/A

Plotted in Fig. 14b are both the scatterplot points and a linear regression fit. As expressed, the regression curve is inverted such that SPT-N is the dependent variable and elevation is the independent variable. The detrending process is carried out by considering each measured SPT-N value, using the associated elevation to evaluate the inverted regression expression, and then subtracting the inverted function value from the measured SPT-N value. The difference between these two values (inverted expression evaluation and measured value) is referred to as the residual.

Carrying out the detrending process for the 51 SPT-N blow counts produces the scatterplot of residuals shown in Fig. 14c. The qualitative distribution of the residuals resembles that of "white noise" compared to depth (Fig. 14a); however the new residual data may still exhibit correlation between pairs (evident from variogram). However, the collection of residuals (Fig. 14c) approximately uphold stationarity, whereas stationarity is not present among the trend-laden measurements of SPT-N blow counts. Also, the variogram does not reach a constant sill value (recall Fig. 9c). Therefore, the residual data—as opposed to the measured SPT-N values—are used when trends are present among measured values used to form z-scores (discussed immediately below), and subsequently, to form experimental variograms and estimates of properties. The estimates of values for SPT-N (or rock strength, etc.) will have the trend added back prior to pile/shaft capacity estimation. Finally, if trends are not present among the "raw" measurements, then the detrending process is not necessary. The GeoStat software is configured such that any given layer of soil or rock data may or may not be detrended for the purpose of variogram formation, at the discretion of the engineer.

2.5.4.2 Normal Score (Z-Score)

Recall from the step-by-step listings of variogram formation (Fig. 11, Fig. 12) that the z-score transformation (mean of zero, standard deviation of unity) of data points rather than the measured values themselves are used when forming experimental variogram points. As illustrated in previous sections, this approach allows for more consistent interpretations of variograms and adds convenience when selecting theoretical variogram features such as sills. To carry out normal score (z-score) calculation given a data point (q), the following expression is evaluated:

$$Z_{score} = \frac{q - \mu}{\sigma} \tag{12}$$

where the z-score (Z_{score}) is a dimensionless quantity. When detrending is not carried out on a data set, z-scores are computed using the "raw" data (e.g., SPT-N, q_u). However, when detrending is carried out on a data set, z-scores are determined (for the purpose of forming variograms) using residuals rather than the measured data.

As illustration, plotted in Fig. 15 are the z-scores corresponding to the residuals of the 51 SPT-N data points from Fig. 14. Because the mean of the residuals is approximately zero-valued for this illustrative data set, the plots of residuals and the z-scores are proportional to one another.
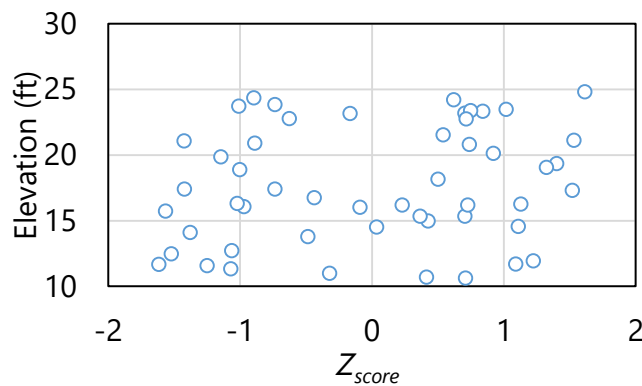
Figure 15. Normal score (Z_{score}) of residuals for illustrative set of 51 SPT-N blow counts (elevation range: 30 ft to 10 ft)

2.6 Stochastic Simulation

Axial resistances of deep foundation members are determined in GeoStat by stochastically simulating realizations (profiles) of geotechnical site data (SPT-N, q_u); empirically relating geotechnical site data to unit quantities of side and tip resistance (skin friction, f_s; tip resistance, q_{tip}); and, then integrating the unit quantities. Introduced in Sec. 2.6.1 and Sec. 2.6.2 are the means by which probabilistic simulation can be conducted using GeoStat (unconditional and conditional, respectively). Additional considerations for conducting stochastic simulation (with focus on worst case conditions regarding variability and uncertainty) are documented in Sec. 2.6.3. See Sec. 2.7 for documentation of the empirical relationships used in relating between layer-specific soil or rock parameter values and unit quantities of side and tip resistance.

2.6.1 Unconditional Simulation

Unconditional simulation is analogous to simulation of spatially varying geotechnical properties with complete knowledge of a site (McVay et al. 2012). Further, for unconditional

simulation, the plan-view foundation location is unknown. Stated alternatively, unconditional simulation involves generation of random variable values on a specified geometric grid such that the probability distribution functions (PDFs) and correlation structures of the available points of measured data are (on average) reproduced. Further, results from unconditional simulation represent typical site or zone properties, and the associated LRFD-ϕ value. These aspects of unconditional simulation are in contrast to those of conditional simulation (discussed in Sec. 2.6.2), where realizations of soil or rock profile data are conditioned to specific boring values.

Unconditional simulation is implemented in GeoStat via use of the lower-upper triangular matrix decomposition algorithm (i.e., the *LU* algorithm), and in turn, produces spatially varying vertical profiles of soil or rock parameters that satisfy the variogram of the site (or zone, layers, etc.). The overall unconditional simulation procedure is illustrated in Fig. 16. Major steps include: generation of a geometric grid; generation of covariance matrices (per soil or rock layer); and then, performance of stochastic simulation. In addition, as part of the overall unconditional simulation procedure, vertical variograms (discussed in Sec. 2.5) play an important role, as highlighted in Fig. 16 (upper-right).

As the first major step in the unconditional simulation procedure (Fig. 16, upper-left), a geometric location grid is formed. For a range of candidate embedment lengths (as specified by the engineer), only the corresponding elevations, {*elevation*}, are accumulated. In GeoStat, the associated elevations that fall within each soil or rock layer are subdivided into 0.5-ft increments.

As the second major step (Fig. 16, middle-left), covariance matrices, [*C*], are formed for each soil or rock layer. More specifically, for each of n_{layers}, the corresponding subsets of {*elevation*} values are expanded into matrix form. Here, such expansion denotes that the matrices house columnated differences in vertical position for each location of interest (i.e., each diagonal entry), relative to every other location of interest (i.e., all other column entries). That is, the {*easting*} vector is expanded using the following expression:

$$[\Delta_{elev}] = \{elevation\} \cdot \{1\}^T - (\{elevation\} \cdot \{1\}^T)^T \qquad (13)$$

where [Δ_{elev}] is a matrix of differences in elevation; {*1*} is a vector of unity-valued entries; and, the superscript "T" denotes the transpose operation.

At this stage, the vertical variogram of the current layer holds significance (Fig. 16, upper-right; see Sec. 2.5 regarding formation of variograms). Subsequent to formation of the elevation-difference matrix, all terms are squared and normalized by the square of the range of the theoretical, vertical variogram (a_v):

$$[h_{norm}]_{jk} = ([\Delta_{elev}]^2_{jk}/a_v^2)^{0.5} \qquad (14)$$

where $[h_{norm}]$ is a symmetric matrix of the normalized vertical distance between each location of interest, relative to every other location considered (within the current layer). The subscripts "jk" denote that the total distance is computed on an entry by entry basis. In certain instances, vertical variograms may be formed within a given layer and exhibit features such as the nugget effect (as introduced in Sec. 2.5). For these instances, a normalization scheme analogous to that described above for the vertical range (a_v) is carried out.
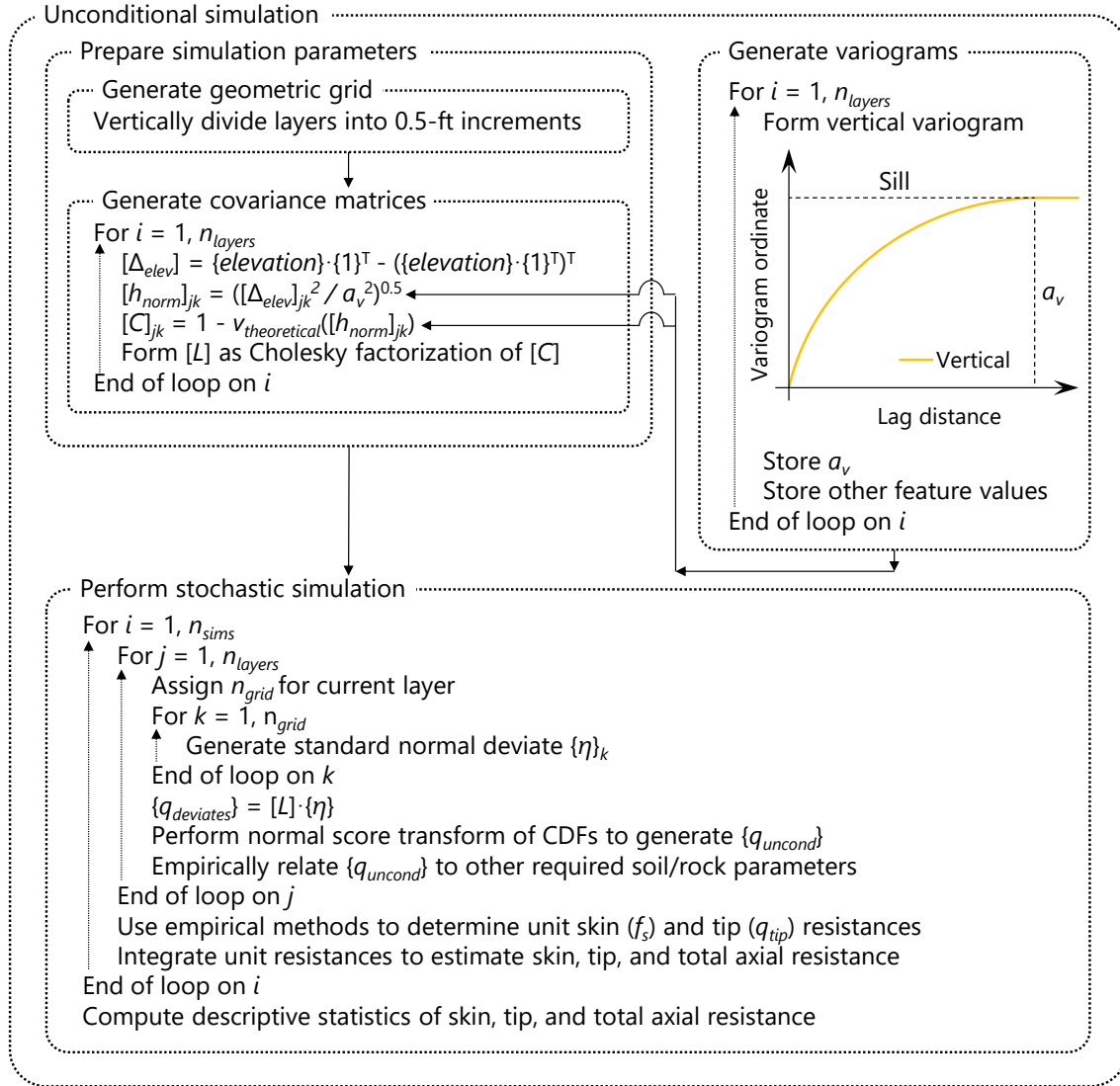

Figure 16. Unconditional simulation procedure

Having formed the matrix of normalized vertical distance for every location of interest within a layer (relative to every other location of interest), the selected form of the theoretical variogram, $v_{theoretical}$, is evaluated (exponential, spherical; as introduced in Sec. 2.5). Recall that,

when forming the entries of $[h_{norm}]$, variogram range values (a_v) are used for normalization. Therefore, evaluations of the theoretical variogram are carried out without direct use of the respective variogram range values. For example, consider a scenario where the exponential form is made use of when forming the theoretical variograms within a given layer. Then solely for the purposes of evaluating the vertical variogram using entries of $[h_{norm}]$ within said layer, the theoretical variogram is modified from that of Eqn. 11 to:

$$v_{theoretical}\big([h_{norm}]_{jk}\big) = 1 - exp(-[h_{norm}]_{jk}) \qquad (15)$$

Relative to the variogram definition from Eqn. 9, the variance (σ^2) of all measured data for all locations of interest within the layer is not directly present in Eqn. 15. This is because, as discussed in Sec. 2.5, the variogram formation process in GeoStat involves subjecting measured geotechnical site data to a separate normalization process. As an additional artifact of data normalization, during variogram formation in GeoStat, entries of the covariance matrix, $[C]$, can also be formed without direct use of the data variance:

$$[C]_{jk} = 1 - v_{theoretical}\big([h_{norm}]_{jk}\big) \qquad (16)$$

The covariance matrix is symmetric and positive definite due to the choice of the $v(h)$ functional form (experimental, spherical). Therefore, Cholesky decomposition is next carried out to obtain the (factorized) lower triangular form of the covariance matrix, $[L]$. As emphasis, formation of the lower triangular matrix is repeated for each layer.

The stochastic simulation is then undertaken (Fig. 16, bottom) for the desired number of soil or rock profiles to be realized (n_{sims}). For each realization, the system layers (n_{layers}) are iterated through. For each layer considered, the number of locations in the geometric grid (n_{grid}) is first assigned, and in turn, iterated through. At this tertiary loop-level, independent values of standard normal deviates are sampled n_{grid} times and stored in vector form $\{\eta\}$. As context, a standard normal deviate is a value sampled from the standard normal distribution (i.e., a unitless normal distribution with mean of 0 and standard deviation of 1). The independently sampled deviate values are then used along with the layer-specific lower-triangular matrix of covariance, $[L]$, to form simulated values of measured properties:

$$\{q_{deviates}\} = [L] \cdot \{\eta\} \qquad (17)$$

where $\{q_{deviates}\}$ is the collection of layer-specific, simulated values of soil properties.

The terms in $\{q_{deviates}\}$ are obtained by operating (in part) on normally distributed data (i.e., $\{\eta\}$). However, physically measured data, $\{q\}$, within a given layer may or may not be normally distributed (distribution types such as log-normal are more commonly applicable to strength quantities). Therefore, a normal score transformation is carried out to map from the normally

distributed values making up {$q_{deviates}$} to a distribution that reflects the ensemble of layer-specific physical measurements, {q}. This procedure is depicted in Fig. 17 for a mapping between normally distributed values of {$q_{deviates}$} and an illustrative set of physical, log-normally distributed data {q}. Note that the use of a log-normal distribution is utilized here purely as illustration; this transformation procedure applies to other distributions as well.
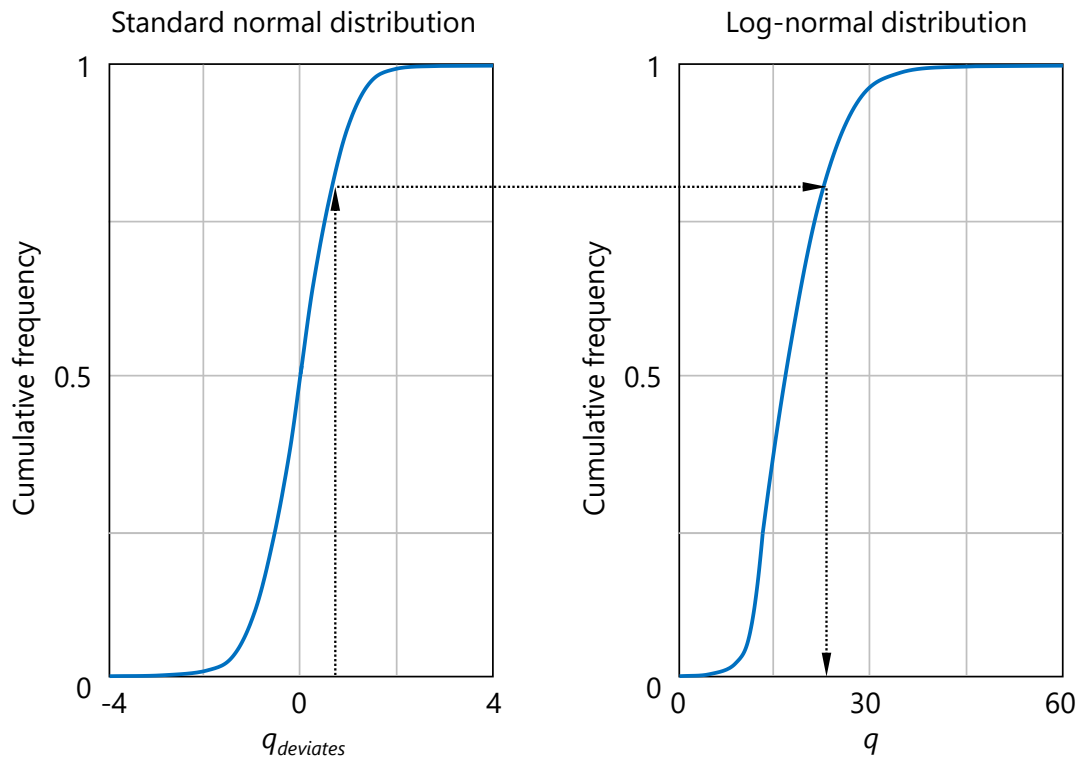
Figure 17. Illustrative normal score transformation (from normal to log-normal) using cumulative distribution functions

The mapping procedure (Fig. 17) involves permuting through each entry of {$q_{deviates}$}. For each entry, the associated CDF value of the normally distributed data (Fig. 17, left) is determined. Then, the ordinate axis of the log-normally distributed data is entered at the same cumulative frequency value (Fig. 17, right). The unconditional simulation value is then assigned by honoring the CDF of the physically measured values. The set of values simulated in this manner constitute the unconditionally simulated values {q_{uncond}} for the layer currently being considered.

At this step in the unconditional simulation process, the simulated values, {q_{uncond}}, always correspond to either SPT-N blow counts or unconfined compression strengths of rock, q_u. For the purpose of building up required soil or rock parameters within a layer, beyond those of SPT-N and q_u values, it is necessary to make use of empirical relations. That is, the SPT-N and q_u values are used along with empirical relationships to estimate the other required soil or

28

rock parameters. Additional details of the required parameters, and associated empirical relationships, are provided in Sec. 2.7.

Continuing with the unconditional simulation procedure (Fig. 16, bottom)—after all layers are iterated through—empirical methods are utilized to relate profiles of soil or rock strength parameters to unit skin friction (f_s) and tip resistance (q_{tip}) quantities. Then, the unit quantities are integrated to form estimates of pile/shaft axial resistance for the current simulation (i.e., pile/shaft configuration and candidate embedment length). The axial capacity calculation software FB-Deep is used for this purpose. See the FB-Deep Help Manual for details regarding empirical determination of unit resistance quantities and integration of these quantities to determine axial, tip, and total resistances of piles/shafts.

The final step of the unconditional simulation procedure (Fig. 16, bottom) is to form descriptive statistics of skin, tip, and total resistances for the pile/shaft section and range of embedment lengths being analyzed. As a result, through-depth profiles of mean-valued resistance are formed. As direct measures of spatial variability, through-depth profiles of variance and coefficient of variation are also quantified. Regarding uncertainty, profiles of LRFD resistance factors (ϕ) are produced as well (see Sec. 2.8 for additional details regarding uncertainty calculations).

2.6.2 Conditional Simulation

Conditional simulation is analogous to conditioning to a specific boring location, where the simulated values of soil or rock strength parameters at said location reproduce corresponding measured values (McVay et al. 2012). As a precursor to conditional simulation, a boring of interest is identified and the plan-view location (easting, northing) is cataloged. This is in contrast to unconditional simulation (discussed in Sec. 2.6.1), where complete site knowledge is assumed, and no plan-view location is specified. Even so, the major steps associated with the conditional simulation procedure (Fig. 18) are similar to those detailed above for unconditional simulation (recall Fig. 16).

In GeoStat, conditional simulation makes use of the *LU* algorithm for producing spatially varying vertical profiles of soil or rock parameters. Major steps include: generation of a geometric grid; generation of covariance matrices (per soil or rock layer); and then, performance of stochastic simulation. In contrast to that of unconditional simulation, both horizontal and vertical variograms play a significant role when conducting conditional simulation. Therefore, conditional simulation should only be conducted if representative variograms can be formed in both the horizontal and vertical directions.

The first major step in the conditional simulation procedure (Fig. 18, upper-left) consists of generating a geometric grid of boring location data. From the plan-view perspective, sets of eastings, {*easting*}; and, northings, {*northing*}, are accumulated to represent all boring

locations. Then, over a range of candidate embedment lengths (as specified by the engineer), corresponding elevations, {*elevation*}, are assembled in the vertical dimension, resulting in n_{grid} geometric location data points. Next, in the GeoStat implementation, the elevation range associated with the current layer is divided into 0.5-ft increments. Note that this subdivision does not affect previously assembled entries of {*elevation*}. Rather, the 0.5-ft increments in elevation are used to augment the layer-specific {*elevation*} vector with n_{cond} additional entries. A corresponding number of plan-view position values are used to augment the {*easting*} and {*northing*} vectors. However, the newly added northing and easting values are all set equal to those of the boring selected for conditioning upon.

As the second major step (Fig. 18, middle-left), covariance matrices, [*C*], are formed for each soil or rock layer. More specifically, for each of n_{layers}, the corresponding subsets of position arrays ({*easting*}, {*northing*}, and {*elevation*}) are expanded into matrix form. This expansion denotes that the matrices house columnated differences in position for each location of interest (i.e., each diagonal entry), relative to every other location of interest (i.e., all other column entries). For example, the {*easting*} array is expanded to form:

$$[\Delta_{east}] = \{easting\} \cdot \{1\}^T - (\{easting\} \cdot \{1\}^T)^T \tag{18}$$

where [Δ_{east}] is a matrix of differences in easting; {*1*} is a vector of unity-valued entries; and, the superscript "T" denotes the transpose operation. The same manner of expansion is carried out to form the matrix of differences in northing, [Δ_{north}], and elevation, [Δ_{elev}], pertaining to the current layer.

At this stage, the horizontal and vertical variograms of the layer hold significance (Fig. 18, upper-right; see Sec. 2.5 regarding formation of variograms). Subsequent to formation of the location-difference matrices, horizontal difference terms (in [Δ_{east}] and [Δ_{north}]) are normalized by the range of the theoretical, horizontal variogram (a_h). Likewise, vertical difference terms are normalized by the range of the theoretical, vertical variogram (a_v).

Next, the matrices containing the (normalized) location-difference terms are amalgamated into a total difference of distance:

$$[h_{norm}]_{jk} = ([\Delta_{east}]_{jk}^2 + [\Delta_{north}]_{jk}^2 + [\Delta_{elev}]_{jk}^2)^{0.5} \tag{19}$$

where [h_{norm}] is a symmetric matrix of the normalized total distance between each location of interest, relative to every other location considered (within the current layer). The subscripts "*jk*" denote that the total distance is computed on an entry by entry basis. The normalization scheme discussed here pertains to scenarios where different values are selected for the ranges a_h and a_v. In certain instances, horizontal and vertical variograms may be formed within a given layer and exhibit features such as the nugget effect (as introduced in Sec. 2.5). For these

instances, normalization schemes analogous to that described above for differing range values (a_h, a_v) are carried out.

Conditional simulation

Prepare simulation parameters

Generate geometric grid

For i = 1, n_{layers}
Assemble n_{grid} entries for {$easting$}, {$northing$}, and {$elevation$} for measured data in layer
Vertically divide layer into 0.5-ft increments
Augment {$easting$}, {$northing$}, and {$elevation$} arrays with n_{cond} location data points
End of loop on i

Generate covariance matrices

For i = 1, n_{layers}
$[\Delta_{east}]$ = {$easting$}·{1}^{T} - ({$easting$}·{1}^{T})^T
$[\Delta_{north}]$ = {$northing$}·{1}^{T} - ({$northing$}·{1}^{T})^T
$[\Delta_{elev}]$ = {$elevation$}·{1}^{T} - ({$elevation$}·{1}^{T})^T
Normalize $[\Delta_{east}]$, $[\Delta_{north}]$ by a_h; $[\Delta_{elev}]$ by a_v
$[h_{norm}]_{jk}$ = ($[\Delta_{east}]_{jk}^2$ + $[\Delta_{north}]_{jk}^2$ + $[\Delta_{elev}]_{jk}^2$)$^{0.5}$
$[C]_{jk}$ = 1 - $v_{theoretical}([h_{norm}]_{jk})$
Form $[L]$ as Cholesky factorization of $[C]$
End of loop on i

Generate variograms

For i = 1, n_{layers}
Form variograms

— Horizontal — Vertical

Sill

a_v a_h

Variogram ordinate

Lag distance

Store a_h, a_v
Store other feature values
End of loop on i

Perform stochastic simulation

For i = 1, n_{sims}
For j = 1, n_{layers}
Assign n_{grid} and n_{cond} for current layer
Determine ordinary kriging weights
For k = 1, n_{grid} + n_{cond}
Generate standard normal deviate {η}$_k$
End of loop on k
{$q_{deviates}$} = $[L]$·{η}
Generate ordinary kriging prediction {q_{krig}}
Generate ordinary kriging prediction {$q_{krig\_deviates}$} using unconditional prediction
{$q_{normdist}$} = {q_{krig}} + {$q_{deviates}$} - {$q_{krig\_deviates}$}
Perform normal score transform of CDFs to generate {q_{cond}}
Empirically relate {q_{cond}} to other required soil/rock parameters
End of loop on j
Use empirical methods to determine unit skin (f_s) and tip (q_{tip}) resistances
Integrate unit resistances to estimate skin, tip, and total axial resistance
End of loop on i
Compute descriptive statistics of skin, tip, and total axial resistance
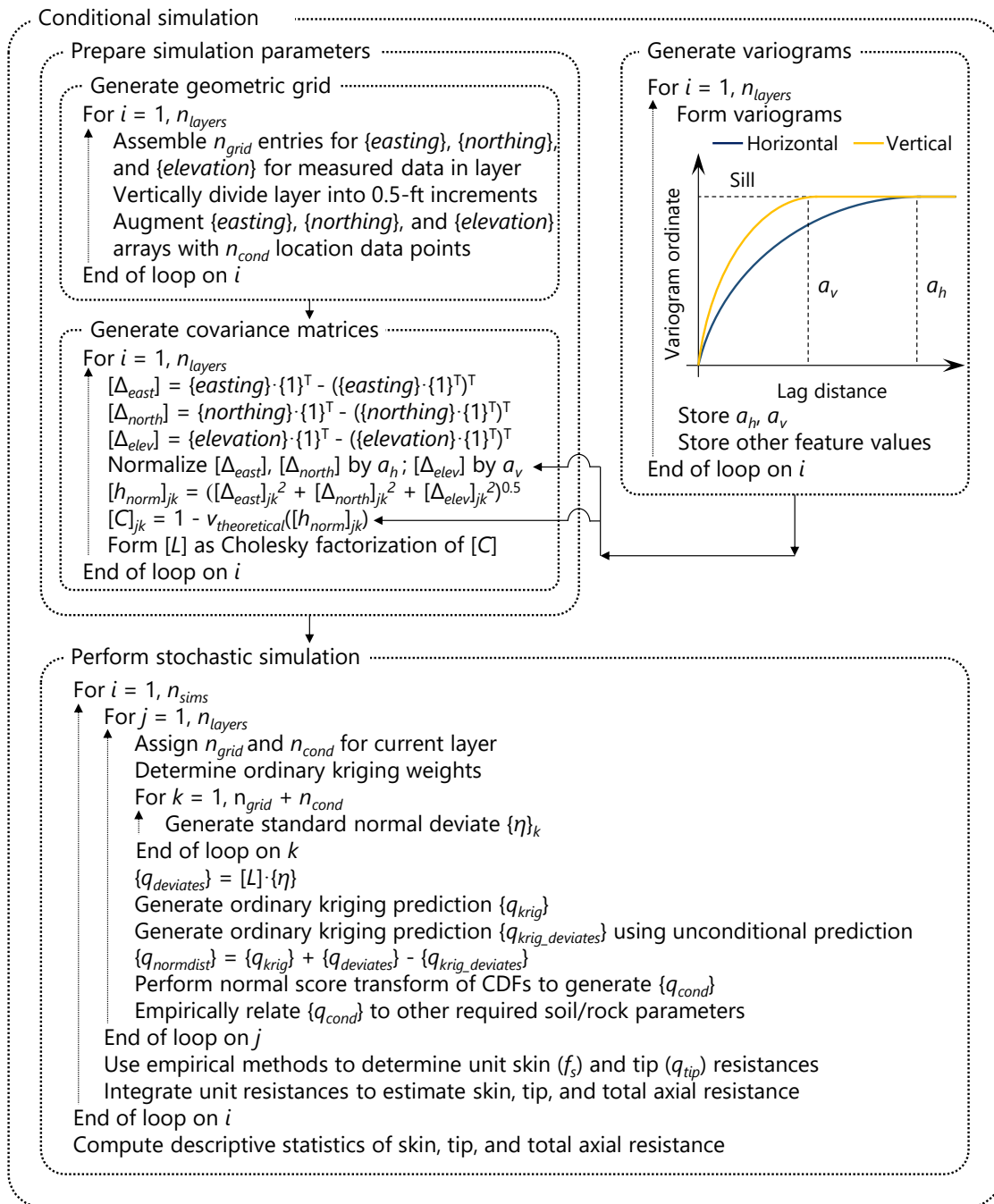
Figure 18. Conditional simulation procedure

Having formed the matrix of normalized total distance for every location of interest within a layer (relative to every other location of interest), the selected form of the theoretical variogram, $v_{theoretical}$, is evaluated (exponential, spherical; as introduced in Sec. 2.5). Recall that,

when forming the entries of $[h_{norm}]$, variogram range values (a_h, a_v) are used for normalization. Therefore, evaluations of the theoretical variogram are carried out without direct use of the respective variogram range values. For example, consider a scenario where the spherical form is made use of when forming the theoretical variograms within a given layer. Then solely for the purposes of evaluating entries of $[h_{norm}]$ within said layer, the theoretical variogram is modified from that of Eqn. 10 to:

$$v_{theoretical}\big([h_{norm}]_{jk}\big) = \begin{cases} \Big(1.5[h_{norm}]_{jk} - 0.5\big([h_{norm}]_{jk}\big)^3\Big)\,;\ [h_{norm}]_{jk} < 1 \\ 1\,;\ [h_{norm}]_{jk} \geq 1 \end{cases} \qquad (20)$$

Relative to the variogram definition from Eqn. 10, the variance of all measured data for all locations of interest within the layer (σ^2) is not directly present in Eqn. 20. This is because, as discussed in Sec. 2.5, the variogram formation process in GeoStat involves subjecting measured geotechnical site data to a separate normalization process. As an additional artifact of data normalization during variogram formation in GeoStat, entries of the covariance matrix, $[C]$, can also be formed without direct use of the data variance (σ^2):

$$[C]_{jk} = 1 - v_{theoretical}\big([h_{norm}]_{jk}\big) \qquad (21)$$

Subsequent to formation of the covariance matrix, which is symmetric and positive definite, Cholesky decomposition is carried out to obtain the (factorized) lower triangular form of the covariance matrix, $[L]$. As emphasis, the lower triangular matrix is uniquely formed for each soil or rock each layer.

The stochastic simulation is then undertaken (Fig. 18, bottom) for the desired number of soil or rock profiles to be realized (n_{sims}). For each realization, the system layers (n_{layers}) are iterated through. For each layer considered, the number of locations in the geometric grid (n_{grid}) and the number of layer-specific locations along the boring being conditioned upon (n_{cond}) are assigned. Ordinary kriging weights are then determined. In GeoStat, the weights are solved in the same manner as that presented in Faraone (2014) and Goovaerts (1997):

$$\sum_{j=1}^{n_{cond}} \omega_j\,(x_g) \cdot [C]_{ij} + \lambda = [C]_{ig} \ \ \forall\ i = 1, \ldots, n_{grid} \qquad (22)$$

where ω_j is the ordinary kriging weight. The presence of (x_g) signifies that n_{cond} weights are assigned at each grid location (corresponding to the first n_{grid} entries in {*easting*}, {*northing*}, and {*elevation*}), and relative to the location of the boring being conditioned upon. The sum of all kriging weights associated with a given location, x_g, must equal unity. Continuing from left to right in Eqn. 22, λ is a Lagrangian operator. On the right-hand side of Eqn. 22, the subscripts "*ig*" are assigned to the covariance matrix. The second subscript "*g*" in particular

signifies correspondence with the location, x_g. As a more physical interpretation, the kriging weights constitute a relative spatial correlation structure between the 3D locations of the boring being conditioned upon and the 3D locations of all other borings that are pertinent to the layer being considered.

As the next step in conditional simulation, independent values of standard normal deviates are sampled n_{grid} + n_{cond} times and stored in vector form $\{\eta\}$. The independently sampled deviate values are then used along with the layer-specific lower-triangular matrix of covariance, $[L]$, to form simulated values of measured properties:

$$\{q_{deviates}\} = [L] \cdot \{\eta\}$$ (23)

where $\{q_{deviates}\}$ is the collection of layer-specific, normally distributed, and unconditionally simulated values of soil properties. The length of $\{q_{deviates}\}$ is equal to the sum of n_{grid} and n_{cond}.

To convert the values associated with unconditional simulation to that of conditional simulation, the previously computed kriging weights are utilized. In particular, as the next step in the conditional simulation process (Fig. 18, bottom), a set of n_{cond} ordinary kriging predictions, $\{q_{krig}\}$, is generated as:

$$\{q_{krig}\}_i = \sum_{j=1}^{n_{grid}} \omega_j^{\langle i \rangle} \cdot Z_{score}(\{q\}_j)$$ (24)

where, relative to Eqn. 22, the kriging weights are expressed such that the superscript, $\langle i \rangle$, signifies the ith column from the kriging weights in matrix form (n_{grid} rows by n_{cond} columns) . Also, recalling Eqn. 12, the term $Z_{score}()$ indicates evaluation of the standard normal score (z-score) for physically measured data points, $\{q\}$, that fall within the current layer.

As an additionally required conversion quantity (unconditional to conditional), a separate set of ordinary kriging predictions are generated, but with use of $\{q_{deviates}\}$:

$$\{q_{krig\_deviates}\}_i = \sum_{j=1}^{n_{grid}} \omega_j^{\langle i \rangle} \cdot Z_{score}(\{q_{deviates}\}_j)$$ (25)

A set of conditionally simulated—but normally distributed—soil or rock parameter values are then obtained by combining the n_{cond} entries of $\{q_{krig}\}$, $\{q_{deviates}\}$, and $\{q_{krig\_uncond}\}$ that are associated with the boring being conditioned upon:

$$\{q_{normdist}\} = \{q_{krig}\} + \{q_{deviates}\} - \{q_{krig\_deviates}\}$$ (26)

33

where contributing terms are combined in this manner to eliminate the smoothing effect from the ordinary kriging operator, $\{q_{krig}\}$; and, to reinstate the spatial variability of the process in the random field (Faraone, 2014).

The terms in $\{q_{normdist}\}$ are obtained by operating (in part) on normally distributed data. However, physically measured data, $\{q\}$, within a given layer may or may not be normally distributed. Therefore, a normal score transformation is carried out to map from the n_{cond} normally distributed values making up $\{q_{normdist}\}$ to a distribution that reflects the ensemble of n_{grid} layer-specific physical measurements, $\{q\}$. Refer to Fig. 17 (as part of the discussion for unconditional simulation) for details of the mapping procedure, which in the present discussion produces conditionally simulated values $\{q_{cond}\}$.

The simulated values, $\{q_{cond}\}$, always correspond to either SPT-N blow counts or unconfined compression strengths of rock, q_u. For the purpose of building up required soil or rock parameters within a layer, beyond those of SPT-N and q_u values, it is necessary to make use of empirical relations. That is, the SPT-N and q_u values are used along with empirical relationships to estimate the other required soil or rock parameters. Additional details of the required parameters, and associated empirical relationships, are provided in Sec. 2.7.

After all layers are iterated through in the conditional simulation procedure (Fig. 18, bottom), empirical methods are utilized to relate profiles of soil or rock strength parameters to unit skin friction (f_s) and tip resistance (q_{tip}) quantities. Then, the unit quantities are integrated to form estimates of pile/shaft axial resistance for the current simulation (i.e., pile/shaft configuration and candidate embedment length). The axial capacity calculation software FB-Deep is used for this purpose. See the FB-Deep Help Manual for details regarding empirical determination of unit resistance quantities and integration of these quantities to determine axial, tip, and total resistances of piles/shafts.

The final step of the conditional simulation procedure (Fig. 18, bottom) is to form descriptive statistics of skin, tip, and total resistances for the pile/shaft section and range of embedment lengths being analyzed. As a result, through-depth profiles of mean-valued resistance are formed. As direct measures of spatial variability, through-depth profiles of variance and coefficient of variation are also quantified. Regarding uncertainty, profiles of LRFD resistance factors (ϕ) are produced as well (see Sec. 2.8 for additional details regarding uncertainty calculations).

2.6.3 Special Considerations for Worst Case Conditions

In the case where no acceptable theoretical variogram can be fit to the experimental variogram points (e.g., availability of little, if any, site data), "worst case" conditions can be simulated. In this context, the phrasing "worst case" signifies consideration of: 1) upper bound

estimates of spatial variability (e.g., long correlation lengths); and, 2) upper bound estimates of uncertainty which result in lower bound estimates of LRFD resistance factor, ϕ. Consequently, stochastic simulation using worst case conditions tends to require longer piles/shafts to achieve a given magnitude of axial resistance.

The option to conduct unconditional simulation under worst case conditions is available in the GeoStat software, and is implemented consistent with recommendations from McVay et al. (2012) and Faraone (2014). Selection of worst conditions can be made on a layer by layer basis in GeoStat, and with respect to either (or both) the horizontal and vertical directions. Whenever the worst case conditions are applied to the vertical search direction, within a given layer, the range (a_v) is constrained to a large number relative to pile/shaft length (10,000 ft). Regarding the horizontal search direction, if unconditional simulation is being carried out, then horizontal range is constrained to a large number relative to pile/shaft width (again, 10,000 ft). However, when the worst case scenario is assigned for the horizontal search direction within a given layer, and conditional simulation is conducted, then the horizontal range is set to the vertical range ($a_h = a_v$).

2.7 Realization of Layer Data

As part of both the unconditional and conditional simulation procedures (recall Fig. 16 and Fig. 18, respectively), it is necessary for "base" sets of soil or rock parameters to be related to all other required parameters through use of empirical relationships. Recall that the base parameters are SPT-N blow counts and unconfined compression strength (q_u). In the following, all empirical relationships that are made use of during stochastic simulation are delineated. More specifically, listings and discussion are provided concerning: 1) the types of soil or rock layers that can be modeled in GeoStat; 2) the associated (layer-specific) soil or rock parameters required for estimating unit measurements of axial resistance (skin, tip); and, 3) empirical relationships adopted for using SPT-N (and/or q_u) values to estimate all other required soil or rock parameters throughout vertically subdivided profiles (in 0.5-ft increments).

Consistent with the axial capacity calculation software, FB-Deep, an integer mapping scheme is adopted in GeoStat in assigning available soil or rock types to a given profile layer. The listing is provided in Table 4. Considerations for each of the available layer types, within the context of performing stochastic simulation using GeoStat, are presented immediately below.

Table 4. Integer mappings for available soil and rock layer types in GeoStat

Soil or rock type	Integer mapping
Plastic clay	1
Clay and silty sand	2
Clean sand	3
Limestone and very shelly sand	4

2.7.1 Plastic Clay

Stochastic simulations involving Plastic Clay layers (type 1 from Table 4) require the parameters listed in Table 5. The required parameters, as listed, are consistent with that discussed in Sec. 4.2.4.4 of McVay et al. (2012). Namely, for simulations involving driven piles, only values of C_u (undrained shear strength) are required along the vertical dimension of the Plastic Clay layer. For simulations involving drilled shaft foundation members, both γ (unit weight) and C_u (undrained shear strength) are required. During simulation, realizations of SPT-N blow counts are used along with the empirical relationship from (Terzaghi and Peck 1967) to estimate C_u in units of tsf:

$$C_u = 0.063 \cdot \text{SPT-N} \tag{27}$$

Table 5. Parameters for Plastic Clay layers

Parameter	Piles	Shafts
γ		✓
C_u	✓	✓

Regarding required values for unit weight, γ: mean values and corresponding COVs are directly provided by the engineer as part of the layer definition (see the Help Manual for additional details). Then, for each elevation of interest during the simulation, the input values (mean, COV) are used to form and sample from a lognormal distribution, and in turn, produce statistically independent values for unit weight.

2.7.2 Clay and Silty Sand

For Clay and Silty Sand layers (type 2 from Table 4), the required parameters are identical to those of Plastic Clay. Unit weight (γ) and undrained shear strength (C_u) properties are required for drilled shafts, while only C_u (as correlated from SPT-N) is required for simulations involving driven piles. In addition, the correlation from Terzaghi and Peck (1967) is again used when estimating C_u values. Specific to simulations of drilled shaft foundations, values of unit weight (γ) are generated in the same manner as that described above for Plastic Clay layers.

2.7.3 Clean Sand

As listed in Table 6, two parameters are required for embedment depths that correspond to Clean Sand. For driven pile foundations, only SPT-N blow counts are necessary for simulation purposes. When drilled shafts are considered, through-depth values of both the unit weight (γ) and SPT blow count (SPT-N) are required. Vertical profiles of SPT-N blow counts are generated as described previously for unconditional and conditional simulation. Values of unit weight are generated using the same approach as that documented for Plastic Clay layers.

Table 6. Parameters for Clean Sand layers

Parameter	Piles	Shafts
γ		✓
SPT-N	✓	✓

2.7.4 Limestone and Very Shelly Sand

Layers designated as Limestone and Very Shelly Sand maintain substantially different input parameter requirements depending on the foundation member type (Table 7). When pile foundation members are considered, only values of SPT-N are necessary. The procedures for simulating vertical profiles of SPT-N values are the same as those described previously for unconditional and conditional simulation.

For shaft member portions embedded in Limestone and Very Shelly Sand layers, the "base" parameter q_u is drawn upon, which is in contrast to the approach adopted for processing of all other layer types and foundation configurations. The implementation in GeoStat for generating required simulation parameters (for drilled shafts in Limestone and Very Shelly Sand) is consistent with the approach presented in Sec. 4.2.4 of McVay et al. (2012). Accordingly, several types of parameters must be empirically determined prior to computation of unit skin and tip resistance quantities. The required parameters include (Table 7): unit weight (γ), unconfined compression strength (q_u), split tensile strength (q_t), mass modulus (E_m), rock quality designation (RQD), and *recovery*.

Table 7. Parameters for Limestone and Very Shelly Sand layers

Parameter	Piles	Shafts
γ		✓
SPT-N	✓	
q_u		✓
q_t		✓
E_m		✓
RQD		✓
recovery		✓

Simulated realizations (vertical profiles) of unit weight (γ) are generated in the same manner as that documented above for Plastic Clay layers. In addition, realizations of unconfined compression strength, q_u, are generated using the procedures detailed previously for unconditional (Fig. 16) and conditional (Fig. 18) simulation.

2.7.4.1 Split Tensile Strength (q_t)

The procedure implemented in GeoStat for simulating values of split tensile strength, q_t, is delineated in Fig. 19. Overall, the procedure incorporates site-specific characterization of the strength of correlation that is present between physically measured values of q_t and unconfined compression strength, q_u. Major steps involved in simulating q_t values consist of preparing relevant simulation parameters and then performing stochastic simulation.
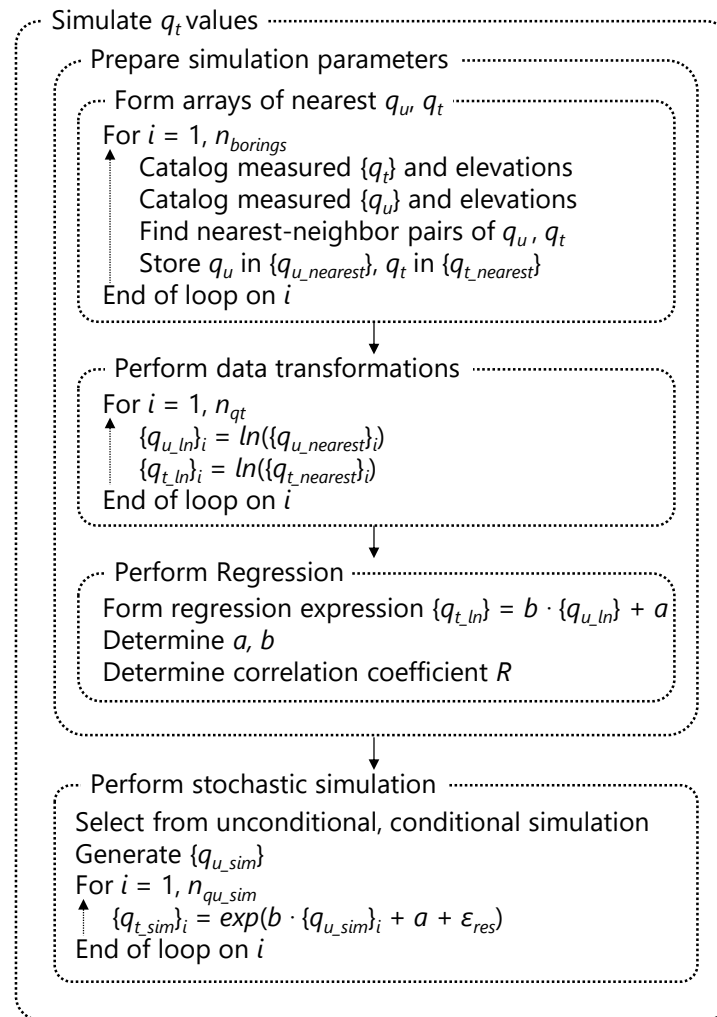

Figure 19. Simulation of split tensile strength, q_t

As the first step in preparing simulation parameters (Fig. 19, top), all borings considered for analysis are iterated through to identify pairs of physically measured q_u and q_t values, which are stored (respectively) in $\{q_{u\_nearest}\}$ and $\{q_{t\_nearest}\}$. To illustrate the manner by which physical measurements of q_u and q_t are paired together, consider the illustrative core-run data listed in Table 8. Labels listed beneath the Sample column denote the order in which specimen data are reported (1 through 9). Also, the letter "T" signifies that the specimen is used for

conducting a split tensile test (to produce q_t). The letter "U" signifies conduction of an unconfined compression strength test to produce q_u.

While core runs are typically 5 ft in length, the summed length of all recovered specimens within the run do not typically reach 5 ft. Such is the case for the illustrative core run data of Table 8. Further, the top-to-bottom order of a given set of core run data may or may not be available. Therefore, it is assumed (in this illustrative scenario) that the specimen data are ordered from top to bottom of the run (Fig. 20). Based on these assumptions, a nearest-neighbor search is carried out to identify pairs of measured q_u and q_t data.

Table 8. Illustrative laboratory test data for a coring run (adapted from McVay et al. 2012)

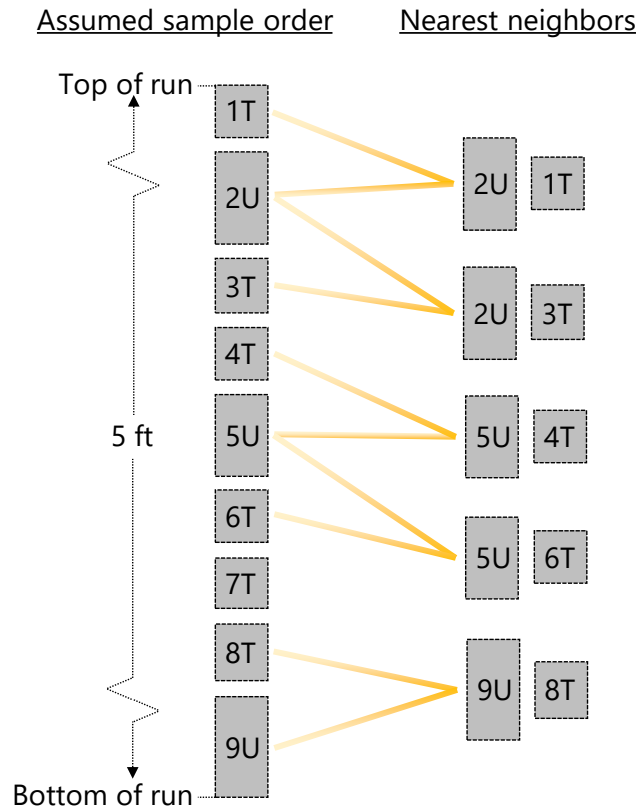| Sample	Length (in)	q_t (psi)	q_u (psi)
1T	2.495	150.3842	--
2U	4.376	--	439.014
3T	2.621	128.7227	--
4T	2.492	353.7287	--
5U	3.913	--	454.679
6T	2.473	252.8827	--
7T	2.404	252.7647	--
8T	2.658	281.5633	--
9U	4.811	--	711.509

Figure 20. Illustrative core run specimens with nearest-neighbor pairings for q_u and q_t

Paired values identified as part of a nearest-neighbor search (using the illustrative data set) are depicted in the right portion of Fig. 20. As is the case here, data obtained from an unconfined compression test (q_u) may be identified for use in multiple pairings. For example, specimen 2U is paired with specimen 1T, and independently, specimen 2U is paired with specimen 3T. For instances where more than two consecutive specimens are used to conduct the same type of testing, then no pairings are identified for the intermediately positioned specimens. For example, specimens 6T, 7T, and 8T are all used for measuring split tensile strength, q_t. Because specimen 7T is bounded (above and below) by two specimens of the same test type, no pair is assigned to the 7T specimen. If it is desired to explicitly pair two measured q_u and q_t values, then the nearest-neighbor search algorithm can be overridden in GeoStat by simply defining said q_u and q_t values at the same elevation (see the Help Manual for details regarding how boring data are input in GeoStat models).

Subsequent to finding nearest neighbors of measured data values across the set of site borings, and forming the $\{q_{u\_nearest}\}$ and $\{q_{t\_nearest}\}$ quantities, the next step in the overall q_t simulation procedure is carried out (Fig. 19, middle). Namely, each entry in $\{q_{u\_nearest}\}$ and $\{q_{t\_nearest}\}$ is transformed (using natural log) to produce $\{q_{u\_ln}\}$ and $\{q_{t\_ln}\}$. Then, regression is carried out upon the transformed data, where entries in $\{q_{t\_ln}\}$ are treated as the dependent variable. The form of the regression expression is:

$$\{q_{t\_ln}\} = b \cdot \{q_{u\_ln}\} + a \tag{28}$$

where, respectively, *a* and *b* are the intercept and slope of the regression line fitted to the transformed data. Regression terms for slope (*b*), intercept (*a*), and correlation coefficient (*R*) are retained from this step in the overall procedure, and are made use of during the subsequently conducted stochastic simulation (Fig. 19, bottom).

Having completed preparation of relevant simulation data, either unconditional or conditional simulation is then conducted (recall Fig. 16 and Fig. 18, respectively) to produce a realization of n_{qu_sim} simulated q_u values, $\{q_{u\_sim}\}$. Next, for each entry in $\{q_{u\_sim}\}$, corresponding values of q_t are computed to populate $\{q_{t\_sim}\}$:

$$\{q_{t\_sim}\}_i = exp\left(b \cdot \{q_{u_{sim}}\}_i + a + \varepsilon_{res}\right) \tag{29}$$

where the previously determined components of the regression expression (*a*, *b*) are utilized. Additionally, a residual error term, ε_{res}, is introduced. More specifically, for each simulated value of q_t, a corresponding residual term is sampled from a normal distribution with mean of zero and variance, σ_{res}^2, of:

$$\sigma_{res}^2 = \sigma_{qt\_ln}^2 \cdot (1 - R^2)^2 \tag{30}$$

where $\sigma_{qt\_ln}^2$ is the variance of the transformed physical measurements of q_t, and the previously determined correlation coefficient (*R*) is utilized for scaling.

2.7.4.2 Mass Modulus (*E_m*)

The procedure implemented in GeoStat for simulating values of rock mass modulus, E_m, is delineated in Fig. 21. As implemented, the approach automates site-specific characterization of the strength of correlation that is present between physically measured values of E_m and unconfined compression strength, q_u. Major steps involved in simulating E_m values consist of preparing relevant simulation parameters and then performing stochastic simulation.
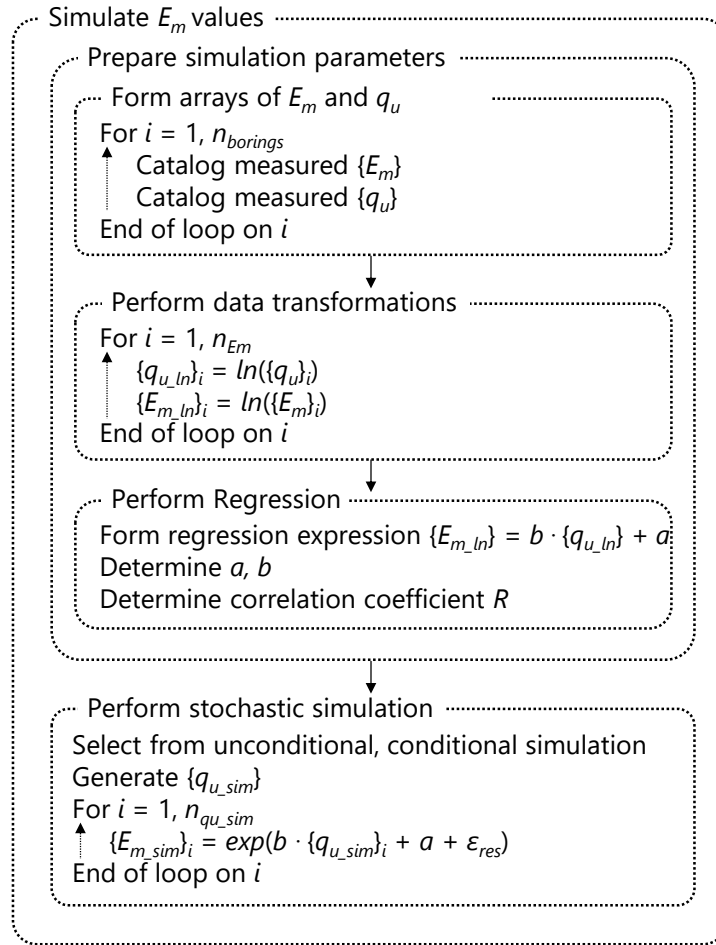
Figure 21. Simulation of mass modulus, E_m

In contrast to simulation of q_t values, pair matching (i.e., nearest-neighbor searching) is not necessary for simulating E_m values. This is because mass modulus is typically determined relative to unconfined compression strength (q_u). Consequently, for all borings considered, measured values of E_m and q_u can be directly cataloged (Fig. 21, top).

Subsequently, each cataloged entry of $\underline{q_u}$ and E_m is transformed (using natural log) to produce $\{q_{u\_ln}\}$ and $\{E_{m\_ln}\}$. Then, regression is carried out upon the transformed data (Fig. 21, middle), where entries in $\{E_{m\_ln}\}$ are treated as the dependent variable. The form of the regression expression is:

$$\{E_{m\_ln}\} = b \cdot \{q_{u\_ln}\} + a \tag{31}$$

where, respectively, a and b are the intercept and slope of the regression line fitted to the transformed E_m and q_u data. The slope (b), intercept (a), and correlation coefficient (R) are retained, and are made use of during stochastic simulation (Fig. 21, bottom).

Either unconditional or conditional simulation is then conducted (recall Fig. 16 and Fig. 18, respectively) to produce a realization of n_{qu_sim} values of unconfined compression strength, $\{q_{u\_sim}\}$. Next, for each entry in $\{q_{u\_sim}\}$, corresponding values of E_m are computed to populate $\{E_{m\_sim}\}$:

$$\{E_{m\_sim}\}_i = exp\left(b \cdot \{q_{u_{sim}}\}_i + a + \varepsilon_{res}\right) \tag{32}$$

where the previously determined components of the regression expression (a, b) are utilized. Additionally, a residual error term, ε_{res}, is introduced, and is sampled from a normal distribution with mean of zero and variance, σ_{res}^2, of:

$$\sigma_{res}^2 = \sigma_{Em\_ln}^2 \cdot (1 - R^2)^2 \tag{33}$$

where $\sigma_{Em\_ln}^2$ is the variance of the transformed boring data for E_m, and the previously determined correlation coefficient (R) is utilized for scaling.

2.7.4.3 RQD and Recovery

Regarding Florida limestone, McVay et al. (2012) found no significant correlations between unconfined compression strength (q_u) and RQD (nor q_u and *recovery*). In GeoStat, random selection of the site-wide collection of RQD and *recovery* values is carried out, when such values are required, during simulation. However, if so desired, this process can be overridden in GeoStat by simply defining said RQD and *recovery* values at the same elevation as a given, measured value of q_u.

For example, consider a q_u value and associated elevation, such as would be defined in the Boring Data dialog (see the Help Manual). If an RQD (and/or *recovery*) value is input at that same elevation, then the RQD (and/or *recovery*) value will be associated with the q_u value. Otherwise, when GeoStat carries out the process to pair q_u values and RQD (and/or *recovery*) values, the RQD (and *recovery*) values are selected from the general set of values defined across all currently enabled boring locations.

2.8 Resistance Factor (ɸ)

The preceding subsections of Ch. 2 document modeling techniques and simulation procedures for characterizing variability (i.e., spatial variability of geotechnical site data). However, the uncertainty associated with a given estimate of pile (or shaft) axial resistance is also critical to foundation design. In LRFD approaches, resistance factors (ɸ) encapsulate both variability and uncertainty phenomena. Further, resistance factors (ɸ) typically range from 0 to 1. The product of computed values of nominal resistance and ɸ produce factored resistance, where the latter quantity is then used for member design. Note that

program-generated resistance (ϕ) factors should only be used in conjunction with Owner's guidelines.

The expression used for resistance factor, ϕ, evaluation in GeoStat is adopted from McVay et al. (2012):

$$\phi = \frac{(\gamma_D \cdot \frac{Q_D}{Q_L} + \gamma_L) \cdot \sqrt{\frac{1 + COV_Q^2}{1 + COV_R^2}}}{(\lambda_{QD} \cdot \frac{Q_D}{Q_L} + \lambda_{QL}) \cdot exp\left(\beta \cdot \sqrt{ln\left((1 + COV_R^2) \cdot (1 + COV_Q^2)\right)}\right)} \tag{34}$$

$$COV_Q^2 = \frac{(\lambda_{QD} \cdot \frac{Q_D}{Q_L} \cdot COV_{QD})^2 + (\lambda_{QL} \cdot COV_{QL})^2}{(\lambda_{QD} \cdot \frac{Q_D}{Q_L})^2 + 2 \cdot \frac{Q_D}{Q_L} \cdot \lambda_{QD} \cdot \lambda_{QL} + \lambda_{QL}^2} \tag{35}$$

where COV_R is the coefficient of variation of the nominal resistance (quantified, in part, through spatial variability characterization); COV_Q is the coefficient of variation with respect to loading as stipulated by Styler (2006). The first-order second-moment (FOSM) LRFD-ϕ, using the Styler (2006) representation of COV_Q, has been shown to be within 3% of the first order reliability method (FORM) LRFD-ϕ (Styler 2006). All other component terms used in calculating ϕ are listed in Table 9. Values of component terms are taken from McVay et al. (2012).

Table 9. Component terms for evaluation of LRFD resistance factors, ϕ

Term description	Symbol	Value
Dead load factor	γ_D	1.25
Live load factor	γ_L	1.75
Dead to live load ratio	Q_D/Q_L	2.00
Dead load bias factor	λ_{QD}	1.08
Live load bias factor	λ_{QL}	1.15
Mean resistance bias factor	λ_R	1.0
Dead load coefficient of variation	COV_{QD}	0.128
Live load coefficient of variation	COV_{QL}	0.18
Target reliability index	β	3.0

In Eqn. 34, the term COV_R is contributed to by: 1) spatial variability of site data (quantified as part of stochastic simulation); and, 2) inherent error that arises due to use of empirical methods. Discussion of the latter phenomenon is provided in Ch. 3.

CHAPTER 3
METHOD ERROR ANALYSIS

3.1 Overview

For estimating axial resistances of deep foundation members, total uncertainty of design resistance is comprised of both spatial variability and the uncertainty of "method error". Method error is defined in McVay et al. (2012) as the total difference between predicted design resistance and the corresponding (physically measured) load-tested resistance. The manner in which method error is utilized when estimating pile (or shaft) axial resistance, as originally developed in McVay et al. (2012), is adopted in the GeoStat implementation. Sources of method error relevant to use of the GeoStat software include: 1) measurement error associated with in-situ testing; 2) intrinsic error in empirical relationships that are used for relating physical measurements to unit resistance quantities; and, 3) intrinsic error in empirical methods used in integrating unit resistance quantities to calculate member-level estimates of pile/shaft axial resistance.

Determination of method error necessitates use of regression concepts. For example, regression analysis of predicted shaft axial resistance versus measured load-test data may be utilized in forming method error relationships for use in design. Accordingly, pertinent concepts of regression analysis are discussed in Sec. 3.2. Sections of Ch. 3 beyond Sec. 3.2 focus on expressions of method error, which are implemented in GeoStat, and further, are specific to foundation member type and the surrounding soil or rock medium. Development of a representative regression curve for axial resistances of driven piles is documented in Sec. 3.3, while considerations for portions of embedded shafts in sand, clay, and rock layers are presented in Sec. 3.4 through Sec. 3.6, respectively. Considerations for incorporating results from custom regression analysis into method error (e.g., from load tests) is discussed in Sec. 3.7. Expressions for quantifying the combined effects of spatial variability and method error of pile/shaft axial resistances (i.e., total uncertainty) are provided in Sec. 3.8. Also indicated in Sec. 3.8 is the significance of total uncertainty with respect to computing LRFD resistance factors (ϕ).

3.2 Regression Analysis

Consider the illustrative schematic of predicted (q_{pred}) and physically measured (q_{meas}) axial resistances plotted in Fig. 22. A linear regression curve passing through the data is also plotted in Fig. 22. All points along the regression curve are described (for this illustration) using intercept, a, and slope, b. While many other regression curve types are possible (e.g., exponential, power functions), the same general concepts as those discussed immediately below remain applicable.

Returning the illustrative data set of Fig. 22, for each plotted point of q_{pred} and $q_{measured}$, the difference between the regression curve ordinate and the physically measured resistance (q_{meas}) is referred to as the error (ε) of the regression. To calculate a given value of physically measured resistance (q_{meas}) using the respective prediction (q_{pred}), the regression curve, and regression error (ε), the following expression is utilized:

$$q_{meas} = a + b \cdot q_{pred} + \varepsilon \tag{36}$$

Due to variations across the set of q_{pred} and q_{meas} values, the regression error (ε) varies from point to point. For regression analysis, it is typically desired for the regression expression parameters (a, b) to be selected such that the summation of the squares of errors ($\sum \varepsilon^2$) across all pairs of q_{pred} and q_{meas} is minimized.
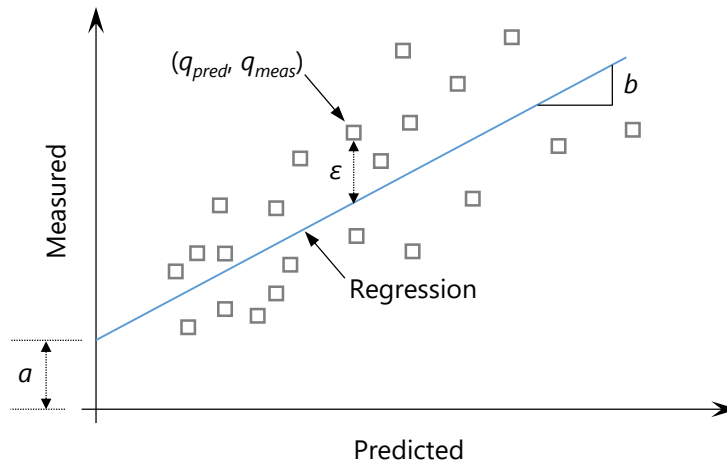

Figure 22. Illustrative scatterplot of measured (q_{meas}) and predicted (q_{pred}) resistances

Recalling the definition of the correlation coefficient (R) from Ch. 2, the slope of the regression curve that satisfies the least-squares error criterion is given as:

$$b = R \cdot \frac{\sigma_{meas}}{\sigma_{pred}} \tag{37}$$

where R is the correlation coefficient between the set of values; σ_{meas} is the standard deviation of all q_{meas} values; and, σ_{pred} is the standard deviation of the corresponding q_{pred} values. Furthermore, the intercept of the regression curve is:

$$a = \bar{q}_{meas} - b \cdot \bar{q}_{pred} \tag{38}$$

where $\bar{q}_{meas}$ is the mean of all q_{meas} values, and $\bar{q}_{pred}$ is the mean of the corresponding q_{pred} values. The variance of the regression error (σ_ε^2) can be related to the variance of the measured data (σ_{meas}^2) by:

$$\sigma_\varepsilon^2 = \sigma_{meas}^2 \cdot (1 - R^2)^2 \tag{39}$$

Documented in the following are regression analyses of collections of measured and predicted axial resistances of deep foundation members, where the concepts, types of quantities, and curve components employed are analogous to those introduced above. Sets of data pertaining to pile and shaft foundation member types, embedded in various media, are analyzed. Additionally, representative regression curves are identified, in relation to method error characterization, for each considered member type and surrounding medium (e.g., clay, sand, limestone).

3.3 Driven Piles

Plotted in Fig. 23 are pairs of predicted and measured (total) axial resistance pertaining to physically constructed concrete piles, which in turn, are distributed across several bridge sites. The 48 data points (q_{pred}, q_{meas}) were originally gathered from the literature as part of McVay et al. (2012). Also reported in McVay et al. (2012) a representative best-fit regression curve to the 48 predicted and measured (i.e., Davisson) capacity values.
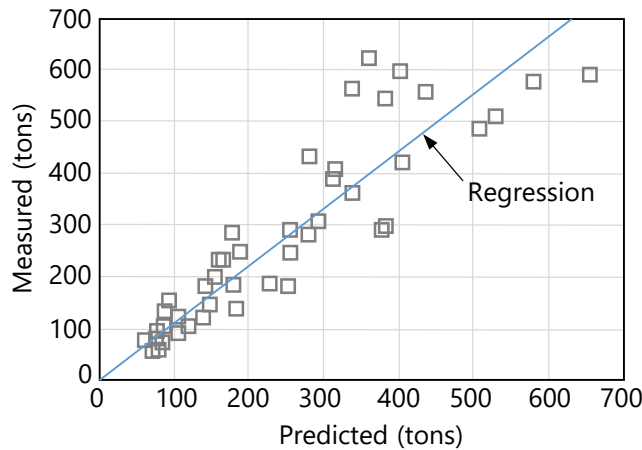

Figure 23. Regression analysis for total axial resistance of concrete piles (McVay et al. 2012)

The form of the regression curve is the product of exponential and power terms. Predicted values of axial resistance (q_{pred}) are taken as the independent variable, and computed values of measured resistance (as opposed to physically measurements of resistance), $\hat{q}_{meas}$, are produced:

$$\hat{q}_{meas} = exp(a) \cdot q_{pred}^b \tag{40}$$

where recommended values for the regression terms a and b of the (n = 48) driven pile data set are listed in Table 10. Also listed in Table 10 is the coefficient of variation of the regression error (COV_ε):

$$COV_\varepsilon = \sqrt{exp(\sigma^2_{\varepsilon\_ln}) - 1} \qquad (41)$$

where COV_ε is a function of the log-transformed variance of the regression error, $\sigma_{\varepsilon\_ln}{}^2$.

Table 10. Regression parameter values for total axial resistance of concrete piles (McVay et al. 2012)

Parameter	Value
a	0.17
b	0.99
COV_ε	0.24
n	48

Together, Eqn. 40, Eqn. 41, and the parameter values listed in Table 10 constitute a representative means of relating between predicted and measured axial resistances of driven piles. See Sec. 3.8 for the means by which selected terms from the representative regression expression are utilized when characterizing total uncertainty.

3.4 Drilled Shafts in Sand

Pairs of total predicted and measured axial resistance pertaining to physically constructed drilled shafts in sand are plotted in Fig. 24. The (n = 31) data points (q_{pred}, q_{meas}) are directly excerpted from the previously conducted data gathering efforts of McVay et al. (2012). A representative best-fit regression curve to the 31 points, as originally developed in McVay et al. (2012), is:

$$\hat{q}_{meas} = exp(a) \cdot q^b_{pred} \qquad (42)$$

where the form of the regression expression is defined as the product of exponential and power terms. Recommended values (McVay et al. 2012) for the argument of the exponential function, a, and the exponent, b, are listed in Table 11.

Also listed in Table 11 is the coefficient of variation of the regression error (COV_ε), which is the same (in form) as that given above for driven piles:

$$COV_\varepsilon = \sqrt{exp(\sigma_{\varepsilon\_ln}^2) - 1} \tag{43}$$

where $\sigma_{\varepsilon\_ln}^2$ is the log-transformed variance of the regression error for drilled shafts in sand. See Sec. 3.8 for the manner in which terms associated with the representative regression expression for drilled shafts in sand are carried forward into the characterization of total uncertainty.
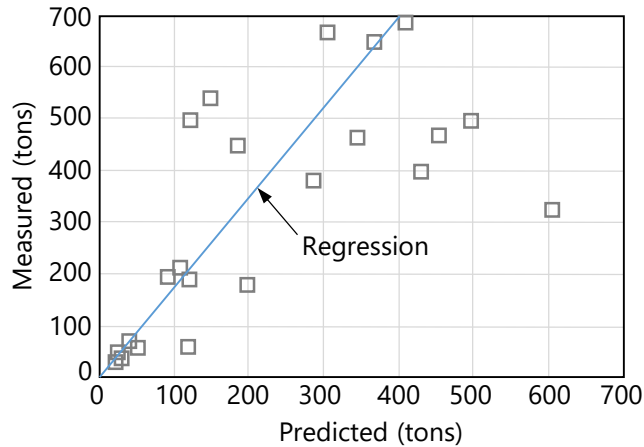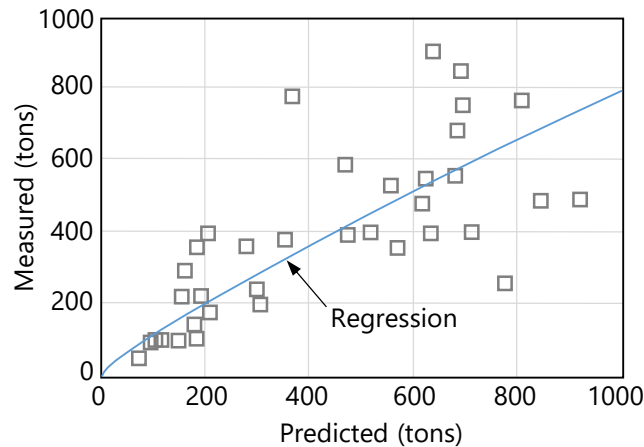

Figure 24. Regression analysis for total axial resistance of drilled shafts in sand (McVay et al. 2012)

Table 11. Regression parameter values for total axial resistance of drilled shafts in sand (McVay et al. 2012)

Parameter	Value
a	0.66
b	0.98
COV_ε	0.68
n	31

3.5 Drilled Shafts in Clay

Shown in Fig. 25 are (n = 38) predicted and measured values of total axial resistance pertaining to physically constructed drilled shafts in clay. The plotted (q_{pred}, q_{meas}) data points are taken directly from McVay et al. (2012). A representative best-fit regression curve to the 38 points, as reported by McVay et al. (2012), is:

$$\hat{q}_{meas} = exp(a) \cdot q_{pred}^b \tag{44}$$

where the form of the regression expression is defined as the product of exponential and power terms. McVay et al. (2012) recommended values for regression coefficients, a and b, as

listed in Table 12. Also listed therein is COV_ε, the coefficient of variation of the regression error. The COV_ε term for drilled shafts in clay takes the same form as that given above for driven piles and drilled shafts in sand:

$$COV_\varepsilon = \sqrt{exp(\sigma^2_{\varepsilon\_ln}) - 1} \tag{45}$$

where $\sigma_{\varepsilon\_ln}^2$ is the log-transformed variance of the regression error (specific to drilled shafts in clay). Use of the regression analysis results for characterization of total uncertainty, concerning drilled shafts in clay, is discussed in Sec. 3.8.

Figure 25. Regression analysis for total axial resistance of drilled shafts in clay (McVay et al. 2012)

Table 12. Regression parameter values for total axial resistance of drilled shafts in clay (McVay et al. 2012)

Parameter	Value
a	0.73
b	0.86
COV_ε	0.41
n	38

3.6 Drilled Shafts in Limestone

In contrast to the considerations for the combinations of member types and soil types discussed above, relatively more pronounced distinctions are made in regards to method error calculations for drilled shaft portions embedded in limestone layers. More specifically, separate treatments are given for method error arising due to skin friction resistance and end bearing resistance. Considerations for each form of resistance are documented in Sec. 3.6.1 (skin friction) and Sec. 3.6.2 (end bearing).

3.6.1 Skin Friction

Plotted Fig. 26 are predicted and measured values of McVay skin friction resistance pertaining to ($n = 18$) physically constructed drilled shafts embedded in limestone. All plotted (q_{pred}, q_{meas}) data points are taken directly from McVay et al. (2012). Additionally, a representative best-fit regression curve to the 18 points is superimposed on the plot, where the regression analysis was originally conducted in McVay et al. (2012).
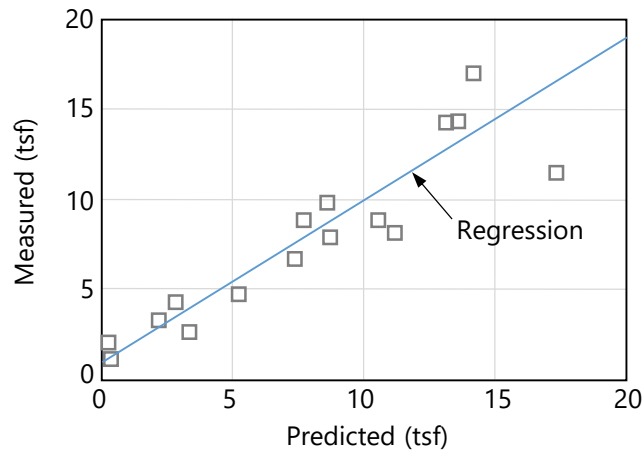

Figure 26. Regression analysis for McVay skin friction of drilled shafts in limestone (McVay et al. 2012)

The regression curve for skin friction (Fig. 26) is linear in form, and is given as:

$$\hat{q}_{meas} = a + b \cdot q_{pred} \tag{46}$$

where $\hat{q}_{meas}$ is the computed value of skin friction obtained from evaluation of the trend line. Parameter values for the regression coefficients included in Eqn. 46 (i.e., a, b) are listed in Table 13.

Table 13. Regression parameter values for McVay skin friction of drilled shafts in limestone (McVay et al. 2012)

Parameter	Value
a	0.90
b	0.90
σ_ε^2	4.52
n	18

Three sequentially evaluated expressions are employed for calculating the method error associated with skin friction resistance (and specific to drilled shafts in limestone). First, the error of the linear regression curve itself is expressed in terms of variance, σ_{reg}^2:

$$\sigma_{reg}^2 = \frac{n-1}{n-2} \cdot \sigma_{q_{meas}}^2 \cdot (1 - R^2) \tag{47}$$

where n is the number of available data points associated with physical measurements (e.g., load test data for skin friction); σ_{meas}^2 is the variance of the collection of q_{meas} values; and, R is the correlation coefficient associated with the pairs of q_{pred}, q_{meas}. Next, the variance of the error associated with evaluation of the regression expression ($\sigma_{\hat{q}_{meas}}^2$) is determined using:

$$\sigma_{\hat{q}_{meas}}^2 = \sigma_{reg}^2 \cdot \left(\frac{1}{n} + \frac{(q_{pred} - \bar{q}_{pred})^2}{(n-1) \cdot \sigma_{pred}^2} \right) \tag{48}$$

where $\bar{q}_{pred}$ is the mean of the collection of q_{pred} values; and, σ_{pred}^2 is the variance of the collection of q_{pred} values. The method error attributed to skin friction resistance, for drilled shafts in limestone, is then calculated as:

$$\sigma_\varepsilon^2 = \sigma_{\hat{q}_{meas}}^2 + \sigma_{reg}^2 \tag{49}$$

Note that method error, for these scenarios, is represented using variance rather than COV. Use of the variance attributed to (skin friction) method error in calculation of total uncertainty for drilled shafts in limestone is discussed in Sec. 3.8.

3.6.2 End Bearing

Presented in Fig. 27 are predicted and measured values of O'Neill end bearing resistance for (n = 11) physically constructed drilled shafts embedded in limestone. All plotted (q_{pred}, q_{meas}) data points are taken directly from McVay et al. (2012). Also plotted in Fig. 27 is a representative best-fit regression curve to the 11 points. Regression analysis for the 11 points, originally conducted in McVay et al. (2012), is reviewed below.

The regression curve for end bearing (Fig. 27) is linear in form, and is given as:

$$\hat{q}_{meas} = a + b \cdot q_{pred} \tag{50}$$

where $\hat{q}_{meas}$ is the computed value of end bearing obtained from evaluation of the trend line. The corresponding parameter values for the regression coefficients a and b) are listed in Table 14. Note that the value of a is defaulted to zero rather than 20.5 in GeoStat to prevent

potentially unconservative adjustments to resistance when tip resistance is not a significant contributor total resistance.

Three expressions are employed for calculating the method error associated with end bearing resistance (specific to drilled shafts in limestone). First, the error of the linear regression curve itself is expressed in terms of variance, σ_{reg}^2:

$$\sigma_{reg}^2 = \frac{n-1}{n-2} \cdot \sigma_{q_{meas}}^2 \cdot (1 - R^2) \tag{51}$$

where n is the number of available data points associated with physical measurements (e.g., load test data for end bearing); σ_{meas}^2 is the variance of the collection of q_{meas} values; and, R is the correlation coefficient associated with the pairs of q_{pred}, q_{meas}. Next, the variance of the error associated with evaluation of the regression expression ($\sigma_{\hat{q}_{meas}}^2$) is determined using:

$$\sigma_{\hat{q}_{meas}}^2 = \sigma_{reg}^2 \cdot \left(\frac{1}{n} + \frac{(q_{pred} - \bar{q}_{pred})^2}{(n-1) \cdot \sigma_{pred}^2} \right) \tag{52}$$

where $\bar{q}_{pred}$ is the mean of the collection of q_{pred} values; and, σ_{pred}^2 is the variance of the collection of q_{pred} values.
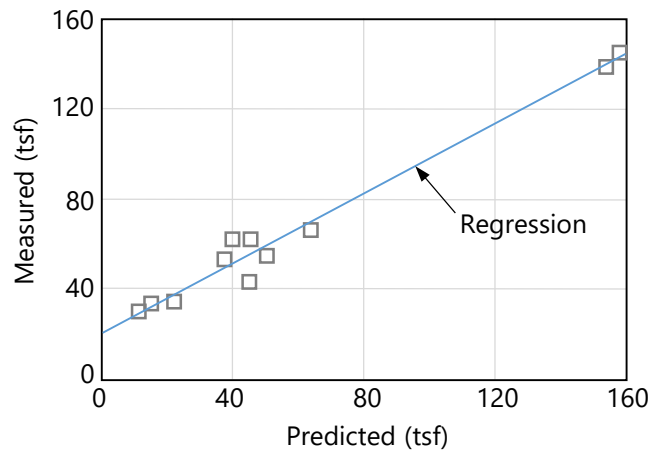

Figure 27. Regression analysis for O'Neill end bearing of drilled shafts in limestone (McVay et al. 2012)

Table 14. Regression parameter values for O'Neill end bearing of drilled shafts in limestone (McVay et al. 2012)

Parameter	Value
a	20.50
b	0.77
σ_ε^2	48.89
n	11

The method error attributed to end bearing resistance, for drilled shafts in limestone, is then calculated as:

$$\sigma_\varepsilon^2 = \sigma_{\hat{q}_{meas}}^2 + \sigma_{reg}^2 \qquad (53)$$

As with considerations for skin friction, method error for end bearing resistance of drilled shafts in limestone is represented using variance rather than COV. Use of the variance attributed to (end bearing) method error in calculation of total uncertainty for drilled shafts in limestone is discussed in Sec. 3.8.

3.7 Custom Characterization of Method Error

In the event that axial load test data are available for the planned foundation members of a given bridge site, then regression analysis of said data may lead to regression curve parameters different from those presented in Sec. 3.3 through Sec. 3.6. However, for a given member type and surrounding soil or rock layers, the same overall manner of performing regression analysis as that described above can be carried out. That is, if a set of measured and predicted resistances are known for a site, then (for a given foundation member type) the processes documented above can be utilized to conduct customized regression analysis.

Results obtained from "custom" regression analysis can, in turn, be used to model custom (i.e., site-specific) method error in GeoStat. If axial load test data are available for driven piles, then the process described in Sec. 3.3 can be utilized (but with use of the site-specific data). Likewise, processing of site-specific axial load test data for drilled shafts in sand and clay can be carried out using the processes described in Sec. 3.4 and Sec. 3.5, respectively. For portions of drilled shafts in limestone, and for instances where load test measurements can be categorized into skin friction and end bearing, the process documented in Sec. 3.6 can be utilized.

Consider, for example, the procedure for site-specific characterization of method error (Fig. 28) when analyzing driven piles or portions of drilled shafts embedded in sand (and/or clay). As precursors to the method error characterization, a foundation member type (pile, shaft) is selected and n values of q_{meas} are assembled into $\{q_{meas}\}$. The characterization procedure then begins with determination of corresponding sets of predicted values, $\{q_{pred}\}$, (Fig. 28, top). In addition, sets of log-transformed values are generated for measured data, $\{q_{meas\_ln}\}$, and predicted data, $\{q_{pred\_ln}\}$.

Next, regression parameter values are determined for each of the number of required regression analyses (n_{reg}). For driven piles, n_{reg} is equal to 1 since only a single regression analysis is necessary along the entire pile embedment length. Similarly, for drilled shafts embedded in only sand (or only clay) layers, n_{reg} is also equal to 1. However, for drilled shafts

embedded in soil profiles that include both sand and clay layers, generation of two sets of regression analysis parameters are required (one set shaft portions embedded in sand, one set for portions embedded in clay).

For each iteration through the loop on n_{reg} (Fig. 28, middle), the remainder of the current regression analysis is divided into two parts: 1) determination of descriptive statistics; and, 2) determination of regression values. For determination of descriptive statistics, and for iteration i within the loop on n_{reg}, the subsets for each of $\{q_{pred}\}$ and $\{q_{meas}\}$ are first identified. Then, the mean values ($\bar{q}_{pred}$, $\bar{q}_{meas}$) and standard deviations (σ_{pred}, σ_{meas}) are calculated for the as-identified data subsets. The same identification and calculation steps are carried out with use of the log-transformed data to produce mean (subset) values, ($\bar{q}_{pred\_ln}$ and $\bar{q}_{meas\_ln}$), and standard deviation values, (σ_{pred_ln} and σ_{meas_ln}).

```
Example method error characterization procedure
    Generate predicted and log-transformed data
    Given a type of foundation member and {q_meas}
    For i = 1, n
        Calculate {q_pred}_i
        {q_meas_ln}_i = ln({q_meas_ln}_i)
        {q_pred_ln}_i = ln({q_pred_ln}_i)
    End of loop on i

    Perform regression(s)
    For i = 1, n_reg
        Determine descriptive statistics
        Identify subset of {q_pred} and {q_meas}
        Calculate correlation coefficient R
        Calculate q̄_pred , q̄_meas
        Calculate σ_pred , σ_meas
        Identify subset {q_pred_ln} and {q_meas_ln}
        Calculate correlation coefficient R_ln
        Calculate q̄_pred_ln , q̄_meas_ln
        Calculate σ_pred_ln , σ_meas_ln

        Determine regression values
        Use q̂_meas = exp(a) · q_pred^b
        Find a, b that minimize σ_ε
        Perform linear regression on {q_meas_ln}, {q_pred_ln}
        Use σ_ε_ln from linear regression to find COV_ε
    End of loop on i
```

Figure 28. Example method error characterization procedure for driven piles, drilled shafts in sand, and drilled shafts in clay

Next, the associated regression values (*a*, *b*) are determined (Fig. 28, bottom) using the same form of regression expression as that given in (for example) Eqn. 40. Also, a separate, linear regression is carried out using the log-transformed data ({q_{pred_ln}} and {q_{meas_ln}}) to find the minimum value of σ_{ε_ln} and corresponding regression coefficient, R_{ln}. Then, COV_{ε} is calculated (e.g., as given in Eqn. 41) as a summary representation of the method error for the current iteration through the loop on n_{reg}.

3.8 Total Uncertainty

Recall from Ch. 2 that the LRFD resistance factor (ϕ) represents the total uncertainty attributed to a given resistance quantity. Further, the product of nominal resistance and ϕ gives the (factored) design resistance. The expression for ϕ that is implemented in GeoStat (and adopted from McVay et al. 2012) is repeated here for convenience:

$$\phi = \frac{(\gamma_D \cdot \frac{Q_D}{Q_L} + \gamma_L) \cdot \sqrt{\frac{1 + COV_Q^2}{1 + COV_R^2}}}{(\lambda_{QD} \cdot \frac{Q_D}{Q_L} + \lambda_{QL}) \cdot exp\left(\beta \cdot \sqrt{ln\left((1 + COV_R^2) \cdot (1 + COV_Q^2)\right)}\right)} \tag{54}$$

where all constituent terms are defined as part of documenting Eqn. 34 in Ch. 2. Of particular relevance to method error is the coefficient of variation of member axial resistance, COV_R, which reflects both spatial variability and method error phenomena. Various expressions of COV_R—and terms directly relevant to COV_R—are given immediately below for each foundation member type and soil or rock medium that can be analyzed in GeoStat.

3.8.1 Driven Piles, Drilled Shafts in Sand, and Drilled Shafts in Clay

For driven piles embedded in media consisting of one or more sand, clay, or limestone layers, spatial variability and method error phenomena are combined into COV_R, as presented in Eqn. 55. The expression in Eqn. 55 is also applicable to drilled shaft portions that are embedded in sand or clay layers:

$$COV_R = \frac{\sqrt{exp(a)^2 \cdot \sigma_{\bar{q}_{sim}}^2 + (COV_{\varepsilon} \cdot \bar{q}_{sim})^2}}{exp(a) \cdot exp(a)^2 \bar{q}_{sim}^b} \tag{55}$$

where *a* and *b* are regression coefficients between measured and predicted values of resistance, with use of the form given in (for example) Eqn. 40; $\sigma_{\bar{q}_{sim}}^2$ is the variance about the mean of a corresponding set of simulated resistance values (e.g., from unconditional simulation, conditional simulation); and, $\bar{q}_{sim}$ is the mean value of simulated resistance. Stated

another way, the terms $\bar{q}_{sim}$ and $\sigma^2_{\bar{q}_{sim}}$ are obtained directly (i.e., without adjustment) from stochastic simulation, and represent contributions to total uncertainty from spatial variability phenomena. Furthermore, the terms *a*, *b*, and COV_ε are dependent on foundation member type (and soil type for drilled shafts), and signify method error contributions to total uncertainty.

3.8.2 Drilled Shafts in Limestone

For drilled shaft portions that are embedded in limestone layers, total uncertainty is divided into side (skin friction) and tip (end bearing) components.

3.8.2.1 Skin Friction

Specifically, the total uncertainty contributions from spatial variability and method error of skin friction are combined into an expression of COV_R as:

$$COV_R = \frac{\sqrt{\sigma^2_{skin}}}{A_{skin} \cdot \left(a_{skin} + b_{skin} \cdot \bar{q}_{sim\_skin}\right)} \tag{56}$$

where $\bar{q}_{sim\_skin}$ is the mean value of simulated (unit) skin resistance along some portion of the shaft length; A_{skin} is the shaft surface area along that same portion; a_{skin} and b_{skin} are associated regression coefficients (corresponding to *a* and *b* in Eqn. 46); and, σ^2_{skin} is a variance term defined as:

$$\sigma^2_{skin} = A^2_{skin} \cdot \left(\sigma^2_{sim\_skin} + \sigma^2_{\varepsilon\_skin}\right) \tag{57}$$

where $\sigma^2_{sim\_skin}$ is the variance of the simulated set of unit skin friction resistances; and, $\sigma^2_{\varepsilon\_skin}$ is the variance associated with method error and skin friction resistance (corresponding to σ^2_ε in Eqn. 49).

3.8.2.2 End Bearing

An alternative form of COV_R, which describes the total uncertainty contribution from tip resistance, is expressed as:

$$COV_R = \frac{\sqrt{\sigma^2_{tip}}}{A_{tip} \cdot \left(a_{tip} + b_{tip} \cdot \bar{q}_{sim\_tip}\right)} \tag{58}$$

where $\bar{q}_{sim\_tip}$ is the mean value of simulated, unit end bearing shaft resistance; A_{tip} is the shaft area available for tip resistance; a_{tip} and b_{tip} are associated regression coefficients (corresponding to a and b in Eqn. 50); and, σ_{tip}^2 is a variance term defined as:

$$\sigma_{tip}^2 = A_{tip}^2 \cdot \left(\sigma_{sim\_tip}^2 + \sigma_{\varepsilon\_tip}^2\right) \tag{59}$$

where $\sigma_{sim\_tip}^2$ is the variance of the simulated set of unit end bearing resistances; and, $\sigma_{\varepsilon\_tip}^2$ is the variance associated with method error and end bearing resistance (corresponding to σ_ε^2 in Eqn. 53).

The total uncertainty contribution for total (combined skin and tip) resistance, expressed as another alternative form of the coefficient of variation, COV_R, is given as:

$$COV_R = \frac{\sqrt{\sigma_{total}^2}}{A_{skin} \cdot \left(a_{skin} + b_{skin} \cdot \bar{q}_{sim\_skin}\right) + A_{tip} \cdot \left(a_{tip} + b_{tip} \cdot \bar{q}_{sim\_tip}\right)} \tag{60}$$

where σ_{total}^2 is a variance term that includes cross-correlation between skin and tip resistance, and is defined as:

$$\sigma_{total}^2 = \sigma_{skin}^2 \cdot + \sigma_{tip}^2 + 2 \cdot R_{skin\_tip} \cdot \sigma_{skin} \cdot \sigma_{tip} \tag{61}$$

where R_{skin_tip} is the correlation coefficient between the respective sets of simulated values, q_{sim_skin} and q_{sim_tip}.

CHAPTER 4
MODELING OF EXAMPLE SITE A

4.1 Overview

Presented in Ch. 4 is a detailed walkthrough of geotechnical site modeling and axial resistance simulation for an example bridge site. The data sets discussed herein represent one instance of the types and ranges of geotechnical site data that may be collected when investigating the foundations of a bridge site, but for when only a relatively small set of site data is available. In addition, portions of the overall data set exhibit high levels of variability. Use of the associated site data—within the context of modeling and simulation in GeoStat—is divided into several steps, where such division reflects the left-to-right progression across the seven tabs of the GeoStat user interface (UI). See the Help Manual for detailed descriptions of the GeoStat UI layout.

The site of interest is referred to as Example Site A (or, Site A). Cataloging of the available collection of Site A data for modeling within GeoStat is discussed in Sec. 4.2. Initial selection of boundary soil and rock (limestone) layer elevations is discussed in Sec. 4.3. Also documented in Sec. 4.3 are layer-related considerations specific to the type of foundation member being considered (pile, shaft). Initial formation of spatial correlation structures (i.e., variograms) for each defined layer is then discussed in Sec. 4.4.

As will be demonstrated, the relatively limited data set gives way to multiple, possible interpretations concerning layer definitions. A set of alternative layer definitions is presented in Sec. 4.5. Associated geostatistical parameters (obtained using the alternative layer definitions) are documented in Sec. 4.6. Zonal issues are not anticipated for the Site A data set (see Ch. 5 for a detailed guide for modeling of zones). Purely for illustration of the concepts and process, a cursory examination of the Site A data set is given in Sec. 4.7 within the context of assessing the presence of zones.

Subsequent to definition of representative layers and characterization of layer-specific correlation structures, the focus of the walkthrough for Site A shifts to stochastic simulation of axial resistance in Sec. 4.8. Interpretation of simulated profiles of axial resistance, which reflect spatial variability phenomena, is provided in Sec. 4.9. Considerations for incorporating method error phenomena into the simulated results are detailed in Sec. 4.10. The combined effects of spatial variability and method error upon computed axial resistance, culminating in profiles of both resistance factors (ϕ) and factored axial resistance, are examined in Sec. 4.11.

4.2 Cataloging Site Data

Shown in Fig. 29 is the first (leftmost) tab encountered within the GeoStat UI, referred to as the Project Information tab. This region of the GeoStat UI facilitates input and organization of

all data obtained from geotechnical investigation of the site. The foundation type is also selected in the Project Information tab (Fig. 29, upper-right).

For Site A, a drilled shaft foundation type is selected. However, throughout Ch. 4, when distinct considerations are required that depend on the selected foundation type (piles, shafts), such distinctions are noted. Otherwise, documentation of parameters selected for site modeling and interpretation of simulation results are generally applicable regardless of the selection for type of foundation member.

4.2.1 Initial Visual Assessment of Site A

For the start of the analysis, all borings for the site should be active. Accordingly, as a starting point, initial characterization of the site data (through the step of forming variograms) is carried out using all available measurements from across the 14 boring locations. Data from 14 unique boring locations are cataloged for Site A, including both SPT-N blow counts and rock-related measurements obtained from numerous core runs (e.g., unconfined compression strength, q_u). Values of undrained shear strength (C_u) are not available among the site data. However, as discussed in Sec. 2.7, blow count values are simulated and then empirically related to undrained shear strength. The geotechnical investigation of Site A indicates the presence of interspersed bands and layers of clay and limestone across the 14 boring locations. Given the prevalence of limestone throughout Site A, emphasis is initially placed on available measurements of rock strength (as discussed below) when forming components of the GeoStat model.

The plan-view boring locations for Site A are distributed across a footprint, that in turn, extends along several bridges spans (particularly with respect to northing values). A plan view of the 14 boring locations is plotted in the left portion of the Project Information tab, and a corresponding plot of eastings and northings for the boring locations is shown in Fig. 30. As listed in the table on the right portion of the Project Information tab (Fig. 29, right), northing values range from 0 ft to approximately 1500 ft, and easting values range from (approximately) -75 ft to 75 ft. Further, the ground surface elevations across the 14 borings range from 78 ft to 98 ft.

On the Project Information tab (Fig. 29) scatterplot data associated with any currently selected (and active) boring location is highlighted, and can be used to quickly identify borings that contain outlier data or are associated with a unique zone. For each of the 14 boring locations, the respective (boring-specific) geotechnical site data are input in GeoStat using the Boring Data dialog. This dialog is accessible from the upper-right portion of the Project Information tab. For example, site data measured at boring location B-1 (easting of 64 ft; northing of 427 ft) consists of through-depth SPT-N blow count values, and is cataloged as shown in Fig. 31. An additional example is provided in Fig. 32 for boring location B-4 (easting of -24 ft;

northing of 360 ft), which contains a mixture of SPT-N blow count and core run data (e.g., unconfined compression strength, q_u, split tensile strength, q_t, RQD, *recovery*).

The rightmost plot in the Project Information tab (Fig. 29, middle) facilitates plotting of collections of the desired type of site measurement (e.g., SPT-N, q_u). In addition, data pertaining to any boring location of interest are highlighted (using solid blue plot points), as exemplified for boring location B-1 in Fig. 29.
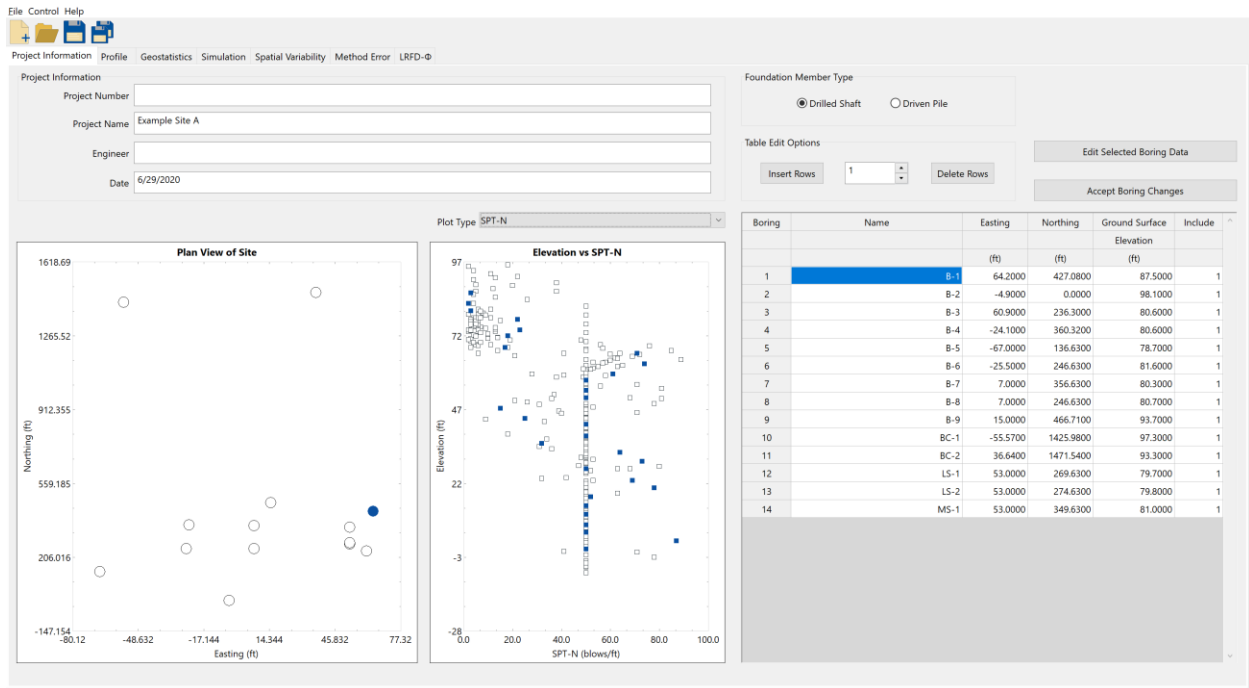

Figure 29. Project Information tab
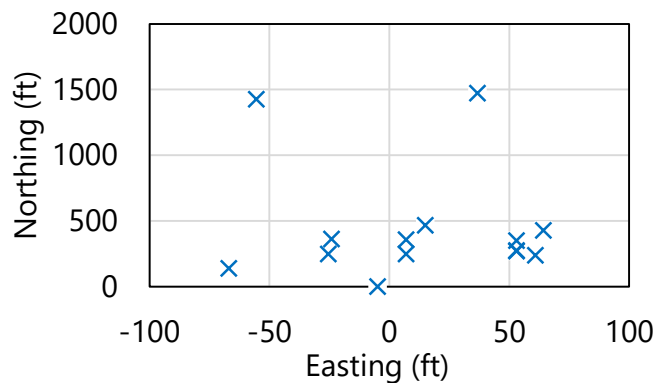
Figure 30. Plan view of 14 boring locations for Site A

Boring Data - B-1   ✕

Table Edit Options

Insert Rows | 1 | Delete Rows

Default RQD and Recovery To 1

Notes

1. Input all available data for the boring within the table below.

2. For any depths where a given soil property is not available, then leave the corresponding cell blank.

3. Soil Types: 1 = Plastic Clay | 2 = Clay and Silty Sand | 3 = Clean Sand | 4 = Limestone and Very Shelly Sand.

Number	Elevation	Depth	Soil Type [1|2|3|4]	N. Blows	Unit Weight	Cu	qu	qt	qb	Em	RQD [0.0 to 1.0]	Socket Roughness [0 | 1]	Rock Recovery [0.0 to 1.0]
	(ft)	(ft)		(blows/ft)	(pcf)	(tsf)	(tsf)	(tsf)	(tsf)	(ksi)			
1	86.5000	1.0000	2	3									
2	83.0000	4.5000	2	2									
3	80.5000	7.0000	2	3									
4	77.5000	10.0000	2	22									
5	74.0000	13.5000	2	23									
6	72.0000	15.5000	2	18									
7	68.0000	19.5000	2	17									
8	66.0000	21.5000	2	71									
9	62.5000	25.0000	2	74									
10	59.0000	28.5000	2	61									
11	57.0000	30.5000	2	50									
12	53.5000	34.0000	2	50									
13	51.0000	36.5000	2	50									
14	47.5000	40.0000	1	15									
15	44.0000	43.5000	1	25									
16	42.0000	45.5000	1	50									
17	38.0000	49.5000	1	50									
18	35.5000	52.0000	1	32									

OK | Cancel

Figure 31. Boring Data dialog for boring location B-1

Boring Data - B-4   ✕

Table Edit Options

Insert Rows | 1 | Delete Rows

Default RQD and Recovery To 1

Notes

1. Input all available data for the boring within the table below.

2. For any depths where a given soil property is not available, then leave the corresponding cell blank.

3. Soil Types: 1 = Plastic Clay | 2 = Clay and Silty Sand | 3 = Clean Sand | 4 = Limestone and Very Shelly Sand.

Number	Elevation	Depth	Soil Type [1|2|3|4]	N. Blows	Unit Weight	Cu	qu	qt	qb	Em	RQD [0.0 to 1.0]	Socket Roughness [0 | 1]	Rock Recovery [0.0 to 1.0]
	(ft)	(ft)		(blows/ft)	(pcf)	(tsf)	(tsf)	(tsf)	(tsf)	(ksi)			
1	79.7000	0.9000	2	8									
2	76.6000	4.0000	2	6									
3	73.4000	7.2000	3	13									
4	70.5000	10.1000	3	19									
5	67.0000	13.6000	3	14									
6	64.3000	16.3000	1	63									
7	61.5000	19.1000	1	63									
8	58.0000	22.6000	1	38									
9	55.5000	25.1000	1	71									
10	53.1833	27.4167	4		103.2000			5.0184			0.5000		0.2200
11	52.3500	28.2500	4		109.3000		60.9264				0.5000		0.2200
12	51.5167	29.0833	4		104.3000			9.3600			0.5000		0.2200
13	50.6833	29.9167	4										
14	49.8500	30.7500	4		102.2000			6.2424			0.5000		0.2200
15	49.0167	31.5833	4		102.1000			6.7896			0.5000		0.2200
16	47.8222	32.7778	4		91.8000			0.6120			1.0000		0.6700
17	47.2667	33.3333	4		95.8000			1.6848			1.0000		0.6700
18	46.7111	33.8889	4		102.8000		23.4792				1.0000		0.6700

OK | Cancel

Figure 32. Boring Data dialog for boring location B-4

Documented in the remainder of Sec. 4.2 are initial characterizations of the various types of measured site data available for Site A. Data are presented in scatterplot form, or as through-depth profiles of measurements accumulated across all 14 boring locations. In this way, initial characterization of trends or groupings among the site data are qualitatively identified, where such identification is necessary (for example) in defining soil or rock layering.

4.2.2 Site Data for Shafts in Limestone

As aforementioned, initial efforts toward characterizing the site emphasize examination of available rock strength data (e.g., q_u), given the frequent occurrence of limestone throughout Site A. Shown in Fig. 33 are measurements of rock strength obtained across the 14 boring locations (and associated core runs) of Site A. For unconfined compression strength, q_u, 152 measurements are available (Fig. 33a). Also, 191 measurements of split tensile strength, q_t, are available (Fig. 33b).

No immediately apparent q_u-q_t correlations are identified between the scatterplots in Fig. 33. However, while the majority of measured q_u values are less than approximately 10 tsf, relatively higher compression strength values (between approximately 25 tsf and 325 tsf) are concentrated over the approximate elevation range of 45 ft to 30 ft.

Plotted in Fig. 34 are additional measurements pertaining to rock strength, as gathered from across the core runs of Site A. Concerning rock quality designation (RQD), 338 values are taken from the collection of core runs (Fig. 34a). Correspondingly, 338 values of *recovery* are included for use in GeoStat modeling of the site (Fig. 34b).

Many interspersed groupings of both RQD and *recovery* values are distributed throughout the scatterplots, and decimal values generally range from (approximately) 0.2 to 1.0. Stated alternatively, despite the relatively large number of measured values available for RQD and *recovery*, no overtly discernible trends or groupings of values are apparent from visual inspection of the scatterplots.

Measured values of unit weight are also examined, but are considered secondary (e.g., for establishment of layering) to measured rock strengths. Depicted in Fig. 35 are measured values of unit weight, γ, available over the elevation range of 67 ft to 9 ft. Relatively weak groupings of values are qualitatively identified over the elevation range of approximately 67 ft to 45 ft, and separately, 45 ft to approximately 9 ft. The 338 measured values of unit weight (γ) vary, approximately, from 90 lb/ft^3 to 160 lb/ft^3.
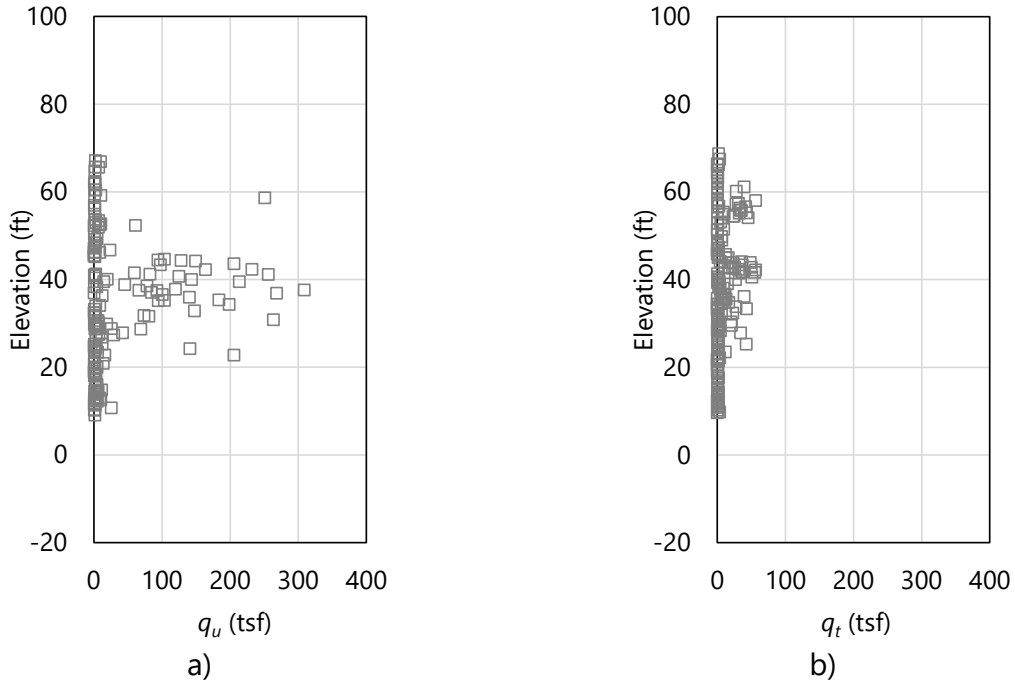
Figure 33. Scatterplots of limestone strength parameters: a) 152 values for unconfined compression strength, q_u, (elevation range: 67 ft to 9 ft); b) 191 values for split tensile strength, q_t, (elevation range: 53 ft to 25 ft)
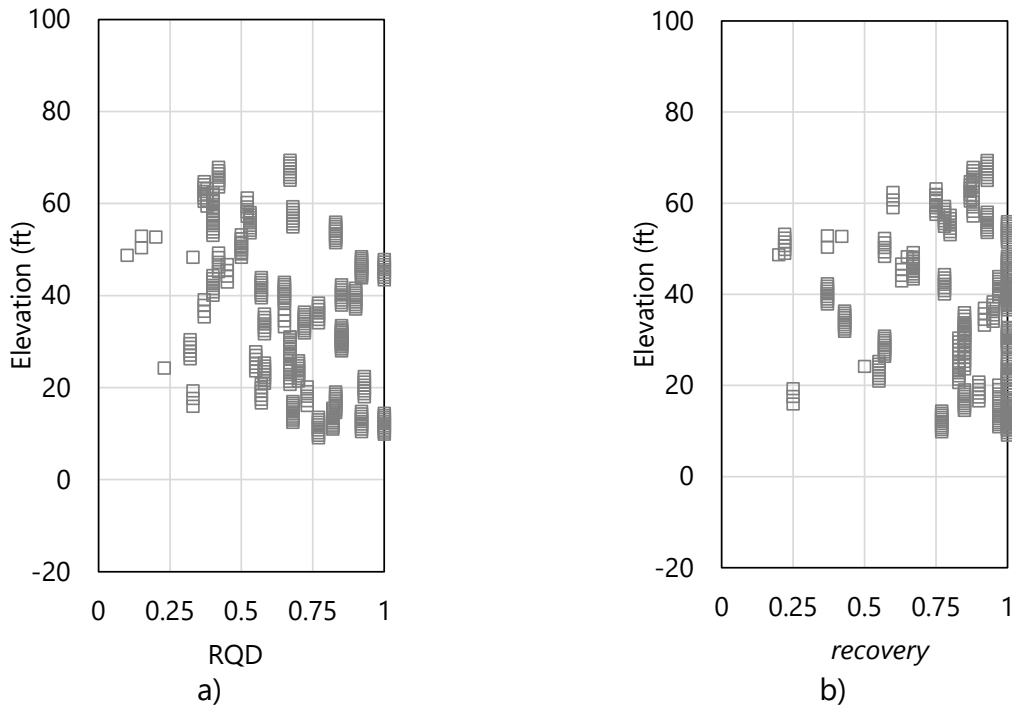
Figure 34. Scatterplots of limestone strength parameters: a) 338 values for RQD (elevation range: 67 ft to 9 ft); b) 338 values for *recovery* (elevation range: 67 ft to 9 ft)
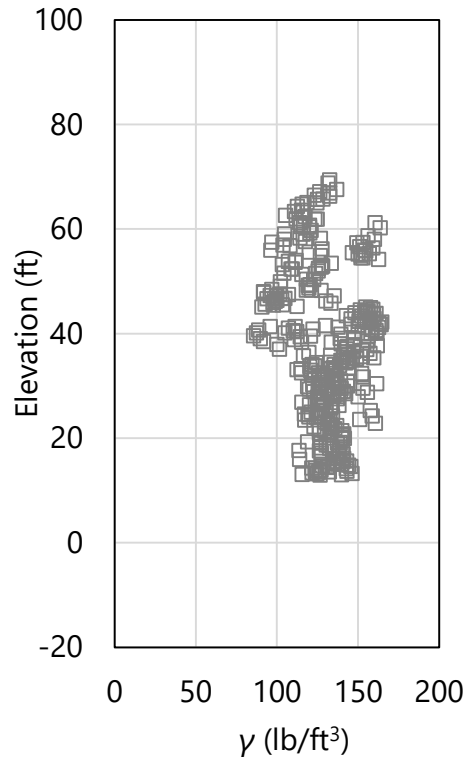
Figure 35. Scatterplot of 338 values of unit weight, γ, (elevation range: 67 ft to 9 ft)

4.2.3 Site Data for Shafts in Clay, Shafts in Sand, and Driven Piles

For portions of drilled shafts and piles embedded in clay and sand, SPT-N blow count values are most pertinent in computing axial resistances from within GeoStat. As noted above, values of undrained shear strength (C_u) are not available among the site data, but rather, are estimated via empirical correlation to SPT-N blow count values (see Sec. 2.7 for additional discussion). Plotted in Fig. 36 are 271 SPT-N blow count values, as collected across the 14 boring locations of Site A. Blow count values range from 0 blows/ft to approximately 90 blows/ft. Per the available site data, a relatively high prevalence of blow count values are attributed to refusal-like conditions and thus reported as 50 blows/ft.

A qualitative grouping of SPT-N blow count values is apparent from elevations of 97 ft to approximately 65 ft. An additional grouping is identified from 65 ft to approximately 45 ft, and a third qualitative grouping occurs (approximately) from 45 ft to 20 ft. These visually identified groupings are revisited later as part of defining representative layering for the available Site A data.
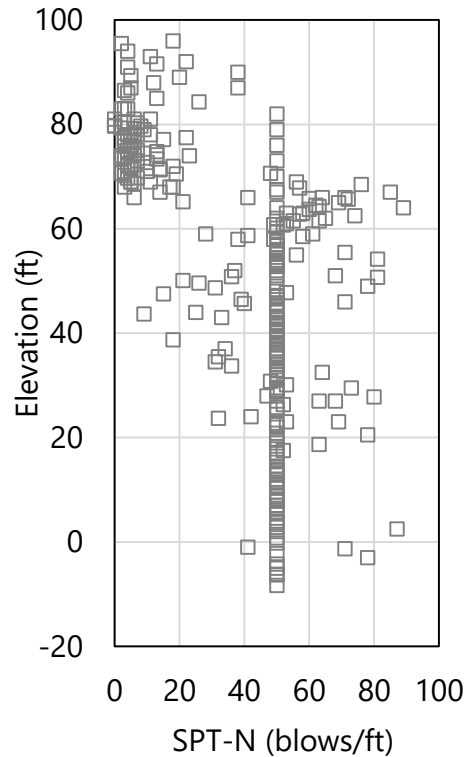
Figure 36. Scatterplot of 271 SPT-N blow counts (elevation range: 96 ft to -10 ft)

4.3 Initial Definition of Soil or Rock Layering

The second of seven tabs (from left to right) in the GeoStat UI is the Profile tab (Fig. 37). Using the controls within this tab, a representative soil or rock layering is defined. Scatterplots of the previously cataloged site data are utilized here (Fig. 37, left and middle) to aid in selection of boundary layer elevations. Layer bottom elevations can be defined through graphical selection within the profile plots. Additionally, all required parameter values for a given layer (e.g., soil or rock type, top elevation, bottom elevation) can be input in the layer data table (Fig. 37, right).

As a first attempt at establishing layer definitions for Site A, consider the soil or rock types and layer elevations given in Table 15. Based on the cataloged site data, with emphasis on rock strengths, four layers are defined and consist of either clay (layer 1) or limestone (layer 2, layer 3, and layer 4). Layer top and bottom elevations span the ranges of elevations identified during the initial review of the site data (documented above). Additional discussion regarding initial selections of the boundary layer elevations is provided in the remainder of Sec. 4.3. Still further considerations are documented in Sec. 4.4, as part of forming the initial (layer-specific) variograms.
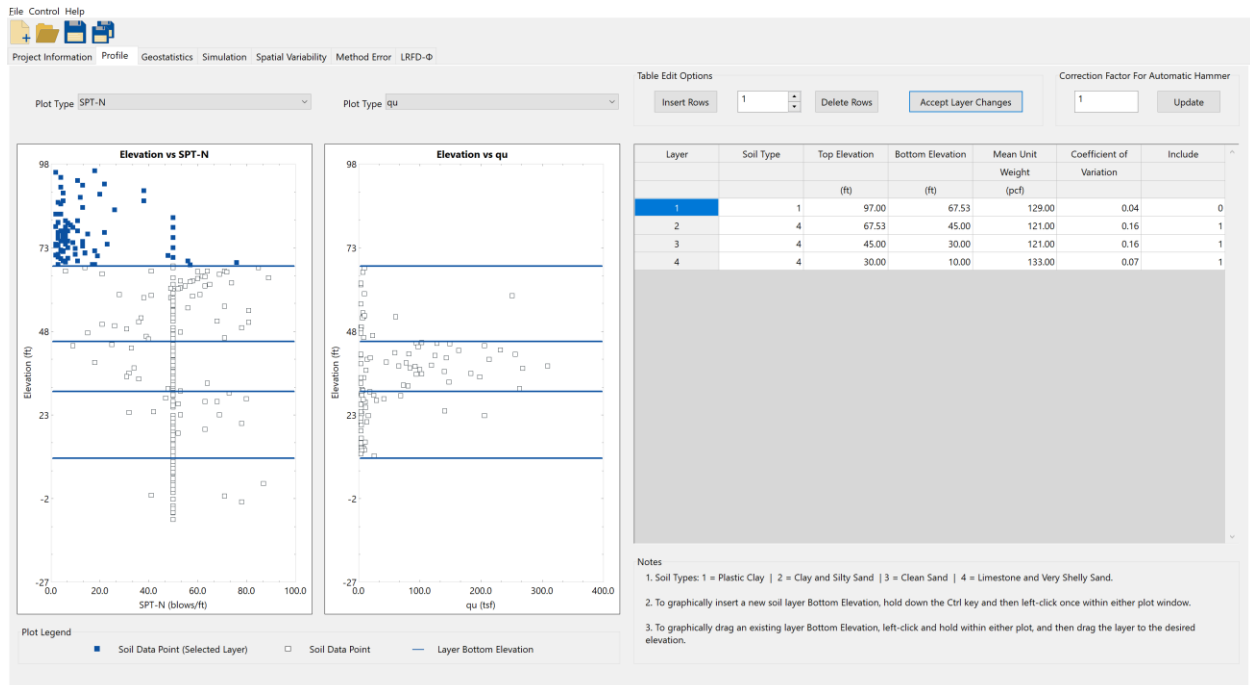
Figure 37. Profile tab

Table 15. Initial selection of layer types and elevation ranges

Layer	Layer type	Top elevation (ft)	Bottom elevation (ft)
1	Clay	97.0	67.5
2	Limestone	65.0	45.0
3	Limestone	45.0	30.0
4	Limestone	30.0	10.0

4.3.1 Initial Selection of Layer Elevations

Selected geotechnical data pertaining to rock strength are made use of for initial definition of the boundary layer elevations. In particular, plotted in Fig. 38 are the layer divisions and ensemble of 152 measurements for unconfined compression strength, q_u. Qualitatively, three through-depth groupings are identified. For example, from approximately 67.5 ft to 45 ft, measured q_u values are generally less than 10 tsf. In accordance with observations made from the review of the full catalog of site data, a concentrated region of relatively higher-magnitude q_u values is designated as a distinct limestone layer. Consequently, layer 2 is defined as a limestone layer from 67.5 ft to 45 ft, and layer 3 (also limestone) is defined as spanning the elevations from 45 ft to 30 ft.

Continued visual inspection of q_u values in Fig. 38 reveals additional groupings of significance for data positioned at elevations below 30 ft. Measurements of q_u, associated with rock strength are generally of low magnitude (i.e., less than 10 tsf). Therefore, layer 4 is defined for

data below 30 ft down to a practical limit for embedment depths (i.e., layer 4 is defined between 30 ft and 10 ft), and is defined as a limestone layer.
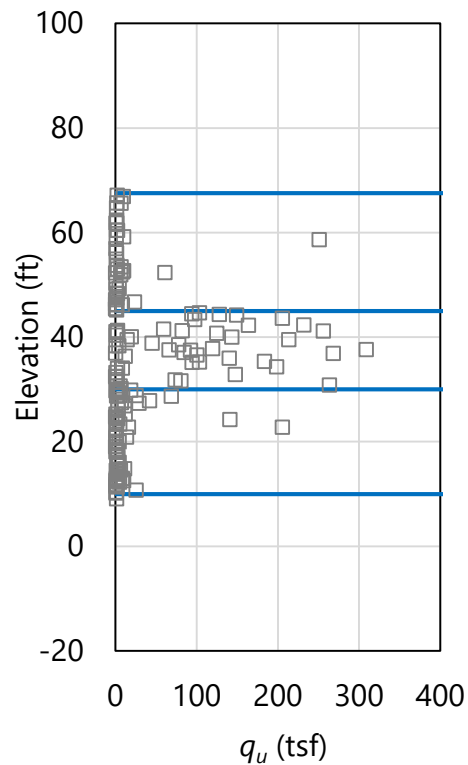
Figure 38. Scatterplot of 152 values for unconfined compression strength, q_u, (elevation range: 67.5 ft to 9 ft) with layer bottom elevations (blue horizontal lines)

The 271 SPT-N blow counts associated with the 14 boring locations of Site A are also examined (secondary to q_u values for this initial examination). A scatterplot of the SPT-N values, along with layer bottom elevations (blue horizontal lines), is presented with respect to elevation in Fig. 39. Consistent with the initial review of the cataloged SPT-N data for Site A, the selected layer divisions are positioned in accordance with qualitative groupings of the SPT-N blow counts. For example, a distinct grouping of blow counts is apparent between 97 ft and 67.5 ft, in comparison to those values cataloged below 67.5 ft. Thus, Layer 1 is defined between 97 ft and 67.5 ft. Similarly, the qualitative grouping of SPT-N blow counts positioned between 67.5 ft and 45 ft (complementary to the above examination of q_u values) further motivates designation of the boundary elevations for layer 3 (45 ft to 30 ft).
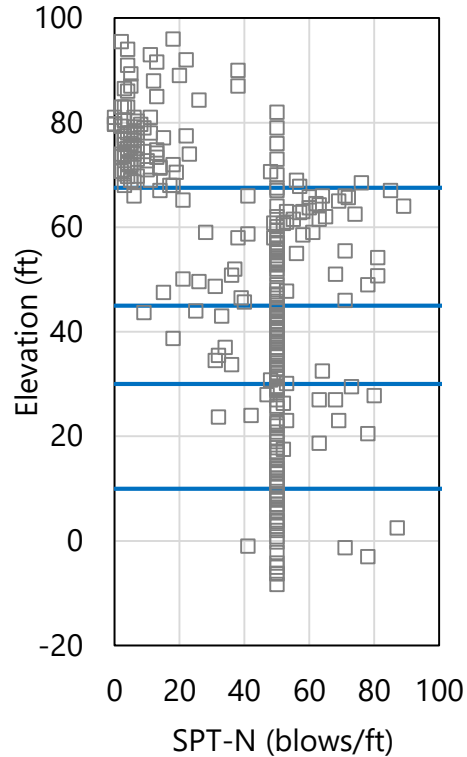
Figure 39. Scatterplot of 271 SPT-N blow counts (elevation range: 96 ft to -10 ft) with layer bottom elevations (blue horizontal lines)

4.3.2 Specifying Unit Weight per Layer when Modeling Drilled Shafts

Axial resistances for both driven piles and drilled shafts can be computed using the GeoStat software. For instances where driven piles are being considered, only the layer types (e.g., clay, sand, limestone) and boundary elevations are required for layer definitions. However, for drilled shafts, descriptive statistics pertaining to unit weight, γ, are additionally required for each defined layer. The descriptive statistics are input in the GeoStat UI (per layer) in the same location as the respective layer top and bottom elevations (recall Fig. 37, right). Required statistics include the mean value of unit weight and the associated COV.

As illustration of how the descriptive statistics are formed when drilled shafts are selected as the foundation type, consider the scatterplot of 338 unit weight (γ) values for Site A (and layer bottom elevations) in Fig. 40. Formation of descriptive statistics for each layer is carried out by: 1) identifying those values of unit weight (γ) that are positioned within the layer; 2) calculating the mean value of the identified γ values; 3) calculating the standard deviation; and, 4) calculating the COV.

69
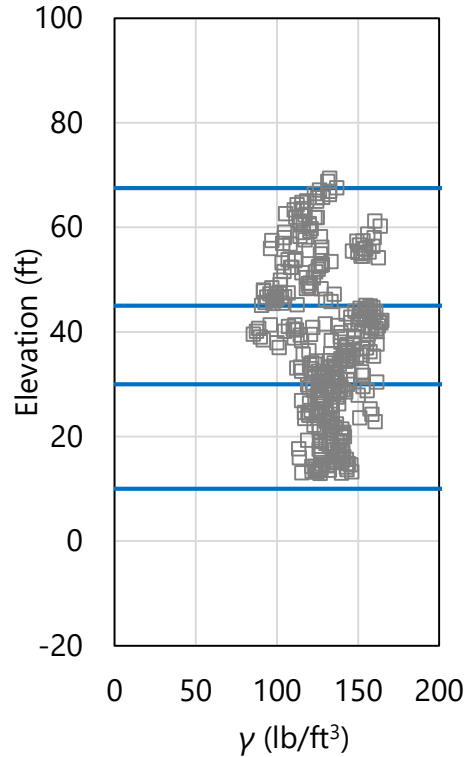
Figure 40. Scatterplot of 338 values of unit weight, γ, (elevation range: 67.5 ft to 9 ft) with layer bottom elevations (blue horizontal lines)

Continuing the illustration, consider the 147 unit weight values (γ) exclusive to layer 4 (Fig. 41). A corresponding histogram of the 147 values is shown in Fig. 42. The distribution of unit weight values, γ, in layer 4 (Fig. 42) qualitatively resembles that of a right-skewed lognormal distribution. Further, the histogram does not exhibit conspicuous features such as bimodal frequency peaks, which if present, would potentially require revisions to the layer elevations defined in Table 15. The mean of the layer 4 unit weight data is calculated as 133 lb/ft^3; the standard deviation is calculated as 9.3 lb/ft^3; and, the COV is calculated as 0.07. Both the mean and COV values for unit weight, γ, are supplied as part of the layer 4 definition, given that drilled shafts (as opposed to driven piles) are being investigated for Site A.
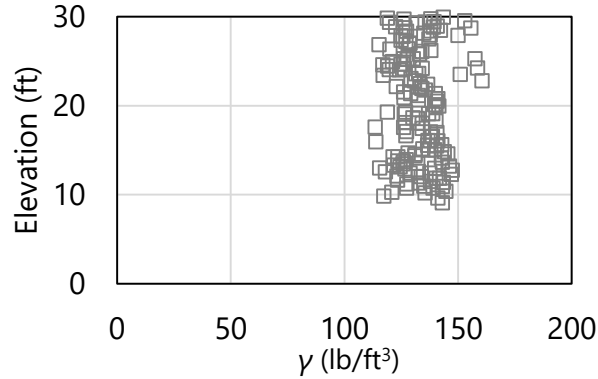
Figure 41. Scatterplot of 147 values of unit weight, γ, (elevation range: 30 ft to 9 ft) within layer 4
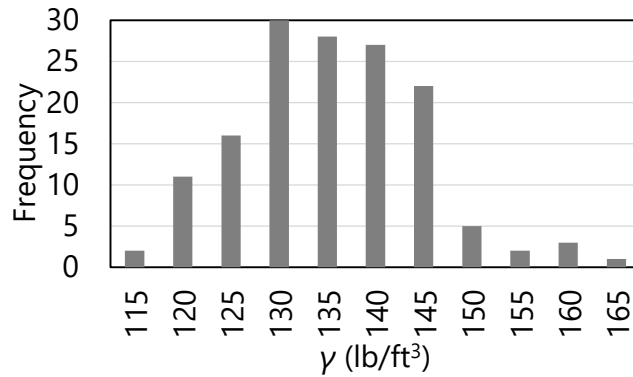
Figure 42. Histogram of 147 values of unit weight, γ, (elevation range: 30 ft to 9 ft) within layer 4

The same procedure as detailed above for layer 4 is carried out for all defined layers of Site A. Respective values of mean unit weight and COV are listed for layer 1 through layer 4 in Table 16. The dispersion of the layer-specific values for unit weight, expressed as COV, range between 0.04 (layer 1) and 0.16 (layer 2). As discussed previously in Ch. 2, these descriptive statistics are utilized when simulating log-normally distributed values of unit weight (γ), as part of stochastic simulation of axial resistance for drilled shaft members.

Table 16. Descriptive statistics for unit weight for each layer

Layer	Mean unit weight (lb/ft^3)	COV
1	129	0.04
2	121	0.16
3	137	0.14
4	133	0.07

71

4.3.3 Accounting for Steel Casings when Modeling Drilled Shafts

As an additional consideration when modeling axial resistances of drilled shafts, it may be desirable to neglect skin friction resistance near upper portions of the shaft when steel casings are present. As a convenience, for such instances, the option is available to exclude any defined layer from the resistance computation procedures implemented in GeoStat.

For example, if a drilled shaft foundation type is considered for Site A, and a casing is present from the ground surface down to the rock layer (i.e., layer 2), then layer 1 is excluded from axial resistance calculations by setting the Include flag to 0 (as opposed to 1, which signifies inclusion) within the layer data table of the Profile tab (Fig. 37, far right).

4.4 Initial Selection of Geostatistical Parameter Values

Having defined an initial layering for the Site A geotechnical data, focus of the modeling efforts within GeoStat continues onward to the formation of layer-specific spatial correlation structures (i.e., variograms). Although, as part of the variogram formation for each layer, additional checks are conducted regarding the previously defined layering (as discussed in Sec. 4.4.1).

Variogram formation for each layer is carried out within the Geostatistics tab (Fig. 43) of the GeoStat UI. For any layer that is to be included for simulating axial resistance, various graphical depictions are provided in the bottom region of the Geostatistics tab. From left to right (Fig. 43, bottom), the layer-specific graphical depictions include a scatterplot of the relevant soil or rock parameter, corresponding histogram, horizontal variogram, and vertical variogram.

While the scatterplot and histogram are dictated by the previously cataloged site data and initial layer definitions, the (experimental) variogram points are dependent on selection of variogram parameter values in the table located above the plots (Fig. 43, middle). Documentation of the selection of variogram parameter values for the initial Site A layering is provided later.

However, for drilled shaft portions embedded in limestone layers, values of unconfined compression strength (q_u) are used for computation of variogram points. When forming spatial correlation structures for driven pile foundation members, SPT-N blow count values are utilized in forming variograms. Likewise, for drilled shaft portions embedded in clay layers and drilled shaft portions embedded in sand layers, SPT-N blow count values are again utilized.

For the modeling of Site A, recall that a drilled shaft is selected as the foundation member type. Given the initial (limestone) layer definitions for layer 2, layer 3, and layer 4, variograms

72

would be formed based on layer-specific ensembles of unconfined compression strength (q_u). Also, because steel casing is assumed to be present down to the rock layer (layer 2), there is no need to form spatial correlation structures for layer 1.

Layer	Detrend	Detrend Polynomial Degree	Variogram Model	Horizontal Lag (ft)	Number of Horizontal Lags	Horizontal Tolerance (ft)	Horizontal Bandwidth (ft)	Horizontal Range	Horizontal Nugget	Horizontal Sill	Horizontal Worst Case	Vertical Lag (ft)	Number of Vertical Lags	Vertical Tolerance (ft)	Vertical Bandwidth (ft)	Vertical Range	Vertical Nugget	Vertical Sill	Vertical Worst Case	Status
1	No	1	Spherical	20.00	10	10.00	10.00	60.00	0.00	1.00	No	5.00	10	2.50	2.50	10.00	0.00	1.00	No	Not Included
2	Yes	1	Spherical	5.00	20	3.00	5.00	0.01	0.00	3.00	Yes	2.50	5	1.25	0.00	6.05	0.00	1.00	No	Completed
3	Yes	1	Spherical	5.00	20	2.50	2.00	0.01	0.00	1.00	Yes	2.50	4	1.25	0.00	3.63	0.00	1.00	No	Completed
4	No	1	Spherical	5.00	20	3.00	5.00	60.00	0.00	1.00	Yes	1.50	8	0.75	0.00	5.63	0.00	1.00	No	Completed

Elevation vs qu for Layer 3 — Histogram for Layer 3 — Horizontal Variogram for Layer 3 — Vertical Variogram for Layer 3

Mean	88.43	
Coefficient of Variation	0.94	
Variance	6976.44	
Number of samples	52	

Number of Points	2	
Minimum Number of Pairs	9	
Maximum Number of Pairs	18	
Average Number of Pairs	13	

Number of Points	4	
Minimum Number of Pairs	19	
Maximum Number of Pairs	66	
Average Number of Pairs	42	

Figure 43. Geostatistics tab

4.4.1 Examining Initial Definition of Layer Data

Prior to selecting variogram parameter values for each layer, both the descriptive statistics and graphical depictions of the layer-specific collections of q_u values are examined. Summary statistics for the relevant types of soil or rock measurements of each layer (q_u, given the initial layer definitions) are listed in Table 17. The sample sizes (i.e., number of measured values) per layer range from 38 to 61 across layers 2 through 4. Values pertaining to layer 1 are not applicable (N/A) because the layer is excluded from the Site A analysis to reflect the presence of a steel casing.

The dispersions associated with layers 2 and 4 are markedly high (COV values are 3.50 for layer 2, 2.63 for layer 4) Such large magnitudes of COV, in part, motivate assessment of the Site A data for alternative layer definitions (as discussed later). The unconfined compression strength value associated with layer 3 also exhibits large variations in an absolute sense (the COV value is 0.94); however, this latter dispersion value is less than (approximately) unity, and so, is less conspicuous.

Concerning examination of graphical depictions of layer-specific data (again, only q_u is applicable here), the scatterplot (e.g., Fig. 43, bottom-left) serves to reveal if trends are present

among the layer data. In the event that a trend is observed among the data attributed to a layer, then detrending is necessary. The detrending process (documented in Ch. 2) is automated in the GeoStat UI. Recalling Fig. 43 (middle-left), if detrending is desired for the data of a given layer, then the respective entry in the Detrend column of the layer data table is set to Yes (as opposed to No). Further, the polynomial degree of the trend is specified. Typically, linear detrending is sufficient for instances when detrending is necessary.

Table 17. Summary statistics for defined layers

Layer	Physical measurement	Sample size	Mean	COV
1	N/A	N/A	N/A	N/A
2	q_u (tsf)	38	11.7	3.50
3	q_u (tsf)	52	88.4	0.94
4	q_u (tsf)	61	12.4	2.63

Regarding the histograms of layer-specific data (e.g., Fig. 43, bottom-center), these plots allow for conspicuous frequency-related features (i.e., bimodal peaks) to be identified. More broadly, in the event that the data distribution for a given layer does not roughly exhibit a lognormal shape, then revisions to the layer definitions (and particularly the layer elevations) may need to be carried out. When conspicuous features are present in a layer-specific histogram, then it may also be necessary to assess the site data for the presence of distinct geological zones. If zones are identified, then modeling of each zone (one subset of boring locations at a time) can lead to more representative layers for a given region within the site, and also, to relatively smaller values of COV for layer-specific data. As a tradeoff though, the number of data points per layer will be reduced as the data set is further subdivided. See Ch. 5 for additional details regarding modeling of zones within sites.

4.4.1.1 Layer 2

A scatterplot of the 38 unconfined compression strength (q_u) values positioned within layer 2 is presented in Fig. 44. All but three values are less than approximately 10 tsf. As part of the present examination it is confirmed that the q_u values are generally contributed to from across all boring locations that contain core run data. That is, if any one boring location containing core run data is deactivated, no visual changes are observed within the scatterplot of q_u values. A very weak trend is present in the data that indicates decreases in q_u with increasing depth.

A histogram of the 38 measured q_u values pertaining to layer 2 is presented in Fig. 45. To better reveal the qualitative characteristics of the distribution, the histogram excludes the three q_u values that are greater than approximately 10 tsf. The overall histogram (roughly) resembles that of log-normally distributed data, and possesses a pronounced right skew. Given the absence of conspicuous features (such as bimodal phenomena) in the layer 2 histogram, no revisions are made regarding the initial selection of boundary elevations for layer 2.
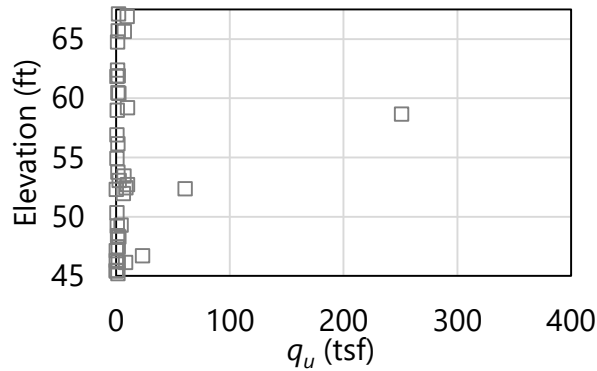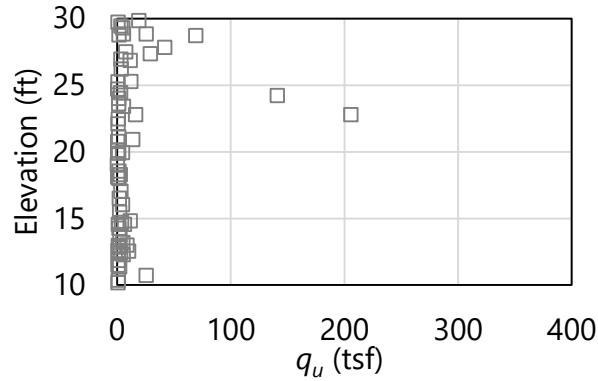
Figure 44. Scatterplot of 38 unconfined compression strength, q_u, values (elevation range: 67.5 ft to 45 ft) within layer 2
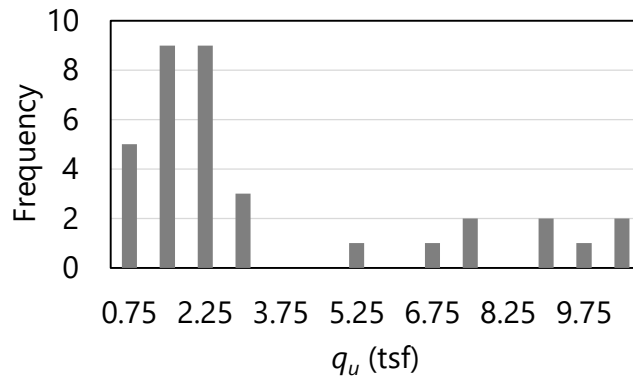

Figure 45. Histogram of 38 q_u values (elevation range: 67.5 ft to 45 ft) within layer 2

4.4.1.2 Layer 3

A scatterplot of the 52 unconfined compression strength (q_u) values positioned within layer 3 is presented in Fig. 46. The relatively higher-magnitude values of q_u in layer 3 (i.e., those greater than approximately 50 tsf) are confirmed to be contributed to from across the data sets of all boring locations, that in turn, include core run data. A significant number of q_u values of magnitudes less than approximately 10 tsf are also present, and a very weak trend is present (where q_u values decrease with increasing depth).

A histogram of the 52 measured q_u values pertaining to layer 3 is presented in Fig. 47. Visual inspection of the histogram indicates (approximately) log-normally distributed data with a right skew. Therefore, no revisions are made to the initial selections of boundary elevations for layer 3.
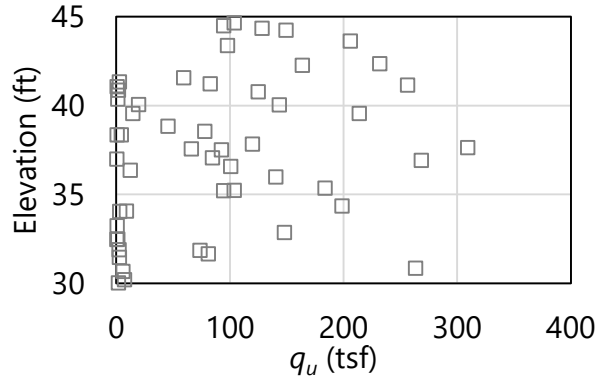
Figure 46. Scatterplot of 52 unconfined compression strength, q_u, values (elevation range: 45 ft to 30 ft) within layer 3
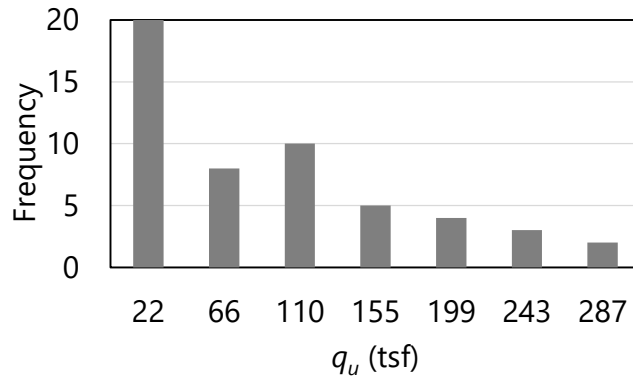
Figure 47. Histogram of 52 unconfined compression strength, q_u, values (elevation range: 45 ft to 30 ft) within layer 3

4.4.1.3 Layer 4

A scatterplot of the 61 unconfined compression strength (q_u) values positioned within layer 4 is presented in Fig. 48. All but 7 values are less than approximately 20 tsf. As with layer 2 and layer 3, it is likewise confirmed for layer 4 that the q_u values are generally contributed to from across all boring locations that contain core run data. Also, no apparent trend is observed within the layer 4 scatterplot.

A histogram of the 61 measured q_u values pertaining to layer 4 is presented in Fig. 49. To better reveal the qualitative characteristics of the distribution, the histogram excludes the seven q_u values that are greater than approximately 20 tsf. The overall histogram (roughly) resembles that of log-normally distributed data, with a pronounced right skew. Given the absence of conspicuous features (such as bimodal phenomena) in the layer 4 histogram, no revisions are made regarding the initial selection of boundary elevations for layer 4.

76

Figure 48. Scatterplot of 61 unconfined compression strength, q_u, values (elevation range: 30 ft to 10 ft) within layer 4
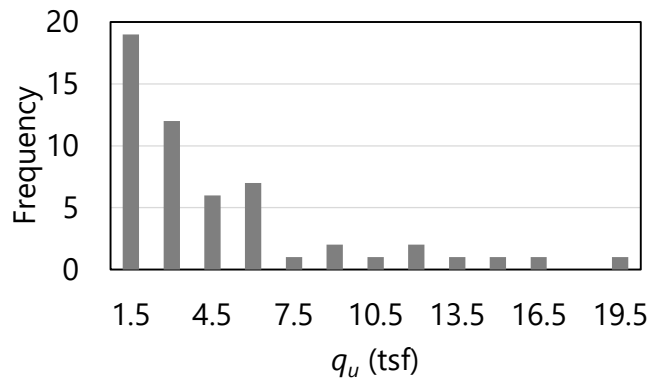
Figure 49. Histogram of 61 unconfined compression strength, q_u, (elevation range: 30 ft to 10 ft) within layer 4

4.4.2 Forming Variograms using Initial Layer Definitions

The above examination reaffirms the initial selections of layer elevations for the geotechnical data of Site A. Despite this reaffirmation, the COV values of q_u for layer 2 and layer 4 (recall Table 17) are conspicuously large and require further consideration, as provided later. As the immediate next step though, the process of forming variograms is undertaken for layer 2 through layer 4.

4.4.2.1 Limitations of the Site A Data Set

Recalling Fig. 30, geotechnical data are available for only 14 boring locations, and those locations are distributed across a plan-view area of approximately 150 ft by 1500 ft. Consequently, the prospect of forming representative spatial correlation structures in the horizontal direction is precluded for Site A. Importantly, this is not to say that the horizontal variograms are neglected. Rather, worst case conditions (conceptually introduced in Ch. 2) are

77

applicable to the horizontal variograms. More specifically, worst case conditions are applicable to the horizontal variograms because insufficient data are available across the 14 borings of Site A for the purpose of constructing well-formed horizontal variograms. Further recall from Ch. 2 that worst case conditions constitute upper-bound conservativism; worst case conditions are associated with maximally conservative (i.e., highest-valued) variability, lowest-valued resistance factors (ϕ), and ultimately, lowest-valued factored resistances. Use of worst case conditions may lead to designs that are not cost effective due to the associated levels of conservatism.

As detailed in Ch. 2, unconditional (stochastic) simulation for estimating foundation member axial resistance makes use of spatial correlation structures in the vertical direction, as opposed to variograms in the horizontal and vertical directions. Unconditional simulation is elected for Site A to avoid the prospect of generating factored axial resistances under worst case conditions (with respect to the horizontal variograms). Given the small number of relatively distant boring locations (in plan-view) for Site A, focus is given below to formation of vertical variograms. However, the same general concepts apply for instances where sufficient site data are available to construct both horizontal and vertical variograms for a site.

4.4.2.2 Summary of Initial Selections for Variogram Parameter Values

Vertical variogram parameters initially selected for layer 2 through layer 4 of Site A are listed in Table 18. As discussed in Ch. 2, the lag distance, number of lags, tolerance, and bandwidth are all instrumental in forming points of the experimental variogram. Vertical variogram values for range and sill are listed per layer in Table 19, where these values are more strongly related (in GeoStat) to the theoretical variogram (see Ch. 2 for additional details).

Table 18. Layer-specific parameters for vertical variograms

Layer	Lag (ft)	Number of lags	Tolerance (ft)	Bandwidth (ft)
1	N/A	N/A	N/A	N/A
2	2.5	5	1.25	0.0
3	2.5	4	1.25	0.0
4	1.0	8	0.50	0.0

Table 19. Vertical variogram ranges and sills for layers

Layer	Vertical range (ft)	Vertical sill
1	N/A	N/A
2	5.5	1.0
3	3.6	1.0
4	5.6	1.0

As listed above in Table 18, lag distances (i.e., the abscissa spacing between points of the variogram) are selected to range between 1 ft and 5 ft. Selection of these distance values is

motivated by characteristic lengths that are relevant to spacings between reported measurements along core runs. For example, with regards to layer 2, a lag distance of 2.5 ft is on the order of that associated with typical core run lengths (5 ft).

As detailed for each layer in the content below, use of the above lag distances leads to well-formed vertical variograms for the initial layering of Site A. Regardless, it is recommended that multiple candidates for lag distance be considered prior to finalizing the variogram for a given layer and variogram direction. Furthermore, for each candidate lag distance considered, it is necessary to update the values for tolerance and bandwidth.

Recommendations are given in McVay et al. (2012) for determining values of tolerance and bandwidth, given a candidate value of lag distance. For example, for the selected lag distance of 2.5 ft that is associated with the layer 2 vertical variograms, the tolerance is set to one-half the magnitude of the lag distance (i.e., 1.25 ft) and the bandwidth is set to 0 ft. In particular, setting the bandwidth to 0 ft when constructing vertical variograms is recommended given typical horizontal spacings between boring locations, relative to vertical spacings between data measurements (SPT-N, q_u). Considerations for the number of lags (Table 18); and, values for vertical range and vertical sill (Table 19) are discussed below on an individual layer basis.

4.4.2.3 Layer 2

Vertical variogram points for layer 2 are based upon (vertical) distance-based pairings of measured q_u values. The experimental variogram points for layer 2 are listed in Table 20 and plotted in Fig. 50, and are generated with use of linear data detrending. Also listed in Table 20 are the pairs associated with each variogram point. The data listed in Table 20 are obtained directly from the GeoStat UI by entering the Variogram Data dialog (Fig. 43, top-left).

Table 20. Vertical variogram data for layer 2 (elevation range: 67.5 ft to 45 ft)

Abscissa (ft)	Ordinate	Pairs
2.5	0.87	24
5.0	0.70	22
7.5	1.00	25
10.0	0.88	12
10.0	1.02	15

As discussed in Ch. 2, the number of measured data pairs used in forming an experimental variogram point reflect the strength (or significance) of said point. Further, as is the case for the variogram plots within the GeoStat UI (recall Fig. 43), the experimental variogram point symbols in Fig. 50 are sized (scaled) based on the respective number of pairs used in forming said points. The scaling visually signifies the strength or significance of each variogram point. A threshold value of approximately 30 (pairs) is recommended in McVay et al. (2012) when judging the significance of an experimental variogram point.

Specific to the vertical variogram for layer 2, pair counts steadily reduce from 24 at a distance of 2.5 ft down to 15 at a distance of 12.5 ft (Table 20). The variogram points roughly indicate convergence toward a sill value of unity, and so, the five generated points along the variogram (i.e., 5 lags) are considered sufficient.

a)

b)
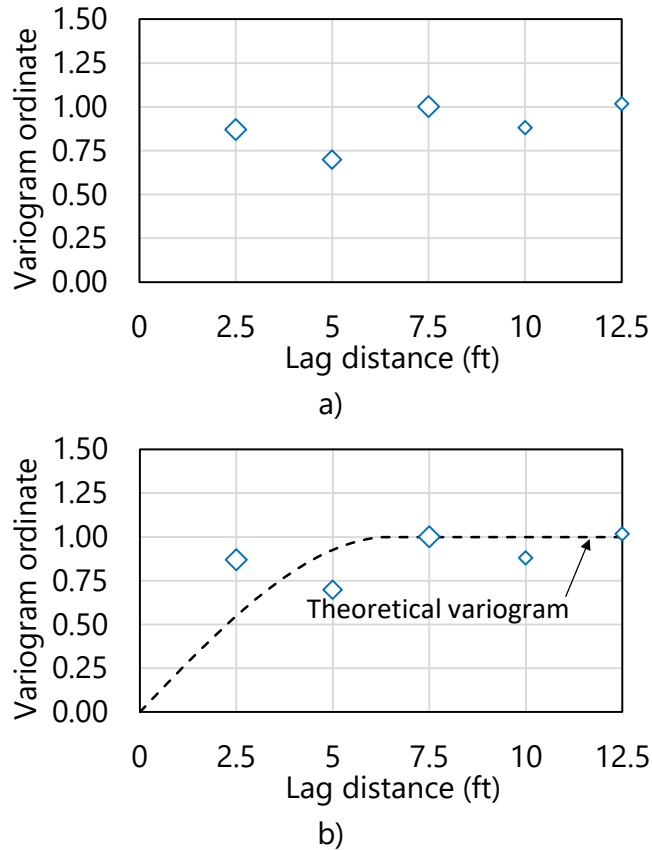
Figure 50. Vertical variogram for layer 2 (elevation range: 67.5 ft to 45 ft): a) Experimental variogram points; b) Experimental variogram points and theoretical (spherical) fit

The experimental variogram points approach the data-wide variance (i.e., a sill value of 1.0) between the second and third variogram points (Fig. 50a). Approximately asymptotic behavior is apparent for increasing vertical distance. As a counterpart, the theoretical variogram selected for layer 2 is displayed in Fig. 50b. The theoretical variogram is graphically fit from within the GeoStat UI by left-clicking and dragging the curve directly within the vertical variogram plot (e.g., Fig. 43, bottom-right). Care is taken to ensure that the theoretical variogram passes through those experimental variogram points possessing the pair counts nearest to 30. As a result, the range and sill values are automatically quantified as 5.5 ft and 1.0, respectively.

4.4.2.4 Layer 3

Vertical variogram points for layer 3 are listed in Table 21 and plotted in Fig. 51. Similar to that of layer 2, initial formation of the (experimental) vertical variogram for layer 3 is based upon identified pairs of unconfined compression strength (q_u). The variogram points are generated (automatically from within GeoStat) using first-order (linear) detrending of the layer data. Also listed in Table 21 are the pairs associated with each layer 3 variogram point.

The pair counts associated with each variogram point steadily reduce from 66 at a distance of 2.5 ft down to 19 at a distance of 10.0 ft. The variogram gives clear convergence toward a sill value of unity, and so, four points along the variogram (i.e., 4 lags) are considered sufficient.

Table 21. Vertical variogram data for layer 3 (elevation range: 45 ft to 30 ft)

Abscissa (ft)	Ordinate	Pairs
2.5	0.87	66
5.0	1.14	50
7.5	1.05	34
10.0	1.01	19
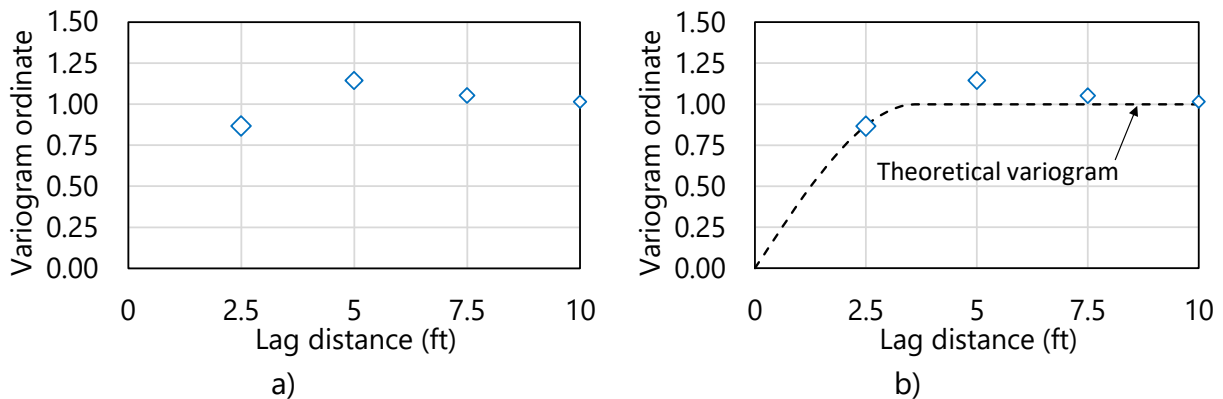
Figure 51. Vertical variogram for layer 3 (elevation range: 45 ft to 30 ft): a) Experimental variogram points; b) Experimental variogram points and theoretical (spherical) fit

The experimental variogram points for layer 3 (Fig. 51a) are fitted with a theoretical variogram (Fig. 51b). Convergence to the sill value (of unity) is judged to occur between the first and second points of the experimental variogram. The range (3.6 ft) and sill (1.0) values are automatically quantified by virtue of employing the graphical selection feature (for characterizing theoretical variograms) implemented in the GeoStat UI.

4.4.2.5 Layer 4

Vertical variogram points for the initial definition of layer 4 are listed in Table 22 and plotted in Fig. 52. Similar to that of layer 2 and layer 3, vertical variogram formation for layer 4 is

based upon identified pairs (based on distances between measurements) of q_u values. However, no detrending is included prior to generation of variogram points for layer 4. Also listed in Table 22 are the pair counts associated with each layer 4 (experimental) variogram point.

The pair counts associated with each variogram point consistently reduce from 47 at a distance of 1.5 ft down to 20 at a distance of 12.0 ft. Despite the presence of mild cyclicity, the experimental variogram points clearly trend toward a sill value of unity. As plotted in Fig. 52b, a theoretical (vertical) variogram is generated through use of the graphical fit feature in the GeoStat UI. The corresponding range of the theoretical variogram for layer 4 is defined (graphically) as 5.6 ft.

Table 22. Vertical variogram data layer 4 (elevation range: 30 ft to -10 ft)

Abscissa (ft)	Ordinate	Pairs
1.5	0.40	47
3.0	0.74	42
4.5	0.90	38
6.0	0.80	32
7.5	0.83	29
9.0	1.03	26
10.5	1.02	21
12.5	0.92	20
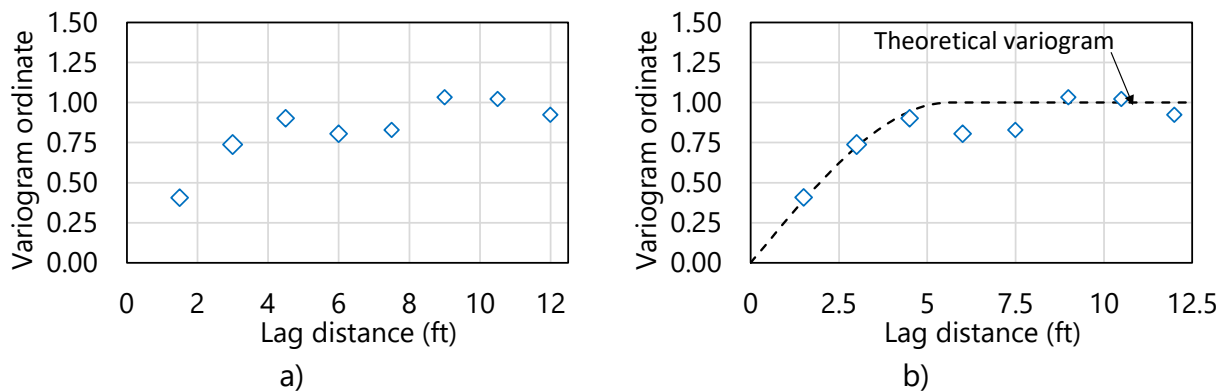
Figure 52. Vertical variogram for layer 4 (elevation range: 30 ft to -10 ft): a) Experimental variogram points; b) Experimental variogram points and theoretical (spherical) fit

4.4.3 Observations Regarding Initial Layer Definitions and Variograms

As noted previously, the volume of available data for Site A is relatively limited, which leads to conspicuously large COV values for the q_u data of layer 2 and layer 4 (recall Table 17). Furthermore, scrutiny of the selected layer elevations (discussed, and reaffirmed, above) does not provide justification for further subdividing the initial selections of layer elevations. In

other words, the large COV values for layer 2 (3.49) and layer 4 (2.63) cannot be attributed to the need to further subdivide the layers.

Therefore, with regard to characterization of the relatively limited volume of site data, two options remain at this stage (given that zonal issues are not present): 1) accept the initial layer definitions (soil or rock types; elevations), and the associated (large) magnitudes of COV values for layer 2 and layer 4; or, 2) explore a modification to the layer definitions for layer 2 and layer 4. The latter option is elected and discussed in the following.

4.5 Alternative Definition of Soil or Rock Layering

Recalling that bands and layers of clay are prevalent (along with limestone) among the Site A data, the layer types assigned to layer 2 and layer 4 are modified to clay. Consequently, the relatively more numerous measurements of SPT-N values (as opposed to q_u values) are drawn upon in constructing variograms using the alternative definitions of layer 2 and layer 4.

Scatterplots of the previously cataloged site data are again utilized (recall Fig. 37, left and middle) to aid in selection of boundary layer elevations. Alternative layer definitions formed for Site A are listed in Table 23. Based on the cataloged site data, four layers are defined and consist of either clay (layer 1, layer 2, and layer 4) or limestone (layer 3). Layer top and bottom elevations span the ranges of elevations identified during the initial review of the site data documented above. The only modification (relative to the initial layer definition) is to slightly adjust the bottom of layer 1 to 65 ft. Additional discussion regarding the selections of the boundary layer elevations is provided in the remainder of Sec. 4.5. Still further considerations are documented in Sec. 4.6, as part of forming variograms (based on the alternative layer definitions).

Table 23. Selected layer types and elevation ranges

Layer	Layer type	Top elevation (ft)	Bottom elevation (ft)
1	Clay	97.0	65.0
2	Clay	65.0	45.0
3	Limestone	45.0	30.0
4	Clay	30.0	-10.0

4.5.1 Selecting Alternative Layer Elevations

The 271 SPT-N blow counts associated with the 14 boring locations of Site A, along with layer divisions (blue horizontal lines), are plotted with respect to elevation in Fig. 53. Values of SPT-N blow counts are focused upon because values of undrained shear strength (C_u) are not available for Site A. As an alternative, SPT-N blow counts are examined, simulated, and then empirically related to C_u values (as discussed in Sec. 2.7). Consistent with the initial review of the cataloged SPT-N data for Site A, the selected layer divisions are positioned in accordance

with qualitative groupings of the SPT-N blow counts. For example, a distinct grouping of blow counts is apparent between 97 ft and 65 ft, in comparison to those values cataloged below 65 ft. Thus, Layer 1 is defined between 97 ft and 65 ft.
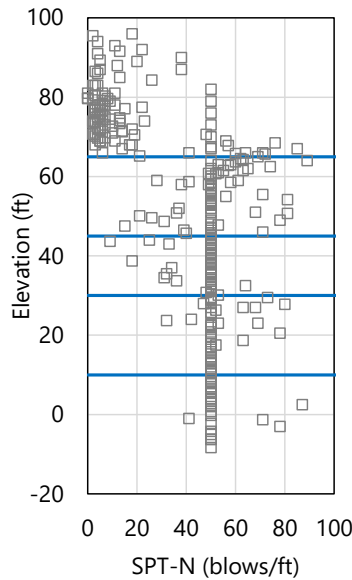
Figure 53. Scatterplot of 271 SPT-N blow counts (elevation range: 96 ft to -10 ft) with layer bottom elevations (blue horizontal lines)

The qualitative grouping of SPT-N blow counts positioned between 65 ft and 45 ft motivates designation of the boundary elevations for layer 2. Regarding layer 3, and because this layer type remains designated as limestone, no modifications are made relative to the initial layer definition (with elevations of 45 ft to 30 ft). The SPT-N blow counts below 30 ft are generally associated with refusal-like conditions. Therefore, layer 4 is defined to bound all data at and below 30 ft (i.e., layer 4 is defined between 30 ft and -10 ft), and is defined as a clay layer (as opposed to limestone). Mean and COV values for unit weight, γ, for all layers are maintained relative to the initial layer definitions (recall Table 16).

4.6 Alternative Selection of Geostatistical Parameter Values

Having defined an alternative layering for the Site A geotechnical data, focus of the modeling efforts within GeoStat continues onward to the formation of layer-specific spatial correlation structures (i.e., variograms). As part of the variogram formation for each layer, additional checks are conducted regarding the revisions to the layering definitions (as discussed in Sec. 4.6.1). Also, consistent with the investigation of the initial layer definitions, focus is given to vertical variogram formation. This focus is motivated by the fact that insufficient volumes of Site A data are available for the purpose of constructing horizontal variograms. Importantly, horizontal variograms are not neglected, but rather, are associated with worst case conditions (as introduced in Ch. 2). So as to avoid the potentially extreme conservatism that accompanies

use of worst case conditions, unconditional simulation is again elected, and as a result, only the vertical variograms are made use of during simulation.

For the modeling of Site A, recall that a drilled shaft is selected as the foundation member type. Therefore, for layer 2 and layer 4 (of type clay), variograms are formed based on layer-specific ensembles of SPT-N blow count values. Variogram formation for layer 3 is based upon values of unconfined compression strength (q_u). Also, because (for illustration) steel casing is assumed to be present down to the rock layer (layer 3), there remains no need to form spatial correlation structures for layer 1.

4.6.1 Examining Alternative Layer Data

Prior to selecting variogram parameter values for the alternative layer definitions, both the descriptive statistics and graphical depictions of the layer specific collections of SPT-N blow counts (or q_u values) are examined. Summary statistics for the relevant types of soil or rock measurements of each layer (either SPT-N or q_u) are listed in Table 24. The sample sizes (i.e., number of measured values) per layer range from 52 to 63 across layers 2 through 4. Values pertaining to layer 1 are not applicable (N/A) because the layer is excluded from the Site A analysis to reflect the presence of steel casing.

The dispersions associated with layers 2 and 4 are relatively low (COV values are 0.26 for layer 1, 0.18 for layer 4). The reduction in dispersions partly remedies reservations associated with the initial layer definitions. However, the reduced values of COV in layer 2 and layer 4 (relative to those of the initial layer definitions) are due in some measure to the prevalence of SPT-N blow counts equal to 50, which are distributed throughout each layer. As with the initial layering, the unconfined compression strength values associated with the limestone layer (layer 3, Table 24) exhibit relatively large variations (the COV value is 0.98).

Table 24. Summary statistics for defined layers

Layer	Physical measurement	Sample size	Mean	COV
1	N/A	N/A	N/A	N/A
2	SPT-N (blows/ft)	63	52.4	0.26
3	q_u (tsf)	52	88.4	0.98
4	SPT-N (blows/ft)	63	53.2	0.18

4.6.1.1 Layer 2

A scatterplot of the 63 SPT-N blow counts positioned within layer 2 is presented in Fig. 54. A relatively large portion of the SPT-N blow count data is equal to 50 blows/ft. As part of the present examination, it is confirmed that the blow count data points of 50 blows/ft are generally contributed to from across the 14 boring locations. Also, owing in part to the prevalence of SPT-N blow count measurements recorded at 50 blows/ft, no apparent trend is observed for the layer 2 scatterplot.

85
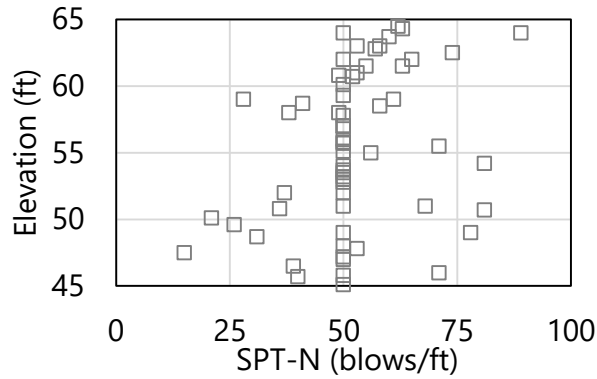
Figure 54. Scatterplot of 63 SPT-N blow count values (elevation range: 65 ft to 45 ft) within layer 2

A histogram of the 63 measured SPT-N blow count values pertaining to layer 2 is presented in Fig. 55. Although a pronounced frequency peak is present for blow count values of 50 blows/ft, the overall histogram (roughly) resembles that of normally or log-normally distributed data. Given the absence of conspicuous features (such as bimodal phenomena) in the layer 2 histogram, no revisions are made regarding the boundary elevations for layer 2 listed in Table 23.
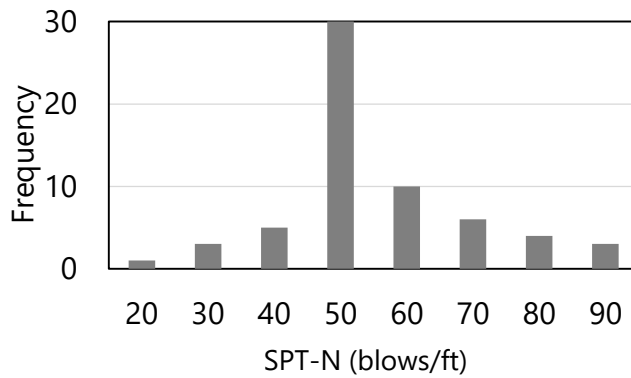
Figure 55. Histogram of 63 SPT-N blow count values (elevation range: 65 ft to 45 ft) within layer 2

4.6.1.2 Layer 3

The layer type (limestone) and elevations (45 ft to 30 ft) initially assigned to layer 3 remain unchanged in the alternative layer definition. Therefore, examination of q_u values positioned within layer 3 is identical to that discussed above in association with the initial layer definition. Stated alternatively, the previous assessment of q_u values within layer 3 still holds, and no modifications are made to layer 3 (relative to the listings of Table 23).

86

4.6.1.3 Layer 4

A scatterplot of the 63 SPT-N blow counts positioned within layer 4 is presented in Fig. 56. The vast majority of the SPT-N blow count data is equal to 50 blows/ft. As part of the present layer examination, it is confirmed that the blow count data points of 50 blows/ft are generally contributed to from across the 14 boring locations throughout Site A. Also, owing in part to the abundance of SPT-N blow count measurements recorded at 50 blows/ft, no apparent trend is observed for the layer 4 scatterplot.

A histogram of the 63 measured SPT-N blow count values pertaining to layer 4 is presented in Fig. 57. Although a predominant frequency peak is present for blow count values of 50 blows/ft, the overall histogram (roughly) resembles that of log normally distributed data. Given the absence of other conspicuous features in the layer 4 histogram, no revisions are made regarding the boundary elevations for layer 4 (Table 23).
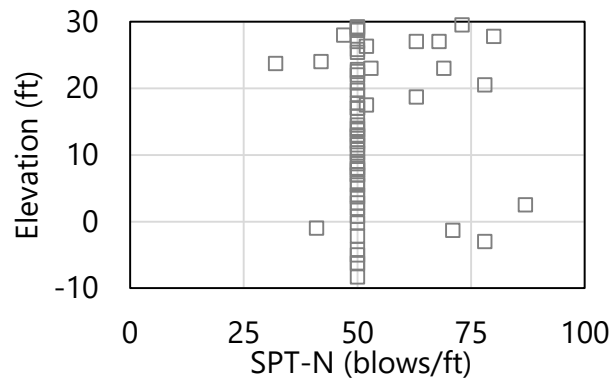
Figure 56. Scatterplot of 63 SPT-N blow count values (elevation range: 30 ft to -10 ft) within layer 4
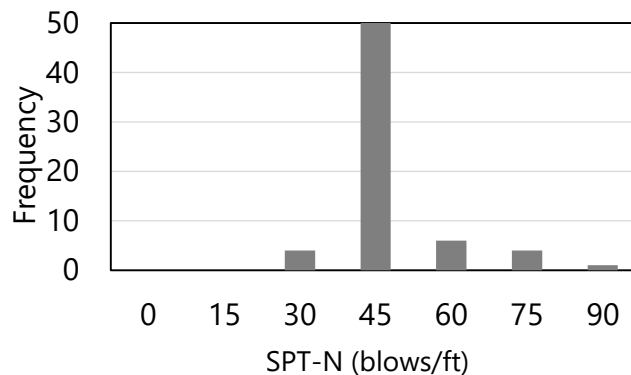
Figure 57. Histogram of 63 SPT-N blow count values (elevation range: 30 ft to -10 ft) within layer 4

4.6.2 Forming Variograms using Alternative Layering

Vertical variogram parameters selected for the alternative definitions of layer 2 through layer 4 of Site A are listed in Table 25. As discussed in Ch. 2, the lag distance, number of lags, tolerance, and bandwidth are all instrumental in forming points of the experimental variogram. Vertical variogram values for range and sill are listed per layer in Table 26, where these values are more strongly related (in GeoStat) to the theoretical variogram (see Ch. 2 for additional details).

Table 25. Layer-specific parameters for vertical variograms

Layer	Lag (ft)	Number of lags	Tolerance (ft)	Bandwidth (ft)
1	N/A	N/A	N/A	N/A
2	2.5	6	1.25	0.0
3	2.5	7	1.25	0.0
4	2.5	8	1.25	0.0

Table 26. Vertical variogram ranges and sills for layers

Layer	Vertical range (ft)	Vertical sill
1	N/A	N/A
2	3.2	1.0
3	4.7	1.0
4	2.3	1.0

As listed above in Table 25, a lag distance of 2.5 ft is selected for the variograms of layer 2 through layer 4. Selection of this distance value is motivated by characteristic lengths that are relevant to spacings between reported SPT measurements. Also, McVay et al. (2012) recommended using lag distances of 2.5 ft when constructing variograms with use of SPT-N blow counts. With regards to layer 3 (which emphasizes q_u values), a lag distance of 2.5 ft is on the order of that associated with typical core run lengths (5 ft). If core run data are positioned over different intervals, then such intervals should be taken into account when selecting a lag distance for modeling of drilled shaft portions in limestone layers.

As detailed for each layer in the content below, use of a uniform lag distance across all layers leads to reasonably well-formed vertical variograms for the Site A modeling. Recommendations given in McVay et al. (2012) are again utilized for determining vertical variogram values of tolerance and bandwidth, given values of lag distance in Table 25. For example, for the selected lag distance of 2.5 ft, the tolerance is set to one-half the magnitude of the lag distance (i.e., 1.25 ft) and the bandwidth is set to 0 ft. Considerations for the number of lags (Table 25); and, values for vertical range and vertical sill (Table 26) are discussed below on an individual layer basis.

4.6.2.1 Layer 2

Vertical variogram points for layer 2 are based upon (vertical) distance-based pairings of measured SPT-N blow count values. The experimental variogram points for layer 2 are listed in Table 27 and plotted in Fig. 58. Also listed in Table 27 are the pairs associated with each variogram point. Pair counts steadily reduce from 51 at a distance of 2.5 ft down to 6 at a distance of 17.5 ft. Beginning at a distance of 12.5 ft, consecutive points of greater distance correspond to pair counts well below the threshold value of 30 pairs. Therefore, 7 points along the variogram (i.e., 7 lags) are considered sufficient for the vertical variogram of layer 2.

While the experimental variogram points approach the data-wide variance (i.e., a sill value of 1.0) at the first variogram point (Fig. 58a), approximately asymptotic behavior is apparent for increasing vertical distance. As a counterpart, the theoretical variogram selected for layer 2 is displayed in Fig. 58b. Care is taken to ensure that the theoretical variogram passes through those experimental variogram points possessing the pair counts greater than 30. As a result, the range and sill values are automatically quantified as 3.2 ft and 1.0, respectively.

Table 27. Vertical variogram data for layer 2 (elevation range: 65 ft to 45 ft)

Abscissa (ft)	Ordinate	Pairs
2.5	0.94	51
5.0	1.00	40
7.5	0.97	22
10.0	1.18	29
12.5	1.11	21
15.0	1.88	14
17.5	0.96	6
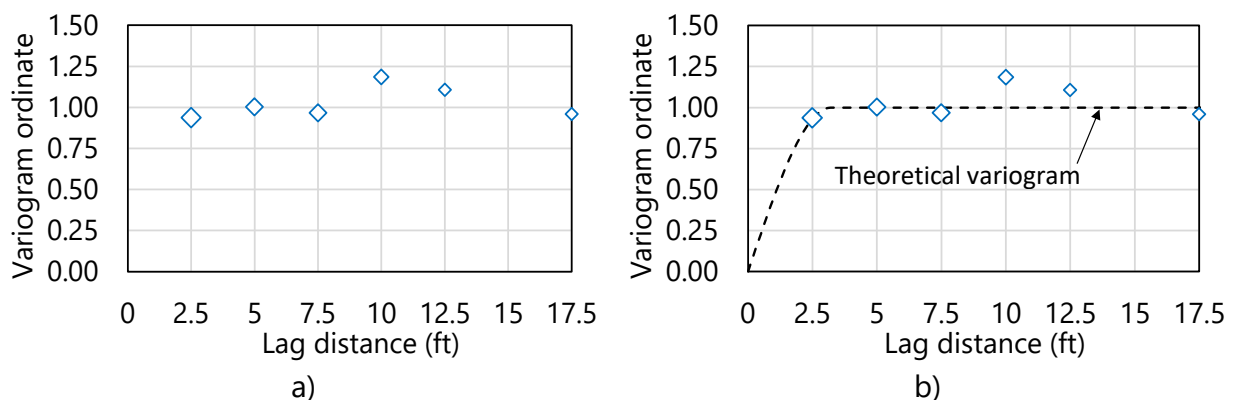
Figure 58. Vertical variogram for layer 2 (elevation range: 65 ft to 45 ft): a) Experimental variogram points; b) Experimental variogram points and theoretical (spherical) fit

4.6.2.2 Layer 3

As aforementioned, the layer type and elevations initially assigned to layer 3 (limestone; 45 ft to 30 ft) remain unchanged in the alternative layer definition. Therefore, the variogram formed for layer 3 is identical to that discussed above in association with the initial layer definition. Stated alternatively, the vertical variogram constructed using q_u values within layer 3 and the initial layer definition still holds.

4.6.2.3 Layer 4

Vertical variogram points for layer 4 are listed in Table 28 and plotted in Fig. 59. Similar to that of the layer 2 definition, vertical variogram formation for layer 4 is based upon identified pairs (based on distances between measurements) of SPT N blow count values. Also listed in Table 28 are the pair counts associated with each layer 4 (experimental) variogram point. The pair counts associated with each variogram point steadily reduce from 46 at a distance of 2.5 ft down to 22 at a distance of 20.0 ft. Beginning at a distance of 17.5 ft, consecutive variogram points of greater distance correspond to pair counts well below the threshold value of 30 pairs. Therefore, 8 points along the variogram (i.e., 8 lags) are considered sufficient for the vertical variogram of layer 4.

The experimental variogram points for layer 4 (Fig. 59a) exhibit slight undulations, but overall asymptotic behavior. With the exception of a single point (7.5 ft, 0.79), experimental variogram points values generally converge to the normalized sill value of 1.0. The theoretical variogram for layer 4 (Fig. 59b) is generated through use of the graphical fit feature in the GeoStat UI. Given the relatively large number of pairs and ordinate associated with the point (2.5 ft, 1.09), the theoretical variogram is constructed to reach a sill of 1.0 at a distance slightly less than 2.5 ft. The corresponding range of the theoretical variogram for layer 4 is defined as 2.3 ft.

Table 28. Vertical variogram data layer 4 (elevation range: 30 ft to -10 ft)

Abscissa (ft)	Ordinate	Pairs
2.5	1.09	46
5.0	1.16	46
7.5	0.79	34
10.0	1.12	38
12.5	1.07	31
15.0	1.12	32
17.5	1.10	23
20.0	0.92	22
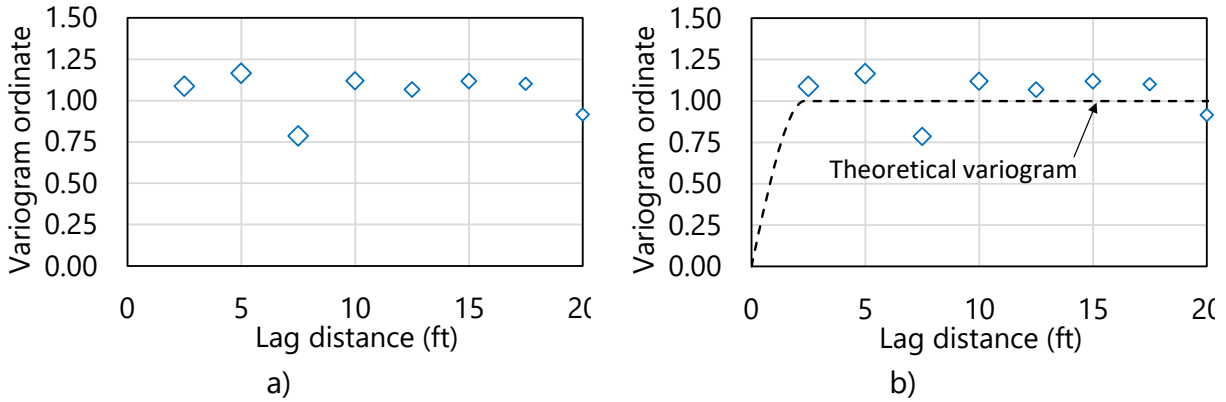
Figure 59. Vertical variogram for layer 4 (elevation range: 30 ft to -10 ft): a) Experimental variogram points; b) Experimental variogram points and theoretical (spherical) fit

4.7 Cursory Examination of the Site A Data for Identifying Zones

Zonal issues are not anticipated in association with modeling of the Site A data (see Ch. 5 for a detailed example of modeling zones). Solely for illustration purposes, prior to moving beyond variogram formation for the alternative layer definitions, a cursory assessment of the available Site A data is carried out to ensure that no distinct geological zones are present. Highlighted in Fig. 60 are two boring locations from within Site A that are relatively far from the remaining 12 boring locations. These two boring locations are excluded from the site modeling and the vertical variograms are reformed using the remaining 12 borings. Note that it is also confirmed that removal of the two borings does not affect the selections for layer elevations (with considerations similar to those documented above). Comparisons between the two sets of variograms are compared in (Table 29, Table 30, Fig. 61, and Fig. 62).
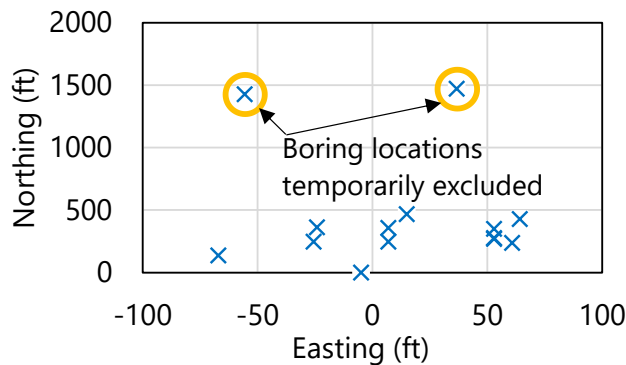
Figure 60. Site A boring locations with indication of temporarily excluded borings

In the comparisons of (experimental) vertical variograms, focus is given to layer 3 and layer 4. This is because resistances from layer 1 and layer 2 are not anticipated to appreciably contribute to the axial resistance of the drilled shaft. More specifically, resistances associated with layer 1 are neglected due to the presence of a steel casing. Resistances attributable to

91

layer 2 are anticipated to be small relative to those attained for embedded shaft portions in the limestone layer (layer 3).

Table 29. Comparison of vertical variogram data for layer 3 when all 14 boring locations are considered versus when two borings are excluded

| | All borings | | Two borings excluded | |
Abscissa (ft)	Ordinate	Pairs	Ordinate	Pairs
2.5	0.87	66	0.87	66
5.0	1.14	50	1.14	50
7.5	1.05	34	1.05	34
10.0	1.01	19	1.01	19

Table 30. Comparison of vertical variogram data for layer 4 when all 14 boring locations are considered versus when two borings are excluded

| | All borings | | Two borings excluded | |
Abscissa (ft)	Ordinate	Pairs	Ordinate	Pairs
2.5	1.09	46	1.04	44
5.0	1.16	46	1.09	45
7.5	0.79	34	0.75	34
10.0	1.12	38	1.10	38
12.5	1.07	31	1.03	31
15.0	1.12	32	1.07	32
17.5	1.10	23	1.07	23
20.0	0.92	22	0.88	22
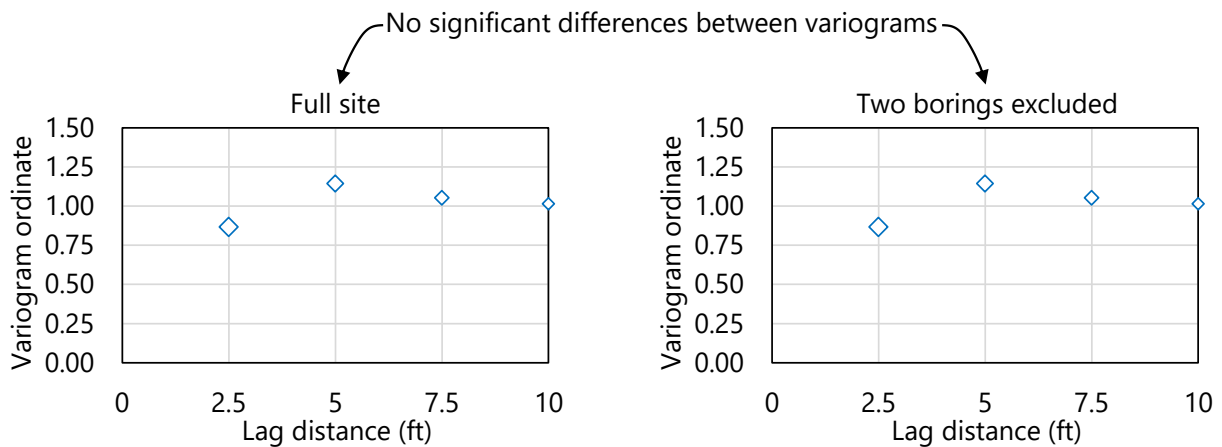
Figure 61. Comparison of experimental vertical variogram points for layer 3 when all boring locations are considered versus when two boring locations are excluded
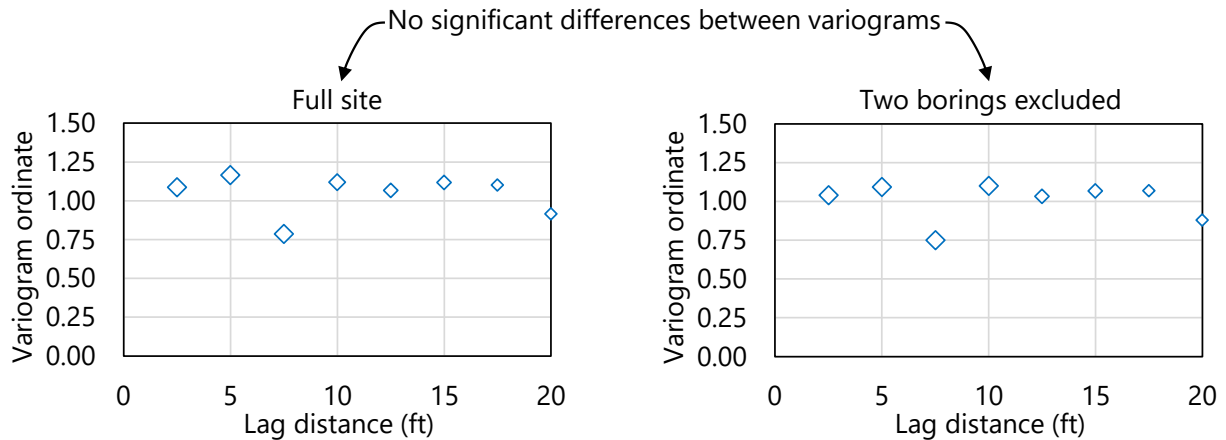
Figure 62. Comparison of experimental vertical variogram points for layer 4 when all boring locations are considered versus when two boring locations are excluded

Exclusion of the two boring locations indicated in Fig. 60 has practically no effect on the vertical variogram of layer 3 (Table 29, Fig. 61). This is because the two excluded borings do not contain any core run data. The effect that removing the two boring locations has upon the layer 4 variogram (Table 30, Fig. 62) is relatively small.

The variogram ordinate values of layer 4, for a given distance, remain within 6% of one another. Also, the pair counts remain with 5% of one another. While the above assessment is cursory, and solely for illustration, outcomes from the assessment do not indicate zonal issues. In other words, the assessment supports that the 14 boring locations of Site A can be treated as if the collective geotechnical site data originate from the same, single geological zone. Detailed documentation for modeling of zones within sites is provided in Ch. 5.

4.8 Performing Stochastic Simulation

Using the alternative layering and vertical variograms for the available geotechnical data of Site A, stochastic simulation of axial resistance is carried out in GeoStat as the next major step. Shown in Fig. 63 is the fourth of seven tabs (from left to right) in the GeoStat UI, referred to as the Simulation tab. Discussed below are selections made for relevant foundation member parameters, as well as initial considerations for carrying out simulations.

93
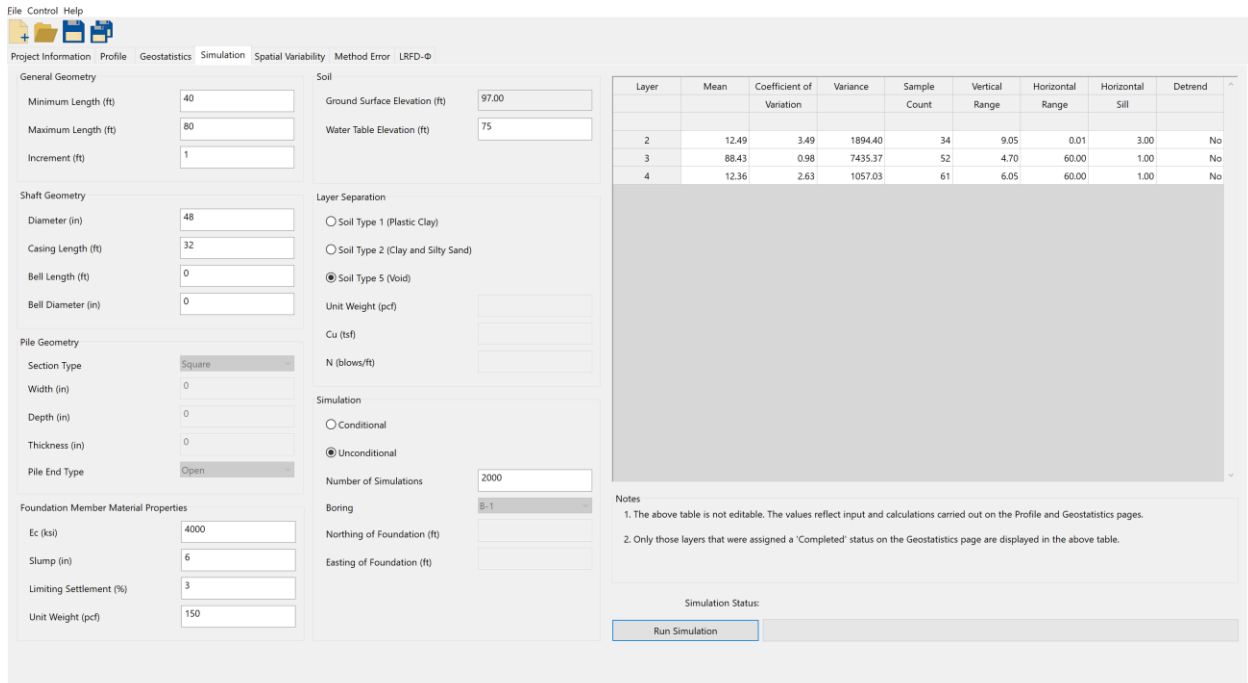
Figure 63. Simulation tab

4.8.1 Selecting the Embedment Range and Interval

For the drilled shaft foundation member being investigated in association with Site A, embedment lengths ranging from 40 ft to 90 ft are considered. Despite the emphasis on modeling of drilled shaft foundations, the following discussion is generally applicable regardless of the type of foundation member being considered. Along these lines, an embedment interval of 1 ft is selected, signifying that axial resistances are to be computed in 1-ft intervals between the 40-ft and 90-ft embedment range. Interval lengths that are small relative to the layer heights are generally recommended for conducting simulations in GeoStat.

Recall that the ground surface elevation is defined as 97 ft (the water table elevation is defined as 75 ft). Candidate shaft configurations for Site A therefore terminate (approximately) at elevations ranging from the center of layer 2 and extending down into layer 4. This range of embedments (40 ft to 90 ft) is considered as it allows for axial resistances to be determined for shafts terminating at a relatively small distance above the limestone layer (Fig. 64), as well as for shaft embedments that extend into and beyond the limestone layer.
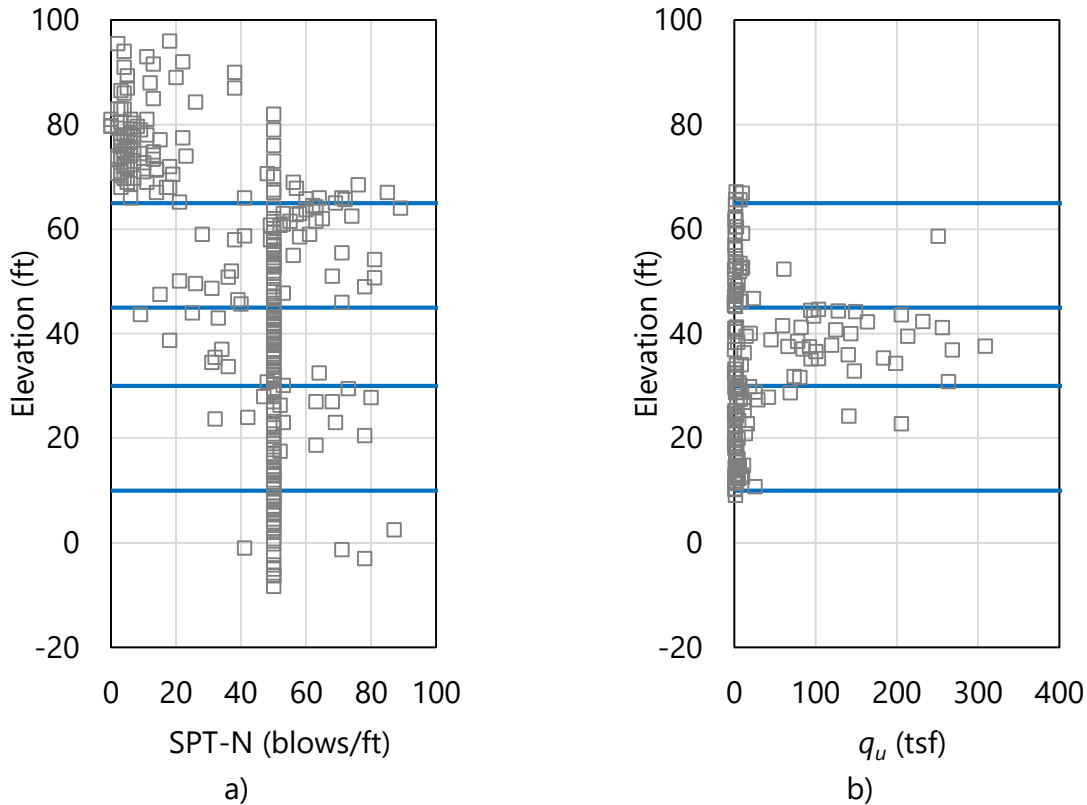
Figure 64. Scatterplots of soil and limestone strength parameters with layer bottom elevations (blue horizontal lines): a) SPT-N blow counts; b) Unconfined compression strength, q_u

4.8.2 Foundation Member Cross-Section

The middle-left portion of the Simulation tab (recall Fig. 63) contains input controls that allow for definition of the foundation member cross-section. Because a drilled shaft is being considered for Site A, only the shaft diameter and casing length are necessary to define the cross-section. These are defined as 48 in. and 32 ft, respectively. For scenarios where a driven pile is selected as the type of foundation member, required inputs for the cross-section geometry vary by the type of pile being considered (e.g., square, cylindrical, h-pile). Additional details for the required input parameters of driven pile cross-sections are detailed in the Help Manual.

4.8.3 Foundation Member Material Properties

GeoStat UI controls positioned in the bottom-left portion of the Simulation tab (recall Fig. 63) pertain to the definition of the foundation member material properties. For driven piles, only the pile unit weight is required. For drilled shafts, unit weight (150 lb/ft³) is also required. Values of shaft elastic modulus, concrete slump, and limiting shaft settlement are additionally

95

required for drilled shafts. These values, respectively, are input as 4000 ksi, 6 in., and 3%, and are necessary for computing shaft end bearing resistance.

4.8.4 Layer Separation

Included among the simulation parameters input on the Simulation tab (Fig. 63, middle) is selection of a soil type for modeling of layer separations. Recall from Fig. 37 that soil or rock layerings are defined from within the Profile tab of the GeoStat UI. Furthermore, layers can be defined as consisting of one of four possible soil or rock types. For generation of analysis model files during stochastic simulation, the "physical" layers are subdivided into 0.5-ft increments (referred to in this context as sublayers).

A subset of the available layer types may be specified for defining those sublayers that fall at the boundaries of layers that are defined on the Profile tab. For use of the GeoStat software in design applications, it is recommended that these sublayers (or, layer separators) be designated as Soil Type 5 (Void). If it is alternatively desired that layer separations not be designated as Soil Type 5 (Void), then additional properties must be specified as delineated (along with additional contextual discussion) in the Help Manual.

4.8.5 Selecting the Simulation Type

As detailed in Ch. 2, either unconditional or conditional (stochastic) simulation can be conducted using GeoStat software. However, as established above, conditional simulation (which requires construction of well-formed horizontal and vertical variograms) is not practical given the available volume of geotechnical data for Site A. When conducting unconditional simulation, only the number of realizations to be generated during simulation must be specified (Fig. 63, bottom-center). Additional considerations for deciding upon the suitable number of realizations for simulation are provided in Sec. 4.9. Input parameters required for conducting conditional simulation are detailed in the Help Manual.

4.9 Viewing Spatial Variability Results

Shown in Fig. 65 is the fifth of seven tabs (left to right) in the GeoStat UI, referred to as the Spatial Variability tab. This tab is intended for use in viewing profiles of computed axial resistance, where the resistance values take into account spatial variability phenomena. Plots of spatial resistance are divided into skin friction (side) resistance, end bearing (tip) resistance, and total resistance. For each type of resistance (skin, tip, total), profile plots of the mean, variance, COV, and ϕ (reflecting spatial variability only) are provided. In other words, resistance-related quantities plotted on the Spatial Variability tab facilitate visual review of profiles of descriptive statistics obtained from the "raw" simulation results.
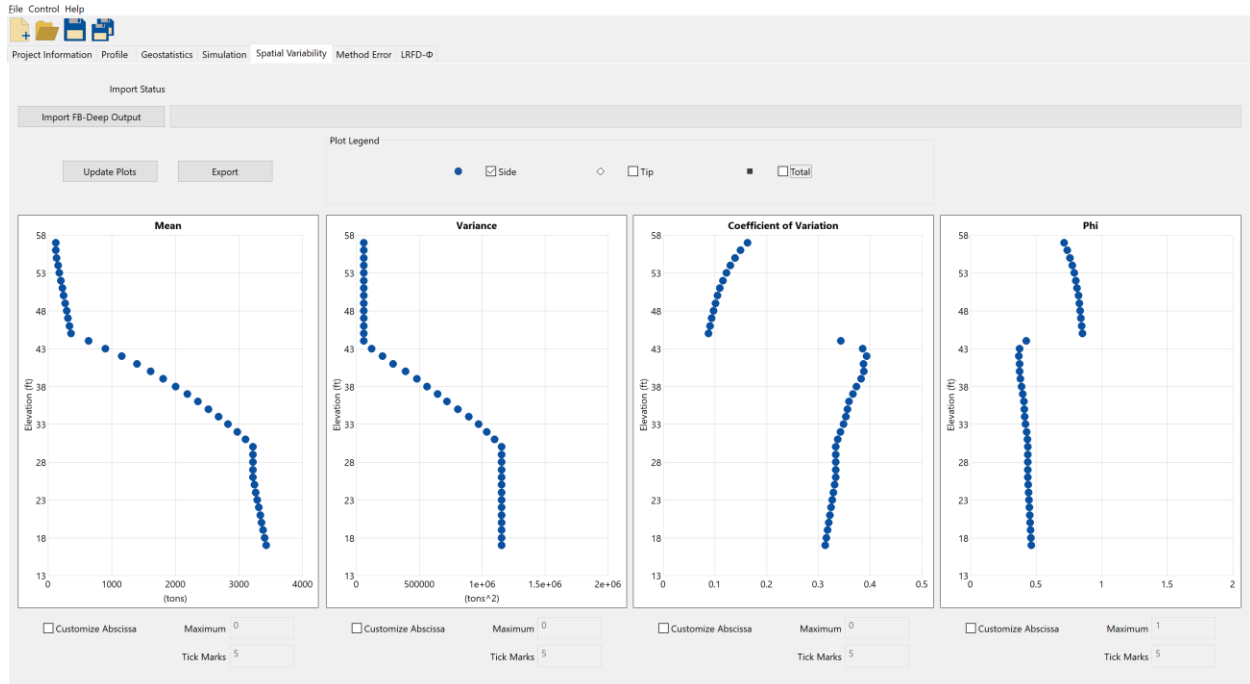
Figure 65. Spatial variability tab

4.9.1 Profiles of Computed Resistance

Profile plots of computed results are presented in Fig. 66 and Fig. 67. Profiles of skin and total resistance quantities—obtained from unconditional simulation with 2000 realizations—are displayed. Also, layer divisions (blue horizontal lines) are superimposed atop the profile plots to distinguish layer 2 from layer 3, and layer 3 from layer 4. The results shown are associated with both the initial (limestone) and the alternative (clay-limestone-clay) layerings developed above.

For the shaft configuration and soil or rock layering considered, skin resistance is clearly the dominant contributor to the mean (Fig. 66a, Fig. 67a) and variance (Fig. 66b, Fig. 67b) quantities for total resistance. Note though that the clay-limestone-clay layering leads to a relatively small proportion of contributions to resistance from end bearing. For the two layerings analyzed, trends in the computed skin and total resistances undergo abrupt shifts as embedment lengths progress into each of layer 2, layer 3, and layer 4.

Relatively substantial increases in resistance (from approximately 500 tons to 3200 tons) occur with respect to shaft embedment depths within the limestone layer (layer 3) of both layerings. Unfactored unit side friction throughout layer 3 is approximately 14 tsf. Only moderate increases in computed resistance (less than 1000 tons total) occur with respect to depth for embedment depths that terminate within layer 2 and layer 4 (regardless of layer definition). Based on these results, the greatest efficiencies with respect to shaft length may correspond to shaft termination within or below the limestone layer.
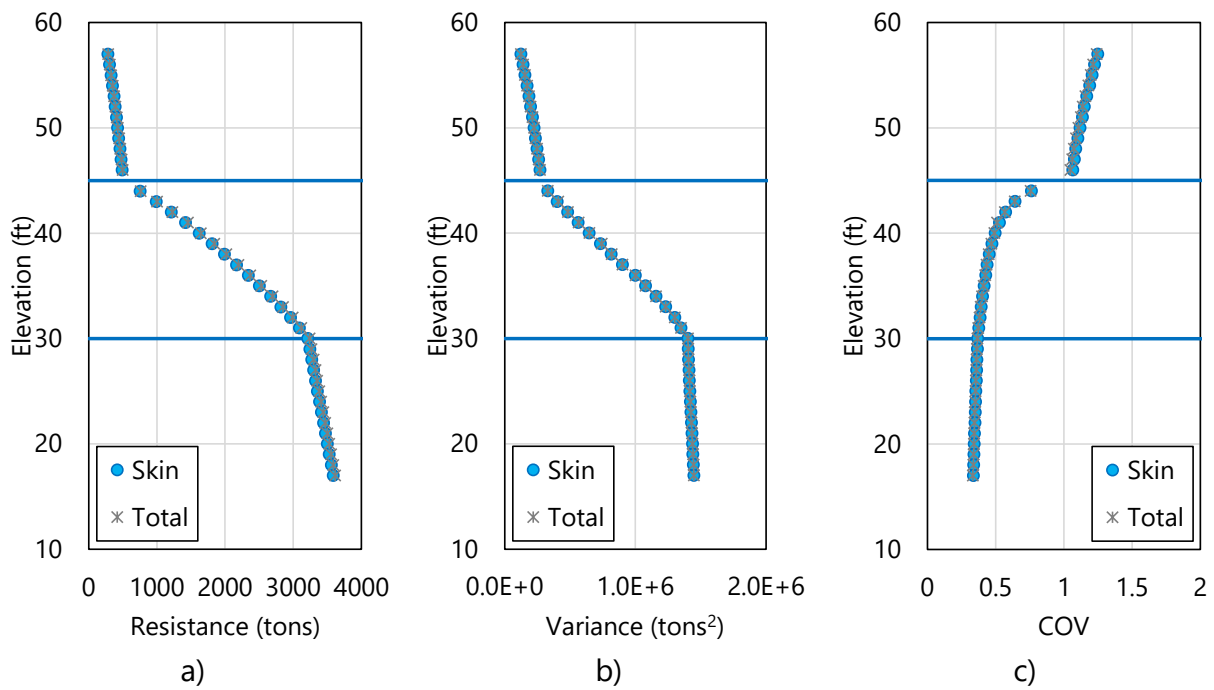
Figure 66. Profile plots obtained from unconditional simulation with limestone layering: a) Mean resistance (spatial variability only); b) Variance; c) COV
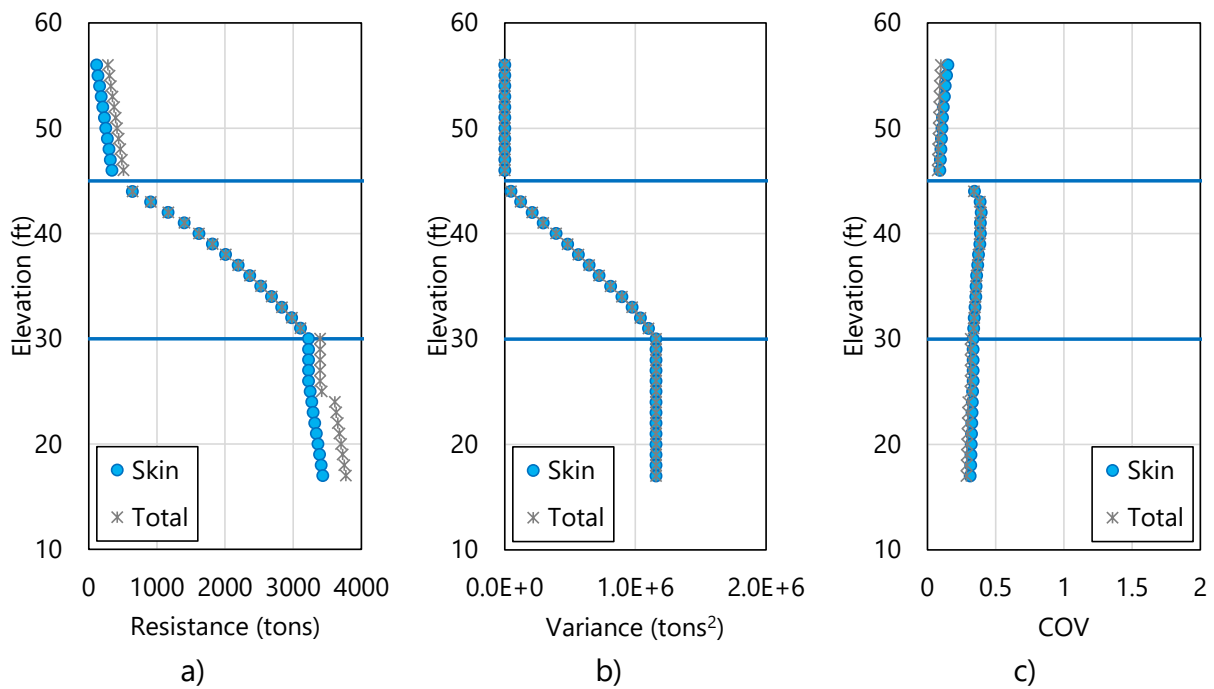
Figure 67. Profile plots obtained from unconditional simulation with clay-limestone-clay layering: a) Mean resistance (spatial variability only); b) Variance; c) COV

Regarding the profile of COV values (Fig. 66c, Fig. 67c), within a given layer, the variability of the computed resistance generally decreases with depth. As an exception for the clay-limestone-clay layering (Fig. 67c), profiles of COV values exhibit localized increases at and near the top portions of the limestone layer. As discussed in Ch. 2 and Ch. 3, smaller COV values associated with estimates of axial resistance correspond to relatively larger values of resistance factors, ϕ. Therefore, both layer interpretations support extending the shaft a considerable distance into or beyond the limestone layer (and further reducing the associated COV) so as to produce relatively more favorable estimates of factored axial resistance.

4.9.1.1 Determining a Suitable Number of Realizations for Simulation

Plotted in Fig. 68 are profiles of total resistance quantities, as obtained from conducting unconditional simulations with 100, 1500, and 2000 realizations, and use of the alternative layering. Visual inspection of the mean total resistance does not reveal appreciable sensitivities with respect to the number of realizations. Critically, though, the variance of the computed resistance Fig. 68b changes substantially when transitioning from 100 realizations to either 1500 or 2000 realizations. In contrast, only slight differences are present with respect to the variance profiles of 1500 and 2000 realizations.
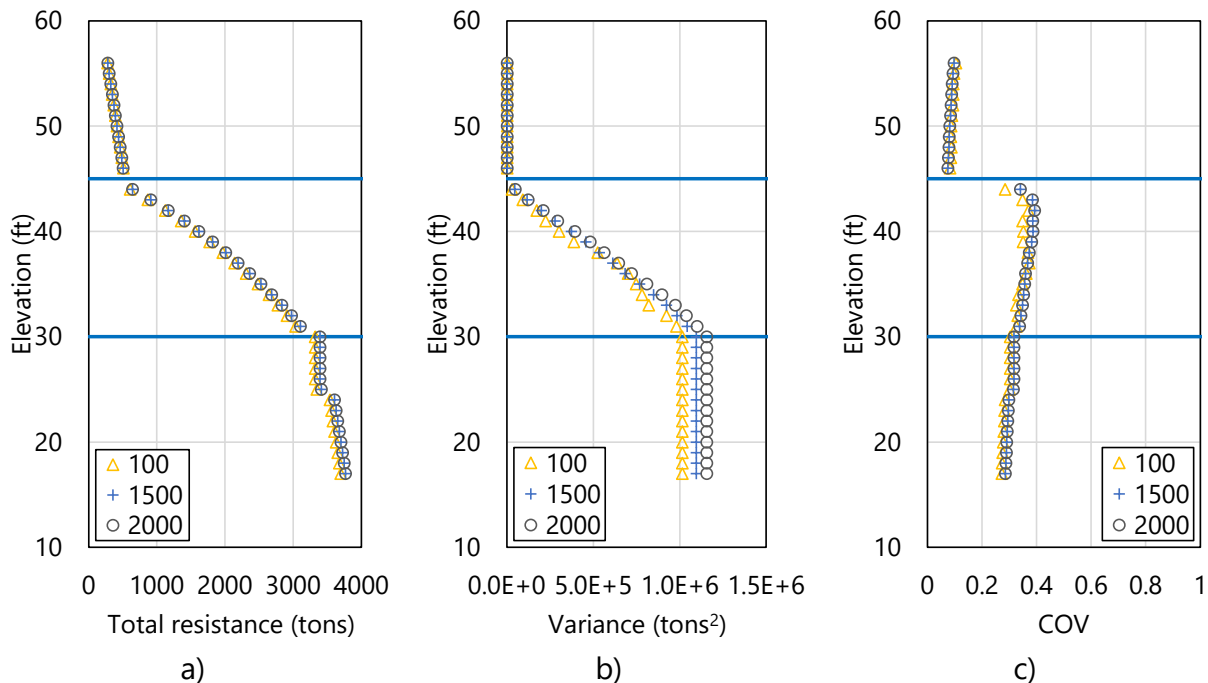
Figure 68. Profile plots obtained from unconditional simulation with 100, 1500, and 2000 realizations: a) Mean total resistance (spatial variability only); b) Variance; c) COV

For all demonstration cases reported in McVay et al. (2012), the associated number of realizations was set to 2000. Further, Faraone (2014) recommended that a minimum of 1000

realizations be considered when conducting stochastic simulation. For use of GeoStat in design applications, it is recommended that 2000 realizations be considered. However, it can always be verified that iterative increases in the number of realizations do not lead to appreciable changes in variance for the computed profiles of resistance.

4.9.2 Resistance Factor (φ), Spatial Variability Only

Presented in Fig. 69 are profile plots of resistance factors, φ, for skin and total resistance, as obtained from unconditional simulation with 2000 realizations. The plotted profiles only take into account spatial variability, as opposed to the total uncertainty associated with combined spatial variability and method error. As a mirror to the profiles of COV values (recall Fig. 66c, Fig. 67c), the profiles of computed resistance factors, φ (spatial variability only), generally increase with respect to depth. Such mirroring includes (for the clay-limestone-clay layering, Fig. 69b) localized increases of φ values near the top portions of the limestone in layer 3.

For the limestone layering (Fig. 69a), values of φ dramatically increase (from approximately 0.1 to 0.4) in layer 3. For embedments within the limestone layer of the clay-limestone-clay layering (Fig. 69b), values of φ range from approximately 0.38 to 0.48 throughout layer 3. For shaft lengths that extend into layer 4, moderate increases in resistance factors occur, reaching values up to 0.44 (Fig. 69a) and 0.53 (Fig. 69b). Given the absence of zones in the Site A data, influence upon the resistance factors (φ) can be attributed, in part, to the relatively high COV values associated with the q_u values of relevant layers (e.g., recall Table 24).
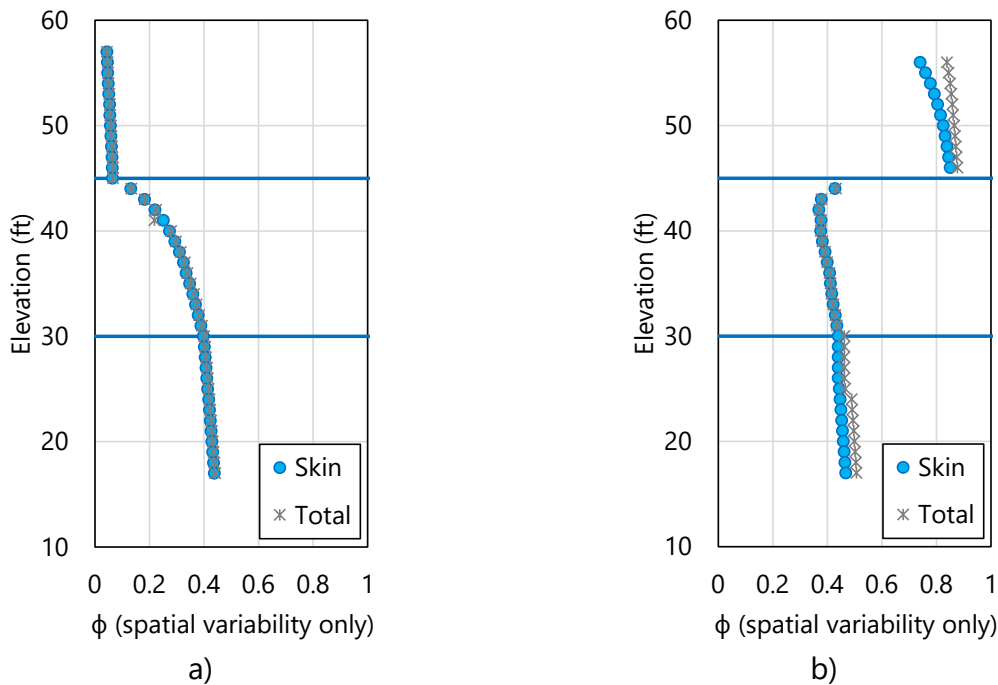
Figure 69. Profile plot of resistance factor, φ spatial variability only, obtained from unconditional simulation: a) Limestone layering; b) Clay-limestone-clay layering

100

Two general strategies are worth emphasizing at this stage for potentially producing relative increases in resistance factors (φ). First, if geological zones are present among the site data being characterized, then isolating the zones and repeating the modeling (and simulation) efforts may be of benefit. Second, additional layers may be defined throughout the range of candidate embedment lengths, or the layer definitions may be otherwise modified, to reduce the COV of the measured data per layer.

4.10 Incorporating Method Error

As documented in Ch. 3, two contributors to total uncertainty for estimates of foundation member axial resistance are spatial variability and method error. Method error calculations serve to adjust the "raw" results obtained from stochastic simulation, and in addition, contribute to the calculation of resistance factors (φ). In the GeoStat UI, parameters related to method error are specified in the sixth of seven (left to right) program tabs (Fig. 70).

As also detailed in Ch. 3, characterization of method error phenomena in GeoStat is divided into regression expressions for: driven piles, drilled shafts in clay, drilled shafts in sand, McVay skin friction of drilled shafts in limestone, and O'Neill end bearing for drilled shafts in limestone. Of relevance to the Site A models (initial layering, alternative layering) are portions of drilled shafts in clay and portions of drilled shafts in limestone. Considerations for layer-specific contributions to method error for Site A (including selection of regression parameter values) are discussed immediately below.
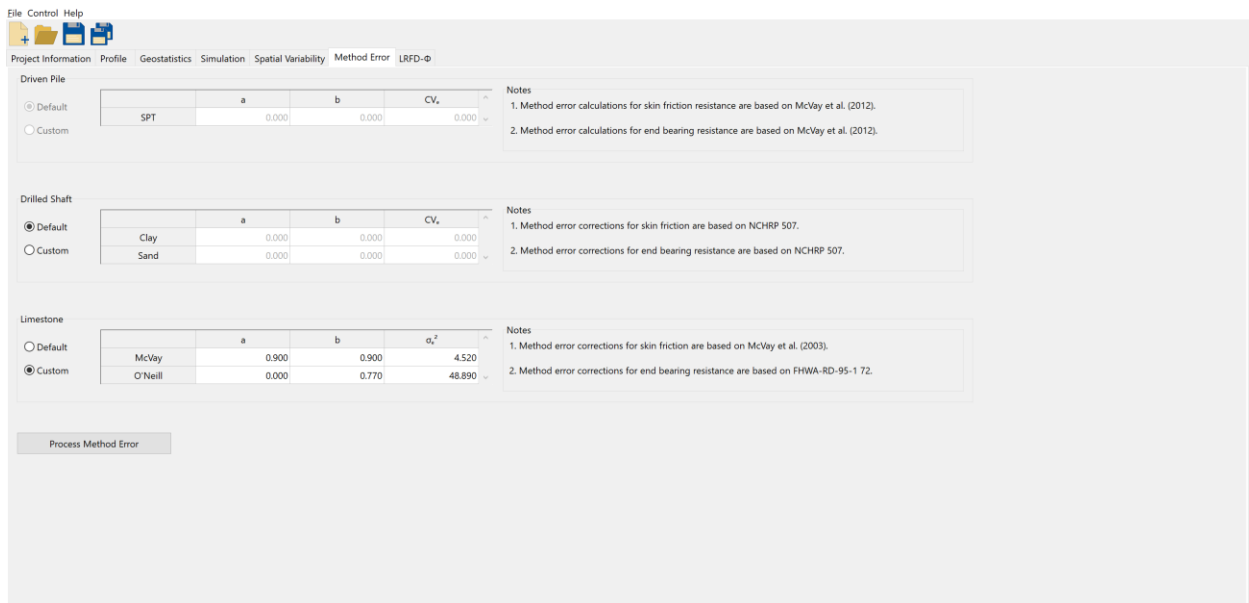
Figure 70. Method Error tab

4.10.1 Shaft Portions in Clay

Regression values pertaining to method error calculations, for portions of the drilled shaft embedded in clay (layer 2, layer 4 of the clay-limestone-clay layering), are listed in Table 31. Lacking numerous instances of load test data for Site A, the listed values correspond to the default regression parameters implemented in GeoStat (and originally recommended in McVay et al. 2012). Additional discussion of how these parameters influence resistance quantities (including ϕ) is provided in Ch. 3.

Table 31. Method error parameter values for shaft portions embedded in clay

Parameter	Value
a	0.73
b	0.86
COV_ε	0.41

4.10.2 Shaft Portions in Limestone

Regression values pertaining to method error calculations, for portions of the drilled shaft embedded in limestone (applicable to both layer definitions), are listed in Table 32 (skin) and Table 33 (tip). Default regression parameters implemented in GeoStat are utilized for method error calculations associated with skin friction. For end bearing resistance, all parameters except set to match the default values implemented in GeoStat. Note that the intercept (a) of the regression expression is defined as 0 instead of the value of 20.5 (from O'Neill). This deviation is elected because end bearing does not substantially contribute to the total resistance for the Site A analyses (recall Fig. 66a, Fig. 67a), particularly for shaft embedments that terminate within layer 3.

Table 32. Method error parameter values for skin friction of shaft portions embedded in limestone

Parameter	Value
a	0.90
b	0.90
σ_ε^2	4.52

Table 33. Method error parameter values for end bearing of the shaft in limestone

Parameter	Value
a	0.00
b	0.77
σ_ε^2	48.89

4.11 Viewing Final Results

Shown in Fig. 71 is the rightmost (seventh) tab in the GeoStat UI. Profile plots located within this tab facilitate viewing of total resistance quantities that reflect spatial variability phenomena as well as computed results associated with total uncertainty (spatial variability and method error combined). Presented below are profile plots for both the initial (limestone) and alternative (clay-limestone-clay) layer definitions. The types of profile plot data available for viewing include unfactored resistance (e.g., Fig. 72, Fig. 73); corresponding COV values (Fig. 74, Fig. 75); corresponding resistance factors, ϕ, (Fig. 76, Fig. 77); and, factored resistance (Fig. 78, Fig. 79). All plotted results in Fig. 72 through Fig. 79 are associated with unconditional simulation and 2000 realizations.

Trends and phenomena that pertain to the profile plots of mean total resistance, COV, and ϕ values are analogous to those documented above in Sec. 4.9. Of note, however, is that total uncertainty (versus spatial variability alone) tends to more heavily penalize (reduce) computed resistance values. This phenomenon is particularly present in the profile plots of factored resistance for the clay-limestone-clay layering (Fig. 79). Also of note is that the profile of resistance factors (ϕ) varies with respect to depth (Fig. 76, Fig. 77). Computation of profiles of ϕ values is uniquely facilitated through use of GeoStat, and the depth-dependent profiles are more reflective of the site-specific characteristics versus application of a single, prescriptive resistance factor (e.g., a single, prescribed ϕ value).
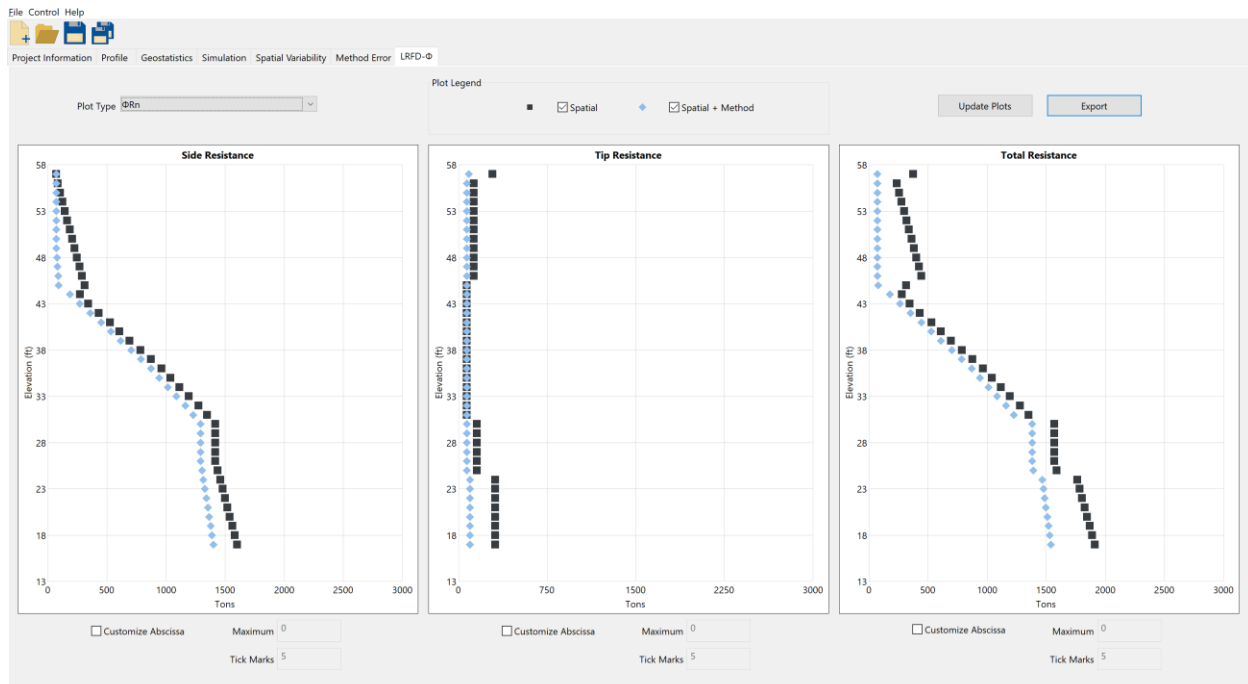
Figure 71. LRFD-ϕ tab for plotting profiles of resistance factors, ϕ, and factored resistances
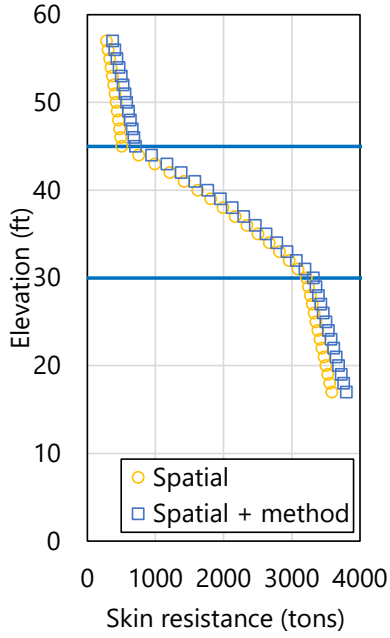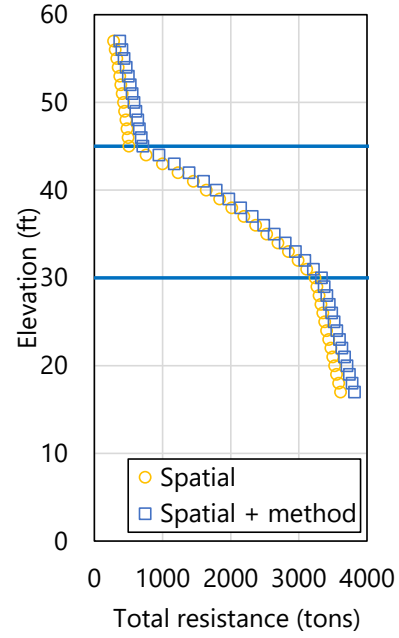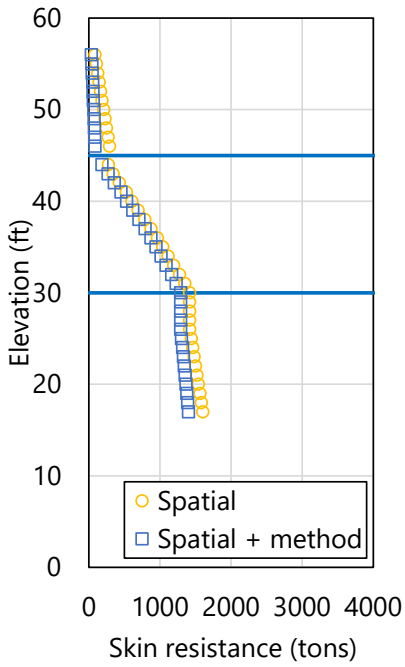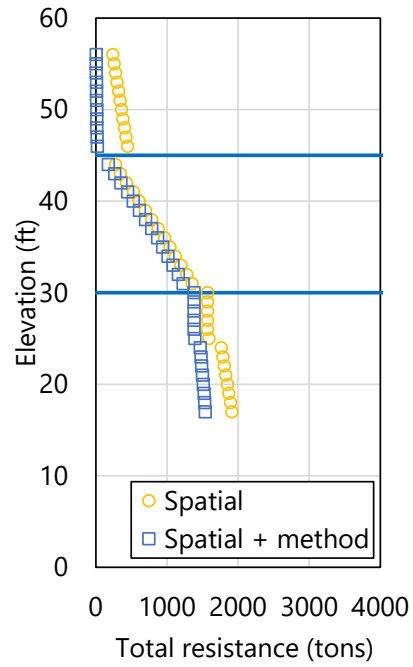
Figure 72. Profile plots of unfactored mean resistance for limestone layering: a) Skin; b) Total
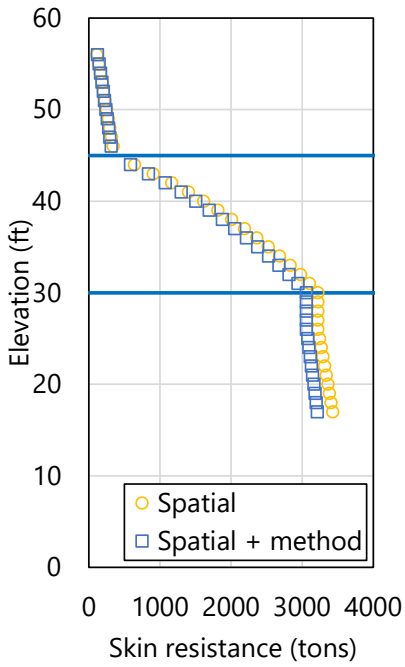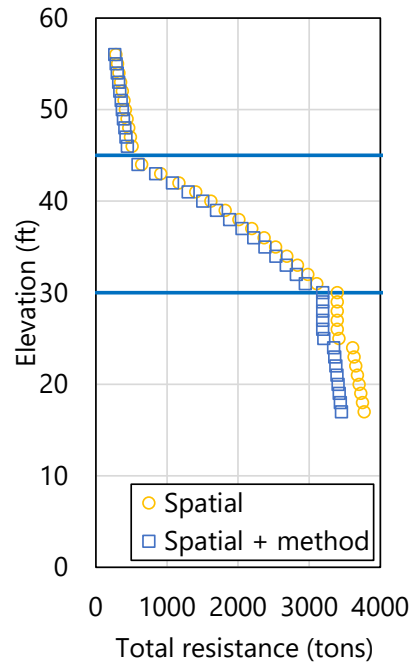
Figure 73. Profile plots of unfactored mean resistance for clay-limestone-clay layering: a) Skin; b) Total
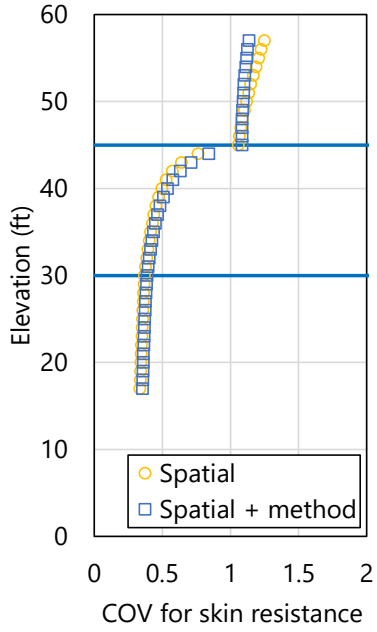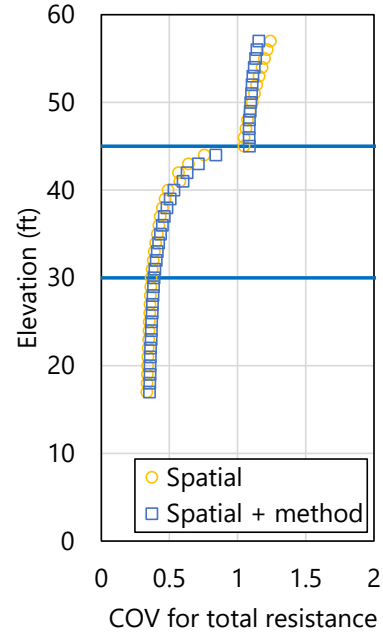
Figure 74. Profile plots of COV for unfactored mean resistance for limestone layering: a) Skin; b) Total
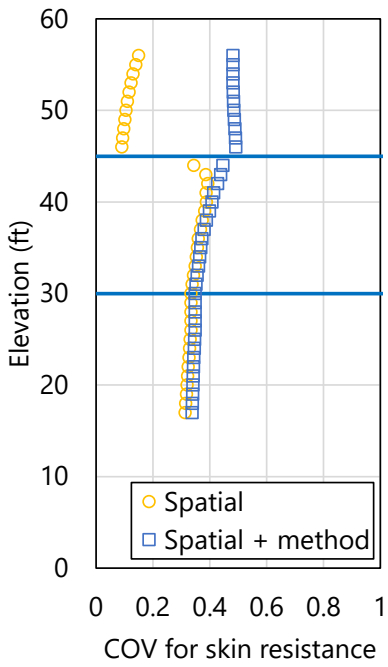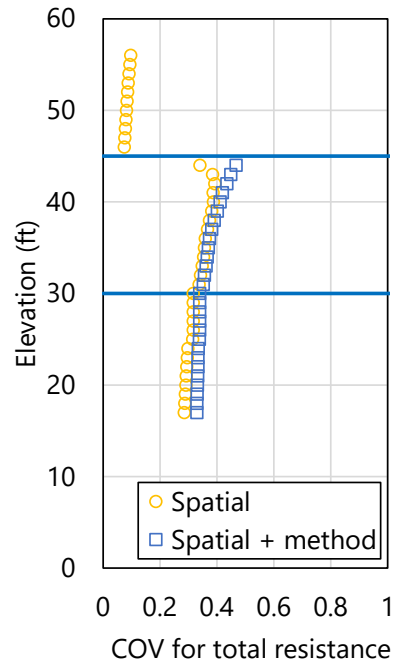
Figure 75. Profile plots of COV for unfactored mean resistance clay-limestone-clay: a) Skin; b) Total

105
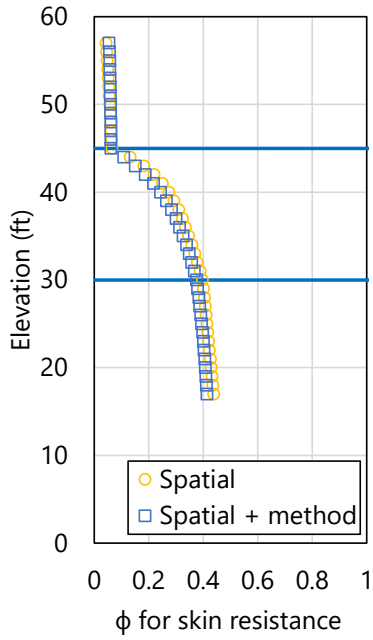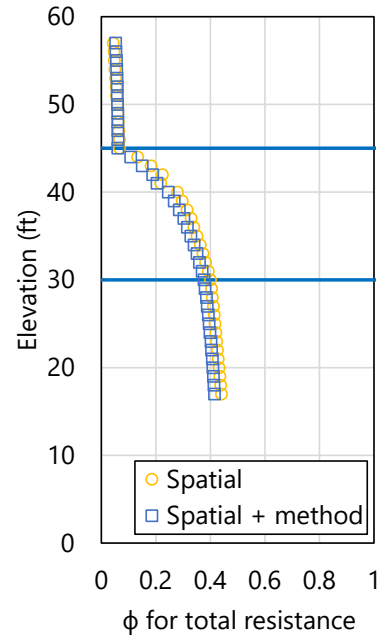
Figure 76. Profile plots of resistance factor, ϕ, for limestone layering: a) Skin; b) Total
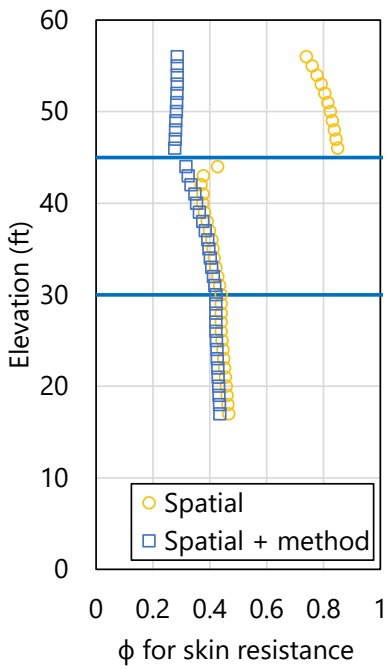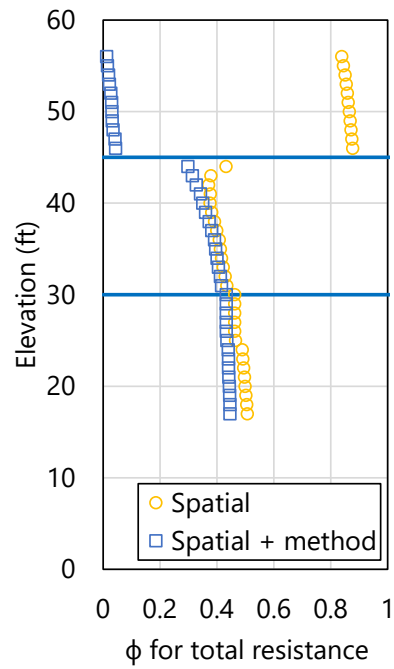
Figure 77. Profile plots of resistance factor, ϕ, for clay-limestone-clay layering: a) Skin; b) Total
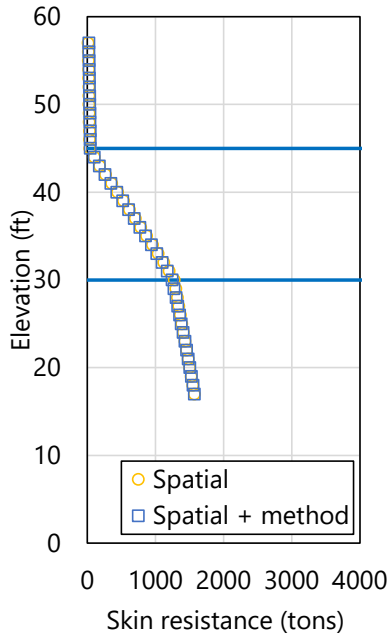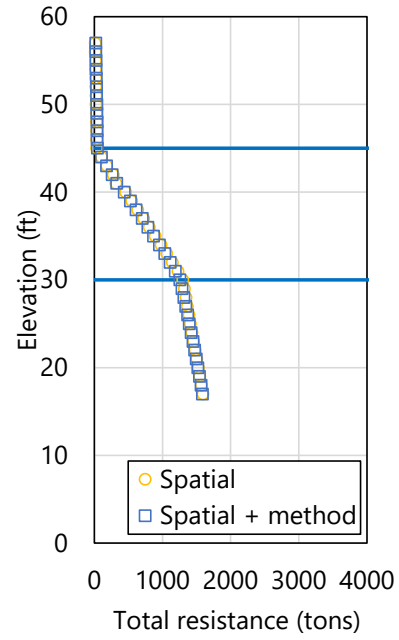
Figure 78. Profile plots of ϕ-factored mean resistance for limestone layering: a) Skin; b) Total

Figure 79. Profile plots of ϕ-factored mean resistance for clay-limestone-clay layering: a) Skin; b) Total

As additional comparisons of the two sets of results, note that initial (limestone) layer definitions produce profiles of unfactored resistance that are of relatively larger magnitude. For example, through the bottom of layer 2, use of the initial layer definitions leads to increased unfactored resistances (by approximately 5% to 10%; Fig. 72 versus Fig. 73), as compared to those obtained from use of the alternative layer definitions (discussed in Sec. 4.5 through Sec. 4.6).

Such differences stem from the use of different empirical expressions for limestone (i.e., McVay side friction) throughout the profile for the initial (limestone) layering, versus the clay portions of the clay-limestone-clay profile for the alternative layering (which make use of the Alpha, α, method). In other words, the clay layers do not contribute as much to unit side resistance as compared to those contributions from the limestone layers. Along these same general lines, different regression expressions are applied when incorporating method error into layer 2 and layer 4 of the clay-limestone-clay profile (versus layer 2 and layer 4 of the limestone profile). This difference, in turn, leads to differences in the profiles when considering spatial-only results versus combined spatial variability and method error phenomena.

Comparing (limestone) Fig. 74 and (clay-limestone-clay) Fig. 75, the COV profile for the limestone layering indicates much more pronounced reductions in COV values within layer 3. As noted above, the profiles of resistance factors (ϕ) mirror the profiles of COV values. The relative increases in mean resistance (with use of initial layer definitions) are offset by relatively smaller values (approximately 5%) for resistance factors (ϕ). As a result, the factored skin and total resistance profiles are (overall) within approximately 5% of one another (Fig. 78 versus Fig. 79) regardless of the use of the initial or alternative layering definitions (and associated sets of vertical variograms). This suggests that the limestone in layer 3 is a primary driver of axial resistance.

CHAPTER 5
MODELING OF EXAMPLE SITE B

5.1 Overview

Presented in Ch. 5 is a second, detailed walkthrough of geotechnical site modeling and axial resistance simulation for an example bridge site. The data sets discussed in Ch. 5 represent one instance of the ranges and types of geotechnical site data that may be collected when investigating the foundations of a bridge site possessing medium variability. An example site exhibiting high variability is discussed in Ch. 4. In addition, the extent or size of the site of interest in Ch. 5 is large relative to that discussed in Ch. 4. Within the context of modeling and simulation in GeoStat, use of the associated (medium variability, large extent) site data is divided into several steps. Such division reflects the left-to-right progression across the seven tabs of the GeoStat user interface (UI), where the layout of the GeoStat UI is detailed in the program Help Manual.

The site of interest in Ch. 5 is referred to as Example Site B, or, Site B. Cataloging of the available Site B data for modeling within GeoStat is discussed in Sec. 5.2. Initial selection of boundary soil and rock (limestone) layer elevations is discussed in Sec. 5.3. Also documented in Sec. 5.3 are layer-related considerations specific to the type of foundation member being considered (pile, shaft).

Initial formation of spatial correlation structures (i.e., variograms) for each defined layer, and solely for the purpose of identifying geological zones, is then discussed in Sec. 5.4. Observations and considerations related to the identification of geological zones within Site B are discussed in Sec. 5.5. These considerations include assessment of zonal anisotropy and illustration of how zones are defined (modeled) within GeoStat. Two zones are identified among the Site B data set, where detailed walkthroughs of characterizing zone-specific layer definitions and variograms are illustrated in Sec. 5.6 (for zone 1) and Sec. 5.7 (for zone 2). For each of the two illustrations, comparisons are made to respective quantities obtained from the site-wide data set to demonstrate the importance of accounting for geological zones. Summary observations regarding the site-wide, zone 1, and zone 2 data sets (with respect to variograms) are provided in Sec. 5.8.

The focus of the walkthrough for Site B then shifts to stochastic simulation of axial resistance in Sec. 5.9, where one set of simulations is conducted for each of zone 1 and zone 2. Interpretation of simulated profiles of axial resistance, which reflect spatial variability phenomena of the zone-specific data, is provided in Sec. 5.10.

Comparisons are subsequently made between zone-specific simulation results to further emphasize the importance of accounting for distinct geological zones. Considerations for incorporating method error phenomena into the simulated, zone-specific results are detailed

in Sec. 5.11. The combined effects of spatial variability and method error upon computed axial resistance, culminating in profiles of both resistance factors (ϕ) and factored axial resistance, are examined in Sec. 5.12.

5.2 Cataloging Site Data

Shown in Fig. 80 is the first (leftmost) tab encountered within the GeoStat UI, referred to as the Project Information tab. This region of the GeoStat UI facilitates input and organization of all data obtained from geotechnical investigation of the site. The foundation type is also selected in the Project Information tab (Fig. 80, upper-right).

For Site B, a drilled shaft foundation type is selected. See the Example Site A walkthrough (Ch. 4) for documentation of when distinct considerations are required depending on the selected foundation type (piles, shafts). Even so, documentation of parameters selected for site modeling and interpretation of simulation results in Ch. 5 are generally applicable regardless of the selection for type of foundation member.

5.2.1 Initial Visual Assessment of Site B

For the start of the analysis, all borings for the site should be active (included) and zonal issues should be identified from variograms (e.g., recall Fig. 8c) or comparison of properties with depth from boring to boring (i.e., permuting through borings and viewing the scatterplot in Fig. 80). Accordingly, as a starting point, initial characterization of the site data (through the step of forming variograms) is carried out using all available measurements from across the 90 boring locations. Even so, given the large footprint of the site data, the need to divide the site into zones is anticipated.

Data from 90 unique boring locations are cataloged for Site B, including both SPT-N blow counts and rock-related measurements obtained from numerous core runs (e.g., unconfined compression strength, q_u). The geotechnical investigation of Site B indicates the presence of silty sands at relatively shallow depths. Limestone is commonly encountered at deeper depths, either in the form of relatively thin bands or thick layers across the 90 boring locations. Given the prevalence of limestone throughout Site B, emphasis is initially placed on available measurements of rock strength (as discussed below) when forming components of the GeoStat model.

A plan view of the 90 boring locations is plotted in the left portion of the Project Information tab, and a corresponding plot of eastings and northings for the boring locations is shown in Fig. 81. As listed in the table on the right portion of the Project Information tab (Fig. 80, right), easting values range from 0 ft to approximately 9500 ft, and northing values range from (approximately) 0 ft to 2500 ft. Further, the ground surface elevations across the 90 borings

range from 5 ft to 33 ft. This range of ground surface elevations (nearly 30 ft) is one of several indicators that motivate assessment of the site for division into distinct geological zones.

For each of the 90 boring locations, the respective (boring-specific) geotechnical site data are input in GeoStat using the Boring Data dialog. This dialog is accessible from the upper-right portion of the Project Information tab. For example, site data measured at boring location TS-1 (easting of 799 ft; northing of 339 ft) consists of a mixture of through-depth SPT-N blow count values at shallower depths (as shown in the excerpt of Fig. 82), and core run data from thick limestone layers at deeper depths. An additional example is provided in Fig. 83 for boring location B-705 (easting of 7197 ft; northing of 403 ft), which contains a mixture of SPT-N blow count and core run data from core run data from thin bands of limestone (e.g., unconfined compression strength, q_u; split tensile strength, q_t, RQD, *recovery*).

The rightmost table column of the Project Information tab allows for any subset of borings (or all borings) to be included or excluded from the site/zone modeling. For instance, in the case of zonal anisotropy, only the borings within the zone of interest would be included (i.e., value set to 1 in far-right table column for two or more borings) for development of summary statistics, variograms, and estimated pile/shaft capacities. The result is then saved in a uniquely named model file, such as Site B – zone 1. Subsequently, other borings would be turned on and prior borings turned off for other zone analyses. On the Project Information tab (Fig. 80) scatterplot data associated with any currently selected (and active) boring location is highlighted, and can be used to quickly identify borings that contain outlier data or are associated with a unique zone.

The rightmost plot in the Project Information tab (Fig. 80, middle) facilitates plotting of collections of the desired type of site measurement (e.g., SPT-N, q_u). In addition, data pertaining to any boring location of interest are highlighted (using solid blue plot points), as exemplified for boring location TS-1 in Fig. 80.

Documented in the remainder of Sec. 5.2 are initial characterizations of the various types of measured site data available for Site B. Data are presented in scatterplot form, or as through-depth profiles of measurements accumulated across all 90 boring locations. In this way, initial characterization of trends or groupings among the site data are facilitated, where such characterization is necessary (for example) to identify zones and define soil or rock layering.
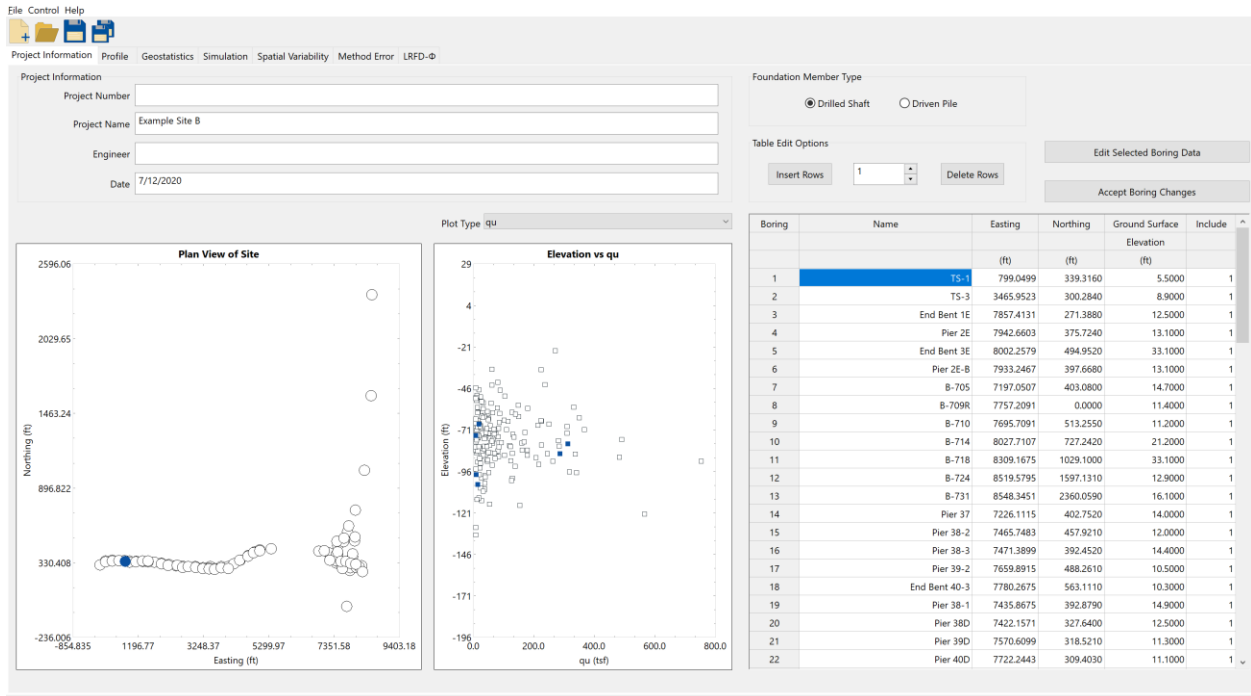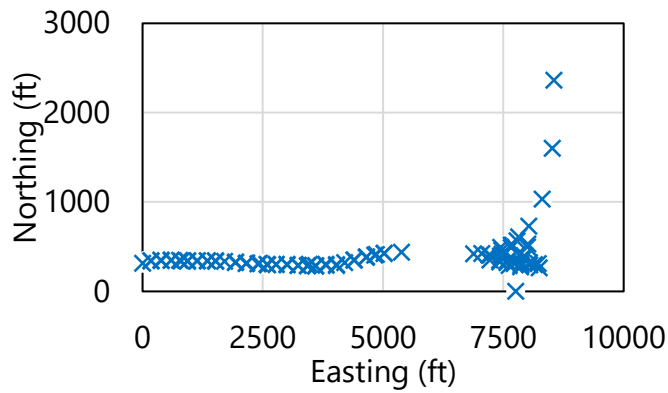
Figure 80. Project Information tab

Figure 81. Plan view of 90 boring locations for Site B

Table Edit Options

Insert Rows | 1 | Delete Rows

Default RQD and Recovery To 1

Notes

1. Input all available data for the boring within the table below.

2. For any depths where a given soil property is not available, then leave the corresponding cell blank.

3. Soil Types: 1 = Plastic Clay | 2 = Clay and Silty Sand | 3 = Clean Sand | 4 = Limestone and Very Shelly Sand.

Number	Elevation	Depth	Soil Type	N. Blows	Unit Weight	Cu	qu	qt	qb	Em	RQD	Socket Roughness	Rock Recovery
			[1 | 2 | 3 | 4]								[0.0 to 1.0]	[0 | 1]	[0.0 to 1.0]
	(ft)	(ft)		(blows/ft)	(pcf)	(tsf)	(tsf)	(tsf)	(tsf)	(ksi)			
1	0.5000	5.0000	2	13									
2	-1.0000	6.5000	3	13									
3	-2.5000	8.0000	2	13									
4	-7.5000	13.0000	2	14									
5	-9.5000	15.0000	2	19									
6	-12.5000	18.0000	2	16									
7	-14.5000	20.0000	2	19									
8	-16.5000	22.0000	2	7									
9	-18.5000	24.0000	2	8									
10	-20.5000	26.0000	1	0									
11	-24.5000	30.0000	1	0									
12	-26.5000	32.0000	1	0									
13	-29.5000	35.0000	4	10									
14	-31.5000	37.0000	4	11									
15	-33.5000	39.0000	4	15									
16	-35.5000	41.0000	4	28									
17	-37.5000	43.0000	4	34									
18	-39.5000	45.0000	4	22									

OK | Cancel

Figure 82. Boring Data dialog for boring location TS-1

Table Edit Options

Insert Rows | 1 | Delete Rows

Default RQD and Recovery To 1

Notes

1. Input all available data for the boring within the table below.

2. For any depths where a given soil property is not available, then leave the corresponding cell blank.

3. Soil Types: 1 = Plastic Clay | 2 = Clay and Silty Sand | 3 = Clean Sand | 4 = Limestone and Very Shelly Sand.

Number	Elevation	Depth	Soil Type	N. Blows	Unit Weight	Cu	qu	qt	qb	Em	RQD	Socket Roughness	Rock Recovery
			[1 | 2 | 3 | 4]								[0.0 to 1.0]	[0 | 1]	[0.0 to 1.0]
	(ft)	(ft)		(blows/ft)	(pcf)	(tsf)	(tsf)	(tsf)	(tsf)	(ksi)			
1	6.7000	8.0000	2	5									
2	4.7000	10.0000	2	4									
3	-0.3000	15.0000	2	7									
4	-5.3000	20.0000	2	11									
5	-10.3000	25.0000	2	0									
6	-15.3000	30.0000	2	3									
7	-20.3000	35.0000	4	68									
8	-21.8000	36.5000	4		128.3000						0.3200		0.4800
9	-23.3000	38.0000	4				271.3680						
10	-25.3000	40.0000	4					57.2400					
11	-30.3000	45.0000	4	50									
12	-35.3000	50.0000	4	50									
13	-37.3000	52.0000	4	50									
14	-39.3000	54.0000	4	50									
15	-41.3000	56.0000	4	50									
16	-43.3000	58.0000	4	50									
17	-45.3000	60.0000	4	50									
18	-47.3000	62.0000	4	50									

OK | Cancel

Figure 83. Boring Data dialog for boring location B-705

113

5.2.2 Site Data for Shafts in Limestone

As noted previously, initial efforts toward characterizing the site emphasize examination of available rock strength data (e.g., q_u), given the frequent occurrence of limestone bands and layers throughout Site B. Although, initially, the full collection of available site data is examined, considerations are given later to determine whether or not zones are present. Shown in Fig. 84 are measurements of rock strength obtained across the 90 boring locations (and associated core runs). For unconfined compression strength, q_u, 186 measurements are available (Fig. 84a). Also, 187 measurements of split tensile strength, q_t, are available (Fig. 84b). From a qualitative standpoint, measured values of q_t tend to increase with increasing values of q_u. Additionally, while the majority of measured q_u values are less than approximately 100 tsf, relatively higher compressive strength values (between approximately 100 tsf and 750 tsf) are measured over the approximate elevation range of -40 ft to -135 ft.

Plotted in Fig. 85 are additional measurements pertaining to rock strength, as gathered from across all core runs of Site B. Concerning rock quality designation (RQD), 364 values are taken from the collection of core runs (Fig. 85a). Correspondingly, 364 values of *recovery* are included for use in GeoStat modeling of the site (Fig. 85b). Ranges for both the RQD and recovery measurements encompass decimal values from approximately 0.05 to 1.0. Despite the relatively large number of measured values available for RQD and *recovery*, no overtly discernible trends or groupings of values are apparent from visual inspection of the scatterplots.

Depicted in Fig. 86 are measured values of unit weight, γ, available over the elevation range of -15 ft to -102 ft. The 23 measured values of unit weight (γ) vary, approximately, from 105 lb/ft^3 to 150 lb/ft^3. Values of unit weight are considered as secondary to rock strength measurements (q_u, q_t) for activities such as defining layers. Additionally, relatively few measured values of unit weight (23) are available from the Site B data set, and so, visual identification of qualitative trends or groupings is precluded.
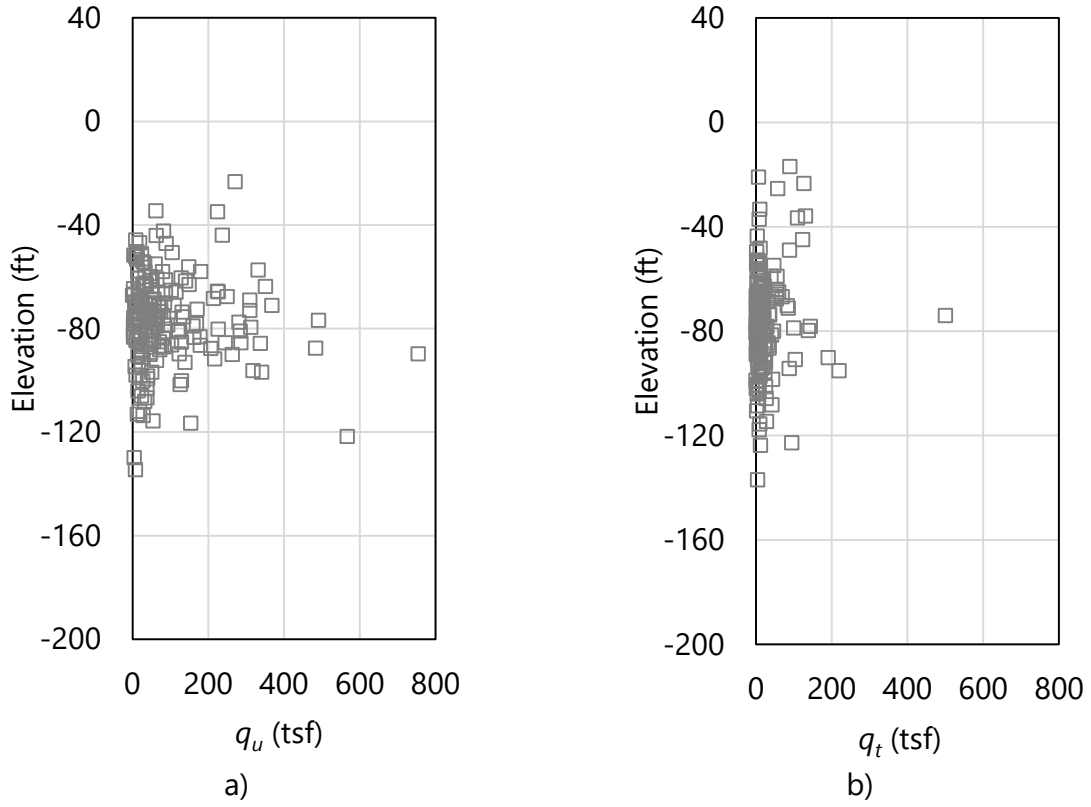
Figure 84. Scatterplots of limestone strength parameters: a) 186 values for unconfined compression strength, q_u, (elevation range: -23 ft to -134 ft); b) 187 values for split tensile strength, q_t, (elevation range: -17 ft to -137 ft)
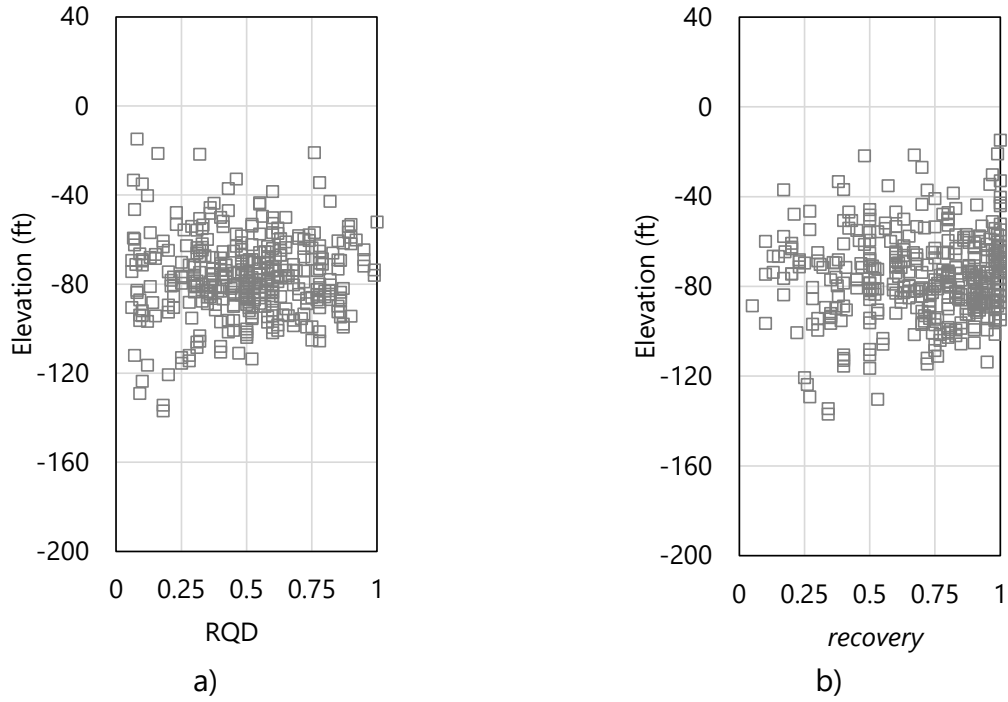
Figure 85. Scatterplots of limestone strength parameters: a) 364 values for RQD (elevation range: -17 ft to -137 ft); b) 364 values for *recovery* (elevation range: -17 ft to -137 ft)
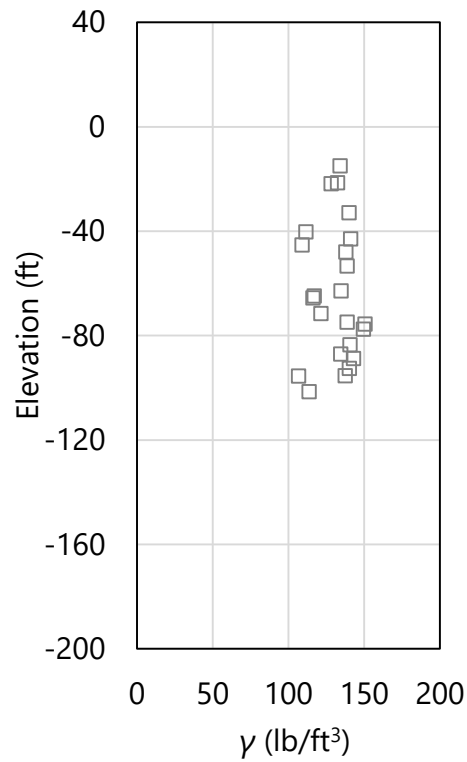
Figure 86. Scatterplot of 23 values of unit weight, γ, (elevation range: -15 ft to -102 ft)

5.2.3 Site Data for Piles, Shafts in Clay, and Shafts in Sand

For portions of drilled shafts and piles embedded in clay and sand, SPT-N blow count values are most pertinent in computing axial resistances from within GeoStat. Plotted in Fig. 87 are 3144 SPT-N blow count values, as collected across the 90 boring locations of Site B. Blow count values range from 0 blows/ft to approximately 95 blows/ft. Per the available site data, a relatively high prevalence of blow count values are attributed to refusal-like conditions and thus reported as 50 blows/ft (e.g., over the elevation range of -10 ft to -160 ft).

A qualitative grouping of SPT-N blow count values is apparent from elevations of 10 ft to approximately -50 ft. For elevations below -50 ft, relatively high levels of dispersion are present among the collection of SPT-N blow counts. These visually identified groupings are revisited later as part of defining representative layering for the available Site B data, and when investigating the presence of zones.
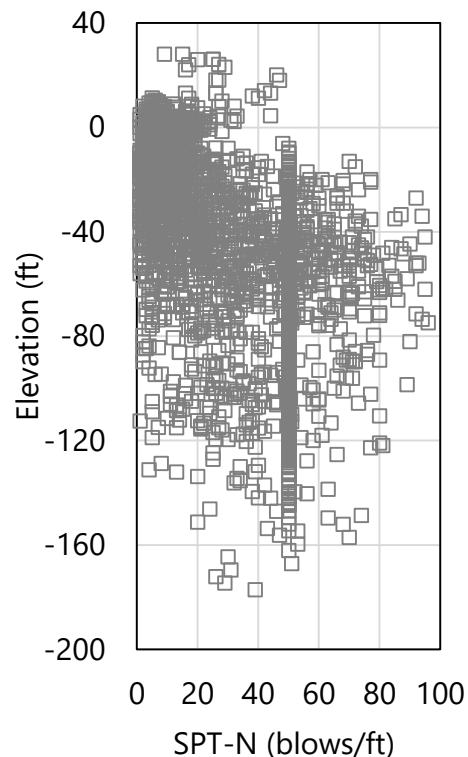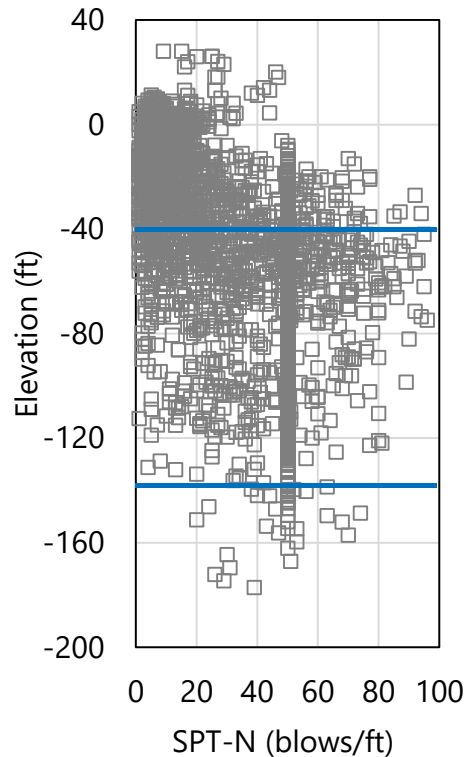

Figure 87. Scatterplot of 3144 SPT-N blow counts (elevation range: 33 ft to -177 ft)

5.3 Initial Definition of Soil or Rock Layering

The second of seven tabs (from left to right) in the GeoStat UI is the Profile tab (Fig. 88). Using the controls within this tab, a representative soil or rock layering is defined. Scatterplots of the previously cataloged site data are utilized here (Fig. 88, left and middle) to aid in selection of boundary layer elevations. Layer bottom elevations can be defined through graphical

selection within the profile plots. Additionally, all required parameter values for a given layer (e.g., soil or rock type, top elevation, bottom elevation) can be input in the layer data table (Fig. 88, right).

As a first attempt at establishing layer definitions for Site B, consider the soil or rock types and layer elevations given in Table 34. Based on the cataloged site data, two layers are defined and consist of either silty sand (layer 1) or limestone (layer 2). Layer top and bottom elevations span the ranges of elevations identified during the initial review of the site data documented above. Additional discussion regarding the selections of the boundary layer elevations is provided in the remainder of Sec. 5.3. Still further considerations are documented in Sec. 5.4, as part of the initial formation of layer-specific variograms.
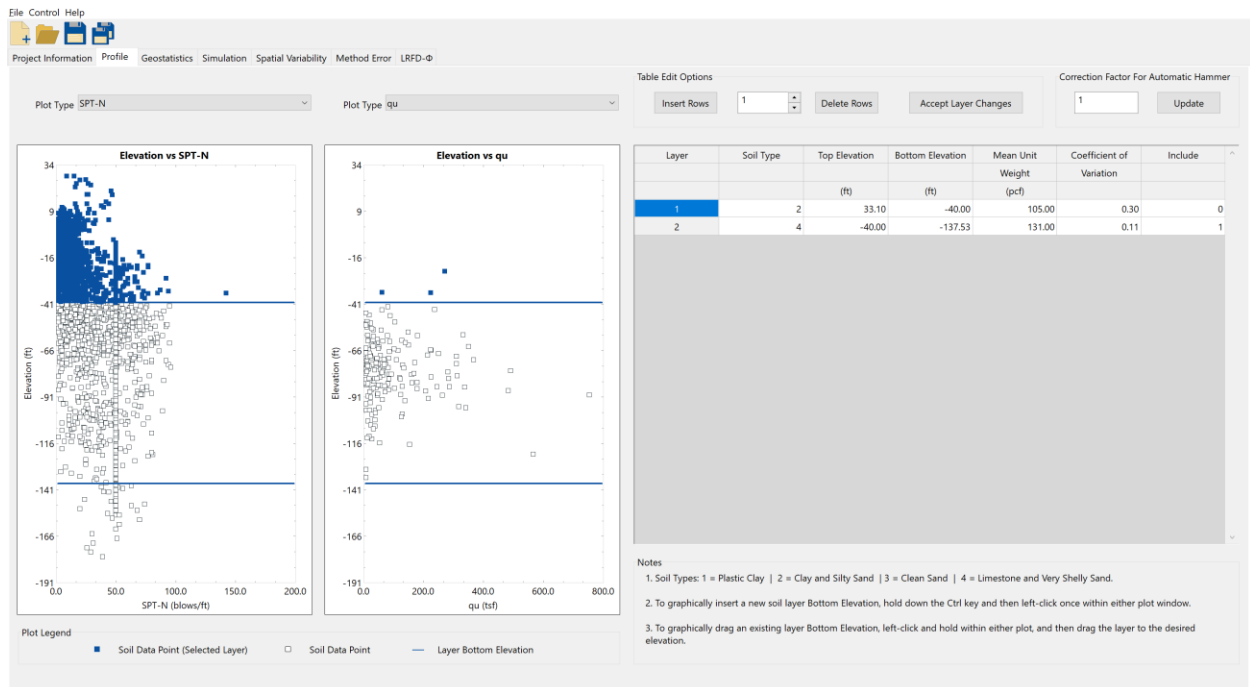
Figure 88. Profile tab

Table 34. Selected layer types and elevation ranges

Layer	Layer type	Top elevation (ft)	Bottom elevation (ft)
1	Silty sand	33.1	-40.0
2	Limestone	-40.0	-137.0

5.3.1 Initial Selection of Layer Elevations

Selected geotechnical data pertaining to rock strength are made use of for initial definition of the boundary layer elevations. Plotted in Fig. 89 are the layer divisions and ensemble of 186 measurements for unconfined compression strength, q_u, and split tensile strength, q_t.

118

Consistent with the initial review of the cataloged for Site B, the selected layer divisions are positioned in accordance with qualitative groupings identified above. For example, in accordance with observations made from the initial review of the cataloged site data, the concentrated region of relatively higher-magnitude q_u values is designated as a distinct limestone layer, with top elevation of -40 ft. The bottom elevation of layer 2 is defined to encompass the available values of q_u and q_t (i.e., -137 ft in Fig. 89b).

The 3144 SPT-N blow counts associated with the 90 boring locations of Site B, along with layer divisions (blue horizontal lines), are plotted with respect to elevation in Fig. 90. For example, a trend (albeit weak, with pronounced scatter) is discernible among the blow counts between 33 ft and -40 ft, in comparison to the relatively high levels of scatter present for values cataloged below -40 ft. Thus, Layer 1 is defined between 33 ft and -40 ft.
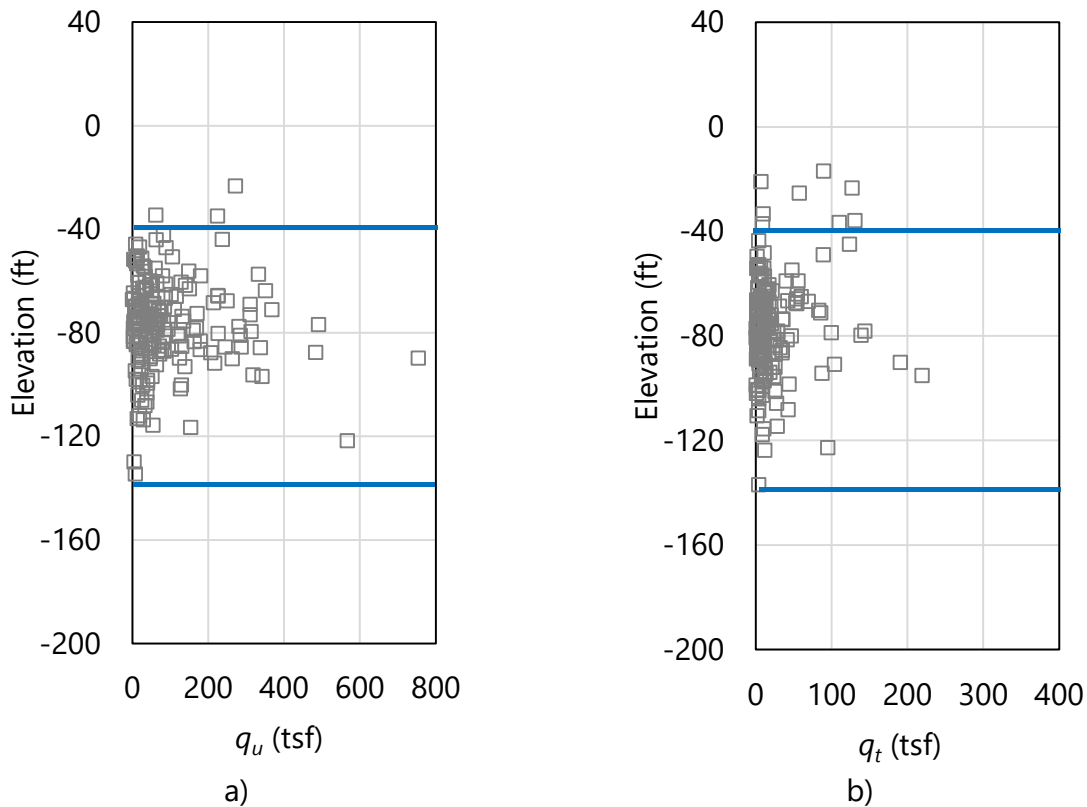
Figure 89. Scatterplot of measured rock strengths with layer bottom elevations (blue horizontal lines): a) 186 values for unconfined compression strength, q_u, (elevation range: -23 ft to -134 ft); b) 187 values for split tensile strength, q_t, (elevation range: -17 ft to -137 ft)

Figure 90. Scatterplot of 3144 SPT-N blow counts (elevation range: 33 ft to -177 ft) with layer bottom elevations (blue horizontal lines)

5.3.2 Specifying Unit Weight per Layer when Modeling Drilled Shafts

For modeling of drilled shafts in GeoStat, descriptive statistics pertaining to unit weight, γ, are required in addition to the boundary elevations of each defined layer. The descriptive statistics are input in the GeoStat UI (per layer) in the same location as the respective layer top and bottom elevations (recall Fig. 88, right). Required statistics include the mean value of unit weight and the associated COV.

As illustration of how the descriptive statistics are formed when drilled shafts are selected as the foundation type, consider the scatterplot of 23 unit weight (γ) values for Site B (and layer divisions) in Fig. 91. Formation of descriptive statistics for each layer is carried out by: 1) identifying those values of unit weight (γ) that are positioned within the layer; 2) calculating the mean value of the identified γ values; 3) calculating the standard deviation; and, 4) calculating the COV.

Continuing the illustration, consider the 17 unit weight values (γ) exclusive to layer 2 (Fig. 92). A corresponding histogram of the 17 values is shown in Fig. 93. Given the relatively few available measurements of unit weight, γ, assessment of the histogram is of limited utility.

120

Even so, descriptive statistics for the unit weight values positioned in layer 2 are assumed to be somewhat representative for the Site B data. The mean of the layer 2 unit weight data is calculated as 131 lb/ft³; the standard deviation is calculated as 14.4 lb/ft³; and, the COV is calculated as 0.11. Both the mean and COV values for unit weight, γ, are supplied as part of the layer 2 definition.

Of the 23 available values of unit weight, γ, only 6 values fall within the elevation range defined for layer 1. Engineering judgement is therefore exercised to estimate descriptive statistics for layer 1. Given that layer 1 is defined as silty sand, the mean unit weight is defined as 105 lb/ft³, and a relatively high value of COV (relative to layer 2) is assumed as 0.3. The descriptive statistics for layer 1 and layer 2 are listed in Table 35. As discussed previously in Ch. 2, these descriptive statistics are utilized when simulating log-normally distributed values of unit weight (γ), as part of stochastic simulation of axial resistance for drilled shaft members.
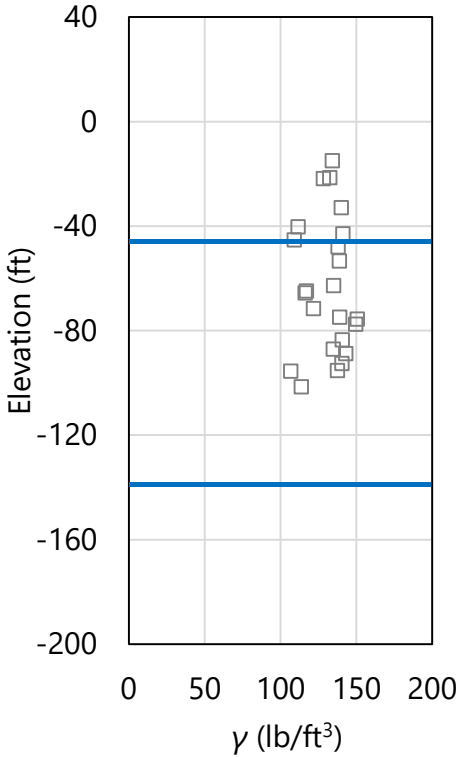
Figure 91. Scatterplot of 23 values of unit weight, γ, (elevation range: -15 ft to -102 ft) with layer bottom elevations (blue horizontal lines)
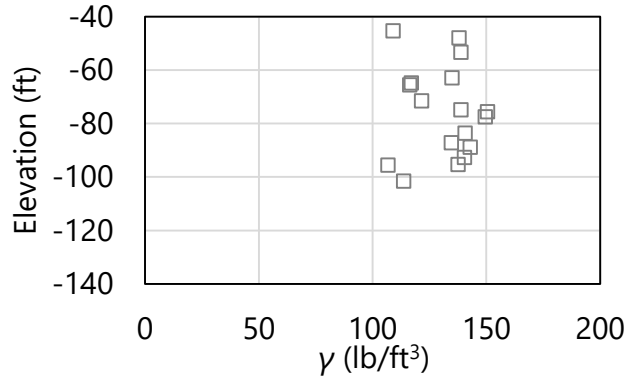
Figure 92. Scatterplot of 17 values of unit weight, γ, (elevation range: -45 ft to -102 ft) within layer 2
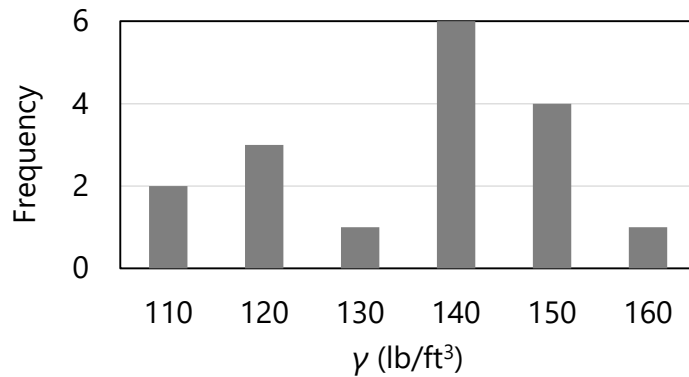
Figure 93. Histogram of 17 values of unit weight, γ, (elevation range: -45 ft to -102 ft) within layer 2

Table 35. Descriptive statistics for unit weight, γ, for each layer

Layer	Mean unit weight (lb/ft³)	COV
1	105	0.3
2	131	0.11

5.3.3 Accounting for Steel Casings when Modeling Drilled Shafts

As an additional consideration when modeling axial resistances of drilled shafts, it may be desirable to neglect skin friction resistance near upper portions of the shaft when steel casings are present. As a convenience, for such instances, the option is available to exclude any defined layer from the resistance computation procedures implemented in GeoStat.

For example, a drilled shaft foundation type is considered for Site B, and a casing is assumed to be present from the ground surface down to the rock layer (i.e., layer 2). Consequently, layer 1 is excluded from axial resistance calculations by setting the Include flag to 0 (as

122

opposed to 1, which signifies inclusion) within the layer data table of the Profile tab (Fig. 88, far right).

5.4 Initial Selection of Geostatistical Parameter Values

Having defined an initial layering for the Site B geotechnical data, focus of the modeling efforts within GeoStat continues onward to the formation of layer-specific spatial correlation structures (i.e., variograms). Recalling the relatively large plan-view area associated with Site B, the need to divide the site data into zones is anticipated, and so, initial formation of variograms (using all Site B data) is carried out to demonstrate such need. As part of the variogram formation for each applicable layer, additional checks are conducted regarding the previously defined layering (as discussed in Sec. 5.4.1). Variogram formation for each layer is carried out within the Geostatistics tab (Fig. 94) of the GeoStat UI.
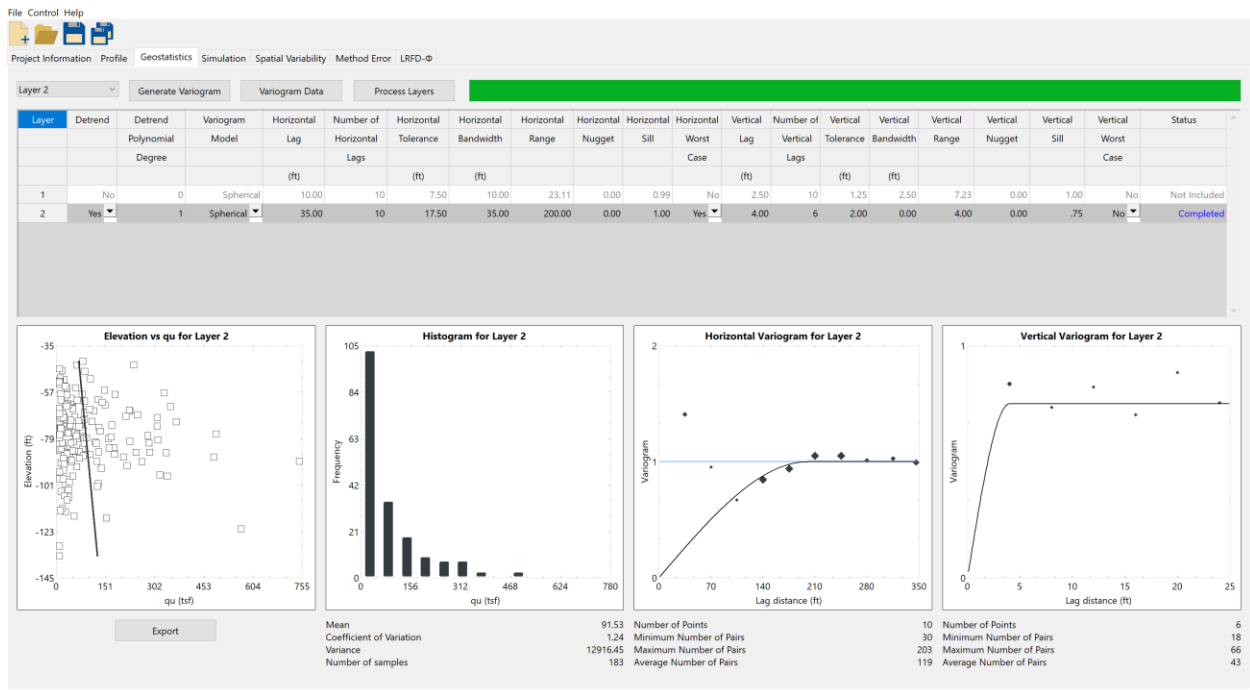
Figure 94. Geostatistics tab

For any layer that is to be included for simulating axial resistance, various graphical depictions are provided in the bottom region of the Geostatistics tab. From left to right (Fig. 94, bottom), the layer-specific graphical depictions include a scatterplot of the relevant soil or rock parameter, corresponding histogram, horizontal variogram, and vertical variogram. While the scatterplot and histogram are dictated by the previously cataloged site data and previously formed layer definitions, the (experimental) variogram points are dependent on selection of variogram parameter values in the table located above the plots (Fig. 94, middle).

When forming spatial correlation structures for drilled shaft portions embedded in sand layers, SPT-N blow count values are utilized. For drilled shaft portions embedded in clay layers, SPT-N blow counts are again utilized, but then empirically related to undrained shear strength (C_u). However, for drilled shaft portions embedded in limestone layers, values of unconfined compression strength (q_u) are used for computation of variogram points. For the modeling of Site B, recall that a drilled shaft is selected as the foundation member type, and that steel casing is present from the ground surface down to the top of layer 2. Therefore, no considerations are necessary in relation to layer 1 (silty sand). Initial formation of variograms for layer 2 (limestone) is based upon values of unconfined compression strength (q_u).

5.4.1 Examining Initial Definition of Layer Data

Prior to selecting variogram parameter values for layer 2, both the descriptive statistics and graphical depictions of the layer-specific collections of q_u values are examined. Summary statistics for the relevant types of soil or rock measurements for layer 1 and layer 2 are listed in Table 36. Values pertaining to layer 1 are not applicable (N/A) because the layer is excluded from the Site B analysis to reflect the presence of a steel casing. The level of dispersion associated with the q_u data of layer 2 is relatively high (COV value is 1.25). Such a relatively large value of COV, in part, motivates assessment of the Site B data for the purpose of identifying distinct geological zones (as discussed in Sec. 5.5).

Table 36. Summary statistics for defined layers

Layer	Physical measurement	Sample size	Mean	COV
1	N/A	N/A	N/A	N/A
2	q_u (tsf)	180	91.5	1.25

Concerning examination of graphical depictions of layer 2 data (q_u), the scatterplot (e.g., Fig. 94, bottom-left) serves to reveal if trends are present among the layer data. In the event that a trend is observed among the data attributed to a layer, then detrending is necessary. The detrending process (documented in Ch. 2) is automated in the GeoStat UI. Recalling Fig. 94 (middle-left), if detrending is desired for the data of a given layer, then the respective entry in the Detrend column of the layer data table is set to Yes (as opposed to No). Further, the polynomial degree of the trend is specified. Typically, linear detrending is sufficient for instances when detrending is necessary.

Regarding the histograms of layer-specific data (e.g., Fig. 94, bottom-center), these plots allow for conspicuous frequency-related features (i.e., bimodal peaks) to be identified. More broadly, in the event that the data distribution for a given layer does not exhibit (roughly) a lognormal shape, then revisions to the layer definitions (and particularly the layer elevations) may need to be carried out. When conspicuous features are present in a layer-specific histogram, then it may be necessary to assess the site data for the presence of distinct geological zones (as discussed for Site B in Sec. 5.5). If zones are identified, then modeling of

each zone (one subset of boring locations at a time) can lead to more representative layers for a given region within the site, and also, relatively smaller values of COV for layer-specific data. Subdivision of the site into zones, though, tends to reduce the number of data points available for modeling of a given layer (and can hinder the formation of variograms). Stated alternatively, a balance is required between subdivision of site data and available data points per layer.

5.4.1.1 Layer 2

A scatterplot of the 183 unconfined compression strength, q_u, values positioned within layer 2 is presented in Fig. 96. Visual examination of the scatterplot (Fig. 96) confirms the relatively high level of dispersion (COV of 1.25) reported in Table 36. Also, owing in part to the level of dispersion among the collected data, only a weak trend (increasing q_u values with increasing depth) is observed from the scatterplot.
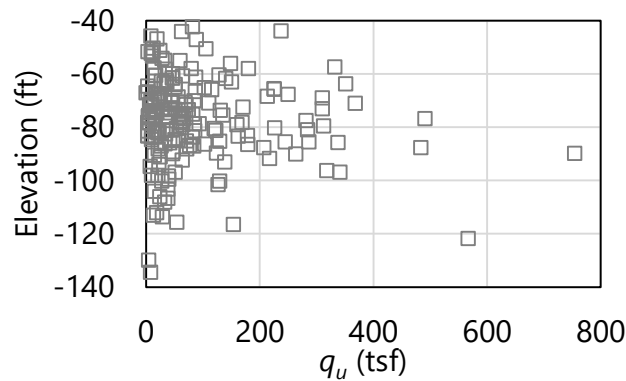
Figure 95. Scatterplot of 183 unconfined compression strength, q_u, values (elevation range: -40 ft to -134 ft) within layer 2

A histogram of the 183 measured q_u values pertaining to layer 2 is presented in Fig. 96. Despite the far-left, pronounced frequency peak for q_u values of approximately 50 tsf, the overall histogram (roughly) resembles that of log-normally distributed data. Furthermore, the right skew of the histogram is markedly elongated and contributes to the associated COV value of 1.25. These observations provide sustained motivation for assessment of distinct geological zones for Site B. However, given the absence of conspicuous features (such as bimodal phenomena) in the layer 2 histogram, no revisions are made regarding the initial selections of boundary elevations for layer 2.
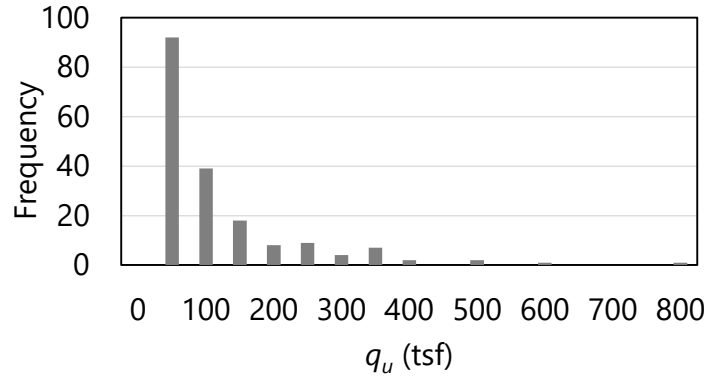
Figure 96. Histogram of 183 unconfined compression strength, q_u, values (elevation range: -40 ft to -134 ft) within layer 2

5.4.2 Forming Variograms using Initial Layer Definitions

The above examination reaffirms the initial selections of layer elevations for the geotechnical data of Site B. The process of forming variograms is next undertaken for layer 2, but solely for the purpose of demonstrating the need to divide the site into zones. Recalling Fig. 81, geotechnical data are available for a relatively large number of boring locations (90). Accordingly, consideration is given to forming initial spatial correlation structures in both the horizontal and vertical directions. Variogram parameters initially selected for layer 2, with consideration of all (90) Site B borings, are listed in Table 37.

Table 37. Layer-specific parameters for variograms with consideration of all Site B borings

Layer	Type	Lag (ft)	Number of lags	Tolerance (ft)	Bandwidth (ft)
1	N/A	N/A	N/A	N/A	N/A
2	Horizontal	35	10	17.5	35.0
2	Vertical	4	6	2.0	0.0

Table 38. Variogram ranges and sills for all Site B borings

Layer	Type	Range (ft)	Sill
1	N/A	N/A	N/A
2	Horizontal	200	1.0
2	Vertical	4.0	0.75

As discussed in Ch. 2, the lag distance, number of lags, tolerance, and bandwidth are all instrumental in forming points of the experimental variogram. Recommendations given in McVay et al. (2012) are utilized in selecting tolerance and bandwidth values listed in Table 37 (detailed for layer 2 below). Variogram values for range and sill are not listed as these values (range, sill) are more strongly related to the theoretical variogram in GeoStat (see Ch. 2 for additional details).

5.4.2.1 Layer 2

As listed above in Table 37, a horizontal lag distance (i.e., the abscissa spacing between points of the horizontal variogram) is selected as 35 ft for the horizontal variogram of layer 2. A relatively large horizontal lag distance (versus vertical lag distance of 4 ft) is selected to reflect the plan-view distances of borings distributed across Site B. The vertical lag distance of 4 ft is selected to be on the order of the distances associated with core runs (5 ft).

Use of the lag distances specified above lead to qualitatively apparent trends in the respective experimental variograms (presented later). However, it is recommended that multiple candidates for lag distance be considered prior to finalizing the variogram for a given layer and variogram direction. Furthermore, for each candidate lag distance considered, it is necessary to update the values for tolerance and bandwidth.

Recommendations are given in McVay et al. (2012) for determining values of tolerance and bandwidth, given a candidate value of lag distance. Distinctions are made between recommendations for horizontal and vertical variogram parameters. For example, for the selected (vertical) lag distance of 4 ft, the tolerance is set to one-half the magnitude of the lag distance (i.e., 2 ft) and the bandwidth is set to 0 ft. As an additional example, for the horizontal variogram of layer 2, the tolerance (17.5 ft) is again set to one-half of the respective lag distance (35 ft).

Variogram points for layer 2 are calculated, in part, using distance-based pairings of measured q_u values. Linear detrending is applied to the data set (as automated in GeoStat) for the purpose of forming variogram points. The horizontal and vertical (experimental) variogram points for layer 2 are listed in Table 39 and Table 40, respectively. Corresponding plots of the experimental variograms are presented in Fig. 97 (horizontal) and Fig. 98 (vertical). Also listed in Table 39 and Table 40 are the pairs associated with each variogram point. The data listed in Table 39 and Table 40 are obtained directly from the GeoStat UI by entering the Variogram Data dialog (Fig. 94, top-left).

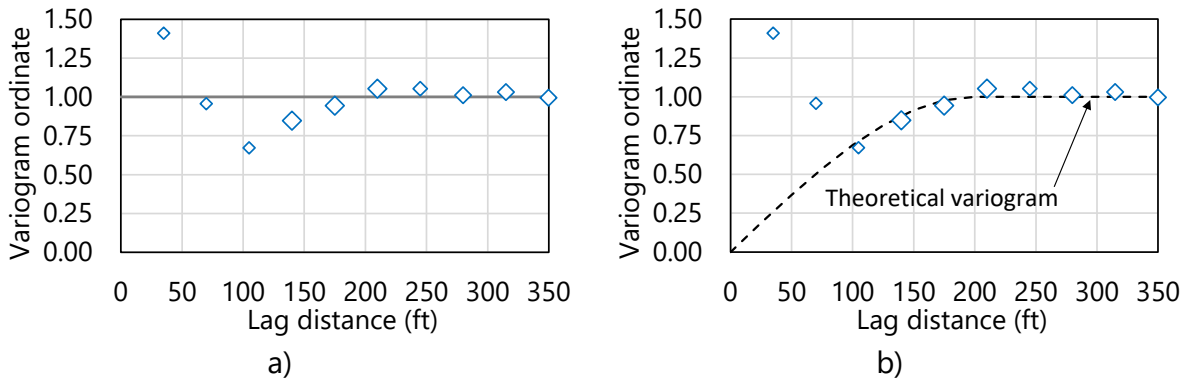Table 39. Horizontal variogram data for layer 2 (elevation range: -40 ft to -137 ft) with consideration of all Site B borings

Abscissa (ft)	Ordinate	Pairs
35	1.41	66
70	0.96	60
105	0.67	30
140	0.85	157
175	0.94	187
210	1.05	203
245	1.05	174
280	1.01	101
315	1.03	98
350	0.99	122

Table 40. Vertical variogram data for layer 2 (elevation range: -40 ft to -137 ft) with consideration of all Site B borings

Abscissa (ft)	Ordinate	Pairs
4	0.84	66
8	0.74	62
12	0.82	54
16	0.70	32
20	0.88	30
24	0.76	18

As discussed in Ch. 2, the number of measured data pairs used in forming an experimental variogram point reflect the strength (or significance) of said point. Further, as is the case for the variogram plots within the GeoStat UI (recall Fig. 94), the experimental variogram point symbols in Fig. 94 are sized (scaled) based on the respective number of pairs used in forming said points. The scaling visually signifies the strength or significance of each variogram point. A threshold value of approximately 30 (pairs) is recommended in McVay et al. (2012) when judging the significance of an experimental variogram point.

For the layer 2 horizontal variogram of Site B, pair counts well in excess of 30 are generally produced across the variogram points (Table 39), particularly for distances equal to or greater than 140 ft. Points at distances greater than 100 ft conform to asymptotic behavior, with a sill value of unity. A theoretical is fit to the horizontal variogram points, with range of 200 ft and sill of unity. Regarding the vertical variogram for layer 2 (Table 40, Fig. 98), ordinate values considerably less than unity (0.70 to 0.88) occur across all lag distances. For increasing lag distances, the variogram ordinates appear to converge toward an ordinate value of approximately 0.75. Accordingly, a theoretical variogram is fit to the variogram points, with a range of 4 ft and sill of 0.75.

Comparing horizontal (Fig. 97) and vertical (Fig. 98) variogram plots for layer 2 (when considering all 90 boring locations), zonal anisotropy is apparent. Of greatest significance, the sills of the horizontal (1.0) and vertical (0.75) variograms do not converge to the same ordinate value. As detailed in Ch. 2, zonal anisotropy is present when the ordinates of the variograms for a given layer do not converge to the same sill (Fig. 99). Alternatively stated, when data sets exhibit zonal anisotropy, then the corresponding variances are direction dependent. Additionally, it is very likely due to proportionality (i.e., COV, or standard deviation divided by the mean) that if the sill (variance, or, standard deviation squared) is different, then the means will differ by zone and, ultimately, so will the estimated shaft capacities. Still further, if carried forward when zonal anisotropy is present, the overall variance of the data may adversely affect terms that contribute to total uncertainty when calculating LRFD resistance (via the resistance factor, ϕ).

Figure 97. Horizontal variogram for layer 2 (elevation range: -40 ft to -137 ft) with consideration of all Site B boring locations: a) Experimental; b) Experimental with fit
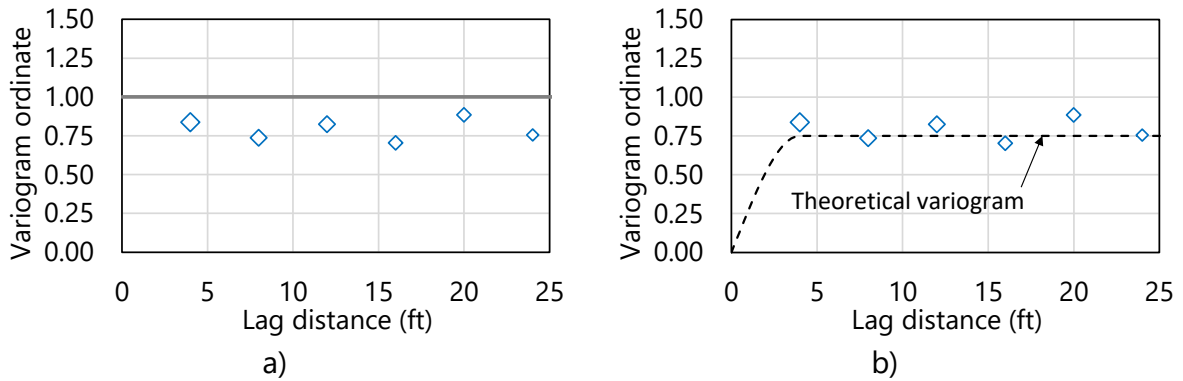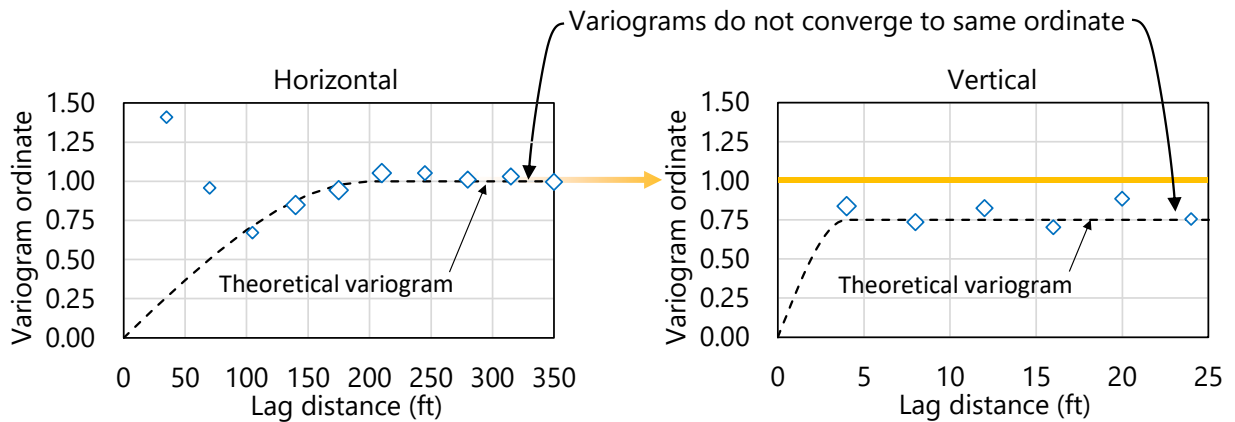

Figure 98. Vertical variogram for layer 2 (elevation range: -40 ft to -137 ft) with consideration of all Site B boring locations: a) Experimental; b) Experimental with fit

Figure 99. Zonal anisotropy of variograms when all Site B boring locations are considered

129

Returning to the 90 borings distributed across Site B, differences in the sills of the horizontal and vertical variograms suggest that Site B encompasses multiple geological zones. Therefore, further division of the Site B data, with respect to plan-view positioning, is necessary. As a result, one data subset is defined for each zone (see Sec. 5.6, Sec. 5.7). Summary comparisons of the site-wide and zone-specific data sets are documented in Sec. 5.8.

5.5 Identifying Geological Zones

Three possible means of identifying the need to divide site data into zones are: 1) examination of through-depth scatterplots and histograms of available site data; 2) assessment of the sensitivity to variograms to removal of a subset of boring locations from the variogram formation process; and, 3) identification of variogram phenomena such as zonal anisotropy. Given the presence of zonal anisotropy within the variograms of the Site B data set, further assessment of the available data is carried out to identify distinct geological zones.

Among the 90 borings distributed across Site B, 48 are located along a relatively narrow band of northings (with eastings ranging from 0 ft to approximately 5500 ft). The 48 borings positioned along this "strip" are highlighted in Fig. 100, and are focused upon in the Ch. 5 documentation for modeling of zones. More specifically, to illustrate the process of modeling zone-specific data sets, two distinct zones from within Site B are identified in the following.

Commentary is provided regarding selection of borings that are included in each of the two zones. Also, for each zone, layerings are defined and spatial correlation structures (variograms) are formed. The same general concepts (and overall process) documented below can be applied when investigating and modeling zones in other sites.
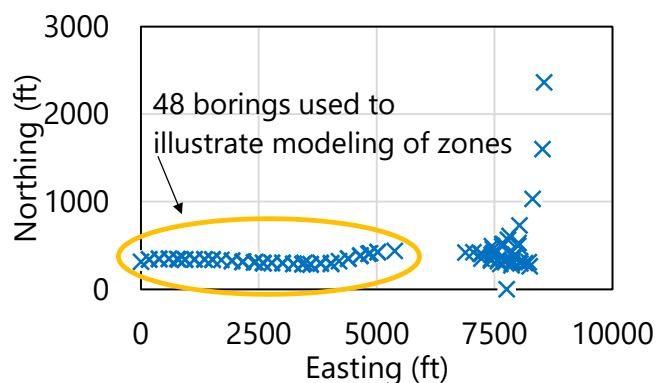
Figure 100. Plan view of Site B boring locations with indication of 48 borings used to illustrate modeling of zones

5.5.1 Recommendation for Model File Handling when Zones are Detected

In general, for each zone identified, it is recommended that a separate GeoStat model be created, where only the boring locations associated with said zone are included for site modeling. A straightforward means for selection of subsets of boring locations is implemented in GeoStat, where data from only those locations are carried forward into site modeling (layer definition and variogram formation) and stochastic simulation processes.

Recalling the Project Information tab (Fig. 80), indication of each boring location that is to be utilized for site modeling and simulation is signified by supplying a value of 1 beneath the Include column (Fig. 80, right). In this way, data from all boring locations across the site can be retained in the zone-specific GeoStat model (if desired). Then, for each identified zone, the associated GeoStat model is configured such that only those boring locations within said zone are assigned a value of 1 beneath the Include column on the Project Information tab.

5.6 Characterizing Site Data for Zone 1

As a practical measure, the "strip" of 48 borings (recall Fig. 100) is divided into two portions, with the leftmost boring locations constituting a candidate zone (referred to as zone 1). This subset of borings is investigated as a candidate, distinct zone by reexamining layering and reforming variograms. Considerations for the remainder of the 48 borings are discussed in Sec. 5.7. As highlighted in Fig. 101, 23 boring locations from within Site B are identified based on visually recognition of clusters of borings in plan-view, followed by practical considerations to divide those clusters into candidate zones. Summarily, the 23 borings making up zone 1 are selected: 1) to illustrate the overall process of modeling zones within a site; and, 2) based on close proximity to one another, or adherence to a plan-view grouping, relative to other boring locations.
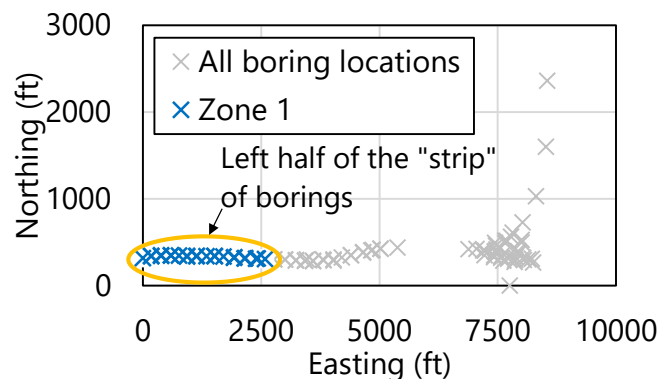
Figure 101. Plan view of Site B boring locations with indication of 23 boring locations that comprise zone 1

In the following, variograms are reformed using the 23 borings selected to comprise zone 1. Subsequently, the variograms pertaining to zone 1 are compared to those previously generated with consideration of all 90 borings from Site B. The effect of isolating the 23 borings, with regard to selecting layer elevations, is also assessed. Detailed comparisons between the site-wide data and zone 1 are presented immediately below. See Sec. 5.8 for summary comparisons between the site-wide and zone-specific data sets.

5.6.1 Defining Soil or Rock Layering for Zone 1

Prior to forming variograms specific to zone 1, the previously defined layering (obtained from examination of all Site B data) is reassessed. The reassessment begins with calculation of the layer summary statistics, but with use of geotechnical site data that are specific to the 23 borings of zone 1. Summary statistics that are obtained when considering all 90 borings of Site B, versus those obtained from the 23 borings making up zone 1, are compared in Table 41.

Table 41. Comparisons of summary statistics for defined layers (all borings versus Zone 1 borings)

Layer	Physical measurement	All borings			Zone 1 borings		
		Sample size	Mean	COV	Sample size	Mean	COV
1	N/A	N/A	N/A	N/A	N/A	N/A	N/A
2	q_u (tsf)	183	91.5	1.25	48	62	0.80

Recall that a casing is assumed to be present throughout the layer 1 elevation range, and so, no additional considerations are necessary with respect to layer 1. All of the sample size, mean, and COV for layer 2 decrease when transitioning from site-wide analysis to zone 1 analysis. The decrease in COV value corresponds to more favorable (i.e., reduced) estimates of total uncertainty when conducting stochastic simulation. Regardless, further examination of the measured site data within layer 2 is necessary.

5.6.1.1 Layer 2

Scatterplots of the measured q_u values that are positioned within layer 2 (site-wide versus zone 1) are presented in Fig. 102. The q_u values specific to zone 1 begin at an elevation of approximately -50 ft and extend down to approximately 120 ft. Within the range of 100 tsf to 400 tsf, a relatively larger number of measured q_u values are present among the site-wide data (Fig. 102a). Also, the site-wide data set contains many more measured values of q_u that exceed 200 tsf. This difference is reflected in the means (91 tsf versus 62 tsf) and COV values (1.25 versus 0.8). In contrast to the relatively pronounced scatter of the site-wide data, a trend is apparent among the zone 1 data, where q_u values tend to increase with respect to increasing depth (Fig. 102b).

132
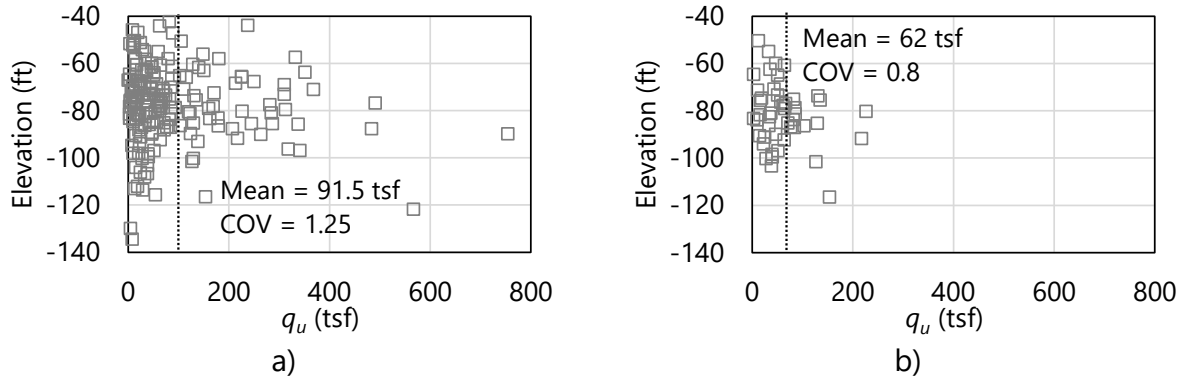
Figure 102. Scatterplots of unconfined compression strength, q_u, values (elevation range: -40 ft to -137 ft) within layer 2: a) All boring locations; b) Zone 1

Histograms of the q_u values pertaining to layer 2, when formed using all 90 borings and when using the 23 borings of zone 1, are presented in Fig. 103. As anticipated, reduced frequency counts are observed for the zone 1 data (Fig. 103b) relative to the site-wide data (Fig. 103a). While the histogram associated with zone 1 (Fig. 103b) qualitatively retains a log-normally distributed shape, the right skew is much less pronounced than that of the histogram for the site-wide data. The less pronounced skew is signified by the relative reduction in both the mean value and COV (recall Table 41).

Based on comparisons of the scatterplots and histograms, two modifications are made to the layer 2 definition: 1) the top and bottom elevations are updated; and, 2) linear detrending is carried out when forming variograms (where the variogram formation is discussed later). The layer 1 definition remains unchanged as a casing is positioned to the top of layer 2. A summary of the revised layer definitions, specific to zone 1, is given in Table 42. Regarding unit weights per layer (as required when modeling drilled shafts in GeoStat), no measurements are available among the zone 1 data set. Consequently, the mean and COV values of unit weight, calculated using the site-wide data set, are utilized (recall Table 35).
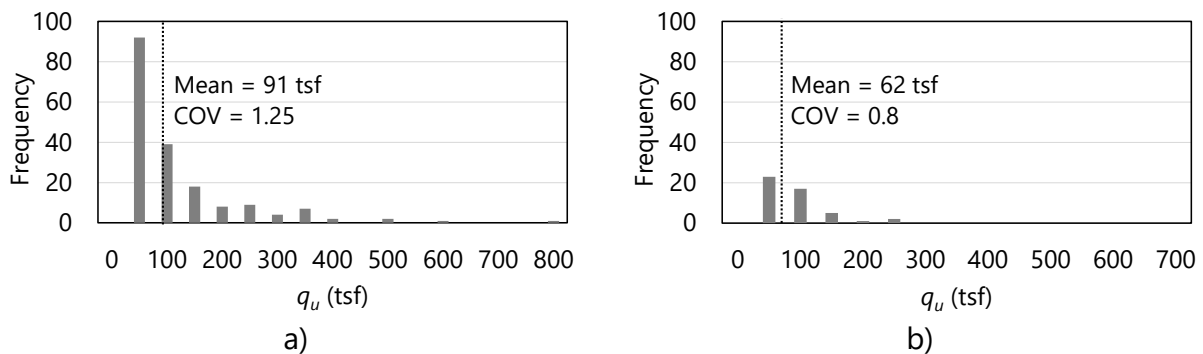
Figure 103. Histograms of unconfined compression strength, q_u, values within layer 2: a) All boring locations; b) Zone 1

133

Table 42. Selected layer types and elevation ranges for zone 1			
Layer	Layer type	Top elevation (ft)	Bottom elevation (ft)
1	Silty sand	3.0	-50.0
2	Limestone	-50.0	-120.0

5.6.2 Selecting Geostatistical Parameter Values for Zone 1

Having revised the previously defined layer elevations for Site B to reflect the q_u values from the 23 borings of zone 1, the process of forming variograms specific to zone 1 is next undertaken. Recall that a casing is assumed to be present down to the top of layer 2, and so, focus is given to layer 2 in the following discussion. As highlighted in Fig. 101 above, geotechnical data are available for 23 (out of 90) boring locations, and those locations are distributed across a plan-view area of approximately 50 ft by 2500 ft. While the 23 borings constitute a considerable number of locations, no well-formed spatial correlation structures (variograms) are found in the horizontal direction for zone 1. Note that horizontal variograms are not neglected, but rather, worst case conditions (conceptually introduced in Ch. 2) are applicable to the horizontal variograms. More specifically, worst case conditions are assigned to the horizontal variograms only after unsuccessfully iterating upon several trial constructions of the horizontal variograms for zone 1.

As detailed in Ch. 2, unconditional (stochastic) simulation for estimating foundation member axial resistance makes use of spatial correlation structures in the vertical direction, as opposed to variograms in the horizontal and vertical directions. Stated another way, unconditional simulation (discussed later) is elected for zone 1 to avoid the prospect of generating factored axial resistances under worst case conditions (for the horizontal variograms). Therefore, focus is given below to formation of vertical variograms. However, the same general concepts apply for instances where sufficient site data are available to construct both horizontal and vertical variograms for a site.

5.6.2.1 Constructing Variograms for Zone 1

Vertical variogram parameters selected for layer 2, with consideration of the 23 borings making up zone 1, are listed in Table 43 and Table 44. The variogram parameter values are selected in a manner that is, overall, analogous to that detailed previously when considering the site-wide data set (as well as that documented for Example Site A in Ch. 4). The lag distance selected for layer 2 is larger than, but still on the order of, typical lengths for core run data (5 ft). More broadly, lag distances closer to (or even less than) 5 ft are typical when forming vertical variograms, and should be selected whenever feasible.

Parameter values selected for the vertical variograms of zone 1 (Table 43) differ substantially from respective values selected when considering all 90 borings of Site B (recall Table 37).

Given well-formed vertical variograms for zone 1 (presented below) division of Site B into zones is substantiated by these differences.

Table 43. Layer-specific parameters for vertical variograms of zone 1

Layer	Lag (ft)	Number of lags	Tolerance (ft)	Bandwidth (ft)
1	N/A	N/A	N/A	N/A
2	8	5	4.0	0.0

Table 44. Vertical variogram ranges and sills for zone 1 layers

Layer	Range (ft)	Sill
1	N/A	N/A
2	15.5	1.0

Listings of experimental vertical variogram points for layer 2 are provided in Table 45. Included among the listings are variogram points (and pairs) generated when considering all 90 borings from Site B and when considering the 23 borings from zone 1. Reductions consistently occur in the pair count values when transitioning from the site-wide data to the zone 1 data. This reduction is expected as only 23 boring locations are considered for zone 1, versus the 90 locations that make up the site-wide data. Despite the presence of pair counts below 30 for lag distances approaching 40 ft, the trend in the vertical variogram ordinate values for zone 1 (Table 45) indicate much more clearly distinguishable convergence toward a sill value of 1.

Table 45. Comparison of vertical variogram data for layer 2 when all borings are considered versus when zone 1 borings are considered

All borings			Zone 1 borings		
Abscissa (ft)	Ordinate	Pairs	Abscissa (ft)	Ordinate	Pairs
4	0.84	66	8.0	0.77	30
8	0.74	62	16.0	0.96	26
12	0.82	54	24.0	0.95	11
16	0.70	32	32.0	0.89	9
20	0.88	30	40.0	1.03	3
24	0.76	18	--	--	--

Comparative plots of the experimental, vertical variograms (all borings versus zone 1 borings) are presented in Fig. 104. Additionally, the variogram ordinate value of 1.0 is visually emphasized in each plot. Visual comparison of the vertical variogram points (Fig. 104a, Fig. 104b) reveals that the zone 1 variogram converges to unity while the site-wide variogram converges to a value less than unity (0.75). The vertical variogram associated with layer 2 (of zone 1) is generated with linear detrending of the q_u values (recall Fig. 102b), and is replotted in Fig. 105. The act of detrending tends to reduce the COV of the data set. In this case, the

COV (i.e., the standard deviation of the detrended data divided by the mean of the physical measurements) marginally reduces the COV value for layer 2, from 0.80 to 0.78.

The fitted theoretical variogram is of exponential form (as opposed to spherical) as the exponential expression (defined in Ch. 2) better conforms to the experimental variogram points. The range value associated with the theoretical variogram of zone 1 (15.5 ft in Fig. 105) is smaller than the largest abscissa value generated for the experimental variogram (40 ft). This serves to verify that a sufficient number of lag distances are specified as listed in Table 43 above.
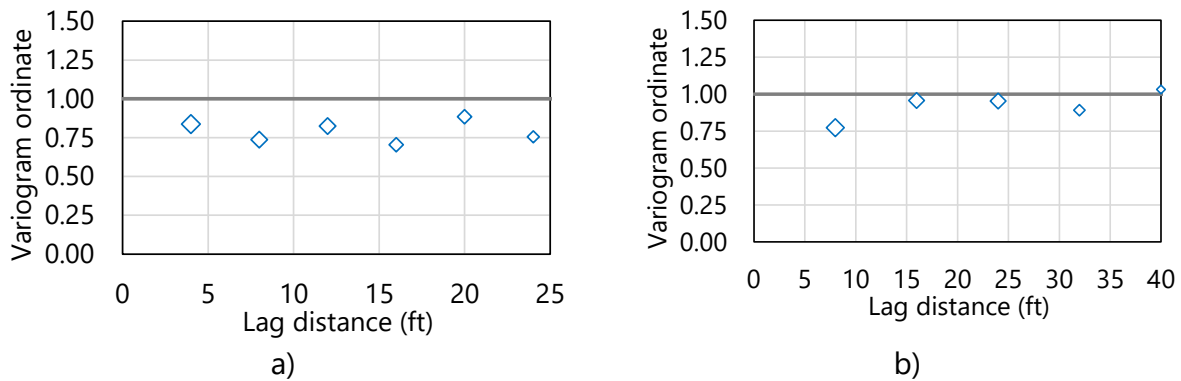
Figure 104. Comparison of vertical variogram points for layer 2: a) All borings; b) Zone 1
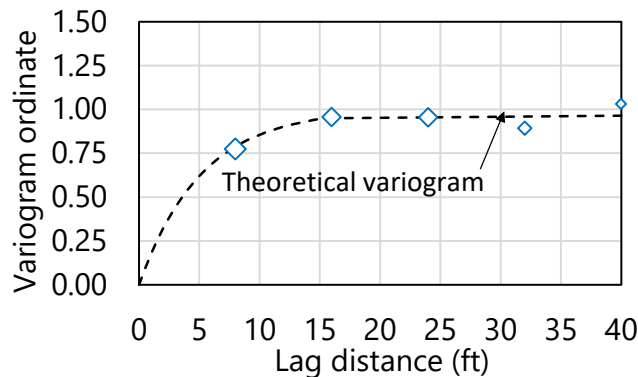
Figure 105. Vertical variogram for layer 2 of zone 1 (elevation range: -50 ft to -120 ft)

Given the well-formed vertical variogram for layer 2 of zone 1, which converges at a sill value of unity, it is reasonable to divide Site B into distinct geological zones. The process of defining and assessing various spatially varying quantities (layers, variograms) for other potential zones within Site B is analogous to that detailed above for zone 1. Discussed immediately below is utilization of similar concepts, relative to those applied above, to investigate an additional zone within Site B. Subsequently, the site-wide and zone-specific variograms are compared

in Sec. 5.8. Further, in Sec. 5.9, data sets for zone 1 and zone 2 are utilized to perform stochastic simulations, and ultimately, compute zone-specific estimates of factored axial resistances for drilled shaft foundations.

5.7 Characterizing Site Data for Zone 2

Recall from Fig. 100 that a "strip" of 48 borings from Site B is divided into two portions, with the 23 leftmost boring locations constituting zone 1. Considerations for the remainder of the 48 borings are discussed throughout Sec. 5.7, where these 25 borings comprise zone 2 (Fig. 106). The 25 borings making up zone 2 are selected: 1) to provide a second illustration of the overall process of modeling zones within a site; and, 2) based on close proximity to one another, or adherence to a plan-view grouping, relative to other boring locations of Site B.
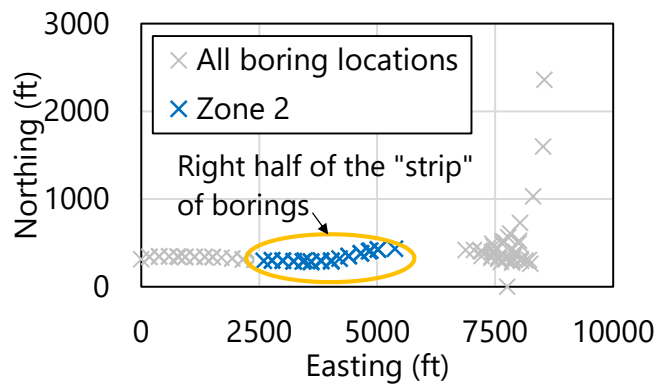
Figure 106. Plan view of Site B boring locations with indication of 25 boring locations that comprise zone 2

In the following, variograms are reformed using the 25 borings selected to comprise zone 2. Subsequently, the variograms pertaining to zone 2 are compared to those previously generated with consideration of all 90 borings across Site B. The effect of isolating the 25 borings, with regard to selecting layer elevations, is also assessed in the following. Here, again, comparisons are made relative to layer definitions associated with the site-wide data. See Sec. 5.8 for comparisons between the site-wide, zone 1, and zone 2 data sets.

5.7.1 Defining Soil or Rock Layering for Zone 2

Prior to forming variograms specific to zone 2, the initial layering definitions produced from examination of all Site B data are reassessed. This reassessment begins with calculation of the layer summary statistics, but with use of geotechnical site data that are specific to the 25 borings of zone 2. Summary statistics that are obtained when considering all 90 borings of Site B, versus those obtained from the 25 borings making up zone 2, are compared in Table 46.

Recall that a casing is assumed to be present throughout the layer 1 elevation range, and so, no additional considerations are necessary with respect to layer 1. All of the sample size, mean, and COV for layer 2 decrease when transitioning from site-wide analysis to zone 2 analysis. The decrease in COV value is not as substantial as that attributed to zone 1 (recall Table 42), and ideally should fall at or below a value of approximately 1.0. Even so, the COV for zone 2 corresponds to more favorable (i.e., reduced) estimates of total uncertainty when conducting stochastic simulation. Especially because the value of COV is greater than 1.0 when considering the zone 2 data set, further examination of the measured site data within layer 2 is necessary.

Table 46. Comparisons of summary statistics for defined layers (all borings versus Zone 2 borings)

Layer	Physical measurement	All borings			Zone 2 borings		
		Sample size	Mean	COV	Sample size	Mean	COV
1	N/A	N/A	N/A	N/A	N/A	N/A	N/A
2	q_u (tsf)	183	91.5	1.25	46	63	1.15

5.7.1.1 Layer 2

Scatterplots of the measured q_u values that are positioned within layer 2 (site-wide versus zone 2) are presented in Fig. 107. Within zone 2, q_u values begin at an elevation of approximately -45 ft and extend down below -100 ft. Within the range of 100 tsf to 400 tsf, a considerably larger number of measured q_u values are present among the site-wide data (Fig. 107a). Also, the full data set of Site B contains many more measured values of q_u greater than approximately 150 tsf. Consequently, both the mean and COV of the site-wide data (91.5 tsf, 1.25) exceed those of zone 2 (63 tsf, 1.15). In contrast to the relatively pronounced scatter of the site-wide data, a more pronounced trend is apparent among the zone 2 data, indicating an increase (despite still discernible scatter) with respect to increasing depth (Fig. 107b).
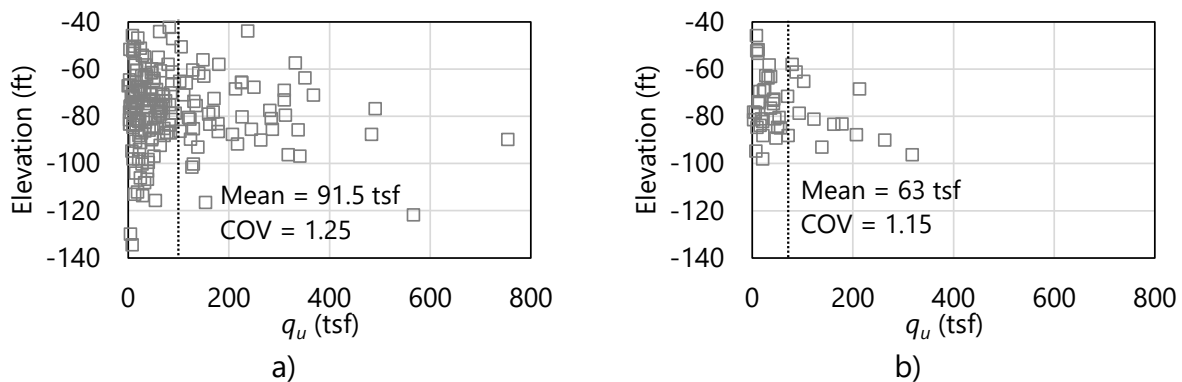
Figure 107. Scatterplots of unconfined compression strength, q_u, values within layer 2: a) All boring locations; b) Zone 2

Histograms of the q_u values pertaining to layer 2, when formed using all 90 borings and when using the 25 borings of zone 2, are presented in Fig. 108. As anticipated, reduced frequency counts are observed for the zone 2 data (Fig. 108b) relative to the site-wide data (Fig. 108a). While the histogram associated with zone 2 (Fig. 108b) qualitatively retains a log-normally distributed shape, the right skew is much less pronounced than that of the histogram for the site-wide data. The less pronounced skew is signified by the relative reduction in both the mean value and COV (recall Table 46).
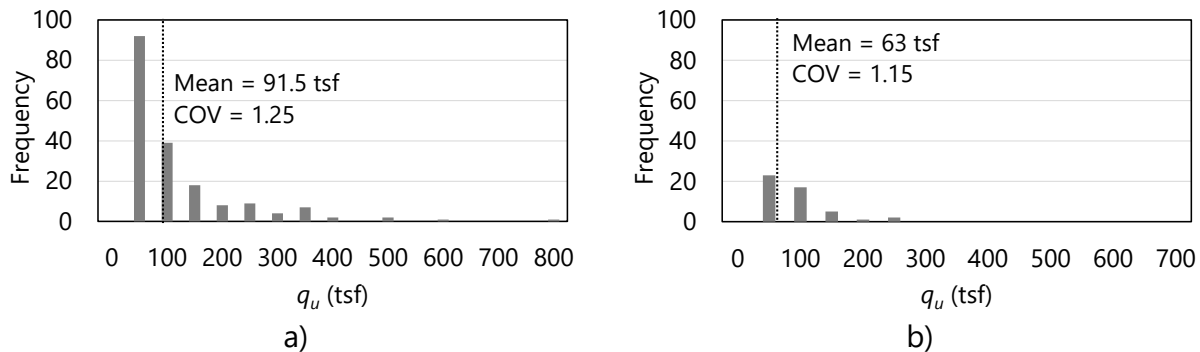
Figure 108. Histograms of unconfined compression strength, q_u, values within layer 2: a) All boring locations; b) Zone 2

Table 47. Selected layer types and elevation ranges for zone 2

Layer	Layer type	Top elevation (ft)	Bottom elevation (ft)
1	Silty sand	9.0	-45.0
2	Limestone	-45.0	-105.0

Based on comparisons of the scatterplots and histograms, two modifications are made to the layer 2 definition: 1) the top and bottom elevations are updated; and, 2) linear detrending is carried out when forming variograms (where the variogram formation is discussed later). The layer 1 definition remains unchanged as a casing is positioned to the top of layer 2. A summary of the revised layer definitions, specific to zone 2, is given in Table 47. Regarding unit weights per layer (as required when modeling drilled shafts in GeoStat), no measurements are available among the zone 2 data set. Consequently, the mean and COV values calculated across the site-wide data set are again utilized for unit weights (recall Table 35).

5.7.2 Selecting Geostatistical Parameter Values for Zone 2

Having revised the previously defined layer elevations for Site B to reflect the q_u values from the borings of zone 2, the process of forming variograms specific to zone 2 is next undertaken. Recall that a casing is assumed to be present down to the top of layer 2, and so, focus is given to layer 2 in the following discussion. As highlighted in Fig. 106 above, geotechnical data are

139

available for 25 (out of 90) boring locations, and those locations are distributed across a plan-view area of approximately 140 ft by 2700 ft.

Critically, horizontal variograms for zone 2 are not neglected. On the contrary, numerous iterative attempts to construct well-formed horizontal variograms are first undertaken. Having unsuccessfully formed any promising horizontal variograms, and owing to the relatively smaller data set available to zone 2 (relative to the site), worst case conditions are assigned. Furthermore, unconditional simulation (discussed later) is elected for zone 2 to avoid the prospect of generating factored axial resistances under worst case conditions (for the horizontal variograms). Accordingly, focus is given below to formation of well-constructed vertical variograms. Even so, the same general concepts apply for instances where sufficient site data are available to construct both horizontal and vertical variograms for a site.

5.7.2.1 Constructing Variograms for Zone 2

Vertical variogram parameters selected for layer 2, with consideration of the 23 borings making up zone 2, are listed in Table 48 and Table 49. The variogram parameter values are selected in a manner analogous to that detailed previously when considering the zone 1 data set. The lag distance selected for layer 2 (in zone 2) is selected as 2.5 ft, which is on the order of typical lengths for core run data (5 ft). Selection of this lag distance is typically more desirable than, for example, the relatively large lag distance selected for zone 1 (recall Table Table 43). The wider set of parameter values selected for the vertical variograms of zone 2 (Table 48) differ substantially from respective values selected when considering all 90 borings of Site B (recall Table 37). Also, the variogram parameters selected for zone 2 differ from those of zone 1 (recall Table 43). Given reasonably well-formed vertical variograms for zone 2 (presented below) division of Site B into zones is further substantiated by such differences.

Table 48. Layer-specific parameters for vertical variograms of zone 2

Layer	Lag (ft)	Number of lags	Tolerance (ft)	Bandwidth (ft)
1	N/A	N/A	N/A	N/A
2	2.5	6	1.25	0.0

Table 49. Vertical variogram ranges and sills for zone 2 layers

Layer	Range (ft)	Sill
1	N/A	N/A
2	5.0	1.0

Listings of experimental vertical variogram points for layer 2 are provided in Table 50. The variogram points for zone 2 are obtained with detrending of the q_u values, where detrending reduces the COV of layer 2 (zone 2) from 1.15 to 1.08. Included among the listings are variogram points (and pairs) generated when considering all 90 borings from Site B and when considering the 25 borings from zone 2. Substantial reductions consistently occur in the pair

count values when transitioning from the site-wide data to the zone 2 data. For example, only a single pair is identified at 2.5 ft (this point is effectively neglected). Such reductions are somewhat expected as only 25 borings are considered for zone 2, versus the 90 locations throughout Site B. Despite the presence of pair counts below 30 across all lag distances in zone 2, the trend in the vertical variogram ordinate values for zone 2 (Table 50) indicate convergence toward a sill value equal to unity. As an additional observation, several of the variogram ordinate values exceed unity, which suggests the possible presence of layers in the data set. While insufficient data are available to explore this layering for zone 2, burgeoning technologies such as measuring while drilling (MWD) may facilitate such refinements for shaft portions in rock.

Table 50. Comparison of vertical variogram data for layer 2 when all borings are considered versus when zone 2 borings are considered

All borings			Zone 2 borings		
Abscissa (ft)	Ordinate	Pairs	Abscissa (ft)	Ordinate	Pairs
4	0.84	66	2.5	0.13	1
8	0.74	62	5.0	1.19	18
12	0.82	54	7.5	1.23	9
16	0.70	32	10.0	1.04	11
20	0.88	30	12.5	1.10	4
--	--	--	15.0	0.88	9

Comparative plots of the vertical variograms from all of Site B to those of zone 2 are presented in Fig. 109. Additionally, the variogram ordinate value of 1.0 is visually emphasized in each plot. Visual comparison of the vertical variogram points (Fig. 109a, Fig. 109b) reveals that the zone 2 variogram appears to converge toward unity while the site-wide variogram converges to approximately 0.75. The vertical variogram associated with layer 2 (of zone 2) is replotted in Fig. 110, along with the fitted (spherical) theoretical variogram. The range value associated with the theoretical variogram of zone 2 (5.0 ft) is smaller than the largest abscissa value generated for the experimental variogram (15 ft). This serves to verify that a sufficient number of lag distances are specified as listed in Table 50 above.

a)   b)
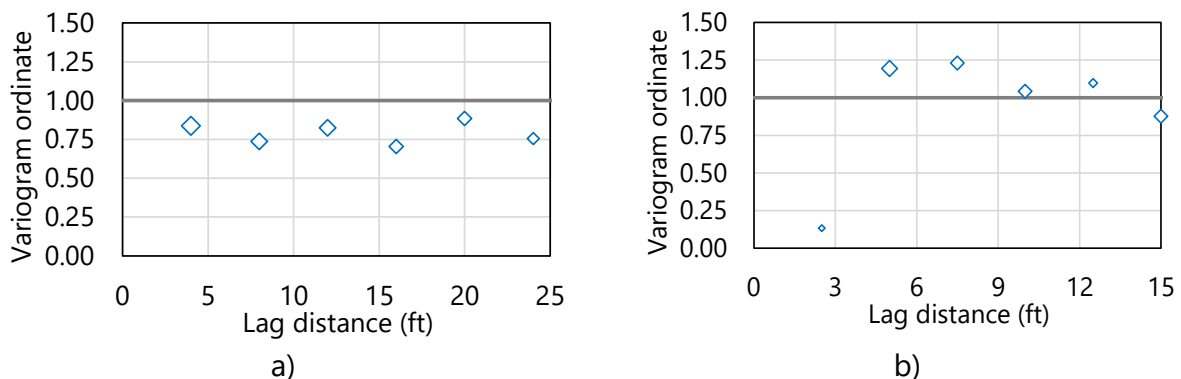
Figure 109. Comparison of vertical variogram points for layer 2: a) All borings; b) Zone 2

141
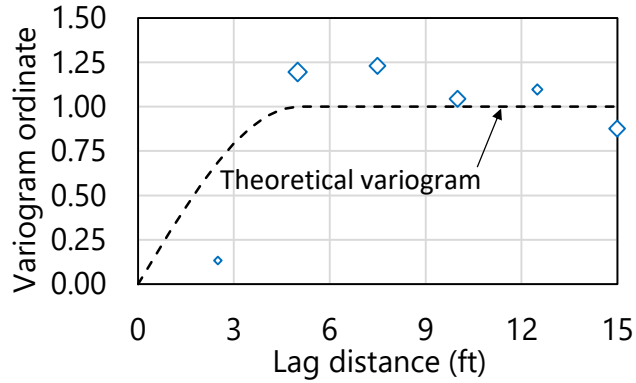
Figure 110. Vertical variogram for layer 2 of zone 2

5.8 Observations Regarding Zonal Issues

Summary comparisons of the site-wide, zone 1, and zone 2 layer data (including variograms) are discussed in the following. These comparisons make clear the need to divide the Site B data set into zones. As demonstrated later in Sec. 5.10, differences in resistance profiles—obtained by performing stochastic simulation for each of zone 1 and zone 2—further substantiate the need to consider the Site B data on a zone by zone basis.

As justification for dividing the site into zones (from the standpoint of layer statistics and spatial correlation structures), consider Fig. 111 through Fig. 113, and Table 51. Presented in Fig. 111 is a scatterplot of the layer 2 data (q_u) when all borings are considered, along with scatterplots of the zone-specific subsets of q_u values. Although qualitative in nature, visual examination of the overlaid scatterplots reveals the presence of more pronounced scatter, across a wider range of values among the site-wide data. Further, it is evident that groupings of the q_u values local to zone 1 include q_u values of larger magnitude relative to those of zone 2.
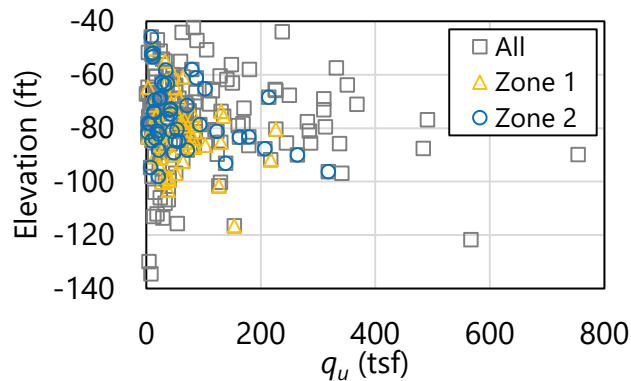
Figure 111. Scatterplots of unconfined compression strength, q_u

142

Descriptive statistics listed across all borings, zone 1, and zone 2 (Table 51) signify (quantitatively) differences in the three collections of q_u values. For example, the mean of the site-wide values (92 tsf) exceeds those of zone 1 (62 tsf) and zone 2 (63 tsf). Also, while the medians of the site-wide data and zone 1 are equal (50 tsf), that of zone 2 is significantly smaller (37 tsf). Further, consistent with the overlaid scatterplots (Fig. 111), the dispersion attributed to the site-wide data (with variance of 13020 tsf^2) is far greater than that of zone 1 (2477 tsf^2). In turn, the variance of zone 1 is approximately half of that for zone 2 (5304 tsf^2). Relative dispersions (i.e., COV values) are comparable between the site-wide data and zone 2 (both exceed 1), while that of zone 1 is relatively smaller (0.8).

Table 51. Summary statistics for layer 2

Borings	Mean (q_u, tsf)	Median (q_u, tsf)	Variance (tsf^2)	COV
All (90)	92	50	13020	1.25
Zone 1 (23)	62	50	2477	0.80
Zone 2 (25)	63	37	5304	1.15

Such widespread differences in the descriptive statistics correspond to differences in the distributions of q_u values. Presented in Fig. 112 are histograms of the layer 2 data associated with all borings, zone 1, and zone 2. To facilitate visual comparisons, the range of q_u values considered is constrained between 25 tsf and 200 tsf. Ordinates consist of relative frequencies because, expectedly, frequency counts associated with the site-wide data (90 borings) far exceed those of zone 1 (23 borings) and zone 2 (25 borings).

Visual examination of the relative frequencies in Fig. 112 makes apparent that significant fractions of the q_u values within the site-wide data set, as well as those of zone 2, are of magnitudes less than approximately 37.5 tsf. For zone 2, this is the case for nearly half of the constituent q_u values. In contrast, values are somewhat evenly (but heavily) distributed across a range of values from 0 tsf to approximately 87.5 tsf. Clearly, these three data sets exhibit distinct statistical properties.
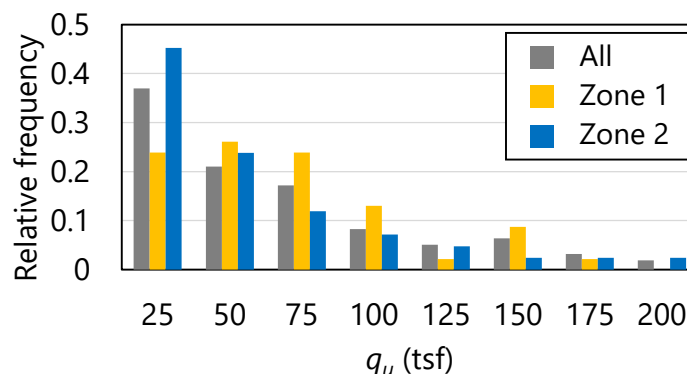
Figure 112. Histograms of unconfined compression strength, q_u, over the range of 25 tsf to 200 tsf

As a culmination of the above discussion, consider the comparative plot of vertical variograms in Fig. 113. Both the experimental variogram points and the theoretical fits are plotted. To facilitate comparisons, the plotted variogram ordinates are not normalized, while the lag distances are normalized (i.e., variogram abscissa values are divided by the maximum abscissa value from the respective set of experimental variogram points). For all variograms, the sill values converge (or should converge) to the variances of the layer data (recall Table 51). As a telling exception, the vertical variogram associated with all borings does not converge to the site-wide variance. This is a strong indicator of zonal issues among the site-wide collection of boring data. Furthermore, the variograms for zone 1 and zone 2 both converge to unique variance values, which are of smaller magnitude than the site-wide variance (as well as that associated with all borings). Therefore, it is concluded that the Site B data set must be divided into zones in order to make representative estimates of axial resistances for deep foundation members.
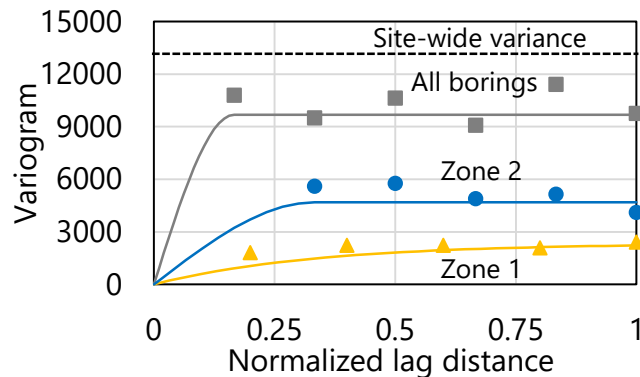
Figure 113. Vertical variograms for layer 2

5.9 Performing Stochastic Simulation

Having established the need to divide Site B into zones, and further, having defined representative layerings and vertical variograms for geotechnical data within zone 1 and zone 2 of Site B, stochastic simulation of axial resistance is carried out in GeoStat as the next major step. In the remainder of Ch. 5 results obtained from stochastic simulation of the zone 1 and zone 2 data sets are documented (and compared). Differences present among the two sets of results clearly demonstrate the need, and value, of dividing sets of site data into zones when appropriate.

Shown in Fig. 114 is the fourth of seven tabs (from left to right) in the GeoStat UI, referred to as the Simulation tab. Data displayed in Fig. 114 corresponds to the zone 1 model. Discussed below are selections made for relevant foundation member parameters specific to zone 1 and zone 2, as well as initial considerations for carrying out the two sets of simulations (again, one set for zone 1 and one set for zone 2).

5.9.1 Selecting Embedment Ranges and Intervals

One drilled shaft foundation member is investigated in association with each of zone 1 and zone 2 from Site B. For the shaft of zone 1, embedment lengths ranging from 55 ft to 110 ft are simulated, where these depths correspond to elevations of -50 ft and -105 ft. For the shaft of zone 2, embedment lengths ranging from 54 ft (elevation of -45 ft) to 114 ft (elevation of -105 ft) are simulated.

Across all shaft lengths considered, an embedment interval of 1 ft is selected. This signifies, for example, that axial resistances in zone 1 are to be computed in 1-ft intervals between the 55-ft and 110-ft embedment range. Interval lengths that are small relative to the layer heights are generally recommended for conducting simulations in GeoStat.

The ground surface elevation is assigned as 5 ft for zone 1 and 9 ft for zone 2. Water table elevations, respectively are assigned as 0 ft and 3 ft for zone 1 and zone 2. Candidate shaft configurations for both zone 1 and zone 2 terminate (approximately) at elevations ranging from the top of layer 2, extending near to the bottom of layer 2 (Fig. 115).
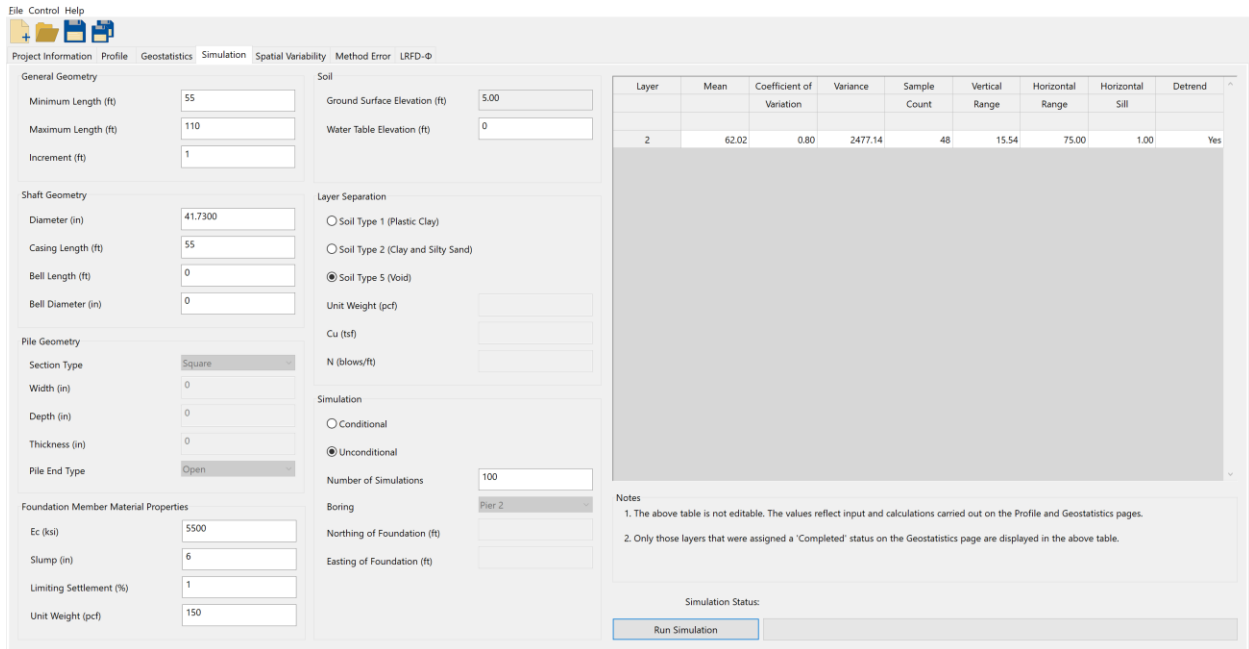
Figure 114. Simulation tab
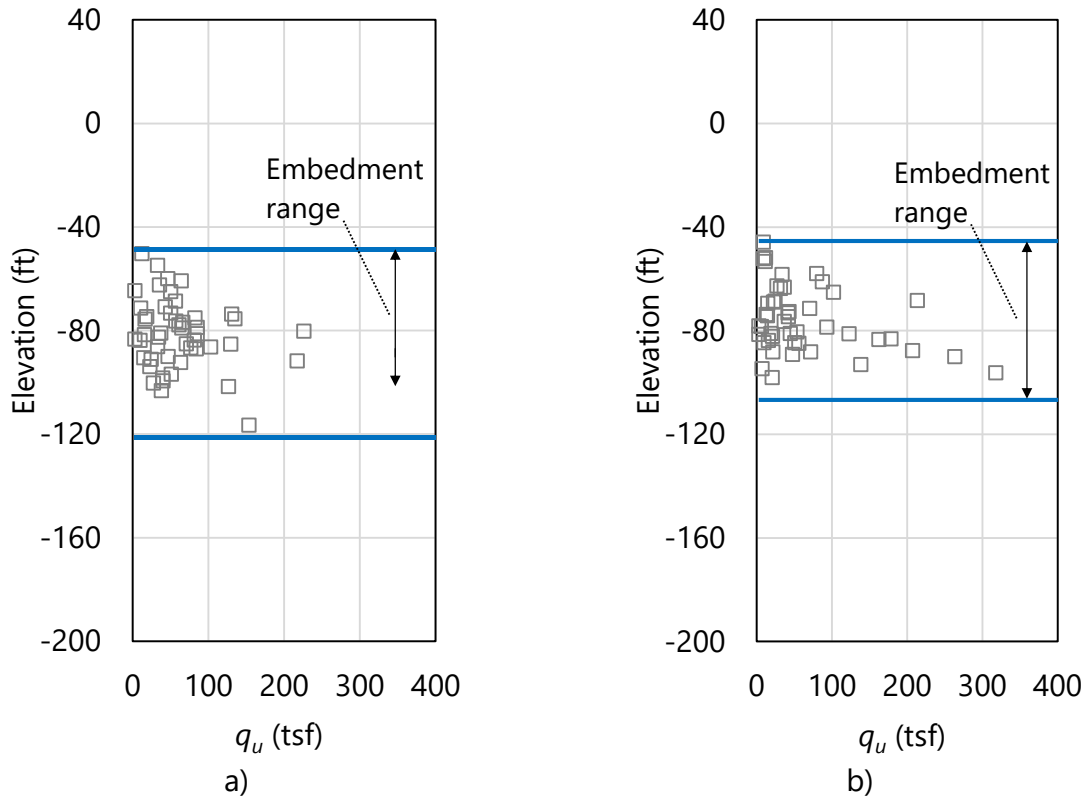
Figure 115. Scatterplots of unconfined compression strength, q_u, with layer divisions (blue horizontal lines): a) Zone 1; b) Zone 2

5.9.2 Foundation Member Cross-Section

The middle-left portion of the Simulation tab (recall Fig. 114) contains input controls that allow for definition of foundation member cross-sections. Because a drilled shaft is being considered for zone 1 and zone 2, only the shaft diameters and casing lengths are necessary to define the cross-section (within the separate model files). Diameters are defined as 41.7 in. for the shafts of zone 1 and zone 2. Casings are also defined in each case, extending down to the top of rock for each zone model. For scenarios where a driven pile is selected as the type of foundation member, required inputs for the cross-section geometry vary by the type of pile being considered (e.g., square, cylindrical, h-pile). Additional details for the required input parameters of driven pile cross-sections are detailed in the Help Manual.

5.9.3 Foundation Member Material Properties

GeoStat UI controls positioned in the bottom-left portion of the Simulation tab (recall Fig. 114) pertain to the definition of the foundation member material properties. For drilled shafts, unit weight (supplied for both zone 1 and zone 2 as 150 lb/ft³) is required. Values of shaft elastic modulus, concrete slump, and limiting shaft settlement are additionally required for drilled shafts. These values, respectively, are input as 4000 ksi, 6 in., and 1% for zone 1;

and, 4000 ksi, 6 in., and 1% for zone 2. Supplying these parameters is only necessary for computing shaft end bearing resistance.

5.9.4 Layer Separation

Included among the simulation parameters input on the Simulation tab (Fig. 114, middle) is selection of a soil type for modeling of layer separations. Recall from Fig. 88 that soil or rock layerings are defined from within the Profile tab of the GeoStat UI. Furthermore, layers can be defined as consisting of one of four possible soil or rock types. For generation of analysis model files during stochastic simulation, the "physical" layers are subdivided into 0.5-ft increments (referred to in this context as sublayers).

A subset of the available layer types may be specified for defining those sublayers that fall at the boundaries of layers that are defined on the Profile tab. For use of the GeoStat software in design applications, it is recommended that these sublayers (or, layer separators) be designated as Soil Type 5 (Void). If it is alternatively desired that layer separations not be designated as Soil Type 5 (Void), then additional properties must be specified as delineated (along with additional contextual discussion) in the Help Manual.

5.9.5 Selecting the Simulation Type

As detailed in Ch. 2, either unconditional or conditional (stochastic) simulation can be conducted using GeoStat software. Unconditional simulation only requires definition of vertical variograms, whereas conditional simulation requires definition of both horizontal and vertical variograms. As discussed previously, unconditional simulation is elected for both the zone 1 and zone 2 models.

When conducting unconditional simulation, only the number of realizations to be generated during simulation must be specified (Fig. 114, bottom-center). For all demonstration cases reported in McVay et al. (2012), the associated number of realizations was set to 2000. Further, Faraone (2014) recommended that a minimum of 1000 realizations be considered when conducting stochastic simulation. For use of GeoStat in design applications, it is recommended that 2000 realizations be considered. However, it can always be verified that further increases in the number of realizations do not lead to appreciable changes in variance for the computed profiles of resistance. Additional considerations for deciding upon the suitable number of realizations for simulation are provided in Ch. 4.

5.10 Viewing Spatial Variability Results

Shown in Fig. 116 is the fifth of seven tabs (left to right) in the GeoStat UI, referred to as the Spatial Variability tab. Results displayed in Fig. 116 correspond to zone 1. This tab is intended for use in viewing profiles of computed axial resistance, where the resistance values take into

account spatial variability phenomena. Plots of spatial resistance are divided into skin friction (side) resistance, end bearing (tip) resistance, and total resistance. For each type of resistance (skin, tip, total), profile plots of the mean, variance, COV, and ϕ (reflecting spatial variability only) are provided.
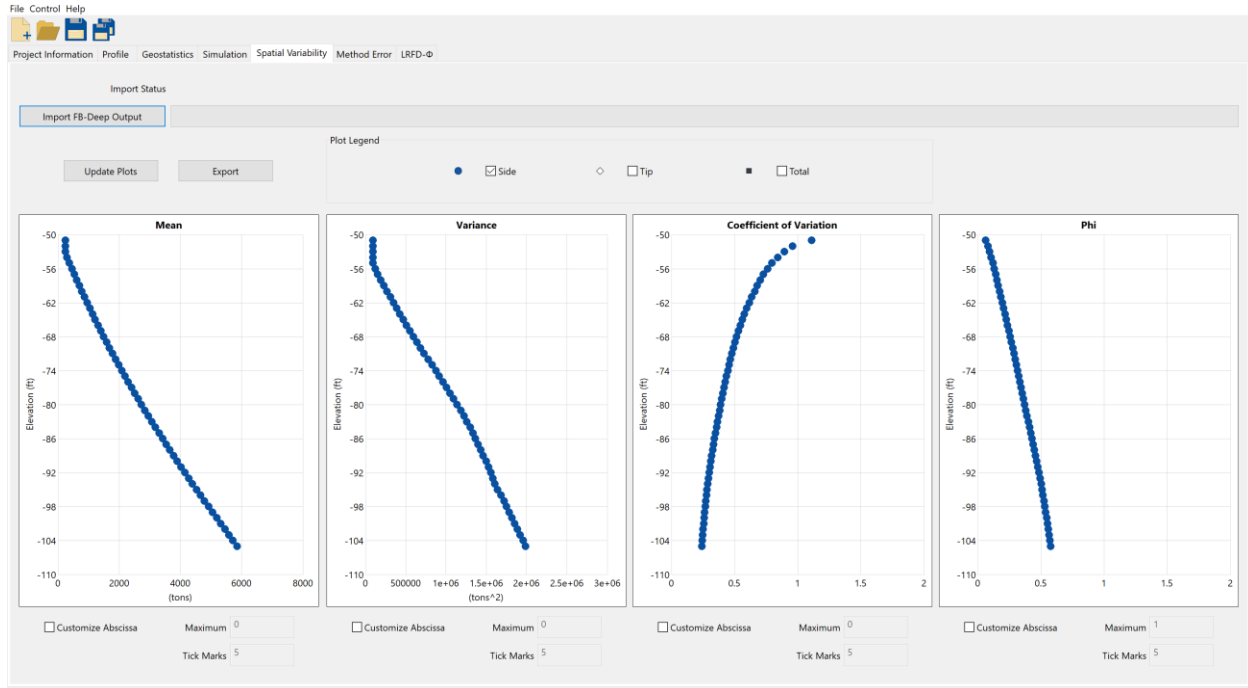

Figure 116. Spatial variability tab

5.10.1 Profiles of Computed Resistance

For both sets of simulation results, physical measurements obtained from test shafts (indicated for each zone in Fig. 117) are available. Also plotted are those borings in closest proximity to the test shaft locations. For zone 1, the constituent borings (Fig. 117a) are roughly positioned to either side of the test shaft location. A similar configuration (with regard to relative positioning) is apparent for the borings comprising zone 2 (Fig. 117b).

Results plots are presented in Fig. 118 for zone 1 and Fig. 119 for zone 2. Namely, profiles of skin and total resistance quantities—obtained from unconditional simulation with 2000 realizations—are displayed. For each shaft configuration and layering considered, skin resistance is clearly the dominant contributor to the mean and variance quantities for total resistance. For the range of zone 1 shaft embedments, resistance increases (from 0 tons to 5900 tons at -105 ft) roughly in proportion to increasing embedment depth within the limestone layer. The shaft associated with zone 2 also exhibits increasing resistance with increasing depth. However, the maximum resistance reaches a substantially smaller magnitude (4260 tons at -105 ft).
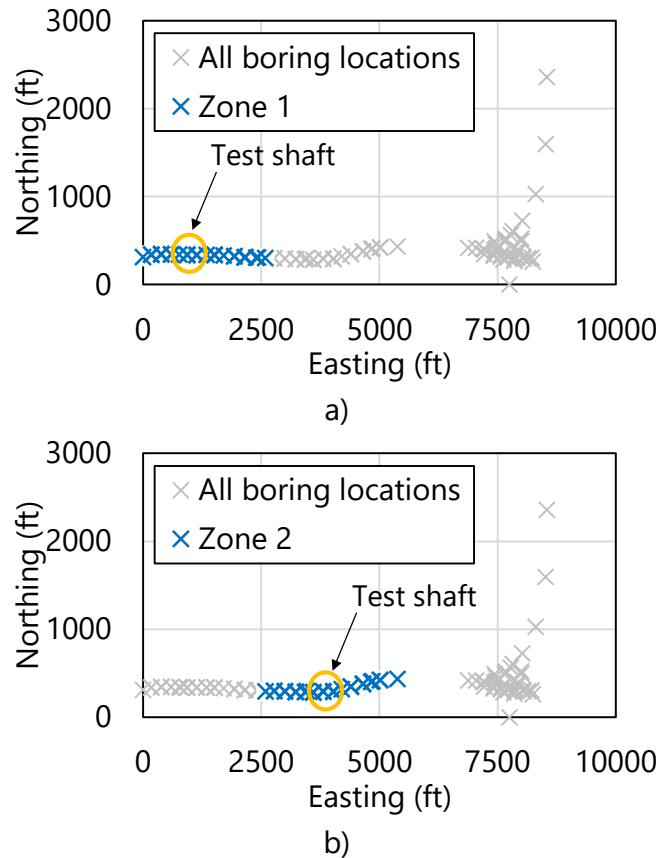
Figure 117. Locations of test shafts in relation to each zone: a) Zone 1; b) Zone 2

Although the shaft for zone 1 possesses the same diameter as that of zone 2 (41.7 in.), it is evident that the limestone in zone 1 allows for relatively greater resistances to be obtained versus that of the limestone in zone 2. Such outcomes would not be discernible without dividing the site into zones, assessing zone-specific spatial variability structures, and then conducting stochastic simulation for each zone.

Regarding computed versus physical measurements, reasonable to favorable comparisons are made between the profiles of computed response and available physical data from the test shaft investigations pertaining to each zone. More specifically, unit side friction quantities are calculated from selected elevation ranges (using the computed profile data), and then compared to corresponding physical data reported among the test shaft results. For zone 1, over the elevation range of -92 ft to -96 ft, the computed profile of side resistance approximately corresponds to 23.5 ksf. The respective value of unit side shear (derived from physical measurements) for the test shaft in zone 1 is 17.5 ksf. As an analogous comparison concerning zone 2, and over the range of -68 ft to -73 ft, the computed results give 12.0 ksf of unit side friction while that of the physical measurements corresponds to 10.4 ksf.
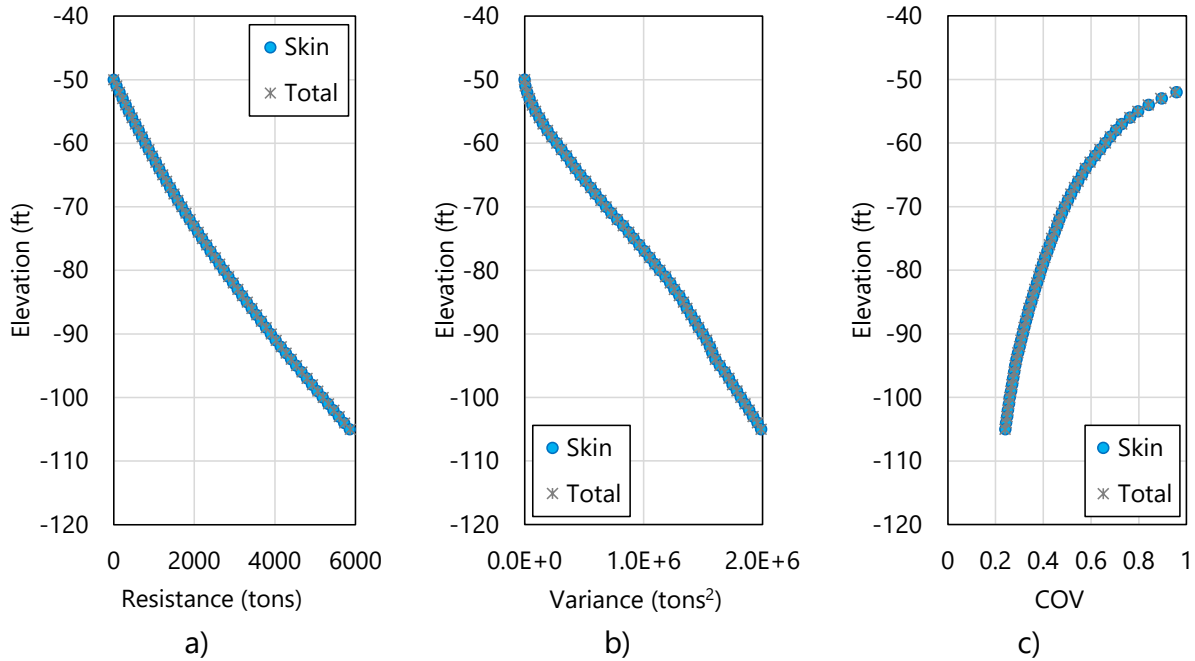
Figure 118. Profile plots obtained from unconditional simulation of zone 1 boring locations with 2000 realizations: a) Mean resistance (spatial variability only); b) Variance; c) COV
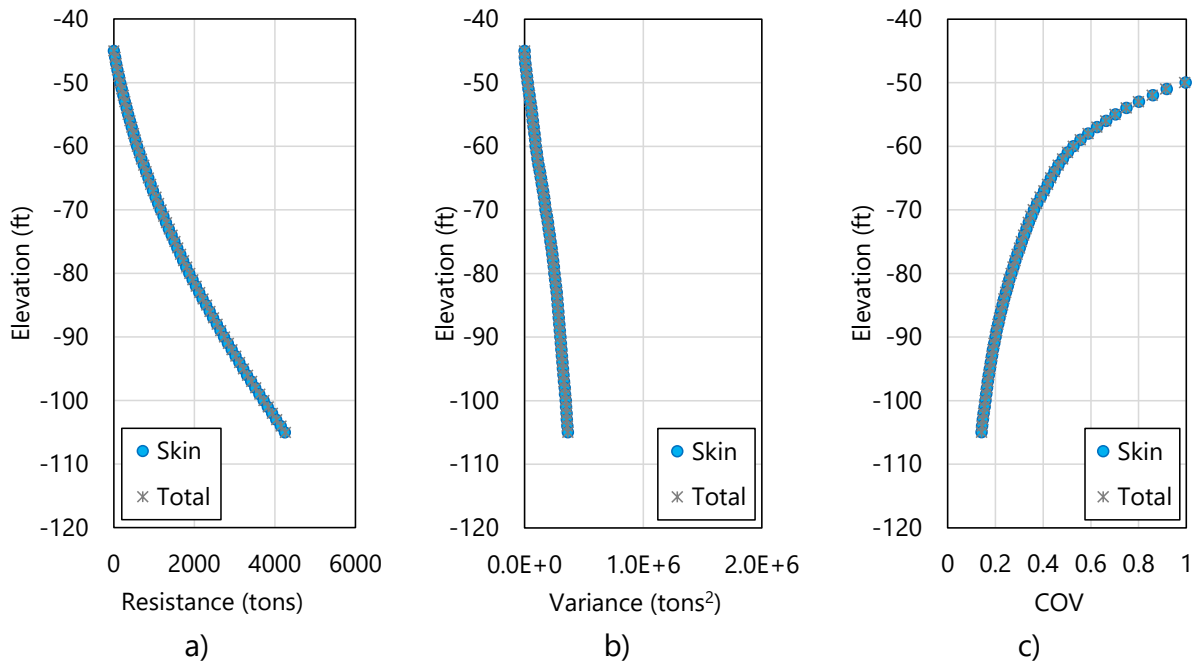
Figure 119. Profile plots obtained from unconditional simulation of zone 2 boring locations with 2000 realizations: a) Mean resistance (spatial variability only); b) Variance; c) COV

Regarding the profiles of variance (Fig. 118b, Fig. 119c), considerably larger magnitudes are computed for zone 1. This is offset though by the relatively larger mean values of resistance computed along the profile of zone 1. Stated another way, for embedment depths corresponding to elevations of approximately -70 ft and below, the COV values associated with each zone are of comparable magnitudes. For the maximum embedments considered, both zones reach COV values of approximately 0.2. As discussed in Ch. 2 and Ch. 3, smaller COV values correspond to relatively larger values of resistance factors, ϕ (and therefore, larger factored resistance values). Therefore, extending the shaft a considerable distance into the limestone layer of each zone (thereby minimizing the associated COVs) may lead to relatively more efficient use of construction materials.

5.10.2 Resistance Factor (ϕ), Spatial Variability Only

Presented in Fig. 120 are profile plots of resistance factors, ϕ, for skin and total resistance, as obtained from unconditional simulation with 2000 realizations. Profile plots are provided for both zone 1 (Fig. 120a) and zone 2 (Fig. 120b). The plotted profiles only take into account spatial variability, as opposed to the total uncertainty associated with combined spatial variability and method error.
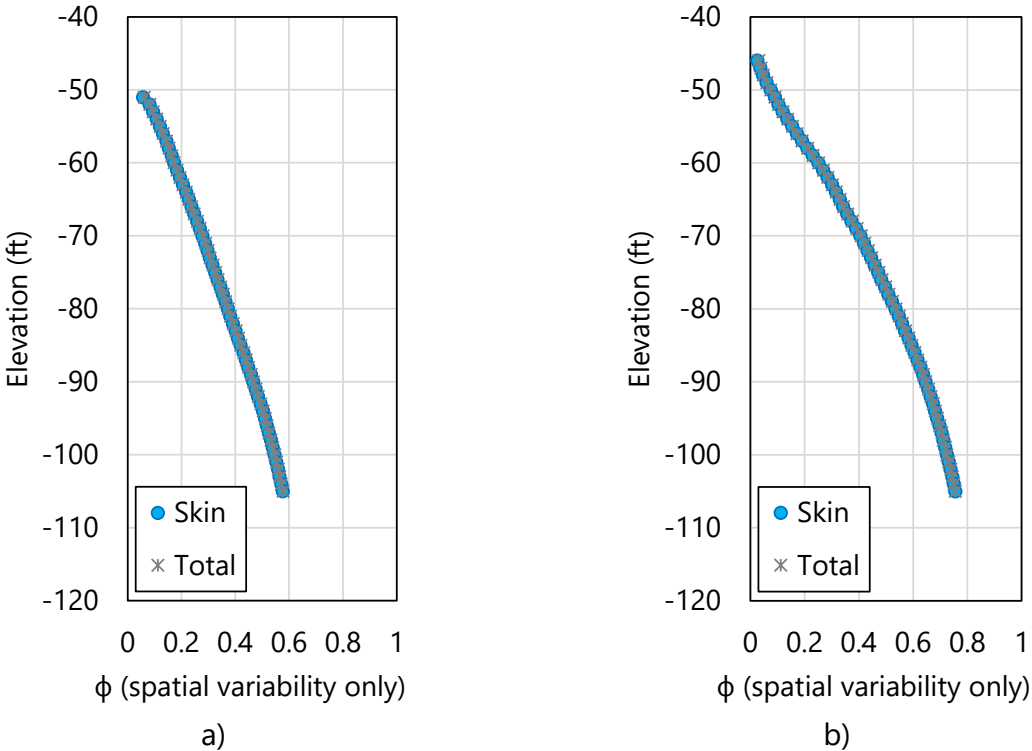
Figure 120. Profile plots of resistance factor, ϕ (spatial variability only), obtained from unconditional simulation with 2000 realizations: a) Zone 1; b) Zone 2

151

In contrast to the profile of COV values (recall Fig. 118c, Fig. 119c), the profiles of computed resistance factors, ϕ (spatial variability only), generally increase with respect to increasing embedment depth. For zone 1, computed values of resistance factors (ϕ) remain relatively low for embedment depths that fall above elevations of approximately -80 ft (zone 1) or -70 ft (zone 2). For the maximum embedment depth considered, however, the resistance factors (ϕ) for both zone 1 and zone 2 approach a more desirable value of approximately 0.6.

Profiles of resistance factors, ϕ, attributable to spatial variability are contributed to, in part, by two factors: 1) the COV of the layer data; and, 2) the range of the variogram. For zone 1, the COV (0.8) is lower than that of zone 2 (greater than 1), but the range assigned to the vertical variogram of zone 1 (15.5 ft) is considerably larger than that of zone 2 (5.0 ft). These two factors offset one another (respectively, in each zone), and as a result, shafts in both zones are able to attain desirable values of resistance factors (ϕ) at maximum embedment depths.

5.10.3 Additional Comparisons of Spatial Variability Results

Accounting for geological zones, isolating the zones, and repeating the variogram modeling efforts is shown to be necessary for the present modeling scenario. Recall (from Table 41) that the COV of the site-wide collection of q_u values in layer 2 is 1.25 while that of q_u values associated with zone 1 is 0.8. The respective COV value for zone 2 is 1.15. The COVs associated with both zone 1 and zone 2 are reduced relative to that of the site-wide data set.

To more fully illustrate the benefit of dividing Site B into zones, consider the two profiles of mean total resistance (spatial variability only) that are plotted in Fig. 121. Here, computed results from zone 1 and zone 2 are plotted together to accentuate comparisons. Clearly, the limestone layer in zone 1 produces greater resistance than that of zone 2.

As one insight into why the two zones produce such different profiles of mean resistance, consider the relative cumulative frequency plots of q_u and q_t in Fig. 122. Recalling Table 41 (for zone 1) and Table 46 (for zone 2), the mean values of q_u for zone 1 (62 tsf) and zone 2 (63 tsf) are of comparable magnitude. However, the distributions of q_u values differ substantially, particularly up to a relative cumulative frequency of 0.75. For example, the median q_u value for zone 1 is 50 tsf, while that of zone 2 is 37 tsf. As detailed in Ch. 2, the distribution of the layer data (e.g., q_u, SPT-N) plays an important role in stochastic simulation (namely, by relating simulated standard normal values to the layer-specific distribution of the physically measured values). Furthermore, the McVay empirical limestone model is used in computing unit side friction ($0.5\sqrt{q_u q_t}$) for the shafts. Given all of the above, it follows that differences in the distributions of q_u values influence the profiles of (integrated) mean total resistance.
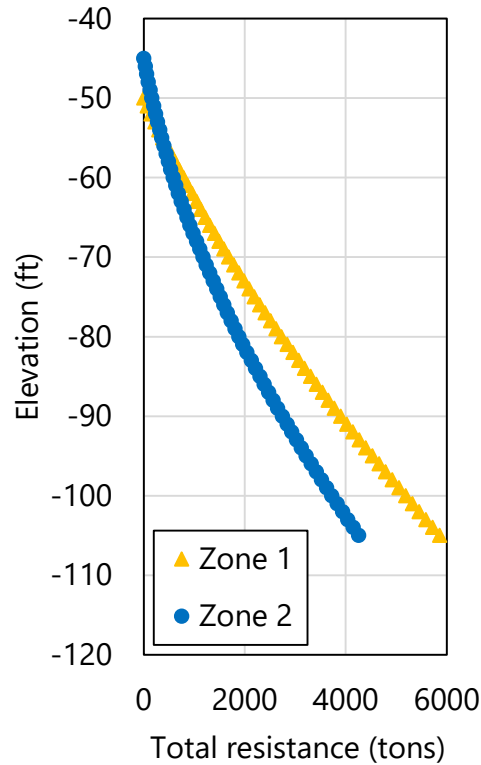
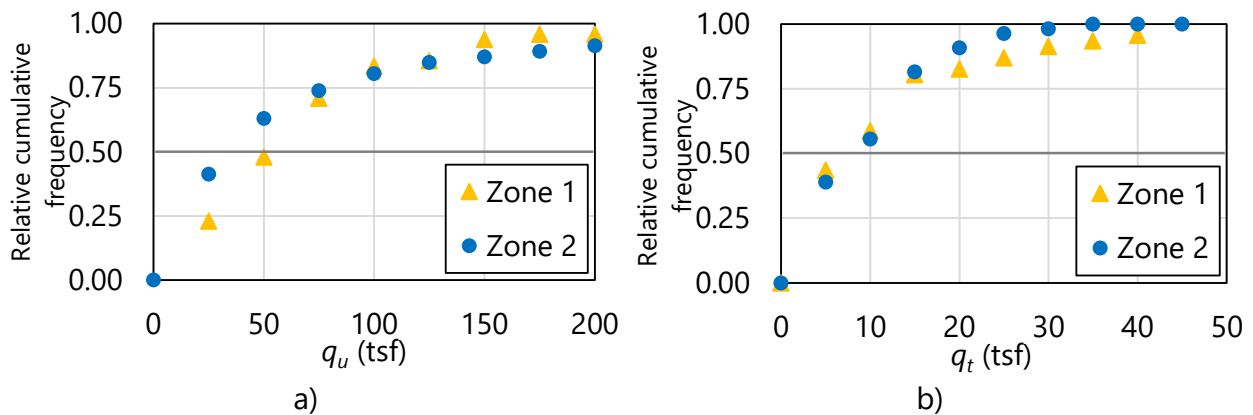Figure 121. Profile plots of mean resistance (spatial variability only)

a)

b)

Figure 122. Relative cumulative frequency functions for rock strengths in layer 2: a) q_u; b) q_t

5.11 Incorporating Method Error

As documented in Ch. 3, two contributors to total uncertainty for estimates of foundation member axial resistance are spatial variability and method error. Method error calculations serve to adjust the "raw" results obtained from stochastic simulation, and in addition, contribute to the calculation of resistance factors (φ). In the GeoStat UI, parameters related to method error are specified in the sixth of seven (left to right) program tabs (Fig. 123).

153
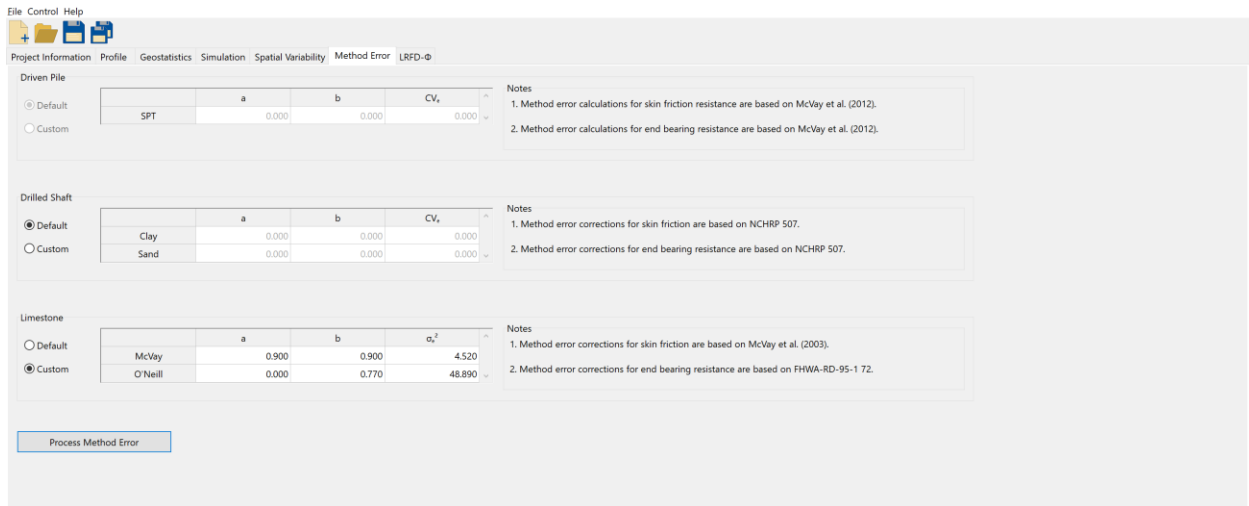
Figure 123. Method Error tab

As also detailed in Ch. 3, characterization of method error phenomena in GeoStat is divided into regression expressions for: driven piles, drilled shafts in clay, drilled shafts in sand, McVay skin friction of drilled shafts in limestone, and O'Neill end bearing for drilled shafts in limestone. Of relevance to both zone and zone 2 are portions of drilled shafts in limestone.

5.11.1 Shaft Portions in Limestone

Regression values pertaining to method error calculations for portions of the drilled shaft embedded in limestone (layer 2) are listed in Table 52 and Table 53. The same regression values are used for both zones. Default regression parameters implemented in GeoStat are utilized for method error calculations associated with skin friction. For end bearing resistance, all parameters are set to match the default values implemented in GeoStat. Of note, the intercept (a) of the regression expression is defined as 0 instead of the value of 20.5 (from O'Neill). This deviation is elected because end bearing only nominally contributes to the total resistance for the Site B analysis (recall Fig. 118, Fig. 119).

Table 52. Method error parameter values for skin friction of shaft portions embedded in limestone

Parameter	Value
a	0.90
b	0.90
σ_ε^2	4.52

154

Table 53. Method error parameter values for end bearing of the shaft in limestone

Parameter	Value
a	0.00
b	0.77
σ_ε^2	48.89

5.12 Viewing Final Results

Shown in Fig. 124 is the rightmost (seventh) tab in the GeoStat UI. Profile plots located within this tab facilitate viewing of total resistance quantities that reflect spatial variability phenomena as well as computed results associated with total uncertainty (spatial variability and method error combined). The types of profile plot data available for viewing include unfactored resistance (e.g., Fig. 125 for zone 1, Fig. 126 for zone 2); corresponding COV values (Fig. 127, Fig. 128); corresponding resistance factors, ϕ, (Fig. 129, Fig. 130); and, factored resistance (Fig. 131, Fig. 132). All plotted results in Fig. 125 through Fig. 132 are associated with unconditional simulation and 2000 realizations.
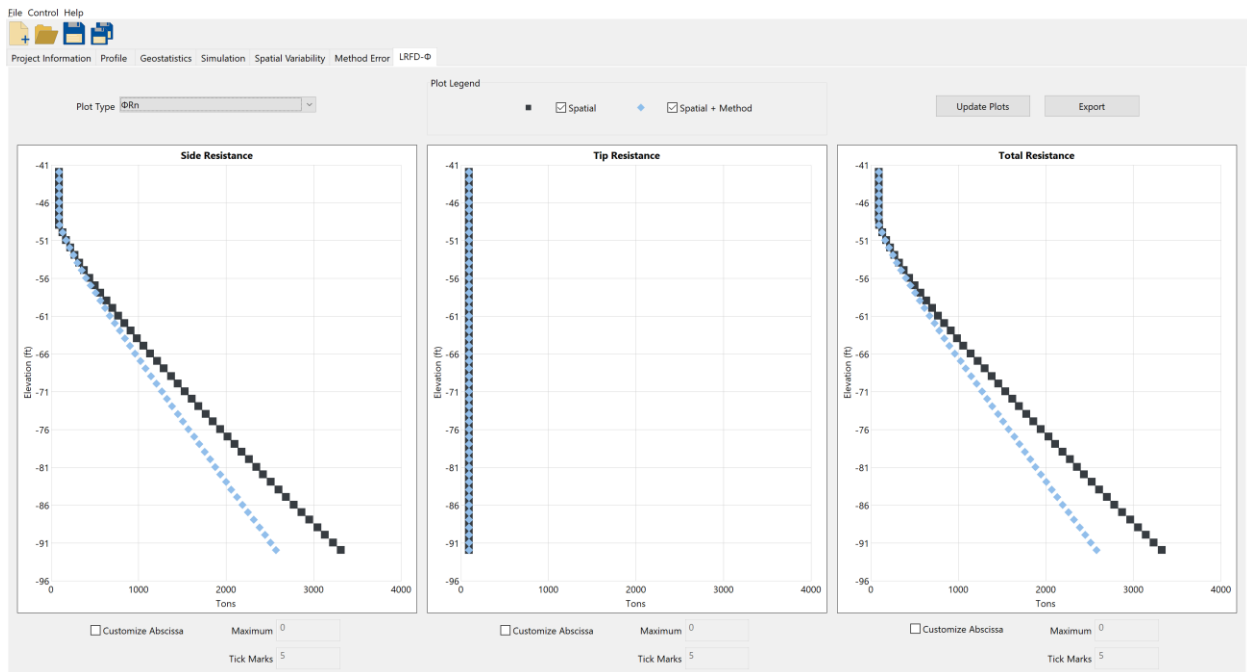
Figure 124. LRFD-ϕ tab for plotting profiles of resistance factors, ϕ, and factored resistances

Trends and phenomena that pertain to the profile plots of mean total resistance, COV, and ϕ values are analogous to those documented above in Sec. 5.10. Of note, however, is that total uncertainty (versus spatial variability alone) tends to more heavily penalize (reduce) computed resistance values. This phenomenon is present in both the profile plots of unfactored (Fig. 125, Fig. 126) and factored resistance (Fig. 131, Fig. 132).
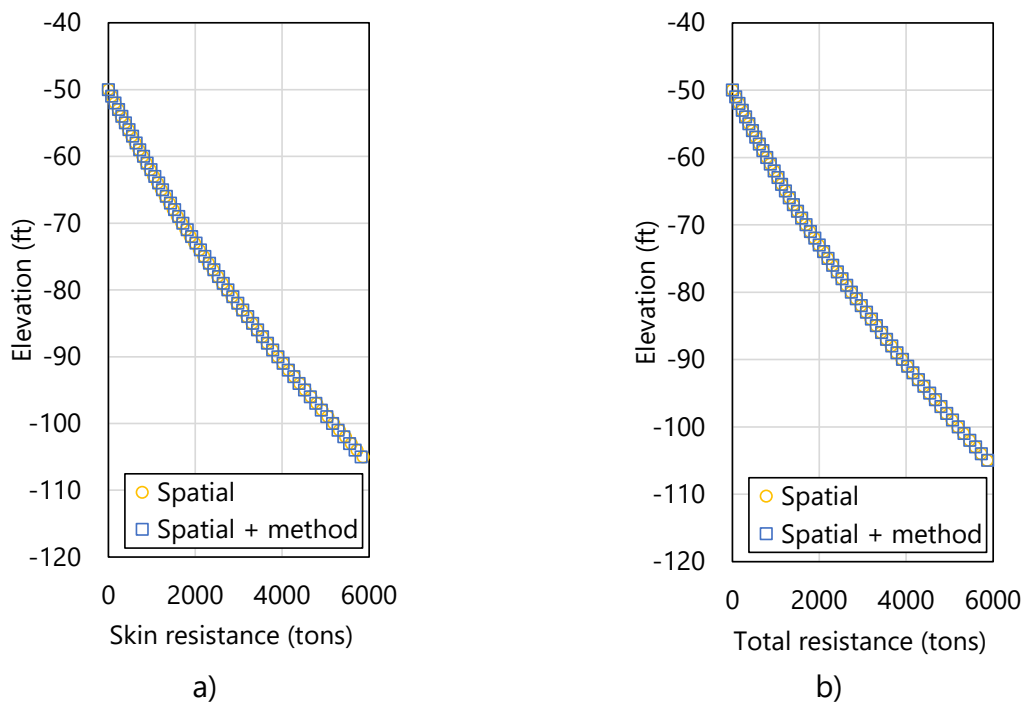
Figure 125. Profile plots of unfactored mean resistance for zone 1: a) Skin; b) Total
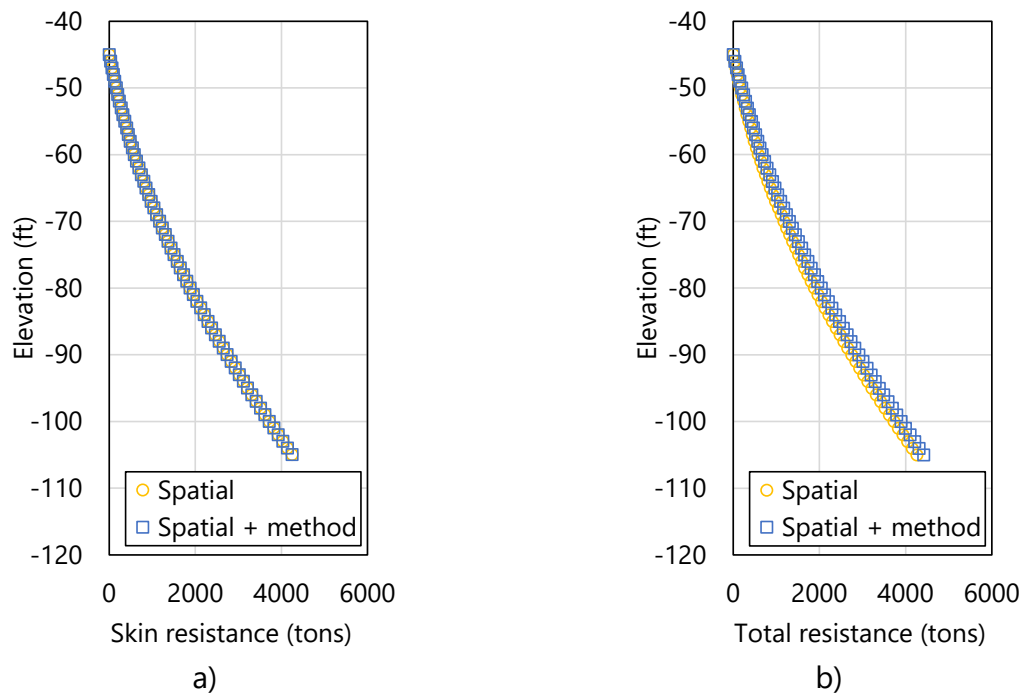
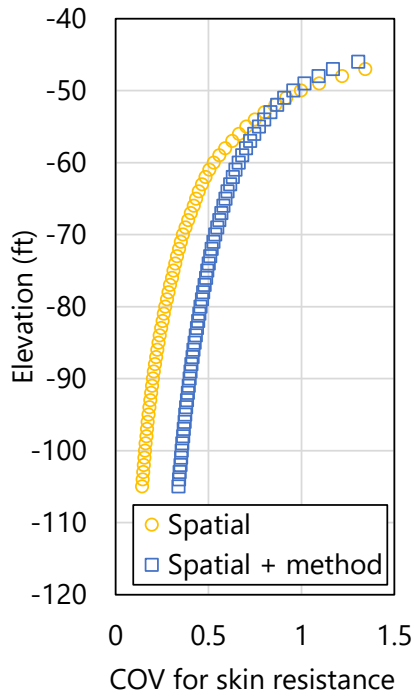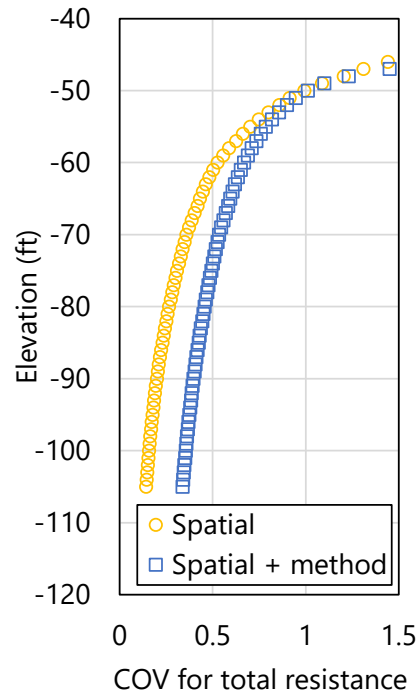Figure 126. Profile plots of unfactored mean resistance for zone 2: a) Skin; b) Total
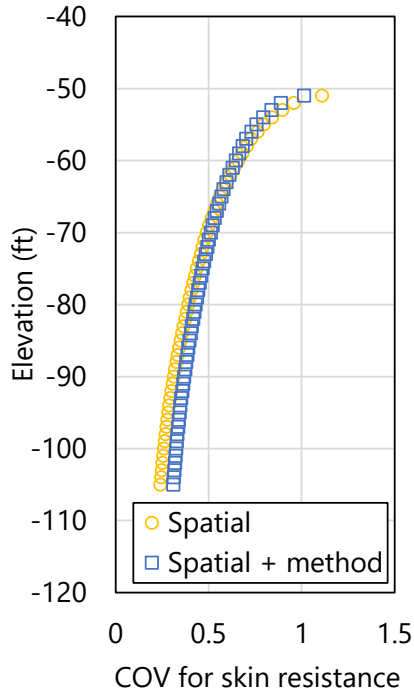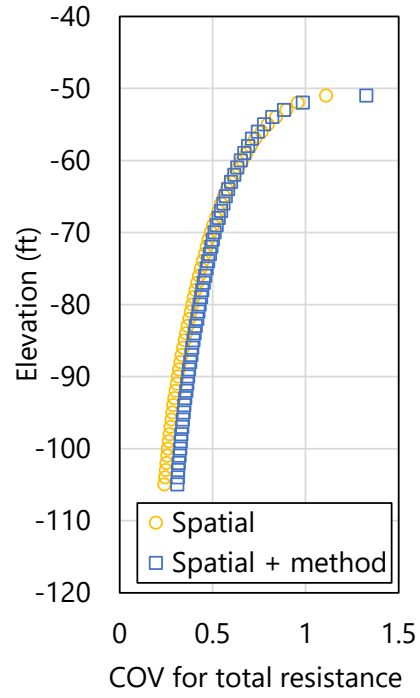
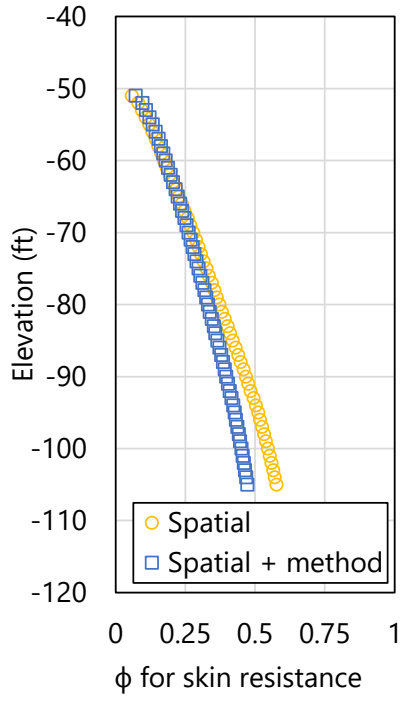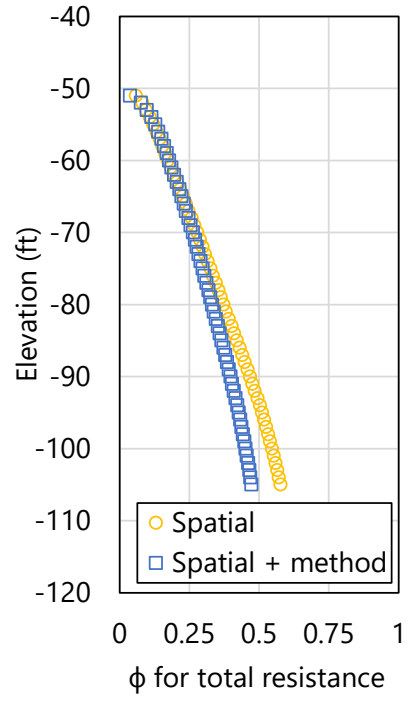Figure 127. Profile plots of COV for zone 1: a) Skin; b) Total

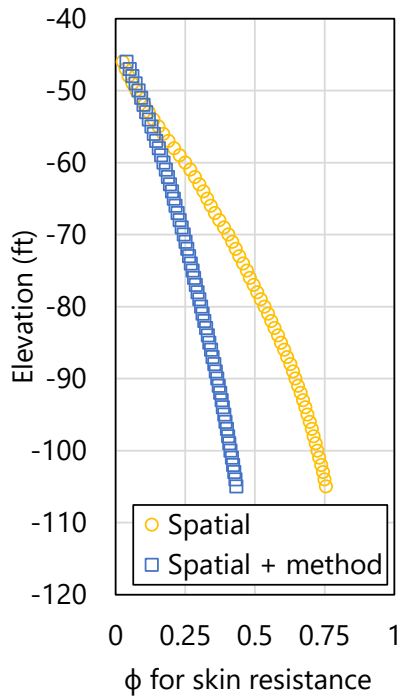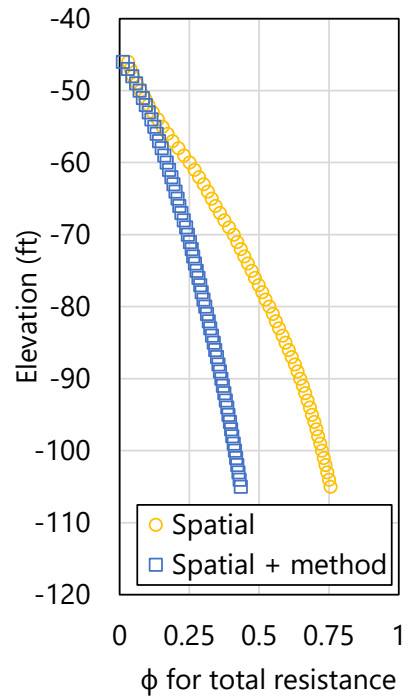Figure 128. Profile plots of COV for zone 2: a) Skin; b) Total

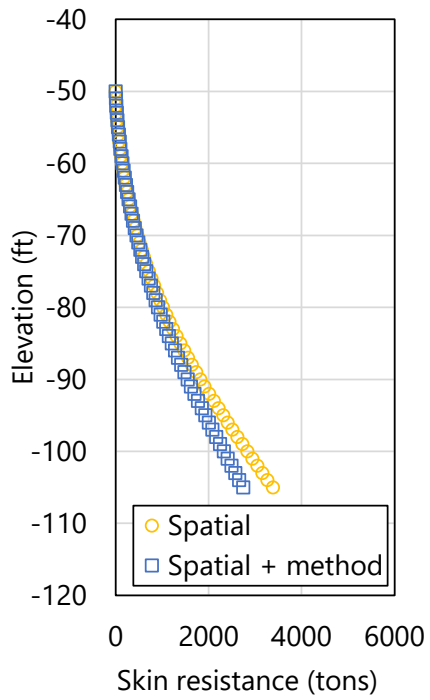Figure 129. Profile plots of resistance factor, ϕ for zone 1: a) Skin; b) Total

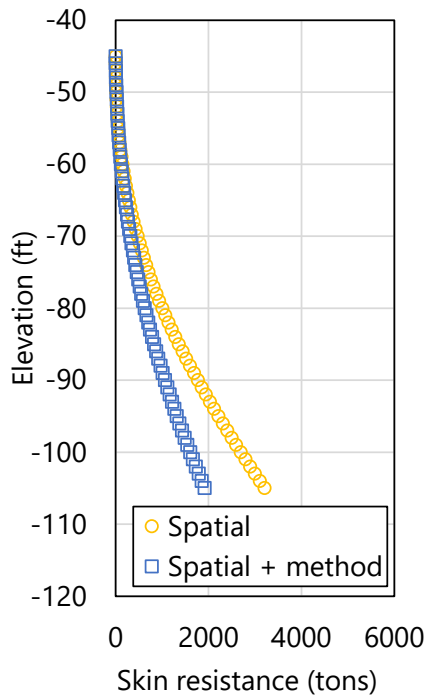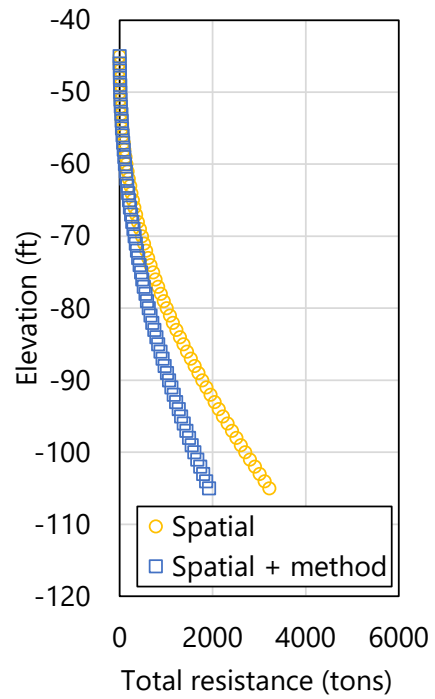Figure 130. Profile plots of resistance factor, ϕ for zone 2: a) Skin; b) Total
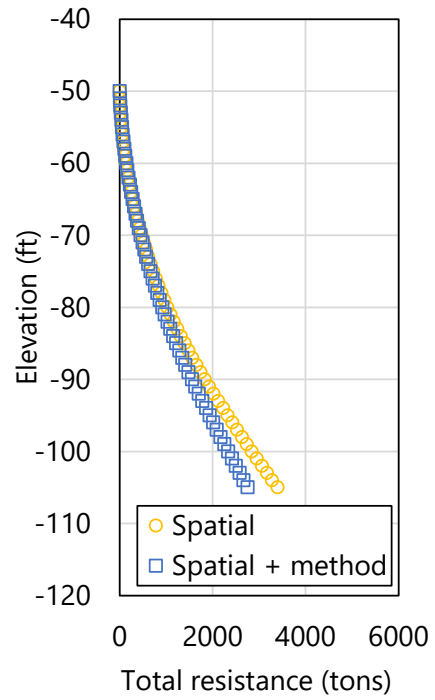
Figure 131. Profile plots of ϕ-factored mean resistance for zone 1: a) Skin; b) Total

Figure 132. Profile plots of ϕ-factored mean resistance for zone 2: a) Skin; b) Total

CHAPTER 6
REFERENCES

AASHTO. (2017). *LRFD Bridge Design Specifications*, 8th Ed. Washington D.C., Published: Washington D.C.

Faraone, M. A. (2014). *Geostatistical Analysis for Reliability Based Design of Foundations*, Dissertation, University of Florida, Gainesville, FL.

FB-Deep [Computer software]. Bridge Software Institute (BSI), University of Florida, Gainesville, FL.

FDOT. (2020). *Structures Design Guidelines*, Structures Manual, Vol. 1, Tallahassee, FL, Published: Tallahassee, FL.

Goovaerts, P. (1997). *Geostatistics for Natural Resources Evaluation*. Oxford University Press.

Gringarten, E., and Deutsch, C. V. (2001). Variogram Interpretation and Modeling, *Mathematical Geology*, 33(4), 507-534.

Klammler, H., McVay, M., Horhota, D., and Lai, P. (2010). "Influence of Spatially Variable Side Friction on Single Drilled Shaft Resistance and LRFD Resistance Factors", *ASCE Journal of Geotechnical and Geoenvironmental Engineering*, 136(8), 1114-1123.

McVay, M., Klammler, H., Bloomquist, D., Otero, J., Faraone, M. A. (2009). *Modifications of LRFD Resistance Factors Based on Site Variability*, FDOT Research Report BD-545 RPW76, Tallahassee, FL.

McVay, M., Klammler, H., Faraone, M. A., Krishmarao, D., Jenneisch, C. (2012). *Development of Variable LRFD ϕ Factors for Deep Foundation Design Due to Site Variability*, FDOT Research Report BDK75 977-23, Tallahassee, FL.

Rivers, B. (2018). Advanced Geotechnical Methods in Exploration (The A-GaME), *49th Annual Southeastern Transportation Geotechnical Engineering Conference* (STGEC), Louisville, KY, Oct. 8-11.

Styler, M. (2006). *Development and Implementation of the DIGGS Format to Perform LRFD Resistance Factor Calibration of Driven Concrete Piles in Florida*. Master's thesis, University of Florida, Gainesville, FL

Terzaghi, K., Peck, R.B. (1967). *Soil Mechanics in Engineering Practice*, 2nd Ed. New York, NY: John Wiley and Sons.